

BBRC

**Bioscience Biotechnology
Research Communications**

SPECIAL ISSUE VOL 13 NO (3) 2020

Print ISSN: 0974-6455

Online ISSN: 2321-4007

CODEN BBRCBA

www.bbrc.in

University Grants Commission (UGC)

New Delhi, India Approved Journal

Bioscience Biotechnology Research Communications Special Issue Volume 13 Number (3) 2020

RECENT ADVANCEMENT IN ELECTRICAL, INFORMATION AND COMMUNICATION TECHNOLOGIES

An International Peer Reviewed Open Access Journal

Published By:
Society For Science and Nature
Bhopal, Post Box 78, GPO,
462001 India

**Indexed by Thomson Reuters, Now
Clarivate Analytics USA**

SJIF 2020=7.728
Online Content Available:
Every 3 Months at www.bbrc.in

Issue Doi: [http://dx.doi.org/10.21786/bbrc/Special Issue Vol 13 No \(3\)](http://dx.doi.org/10.21786/bbrc/Special Issue Vol 13 No (3))



Registered with the Registrar of Newspapers for India under Reg. No. 498/2007
Bioscience Biotechnology Research Communications
SPECIAL ISSUE VOLUME 13 NO (3) 2020

Performance Denoising Filters on MRI Liver Tumor Images B. Sundarambal, R Thalpathi Rajasekaran, R. Balamurali and R. Dhanagopal	01-07
Analysis of Auto Antibody Complex by Pattern of Lacryglobin Spotting C. Narayanan, S.Krishna Priya, A.K. Nivedha, T. Gomathi and V. Boobalan	08-12
HI-TECH Electoral Machine for Election Commission of India P. R. Sivaraman, R. Jaiganesh, P. Ragupathy and R. Ramkumar	13-17
Anti Theft Control of Automatic Teller Machine Using Wireless Sensors R. Jaiganesh, L. Nagarajan, A. Arthi and V. Venkatesh	18-22
Optimization of Clinically Visual Deep Neural Network for the Classification of Liver Tumor Image S.Pavithra, A. Dhanasekaran, Vanisri A and R. Balamurali	23-26
Investigation and Analysis of Path Duration Estimation for Stable Communication Link in VANETS R. Menaka, N. Kandavel, N. Archana, A. Ragini and S. Soundarya	27-31
Scalable and Detect Link-Failure Traffic Balancing Network Using Adaptive Filter R.Purushothaman and R. Narmadha	32-38
Design of Tetra-band Antenna using Complementary Split Ring Resonator V. Ravichandran, M. Suresh, T. Shankar and A. Nazar Ali	39-43
ANN Based MPPT Controller for PEMFC System with Interleaved Resonant PWM High Step up Converter B.Karthikeyan, R. Ramkumar, L. Nagarajan, A. Anton Amala Praveen and S. Vijayalakshmi	44-47
Implementation of High Efficient Single Input Triple output DC-DC Converter A. Rajkumar, R. Jai Ganesh, V. Suresh Kumar, T. Vishnu Kumar and T. Ram Kumar	48-55
Design and Implementation of IOT Based Smart Library Using Android Application R. Ramkumar, B. Karthikeyan, A. Rajkumar, V. Venkatesh and A. Anton Amala Praveen	56-62
Design and Implementation of Tera-Hertz Antenna for High Speed Wireless Communication S. Prasad Jones Christydass, S. Praveen, S. Naveen Kumar, S. Rakesh Kumar and M.Periakaruppan	63-67
TVS Based Technique for Efficient Web Document Clustering in Web Search R Thalpathi Rajasekaran, R. Ramesh, R. Menaka and Vanisri A	68-73
A Survey Paper on Different Feature Extraction Methods in Image Processing N.Hemalatha, T. Menakadevi and A. Kavitha	74-78
Multi Input Dc-Dc Converter for Electric Vehicle Application S. Dineshkumar, K. Sureshkumar, S. Dheepak, and B. Cibishanth	79-81
MMCDM Based Approach for Efficient Web Document Clustering in Web Search R. Siva, T. Thandapani, R. Ramesh and R. Balamurali	82-88



Registered with the Registrar of Newspapers for India under Reg. No. 498/2007
Bioscience Biotechnology Research Communications
SPECIAL ISSUE VOLUME 13 NO (3) 2020

Metamaterial Inspired MIMO Antenna for Radar, Satellite and Terrestrial Communications S.Prasad Jones Christydass, B. Monisha, S. Shanthini and R. Saranya	89-93
Metamaterial Inspired Bandpass Filter for 5G Application S. Prasad Jones Christydass, A. S. Priyanka, S. Sugil and R. Soundharya	94-97
Identification of Diseases in Plant Leaves Using Deep Learning Algorithm R. Lalitha, S. Usha, M. Karthik, B. Pavithra, P. L. Sivagaami and G. Madhumith	98-102
Smart Portable Kidney Dialysis Control and Monitoring System A. Senthil Kumar, G. Keerthi Vijayadhasan D. Rashiga and K. Swetha	103-108
Implementation of Recurrent Controller with Seven Stage Cascaded Converter for Micro Grid Solar Number of Switches Photovoltaic Battery with Reduced M. Hari Prabhu, K. Sundararaju, S. Nagarajan, N. D. Arun, M. Bhuvaneshwaran, and A. Mariya Joseph Sathish	109-120
FPGA Implementation of Adaptive LMS Lattice Filter Sasikala S, Gomathi S, Naveen Kumar D, Praveenraaj R. K and Priyadharshini B	121-125
Secured Iot with Network Intrusion Detection Traffic Control by Data Routing Protocol in Wsn Using Genetic Algorithm S. Manikandan, P. Pushpa and S. Sathish Kumar	126-135
Design and Implementation of Solar Powered Electric Bicycle P. Karthikeyan, Major P. S. Raghavendran and V. Kumaresan	136-140
CSRR Inspired UWB Antenna for Breast Cancer Detection V. Vedanarayanan, G. Arulselvi, D. Poornima and D. Joshua Jeyasekar	141-145
A Novel Control Approach for PV-Grid System in various Atmospheric Conditions Dr. K Balachander, Nagamani Prabu. A and Janarthanan. B	146-151
Enhancing Security Using 3-Kae Algorithm In Wireless Sensor Networks R.Balamurali, S. Rajesh Kannan, R Thalpathi Rajasekaran and R. Ramesh	152-156
Development of Industrial Monitoring System Based on Embedded HTTP Host Using Raspberry Pi S.Bhuvanewari, R. Raghuraman, T. Thandapani and A. Sivabalan	157-161
Device Authentication for IoT Devices using ECC Krithiga J, Krishnan S, Sai Nithisha M, Jeevika Shree A and Lokeswari S	162-166
Detection of Glucose Using Non-Invasive Method and Food Analysis for Diabetic Patients Using IoT N. Suriya, S. Pavithra, K Santhosh Solomon and Yaswanth Reddy	167-171
Framework for Cancer Detection using Deep Wavelet Autoencoder & Neural Network in Brain Images M. Kavitha, S. B.Rajdakshan, S. Tamilselvan and M.Mohamed Fardhin	172-175

Registered with the Registrar of Newspapers for India under Reg. No. 498/2007
Bioscience Biotechnology Research Communications
SPECIAL ISSUE VOLUME 13 NO (3) 2020

Design of Inverted – Dual Band F MIMO Antenna Structure J. Deepa, S. Syedakbar and S. Geerthana	176–179
Powering Smart Street Lighting Cities Using Visible Light Communication and Light Fidelity D. Sivamani, P. Thirusenthil kumaran , C. Gnanavel and L. Nagarajan	180–184
Performance Analysis of Various Photovoltaic Configurations Under Uniform Shading and Rapid Partial Shading Formations A. T. Sankara Subramanian, P. Sabarish, M. D. Udayakumar and T. Vishnu Kumar	185–192
Design of FIR Filter Using High Speed Wallace Tree Multiplier with Fast Adders A. Kavitha, S. Suvathi Priya, S. Naveena, B. Vijiyaprabha and S. Prasheetha	193–196
A New Methodology of Arterial Blood Clot Removal Using Bio Molecular Devices for ATPase Nuclear Motors P. Sabarish, A. T. Sankara Subramanian, S. Murugesan and V. Sureshkumar	197–201
Fractional Order Controlled Multilevel Boost Hybrid Converter S.Jeyasudha, A. Anton Amala Praveen and B. Geethalakshmi	202–210
Design of Triple Layered Antenna for 5G Millimeter Wave Applications Syedakbar. S, Geerthana. S, Arthy. R, Eniyal. S and Mathumitha. B	211–213

EDITORIAL COMMUNICATION

The special issue of Bioscience Biotechnology Research Communications Vol 13 No (3) 2020 on “Recent Advancement in Electrical, Information and Communication Technologies” aims to provide original research articles from scholars, researchers, academia and industry on the emerging technological problems in areas of Electrical, Information and Communication.

This special Issue contains 38 articles on topics of Recent Advancement in Electrical, Information and Communication Technologies. Some of the important research discussions are Filters on MRI Liver Tumor Images, Neural Network, IOT, Tera-Hertz Antenna, Web Document Clustering, Portable Kidney Dialysis, Solar Photovoltaic Battery, Solar Powered Electric Bicycle, Image Processing and Wireless Sensor Networks.

All submissions are well supported by proof with a direct and simulated comparison to the technical solutions, designs and implementations. The articles available in this issue will be helpful for the researchers working in these new emerging areas.

Best wishes and thank you for your contribution to this special issue of Recent Advancement in Electrical, Information and Communication Technologies!

Guest Editors

Mr.S.Prasad Jones Christydass, M.E,(Ph,D)
Assistant Professor, Department of ECE,
K.Ramakrishnan College of Techmology, Tamilnadu, India.

Dr.A.Kavitha, Ph.D
Professor, Department of ECE,
K.Ramakrishnan College of Techmology, Tamilnadu, India.

Dr.R.Dhanagopal, Ph.D
Professor, Department of ECE,
Chennai Institute of Technology, Chennai, India.

CONTENTS



VOLUME 13 • NUMBER 3 • SPECIAL ISSUE 2020

Performance Denoising Filters on MRI Liver Tumor Images.....	01-07
B. Sundarambal, R Thalapathi Rajasekaran, R. Balamurali and R. Dhanagopal	
Analysis of Auto Antibody Complex by Pattern of Lacryglobin Spotting.....	08-12
C. Narayanan, S.Krishna Priya. Nivedha, T. Gomathi and V. Boobalan	
HI-TECH Electoral Machine for Election Commission of India.....	13-17
P. R. Sivaraman, R. Jaiganesh, P. Ragupathy and R. Ramkumar	
Anti Theft Control of Automatic Teller Machine Using Wireless Sensors.....	18-22
R. Jaiganesh, L. Nagarajan, A. Arthi and V. Venkatesh	
Optimization of Clinically Visual Deep Neural Network for the Classification of Liver Tumor Image.....	23-26
S.Pavithra, A. Dhanasekaran, Vanisri A and R. Balamurali	
Investigation and Analysis of Path Duration Estimation for Stable Communication Link in VANETS.....	27-31
R. Menaka, N. Kandavel, N. Archana, A. Ragini and S. Soundarya	
Scalable and Detect Link-Failure Traffic Balancing Network Using Adaptive Filter.....	32-38
R.Purushothaman and R. Narmadha	
Design of Tetra-band Antenna using Complementary Split Ring Resonator.....	39-43
V. Ravichandran, M. Suresh, T. Shankar and A. Nazar Ali	
ANN Based MPPT Controller for PEMFC System with Interleaved Resonant PWM High Step up Converter.....	44-47
B.Karthikeyan, R. Ramkumar, L. Nagarajan, A. Anton Amala Praveen and S. Vijayalakshmi	
Implementation of High Efficient Single Input Triple output DC-DC Converter.....	48-55
A. Rajkumar, R. Jai Ganesh, V. Suresh Kumar, T. Vishnu Kumar and T. Ram Kumar	
Design and Implementation of IOT Based Smart Library Using Android Application.....	56-62
R. Ramkumar, B. Karthikeyan, A. Rajkumar, V. Venkatesh and A. Anton Amala Praveen	
Design and Implementation of Tera-Hertz Antenna for High Speed Wireless Communication.....	63-67
S. Prasad Jones Christydass, S. Praveen, S. Naveen Kumar, S. Rakesh Kumar and M.Periakaruppan	
TVS Based Technique for Efficient Web Document Clustering in Web Search.....	68-73
R Thalapathi Rajasekaran, R. Ramesh, R. Menaka and Vanisri A	
A Survey Paper on Different Feature Extraction Methods in Image Processing.....	74-78
N.Hemalatha, T. Menakadevi and A. Kavitha	
Multi Input Dc-Dc Converter for Electric Vehicle Application.....	79-81
S. Dineshkumar, K. Sureshkumar, S. Dheepak, and B. Cibishanth	
MMCDM Based Approach for Efficient Web Document Clustering in Web Search.....	82-88
R. Siva, T. Thandapani, R. Ramesh and R. Balamurali	
Metamaterial Inspired MIMO Antenna for Radar, Satellite and Terrestrial Communications.....	89-93
S.Prasad Jones Christydass, B. Monisha, S. Shanthini and R. Saranya	

Metamaterial Inspired Bandpass Filter for 5G Application.....	94-97
S. Prasad Jones Christydass, A. S. Priyanka, S. Sugil and R. Soundharya	
Identification of Diseases in Plant Leaves Using Deep Learning Algorithm.....	98-102
R. Lalitha, S. Usha, M. Karthik, B. Pavithra, P. L. Sivagaami and G. Madhumith	
Smart Portable Kidney Dialysis Control and Monitoring System.....	103-108
A. Senthil Kumar, G. Keerthi Vijayadhasan D. Rashiga and K. Swetha	
Implementation of Recurrent Controller with Seven Stage Cascaded Converter for Micro Grid Solar Number of Switches.....	109-120
Photovoltaic Battery with Reduced	
M. Hari Prabhu, K. Sundararaju, S. Nagarajan, N. D. Arun, M. Bhuvaneshwaran, and A. Mariya Joseph Sathish	
FPGA Implementation of Adaptive LMS Lattice Filter.....	121-125
Sasikala S, Gomathi S, Naveen Kumar D, Praveenraj R. K and Priyadharshini B	
Secured Iot with Network Intrusion Detection Traffic Control by Data Routing Protocol in Wsn Using Genetic Algorithm.....	126-135
S. Manikandan, P. Pushpa and S. Sathish Kumar	
Design and Implementation of Solar Powered Electric Bicycle.....	136-140
P. Karthikeyan, Major P. S. Raghavendran and V. Kumaresan	
CSRR Inspired UWB Antenna for Breast Cancer Detection.....	141-145
V. Vedanarayanan, G. Arulselvi, D. Poornima and D. Joshua Jeyasekar	
A Novel Control Approach for PV-Grid System in various Atmospheric Conditions.....	146-151
K Balachander, Nagamani Prabu. A and Janarthanan. B	
Enhancing Security Using 3-Kae Algorithm In Wireless Sensor Networks.....	152-156
R. Balamurali, S. Rajesh Kannan, R Thalapati Rajasekaran and R. Ramesh	
Development of Industrial Monitoring System Based on Embedded HTTP Host Using Raspberry Pi.....	157-161
S. Bhuvaneshwari, R. Raghuraman, T. Thandapani and A. Sivabalan	
Device Authentication for IoT Devices using ECC.....	162-166
Krithiga J, Krishnan S, Sai Nithisha M, Jeevika Shree A and Lokeshwari S	
Detection of Glucose Using Non-Invasive Method and Food Analysis for Diabetic Patients Using IoT.....	167-171
N. Suriya, S. Pavithra, K Santhosh Solomon and Yaswanth Reddy	
Framework for Cancer Detection using Deep Wavelet Autoencoder & Neural Network in Brain Images.....	172-175
M. Kavitha, S. B.Rajdakshan, S. Tamilselvan and M.Mohamed Fardhin	
Design of Inverted - Dual Band F MIMO Antenna Structure.....	176-179
J. Deepa, S. Syedakbar and S. Geerthana	
Powering Smart Street Lighting Cities Using Visible Light Communication and Light Fidelity.....	180-184
D. Sivamani, P. Thirusenthil Kumaran, C. Gnanavel and L. Nagarajan	
Performance Analysis of Various Photovoltaic Configurations Under Uniform Shading and Rapid Partial Shading Formations.....	185-192
A. T. Sankara Subramanian, P. Sabarish, M. D. Udayakumar and T. Vishnu Kumar	
Design of FIR Filter Using High Speed Wallace Tree Multiplier with Fast Adders.....	193-196
A. Kavitha, S. Suvathi Priya, S. Naveena, B. Vijiyaprabha and S. Prasheetha	
A New Methodology of Arterial Blood Clot Removal Using Bio Molecular Devices for ATPase Nuclear Motors.....	197-201
P. Sabarish, A. T. Sankara Subramanian, S. Murugesan and V. Sureshkumar	
Fractional Order Controlled Multilevel Boost Hybrid Converter.....	202-210
S.Jeyasudha, A. Anton Amala Praveen and B. Geethalakshmi	
Design of Triple Layered Antenna for 5G Millimeter Wave Applications.....	211-213
Syedakbar. S, Geerthana. S, Arthy. R, Niyal. S and Mathumitha. B	

Performance Denoising Filters on MRI Liver Tumor Images

B. Sundarambal^{1*}, R Thalapathi Rajasekaran², R. Balamurali³ and R. Dhanagopal⁴

^{1,2}Department of CSE, Chennai Institute of Technology, Chennai, Tamilnadu, India.

^{3,4}Department of ECE, Chennai Institute of Technology, Chennai, Tamilnadu, India.

ABSTRACT

Right now, propose a way to deal with location furthermore, division of liver tumors in uproarious registered geology (CT) pictures. Picture division assumes pivotal job in clinical picture preparing applications. Clamor is very normal in clinical pictures. It happens while securing and transmission of pictures. The fundamental objective of this system is to recognize liver malignant growth by portioning liver tumors from boisterous CT filter pictures. Liver division is troublesome assignment in clinical applications in light of the fact that between quiet inconstancy in size, shape and sickness. By and large CT filtering is utilized to investigate liver disease. Right now, the liver tumors are distinguished by the clinical pictures in three phases, pre-handling stage, preparing stage and location arrange. First in pre-handling stage, middle channel is utilized to evacuate the clamor from CT picture, and afterward the denoised picture is fragmented by fluffy c-implies grouping (FCM) calculation. At long last in the identification organize separation regularized level set development (DRLSE) is utilized to remove tumor limits. This calculation is without question valuable for recognizing hepatocellular carcinoma (liver disease). Test results on different loud CT check pictures show that the proposed technique is proficient for removing hepatic tumors from liver.

KEY WORDS: DRLSE, FCM, CT.

INTRODUCTION

Liver tumor pictures are produced because of oppressing the human liver under examining. At this stage, the clamors are added to the examined picture through different reasons, for example, inductive misfortunes, low quality which would influence the clinical pictures (Bakas, S et al, 2015). This is the most well-known issue and it very well may be corrected by pre-handling strategies. Picture pre-taking care of is used generally for system on

pictures at any rate level of reflection. The purpose of pre-taking care of framework is improvement of the image data that smothers undesired bendings or overhauls some image features appropriate for extra getting ready and assessment of division and request. Rather than genuine pixel esteems, pixels in the picture show diverse power esteems. Clamor evacuation method is the way toward expelling or diminishing the commotion from the picture (Chi, D et al, 2010). Denoising diminishes or evacuates the perceivability of clamor by smoothing the whole picture leaving territories close to differentiate limits.

Different segments may be solid for the introduction of disturbance in the clinical picture. The proportion of pixels destroyed in the image would pick the assessment of the disturbance. The fundamental wellsprings of disturbance in the propelled picture are: a) the imaging sensor may be impacted by regular conditions during

ARTICLE INFORMATION

*Corresponding Author: sundarambal@citchennai.net
Received 15th April 2020 Accepted after revision 20th May 2020
Print ISSN: 0974-6455 Online ISSN: 2321-4007 CODEN: BBRCBA

Thomson Reuters ISI Web of Science Clarivate Analytics USA and Crossref Indexed Journal



NAAS Journal Score 2020 (4.31) SJIF: 2020 (7.728)
A Society of Science and Nature Publication,
Bhopal India 2020. All rights reserved.
Online Contents Available at: <http://www.bbrc.in/>

picture making sure about, b) Insufficient light levels and sensor temperature may introduce the fuss in the image, c) Interference in the transmission channel may moreover deteriorate the image and d) If dust particles are accessible on the scanner screen, they can in like manner present upheaval in the image (Deepa, P et al. 2014).

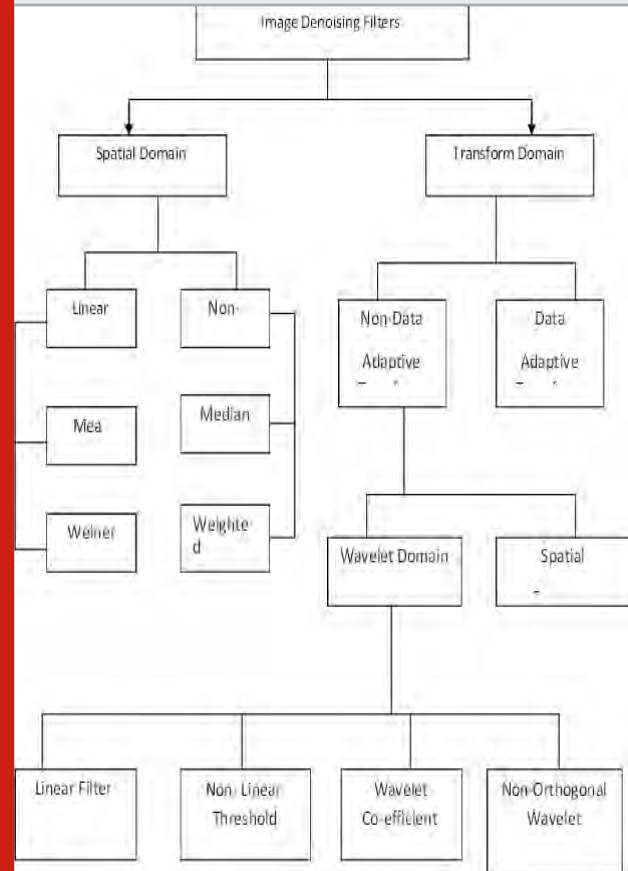
Dependent upon the sort of disturbance, the uproar can impact the image to a substitute degree and it causes undesired effects on the image. The rule central purposes of Denoising are to recognize specific kind of fuss and to apply different frameworks to remove the upheaval. Filtering is a strategy in picture getting ready which is used for different assignments like noise abatement, addition and reevaluating. The choice of channel depends on the sort and proportion of upheaval present in an image considering the way that different channels can empty different sorts of clatter viably. Emptying uninterested change to augment viable sign to-clatter extent is an incredible research zone of energy since the achievement of division, game plan and assessment of liver tumor picture depends upon quiet picture.

The characterization of separating techniques is given in Figure 1. Picture de-noising channel can be arranged into two kinds as spatial area and change space. The spatial area is subdivided into direct and non-straight. A customary method to expel clamor from picture is to utilize spatial channels (Dr. R. Menaka et al,2020; Feng, Y et al,2015). Spatial channels can be additionally characterized into non-straight and direct channels. Straight channels applied to pictures causes too will in general even think about blurring sharp edges, demolish lines and other fine picture subtleties, and perform ineffectively within the sight of sign ward clamor. On account of Non-Linear channels, the clamor can be expelled with no endeavor to recognize the liver tumor picture unequivocally.

Information Adaptive Transforms utilizes a technique called Independent Component Analysis (ICA) that has increased wide spread consideration. The ICA strategy is effectively executed in de-noising Non-Gaussian information. Detriments of ICA based methodologies when appeared differently in relation to wavelet based procedures are the computational cost since they use a sliding window and require trial of commotion free data or if nothing else two picture edges of a comparable scene. In specific applications, it might be difficult to get the fuss free planning data. Non-Adaptive breaking point is a non-flexible comprehensive edge, which depends just on the amount of data centers and it has asymptotic consistency proposing most marvelous execution to the extent MSE when the amount of pixels shows up at ceaselessness.

In electronic picture getting ready, wavelet change is a critical instrument for inspecting the image characteristics. For better examination the image needs to transform from the other space to wavelet region. At the point when everything is said in done, there are numerous progressions that are available like Fourier

Figure 1: Classification of filtering methods



change and Wavelet change. The Fourier change is one of the most extensively used and standard changes for dismembering reason, anyway it gives only the repeat plentifulness depiction and not the time information. Right now, isn't fitting to be used for applications which need both time similarly as repeat information (Goceri, E, et al,2012 ; Gunasundari, S et al, 2012). Wavelet change permits channels to be developed for Stationary (signal that as no adjustment in the properties of sign) just as non-stationary (signal with there is change in the properties of sign). Wavelet changes permit the both the segments of stationary just as non-stationary signs to be examined. Subsequently wavelet change is being favored contrasted with the different changes. Wavelet change application includes signal handling and sifting. It likewise incorporates the other region applications like non-straight relapse and pressure.

In the current research, five unique kinds of channels from all the areas to be specific Median Filter (MF), Mean Filter, Lee Filter, Frost Filter and Fractional Wavelet Filter (FWF) were tried and analyzed. The investigation is done dependent on the exhibition parameters, in particular mean square blunder, PSNR, difference to commotion proportion, quality list and mean total mistake. The partial wavelet channel performs well in de-noising the picture without influencing the edges. This strategy is a pre-preparing venture of division and arrangement of liver tumor pictures.

MATERIALS AND METHODS

2.1 Filter description: In liver tumor pictures, before division and arrangement, commotion evacuation is a significant pre-preparing venture to be finished. By utilizing various kinds of sifting systems clamor can be evacuated. The accompanying area portrays various kinds of channels and best among them is picked to expel the clamor from the liver tumor picture (Ilakkiya, G et al, 2013)

2.2 Median filtering: A non-straight mechanized filtering procedure center isolating is used to remove disturbance from pictures. It is normally used as it is especially valuable at removing uproar while shielding edges. It is practical generally at removing "salt and pepper" type uproar. This channel works by moving from side to side the image pixel by pixel, displacing each pixel regard with the center estimation of the nearest pixels. The model of neighbors is known as the "window", which slides, pixel by pixel over the whole picture pixel and over the whole picture. The center worth is considered by first orchestrating all the pixel regards from the window into numerical solicitation, and thereafter overriding the pixel being considered with the inside (center) pixel regard. For every pixel, a 3x3 neighborhood with the pixel as midpoint is considered. In center isolating, the estimation of the pixel is replaced by the center of the pixel regards in the 3x3 neighborhood (Kumar, SS et al, 2012).

Figure 2: illustration of median filter

123	125	126	130	140	Neighbourhood values: 115, 119, 120, 123, 124, 125, 126, 127, 150 Median value: 124
122	124	126	127	135	
118	120	150	125	134	
119	115	119	123	133	
111	116	110	120	130	

The extents of the entirety of the vectors inside a cover are arranged by the sizes by the middle channel. The pixel esteem with the middle extent is then used to supplant the pixel considered. This channel has a touch of breathing space over the Mean channel since the center of the information is taken as opposed to the mean of an image. The pixel regard with the center degree is then used to override the pixel inspected. The center of a set is continuously incredible with respect to the proximity of uproar. The middle channel is given by

$$\text{Median filter}(x_1 \dots x_N) = \text{Median} (|x_1| |x_2| \dots |x_N|)$$

When isolating using the essential center channel, an exceptional and the consequent filtered pixel of the model have a comparable pixel. A pixel that doesn't

change because of filtering is known as the establishment of the cloak. A most huge piece of breathing space of the center channel over direct channels is that the center channel can diminish the effect of data upheaval regards with extremely huge sizes. Curiously, straight channels are sensitive to this kind of racket i.e., the yield may be defiled intensely by even a little piece of bizarre upheaval regards.

2.3 Mean filter: To diminish the volume of force variety between pixels, i.e., to lessen the commotion in the picture picked mean sifting method is utilized. It is a basic, instinctive and simple to execute technique for picture smoothening. The mean sifting procedure includes changing every pixel esteem in a picture with the mean ('normal') estimation of its neighbors, including its own. This method avoids the estimations of pixels that delude their encompassing regions. Mean separating resembles the convolution channel.

Figure 3: 3x3 averaging kernel used in mean filtering

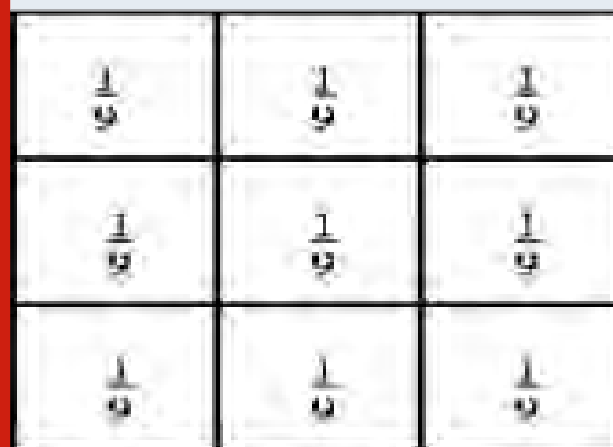


Figure 4 a): Single window values

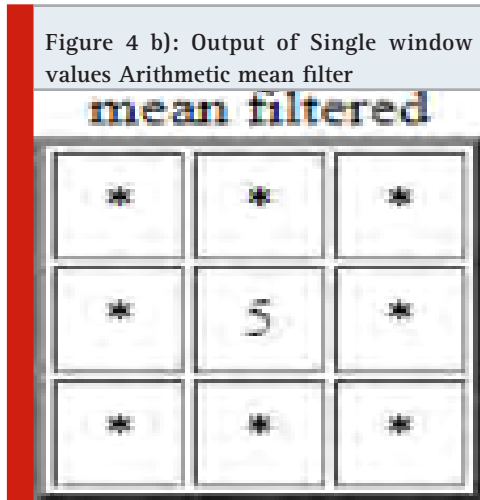
unfiltered values		
5	3	6
2	1	9
8	4	7

Convolution channel figures the mean for inspecting dependent on the bit which speaks to the shape and size of the area to be tested. For instance, 3x3 square bit, as appeared in Figure 3, albeit bigger pieces (for example

5x5 squares) can be utilized for increasingly serious smoothing (Kumar, SS et al , 2011)

An example of mean filtering of a single 3x3 window of values is shown in Figure 4.

$$5 + 3 + 6 + 2 + 1 + 9 + 8 + 4 + 7 = 45 \text{ and } 45 / 9 = 5$$



Number juggling mean channel is the most straightforward type of the mean channels. Let S_{xy} show the arrangement of directions in a rectangular sub picture window of size $m \times n$ and center at point (x, y) . The math mean separating process registers the ordinary estimation of the undermined picture $g(x, y)$ in the zone characterized by S_{xy} . The estimation of the reestablished picture anytime (x, y) is essentially the number-crunching mean determined utilizing the pixels in the district characterized by S . This channel utilizes a veil wherein all the coefficients of the pixels have esteem $1/mn$ (Lu, D et al,2007). The resultant commotion diminished picture got by this channel smoothes the neighborhood changes causing obscuring.

2.4 Geometric mean filter: An image restored using a geometric mean filter is given by the expression

$$\hat{f}(x, y) = \left[\prod_{(s,t) \in S_{xy}} g(s, t) \right]^{\frac{1}{mn}}$$

Right now, pixel is given by the result of the pixels in the sub picture window, raised to the force $1/mn$. A geometric mean channel accomplishes smoothing which is similar to the number juggling mean channel, yet it will in general lose less picture detail simultaneously.

2.5 Harmonic mean filter: The harmonic mean filtering operation is given by the expression

$$\hat{f}(x, y) = \frac{mn}{\sum_{(s,t) \in S_{xy}} \frac{1}{g(s,t)}}$$

The harmonic mean filter provides better results with noises like Gaussian noise, salt noise, but not for pepper noise.

2.6 LEE Filter: Lee channel utilizes neighborhood insights to viably save edges and highlights dependent on the multiplicative spot model. It deals with the premise of the Minimum Mean Square Error (MMSE) which delivers the spot free picture by utilizing the accompanying articulation

$$U(X) = I(x, y) W(x, y) + I'(x, y) (I-W(x, y))$$

where I' is the mean value of the intensity within the filter window, and $W(x, y)$ is the adaptive filter coefficient calculated using the following formula. Lee channel diminishes the spot uproar by applying a spatial direct to each pixel in an image, which channels the data reliant on neighborhood bits of knowledge decided inside a square window. The estimation of within pixel is superseded by a value decided using the neighboring pixels.

Frost Filter: Ice channel diminishes spot clatter and jam huge picture features at the edges with an exponentially damped and circularly symmetric channel that uses close by estimations inside individual channel windows. The Frost channel is furthermore established on the multiplicative spot model and the close by estimations, and it has relative execution to the Lee channel. Scene reflectivity is a critical factor that isolates the Frost channel from the Lee and Kuan channels, which is controlled by getting the watched picture together with the drive response of the system. The Frost channel requires a damping factor which describes the level of exponential damping. The more diminutive the value is, the better the smoothing limit and channel execution.

The Frost channel is a flexible and exponentially weighted averaging channel reliant on the coefficient of assortment, which is the extent of the local standard deviation to the close by mean of the spoiled picture. It replaces the pixel of energy with a weighted entire of the characteristics inside the moving piece and the weighting factors decrease with detachment and addition with the extension in the variance of the bit.

RESULTS AND DISCUSSIONS

3.1 Performance Analysis of Image Denoising Filters:

Measurement of Image quality: the quality of the output images can be measured by the traditional distortion measurements such as MSE, PSNR, CNR, QI and MAE.

3.2 Performance analysis of liver tumor image based on Mean Square Error(MSE):

MSE represents the growing squared error between the compressed and the original image, whereas PSNR represents the computation of the peak error. The subordinate value of MSE indicates the lower error. To calculate The PSNR, the block first calculates the mean-squared error.

3.3 Performance analysis of liver tumor image based on Peak Signal- to- Noise Ratio (PSNR):

PSNR is the proportion between the most extreme conceivable intensity of a sign and the intensity of debasing commotion that influences the loyalty of its portrayal. It processes the pinnacle signal-to-commotion proportion, in decibels, between two pictures. This proportion is regularly utilized as a quality estimation between the first and a compacted picture. The higher PSNR shows the better nature of the packed or recreated picture. At that point the square figures the PSNR utilizing the accompanying condition:

$$PSNR = 10 \log_{10} \left(\frac{R^2}{MSE} \right)$$

$$R = 2n - 1$$

Where n is the number of bits used in representing the pixel of the image. For gray scale image, n is 8.

3.4 Performance of liver tumor image based on Quality Index(QI):

IQI is a proportion of picture quality twisting. Scientifically, it is characterized through demonstrating picture mutilation, which is identified with the reference picture. A reference picture is a blend of loss of relationship, luminance contortion and differentiation bending factors. IQI is the result of three segments, where the main part speaks to connection coefficients and it changes in the range [-1,1]. It is utilized to quantify the level of connection coefficient among pictures f and g. The subsequent segment speaks to how close the luminance is between pictures, it falls in the range [0, 1]. σ_f and σ_g are the evaluations of the difference of f and g. this parameter causes the third part to discover how comparable the differences of the pictures are. Tired part esteem ranges from [0,1]

3.5 Performance of liver tumor image based on Contrast to Noise Ratio:

CNR is a parameter that is utilized to decide the nature of picture. It is the proportion of contrast of sign power between two areas, scaled to picture clamor. In the event that the estimation of CNR is improved, at that point the view of contrast between two unmistakable clinical territories of intrigue is expanded. On the off chance that a picture has higher power, the highlights of the pictures are cleaned out by huge inclination. At that point such a picture ought to have low CNR metric. Contingent upon the nature of picture, the CNR esteem changes.

3.6 Performance of liver tumor image based on Mean Absolute Error (MAE):

MAE evaluates how close the desires are to the certified outcome. In time course of action assessment, it is used to evaluate measure botch. In a great deal of check, it measures the typical degree of the slip-ups . Estimation of the presentation examination of middle, mean, ice, lee, fragmentary wavelet channel is done and computes the quality parameters, for example, MSE, PSNR, MAE, CNR and IQI are determined for a given picture. Tests are directed utilizing Malab (R2013a). Loud pictures are given as contribution for all the five distinct channels. The presentation of the channel is assessed utilizing the quality parameters. The sifted yield of each channel is given underneath in Figures 5, 6, 7, 8 and 9.

Figure 5: Image before and after denoising median filter

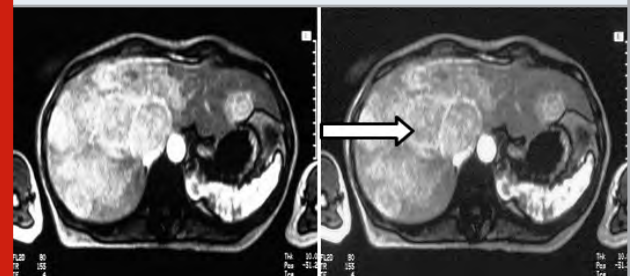


Figure 6: Image before and after denoising using mean

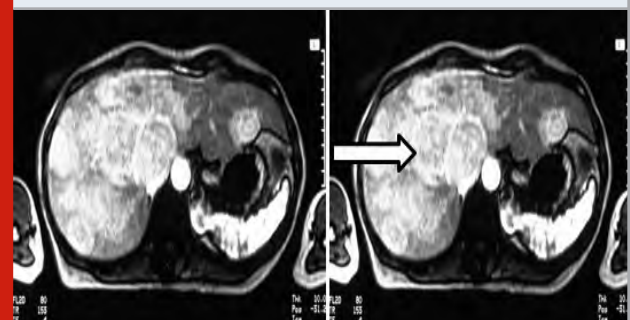


Figure 7: Image before and after denoising using frost

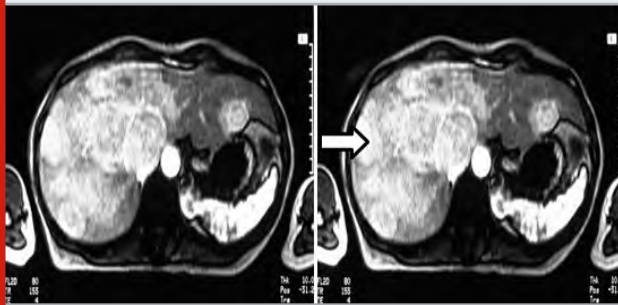


Figure 8: Image before and after denoising using LEE

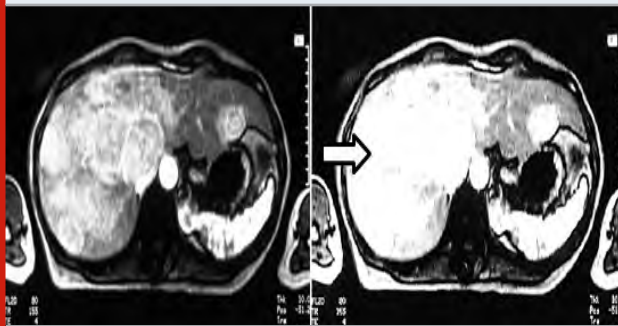


Figure 9: Image before and after denoising using fractional wavelet filters

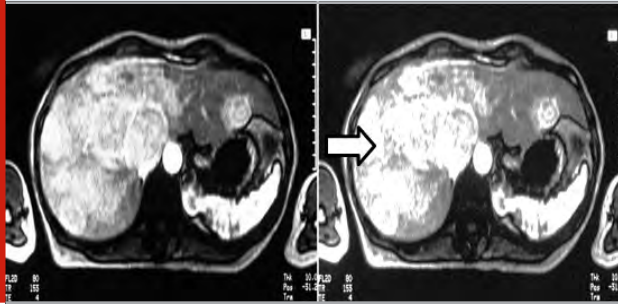


Table 1. Comparison of the Performance of various filter

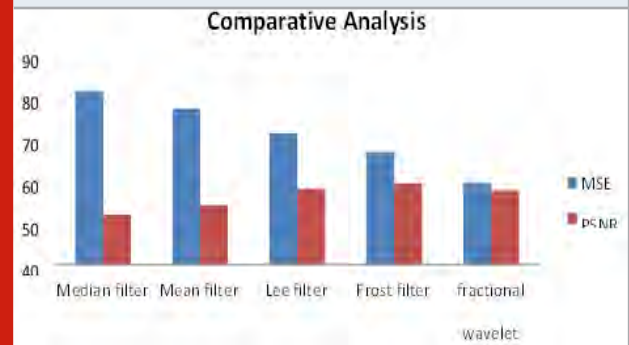
Parameters Filters	MSE	SNR	CNR	IQI	MAE
Median filter	76.8	22.13	45.58	0.75	5.73
Mean filter	69.1	26.25	53.66	0.82	5.84
Lee filter	58.2	33.55	58.54	0.87	3.94
Frost filter	49.7	35.95	57.46	0.89	2.25
Fractional wavelet filters	36.2	32.84	59.47	0.91	1.23

In which the Fractional wavelet filter is found to perform well. The average values for the parameters of the five filters for the given input images are given in Table 1.

The quality parameters such as MSE and PSNR are helpful

to find the efficiency of the filters. The performance of the five different types of filters such as median filter, mean filter, lee filter, frost filter, fractional wavelet filter are shown in Table 1. To evaluate the filter performance, various parameters such as MSE, PSNR, CNR, IQI and MAE are considered.

Figure 10: Comparative Analysis of various filters



CONCLUSION

A monotonous undertaking in the picture handling is expelling the clamor from the liver tumor pictures. For as long as two decades, numerous scientists have been giving adequate plans to the clamor evacuation and sectioning the given info picture. The tumor picture is de-noised by utilizing various sorts of channels, for example, middle channel, mean channel, LEE channel, ice channel and partial wavelet channel. In view of the presentation of channels and classifiers, near and volumetric investigation of the outcome are taken by picking various parameters to guarantee the better outcome.

REFERENCES

Bakas S Chatzimichail K Hunter G Labbe B Sidhu PS & Makris D (2015) Fast semi automatic segmentation of focal liver lesions in contrast enhanced ultrasound based on a probabilistic model Computer Methods in Biomechanics and Biomedical Engineering: Imaging & Visualization Pages 1–10.

Chi D Zhao Y & Li M (2010) Automatic Liver MR Image Segmentation with Self-Organizing Map and Hierarchical Agglomerative Clustering Method Image and Signal Processing Pages 1333-1337.

Deepa P & Suganthi M (2014) Performance Evaluation of Various Denoising Filters for Medical Image” International Journal of Computer Science and Information Technologies vol 5 no 3 Pages 4205-4209.

Dr R Menaka Dr R Janarthanam Dr K Deeba (2020) FPGA implementation of low power and high speed image edge detection algorithm Microprocessors and MicrosystemsVolume 752020103053 ISSN 0141-331.

Feng Y Qin XC Luo Y Li YZ & Zhou X (2015) Efficacy of contrast enhanced ultrasound washout rate in predicting hepatocellular carcinoma differentiation” *Ultrasound Med Biol* vol 41 no 6 Pages 1553–1560.

Goceri E Unlu MZ Guzelis C & Dicle O (2012) An automatic level set based liver segmentation from MRI data sets” *Image Processing Theory Tools and Applications (IPTA) 3rd International Conference on 2012*.

Gunasundari S Suganya M & Ananthi (2012) Comparison and Evaluation of Methods for Liver Tumor Classification from CT Datasets’ *International Journal of Computer Applications (0975 – 8887)* vol 39 no 18.

Ilakkiya G & Jayanthi B (2013) Liver Cancer Classification

Using Principal Component Analysis and Fuzzy Neural Network” *International Journal of Engineering Research & Technology (IJERT)* vol 2 issue 10.

Kumar SS Moni RS & Rajeesh J (2012) Liver Tumor Diagnosis by Gray Level and Contour let Coefficients Texture Analysis *Computing Electronics and Electrical Technologies* Pages 557–562.

Kumar SS Moni RS & Rajeesh J (2011) Automatic Segmentation of Liver and tumor for CAD of Liver” *Journal of Advances in Information Technology* vol 2 no 1.

Lu D (2007) A Fast and Robust Approach to Liver Nodule Detection in MR Images” *Frontiers in the Convergence of Bioscience and Information Technologies*.

Analysis of Auto Antibody Complex by Pattern of Lacryglobin Spotting

C. Narayanan¹, S. Krishna Priya², A.K. Nivedha³, T. Gomathi⁴ and V. Boobalan⁵

Associate Professor¹, Assistant Professor^{2,3,4,5}

^{1,2,3,4}Department Of Biomedical Engineering, Dhanalakshmi Srinivasan Engineering College, Perambalur, Tamil Nadu.

⁵Department Of Biomedical Engineering, Excel Engineering College, Namakkal, Tamil Nadu.

ABSTRACT

Protein profiling utilizing resistant histochemistry takes into consideration representation of the appropriation and relative plentitude of proteins encoded by malignant growth qualities in different tumor tissues. Certain proteins show differential expression between different forms of cancer .In this distribution presence of protein from human tears are taken with various composition or concentration .In that lacryglobin take as biomarker for identification of breast cancer stages.

INTRODUCTION

Bosom malignant growth is a disease that creates in bosom cells. Commonly, the disease frames in either the lobules or the conduits of the bosom. Lobules are the organs that produce milk, and channels are the pathways that carry the milk from the organs to the areola (Jemal A, Bray F, Center MM, Ferlay J, Ward E and Forman D 2011). Bosom malignancy is one of the main demise causes in ladies around the world. The vital prerequisite of its treatability is the early identification. Right now, there are no atomic biomarkers accessible for this reason. Proteomic examination of tear liquid has an incredible potential and advantage due to non-obtrusive example

recovery and low required protein sums (Radpour R, Barekati Z, Kohler C, Holzgreve W and Zhong 2009) .The chemical composition of tear lipids protein and other fluid secreted by glands (Bohm D, Keller K, Boehm N, et al 2000).there are several non specific protein such as lactoferin and glycoprotein for dry eye patient ,in these composition of lacryglobin for abnormal person having cancer cells.

MATERIALS AND METHODS

1. Collection of tear fluid: Tear liquid was gotten from all members utilizing a Schirmer Strip. The Schirmer's test stripis put inside the lower eyelid of the two eyes and the individual is approached to close their eyes.After 5 minutes, strip is expelled. At that point evaluates how far the tears have gone on the paper. After the examples were drawn, the strips were solidified promptly at -80°C to forestall protein corruption.

2. Sample retrieval: For the comparison of protein levels inhealthy women andpatient with primary diagnosed breast carcinoma, every one of the tear elutes were pooled

ARTICLE INFORMATION

*Corresponding Author: kpriya726@gmail.com

Received 15th April 2020 Accepted after revision 20th May 2020

Print ISSN: 0974-6455 Online ISSN: 2321-4007 CODEN: BBRCBA

Thomson Reuters ISI Web of Science Clarivate Analytics USA and Crossref Indexed Journal



NAAS Journal Score 2020 (4.31) SJIF: 2020 (7.728)

A Society of Science and Nature Publication,

Bhopal India 2020. All rights reserved.

Online Contents Available at: <http://www.bbrc.in/>

together in like manner to the gathering and hastened with multiple times the volume of chilled CH₃CO overnight at - 80 °C. The following day, tear proteins were centrifuged at 14000 x g and 4°C to forestall protein debasement. The strips were then washed and separated a subsequent time utilizing the above system and pooled. The Bradford assay was performed on the protein collected from extraction .

3. Estimation of Protein content- Bradford assay: A progression of protein models going in fixation from 0.2 to 1 mg/ml is arranged with the end goal that the last volume for the test is 0.1ml. The obscure examples, both control tear proteins and the tear proteins disengaged from the malignancy patients was additionally arranged likewise with the end goal that the last volume is 0.1ml.. 3.0ml of Bradford reagent was added to each example and standard, vortexed and incubated at room temperature for 30 minutes. The samples were transferred to the cuvettes and the absorbance was measured at 595nm using.

4. Reducing Sodium dodecyl sulfate - Polyacrylamide gel electrophoresis (SDS- PAGE)

4.1.Gel Preparation: For cleaning the glass plates, first it was washed with water followed by di-chromic acid. Wipe the plates to remove organic residues. Again water wash and wipe with ethanol using absorbent cotton and allow to dry. Suitable spacers are placed between the glass plates and damped using clips. Sealed the 3 edges of these set up using 1% agarose. The sealing was done to avoid the leakage. Pour the resolving gel buffer between the glass plates. Stacking gel (5%) was then poured over the resolving gel (12%). Combs were placed into the top of the gel. After the gel setting, the comb and spacers were removed. Glass plates were then carefully transformed to the electrophoresis unit.

4.2.Sample Preparation: 100 µl samples were taken and mixed with loading solution as well as β-mercaptoethanol. It was then allowed to run for 2 hours (100 V). Movement of the bromophenol blue indicated the movement of the proteins. After the sufficient distance of the marker moved, switch off the current. After the removal of glass plates and spacers, gel was immersed in staining solution. Proteins are seen as band in gel after staining the same with Coomassie Brilliant Blue and are visualized under UV transilluminator.

5. Estimation of protein content after elution from SDS PAGE gels

Passive Elution of Proteins from Polyacrylamide Gel Pieces:

1. Place excised gel pieces in clean screw-cap culture or microcentrifuge tubes.
2. Add 0.5-1 ml of elution buffer so that the gel pieces are completely immersed.
3. Crush the gel pieces using a clean pestle and incubate in a rotary shaker at 30°C overnight.
4. Centrifuge at 5,000-10,000 × g for 10 minutes and carefully pipette supernatant into a new

microcentrifuge tube. An aliquot of the supernatant may be tested for the presence of protein by subjecting it to SDS-PAGE. The elutes were then estimated for protein content using Bradford assay.

6. Enzyme Linked ImmunoSorbent Assay (ELISA): ELISA test for CA and CTRL tests were finished utilizing Human tear. This test depends on the sandwich ELISA guideline. Each well of the provided microtiter plate has been pre-covered with an objective explicit catch counter acting agent. Models or tests are added to the wells and the objective antigen ties to the catch immunizer. Unbound Standard or test is washed away. A Horseradish Peroxidase (HRP)- conjugated recognition immune response is then added which ties to the caught antigen. Unbound recognition immune response is washed away. A TMB substrate is then included which responds with the HRP protein bringing about shading improvement. A sulfuric corrosive stop arrangement is added to end shading advancement response and afterward the optical thickness (OD) of the well is estimated at a frequency of 450 nm ± 2 nm. The OD of an obscure example would then be able to be contrasted with the OD of the positive and negative controls so as to decide the nearness or nonattendance of the antigen.

Assay procedure: Carry all reagents and tests to room temperature without extra warming and blended completely by tenderly twirling before pipetting (abstain from frothing). Set up all reagents and tests as coordinated in the past segments.

Set a Blank well with no arrangement.

Add 100 µl of Standard to each well.

Prepare Samples by consolidating 100 µl of Sample Diluent with 10 µl of Sample. Add this 110 µl test to a well. Spread with a plate sealer, and brood for 30 minutes at 37°C. It is enthusiastically suggested that controls and tests are run in copy.

Aspirate the fluid from each well and wash multiple times. Wash by including roughly 200 µl of Wash Buffer utilizing a squirt bottle, multi-channel pipette, complex gadget or robotized washer. Permit each wash to sit for 10 seconds before totally suctioning. After the last wash, suctioning expel any residual Wash Buffer at that point alter the plate and tap against clean permeable paper.

Add 100µl of HRP-conjugate to each well, spread with another plate sealer, and brood for 30 minutes at 37°C.

Wash multiple times as laid out in stage 4.

Add 50µl of Substrate An and 50µl Substrate B to each well, blend well, and hatch in obscurity for 15 minutes at 37°C.

Add 50 µl of Stop Solution to each well. The blue shading will change to yellow right away. In the event that shading change doesn't seem uniform,

tenderly tap the plate to guarantee exhaustive blending. The Stop Solution ought to be added to wells in a similar request and timing just like the substrate arrangement.

Determine the optical thickness (OD estimation) of each well promptly utilizing a microplate peruser set to 450 nm.

The convergence of the disease antigen is straightforwardly relative to the shading power at 450 nm.

RESULTS AND DISCUSSION

1. Collection of tear protein: Tear protein was collected from a 50 year old healthy women as well as a cancer patients with primary diagnosed breast carcinoma using Schirmer Strip .The strip was stored at -800 C and was transported immediately to the laboratory.

Figure 1: Schirmer Strip



2. Retrieval of tear sample: The tear eluates were pooled accordingly and the tear proteins were extracted using chilled acetone overnight precipitation method.

Figure 2: Collection of tear fluid using Schirmer Strip



Figure 3: Showing acetone precipitation at -800 C

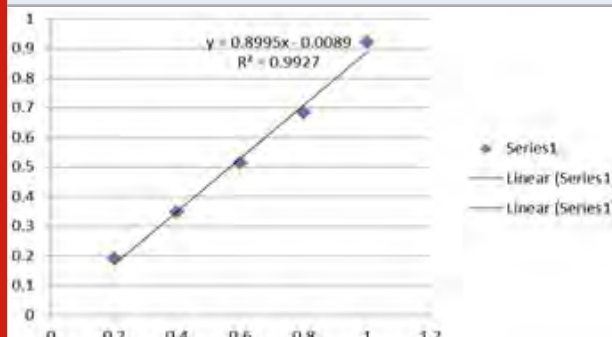


3. Estimation of Protein content using Bradford assay: Estimation of protein was done by Bradford assay, using BSA (Bovine serum Albumin) as a standard (Table:1). Concentration of the test was found to be 0.3545µg/mL and CTRL was found to be 0.5991µg/mL.

Figure 4: Estimation of protein concentration



Figure 5: Standard curve for protein estimation



4. SDS PAGE: After SDS PAGE under reducing conditions, it was found there were almost 30 prominent and clear bands in case of control tear sample, while there is diminution in protein bands in case of tear from cancer patient where there are only around 14 bands present in it (Figure 5). This clearly supports the data from estimation of proteins using Bradford assay.

5. Estimation of protein content after elution from SDS PAGE gels: The protein contents from control and cancer patients were estimated after elution from the gels using Bradford assay. Concentration of the test was found to

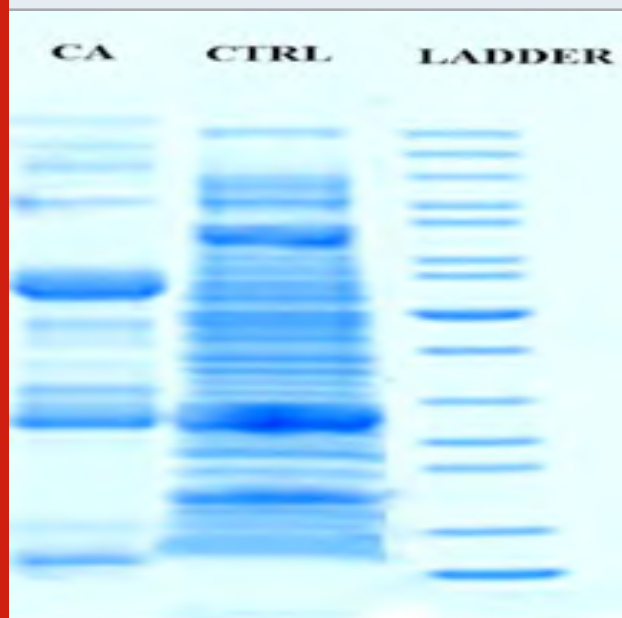
Table 1.

Sl No:	Concentration (µg/ml)	Absorbance @ 595nm
Blank	-	-
S1	0.2	0.19
S2	0.4	0.347
S3	0.6	0.512
S4	0.8	0.684
S5	1	0.921
CTRL	-	0.53
CA	-	0.31

be 0.3422 µg/mL and CTRL was found to be 0.5872 µg/mL which were comparable to the earlier values.

6. Enzyme Linked ImmunoSorbent Assay (ELISA): ELISA test was conducted for the samples (both control and test) using Human CA 15-3 ELISA Kit. It was found that, on addition of cancer tear protein sample to the conjugated ELISA 96 well microtiter plate, the color in the wells changed from blue to light yellow and bright yellow at higher concentrations, while on addition of control tear samples at varying concentration did not exhibit any color change. This clearly indicates the presence of cancer antigen 15-3 in the test sample when compared to the control sample. Thus ELISA test helped in confirmation of the detection of cancer antigen which supports the data from SDS PAGE (Figure 6).

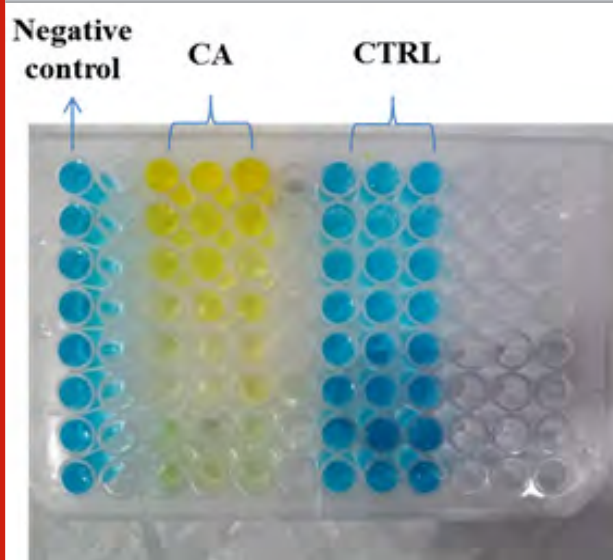
Figure 6: SDS PAGE of tear proteins



As a future prospective, quantitative estimation of the proteins can be done using ELISA kit Curve Expert software or MALDI TOF/SELDI TOF analysis for molecular weight determination and individual component analysis, which may be executed using

SWISS PROT data base system to elucidate the structure of each protein in detail.

Figure 7: ELISA 96 well coated plate. Higher concentrations of samples (Both control and cancer) are loaded at the top of the plate and then keeps decreasing towards the bottom of the microtiter plate.



CONCLUSION

Early discovery of bosom disease lesions bosom malignant growth related mortality. Bosom malignancy biomarkers offer a promising methods for distinguishing this malady at the soonest and most treatable stages . On account of the heterogenous idea of the most tumors, no single tumor marker gives the affectability or particularity required for reaching or screening. Ongoing advances in picture investigation for mass spectrometry and bioinformatics have given the instruments important to high-throughput biomarker disclosure. A few thousand proteins from numerous patients can at the same time be contrasted and broke down with show up at unmistakable phenotypic proteomic profiles that are related with the dangerous state. Contrasted with serum, the examination of tear liquid offers. We found a satisfactory segregation between bosom disease patients and healthy controls. Biomarkers shows an affectability and explicitness of around 70%, from this the immediate involvement of immune system, whereas its component levels are changed in comparison to CTRL subjects.

REFERENCES

- Banks RE Dunn MJ Hochstrasser DF et al (2000) Proteomics new perspectives new biomedical opportunities Lancet 356 1749 1756.
- Bertucci F Birnbaum D and Goncalves A(2006) Proteomics of breast cancer principles and potential clinical applications Mol Cell Proteomics 5 1772-1786.
- Bohm D Keller K Boehm N et al(2011) Antibody

- microarray analysis of the serum proteome in primary breast cancer patient *Cancer Biol Ther* 12 772-779 .
- Brekelmans CT Seynaeve C Bartels CC et al(2001) Effectiveness of breast cancer surveillance in BRCA1/2 gene mutation carriers and women with high familial risk *J Clin Oncol* 19 924-930.
- De Freitas Campos C Cole N Van Dyk D et al(2008) Proteomic analysis of dog tears for potential cancer markers *Res Vet Sci* 85 349-352.
- Diamandis EP Analysis of serum proteomic patterns for early cancer diagnosis drawing attention to potential problems *J Natl Cancer Inst* 96 353-356 2004.
- Downes MR Byrne JC Dunn MJ Fitzpatrick JM Watson RW and Pennington SR(2006) Application of proteomic strategies to the identification of urinary biomarkers for prostate cancer a review *Biomarkers* 11 406-416.
- Elrick MM Walgren JL Mitchell MD and Thompson(2006) DC Proteomics recent applications and new technologies *Basic Clin Pharmacol Toxicol* 98 432-441.
- Harris L Fritsche H Mennel R et al(2007) American Society of Clinical Oncology 2007 update of recommendations for the use of tumor markers in breast cancer *J Clin Oncol* 25 5287-5312.
- Jemal A Bray F Center MM Ferlay J Ward E and Forman D (2011) Global cancer statistics. *CA Cancer J Clin* 61 69-90.
- Lebrecht A Boehm D Schmidt M Koelbl H Schwirz RL and Grus FH(2009) Diagnosis of breast cancer by tear proteomic pattern. *Cancer Genomics Proteomics* 6 177-182.
- Li J Zhang Z Rosenzweig J Wang YY and Chan(2002) DW Proteomics and bioinformatics approaches for identification of serum biomarkers to detect breast cancer *Clin Chem* 48 1296 1304.
- Ramkumar R and N Tejaswini (2016) A novel low cost three arm Ac automatic voltage regulator *Advances in Natural and Applied Sciences* vol.10 no.3
- Ramkuma R et al (2019) Intelligent system to monitor and diagnose performance deviation in Industrial Equipment. *IOPconf.Series:Materials science and Engineering*, Vol 623 Vol 012012.
- Ramkumar, R. et al (2016) PV based SEPIC converter fed four switch BLDC motor drive *Advances in Natural and Applied Sciences* vol. 10 no.3.
- Radpour R Berekati Z Kohler C Holzgreve W and Zhong XY(2009) New trends in molecular biomarker discovery for breast cancer *Genet Test Mol Biomarkers* 13 565-571.
- Shevchenko A Loboda A Ens W Schraven B Standing KG and Shevchenko(2001) Archived polyacrylamide gels as a resource for proteome characterization by mass spectrometry. *Electrophoresis* 22 1194-1203 .
- Tyers M and Mann M(2003) From genomics to proteomics *Nature* 422 193-197.

HI-TECH Electoral Machine for Election Commission of India

Dr. P. R. Sivaraman¹, R. Jaiganesh², P. Ragupathy³ and R. Ramkumar⁴

^{1,2,3,4}Assistant Professor, Department of EEE

^{1,3}Rajalakshmi Engineering College,

^{2,4}K. Ramakrishnan College of Technology.

ABSTRACT

Electronic based voting machines are mostly used for voting during the election period in India. In foreign countries like America they have used forms and internet for voting to reduce the illegal voting. The reason for convenient voting mechanism was reducing the complexity in all over the countries and its better when compared with conventional system. Here this proposed work proposed about e-voting from social websites, through various News channel, Electronic based voting, Electronic based vote checking. It reduces our time and cost moreover. It additionally deals about some upcoming invention howdy tech e-voting based systems which can be used to get better usual voting systems. Bio metric system helps voter to use vote without utilizing internet without location off from a surveying place. More over this proposed system will be a better solution for the issues which arises in previous system in the aspect of security, ease of access, confidentiality and accuracy.

KEY WORDS: E VOTING, FACE RECOGNITION, FINGER PRINT, OTP, RETINA RECOGNITION.

INTRODUCTION

Voting is the primary foundation for every nation. To enhance and make stronger nation the democracy requires as Hi Tech voting techniques. Recently in India utilizing Electronic based machines for the purpose of voting whereas in countries like United States, Switzerland and Canada government using E-voting for voting purposed thereby they attained success also. This E-voting works based private computer network or through internet access throughout the world. Sometimes the Electronic voters may help for disabled voters or less technically

knowledgeable persons and it may be process very fast too(Balkrushna Bhagwatrao et al ,2015).

Currently technologies have been improved a lot so all the people having knowledge on online access, they can able to do banking, shopping and charging through online. From the above statement the people can able to make their vote using E-voting. This E-voting will be very convenience and highly secured(Dipali et al,2015)

In addition the current electronics based voting techniques is called instant way of voting. In this voter can able to select the candidates on their priorities as first order, second order or third order. From the order voters can choose on single candidate. From these techniques, the machine should select and save one candidate as voter preferred and do not save and neglect the rest of the candidate. By the way machine should count for all the voted and need to select the highest voted numbers count to the poll office(Priya Taneja et al,2015). This make some difficult and extent the time. There may be a

ARTICLE INFORMATION

*Corresponding Author:

Received 15th April 2020 Accepted after revision 20th May 2020
Print ISSN: 0974-6455 Online ISSN: 2321-4007 CODEN: BBRCCA

Thomson Reuters ISI Web of Science Clarivate Analytics USA and Crossref Indexed Journal



NAAS Journal Score 2020 (4.31) SJIF: 2020 (7.728)
A Society of Science and Nature Publication,
Bhopal India 2020. All rights reserved.
Online Contents Available at: <http://www.bbrc.in/>

chance of miscounting of the data too. It is necessary to determine (A. Nazar Ali et al,2014) these issues E-Voting system increases the chance of reducing the human error and make the people to vote any where using internet. Even the people live in wherever they can suppose to vote. This system especially creates interest among young students to vote and it creates vote percentage to increase.

What is E-Voting based techniques: The process of voting made through the internet is called E-voting. In developing newer techniques (D. Shyam et al,2019) voted data has been saved, processed and out for the upcoming progress. To make vote and compensate the voted data this technology E-voting is used. Based on this process it is also called as internet voting. This device can be more efficient and it creates a easy path for voters and speed up the election results.

E-voting system advantages: It allows the voters to vote in any places in the world, but one thing is voter should have internet access. It improving the performance of the (A. Nazar Ali et al,2015; AT Sankara Subramanian et al,2017) voting percentage of each state. The printing cost and committing the work with man power can be reduced. It allows the government to publish the election results very easy and short publishing of results. E-Voting system not required more transportation for transport anything. By comparing with conventional Electronics based voting this E-voting having more advantages and convenience for people as well as government. Conventional voting process can be divided into different phases.

1. Authentication: To show the original documents to make them as eligible to vote.
2. Vote: The voted paper should fold and put it to box.
3. Vote tallying: To check the enrollment and how many vote made finally.
4. Verification: Checking for errors and recount for verifications

MATERIALS AND METHODS

Existing Voting Systems in India: Existing voting method was done by putting the voted paper and put it to pool box. From the pool box the voted paper has to be collected and its is moved for counting by hand pick up. By inventing electronics based voting machine the paper has been replaced by pressing the buttons.

The figure 1 shows the existing technique voting machine. This system allows EBM as the abbreviation of Electronic Ballot Marker make voter to select the candidate by touch screen. This technology can speed up the pooling applications reduce the poll staff to compensate and count the vote. It especially helps for physically challenged people and also should be useful for people (S.R. Paveethra et al,2019)

- Electronic based Voting machine
- Electronic based Vote Counting machine
- Voting Through SMS from all over India
- Daily News Polls
- Social networking sites polling

Figure 1: Electronic voting machine



RESULT AND DISCUSSION

Proposed System For E-Voting Techniques in India: In this proposed system different E-voting techniques was discussed especially for India. The techniques discussed are

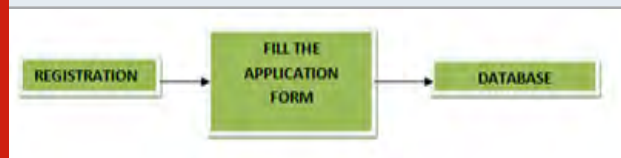
1. OTP (One Time Password) Technique:
2. Face Detection E-Voting:
3. Fingerprint Recognition Based E-Voting:
4. Retina Recognition:

OTP Technique: This technique works based on the message which is received for voter to enroll their voter for authentication. For sending the authentication from government, government needs to collect their database and include their details in database. The database includes their name, address, Date of birth, gender, and unique number given by government of India such as Aadhaar card or smart card and finally the mobile number. The database should be very safe and government should be keep confidentially by keeping the document with password protection or any methods. During the time of voting a four digit or six digits number will be send to voter, using the number the voter can enroll their vote safely and fast. The only thing is the voter should not share their password with anyone. The government also enable the password for some time, after that it automatically disable or not valid. From the next chapter discussed about database registration and step to enroll their vote.

Voter data base registration: This chapter discuss about how to save and register the database of the voters. The database can be collected from form uploaded in government website; there the voters need to register their correct data. That data can be taking an account to voting and possible to send OTP during voting. The user should give correct mobile number. Finally document uploaded by voters can be verified by the

officer for correction. The details of the voter should be enter correct if its an illegal or fake the voters are not able to get their voting rights. The figure 2 shows the database registration of the user and the figure 3 shows the working stages of proposed work

Figure 2: Database Registration



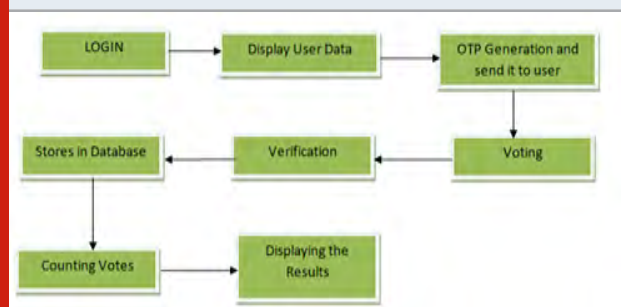
Step 1: The voter should start with entering Aadhaar number. Once its valid the database checks for accessing. Once it's verified it cleared step 1. The voter ID will be enabling thereafter.

Step 2: Once the step 1 cleared, OTP will be received to registered mobile number through the server. The OTP may be looks like a 4 digits or 6 digits it depends on the security purpose.

Step 3: Once the OTP received the voter can supposed to login in machine to make their vote choice. A receipt will come thereafter for ensuring the responses as voter given.

Step 4 : After response from voter, server will check the verification as response and save it in database. The voter can check their results through website once they casted their vote.

Figure 3: Proposed work working progress



Face Detection E-Voting: In initial process of Face detection the captured images was grabbed through an interface. After that the captured image should added for processing to reduce the noise ratio. HSV data's are obtained from the segmentation of RGB color from every pixel. The thresholds takes placed from HSV. Thresholds are nothing but doing segmentation of images. Thresholds help to sharpen the images which were selected. Finally the selection, cropping, sizing has been take place. At last the captured image was compared with processed images for template matching.

For capturing images the voters need to register their data earlier through websites. Then only the server access he voter to make their further process. Base on the process as mentioned above the photo compared with database

for verifications. Once it is cleared the system enables the voter to vote. After them casted vote the database stored and send it to server. It progress the further. This work deals with (A.Nazar Ali et all,2019)the face detection techniques.

Figure 4: Face Detection poses



Figure 5: Finger print based Recognition for people to vote



Fingerprint Recognition Based E-Voting: The requirement for fingerprint recognition based E- voting is listed below Personal computer /Laptop, Finger print scanner with camera. The scanner will scan the finger print of the voter and store it in database. The voter should store earlier before the voting day. At that time of vote the voter needs the identification number for making his thumbs in scanner, so he/she can use the government authorized document like Aadhaar. Once recognition completed voter can make their vote. All the verification completed the voter can be (V.Venkatesh et al,2019) vote and make their choice by pressing over the candidate name or logo. Finally it can be stored in the database and send to server safely. The figure 5 shows the Finger print based Recognition for people to vote

Retina Recognition Based E-Voting:

Step I: Images are capture from sensors and it can be processed for filtering, noise removal and histogram equalization.

STEP II: Once the image was processed the iris part of the image should be separate. The boundaries if iris should be calculated. Once it's calculated the segmentation process will be happen based on the quality of the eye.

STEP III: In last step the iris will be looks normal, it has normal dimensions by that system can obtain the characteristics .Then the iris can be make it for template encode. Once all the process completed the eye image can be extracted and stores it in database. By this way the voter database can be recorded in the database

Figure 6: Retina Recognition

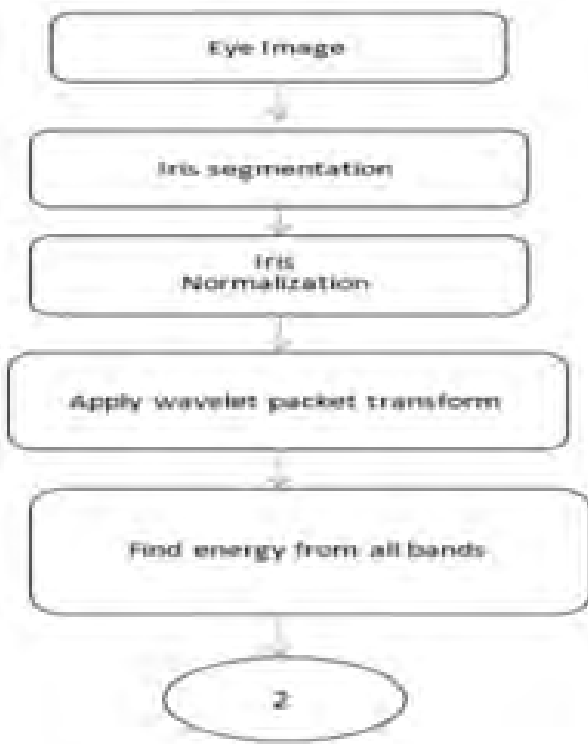


Figure 7: iris based vote casting system



The iris image of each voter is the input to laptop/PC. In database of authority the iris image is compared with stored image. If the image is matched, the system(C. Kalavalli et al,2020) sends the access to the voter for making his vote. If anyone voter tries to cast their vote beyond the time limit, machine will be blocked. If the voter iris pattern is not matched with the stored image, voter may be came as illegal or fake(Sanjay Kumar et al,2013). By that we can find the unusual person from pooling booth. Sample pictorial representation for iris based vote casting system is shown in figure 7.

Advantages of Proposed Hi Tech E-Voting Techniques

- For large populated country like India this Hi tech E- voting machines will help voter to vote fast and secure in anywhere.
- E-voting helps to decrease the human error, the error reduced because of fully automated, transparent and secured system.
- It really works for a disable person to cast vote independently.
- E-voting makes every person who is entitled for vote can create option and it wills consequence in increases the overall voter count.
- Voting from online can view their casted vote once they registered their vote.

Hi Tech Security Requirements For E-Voting Techniques:

The below table I shows the different between conventional and electronics machines system advancement.

CONCLUSION

The HI tech E-Voting system is a newest technique especially good for country like India. That is because the population of India is increasing day by day, surely the automation was required in all parts. Especially while the people making their national duties like voting the technology is required for their betterment. This proposed work really work for the casting the vote through E-voting. This work proposed a way for secured voting from technologies like one time password, Face recognition and detection, Finger print recognition and Retina Recognition techniques. From this study we observed that usage of this Hi Tech technology the voters can n able to vote securely and efficiently. At last it concludes that these technologies surely gain voters in the view of time, cost and accessibility.

REFERENCES

Ali Nazar R Jayabharath MD Udayakumar(2014) An ANFIS Based Advanced MPAGEST Control of a Wind-Solar Hybrid Power Generation SystemInternational review of modelling and simulations vol7 no 4 Pages 638-643.

Balkrushna Bhagwatrao Kharmate Shahebaz Shakil Shaikh Prashant Ravindra Kangane Tushar Anant Lad Prof Ashvini Y Bhamare (2015) A Survey on Smart E-Voting System Based On Fingerprint Recognition

Table 1: Traditional Voting vs. Electronic Voting

NECESSITIES	CONVENTIONAL	ELECTRONIC
Validation	Signature ; Id Card	Password; Electronic Signature
Secrecy	Locks; Envelopes	Encryption Technique
Information Truthfulness	Paper Application	Hash Functions

IJRCCE.

Dipali et al (2015) Mobile Voting System IJETAE.

Kalavalli C SRPaveethraSMurugesan DrANazar Ali (2020) Design And Implementation Of High Efficiency H6 PV Inverter With Dual Axis Tracking International Journal of Scientific & Technology Research Vol 9 issue 02 Pages 4728-31.

Nazar Ali D Sivamani R Jaiganesh M Pradeep (2019) Solar powered air conditioner using BLDC motor IOP Conference Series: Materials Science and Engineering vol 23.

Nazar Ali and R Jayabharath (2014) Performance Enhancement of Hybrid Wind/Photo Voltaic System Using Z Source Inverter with Cuk-sepic Fused Converter Research Journal of APageslied Sciences Engineering and Technology 719 Pages 3964-3970.

Paveethra SR CKalavalli SVijayalakshmi DrANazar Ali DShyam(2020) Evaluation Of Voltage Stability Of Transmission Line With Contingency Analysis International Journal of Scientific & Technology Research Vol 9 issue 02 Pages 4018-22.

Priya Taneja Rajender Kumar Trivedi Rajani Sharma A Proposed method of online voting by face detection IJATES(2015).

Shyam D Premkumar K Thamizhselvan T Nazar Ali A Vishnu Priya M(2019)Symmetrically Modified Laddered H-Bridge Multilevel Inverter with Reduced Configurationally Parameters International journal of engineering and advanced technology Vol 9 issue 1.

Sankara Subramanian AT P Sabarish A Nazar Ali(2017) A power factor correction based canonical switching cell converter for VSI fed BLDC motor by using voltage follower technique IEEE International Conference on Electrical Instrumentation and Communication Engineering (ICEICE) Pages 1-8.

Sanjay Kumar Manpreet Singh (2013) Design a secure electronic voting system using fingerprint technique IJCSI.

Venkatesh A Nazar Ali R Jaiganesh V Indiragandhi (2019) Extraction and conversion of exhaust heat from automobile engine in to electrical energy Energy' IOP Conference Series: Materials Science and Engineering vol 23.

Anti Theft Control of Automatic Teller Machine Using Wireless Sensors

R. Jaiganesh¹, L. Nagarajan², A. Arthi³ and V. Venkatesh⁴

^{1,2}K. Ramakrishnan College of Technology, Assistant Professor/EEE

³M.A.M College of Engineering and Technology, Assistant Professor/CSE

⁴Rajalakhmi Engineering College, Assistant Professor/EEE

ABSTRACT

This paper addresses the security of the Automatic Teller Machine (ATM). The previous methods are having some disadvantages and the robbery has been continued. The objective of the paper is to know the Enhanced smart ATM security system which is developed using Proteus software and advanced technologies. To avoid money theft in the ATM and for protection of the machine, this project approaches some new methodologies using sensors and controllers. Moreover, this project analyses the security systems in the automatic teller machine. In the future, suspicious activities and robbery of thieves will be avoided. For the bank authority, it will be useful for the implementation of their customer services through ATM installation. On the other hand, the footage of the camera in the ATM room can be protected from damage. Still, the robbery in the ATM has been continued even number of protections is there. All the surveillance systems will be monitored successfully by this methodology. Hence the proposed system is the highly secured system for ATMs.

KEY WORDS: AUTOMATIC TELLER MACHINE (ATM), ROBBERY, SURVEILLANCE SYSTEM, PROTEUS SOFTWARE, ARDUINO CONTROLLER.

INTRODUCTION

In the present world, self-governing frameworks are increasing quick prominence. As the social computerization and robotization has been expanded, the ATM cards both debit and credit has been introduced and spread out to variety of banking action. ATM is a Automated Teller Machine that is an automated media communications gadget that gives the clients of a monetary organization

with access to budgetary exchanges in an open space without the requirement for a human representative or bank employee. In ATMs the client is recognized by embeddings a plastic ATM cards with an attractive stripe or a plastic smartcard with a chip (that contains a special card number and some security information) (Bharath E et al., 2012). Since human intervention are minimized the wrong doings for the money related association have been expanded step by step from the year 1999 to 2003, tad diminished in 2004, and afterward expanded again from the year 2005. During the year 2007, there were 2,12,530 of burglary and 4,439 of looter cases filed, and in the 2010 there were 2,69,410 of robbery and 4,409 of looter cases are filed, and further more in the year 2011, there are 2,70,109 of burglary and 4,509 of looter cases filed. These cases in between the year 2007 to 2011 is found increasing later it is being slightly reduced by fixing

ARTICLE INFORMATION

*Corresponding Author: nagarajscorpio@gmail.com

Received 15th April 2020 Accepted after revision 20th May 2020

Print ISSN: 0974-6455 Online ISSN: 2321-4007 CODEN: BBRBCBA

Thomson Reuters ISI Web of Science Clarivate Analytics USA and Crossref Indexed Journal



NAAS Journal Score 2020 (4.31) SJIF: 2020 (7.728)

A Society of Science and Nature Publication,
Bhopal India 2020. All rights reserved.

Online Contents Available at: <http://www.bbrc.in/>

surveillance camera inside and outside the centers but still robbery persons were not caught.

Among the offense for budgetary associations, the instance of burglary and looter have an exceptionally high extent of over 90% and the offense for ATM has located away from the city and on highways. The issue of ATM offense doesn't influence just the bank officials, rather, it is major impact on all parties indirectly involved in the bank action. The cardholder only opens the ATM room and uses it for withdrawing money. As the fraud increases the surveillance and monitoring are mandatory for the ATM area (G.Udaya Sree et al., 2013; Khatmode Ranjit P et al., 2014; M.R.Dineshkumar et al., 2013). This paper ensures the security of the machine in such a way that making sudden protection in milliseconds. All the integrated system is used in three phases like deduction, monitoring and alerting. These are salient for the security enhancement of ATM. The non-contacting technology is used for all the sensors to react within milliseconds. If any suspicious activities made by unauthorized persons the door will get closed automatically. In the future, this proposed work going to be the salient one for the protection of ATM (John Mashurano 1 et al., 2013). Still, the bank authority does not install any ATM center in rural areas due to the robbery. Hereafter these kinds of problems will be avoided and the crime rate in India will be reduced. Hence this system gives solutions for the above problems mentioned (Zaid Imran, et al 2011).

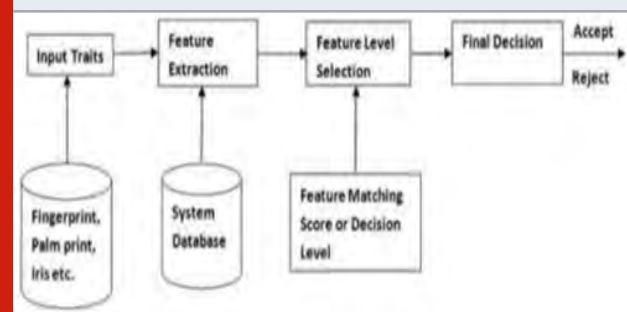
MATERIALS AND METHODS

Existing System: From the literature survey, the following frameworks are available in the current schemes (M. Ajaykumar et al., 2013). The genuine personality of an individual visiting a delicate establishment can be precisely being checked utilizing a blend of the secret key and biometric framework. Secret key personality checks the strategies allude to the utilization of conventional procedures of human character acknowledgment. While biometrics is a robotized strategy for perceiving, an individual dements on a natural or social trademark (Jain, A.K. et al, 2004). Among things to see estimated are the face, palms, DNA, body motion, fingerprints, hand geometry, penmanship, iris, retinal, vein, mark and walk. Biometrics innovations measure and analyze living human body qualities for confirmation, check and ID purposes. ATM is brought in cash exchange easy for clients. In any case, it has the two focal points and weaknesses. Figure 1 shows the block diagram of the existing system. Current ATMs utilize nothing in excess of an entrance card and pin for uniqueness affirmation. This has ATM utilizing face acknowledgement framework exhibit the route to on a ton of phony endeavors and abuse through card burglary, pin robbery, talking and hacking of client's record subtleties and different pieces of security (Suraj B S, et al 2015; Kannan K., 2013; L. Nagarajan et al., 2017).

Recognition: Right now a significant work, acknowledgment utilized in the depiction of biometric frameworks like facial acknowledgement, unique mark

or iris acknowledgement identifying with their key capacity, the nonexclusive term, nonetheless, doesn't really suggest check shut set distinguishing proof or open-set ID.

Figure 1: Block diagram of the existing system



Verification: Here the biometric framework endeavors to affirm an individual has asserted character by contracting a submitted test with at least one recently selected format.

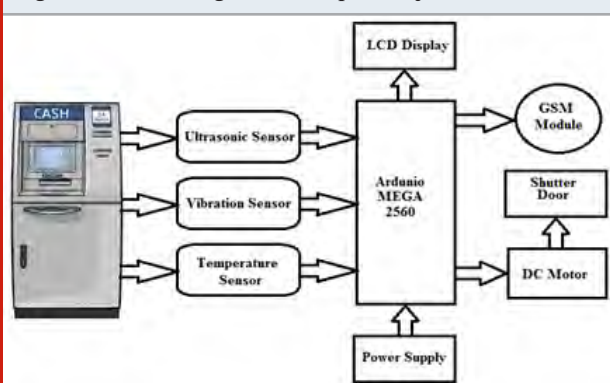
Identification: It is where the biometric framework looks a database for a reference finding a counterpart for the submitted biometric test: a biometric test is gathered and contrasted with all the formats in the database. In the event that it is close-set recognizable proof, the submitted biometric is known to exist in the database. On the off chance that it is open-set distinguishing proof, the submitted biometric test isn't ensured to exist in the database, the framework decides whether the example exists or not. In ATM an idea could be utilized to strengthen the one utilized by ATM's being Card with secret phrase will permit you to get your financial subtleties, as strong as this may appear, on the off chance that somebody approaches the two it will be anything but difficult to get your life investment funds. Nonetheless, if there is one thing one can't get hold of is your face making this an impervious formwork that won't need a lot of preparing time.

Drawbacks of Existing Systems: The possible for recognition of fraud is a significant burden identified with ATM. Fake card perusers called skimmers, are set over the credible peruser to move numbers and codes to nearby ruffian. Secret word voyeurs to gather to get codes additionally utilize spy cameras. Lost access cards are another potential for disoperation. The Federal Trade Commission expresses that individuals are not liable for unapproved utilization of a card in the event that it is accounted for right away. On the off chance that the misfortune is not seen promptly, customers may lose all assets in a record, if notice is not given before cash moves are made. ATMs are a magnet for simply burglary. Burglars are ensured money from purchasers visiting the machines. In spite of the facts that ATM thefts are not normal (just one assaults in each 2.5 million exchange), as per the California Banking Industry, that U.S. Division of Justice (DOJ) reports that around 15% of individuals assaulted and located at ATM stations are slaughtered or harmed. The DOJ guarantees the normal misfortune

is somewhere in the range of \$100 and \$200 (M. Subha et al, 2012; Aru et al., 2014; Patiyoote D.et al.,1998).

Proposed System: The proposed framework will give a propelled ATM burglary security framework. The afflatus for our task is picked up from the news and issue, which are going on in our day-by-day life. Presently ATM thieves or burglary are abundant expanded so because of that we attempting to unveil solution for it. Keeping the strategy of keep it basic in our brain, we suggested a propelled ATM robbery security framework for the ATM machine, beginning from sensor at the passageway to GSM innovation in the ATM machine. Followed by the keen unapproved get to recognition and educated to the closest police headquarters and bank authority. This proposed framework manages the security of ATM from burglary. This framework utilizes an arduino based implanted framework to ongoing information gathered by the vibration sensor, ultrasonic sensor and temperature sensor. When the burglary is distinguished, the siren will begin alarming people in general. The entryway of the ATM will consequently close by utilizing DC motor (R. Jaiganesh., 2017) or three-phase induction motor (L. Nagarajan., 2015). The figure 3 proposes the block diagram of the projected framework with all sensor interfacing between ATM and arduino.

Figure 2: Block diagram of Proposed system



All the sensors and modules integrated with the Arduino controller for the surveillance system of the ATM area. A 6-volt input supply applied to the controller and its output passes to the DC motor (R Jaiganesh., 2018). This DC motor can also be replaced by using a 3Ø induction motor using soft technology (Lasisi H et al., 2012). The core aim of the system is to monitor and protect the ATM area without security. The automated system demands no control room separately. The sensors implemented calculate and process the output within milliseconds and there is no chance for the thief to evade from the location. The sensors integrated with the system reduces every possible way to crack the ATM area.

There are two probabilities to rob the ATM area. By the long-distance hackers and the high hand equipped thief. This system mainly designed to avoid the incidence of the high hand equipped thief. There is also the chance of spraying over the camera to avoid the shoot and there is

another possible way to install the chip and that cracks the circuit and disables the camera recording and enables only the shoot. In some practical cases, a thief enters and tries to fix some false keys and opens the safe and while escaping from the area he breaks the machine. In some exceptional cases, the thief uses some welding and cutting machines to dissect the machine. The temperature sensor and vibration sensor detects the impact and passes the commands to the controller and it closes the door. And by this process, the thief won't escape from the spot. The system also alerts the nearest police station. This concept also catches the thief and avoids the impact on the machine. The system will be super alert when comparing to the conventional system. Even for the small disturbance, the becomes alert. This concept increases the reliability and security of the system.

The police or bank authority should come instantly to the ATM area and have to catch them. If the door once closed it cannot be opened by other people except the bank authority. To open the door there are some techniques can be used such as fingerprint, smart locking system, and hidden locker. The push-button used as the hidden locker and placed behind the shutter.

The door closed in a horizontal manner as the elevator's door. All the integrated sensors connected to the central server. This is going to make a secured transaction of money. ATM is not only used for the withdrawal of money and also used for the deposit of money. Through this, we can know the importance of security for ATM. The near police station authority and banker personal is being alerted by sending message through GSM module. The ATM can be made inactive by entering password and close the gateway as soon as the automatic message is received. The figure 3 shows the way of connecting the motor for automatic operation of the shutter.

Figure 3: Shutter with motor operated



Advantages of the Proposed System: This concept uses highly reliable sensors to sense the different kinds of impact on the ATM machine. This system also protects against the camera shooting hindrance means when the camera lens is sprayed with the paint then the system will come to action and close the door automatically. This system will be responsive even for some minor disturbances. This system won't demand additional human security. The automation will be highly reliable than human intervention.

SIMULATION RESULT AND DISCUSSION

Temperature Sensor: Temperature sensor LM 35 is used to measure the temperature (Kodeeswaran et al.,2017) The following diagram display the temperature when the temperature was measured.Here LCD 16*2 is used to display the result of sensors.Display action is done by the Arduino coding. The figure 4 shows the output of the temperature in the LCD display.

Figure 4: Temperature Sensor Result



Ultrasonic Sensor: This sensor plays a salient role in the measurement of distance.Below figure shows the output of the ultrasonic sensor which is used to identify the obstacle and that distance, It's used for various automobile applications (cars). The figure 5(a) and 5(b) shows the way of incorporation of the Ultrasonic sensor with camera and display of distance in LCD.

Figure 5 (a): Camera with Ultrasonic Sensor



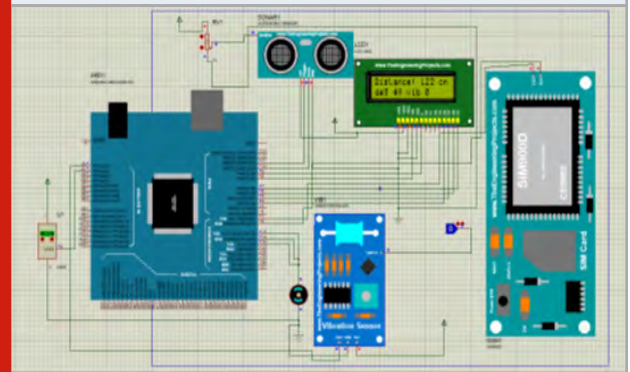
Figure 5 (b): Ultrasonic Sensor Result



Vibration Sensor: The vibration sensor does not only measures the vibration level it also measures tilt motion. This type of sensor mostly used for security purpose, because it measures the vibration level continuously when the vibration exceeds that particular level output system produce the indication.

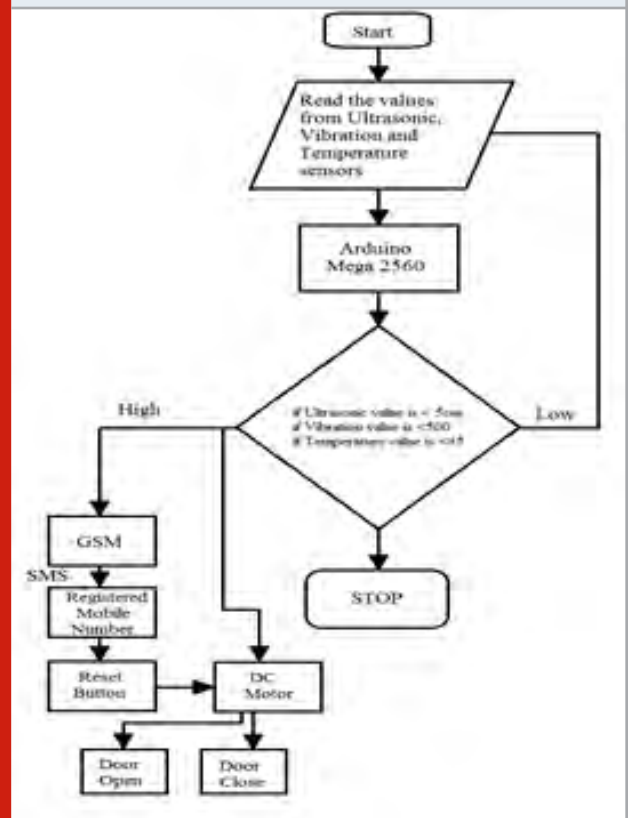
Simulation Result

Figure 6: Simulation Output of Proposed System



Flow Chart: A control flow diagram is a very helpful tool for both systems developers and stakeholders. It shows where control begins and ends, and where it branches on all points in between. The proposed system controlling progress based on the below flowchart. The figure 6 shows the simulation diagram using proteus also the figure 7 represents the flowchart of the sequence of execution.

Figure 7: Flow chart for the proposed system



CONCLUSION

The majority of the ATM has been assaulted by burglaries. Additionally steady builds the robbery of ATM after the step by step. This paper exhibits how mechanization of “ATM THEFT” avoidance from a burglary (or) cheat can

be actualized utilizing GSM technology, vibration sensor, Dc motor, temperature sensor, ultrasonic sensor, signals with arduino can be executed in ATM machine focus. By executing this venture we can get the cheat thefts in ATM itself and further more we can spare our valuable time and cash. In future the ambushes in ATM station can be maintain a strategic distance from by high pitch sound to make them ideal and acquainting some uncommon gas with make them quit.

REFERENCES

- G.Udaya Sree et al (2013) Real Time SMS-Based Hashing Scheme for Securing Financial Transactions on ATM Terminal IJSETR ISSN 2319-8885 Vol.02 Issue.12 pp:1223-1227.
- Khatmode Ranjit P et al (2014) ARM7 Based Smart ATM Access & Security System Using Fingerprint Recognition & GSM Technology ISSN 2250- 2459 Vol. 4 Issue 2.
- M.R.Dineshkumar et al (2013) Protected Cash Withdrawal in ATM Using Mobile Phone ISSN 2319-7242 Vol.2 Issue 4 pp: 1346-1350.
- Zaid Imran, et al (2011) Advance Secure Login International Journal For Science and Research Publications Vol.1 Issue 1.
- M. Ajaykumar et al (2013) Anti-Theft ATM Machine Using Vibration Detection Sensor IJARCSSC Vol.3 Issue 12 ISSN: 2277 128X.
- Suraj B S et al (2015) ARM7 Based Smart ATM Access System International Journal on Recent and Innovation Trends in Computing and Communication Vol.3 Issue 5 ISSN: 2321-8169.
- Kannan K (2013) Microcontroller Based Secure Pin Entry Method For ATM International Journal of Scientific & Engineering Research Vol.4 Issue 8 ISSN 2229-5518.
- L.Nagarajan et al (2017) IoT Based Low Cost Smart Locker Security System International Journal of Advance Research Ideas and Innovations in Technology Vol.3 Issue-6.
- Jain A.K.et al (2004) An Introduction to Biometric Recognition Circuits and Systems for Video Technology IEEE Transactions Vol.14.
- John Mashurano1 et al (2013) ATM Systems Authentication Based On Fingerprint Using ARM Cortex-M3 IJERT Vol. 2 Issue 3 ISSN: 2278-0181.
- M.Subha et al (2012) A study on authenticated admittance of ATM clients using biometrics based cryptosystem IJAET ISSN: 2231-1963 Vol.4 Issue 2 pp 456-463.
- Aru et al (2014) Facial Verification Technology for Use In ATM Transactions AJER ISSN: 2320-0936 Vol.02 Issue-05 pp-188-193.
- L. Nagarajan (2015) Star Delta Starter Using Soft Switch For Low Power Three Phase Induction Motors. Aust. J. Basic & Appl Sci. 9(21) 175-178.
- Lasisi H.et al (2012) Development of stripe biometric based fingerprint authentications systems in Automated Teller Machines Advances in Computational Tools for Engineering Applications (ACTEA) pp.172-175.
- Patiyoot D.et al (1998) Security issues for wireless ATM network Universal Personal Communications.Vol.2.
- Bharath E et al (2012) Automated Teller Machine (ATM) Banking a User friendly ISSN:2230-9519 IJMBS Vol.2 Issue 4.
- Jaiganesh R (2017) Smart Grid System for Water Pumping and Domestic Application using Arduino Controller International Journal of Engineering Research & Technology (IJERT).
- Jaiganesh, R (2018) Grocery Theft and Monitoring Using IoT for Stack Management application International Journal of Engineering Research & Technology (IJERT).
- S Kodeeswaran et al (2017) Precise temperature control using reverse seebeck effect International Conference on Power and Embedded Drive Control (ICPEDC) pp.398-404.

Optimization of Clinically Visual Deep Neural Network for the Classification of Liver Tumor Image

S.Pavithra^{1*}, A. Dhanasekaran², Vanisri A³, and R. Balamurali⁴

¹Department of CSE, Chennai Institute of Technology, Chennai, Tamilnadu, India.

³Department of EEE, Chennai Institute of Technology, Chennai, Tamilnadu, India.

⁴Department of ECE, Chennai Institute of Technology, Chennai, Tamilnadu, India.

²Department of Mechanical Engineering, Chennai Institute of Technology, Chennai, Tamilnadu, India.

ABSTRACT

There are numerous sorts of tumors happening in the liver. Extraordinary tumors have diverse visual appearance and their visual appearance changes after infusion of the differentiation medium. So location of liver tumors is considered as a testing task. Right now, propose a strategy for recognition of liver tumor applicants from CT pictures utilizing a profound convolutional neural system. Experimental outcomes show that we can essentially improve the recognition exactness by utilizing our proposed technique contrasted and the past examines.

KEY WORDS: NEURAL NETWORK, IMAGE PROCESSING, TUMOR.

INTRODUCTION

As of late, liver tumor is one of the significant maladies prompting demise. ID of liver tumor districts precisely from the filtered pictures is viewed as a difficult activity for the specialists. Numerous analysts have revealed different procedures for the recognizable proof of tumor area. The picture de-noising is the fundamental advance to be completed in the clinical picture handling (Chi, D et al ,2010). Picking the reasonable channel for pre-handling is a fundamental undertaking. The separated yield ought to be a de-noised picture. Right now, de-noising is completed by Gabor channel which is trailed by division. The principle target of the division is to

remove the liver tumor area utilizing grouping approach. Division of tissues from customary liver tumor is an exceptionally troublesome and tedious undertaking on account of its composite structure. The greater part of the strategies utilized so far are tedious and they have a few impediments. The k-implies grouping calculation is seen as a less tedious technique when contrasted and other division calculations (Deepa, P et al , 2014; Feng, Y et al,2015)].

Highlight extraction can be completed utilizing GLCM technique. Picking an effective order is a significant job in clinical imaging. Inquires about identified with the created arrangement framework for liver tumor (Filippo Amato et al,2013; Goceri, E et al ,2012) The exhibition of the proposed technique is broke down through the test results are communicated in the area 5.3. At long last, segment 5.4 abridges with a plan to improve the grouping procedure in include.

ARTICLE INFORMATION

*Corresponding Author: pavithras@citchennai.net
Received 15th April 2020 Accepted after revision 20th May 2020
Print ISSN: 0974-6455 Online ISSN: 2321-4007 CODEN: BBRBCA

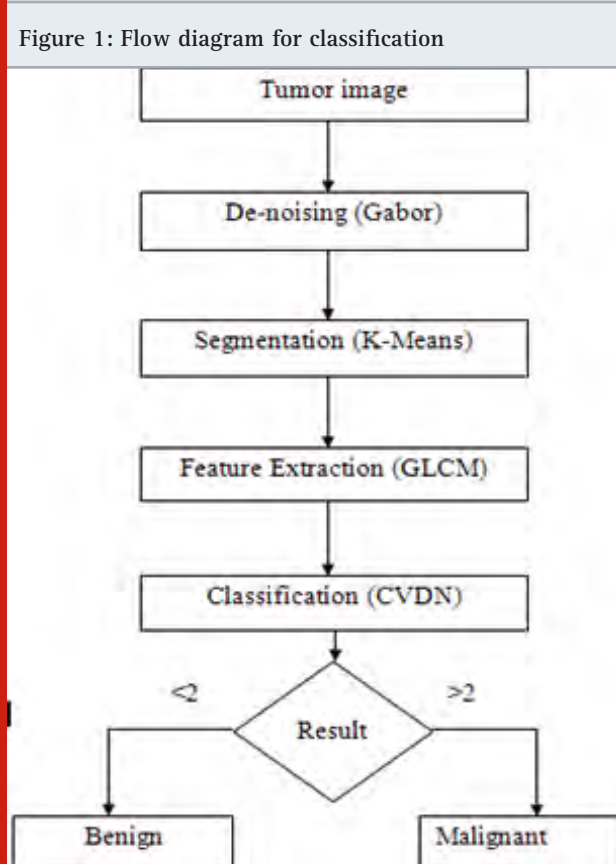
Thomson Reuters ISI Web of Science Clarivate Analytics USA and Crossref Indexed Journal



NAAS Journal Score 2020 (4.31) SJIF: 2020 (7.728)
A Society of Science and Nature Publication,
Bhopal India 2020. All rights reserved.
Online Contents Available at: <http://www.bbrc.in/>

MATERIAL AND METHODS

The stream graph for the proposed CVDN is appeared in Figure 1. The liver tumor picture preparing experiences different procedures, for example, pre-handling, Segmentation, include extraction and arrangement. To improve the exhibition of Liver picture arrangement, inadequate profound neural system order procedure is proposed for staggered Abnormality estimation.



The CVDN technique begins with pre-handling which expels the undesirable commotion from the ultrasound liver picture. To expel the clamor from the info picture, Gabor channel is applied at various level said with various directions. The commotion evacuated picture is then applied with Region based Deep Learning (DL) based element extraction technique for additional investigation. After the component extraction process, CVDN method is utilized to figure the thickness of anomalous pixel esteem. In the Feature order stage, the strategy bunches the smaller scale characterization into various gatherings. The whole procedure is part into three levels, in particular separating with Pre-preparing, Feature extraction utilizing profound learning and highlight characterization utilizing CVDN strategy (Han, XH et al ,2014).

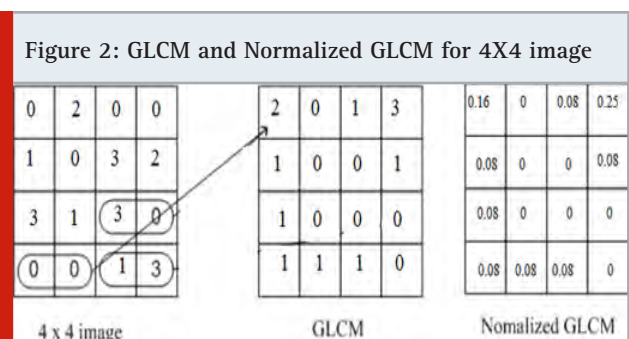
Preprocessing: At the pre-processing stage, the method removes the noise from the image by applying the Gabor filter. The efficiency of Gabor filter is well known and it enhances the image in different adjustments. The magnified image is then used with intensity value based

tumor identification and it removes noise, which improve the quality of input image. The Gabor filter increases the contrast and sharpens the edge to help in the next level edge detection and segmentation process. Finally, the method restores the pixels with the mean value of maximum gray scale value (Ilakkiya, G et al,2013; Karpagachelvi, S et al,2011; Kumar, SS et al.2012).

Segmentation: In the event that the measure of data is littler sum than the whole of the group, at that point it will in general relegate each datum due to the focal point of mass of the bunch. Each focal point of mass can have a gathering name. On the off chance that the measure of data is more prominent than certain bunches, for each datum, it will in general compute the hole to any or all focuses of mass and acquires the base separation. These information are professed to have a place with the bunch that incorporates a base good ways from this information .The base separation calculation depended on the focal point of mass. At that point, that point to dole out all the information to the computerized new focal point of mass. This strategy is steady barely any bunch is moving to an alternate gathering any more.

Feature Extraction and Detection: Highlight extraction is characterized as the blend the pictures into a lot of highlights. It removes the related data to execute the element coordinating. Co-event lattice is alluded as Gray Level Co-event Matrix (GLCM), Gray Level Co-event Histograms (GLCH) and spatial reliance grid. The co-event network or appropriation is a grid or dissemination used to characterize the dispersion of co-happening esteems at a given counterbalance in a picture. The framework C is characterized over a variety of „n X m” of a picture I .

The focus is primarily on GLCM based surface extraction. GLCM is probably the most punctual strategy for include extraction. It contains the data about spatial relationship of pixels in a picture. This spatial data is spoken to as second request measurable minute [16]. A little 4 x 4 sub pictures with 4 dark levels and the comparing GLCM P (I, j/ $\Delta x=1, \Delta y=0$) are appeared in Figure 2.



GLCM is computed for feature extraction using the probability distribution P (d, θ) of clustering image. In this, θ takes the values of 0°, 45°, 90° and 135° while Pt (d, θ) represents the transpose of P (d, θ). The following represents the transpose of P (d, θ):

1. $P(d, 00) = Pt(d, 1800)$
2. $P(d, 450) = Pt(d, 2250)$
3. $P(d, 900) = Pt(d, 2700)$
4. $P(d, 1350) = Pt(d, 3150)$

Using GLCM, Haralick has proposed thirteen statistical features which are known as Haralick texture features. These features are computed from the clustering image: 1. Mean feature, 2. Standard Feature, 3. Entropy Feature, 4. Variance Feature, 5. Correlation Feature, 6. Quadratic mean or RMS Feature, 7. Smoothness, 8. Volume, 9. Breadth, 10. Dimension, 11. Contrast Feature 12. Energy Feature & 13. Homogeneity Feature. Vitality, entropy, complexity, homogeneity and connection highlights are regularly utilized ordinarily among the 13 surface highlights to uncover certain properties with respect to the spatial dissemination of the surface picture. Since clinical picture surfaces normally have numerous different measurements, these surface properties are not self-deciding of one another. For representation, the vitality measure created from dark level co-event lattice is otherwise called homogeneity and change is a proportion of difference in pictures. It uses separation co-event grids to register rakish second minute, complexity, relationship and entropy for grouping errands for a few sorts of pictures. The highlights registered dependent on the co-event lattices have a various types of clinical pictures.

Clinically Visual Deep Neural Network (CVDN): Profound neural systems perform include extraction and gathering of pictures in no problem at all. CVDN strategy takes in to feature depictions from the crude pixels of cell pictures and pixel is acquired from using hand-made framework incorporates as past strategies. Moreover, the portrayal layer is commonly best in class with these part depictions to envision the class for each cell picture. In the ebb and flow inquire about, the going with perspectives are widened : I) a more point-by-point delineation of CVDN classifier structure is displayed, and various key segments for setting up this structure are advised around and likely thought about ii) the piece of data development by methods for rotating cell pictures is dismembered start to finish, and the ampleness of cell picture shroud for this gathering task is analyzed and iii) the shocking adaptability of the CVDN based portrayal system to different datasets is outlined. Despite these, increasingly exploratory connections between's CVDN based structure and the bleeding edge hand-laid out shallower gathering models are coordinated to show the central purposes of the CVDN classifier framework based cell picture order.

After sparsity, to planning tests using the learning references, the CVDN yield including the sparsity level and records of first coefficients in quite a while are utilized as the two courses of action of components for setting up the NN. The proposed scaled down scale CVDN gathering is utilized in a planning pipeline to normally criminologists in 3-D stomach CT pictures. The sectioned highlights are taken care of to CVDN classifier and the loads are refreshed till the CVDN produces result as under

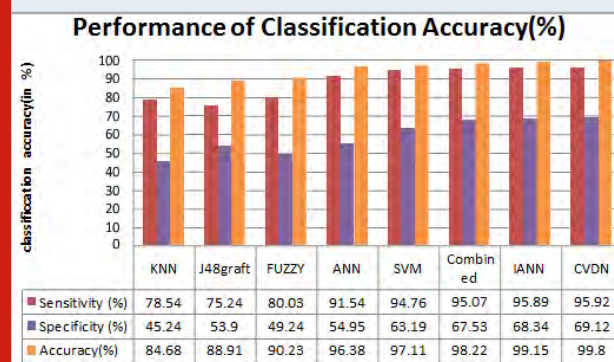
2.0 for amiable cases and more prominent than 2.0 for harmful instances of liver tumor.

RESULT AND DISCUSSIONS

In diagnosing liver tumor, CT has become a significant imaging methodology. Various inquires about have utilized entirely unexpected procedures for characterization of liver development from CT. The exhibition of the proposed technique has been assessed as far as precision, affectability and explicitness. Affectability (Relevant Features) implies what number of liver tumors are acknowledged in the result contrasted and other while explicitness (Irrelevant Features) shows what number of non-liver tumors are dismissed in the result. In general exactness is utilized to the last execution and the affectability is utilized to the acknowledgment ability. Precision is the usually utilized measurement to gauge the exhibition of order. The precision of a classifier relies upon how much characterizing rules square measure genuine.

The element esteems chose for 15 pictures. These element esteems are utilized for the grouping. The adequacy of the proposed strategy has been evaluated utilizing the accompanying measures. The yields of the component extraction vectors are then prepared and the exhibition precision utilizing different classifier techniques is thought about.

Figure 3: Performance comparisons of the Classifiers



The proposed strategy gives better outcomes when contrasted with the current strategies as for affectability and particularity and exactness. Exactness is utilized to estimated how viable the classifier is by indicating the rate. Right now, precision of CVDN and IANN classifier are superior to different classifiers. In this manner, it implies that CVDN classifier could accurately group a greater number of information than different classifiers. Affectability and particularity survey the viability of the classifier.

Figure 3 shows the correlation consequence of grouping exactness and the proposed CVDN strategy has created higher order precision than different strategies. As expressed before, affectability gauges the presentation of the classifier on the measure of effectively ordered kind tumors while explicitness looks at the exhibition

of the classifiers on the measure of accurately grouped harmful tumors. CVDN accomplishes higher estimation of affectability contrasted with different classifiers. Since the reason for the disease location is to distinguish whether the patient has disease or not, which is spoken to by the current of the threatening tumors the most noteworthy accuracy in explicitness is progressively significant in the exploration. The explanation is that patients recognized as malignant growth can be additionally researched to draw out their endurance, yet the patients delegated typical would stay undetected.

CONCLUSION

A proficient liver tumor picture grouping utilizing clinically visual Deep Neural Network is proposed right now. The area is fragmented utilizing K-implies bunching calculation. The highlights were separated utilizing GLCM technique are which is utilized for extricating four Statistical Texture Parameters i.e., entropy, converse contrast minute, precise second minute and relationship. These highlights are valuable in estimation of tumor in Medical Applications. The liver tumor is arranged into considerate and dangerous utilizing CVDN. The order precision is seen as high for the proposed technique when contrasted and the current strategies. This can be additionally improved by the cross breed order strategies.

REFERENCES

- Chi D Zhao Y & Li M (2010) Automatic Liver MR Image Segmentation with Self-Organizing Map and Hierarchical Agglomerative Clustering Method" *Image and Signal Processing* Pages 1333-1337.
- Deepa P & Suganthi M (2014) Performance Evaluation of Various Denoising Filters for Medical Image International Journal of Computer Science and Information Technologies vol 5 no 3 Pages 4205-4209.
- Feng Y Qin XC Luo Y Li YZ & Zhou X (2015) Efficacy of contrast enhanced ultrasound washout rate in predicting hepatocellular carcinoma differentiation" *Ultrasound Med Biol* vol 41 no 6 Pages 1553-1560.
- Filippo Amato Alberto López Eladia María Pena-Mendez Petr Vanhara Ales Hampl & Josef Havel (2013) Artificial neural networks in medical diagnosis" *Journal of Applied Biomedicine*.
- Goceri E Unlu MZ Guzelis C & Dicle O (2012) An automatic level set based liver segmentation from MRI data sets" *Image Processing Theory Tools and Applications (IPTA) 2012 3rd International Conference on 2012*.
- Gonzalez R & Woods R (2008) *Digital Image Processing* Prentice Hall 3rd edition.
- Han XH Wang J Xu G & Chen YW (2014) High-order statistics of micro text on for hep-2 staining pattern classification" *IEEE Trans Biomed Eng* vol 61 Pages 2223-2234.
- Ilakkiya G & Jayanthi B (2013) Liver Cancer Classification Using Principal Component Analysis and Fuzzy Neural Network" *International Journal of Engineering Research & Technology (IJERT)* vol 2 issue 10.
- Karpagachelvi S Arthanari M & Sivakumar M (2011) Classification of ECG Signals Using Extreme Learning Machine" *Computer and Information Science* vol 4 no 1.
- Kumar SS Moni RS & Rajeesh J (2012) Liver Tumor Diagnosis by Gray Level and Contour let Coefficients Texture Analysis" *Computing Electronics and Electrical Technologies* Pages 557-562.

Investigation and Analysis of Path Duration Estimation for Stable Communication Link in VANETS

R. Menaka^{1*}, N. Kandavel², N. Archana³, A. Ragini⁴ and S. Soundarya⁵

^{1,3,4,5}Department of ECE, Chennai Institute of Technology, Chennai, Tamilnadu, India.

²Department of CSE, Chennai Institute of Technology, Chennai, Tamilnadu, India.

ABSTRACT

A mobile wireless network called Vehicular Ad-Hoc network (VANET) in which the vehicles are embedded with the On Board Unit (OBU) on the motherboard that transmit and also receive data packets with the other vehicles. VANET is one of the sub groups of MANETs. All the nodes in the VANET move faster than the nodes in MANETs. In the permanent routes, it is very difficult to receive emergency information and alerts from a identified zones. Therefore, routing plays the important role in VANETs by reducing network overhead, avoids congestion in network, increases congestion in traffic. It is highly appreciable to design a routing protocol that effectively monitors the density of increased traffic and give solutions for VANETs in selecting the appropriate route with high accuracy automatically. VANET is vulnerable to security attacks. Many algorithms were proposed to identify the attacks during transmission with increased overhead. This paper proposes a probabilistic and mathematical analysis of path duration in VANET, based on GA, AODV and DSDV (GAD) based QoS perception routing concept. We derive the probability distribution as well as the expected path duration between source and destination in VANET and solve the Sybil Attack. This reduces the delays that occurs during processing and improves the security in VANETs.

KEY WORDS: VANET, GAD-BASED QOS PERCEPTION ROUTING, NETWORK TOMOGRAPHY, SYBIL ATTACK.

INTRODUCTION

The VANET is the upcoming field now a days. It uses the features of both Ad hc Network and WLAN (Abedi, O et al,2009) All the nodes in VANET are placed randomly in road. They not only communicate with Road Side Units (RSUs) but also with the other nodes through wireless communication (Abedi, O et al,2008) .The three models available for communication in VANET

are: vehicle-to-vehicle (V2V) communication, vehicle-to-infrastructure (V2I) communication and vehicle-to-roadside communication. Since the vehicle nodes can move freely at high speed, the topology can change time to time. The limitations of VANET are reduced by the nodes transmission range, speed, and interferences (Abumansoor, O et al,2011). When the transmitting and receiving nodes are not in the communication region, the network has to find a best route between the two nodes (Bhuvaneswari, R et al,2015). If there is no vehicle in the communication range, the node which carries the information will forward it to RSU, so that it can reach destination vehicle easily.

When the data packets are travelling from source node to destination node in the prescribed path, the transmission delay increases simultaneously. The propagation delay

ARTICLE INFORMATION

*Corresponding Author: menaka.govindaraj@gmail.com

Received 15th April 2020 Accepted after revision 20th May 2020

Print ISSN: 0974-6455 Online ISSN: 2321-4007 CODEN: BBRCBA

Thomson Reuters ISI Web of Science Clarivate Analytics USA and Crossref Indexed Journal



NAAS Journal Score 2020 (4.31) SJIF: 2020 (7.728)

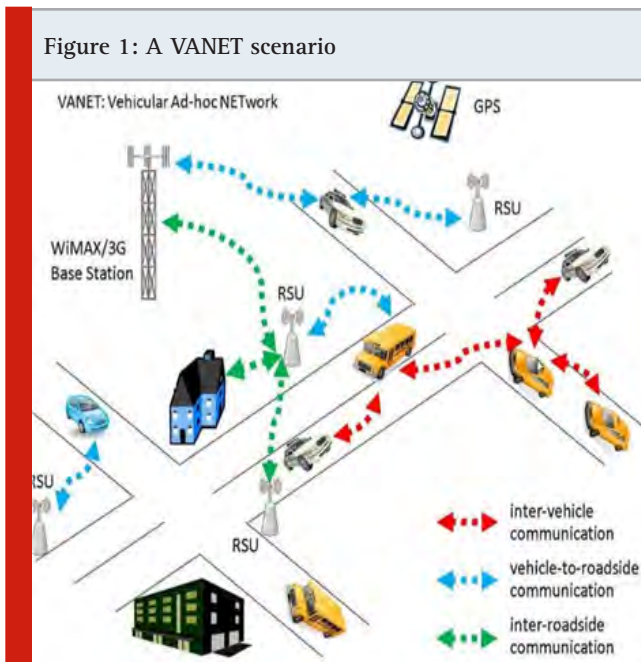
A Society of Science and Nature Publication,
Bhopal India 2020. All rights reserved.

Online Contents Available at: <http://www.bbrc.in/>

can be reduced by selecting the appropriate vehicles with moving with regular density. By designing proper routing protocols for data transmission, this delay issues can be reduced. Many researchers developed various routing protocols as a solution to this issue (Dhanagopal, R et al,2019). Many routing protocols were deigned to work with respect to density of vehicle moving in the path. But the main issue in these protocols is frequent updation required to keep in touch with current vehicle density. Also this information is to be transmitted to all other nodes in the network.

Increase in control packet transmission increases the overhead of the network. This in turn decreases the throughput of the network. So the main of designing routing protocols is to increase the throughput with less delay. Vehicle density that is rapidly changing utilizes more time for convergence in compared with other vehicle density. This is the major reason for the node to obtain in accurate information, as well as the routing behavior will also get affected (Fotohi, R et al,2020) All the node vehicles get information only from nearby nodes and RSUs, this reduces the issues present in the design and only minimum calculations are needed.

All the vehicles in VANETs are normally in contact with fixed nodes on roadsides. As similar to MANET, it is also self organizing network. The structure of VANET is shown in figure 1. During the occurrence of an event in the rode, that particular vehicle will send broadcast messages. On receiving this message, the nearby vehicles or the communicating nodes in the roadside will gain broadcast message, so that the it prevents the other vehicles from crashes. The other vehicles make some calculations and they will take necessary action to prevent the event. The vehicles can also use the fixed stations for connecting to internet.



The traffic jam on the roads is increasing year by year. It is feasible where communications between helps to prevent accidents as well as saving of resources like money, oil etc. Apart from this, the infrastructure management system utilize more funds in developing this structure, since the existing infrastructure does not support for this traffic, which result in planning for new structures of emerging traffic that avoid the dilemmas. VANET's safety is very important that needs to be considered while designing any wireless network. The major drawback of VANETs is the network can be attacked by various kinds of Sybil attacks(Lalitha, R et al,2015). In this paper, it is proposed to design a improved VANET in which new technology can be used to interact with fixed nodes in the network.

Related Workds: The VANET is created by applying the principle of MANET in domain of vehicle communication. The vehicle nodes are moving very fast. The communication between the vehicles during emergency situations is very difficult task to manage. Hence the routing plays a important role in VANET(et ,al,2010). The issues in routing are decreasing the network overhead, increasing the congestion and PDR. Security attacks in VANET network is also a major issue. The P-secure approach is proposed to increases the security in VANET by detecting the DoS attack.

The major problem in VANET network while routing is the moving nodes with the same characteristics as its neighboring nodes (Royer, E. M et al,2000).This paper proposes a location verification protocol to Non line-of-Sight condition among vehicle. The accidents that occur on roads not only affects the human lives but it also affect the public by creating the traffic jam. Since all nodes are mobile nodes in VANET, GSM communication will fail to send messages due to coherence. Other than the GSM communication, the road junction is adopted with sensor for efficient communication between the vehicles. A proximity sensor method is used to collect emergency data and send to fixed nodes in roads. The sensor will be located in road side unit and also in vehicle nodes for immediate response.

A Genetic algorithm to overcome the difficulty in task scheduling for multiprocessor systems. This system includes the key features such as flexibility, adaptive problem representation. By comparing with other traditional scheduling methods shows that the Genetic Algorithm was adapted the changing target nodes automatically. The AODV protocol is widely used in mobile networks. Since there is some issues in testing the protocol in real time scenarios. First, they created a simulation so that it can be used for testing the protocol. After the simulation is completed, it is converted into implementation, some of the changes has to be done in AODV and LINUX environment. This paper proposes and detailed about the modification needs to be done during the implementation of AODV protocol.

AODV is the most efficient and widely used protocol in Adhoc network. Since the AODV is the reactive

protocol, it always transmits the data packet between the neighbor nodes when there is a need. A PAODV approach is proposed which is the improvement on AODV that will make it to adapt for VANET and make more stable routing between the vehicle nodes for the transmission of data packets. The Neighbor discovers distance (NDD) algorithm which detects the information form the sender to receiver without the loss of the data . The detection is made by the many nodes and then join for the improving the detection of the sybil attack very accurately.

The Aim of this research is to improve the shortest routing path for the vehicular network by proposing the GAD (Genetic algorithm, AODV and DSDV) algorithm. The evaluation of network parameters in VANET is tedious because of its dynamic nature of the topology and random mobility of nodes. Hence the Network Tomography is used for the network performance evaluation. In addition to it, the Sybil attack is major issue in the vehicle communication, hence in our proposed method, the Sybil attack can be avoided. These characteristics thus make the proposed method robust and more efficient in the case of the traffic congestion and Road side unit failure.

MATERIAL AND METHODS

The important feature of VANET is to provide improved and safe travel for the travellers. So all the vehicles nodes in the VANET are equipped with wireless communicating devices. This structure should not be like master-slave. Any node can transmit data packet to RSUs and vice versa. The alert messages, road signal information's and also the traffic observation that is captured for some duration are transmitted through such network that give clear details for the vehicles to decide on their route. This system reduces emergency situations in travel time. In this proposed method Modification of AODV is done using GA and DSDV. Therefore this routing technique is called GAD (GA with AODV and DSDV).

Sybil attack is a kind a critical attack where the attackers send the multiple message to the other vehicle. Each message has unique source identity. By sending multiple message to other vehicle creates the traffic jam and confusion by sending wrong message to the other vehicle. Because of the traffic jam the vehicle are forced to take the other best path. The main aim of the attackers is to provide illusion of multiple vehicle with respect to others vehicle so that the vehicle can choose the other best path. With help of GAD we are going to stop this attack. The flowchart of GAD method is shown in figure 2 below.

The basic steps involved in genetic algorithm are as follows:

1. Randomly generate a binary string population
2. For every string, evaluate the fitness in the given population
3. Using reproduction, crossover and mutation operations generate offspring strings.
4. Measure the new strings and compute the fitness

for every string.

5. If the search objective is fulfilled, return the best chromosome as the solution; else go to step 3.

The basic structure of a GA is given in figure 3.

Figure 2: Flowchart for the proposed system

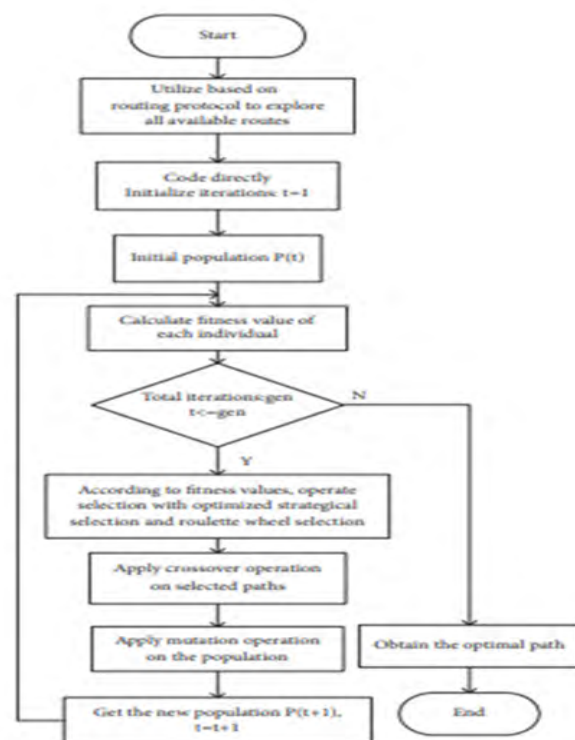
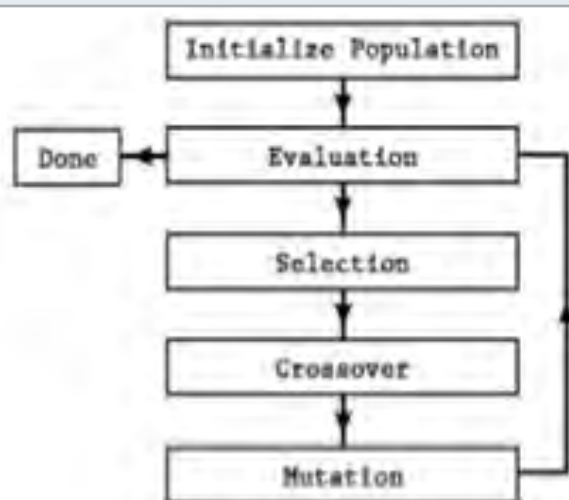


Figure 3: Basic structure of Genetic Algorithm



Simulation result concluded that the path duration will be low for nodes with various / constant relative velocity. When the transmission range is higher, the path duration also will be lower. Thus GA will help for successful communication and reduce the chance of path failure.

RESULTS AND ANALYSIS

The GAD-based QoS perceptive routing approach is evaluated using NS-2 software. Sybil attack make the network weak and unsecure and that weakens the ordinary approaches for the network. In this article we provide a better way to improve the network performance against the sybil attack.

Figure 4 shows Packet Delivery Ratio (PDR). From the following graph it is found that the value of PDR

Figure 4: PDR

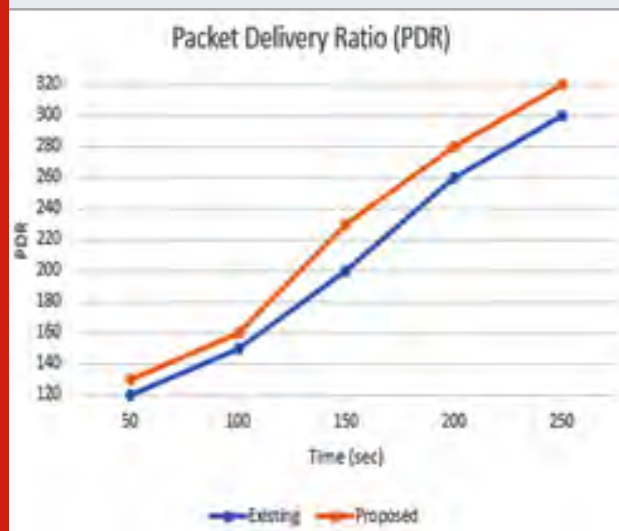
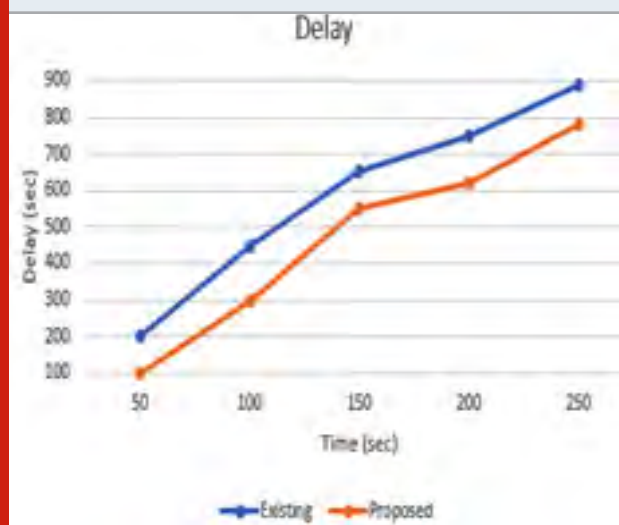


Figure 5: Delay



decreasing with respect to the existing model under attack by varying the pause time. The PDR for the DAD has better improvement than the existing approaches under various attack.

Figure 5 shows e2e_delay. Proposed approach is lower than the existing approaches. The reason is that by

using the proposed algorithm the nodes under suspicion are restricted to send the message and all the intended attacks were easily identified and messages has been sent regarding this.

Figure 6: Energy Consumption

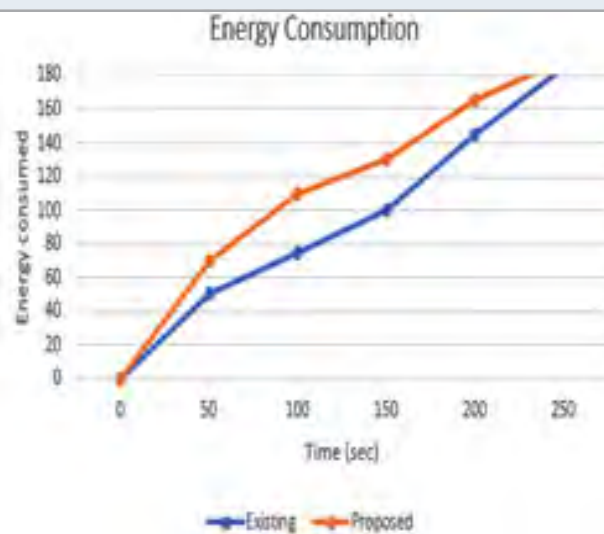


Figure 7: Throughput

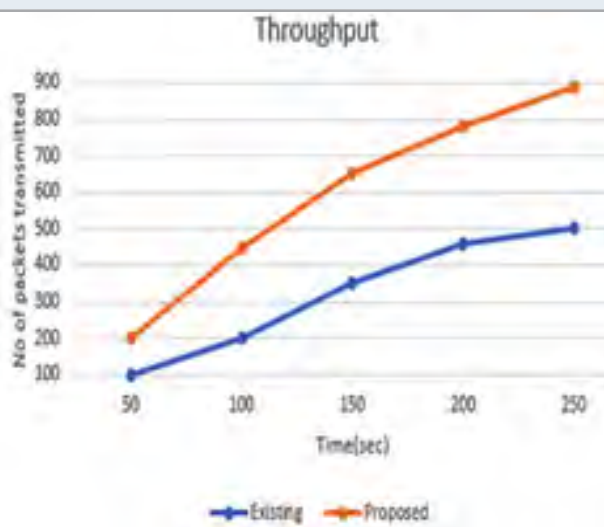


Figure 6 shows Energy consumption is improved than the existing approaches in VANET. Figure 7 shows improved Throughput than the existing approaches in VANET.

CONCLUSION

VANETs are designed to communicate with adjacent vehicle and the vehicle equipped with road side units. In this paper we used the GAD-based QoS perception approach that is used for detecting the sybil attack before the end of transmission time. The GAD based QoS perception routing reduces the processing delay and improves safety and security in VANET. NS-2 simulator was used to illustrate the performance of GAD-based QoS perception routing approach. The simulator result shows

that the GAD-based QoS perception routing approach has more performance than the existing approaches in terms of Throughput, End to end delay and packet drop rate.

REFERENCES

- Abedi O Berangi R & Azgomi M A (2009) Improving route stability and overhead on AODV routing protocol and make it usable for VANET In 2009 29th IEEE International Conference on Distributed Computing Systems Workshops (pp 464-467) IEEE.
- Abedi O Fathy M & Taghiloo J (2008) Enhancing AODV routing protocol using mobility parameters in VANET In 2008 IEEE/ACS International Conference on Computer Systems and Applications Pages 229-235 IEEE.
- Abumansoor O & Boukerche A (2011) A secure cooperative approach for nonline-of-sight location verification in VANET IEEE Transactions on Vehicular Technology 61(1) Pages 275-285.
- Bhuvaneshwari R Balamalathy N Premalatha S Manimozhi V Parvathi S & Kumaresan A (2015) An improve performance discovery and interruption of Sybil attack in MANET Middle-East Journal of Scientific Research 23(7) Pages 1346-1352.
- Dhanagopal R Muthukumar B (2019) A Model for Low Power High Speed and Energy Efficient Early Landslide Detection System Using IoT Wireless Pers Commun.
- Fotohi R Ebazadeh Y & Geshlag M S (2020) A new approach for improvement security against DoS attacks in vehicular ad-hoc network arXiv preprint arXiv:2002.10333.
- Gen M Cheng R & Lin L (2008) Network models and optimization Multiobjective genetic algorithm approach Springer Science & Business Media.
- Lalitha R V S & JayaSuma G (2015) Alleviating the effect of security vulnerabilities in VANETs through proximity sensors In Emerging ICT for Bridging the Future-Proceedings of the 49th Annual Convention of the Computer Society of India (CSI) Volume 1 Pages 31-41 Springer.
- Lequerica I Ruiz P M & Cabrera V (2010) Improvement of vehicular communications by using 3G capabilities to disseminate control information IEEE network 24(1) Pages 32-38.
- Royer E M & Perkins C E (2000 September) An implementation study of the AODV routing protocol In 2000 IEEE Wireless Communications and Networking Conference Conference Record (Cat No 00TH8540) Vol 3 Pages 1003-1008 IEEE.
- Wu A S Yu H Jin S Lin K C & Schiavone G (2004) An incremental genetic algorithm approach to multiprocessor scheduling IEEE Transactions on parallel and distributed systems 15(9) Pages 824-834.

Scalable and Detect Link-Failure Traffic Balancing Network Using Adaptive Filter

R.Purushothaman*¹ and R. Narmadha²

¹Research scholar, Sathyabhama Institute of Science and Technology, Chennai, Tamilnadu, India

²Associate Professor, Sathyabhama Institute of Science and Technology, Chennai, Tamilnadu, India

ABSTRACT

For monitoring the network and its management the Wireless Mesh Network which is based on the Software Defined Radio is widely used. The major advantage of using the SDN based wireless Mesh Network is it makes the management easier but the major disadvantage is it can't able to identify that whether the architecture is for the wired links which can able to handle dynamic topology. The problems such as traffic balancing due to node mobility can be easily overcome with the help of this technique. Another major disadvantage is SDN reaction time in dynamic network topology, which is overcome with the help of supervised two layer gaining knowledge, which monitors the node mobility and chance of failure in the links. Without overloading the control panel, the optimal traffic balance is achieved by an alternative way of route selection method and topology discover is another key area that to be addressed in SDN. In our proposed work, to establish the forwarding decisions, a filter technique which uses the two hop neighbor statistics. The simulated result of end to end delay, network load and throughput clearly shows the parameter are enhanced because of the proposed SDN WMN architecture along with link failure.

KEY WORDS: LINK FAILURE PREDICTION, SOFTWARE-DEFINED NETWORKING (SDN), SUPERVISED LEARNING, WIRELESS MESH NETWORK (WMN).

INTRODUCTION

The programmable network which make use of the centralized management which easily resolve the various requirements such as optimization of traffic engineering network and transportation of data. Such Logical centralized programmable network is used by the software defined radio. But the current network application requires a more scalable means of architecture which can able

to provide a more reliable service for different types of traffic. The above requirement is satisfied with the help of software defined radio architecture since it can able to maintain the entire network states and also it can able to offer flow control for the layers at the bottom level. And another major key point is that it allows the third-party participation in the network application design and exploitation. A new type of network. In the enterprise network for the management and security the centralized controller with flow control management is used which is based on the SDN proposed in the Ethane project.

The element which used in switching is used to carry out the function line forwarding of the packets, but they are controlled and monitored by the controllers. This controller collects the information about the network states and decide how to allocate the network resources.

ARTICLE INFORMATION

*Corresponding Author: purushoth8419@gmail.com
Received 15th April 2020 Accepted after revision 20th May 2020
Print ISSN: 0974-6455 Online ISSN: 2321-4007 CODEN: BBR CBA

Thomson Reuters ISI Web of Science Clarivate Analytics USA and Crossref Indexed Journal



NAAS Journal Score 2020 (4.31) SJIF: 2020 (7.728)
A Society of Science and Nature Publication,
Bhopal India 2020. All rights reserved.
Online Contents Available at: <http://www.bbrc.in/>

And therefore, the SDN makes the switches design and routers design easier since they are dedicatedly used only for the data transfer. SDN directly control the behavior of network and not the behavior of the network resources. In the literature the SDN is studied in terms of wired networks and data centers. However there is some literature which explore the SDN in wireless topology networks. In this paper a survey is presented on usage of SDN in various types of wireless networks. For each type of the wireless network we classify and difference the proposed SD architecture.

We likewise talk about open difficulties and opportunities. Next we consider the utilization of SDN in Wireless Sensor Networks (WSNs) where the essential test spins around dealing with the restricted assets of the sensors as they team up on get-together data about the marvels being observed. These constrained assets intensify adaptability worries with huge systems, as the measure of control traffic important to keep up a state-of-the-art perspective on the system state increments. Sensor organizes additionally require in-arrange preparing for rundown and conglomeration. Further difficulties incorporate supporting numerous applications and empowering various systems to exist together.

MATERIALS AND METHODS

Related Works: In (SoheilHassas et al., 2012) present preventive the straightforwardness of intermittent occasions on the compose plane is vital for understand a versatile Software-Defined Network. One strategy of restricting this overhead is to process visit occasions in the information plane. This requires alter switches and comes at the expense of perceivability in the control level. Taking a substitute course, we propose Kandoo, a structure for saving versatility without adjusting switches. Kandoo has two layers of controllers: (I) the base layer is an assortment of controllers with no interconnection, and no data of the system wide state, and (ii) the top layer is a reasonably brought together controller that keeps up the system wide state. Controllers at the underneath layer run just bound force applications (i.e., applications that can reason utilizing the condition of a solitary switch) close to information ways. These controllers handle the greater part of the regular occasions and effectively shield the top layer. Kandoo's plan empowers arrange administrators to duplicate nearby controllers accessible if the need arises for and lighten the heap on the top layer, that is the handiest conceivable bottleneck regarding versatility. Our evaluations show that a framework constrained by Kandoo has request of size lower sort out channel use contrast with ordinary OpenFlow systems. (Stefano Salsano et al., 2014) presents the Wireless Mesh Routers (WMR) are OpenFlow proficient switches that can be prohibited by SDN controllers, as indicated by the wmSDN engineering that we have presented in a past work. We accept the subject of controller choice in a situation with discontinuous network.

We accept that after some time a solitary WMN can get split in at least two parcels and that different allotments

can converge into a bigger one. We accept that a lot of SDN controllers can conceivably acquire oversee of the WMRs. At a given time just a single controller ought to be the ace of a WMR and it ought to be the most appropriate one as indicated by different measurement. We contend that the cutting-edge answers for "ace political race" among conveyed controllers are not reasonable in a work organizing condition, as they could without much of a stretch be influenced by irregularities. We imagine an "ace determination" approach which is under a gather of each WMR, and assurance that at a concurred time just a single controller will be ace of a WMR. We determined a particular ace determination practice which is exceedingly undemanding as far as the control rationale to be executed in the WMR. We have executed the proposed arrangement and conveyed it over a system emulator (CORE) and over the gathering of two bodily remote proving grounds. (Huawei Huang et al., 2015).

Presents SDN has been imagined as the cutting edge arrange worldview by decoupling control plane and information plane, with the end goal that arrange association and streamlining can be led in a concentrated technique utilizing worldwide system in grouping. Right now, are figuring out how to apply SDN idea to a remote work organize that has been broadly received by different applications. We unique propose a novel design of SD-WMNs, and distinguish various critical difficulties. Since remote range is a defective asset that is public by the two information and arrange move in SD-WMNs, we propose three range distribution and planning calculations, expressly FB-NS, NFB-NS, and NFB-S that coordinate both control and information traffic. At long last, execution is assess by means of broad reenactments In request to show signs of improvement asset activity, we investigate the traffic qualities in SD-WMNs, and propose three novel range allotment and traffic planning calculations, that is, Fixed-Bands Non-Sharing, Non-Fixed-Bands Non-Sharing and Non-Fixed-Bands Sharing calculations, to misuse recurrence and spatial multiplexing.

At last, the exhibition of the proposed three calculations is assessed by broad reproduction. (Golnaz Karbaschi, et al., 2005) presents wireless systems experience the ill effects of irregular varieties in channel and system condition. This prompts lackluster showing in multi-bounce remote systems extraordinarily with a traditional nonflexible steering. To adapt to instability of remote connections, a cross layer directing that ropes adaptivity and enhancement across lower layers of system stack is required. Cross layer directing means to contribute an imperative job in edifying the exhibition of remote systems however requires a cautious consideration on the decision of the measurement. Right now recommend a unique connection quality and blockage mindful measurement for multi-jump remote directing which is gotten from MAC layer. We show that despite everything having a way with sensible length our proposed measurement improves the presentation of steering as far as start to finish postponement and throughput

in contrast with least jump check metric. We contend right now the expended limit ought to be the significant criteria in deciding the best way to any goal.

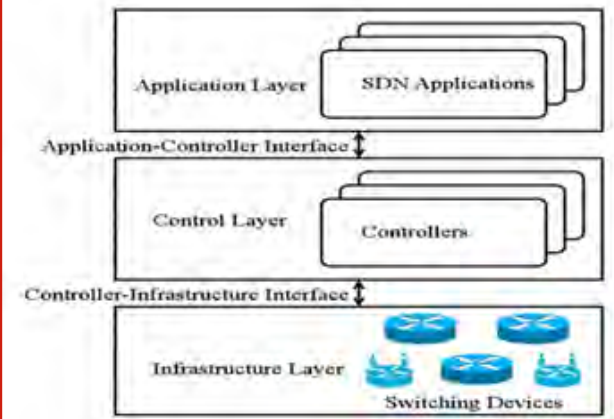
In any case, the proportion of such a criteria isn't straight forward to acquire, as it must consider the connection quality and conflict level of connections. (Xu Li et al., 2014) presents SDN decouples control plane usefulness from the measurements plane and highlights the event of programmable imbecilic system gadgets, which have no or humble acumen and take control orders from a focal controller at the control plane. The focal controller is responsible for controlling information plane equipment and advancing system activity. Incorporated system enhancement and sort out is absurd or infeasible when the system turns out to be excessively extraordinary in measurement or stacking. Circulated arrange advancement comes into take an interest underneath this condition. Totally disseminated arrange advancement requires nearby knowledge at character organize components, against the essential idea of SDN. Right now consider SDN benevolent zone-based dispersed system streamlining and study the essential system zoning trouble, that is, the means by which to assortment organize components into zones, for example, to decrease the straightforwardness of conveyed arrange advancement. We give a numerical definition of the difficulty and show that it is NP supreme. We then close by three heuristic arrangements and assess their exhibition through recreation.

SDN CONCEPT: The Open Networking Foundation (ONF) is a philanthropic consortium excited to development, institutionalization, and commercialization of SDN. ONF has provided the greatest unequivocal and appropriately introduced meaning of SDN as follows: programming program-characterized Networking (SDN) is a developing network design wherein arrange control is decoupled from sending and is legitimately programmable. As in step with this definition, SDN is characterized through two attributes, explicitly decoupling of oversee and information planes, and programmability at the oversee plane. Out of sight of SDN, its uniqueness dwells on the way that it gives programmability through decoupling of control and information planes. In particular, SDN offers uncomplicated programmable system gadgets instead of creation organizing gadgets more multipart as on account of dynamic systems administration.

Additionally, SDN proposes severance of control and information planes in the system design mean. With this expect, arrange control should be possible unconnectedly on the sort out plane without contacting information streams. All things considered, arrange insight can be removed from turning gadgets and situated on controllers. At the coordinating event, exchanging gadgets would now be able to be ostensibly illegal by programming without installed insight. The decoupling of control plane from information plane offers a less complex programmable condition as well as a more noteworthy opportunity for outer programming to characterize the conduct of a system.

SDN MODEL

Figure 1: SDN Model



This copy incorporates three layers, primarily a framework layer, an oversee layer, and an utility layer, stacking over each unique. The framework layer comprises of exchanging gadgets in the information plane. Elements of these exchanging gadgets are generally two-overlay. To begin with, they are responsible for gather arrange status; hoard them transiently in nearby gadgets and sending them to controllers. The system standing may hold onto in grouping, for example, organize topology, traffic insights, and system uses. Second, they are liable for administration holder dependent on rules gave by a controller. The control covering spans the accommodation layer and the framework layer, through its two interfaces. For descending connecting with the framework layer (i.e., the south-sure interface), it determines capacities for controllers to get to abilities outfitted through exchanging devices. The capacities may incorporate introduction arrange status and bringing in bundle sending rules.

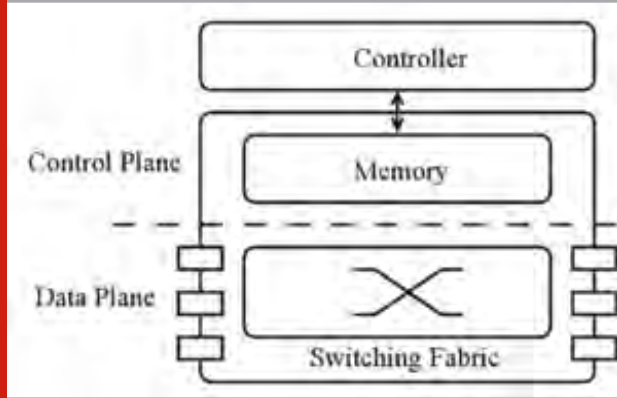
For upward associating with the application layer it offers support passageways in different structures, for instance, an Application Programming Interface. SDN applications would admission be able to organize position data explanation from exchanging gadgets through this API, make conspire modification choices dependent on this in succession, and do these choices by circumstance bundle sending rules to switch gadgets utilizing this API. Since a scope of controllers will make due for a monstrous regulatory system area, an "east-west" declaration interface among the controllers will likewise be attractive for the controllers to disseminate arrange data and synchronize their dynamic procedures.

Switching Device Model in SDN

The building structure of a SDN exchanging gadget, comprising of two sensible parts for the information plane and the control plane is appear in figure Inside the realities plane, the exchanging gadget, in demanding, by means of its processor, plays parcel sending, in view of the sending framework necessary with the guide

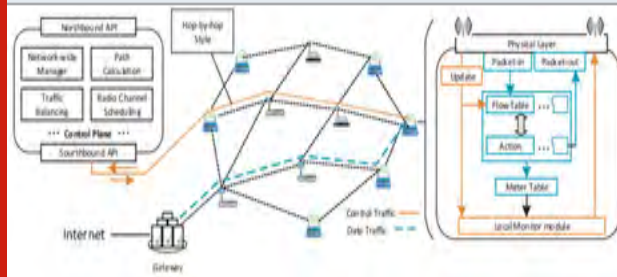
of the control layer. This advanced compositional statute loans SDN forceful focal points. Not at all like traditional exchanging gadgets that additionally run steering conventions to conclude how to advance parcels, directing choice makings are taken from switch gadgets in SDN. As a result, the exchanging gadgets are absolutely responsible for social affair and revealing system position just as preparing parcels dependent on forced sending rules. It goes behind that the SDN switch gadgets are less difficult and will be simpler to fabricate. The amassed intricacy thusly prompts a minimal effort arrangement. This inventive engineering, be that as it may, requires novel equipment structure for SDN-empowered exchanging gadgets. Right now, portray ongoing look at advances in exchanging gadget equipment configuration, focus on both the control plane and the information plane.

Figure 2: Switching Device Model in SDN



SD-WMN architecture

Figure 3: SD-WMN architecture



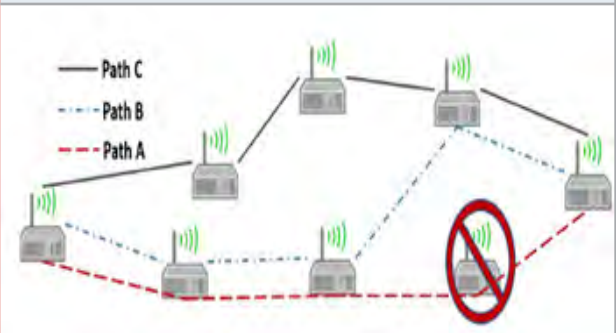
In WMNs, the connection disappointment location is a piece of the steering plans by communicating the HELLO messages to neighboring hubs at a specific recurrence. In any case, the HELLO message presents overhead and postponement as the connection disappointment location profoundly relies upon the sending recurrence of HELLO messages. Some cross-layer connect disappointment recognition plans were proposed in which utilize the ACKs in MAC layer. Be that as it may, these plans utilize a cross-layer convention structure, where a connection disappointment in MAC layer impacts the directing layer execution. The irregularity between the directing and MAC layers as far as connection discovery results may diminish the recognition precision. Besides, utilizing

the ACK alone in MAC layer may not be fitting since some different elements may likewise cause the back to back loss of ACKs. Our proposed two-layer LFP conspire uses the highlights of SD-WMNs by utilizing the coarse forecast in the information plane and fine expectation in the control plane. It depends on the bundle misfortune or debasement insights during information transmissions. An information transmission blunder can be sorted as transient or changeless connection disappointment. The previous speaks to a brief variance of connection quality and doesn't require the difference in the route(s) in the switches. On opposite, last mentioned (i.e., the perpetual disappointment) requires the update of stream tables in the information plane to reroute the information by SDN controller. Our proposed LFP conspire distinguishes the perpetual connection disappointment.

Controller: The intelligently concentrated controller gear the knowledge of the SD-WMN with four boss modules. The universal impression administrators are accountable for checking the absolute system and keep up a system topology that can be utilized to perform worldwide control. The segment of directing way computation can be executing by a pathway looking through calculation, for example, Dijkstra's most limited way calculation, intending to discover a steering way for traffic streams dependent on the all inclusive system review. The exchange planning module plans transmission of both control and information parcels accord to a particular control approach. The past part, range designation, is reliable for arranging range assets in the SD-WMN. What's more, the controller collaborates with a combination of uses in the upper layer through northbound application programming interfaces (APIs), while speak with information plane equipment by means of southbound APIs (e.g., OpenFlow convention).

Traffic during Link Failure

Figure 4: Traffic during Link Failure



For elective course determination, the course length (i.e., the quantity of bounces) ought to be limited. Finding a completely new elective course would produce higher control traffic overhead, since the SDN-FE needs to refresh its stream tables by mentioning information sending rules from the control plane when another information bundle is gotten. Figure 4 shows a case of elective way choice. Expecting that way An is the first way, two elective ways are conceivable (i.e., Paths B

and C) if there should be an occurrence of a connection disappointment. The way B needs to refresh the stream tables for just two hubs, as the rest of the hubs of the first way A stay in way B. Then again, way C needs to refresh the stream tables for the entirety of its hubs, and in this way will produce more control traffic overhead than way B. What's more, way C additionally has higher likelihood of influencing other existing courses because of its bigger extent of connection update.

Connection Failure Prediction in Control Plane: Proposed process based connection disappointment forecast in information plane considers just the neighborhood hub portability, as the information on organize topology isn't accessible in the information plane. To improve the exactness, we additionally perform LFP in control plane. At the point when the portability of a hub is distinguished in information plane, the SDN controller is educated, which at that point checks the SNR estimations of hub's neighbors to affirm its versatility. Since the controller gathers numerous arrangements of SNR estimations, it can settle on an exact choice dependent on the order of the connection quality examples in SNR informational indexes by utilizing the help vector machine which utilizes a directed learning-based characterization

Versatile FILTER: A versatile Filter is a framework with a straight channel that has an exchange highlight constrained by methods for variable parameters and an approach to adjust those parameters as indicated by an improvement set of rules. In light of the multifaceted nature of the improvement calculations, almost all versatile channels are computerized channels. Versatile channels are required for certain applications because of the reality a couple of parameters of the ideal preparing activity are not perceived before or evolving. The finished circle versatile channel off utilizes input inside the type of a mistake sign to refine its switch highlight. Ordinarily talking, the shut circle versatile framework involves the use of a cost work, which is a standard for ideal execution of the channel, to take care of a calculation, which decides how to alter channel move capacity to limit the expense on the following emphasis. The most not bizarre cost work is the mean square of the mistake sign.

TRAFFIC BALANCING OPTIMIZATION: A connection disappointment is anticipated, it is essential to locate the option route(s), which fulfills the accompanying conditions: (1) the most brief way separation, (2) the least control overhead, and (3) minimal effect on other booked information traffic. At the end of the day, the option route(s) should deal with both the steering and traffic designing issues, while limiting the directing overhead. To meet the above conditions, we characterize the steering procedure as an improvement issue which can be illuminated by utilizing the straight programming approach. Right now, first depict the SDN-WMN arrange model for the investigation of online traffic adjusting and

multi-channel asset booking. In view of this model, we will plan a temporary course enhancement calculation to conquer the traffic blockage issue brought about by interface disappointments.

Status Monitoring and Collecting: The worldwide system data is noteworthy for approach projects to figure choices. Status in grouping in the system will be gathered however much as could reasonably be expected, for example, the traffic rate in each connection, rule size in each sending equipment, and range allotment in each radio connection. The position data must be accounted for to the controller through secure channels. The controller may react with novel orders to each gadget. The bidirectional correspondences give to the control move by a non-unimportant portion. Besides, transmission quality is particularly influenced by blockage and interruption in remote connections. Since arrange status data and identical control messages isolate the remote medium with information traffic, advanced planning calculations are attractive to organize traffic in the SD-WMN.

Clog inside the Shared Medium: Other than the checked in succession, the transmission of arrangement rules to coordinate the steering of information traffic is another significant commitment of oversee traffic. As rules are produced to serve the information traffic, the information traffic can get transmitted simply after the equal control traffic are transmitted effectively. That is, arrange trade is more huge than information traffic. A proficient SD-WMN framework ought to bear the cost of higher need to control traffic than to information traffic. It tends to be seen that, contrasted with the customary WMN, more control traffic exists in the system, and it contend with information traffic for radio asset in a SD-WMN. Along these lines, it is conceivable that the control traffic is stuffed with information traffic in occupied association joins, which bring about a long inactivity of control traffic and outcomes in clashing controlling rationales in SDN-empowered systems. This difficulty is far more atrocious in the connections close to passages in a WMN. Clog is probably going to occur right now. Accordingly, control messages and rules will encounter high inactivity

COMPUTATIONAL COMPLEXITY ANALYSIS: We predominantly center around the calculation multifaceted nature investigation for the accompanying three sections: connect quality estimation, SVM-based LFP, and enhancement calculation in the option route(s). In the proposed framework versatile channel method runs at the remote hubs of the information plane for connect quality estimation. Note that the computation of option route(s) is handled in the control plane too. Accordingly, this advancement issue additionally has almost no impact on steering delay since the controller has high computational capacity.

RESULT AND DISCUSSION

Comparison Chart

Figure 5: Number of nodes vs. Throughput

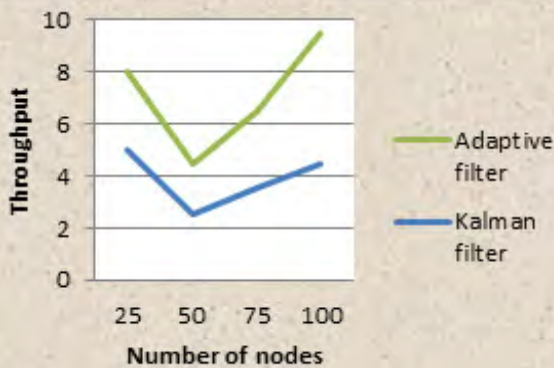
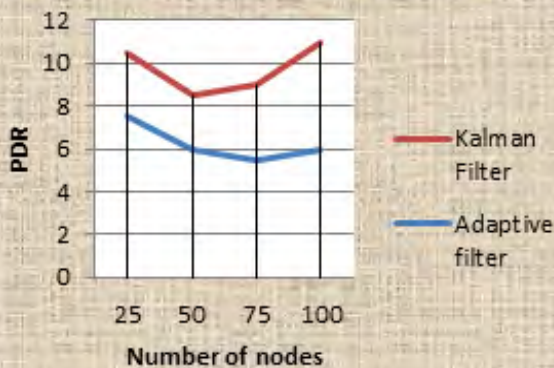


Figure 6: Number of nodes vs. PDR



CONCLUSION

An inventive answer for traffic control was introduced, within the sight of portability in SDN-based WMN. The concentrated SDN control highlights were misused to beat the trouble of taking care of portability issues in WMN. In particular, a SVM based versatile filter followed by an elective course choice plan, in view of the unified traffic designing in charge plane. Our adaptive filter has significantly diminished unnecessary rebroadcasts consequently decreasing the effect of communicate traffic on unicast information transmission. Subsequently, utilizing different channels with a versatile channel is basic to diminish arrange obstruction. Second, when utilizing multi joins with various transfer speed for information transmission, relegating fitting load for each connection is required to limit the absolute transmission delay. Since SDN offers an incredible open door for canny system control, we will utilize new AI models for SD-WMN steering/clog control in future. Additionally, the overhead of control traffic will be additionally diminished by structuring low-unpredictability SDN control plans.

Figure 7: Number of nodes vs. End to End Delay

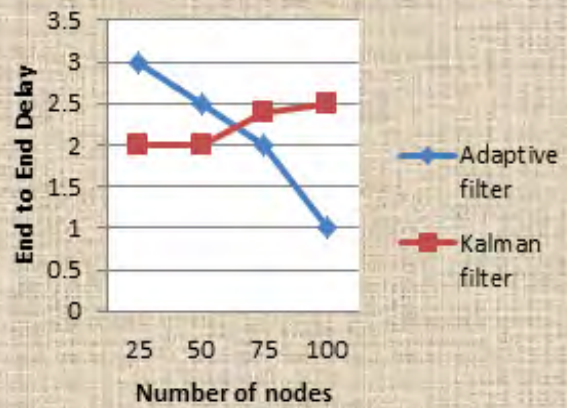


Figure 8: Transmitting message to another node



REFERENCE

- Abolhasan J Lipman W Ni and B Hagelstein (2015) Software-defined wireless networking: Centralized, distributed, or hybrid? IEEE Network vol 29 no 4 Pages 32–38.
- Al-Fares S Radhakrishnan B Raghavan N Huang and A Vahdat (2010) HEDERA: Dynamic flow scheduling for data center networks in NSDI vol. 10 Pages 19–19.
- Cerpa, J L Wong M Potkonjak and D Estrin (2005) Temporal properties of low power wireless links: Modeling and implications on multi-hop routing in 6th ACM International Symp Mobile Ad Hoc Networking and Computing Pages 414–425
- Chen C Wu X Hong Z Lu Z Wang and C Lin (2016) Engineering traffic uncertainty in the openflow data plane in IEEE INFOCOM 2016 Pages. 1–9.
- Costanzo L Galluccio G Morabito and S Palazzo (2012) Software defined wireless networks: Unbridling SDNs in IEEE European Workshop on Software Defined Networking (EWSDN) Pages 1–6.
- Curtis J C Mogul J Tourrilhes P Yalagandula P Sharma and S Banerjee (2011) DEVOFLOW: Scaling flow management for highperformance networks ACM SIGCOMM Computer Communication Review vol. 41

no. 4 Pages. 254–265

De Couto D Aguayo J Bicket and R Morris (2005) A high-throughput path metric for multi-hop wireless routing *Wireless Networks* vol. 11 no 4 Pages 419–434 2005.

Detti C Pisa S Salsano and N Blefari-Melazzi (2013) Wireless mesh software defined networks (WMSDN) in *IEEE 9th International Conf on Wireless and Mobile Computing, Networking and Communications (WiMob)* Pages. 89–95.

Hans G Quer and R R Rao (2017) Wireless SDN mobile ad hoc network: From theory to practice in *IEEE ICC* Pages 1–7.

HassasYeganeh and Y Ganjali (2012) KANDOO: A framework for efficient and scalable offloading of control applications in *ACM 1st Workshop on Hot Topics in Software Defined Networks* Pages. 19– 24.

Huang P Li S Guo and W Zhuang (2015) Software-defined wireless mesh networks: Architecture and traffic orchestration *IEEE Network* vol. 29 no. 4 Pages 24–30.

Karbaschi and A Fladenmuller (2005) A link-quality and congestion-aware cross layer metric for multi-hop wireless routing in *IEEE International Conf on Mobile Adhoc and Sensor Systems 2005* Pages 7–11.

Koponen M Casado N Gude et al. (2010) ONIX: A distributed control platform for large-scale production networks in *OSDI* vol. 10 Pages 1–6.

Labraoui M Boc and A Fladenmuller (2017) Self-configuration mechanisms for SDN deployment in

wireless mesh networks in *IEEE 18th International Symp. World of Wireless Mobile and Multimedia Networks (WoWMoM)* Pages. 1–4.

Li, P Djukic and H Zhang (2014) Zoning for hierarchical network optimization in software defined networks in *IEEE Network Operations and Management Symposium (NOMS)* Pages 1–8.

Lindhorst G. Lukas E Nett and M Mock (2010) Data-mining-based link failure detection for wireless mesh networks in *29th IEEE Symp. Reliable Distributed Systems* Pages 353–357.

Peng L Guo Q Deng Z Ning and L Zhang (2015) A novel hybrid routing forwarding algorithm in SDN enabled wireless mesh networks in *IEEE High Performance Computing and Communications (HPCC)* Pages 1806–1811.

Rasley B Stephens C Dixon E Rozner W Felter K Agarwal J Carter and R Fonseca (2014) PLANCK: Millisecond-scale monitoring and control for commodity networks in *ACM SIGCOMM Computer Communication Review* vol 44 no 4 Pages. 407–418.

Salsano G Siracusano A Detti, C Pisa P L Ventre, and N Blefari Melazzi (2014) Controller selection in a wireless mesh SDN under network partitioning and merging scenarios, *arXiv preprint arXiv:1406.2470*.

Yang Y Li D Jin L Zeng X Wu and A V Vasilakos (2015) Software defined and virtualized future mobile and wireless networks: A survey *Mobile Networks and Applications* vol 20, no 1, Pages 4–18.

Design of Tetra-band Antenna using Complementary Split Ring Resonator

V. Ravichandran¹, M. Suresh², T. Shankar³ and A. Nazar Ali⁴

¹Professor, ^{2,3}Assistant Professor, ⁴Associate Professor

¹Department of ECE, Rover Engineering College, Preambalur, Tamilnadu, India

²Department of ECE, School of communication and computer sciences, Kongu engineering college, Erode, Tamilnadu, India

³Department of ECE, Government College of Engineering, Srirangam, Tamilnadu, India

⁴Department of EEE, Rajalakshmi Engineering College, Chennai, Tamilnadu, India

ABSTRACT

In this paper, a microstrip feed metamaterial inspired antenna for multiband operation is presented. The antenna is fabricated on as substrate of total size 40 x 40 x 1.6 mm³. The projected antenna design is printed on a FR4 substrate which has 4.4 and 0.02 as its relative permittivity value and loss tangent value respectively. In this antenna the circular radiating element is designed and feed with 50-ohm microstrip line to operate at 4.8 GHz. Then, the Complement Split Ring Resonator (CSRR) is introduced in the circular radiating element in order to make the proposed antenna in to multiband resonating antenna. The proposed structure without the CSRR has single resonating frequency at 4.8GHz with operating band from 4 GHz to 4.9 GHz. And after the introduction of CSRR the same antenna is resonating at four bands with resonant frequency at 2.70 GHz, 4.81 GHz, 7.79 GHz and 13.69 GHz. The entire structure is simulated with the assistance of CST studio electromagnetic simulator. The simulated result of return loss, VSWR, 3D radiation pattern, gain, directivity, E plane and H plane radiation pattern are presented. The results clearly illustrate the projected antenna is the best choice for the L band, C band and Ku band applications.

KEY WORDS: MICROSTRIP, METAMATERIAL, CSRR, FR4, CIRCULAR PATCH.

INTRODUCTION

In modern wireless world, the requirement of communication with high data rate and reliability becomes inevitable. The above requirement can be fulfilled with

the antenna with high gain and directivity. The planar antenna are the ideal choice for the modern wireless communication devices. The modern communication devices major requirement is the reduced size and high performance. Because of the reduced size the space for the circuits and antenna available in the devices will be very small, which leads to the need of miniaturized circuits and devices. Such requirement can be fully filled with the help of planar antennas. Metamaterials (Christoph et al., 2006) are the artificial man-made structures that can enhance the EM properties of the antenna. The metamaterial has negative permittivity and permeability because of its structure and not based on its

ARTICLE INFORMATION

*Corresponding Author: raciecev@gmail.com

Received 15th April 2020 Accepted after revision 20th May 2020

Print ISSN: 0974-6455 Online ISSN: 2321-4007 CODEN: BBRCBA

Thomson Reuters ISI Web of Science Clarivate Analytics USA and Crossref Indexed Journal



NAAS Journal Score 2020 (4.31) SJIF: 2020 (7.728)

A Society of Science and Nature Publication,
Bhopal India 2020. All rights reserved.

Online Contents Available at: <http://www.bbrc.in/>

constituents. There are variety of structure are available in the literature which act as metamaterial such as SRR (Prasad et al., 2017), CSRR (Prasad et al., 2017; Prasad et al., 2019; Prasad et al., 2019), S shaped, 8 shaped and omega shaped resonator (Kavitha et al., 2020; Shanthi et al., 2019; Suvadeep et al., 2017; Boopathi et al., 2017; Choi et al., 2009). This resonator shapes can either be printed on a substrates parasitic element or etched from the patch or ground. Both the metamaterial structure and its complementary have same effect in enhancing the EM properties.

In this paper the metamaterial inspired circular printed microstrip patch antenna is proposed for tetra- frequency band application. The entire structure is designed on the substrate made up of FR4 and its height is of 1.6mm. The circular radiating patch of radius 14mm is printed on front of the substrate and on back of the substrate the full ground structure is presented.

MATERIALS AND METHODS

Design of Circular antenna for Tetra-band operating frequency: The projected antenna has two stages of evolution. In the first stage a simple circular patch of radius 14 mm is printed on a substrate made up of FR4 with 1.6 mm height and the size of the substrate is 40 x 40 mm². The entire structure is provided with full ground at the back side of the substrate. The 50-ohm microstrip line feed is used to give the feed for the proposed antenna. The structure of the proposed antenna along with its parameter is presented in figure 1 and the parameter values are presented in Table 1. In figure 2 the picture of the proposed antenna designed in CST studio is given.

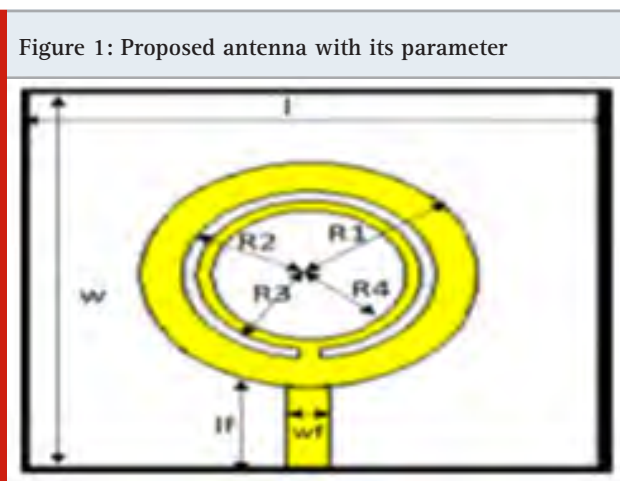
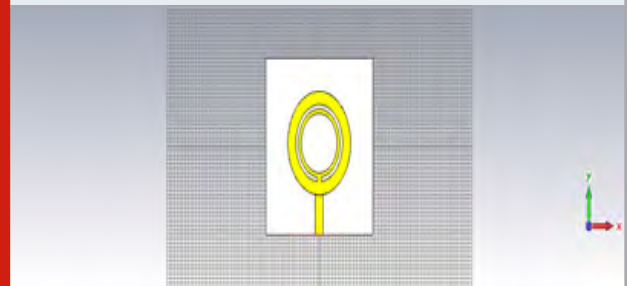


Figure 1: Proposed antenna with its parameter

Table 1. Parameter Value

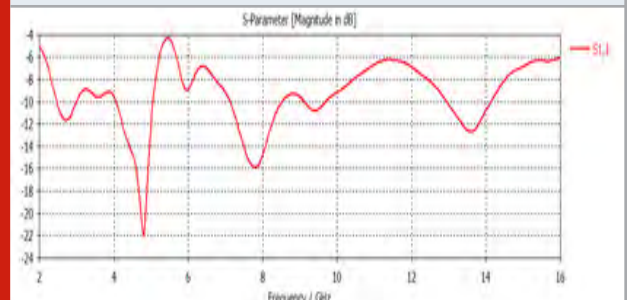
l	w	If	wf	R1
40	40	5	14	14
R2	R3	R4	t	h
13	12.5	12	0.035	1.6

Figure 2: Proposed antenna in CST design studio



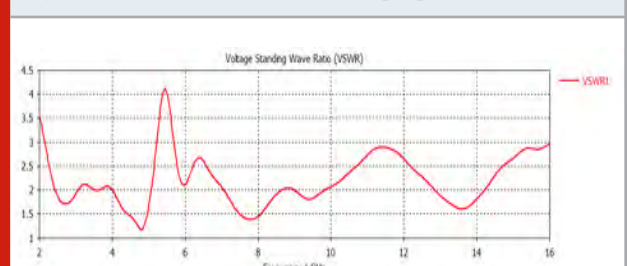
The initial design is simple circular patch feed with 50-ohm microstrip line is capable to operate in the frequency band of 4 GHz to 4.9 GHz with the resonant frequency at 4.78 GHz. Then in order to convert the single band circular patch antenna in to multiband antenna. CSRR is etched in the circular patch. The radius of the circular CSRR is 13mm with the thinness as 1mm. the projected structure with CSRR is operating at 4 band with resonant frequency at 2.70 GHz,4.81 GHz,7.79 GHz and 13.69 GHz which covers the L band, C band and Ku band

Figure 3: s11 (return loss) plot of circular tetra band antenna



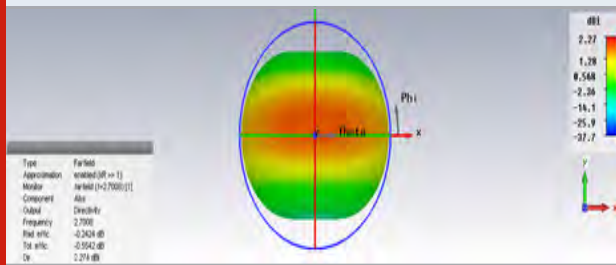
The band with resonance at 2.70 GHz is operating from 2.5 GHz to 2.8 GHz, the band at 4.81GHz is operating from 4 GHz to 4.9 GHz, the band at 7.79 GHz is operating from 7 GHz to 8.3 GHz and finally the 13.61GHz is operating from 12.86GHz to 14.12 GHz. In Figure 3, the return loss plot of the projected antenna is presented, the figure 3 obviously shows that the projected structure is operating in four frequency bands. And in figure 4 the Voltage Standing Wave Ratio (VSWR) plot of the projected antenna is presented which clearly depicts that the VSWR value is less than 2 in all the frequency of operation.

Figure 4: VSWR characteristics of proposed antenna



RESULT AND DISCUSSION

Figure 5: 3 dimensional radiation pattern at 2.70 GHz



In figure 5, the 3 radiation pattern of the proposed antenna at 2.70 GHz is presented. The figure clearly depicted that the radiation is in sheer direction to the proposed antenna. In figure 6, the radiation patten of the antenna is presented which has an omni direction and 8 shaped radiation patten in the E & H - plane radiation patten respectively. The surface current of the proposed antenna at 2.70GHz is presented in figure 7, which clearly depicts that the current maximally concentrated more in the outer copper ring and therefore we can observe that the outer copper ring is responsible for the 2.70 GHz resonating band.

Figure 6: E & H plane pattern at 2.70 GHz

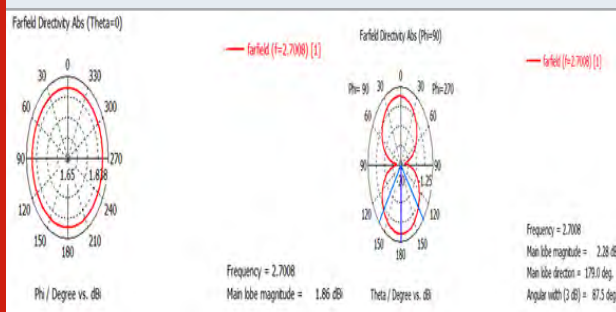
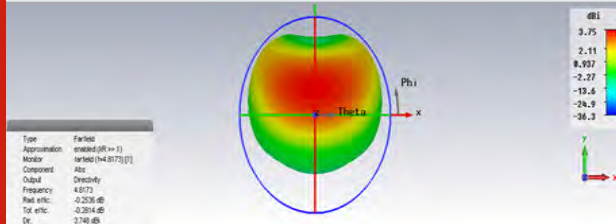


Figure 7: 2.70 GHz Surface current



Figure 8: 3D pattern at 4.81 GHz Figure



In figure 8, the 3-dimensional pattern of the proposed antenna at 4.81 GHz is presented. The figure clearly depicted that the radiation is in vertical direction to the proposed antenna. In figure 9, the radiation patten of the antenna is presented which has an omni direction and 8 shaped radiation patten in the E and H plane radiation patten respectively. The surface current of the proposed antenna at 4.81 GHz is presented in figure 10, which clearly depicts that the current is maximally concentrated more in the outer copper ring and therefore we can observe that the outer copper ring is responsible for the 4.81 GHz resonating band.

Figure 9: E & H plane pattern at 4.81 GHz

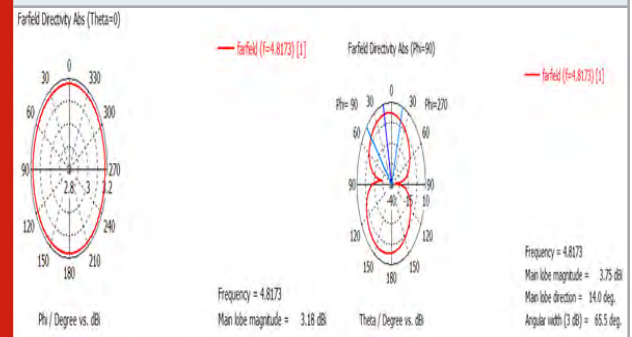


Figure 10: Surface current at 4.81 GHz

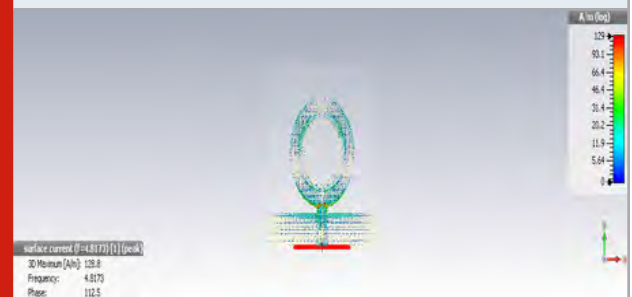
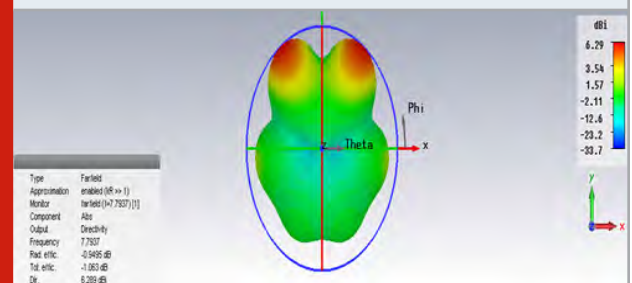


Figure 11: 3 dimensional pattern at 7.79 GHz Figure



In figure 11, the 3- dimensional pattern of the proposed antenna at 7.79 GHz is presented. The figure clearly depicted that the radiation is in parallel direction to the proposed antenna. In figure 12, the radiation patten of the antenna is presented which has an omni direction and 8 shaped radiation patten in the E & H plane radiation patten respectively. The surface current of the proposed antenna at 7.79 GHz is presented in figure 13, which clearly depicts that the current is maximally

concentrated more in the outer copper ring as well as the CSRR and therefore we can observe that the CSRR is responsible for the 7.79 GHz resonating band.

Figure 12: E & H plane radiation pattern at 7.79 GHz

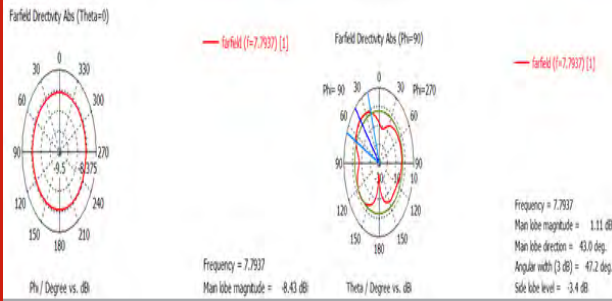
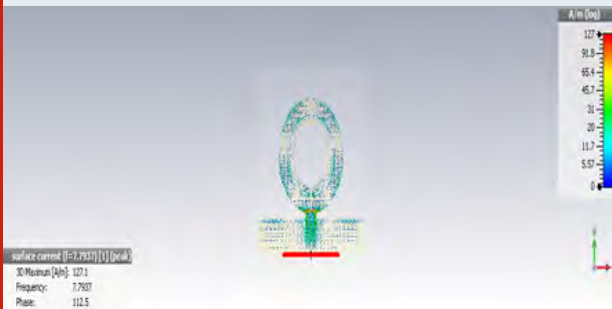


Figure 13: Surface current at 7.79 GHz



In figure 14, the 3-dimensional radiation pattern of the proposed antenna at 13.61 GHz is presented. The figure clearly depicted that the radiation is in parallel direction to the proposed antenna axis. In figure 15, the radiation patten of the antenna is presented which has an omni direction and 8 shaped radiation patten in the E & H plane radiation patten respectively. The surface current of the proposed antenna at 13.61 GHz is presented in figure 16, which obviously portrays that the current is focused more in the outer copper ring as well as the CSRR and therefore we can observe that the CSRR is responsible for the 13.61 GHz resonating band.

Figure 14: 3dimesional pattern at 13.61 GHz

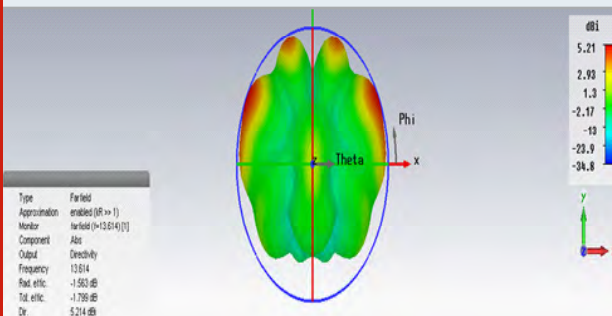


Figure 15: E & H plane radiation pattern at 13.61 GHz

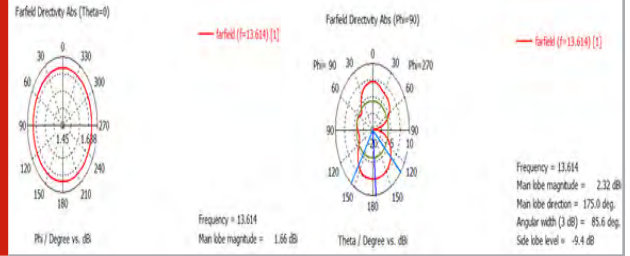


Figure 16: Surface current at 13.61 GHz

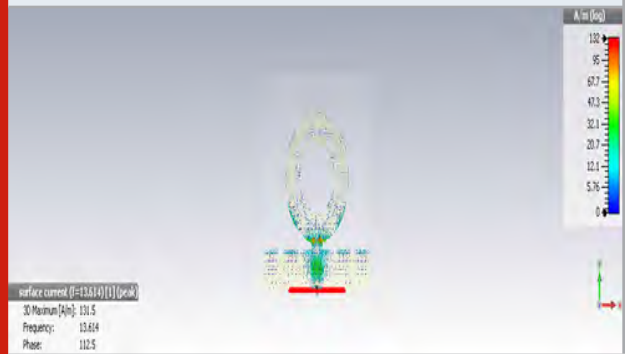
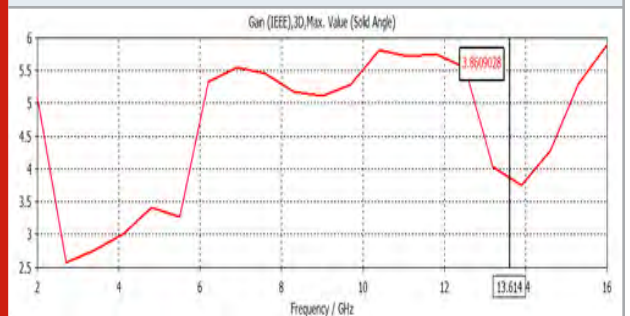
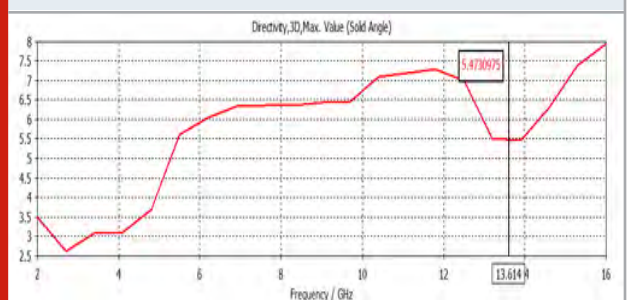


Figure 17: Gain vs Frequency plot



In figure 17 the gain of the projected antenna is presented which clearly depicts that the projected antenna able to achieve a positive gain over the whole frequency band of operation and the gain with maximum value of 5.87dBi. In figure 18, the directivity is plotted with respect to the frequency and it determined directivity of the projected antenna is about 7.3dBi

Figure 18: Directivity vs Frequency plot



CONCLUSION

In this paper, a microstrip feed metamaterial inspired antenna for multiband operation is presented. The entire dimensions of the projection is $40 \times 40 \times 1.6 \text{ mm}^3$. The initial design is simple circular patch feed with 50-ohm microstrip line is capable to operate in the frequency band of 4 GHz to 4.9 GHz with the resonant frequency at 4.78 GHz. Then in order to convert the single band circular patch antenna in to multiband antenna. CSRR is etched in the circular patch. The radius of the CSRR is 13mm with the thickness as 1mm. the proposed structure with CSRR is operating at 4 band with resonant frequency at 2.70 GHz, 4.81 GHz, 7.79 GHz and 13.69 GHz which are in the L band, C band and Ku band. The presented results which clearly proves that the proposed antenna is exhibiting multiple operating frequency because of the CSRR and it also proves that the projected structure is right choice for the wireless application.

REFERENCE

- Boopathi Rani and SK Pandey (2017) A CPW-fed circular patch antenna inspired by reduced ground plane and CSRR slot for UWB applications with notch band Microw Opt Technol Lett 59:Pages 745-749
- Choi ST Hamaguchi K KohnoR (2009) Small printed CPW-fed triangular monopole antenna for ultra-wideband applications Microw Opt Technol Lett;51 Pages 1180-1182
- Christophe Caloz Tatsuo Itoh 2006 Electromagnetic metamaterials: Transmission line theory and microwave applications New York: John Wiley & Sons Inc;
- Kavitha SPrasad Jones Christydass JSilamboli (2020) Metamaterial Inspired Triple Band Antenna for Wireless Communication International Journal of Scientific & Technology Research volume 9 issue 3.
- Prasad Jones Christydass and N Gunavathi (2017) Codirectional CSRR inspired printed antenna for locomotive short range radar International Conference on Inventive Computing and Informatics (ICICI) coimbatore India December 4-5
- Prasad Jones Christydass and N Gunavathi (2017) Design of CSRR loaded multiband slotted rectangular patch antenna IEEE Applied Electromagnetics Conference (AEMC) aurangabad india January 2-5
- Prasad Jones Christydass and Pranit Jeba Samuel (2019) Metamaterial Inspired Slotted Rectangular Patch Antenna for Multiband Operation Biosc Biotech Res Comm Special Issue Vol 12 No(6) Pages 57-62
- Prasad Jones Christydass and Manjunathan(2019) Pentagonal Ring Slot Antenna with SRR for Tri-Band Operation Biosc Biotech Res Comm Special Issue Vol 12 No(6) Pages 26-32
- Shanthi Dr T Jayasankar Prasad Jones Christydass Dr P Maheswara Venkatesh (2019) Wearable Textile Antenna For Gps Application International journal of scientific & technology research volume 8.
- Suvadeep Choudhury and Akhilesh Mohan (2017) Miniaturized sierpinski fractal loaded QMSIW antenna with CSRR in ground plane for WLAN applications Microw Opt Technol Lett 59 Pages 1291-1265

ANN Based MPPT Controller for PEMFC System with Interleaved Resonant PWM High Step up Converter

B.Karthikeyan^{1*}, R. Ramkumar², L. Nagarajan³, A. Anton Amala Praveen⁴ and S. Vijayalakshmi⁵

^{1,2,3,4,5}Assistant Professor, Department of EEE, K. Ramakrishnan College of Technology, Trichy-621112, India.

ABSTRACT

Fossil fuel contributed a major share to energy economy for a last few decades. They are vulnerable due to carbon emission and they will extinct in near future, the people are looking forward to use renewable energy sources for stationary application and transportation. The government also encourages the people to use non-conventional energy resources by providing subsidy for utilizing renewable energy and exempting the tax for renewable energy powered appliances. To promote the purchase of electric vehicles, the Indian government has exempted recently the income tax worth 1.5 lakhs for buying electric vehicles. Hence it is the right time for researchers to give further scope for the fuel cell powered electric vehicles. The alternative sources for the automobile making industry are fuel cell, solar energy, ultra capacitor etc. Among these sources fuel cell is the most attractive because it is 2.5 times efficient than IC engine. Hence PEMFC is taken as input source whose output voltage is not enough to power electrical vehicle motor. An interleaved resonant PWM high step up converter is used to boost the voltage. ANN based MPPT controller is implemented to ensure getting optimum power considering dynamic temperature condition using MATLAB/Simulink Platform.

KEY WORDS: RESONANT PWM, DC-DC CONVERTER, MPPT, PEMFC , ANN

INTRODUCTION

Fossil fuel causes carbon emission, environmental degradation, air pollution etc. In order to overcome these problems, it is necessary to use ecofriendly energy that should not harm the environment. Among the renewable energy resources, fuel cell technology plays a vital role in powering auto mobiles. Because its features like pollution free, noiseless, quick start up, moderate operating

temperature, harmless by-product. The output power of fuel cell depends on various factors like operating temperature, atmospheric pressure, membrane, type of electrode used. Hence it is obvious that the output power will not remain constant if any one of the parameter is varied. In order to extract the maximum power during parameter variation, a number of MPPT algorithms were proposed in the literature.

MATERIALS AND METHODS

(Jyotheeswara et al., 2018) proposed RBFN based MPPT controller for grid-connected PEMFC system with high step-up three-phase IBC. The proposed MPPT controller was analyzed for both standalone system and grid connected system in MATLAB/Simulink platform. The proposed controller was able to inject active and reactive

ARTICLE INFORMATION

*Corresponding Author: karthikeyankrct@gmail.com
Received 15th April 2020 Accepted after revision 20th May 2020
Print ISSN: 0974-6455 Online ISSN: 2321-4007 CODEN: BBRBCA

Thomson Reuters ISI Web of Science Clarivate Analytics USA and Crossref Indexed Journal



NAAS Journal Score 2020 (4.31) SJIF: 2020 (7.728)
A Society of Science and Nature Publication,
Bhopal India 2020. All rights reserved.
Online Contents Available at: <http://www.bbrc.in/>

power during sudden variation of load and dynamic temperature. (Jyotheeswara et al., 2018) proposed ANFIS-MPPT control algorithm for a PEMFC system used in electric vehicle applications. They analyzed the proposed controller by using MATLAB/Simulink platform and prototype hardware. The result of the proposed controller was compared with FLC and the result was evident that their controller was able to extract 1.95% more power than former FLC. (Harrag et al., 2019) A Novel Single Sensor Variable Step Size Maximum Power Point Tracking for Proton Exchange Membrane Fuel Cell Power System. In my point of view, their work was a big mile stone in the fuel cell technology era. Because they were able to prove that a single sensor based controller outperforms the two sensor based controller considering both static and dynamic performance. The proposed technique increased the fuel cell life time by reducing the frequent trip and fuel cell efficiency. (Ahmadi et al., 2017).

Maximum power point tracking of a proton exchange membrane fuel cell system using PSO-PID controller. They were taken operating temperature, membrane water as content as dynamic parameters. Their study confirmed that PSO algorithm can track maximum power from fuel cell with high accuracy, good time response and very power fluctuation. (Abdelghani et al., 2017) proposed How fuzzy logic can improve PEM fuel cell MPPT performances? They compared simulation of conventional step size IC, variable step size IC, fuzzy auto scaled variable step size IC and proposed variable step size fuzzy based MPPT controller in MATLAB/Simulink platform. Their proposed variable step size fuzzy based MPPT controller outperforms other three controllers in terms of response time, overshoot, and ripple reduction which increases life time of the fuel cell. (Harrag, et al., 2019) proposed Variable Step Size IC MPPT Controller for PEMFC Power System Improving Static and Dynamic Performances. The proposed variable step size IC MPPT controller performance was good in terms of response time, overshoot, ripple even in the variation of temperature and hydrogen pressure variation.

In this work Artificial Neural Network based MPPT algorithm is implemented. To validate the performance of MPPT controller, simulation work has been carried out using MATLAB /Simulink Platform. The results obtained from the implemented controller shows better performance than conventional PID controller and FLC controller.

RESULT AND DISCUSSION

Interleaved Resoant Pwm High Step Up Boost Converter

The above Figure represents Interleave Resonant PWM high step up converter in which resonant circuit is designed to achieve ZVS switching of active switches to reduce switching stress. The converted is operated under resonant condition in order to decrease active switch turn off current and duty loss.

Figure 1: Proposed Converter

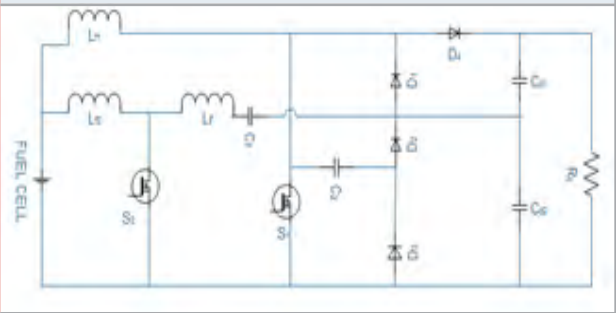


Figure 2: Key waveform of the proposed converter

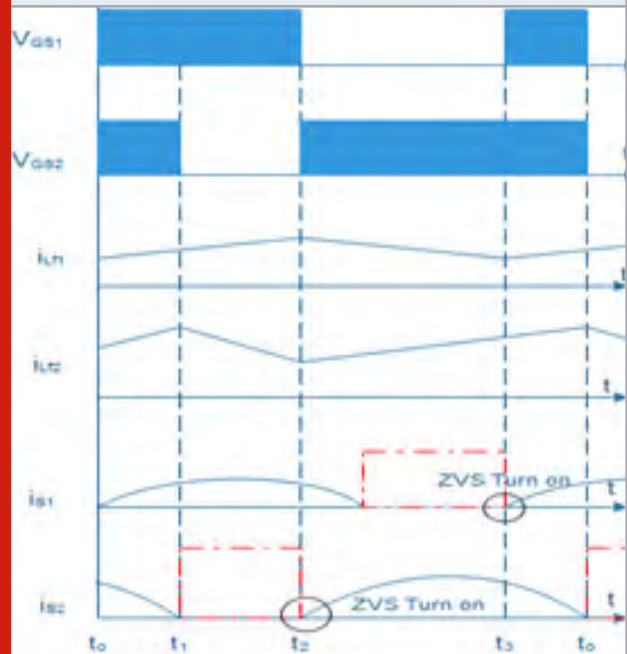


Table1. Performance Comparision

No of switches	2	2
No of Diodes	3	4
No of capacitors	3	5
No of windings	2	3
Voltage gain M	$\frac{2}{1-\alpha}$	$\frac{3}{1-\alpha}$
ZVS switching	NO	YES
Input ripple current	Low	Low
Voltage stress across the diode	$V_o/2$	$V_o/2$
Voltage stress across the switch	High	Lowest

Voltage Gain: The capacitor across C1 and C2 can be approximately written as

$$V_{Co1} = 0.5V_i + V_{L2} \tag{1}$$

$$V_{Co1} = 0.5V_i + \frac{1}{1-d_2} V_i = \frac{0.5}{1-d_2} V_i \tag{2}$$

$$V_{Co2} = 0.5V_i + V_{L1} \tag{3}$$

$$V_{Co1} = 0.5V_i + \frac{1}{1-d_1} V_i = \frac{0.5}{1-d_1} V_i \tag{4}$$

$$V_{O1} = V_i + V_{L1} + V_{Co1} \tag{5}$$

$$V_{O1} = V_i + \frac{d_1}{1-d_1} + \frac{0.5}{1-d_2} V_i \tag{6}$$

$$V_{O1} = V_i + V_{L2} + V_{Co2} \tag{7}$$

$$V_{O2} = V_i + \frac{d_2}{1-d_2} + \frac{0.5}{1-d_1} V_i \tag{8}$$

From the equation (7) and (8),

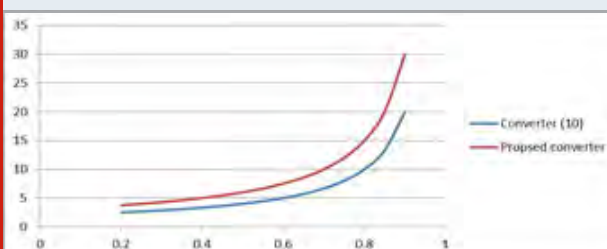
$$V_{O1} = V_{O2} = \frac{1.5}{1-d} V_i \tag{9}$$

$$V_{Out} = V_{O1} + V_{O2} \tag{10}$$

$$M = \frac{3}{1-d} \tag{11}$$

From the above equation (11), it is inferred that the voltage gain of the proposed converter is better than converter cited in article 10. The performance comparison is made and it is listed in the table 1. The voltage gain graph is also shown in figure 3.

Figure 3: Duty cycle with voltage gain.



Simulation Results of Ann Based Mppt Controller

Figure 4: Output voltage across the load

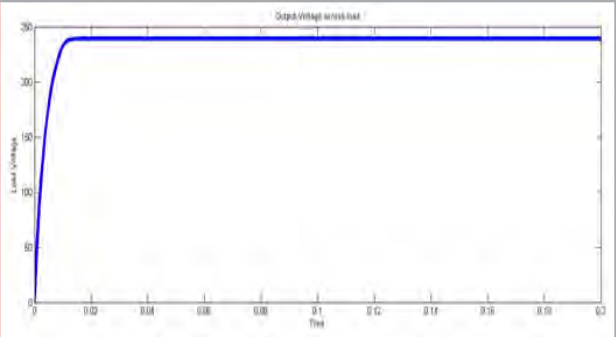


Figure 5: ZVS turn on switches S1 and S2

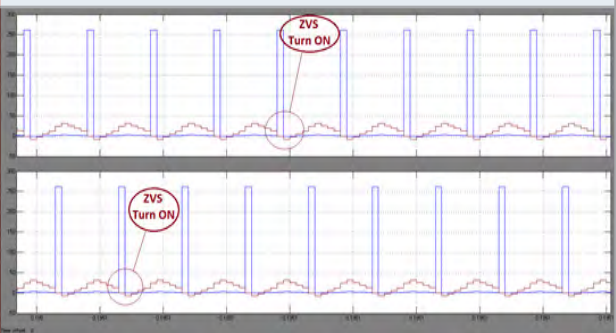


Figure 6: Temperature Variation

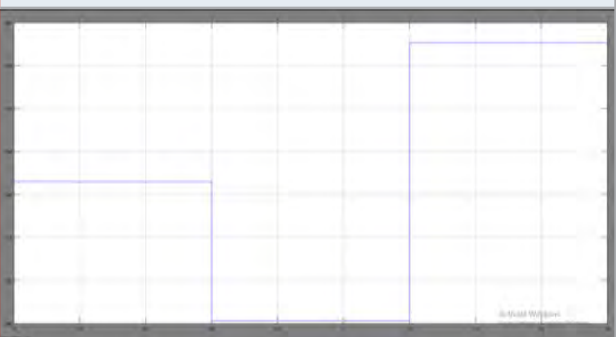


Figure 7: Ouput voltage

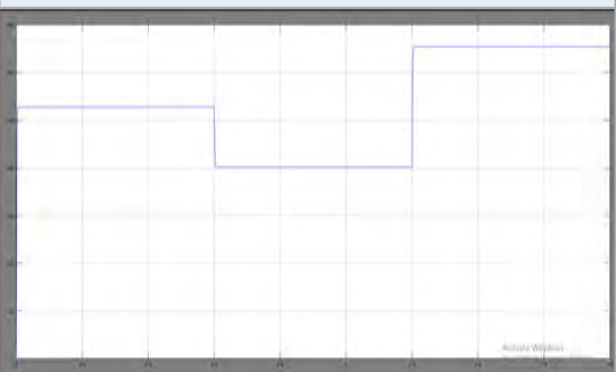


Figure 8: Output current

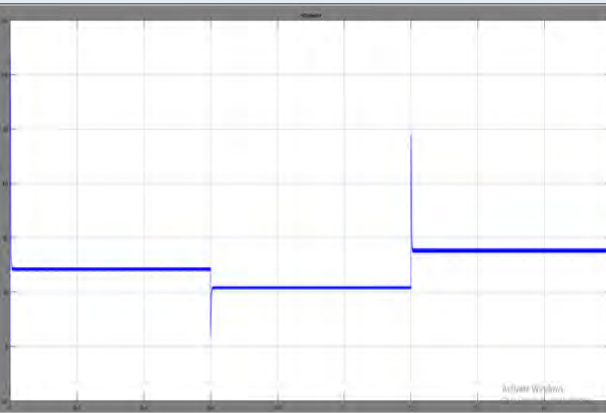
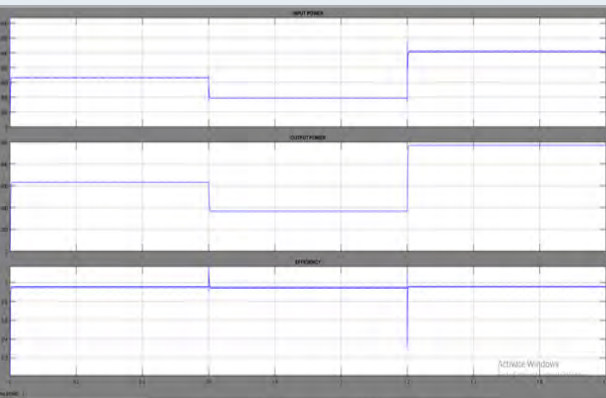


Figure 9: Input power, Output power and efficiency



CONCLUSION

In this article an interleaved Resonant PWM high step up converter performance was analyzed and compared with conventional converter. In order to achieve Zero Voltage Switching, (ZVS) Resonant circuit was designed and ensured to operate under resonant condition. ANN based MPPT controller was implemented to switch the

active switches during dynamic temperature condition using MATLAB/Simulink Platform. The proposed controller extract maximum power during temperature variation condition without affecting efficiency. The future work is to implement the prototype model to validate the result.

REFERENCE

- Abdelghani Harrag and Sabir Messalti (2017)How fuzzy logic can improve PEM fuel cell MPPT performances international journal of hydrogen energy.
- Ahmadi S et al (2017) Maximum power point tracking of a proton exchange membrane fuel cell system using PSO-PID controller international journal of hydrogen energy.
- Harrag,A, S Messalti (2017)Variable Step Size IC MPPT Controller for PEMFC Power System Improving Static and Dynamic Performances FUEL CELLS.
- Harrag,A, H Bahri (2019) A Novel Single Sensor Variable Step Size Maximum Power Point Tracking for Proton Exchange Membrane Fuel Cell Power System FUEL CELLS.
- Jyotheeswara Reddy K N Sudhakar (2018) ANFIS-MPPT control algorithm for a PEMFC system used in electric vehicle applications international journal of hydrogen energy.
- Jyotheeswara Reddy K N Sudhakar (2018) A new RBFN based MPPT controller for grid-connected PEMFC system with high step-up three-phase IBC international journal of hydrogen energy.
- Lakshmi M et al (2018) Non isolated High Gain DC DC Converter for DC Micro grids IEEE transactions on Industrial Electronics Vol 65 No 2 .
- Penghui Ma et al (2019) Interleaved High Step-Up Boost Converter Journal of Power Electronics Vol 19, No 3 pp 665 675.
- Yohan Park et al (2012) Non isolated ZVZCS Resonant PWM DC DC Converter for High Step Up and High Power Applications IEEE Transactions on Power Electronics Vol 27 No 8.

Implementation of High Efficient Single Input Triple output DC-DC Converter

Dr.A. Rajkumar¹, R. Jai Ganesh², V. Suresh Kumar³, T. Vishnu Kumar⁴ and T. Ram Kumar⁵

¹Associate professor, ^{2,3,4,5}Assistant professor

^{1,2,3,4,5}Department of Electrical and Electronics Engineering, K. Ramakrishnan College of Technology, Tiruchirappalli, Tamilnadu, India

ABSTRACT

This study mainly talks a highly efficient one input three-way outputs DC-DC converter with a with two directional current flow and soft switching actions for the high-efficiency power transformation. In wide-ranging the several output voltages require only single input which can be the applications of renewable energy resources such as solar, fuel cell or E- Vehicles. This proposed system has a high voltage transformation to maintain the high voltage dc bus for the employment of DC-AC inverter. This planned system uses a combined inductor with the interleaved topology to obtain the maximum output voltage and to regulate the voltage of the secondary output port incidentally. In addition, the usage of soft switching techniques the proposed system can able to achieve the high efficient power transformation and three output stages as expected. Moreover, the results of the system has been planned to verify by MATLAB simulation and experimental setup.

KEY WORDS: COUPLED INDUCTOR, MATLAB SIMULATION, RENEWABLE ENERGY SOURCES, SINGLE INPUT THREE OUTPUT DC-DC CONVERTER, SOFT SWITCHING.

INTRODUCTION

Several output DC-DC converters have involved an excessive contract of research attention newly, which might be capable to the increasing claim of renewable energy, micro grids, power electronics systems. In associated to discrete DC-DC converters, more port DC-DC converters suggest a dense structure with a slighter cost and less part counts. At additional voltages, switches

voltage tension is a for hemostats for many port DC-DC converters. The reason for that are the troubles such as the cost and the unreachability of high voltage switches, which be able to also have an undesirable outcome on absolute efficiency due to their high forward voltage droplet and ON-state struggle. In addition, the delegate semiconductors used in high voltage claims are IGCT and high power IGBT. Which are not straight outcome for many port DC-DC converters, (A.Rajkumar et al., 2014) owing to the real high converting losses of those changes, their exchange frequency is almost in ad equate to about 1 KHz; as a result, the scope of the inactive components will rise extremely. This knowledge sharp at devious a high-efficiency many port DC-DC converters with dense voltage damage crosswise semiconductor devices and slight inactive components scope. (AT Sankara Subramanian et al., 2017) (A.Nazar Ali et al., 2014).

ARTICLE INFORMATION

*Corresponding Author: rajkumara.eee@krct.ac.in
Received 15th April 2020 Accepted after revision 20th May 2020
Print ISSN: 0974-6455 Online ISSN: 2321-4007 CODEN: BBRCBA

Thomson Reuters ISI Web of Science Clarivate Analytics USA and Crossref Indexed Journal



NAAS Journal Score 2020 (4.31) SJIF: 2020 (7.728)
A Society of Science and Nature Publication,
Bhopal India 2020. All rights reserved.
Online Contents Available at: <http://www.bbrc.in/>

Several outputs DC-DC converters (A.Rajkumar et al., 2015) have been generally used in several submissions, such as combination electric cars, space crafts, ups, and so on. By deal with the difficulty of worldwide warming, fresh drives, such as wind energy, photovoltaic, and, fuel cell etc., have been rapidly expectant. For the growth of the worldwide environmental difficulty and lack of common energy, the development of electric automobiles with renewable drive as a spare for the fossil-fuel automobile has quickly established. The coupled– converters have been studied in the current years in order to achieve high voltage-claims with a low power base. High-converter condition with high-power adaptation, lower efficiency and lower industrial price has risen in the preceding period.

While a 1000W research model was intended for a grid-connected photovoltaic network with a lower input current ripple, it unconditionally increased the industrial price and circuit efficiency by two combined inductors. The consistent condenser with a specific voltage assessment was nominated to validate the safety actions in meanness of an ultra-step-up converter for the high-efficiency claim in.

Although the swapped capacitors in were used to find a minor and lightweight converter, a large quantity of diodes and capacitors in this circuit remained mandatory. In addition, a high performance single-input multi-output converter with the zero-current switching (ZCS) stuff was obtainable. While the use of soft switching methods was developed to minimize switching losses, the option of advanced turn percentages in a current-fed converter could form higher joined losses and leaks.(B. Wanget al., 2016) In addition, the predictable inductor-based enhancement converters for large voltage-ratio submissions are unsatisfactory for staging up the source of input voltage because of significant switching losses and high voltages through power switches. Power switches with small turn-on devices are mandatory as a result to reduce transmission losses and voltage strains. In addition, a great step-up DC-DC converter (C.Kalavalli et al. 2020) was designed for renewable energy claims with the high-efficiency power transmission stuff and varied working range. A hybrid two-output converter with synchronous controls was designed to help reduce transmission losses.

Major intention of the proposed systems is

- To concentrated voltage strain on controls and diodes,
- To concentrated inactive modules size
- To better effectiveness

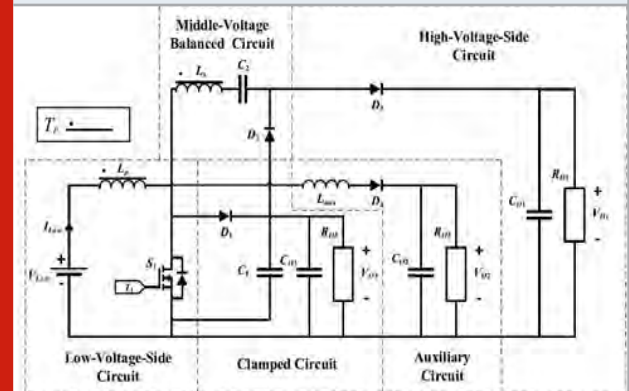
MATERIAL AND METHODS

Proposed System

A. Principle of Operation of Proposed System: The figure 1 shows the high effective one input triple-output DC - DC converter by detailed system configuration. The expression for the proposed converter is listed from the figure 1 i) Small voltage side path ii) Clamped path iii)

Supporting path. Switch S1 represent Low voltage switch, LP is winding for primary side of couple inductor Tr which is fed from the V low i.e., low voltage terminal in input side. The energy from subordinate side winding L of joined inductor Tr is released based on switch on the low voltage switch S. Clamped diode D1, Clamped Capacitor C1, Middle voltage output terminal Vo3, filter capacitor Co3 is composed from clamped circuit. The clamped circuit mostly engages the stored energy in Lk (Main side outflow inductors) which protects the S1 (low voltage switch) that discharge energy to C2 (Central voltage capacitor) and output station of middle of the voltage (Vo3). In addition, stable path has C2 (central voltage capacitor), Central voltage stable diode (D2) and coupled inductor (Tr) along the secondary side winding (Ls). This process mainly absorbs energy in C1 (Clamped circuit) and Co3 (filter capacitor) to boost the conversion process to high dc bus terminal (Vo1). Moreover, at the high voltage side has more voltage on D3 (high voltage diode), Co1, and Vo1. It primarily discharging energy to high dc terminal Vo1 through D3. (J. Reinert et al., 2001)

Figure 1: High efficient single input triple output DC-DC converter



Also, the secondary circuit covers the Laux (secondary inductor), D4 (secondary diode), CO2 (secondary basis filter capacitor), and VO2 (secondary source output terminal). This setup can control the secondary source for secondary apparatus usage. The term VLow and ILow indicates the voltage and current of the input control source at the Low Voltage Source Converter. RO1, RO2, and RO3 direct the corresponding loads for the high-voltage dc bus terminal (VO1), the secondary source output terminal (VO2), and the central -voltage output terminal (VO3), correspondingly. T1 is the energetic signal for the low-voltage control (S1). The planned High Efficient One-Input Three-Output DC-DC Converter has three output ports with dissimilar voltage stages, and only one low-voltage input port. In this learning, the output terminals are distinct as the high-voltage dc bus (VO1), the secondary source (VO2), and the central voltage output terminal (VO3), correspondingly. In order to shorten the account for the output controls of the planned High Effective One-Input Three-Output DC-DC Converter, single output powers can be indicated as

$P_{O1} = V_{2O1} / R_{O1}$ for the high-voltage dc bus terminal, $P_{O2} = V_{2O2} / R_{O2}$ for the secondary source terminal, and $P_{O3} = V_{2O3} / R_{O3}$ for the central -voltage output terminal, correspondingly. Furthermore, the entire output power can be stated as

$$P_{O1} + P_{O2} + P_{O3} = P_{OT}. \quad (1)$$

The planned High Efficient One-Input Three-Output DC-DC Converter (M D Udayakumar et al., 2019) has binary important features for increasing input voltage and making dissimilar voltage stages. To shorten the mathematic sources, entirely of the voltages through a power control and diodes are discounted. (O. Ray et al., 2015) Moreover, it is expected that the compressed capacitor (C1) and the central-voltage capacitor (C2) are big sufficient to be considered as continuous voltage sources VC1 and VC2, correspondingly. For describing the working methods more clearly, the representative waveforms and the operation opinion of the planned High Efficient One-Input Three-Output DC-DC Converter. (P. Sabarish et al., 2019) The correspondent path of the joined inductor (Tr) are collected of the primary-side winding (Lp), the secondary-side winding (Ls), the primary-side attracting inductor (Lm), and the primary-side outflow inductor (Lk). By describing the turns relation (N) to be equivalent N_s/N_p and category the voltage of VLp then VLs across the windings Lp and Ls, the turns ratio (N) be able to denoted as

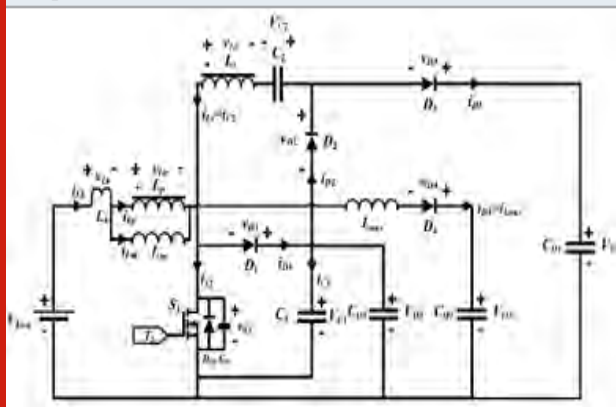
$$V_Ls/V_Lp = N \quad (2)$$

Furthermore, the connection factor of the coupled inductor (Tr) can be stated as

$$k = L_m / (L_k + L_m) \quad (3)$$

CS1 and DS1 are the fundamental capacitance and the body diode of the control switch. In direction to shorten academic examines, the control switch and diodes in the planned converter are reflected as model apparatuses.

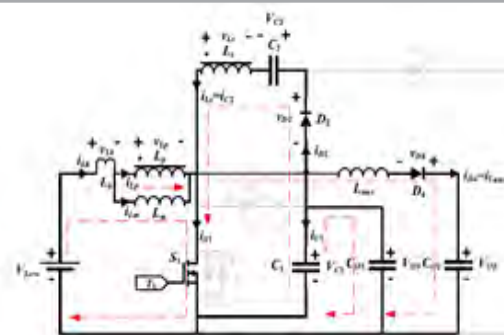
Figure 2: Equivalent circuit of high efficient 1- input 3- output DC-DC converter



The power flow forwards since the Small Voltage Side Converter to the High Voltage Side Converter, the supporting path, and the compressed path, correspondingly, then one labels the working methods via the correspondent circuit in Fig.2. The control (S1) is helped as the highest control and is measured for adaptable the voltages of the High Voltage Side Converter and the middle-voltage output terminal. Furthermore, the diodes (D1, D2, D3, and D4) are directed while the voltages of anodes are greater than the voltages of cathodes. The diodes (D2 and D3) are directed complementarily once the switch (S1) is twisted on-off. (R.-J. Wai et al., 2016)

Mode of Operation: Mode 1 [t0- t1]: At the start of this method, the low-voltage control (S1) is twisted on, and the high-voltage diode (D3) is upturned bias. The input current influences the primary-side attracting inductor (Lm) since the small voltage input source (VLow). The fractional energy of the LVSC transmissions to the subordinate side winding (Ls) through attractivelink; the energy kept in the clamped capacitor (C1) transfers to the middle-voltage capacitor (C2) through the middle-voltage balanced diode (D2), and the fractional drive of the compressed capacitor (C1) likewise issues to the central voltage output terminal (VO3) simultaneously. Furthermore, the energy stored in the supplementary inductor (Laux) still wants to issue energy aimed at charging the supplementary source uninterruptedly. While the current (iLaux) slowly declines to zero, this method ends. (P. Thirusenthil Kumaran et al., 2019)

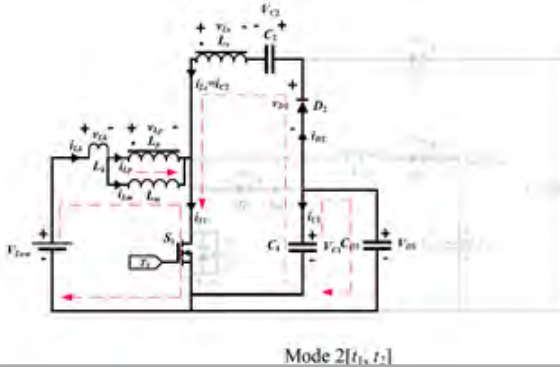
Figure 3: Operation principle of Mode 1



Mode 1 [t0, t1]

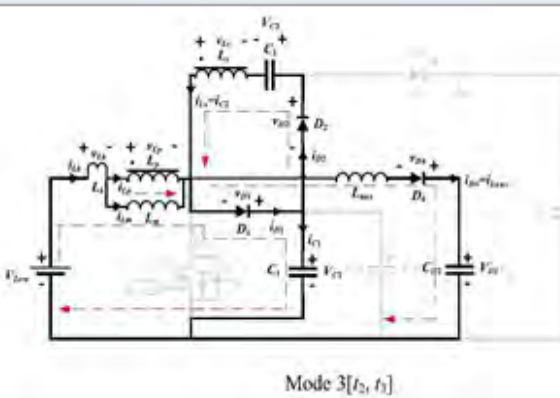
MODE 2 [T1- T2]: By period $t = t_1$, the current (iLaux) has fallen to nil at mode-2. Excepting for the pathway after the supplementary inductor to the supplementary source, extraprocess is like to the one at mode-1. The small voltage input source (VLow) attracts the main side attracting inductor (Lm) uninterruptedly, and the fractional energy of the LVSC still transfers to the subordinate side winding (Ls) through attractivelink. The central voltage stable diode (D2) is directed to convey energy hooked on the central voltage capacitor (C2). The energy kept in the compressed capacitor (C1) issues to the central voltage output terminal (VO3) uninterruptedly.

Figure 4: Operation principle of Mode 2



Mode 3 [t2- t3]: By period $t = t_2$, the short voltage switch (S1) is twisted off. The energy kept in the outflow inductor (L_k) still wants to issue energy, the current way cannot be altered immediately. By way of outcome, the compressed diode (D1) is conducted, and the equivalent energy is engrossed by the compressed capacitor (C1). The partial energy kept in the outflow inductor (L_k) is distributed to the auxiliary circuit for accusing the supplementary source (VO2) via the $L_{aux} - D_4 - V_{Low}$ pathway. The fractional energy kept in the minor side winding (L_s) still wants to issue energy to the central voltage capacitor (C2) via the D1-D2 path. While the minor side current (i_{Ls}) falls to nil and the central voltage stable diode (D2) is inverted bias, this method finishes.

Figure 5: Operation principle of Mode 3



Mode 4 [t3-t4]: By the opening of this method, the energy kept in the main side influencing inductor (L_m) by method of the flyback energy performance is shifted to the secondary side winding (L_s), and the high voltage diode (D3) is frontward bias to convey the energy to the hvsc via the $V_{Low} - L_p - L_s - C_2$ pathway. The outflow inductor (L_k) still wants to issue energy to the compressed capacitor (C1), the central voltage output terminal (VO3), and the secondary source (VO2) continuously.

Mode 5 [t4- t5]: By period $t = t_4$, the energy deposited in the outflow inductor (L_k) has fallen to nil, and the compressed diode (D1) is inverted preference since the voltage (V_{C1}) is developed than the voltage across the small voltage control (v_{S1}). The condition of the HVSC

is the similar as the one at method 4 for providing the energy to the great voltage dc bus (VO1) by the high voltage diode (D3). Furthermore, the small voltage input source (VLow) and the fractional energy of the main side magnetizing inductor (L_m) convey to the secondary source (VO2) over the secondary diode (D4).

Figure 6: Operation principle of Mode 4

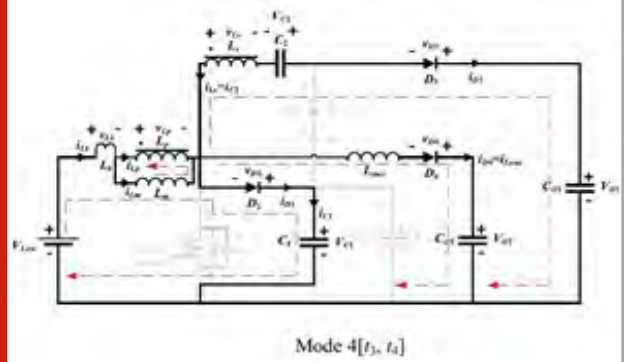
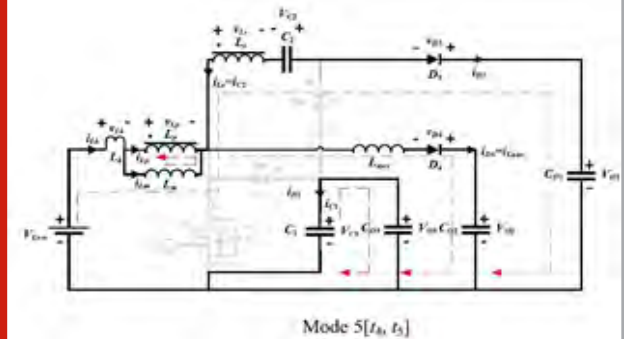


Figure 7: Operation principle of Mode 5



MODE 6 [T5-T6]: The small voltage control (S1) is twisted on by the opening of this system, and the energy held in the secondary inductor (L_{aux}) still wants the secondary diode (D4) to emit to the secondary source (VO2). The small voltage control (S1) is twisted on by the opening of this system, and the energy held in the secondary inductor (L_{aux}) still wants the secondary diode (D4) to emit to the secondary source (VO2). The current dominant angle of i_{Lk} is restricted in the outflow inductor (L_k), then the HVSC, the central voltage stable circuit, and the compressed circuit do not give any current. As a result, the small voltage control (S1) is twisted below the zero current swapping (ZCS) situation to increase the loss from the conversion. In addition, the current in the large voltage diode (i_{D3}) fails to zero, and the current direction of the subordinate side winding (i_{Ls}) variations to conduct the balanced diode (D2) with central voltage. In addition, the current in the large voltage diode (i_{D3}) fails to zero, and the current direction of the subordinate side winding (i_{Ls}) variations to conduct the balanced diode (D2) with central voltage.

Control and Changing Aspects of Proposed System:
A. Secure Loop Control Scheme: In this proposed work technique applied for control scheme is occupied

from the predictable 3 level buck and boost converters. However, due to the innovation of the SIDO TLC, a novel control strategy is essential. As before stated, the planned converter contains of 3 distinct cases.

Figure 8: Operation principle of Mode 6

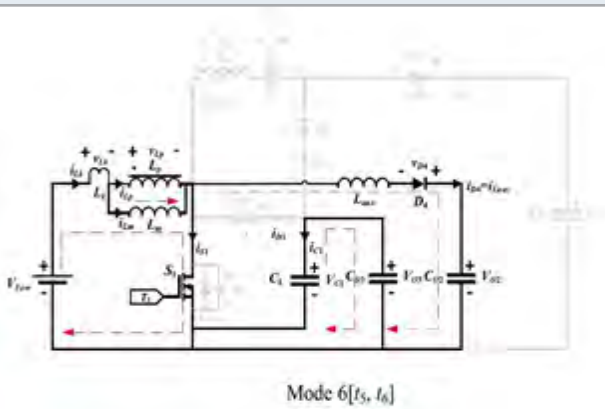
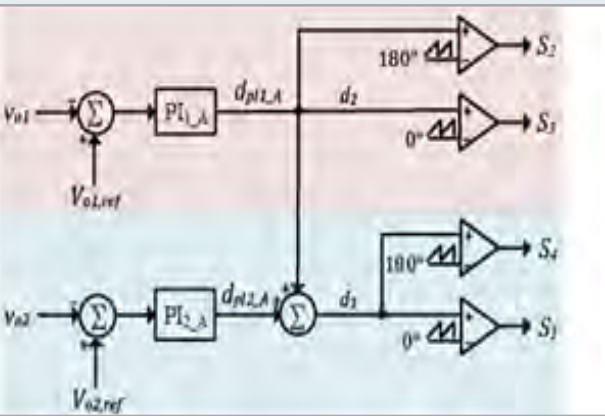
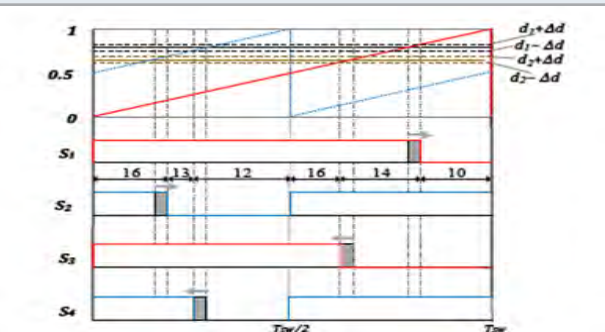


Figure 9: Block diagram of the closed-loop control system



B. Voltage Matching Control Scheme: In exercise, the voltages of the sequence capacitors C11 and C12 will diverge from each other due to the irregularity of the sequence controls and their drive signals as well as the outflow currents of the capacitors. Additional purpose might be the electronic components which are not basically matching despite the fact that their workshop conditions are the similar.

Figure 10: Result of complementary duty-cycle on the switch signals of the control



C. Compensator Design: The process of the SIDO-TLC has been authenticated using a lab model. The converter's stipulations for a strategy model are displayed in Table I. concerning these specifications; the SIDO-TLC functions in situation A. The matching Bode diagrams have also been designed in direction to strategy the optimum control system. As before declared, the stage up output voltage is precise by d2, and the step down cast output voltage is controlled by d1. The control transfer roles with continuous constants are stated at the perfect condition ($\Delta D = 0$) as well as at the situation when the outflow currents of the sequence capacitors are comprised ($\Delta D = 0.004$).

Table 1. Specifications for the SIDO-TLC

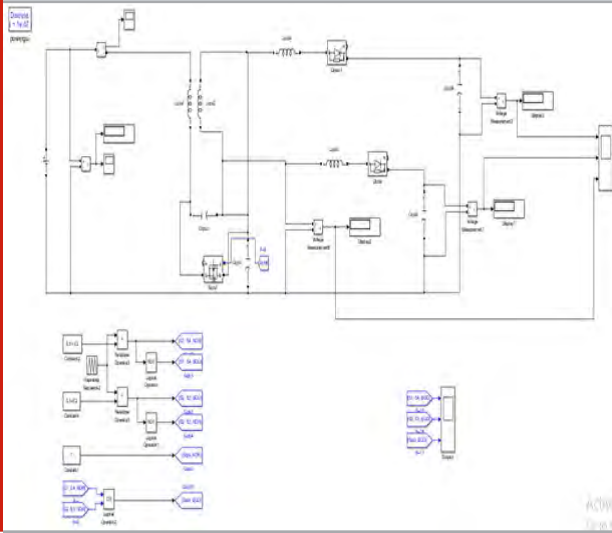
Parameter	Value
Total Output Power (P_o)	300 W
Input Voltage (V_{in})	60 V
Step-Up Output Voltage (V_{o1})	125 V
Step-Down Output Voltage (V_{o2})	36 V
Step-Up Resistive Load (R_{o1})	65 Ω
Step-Down Resistive Load (R_{o2})	20 Ω
Switching Frequency (f_{sw})	20 KHz

RESULTS AND DISCUSSIONS

The equivalent waveforms of the input voltage (V_{Low}) and three output voltages (V_{O1} , V_{O2} and V_{O3}) are shown in Fig 4.5, 4.6, 4.7. The output voltages can be steadily measured to reach the wanted values via the response switch. (S.Vijayalakshmi et al., 2020) The voltage ripple ratios of V_{O1} , V_{O2} and V_{O3} are 0.45%, 0.67%, and 0.50%, respectively. The power switch (S_1) in the planned HSTDC is worked below the ZCS state to decrease the converting loss, and steady output voltage stages can be accurately controlled by the response controller and the strategy of the supporting inductor.

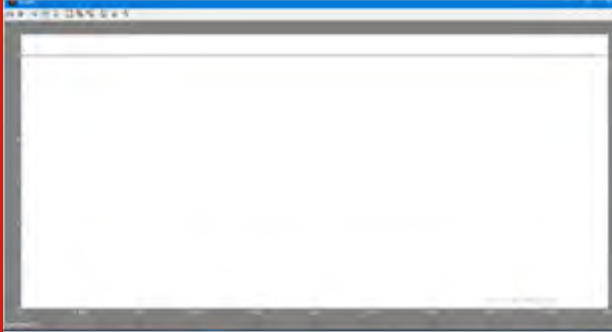
While there are slight voltage differences below input voltage variations since 12V to 13V, 3 output voltages (V_{O1} , V_{O2} and V_{O3}) can be steadily attained at preferred values. By way of input voltage variation from 13V to 11V, 3 output voltages (V_{O1} , V_{O2} and V_{O3}) likewise can be steadily in tune at preferred values. While V_{O1} and V_{O3} are well-ordered by the similar duty cycle of the control switch. The output voltages can be steadily measured below the happening of load differences by the secure loop control procedure. (S.R.Paveethra et al., 2020) Though the output voltage of the secondary circuit one can be attuned at the set range 25V to 30V through the strategy of the secondary inductor, the output voltages of the extraordinary voltage dc bus and the central voltage output station can be exactly measured to be 200V and 40V, correspondingly. (V Venkatesh et al., 2019)

Figure 11: Simulation diagram of the proposed system



A. Simulation Input voltage

Figure 12: Input waveform for planned system



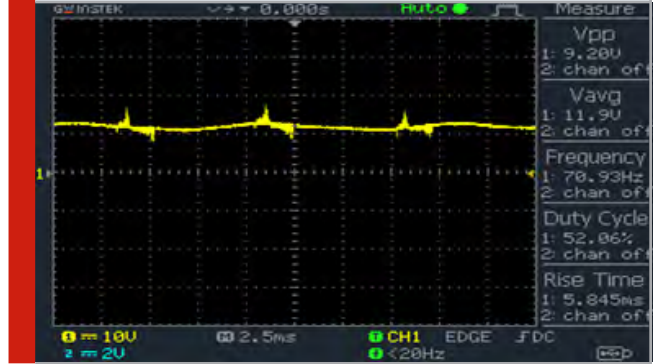
B. PWM Waveform

Figure 13: PWM Pulses for proposed system



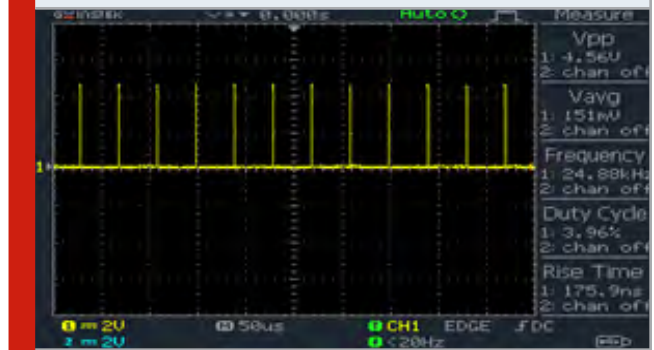
C. Hardware Results of proposed system:
1. Input Voltage:

Figure 14: Input waveform for proposed system



2. Pulse Waveform:

Figure 15: Gate pulse for proposed system



3. Output Voltage V1

Figure 16: Gate pulse for proposed system



4. Output Voltage V2

Figure 17: Gate pulse for proposed system



5. Output Voltage V3

Figure 18: Gate pulse for proposed system



CONCLUSION

This work has effectively established great efficiency 1-input 3-outputs DC-DC converter (HSTDC) for great step-up claims, and this attached inductor-based converter has remained useful well for the submission with great voltage relations and several output stations. The planned HSTDC has a brilliant maintenance under several investigational situations and input voltage differences. In this study, the projected HSTDC integrates an attached inductor, a power control, 4 Schottky diodes, 2 metalized polyester 1m capacitors, and one supplementary inductor to realize the purposes of great competence power translation, zero-current-switching (ZCS) twisted on and one-input 3-outputs feature. Outstanding to the distinctive features of the one-input several outputs process, the planned HSTDC also can be simply cast off for extra great step-up claims. (R. Jai Ganesh et al., 2020).

The main compensations of this learning are shortened as trails: i) the planned converter through only one power control attains the areas of a great step-up percentage, the great efficacy power adaptation, and dissimilar output voltage stages. ii) Meanwhile the voltage strain of the power button can be compressed to be a precise voltage range, the power button with a lesser twisted on resistor can be designated to reduction the transmission loss, and the swapping loss will be lessened through the soft-switching method. iii) A response controller scheme can be employed by a numerical signal computer as an alternative of an old-style analog controller circuit. iv) The secure loop controller system is calculated to steady the output voltage for load differences.

REFERENCE

- A. Rajkumar and B. Karthikeyan (2014) Fuzzy Logic Controller for Fast Transient Response DC DC Converter Adv in Nat Appl Sci 821 65-71.
- AT Sankara Subramanian P Sabarish A Nazar Ali (2017) A power factor correction based canonical switching cell converter for VSI fed BLDC motor by using voltage follower technique IEEE International Conference on Electrical Instrumentation and Communication

Engineering (ICEICE) pp.1-8.

A Rajkumar B Karthikeyan S Senthilkumar (2015) Reliability Analysis of Fuzzy Logic Controlled Fast Transient Response DC- DC Converter. International Journal of Applied Engineering Research 10 85 728-730.

A Nazar Ali R Jeyabharath MD Udayakumar (2016) Cascaded Multilevel Inverters for Reduce Harmonic Distortions in Solar PV Applications Asian Journal of Research in Social Sciences and Humanities Vol 6 pp.703-715.

A Rajkumar B Karthikeyan S Senthilkumar (2015) Fault Tree Based Reliability Analysis of Fast Response DC-DC Converter International Journal of Applied Engineering Research 10 85 731-737.

A Rajkumar B Karthikeyan S Senthil Kumar (2015) Performance Evaluation Fast Transient Response DC-DC Converter using Soft Computing Analysis with PI Controller Australian Journal of Basic and Applied Sciences 9 33 373-379.

A. Nazar Ali R. Sagayaraj and R. Jaiganesh (2018) Analysis the performance of Embedded ZSI fed Induction motor under semiconductor failure condition TAGA JOURNAL VOL 14 1634-1644.

A Ali Nazar R Jayabharath MD Udayakumar (2014) An ANFIS Based Advanced MPPT Control of a Wind-Solar Hybrid Power Generation System international review of modelling and simulations Vol 7 no 4 pp. 638-643.

A Nazar Ali D Sivamani R Jaiganesh M Pradeep (2019) Solar powered air conditioner using BLDC motor IOP Conference Series: Materials Science and Engineering vol 23.

B. Wang V. R. K. Kanamarlapudi L. Xian X. Peng K. T. Tan and P. L. So (2016) Model predictive voltage control for single-inductor multiple-output DCDC converter with reduced cross regulation IEEE Trans. Ind. Electron vol 63 no 7 pp. 4187-4197.

C. Kalavalli S. R. Paveethra S. Murugesan Dr. A. Nazar Ali (2020) Design And Implementation Of High Efficiency H6 PV Inverter With Dual Axis Tracking International Journal of Scientific & Technology Research Vol 9 issue 02 and pages 4728-31

G. R. C. Mouli J. Schijffelen M. V. D. Heuvel M. Kardolus and P. Bauer (2019) A 10kW solar-powered bidirectional EV charger compatible with chademo and COMBO IEEE Trans. Power Electron vol 34 no 2 pp. 1082-1098.

J. Reinert A. Brockmeyer and R. W. A. A. D. Doncke (2001) Calculation of losses in ferro- and ferrimagnetic materials based on the modified Steinmetz equation IEEE Trans. Ind. Appl vol 37 no 4 pp. 1055-1061.

M D Udayakumar et al (2019) IOP Conf. Ser.: Mater. Sci. Eng. 623 012018

M. Pradeep et al (2019) IOP Conf. Ser.: Mater. Sci. Eng. 623 012017

O. Ray A. P. Josyula S. Mishra and A. Joshi (2015) Integrated dual-output converter IEEE Trans. Ind. Electron., vol 62 no 1 pp. 371-382.

R.-J. Wai and J.-J. Liaw (2016) High-efficiency coupled-inductor-based step-down converter IEEE Trans. Power Electron vol 31 no 6 pp. 4265–4279.

P. Thirusenthil Kumaran P. Pushpakarthick G. V. Chidambarathanu M. Venkatachalam Xavier Raja Durai R.Jaiganesh (2019) Power quality in distribution grids International Journal of Innovative Technology and Exploring Engineering (IJITEE) ISSN 2278-3075 Volume 9 Issue 1.

R. Jai Ganesh S. Kodeeswaran M. Kavitha T.Ramkumar(2020) Performance analysis of piezoelectric energy harvesting system employing bridgeless power factor correction boost rectifier <https://doi.org/10.1016/j.matpr.2020.02.085>.

Rajkumar B. Karthikeyan and S. Senthil Kumar (2015) Fuzzy Logic Control of Fast Transient Response DC-DC Converter Middle East J. Sci. Res 23 9 2256-2263.

S.R.Paveethra C.Kalavalli S.Vijayalakshmi Dr.A.Nazar Ali, D.Shyam(2020) Evaluation Of Voltage Stability

Of Transmission Line With Contingency Analysis International Journal of Scientific & Technology Research Vol 9 issue 02.

S. S. Dobakhshari J. Milimonfared M. Taheri and H. Moradisizkoochi (2017) A quasi-resonant current-fed converter with minimum switching losses IEEE Trans. Power. Electron vol 32 no 7 pp. 353–362.

S.Vijayalakshmi P.Sabarish S.R.Paveethra Dr.P.R.Sivaraman Dr.V.Venkatesh (2020) Exploration And Applications Of Electronic Balance For High Power Discharge Lamps At High Frequency Through Power Factor Modification International Journal Of Scientific & Technology Research Volume 9 Issue 02 Issn 2277-8616.

V Venkatesh A NazarAli R Jaiganesh V ndiragandhi (2019)Extraction and conversion of exhaust heat from automobile engine in to electrical energy Energy IOP Conference Series: Materials Science and Engineering vol 23.

Design and Implementation of IOT Based Smart Library Using Android Application

R. Ramkumar¹, B. Karthikeyan², Dr. A. Rajkumar³, V. Venkatesh⁴ and A. Anton Amala Praveen⁵

¹Department of Electricals and Electronics Engineering,

^{1,2,3,5}K.Ramakrishnan college of technology,⁴ Rajalakshmi Engineering College

ABSTRACT

This proposed system is to automate the library and control the lights and fans using voice control and notifying via google assistant. The details of user who lends the book from library will be updated into the database by reading the RFID tags of every user. The RFID tags will be present in the Identity card of every student in the college. The details of book that is lent to the users will be updated to the database by scanning the barcode of every book using barcode scanner. Here, in this proposed system it is also possible to control the electrical apparatus in library by using android application. The details of users who have borrowed and books that is lent from the library will be monitored using the android application which will be interfaced with the database. Updation of these data in the database can also be done.

KEY WORDS: GOOGLE ASSISTANT, RFID, DATABASE, ANDROID APPLICATION

INTRODUCTION

In our proposed project, we are going to automate the library. It will be mainly useful for college libraries and libraries in industry or any organization (Ramkuma R et al.,2019). By using IOT technology incorporated with Google assistant we are going to automate the electrical apparatus inside the library. We will be able to control the lights and fans by voice and texting via android application. The app created by us from MIT app inventor will be having IFTTT. We use Node MCU(ESP 8266) also known as WiFi module as a controller (Premkumar Kamaraj et al 2018). IOT concept will also be used in our proposal for data transmission and reception purposes. RFID tags placed in identity card of that particular student

who is borrowing the book will be read by RFID reader. The book that which is going to be lent will be read by scanning the barcode which will be present on the cover of any book. This two information will be sent to the database via IOT (Nazar Ali A et.al.,2014).

MATERIALS AND METHODS

Principle of Operation: The information of students from the RFID tags and details of the books from the Barcode scanner will be sent to ESP 8266(Wi-FiModule). This WiFi module will send these signals to the database via IOT(Adafruit Platform).These data's from the database will be notified or shown to the librarian or any corresponding personal who runs the library (Ramkumar R et al 2019).

Some specified commands can be sent from smart phones with the help of Google Assistant to the database. Those particular commands will be already programmed with the help of IFTTT platform which is used for connecting our smart phones and Wi-Fi module. When command

ARTICLE INFORMATION

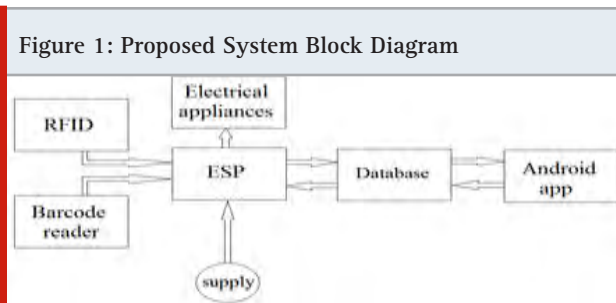
*Corresponding Author: ramkumarr.eee@krct.ac.in
Received 15th April 2020 Accepted after revision 20th May 2020
Print ISSN: 0974-6455 Online ISSN: 2321-4007 CODEN: BBRCBA

Thomson Reuters ISI Web of Science Clarivate Analytics USA and Crossref Indexed Journal



NAAS Journal Score 2020 (4.31) SJIF: 2020 (7.728)
A Society of Science and Nature Publication,
Bhopal India 2020. All rights reserved.
Online Contents Available at: <http://www.bbrc.in/>

is sent from mobile to database, IFTTT will send some signals to the Wi-Fi module which helps us to automate the library. By this concept, we will able to control the electrical apparatus either by voice or by texting. We have also created an App for finding out an exact location of books placed in various shell. (Premkumar et al 2015).



- Main Functions of our Proposed System
- (a) To read the RFID tags from the students
 - (b) To read the ISBN code from the books in library
 - (c) To give the exact location of books using android apk
 - (d) To automate the library
 - (e) To store the datas of students and books in cloud account
- (a) To read the RFID tags from the students

RFID is innovation which deals with radio recurrence and it is utilized for the auto-recognizable proof for the diverse item.

The RFID system mainly consists of two parts.

- 1) RFID Reader or Interrogator
- 2) RFID Tags In this RFID framework



This RFID peruser consistently sends radio floods of a specific recurrence. In the event that the item, on which this RFID tag is connected is inside the scope of this radio waves then it sends the criticism back to this RFID peruser. Furthermore, in light of this input, RFID peruser distinguishes the item.

RFID labels: Now, three various types of RFID labels are financially accessible.

- 1) Passive labels
- 2) Active labels
- 3) Semi-aloof labels

These detached labels don't have any force supply. They used to get their capacity from the approaching radio waves from the Readers. While dynamic labels have a force hotspot for their inside hardware. What's more, for sending the reaction to the peruser likewise, it utilizes its own capacity supply. On account of semi-detached labels, they have a force supply for inner hardware, however for sending the reaction it depends on the radio waves got from the Reader.

Operating Frequency: This RFID system is mainly operated in three frequency bands.

- 1) LF: Low-Frequency band
- 2) HF: High-Frequency band
- 3) UHF: Ultra High-Frequency band

The exact frequency of operation varies from country to country.

Operating Principles: Most of the RFID systems operate on any of this two principles.

- 1) Burden Modulation
 - 2) Backscattered Modulations
- (b) Working principle

Let us see the working standard for this RFID framework. This working standard depends on the repeat of action. Right now, the low and high repeat action the working principle relies upon the inductive coupling. While because of ultra high repeat RFID labels, working rule relies upon electromagnetic coupling.

In this RFID peruser persistently sending radio waves with a specific recurrence. So now this radiowaves which is being sent by this RFID peruser file three needs.

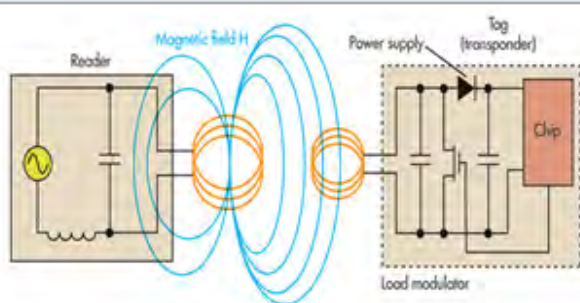
- (i) It incites enough force into the tag.
- (ii) It gives synchronization to the tag.
- (iii) It goes about as a transporter for the information which is returning from the tag.

a) Near Field Coupling: In the event of low and high recurrence activity RFID labels and peruser are near one another. So the working guideline depends on inductive coupling (Sheikh Ghazala et.,al 2015). The field which is produced by this RFID peruser used to get couple with the recieving wire of RFID tag. What's more, due to this common coupling the voltage will ghet incited over the curl of the RFID tag. Presently some bit of the voltage is getting redressed and utilized as a power supply for the controller just as to memory components. Presently as the RFID peruser is sending a radio rushes of a specific recurrence so the voltage that is instigated over the loop is additionally ofa a specific recurrence. So this prompted voltage is likewise used to determine the synchronization clock for the clock. So now , assume in the event that we associate a heap of loop, at that point the present

will begin coursing through this heap and on the off chance that we change the impedance of the heap, at that point the present that is moving through this heap will also get changed.

So now assume if switch on and off this heap and the present will likewise get turned on and off. So this exchanging of current or pace of progress of current additionally produces a voltage in the RFID peruser. So this turning on and off the heap is known as burden regulation. So now assume, if this switch on and off this heap as per the information that is put away inside this RFID tag, at that point the information can be perused by the RFID peruser as voltage. So along these lines utilizing this heap adjustment we are changing the voltage that is produced over the RFID peruser loop. What's more, thusly we are producing adjustment on a transporter signal, so along these lines, in a low and high recurrence RFID labels, utilizing this heap tweak procedure the information is being sent back to the RFID peruser (Premkumar K et al 2018).

Figure 3: Working of RFID reader



b)Far Field Coupling: Let us see the working standard of ultra high recurrence. So for this situation of ultra high recurrence as the separation between the per user and the label will be up to hardly any meters, so the coupling between the per user the loop will be far field coupling. Thus, this RFID per user ceaselessly sending the radio influxes of a specific recurrence towards the tag and accordingly this label will send a feeble sign to the RFID per user. Presently this powerless sign which is being sent back to the RFID per user as known as back dissipated sign and the force of this back dispersed sign relies on the heap coordinating over the curl. Soon the off chance that the heap is coordinated precisely, at that point the power of the back Dissipated sign will be all the more however on the off chance that the heap isn't coordinated precisely, at that point the force of the back dispersed sign will be less.

So along these lines, by changing the state of the heap we can change the power of the back dispersed sign and in the event that we change the state of the heap as per the information that is being put away over this RFID tag, at that point that information can be sent back to the RFID per user. So along these lines, RFID per user can detect that information. Presently in the event of ground-breaking coupling, as the separation between RFID per user and tag is barely any meters, so

the underlying sign which is being sent by the per user ought to be solid with the goal that the back dissipated sign can be recovered by this RFID per user. So this is the manner by which for a situation of far field coupling, the sign is sent back to the RFID per user utilizing this back dispersed regulation system.

(c)To read the ISBN code from the books in library: The guideline behind the CCD innovation isn't in any capacity mind blowing – a CCD scanner utilizes a variety of little light sensors that are pointed at the standardized tag area on an item. The manner in which these scanners work is that they structure a kind of framework of small laser like lights on the outside of the standardized identification part of the item. Since standardized identifications are normally imprinted on white foundations a piece of that light radiated from the scanner is reflected to a recipient inside the leader of the scanner. That light is converted into a voltage utilizing a photovoltaic cell, and that measure of voltage relates to a solitary kind of item in the store.

Figure 4: Barcode scanner with CCD camera



The guideline behind the CCD innovation isn't in any capacity mind blowing – a CCD scanner utilizes a variety of little light sensors that are pointed at the standardized tag area on an item. The manner in which these scanners work is that they structure a kind of framework of small laser like lights on the outside of the standardized identification part of the item. Since standardized identifications are normally imprinted on white foundations a piece of that light radiated from the scanner is reflected to a recipient inside the leader of the scanner. That light is converted into a voltage utilizing a photovoltaic cell, and that measure of voltage relates to a solitary kind of item in the store.

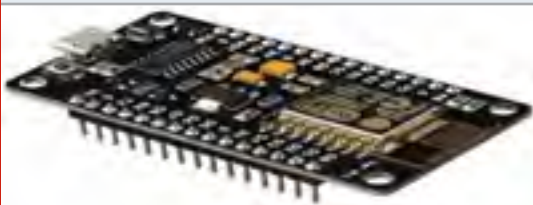
(d)To give the exact location of books using android apk: Application Inventor for Android is an open-source web application at first gave by Google, and now kept up by the Massachusetts Institute of Technology (MIT). It empowers newcomers to PC programming to make programming applications for the Android working structure (OS). It uses a graphical interface, generally equivalent to Scratch and the Star Logo TNG UI, which empowers customers to migrate visual articles to make

an application that can run on Android contraptions. In making App Inventor, Google drew upon basic before explore in informational figuring, similarly as work done inside Google on online improvement circumstances. Application Inventor and the undertakings on which it is based are educated by constructionist learning hypotheses,

which underscores that programming can be a vehicle for connecting influential thoughts through dynamic learning (Ramkuma R et.,al 2019). The Blocks segment enables you to make custom usefulness for your application, so when you press the catches it really accomplishes something with that occasion. The Palette contains the segments to assemble the application configuration like catches, sliders, pictures, names, and so on. It's the Viewer. This is the place you drag the parts to manufacture the application look. Parts. You can see every one of the parts added to your application and how they are sorted out progressively. This is the place you select your segments' properties like shading, size and direction.

(e)To automate the library: NodeMCU Dev Board is based on widely explored esp8266 System on Chip from Expressive. It combined features of WIFI access point and station and microcontroller and uses simple LUA based programming language. ESP8266 NodeMCU offers Arduino like hardware IO, Event-driven API for network applications & then 10 GPIOs D0-D10, PWM functionality, IIC and SPI communication, 1-Wire and ADC A0 etc. all in one board, Wi-Fi networking (can be uses as access point and/or station, host a web server), connect to internet to fetch or upload data. Excellent system on board for InternetofThings(IoT) projects.

Figure 5: WiFi module (Esp 8266)

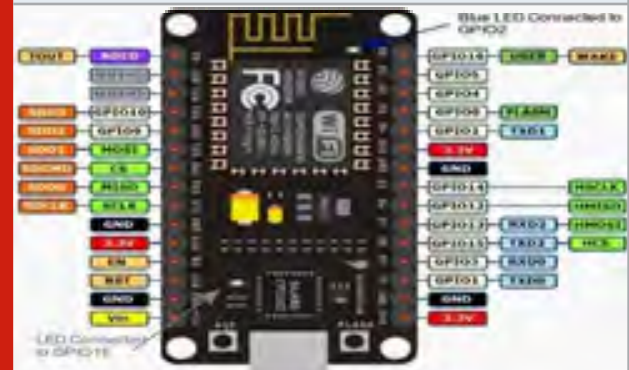


Recently, there has been interest in programming ESP8266 systems using Arduino IDE. Programming, of ESP8266 using Arduino IDE is not very straight forward, until it is properly configured. Especially because, the Input and output pins have different mapping on NodeMCU than those on actual ESP8266 chip.

Here there are three other main important platform for the automation. They are Adafruit , IFTTT and Google Assistant. The IFTTT is used to interconnect the Google Assistant and the Adafruit. The text commands can be given through Adafruit and for the voice commands we must go for the Google Assistant, for the interfacing of the Adafruit and the Google Assistant we need the IFTTT. If This Then That, also known as IFTTT is a free web-based service to create chains of simple conditional

statements, called applets. An applet is triggered by changes that occur within other web services such as Gmail, Facebook, Telegram, Instagram, or Pinterest.

Figure 6: Esp. 8266 Pin Configuration



ESP8266 is a system on a chip (SoC) design with components like the processor chip. The processor has around 16 GPIO lines, some of which are used internally to interface with other components of the SoC, like flash memory. Since several lines are used internally within the ESP8266 SoC, we have about 11 GPIO pins remaining for GPIO purpose. Now again 2 pins out of 11 are generally reserved for RX and TX in order to communicate with a host PC from which compiled object code is downloaded. Hence finally, this leaves just 9 general purpose I/O pins i.e. D0 to D8.

Figure 7: Flowchart for Barcode scanning

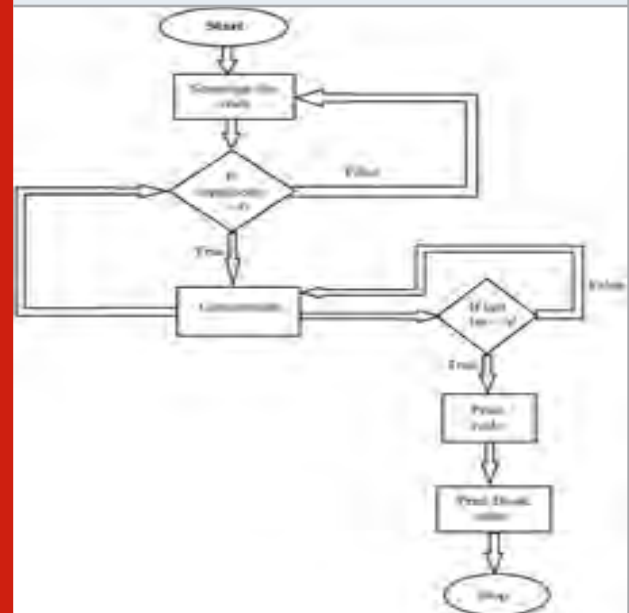
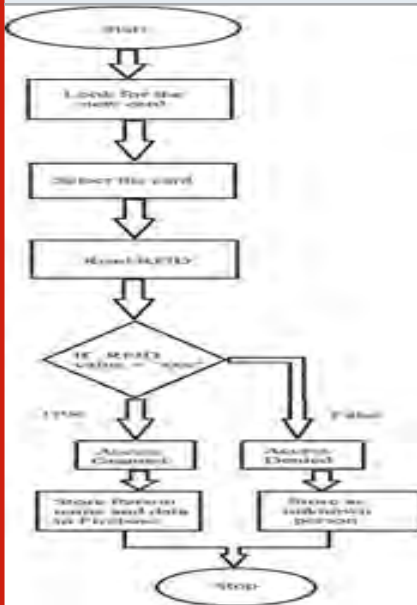


Fig 7 shows the flow chart for Barcode scanning system and Fig 8 shows the flow chart for RFID tag reading system

Figure 8: Flowchart for RFID tagging



transferred to the database. This information will be retrieved and stored in the database.

Figure 10: Adafruit platform

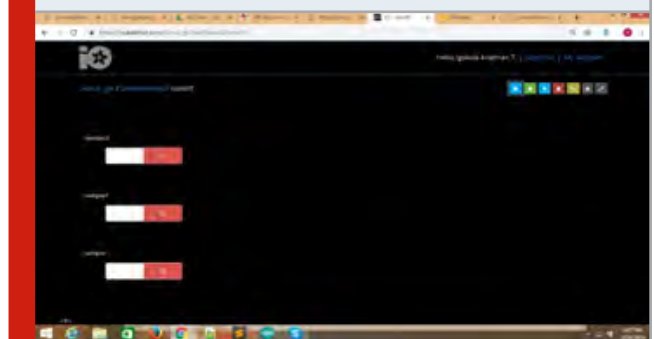
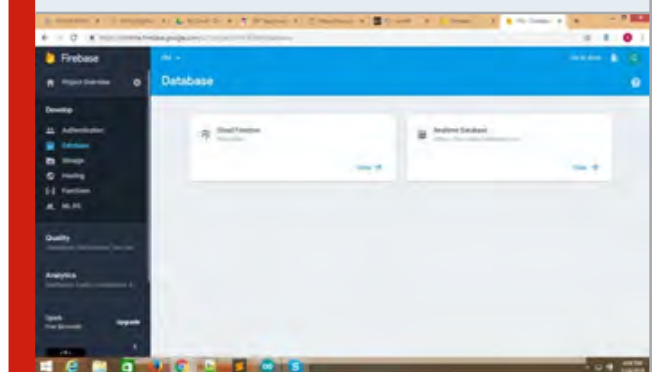


Figure 11: Types of databases



RESULTS AND DISCUSSION

Hardware Results:

Figure 9: RFID database testing

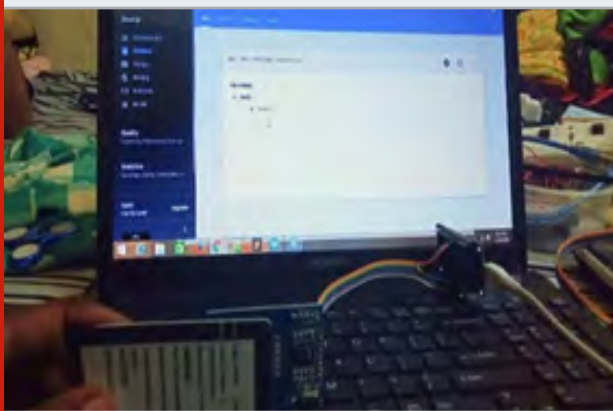


Fig.9 shows the reading the RFID tag using a RFID reader. The RFID tag present in the college Identity card is read by the reader. Fig.10 shows the Adafruit platform responsible for turning on and off the electrical appliances. This figure depicts the number of loads used. Here all the loads are in off condition. If any load is turned on, it would turn green. We can either control the load directly in this platform or by voice and typing via Google assistant.

Figure 11 the two types of databases available in firebase store. One is cloud fire store and real-time database. We use real-time database in our proposed system

Figure 12 depicts once the RFID tags are read by RFID reader, the information obtained by the reader will be

Figure 12: RFID tag stored in database

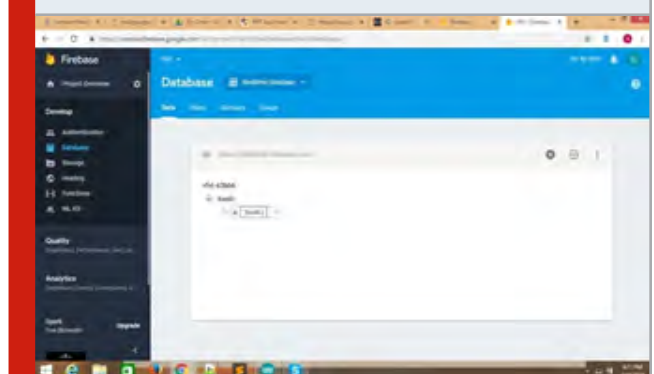


Figure 13: conditions for read/write in firebase

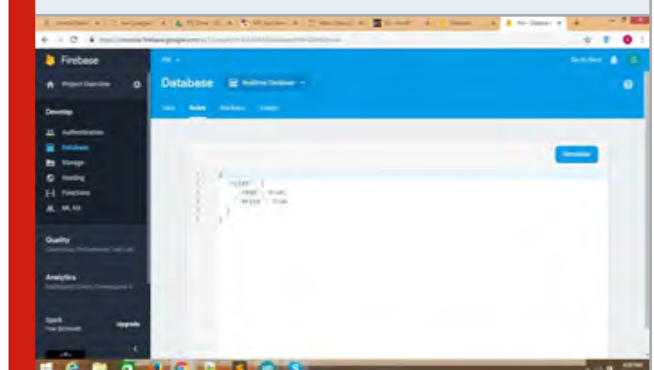


Figure 13 depicts the conditions for read and writes operations in firebase. These rules are responsible for editing and viewing the data which has been stored in the database. Without these rules it will not be possible to view or edit.

Figure 14 shows the Barcode scanner output for the proposed system. To interface our Google Assistant to the Adafruit IO MQTT Broker to permit us to control the lights with voice directions. To do this, we will utilize the IFTTT (If This Then That) stage, which permits many various administrations to trigger activities in an assortment of different administrations.

For trigger, pick "Google Assistant" as the administration; at that point select "Say a straightforward expression" starting from the drop menu of explicit triggers. This will raise another rundown of fields to fill in, including varieties of the actuation expression, the Google Assistant's reaction, and the language. For out initiation phrases, we picked "Turn the light on," "Turn on the light," "Lights on", and "Switch the light on".

The last piece of the applet is the Action, what applet does because of the Trigger. For the administration, pick "Adafruit", and for the particular Action, pick "Send information to Adafruit IO". This will raise two fields that you have to fill in. The first ought to be supplanted with the name of the Adafruit IO feed you need to send information to, right now "off". The subsequent field is the information to send. For this applet, we well send "ON", which is the string our ESP8266 is sitting tight for.

To actuate them, go to the My Applets page on the primary IFTTT site, click on the applet card, and snap set the on-off flip change to "On". On the off chance that it not associated as of now, IFTTT will request to interface with your Adafruit IO and Google Assistant records. Permit the records to be connected, and afterward turn on the subsequent applet too. When the two applets are turned on, the arrangement ought to be finished! Presently the entirety of that is left is to test the framework. To do this, all we need a gadget with the Google Assistant empowered.

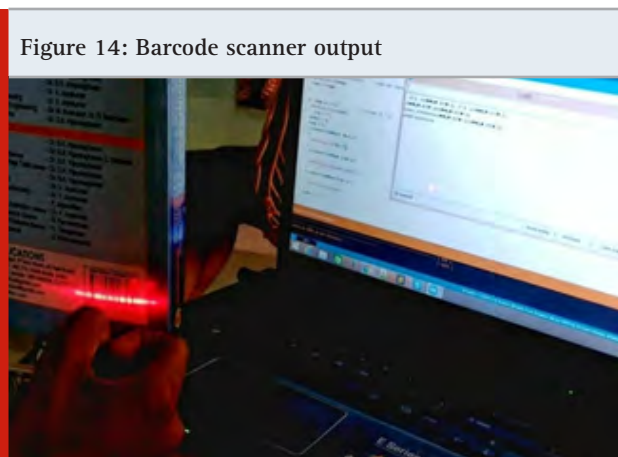


Figure 14: Barcode scanner output

This is incorporated with the most recent adaptations of the Android working framework, just as the Google Home arrangement of gadgets. In the event that it isn't accessible, at that point, the Google Allow informing application, accessible for Android and iOS, likewise incorporates the Google Assistant. Start up the right hand, ensure it's signed into the best possible record, and state the enactment expression you utilized in the past advance. Following a 2-5 second postponement, the light on your ESP8266 board should turn on or off. Attempt the other expression, and ensure it works as well.

CONCLUSION

After working on the hardware of the proposed system, we will be able to control the electrical apparatus like fans, lights, etc very efficiently. The electrical instruments can be controlled either by voice control or typing the command in goggle assistant. The details of students are effectively read with the RFID tag. The RFID tags present in the identity cards of the students will be read and stored in the database. This RFID tag will be read along while reading the barcode scanner of the particular book lent by that particular student. The details of RFID and the ISBN code of book lent both will be stored in the database. By knowing the above details of the student details and ISBN code of the book, we will be able to know who lent which book. Hence there won't be any misjudgment or misunderstanding. The accurate location the book is known by using the library application created. The android application invented will be letting people to know the exact location of the book. It will intimate us about the section, shelf and rack in which the book is located. By using this, it will be easier for the people to know the exact location of book they seek for.

REFERENCES

- Ali Nazar A R Jayabharath MD Udayakumar (2014) An ANFIS Based Advanced MPPT Control of a Wind-Solar Hybrid Power Generation System International review of modelling and simulations. Vol 7 no.4 pp 638-643.
- Kalavalli C S.R.Paveethra S.Murugesan Dr.A.Nazar Ali (2020) Design And Implementation Of High Efficiency H6 PV Inverter With Dual Axis Tracking International Journal of Scientific & Technology Research Vol 9 issue 02 and pages 4728-31.
- Markakis I (2013) RFID enabled library management system using low SAR smart bookshelves Electromagnetic in Advanced Applications (ICEAA) International Conference on IEEE.
- Nazar Ali A D Sivamani R Jaiganesh M Pradeep [2019] Solar powered air conditioner using BLDC motor IOP Conference Series Materials Science and Engineering vol.23.
- Nazar Ali A and R. Jayabharath (2014) Performance Enhancement of Hybrid Wind Photo Voltaic System Using Z Source Inverter with Cuk-sepic Fused Converter." Research Journal of Applied Sciences Engineering and Technology.19:3964-3970.

- Nazar Ali A R Sagayaraj and R Jaiganesh (2018) Analysis the performance of Embedded ZSI fed Induction motor under semiconductor failure condition TAGA JOURNAL VOL 14 : 1634-1644.
- Nazar Ali A R Jeyabharath MD Udayakumar (2016) Cascaded Multilevel Inverters for Reduce Harmonic Distortions in Solar PV Applications Asian Journal of Research in Social Sciences and Humanities Vol 6 pp.703-715.
- Premkumar et al (2015) GA-PSO optimized online ANFIS based speed controller for Brushless DC motor Journal of Intelligent and Fuzzy Systems 28, 6 pages.2839-2850.
- Paveethra S R C.Kalavalli S.Vijayalakshmi Dr A Nazar Ali D.Shyam(2020) Evaluation Of Voltage Stability Of Transmission Line With Contingency Analysis International Journal of Scientific and Technology Research Vol 9 issue 02 and pages 4018-22
- Premkumar Kamaraj et al (2018) Antlion Algorithm Optimized Fuzzy PID Supervised On line Recurrent Fuzzy Neural Network Based Controller for Brushless DC Motor Electric Power Components and Systems, 45,20 pages.2304-2317.
- Premkumar K et al (2018) Novel bacterial foraging based ANFIS for speed control of matrix converter fed industrial BLDC motors operated under low speed and high torque Neural Computing and Applications 29, 12 pages.1411-1434.
- Ramkumar R and N Tejaswini (2016) A novel low cost three arm Ac automatic voltage regulator Advances in Natural and Applied Sciences vol.10 no.3
- Ramkuma R et al (2019) Intelligent system to monitor and diagnose performance deviation in Industrial Equipment.IOPconf.Series:Materials science and Engineering,Vol 623 Vol 012012.
- Ramkumar, R. et al (2016) PV based SEPIC converter fed four switch BLDC motor drive Advances in Natural and Applied Sciences vol. 10 no.3.
- Rajkumar B Karthikeyan and S Senthil Kumar (2015) Fuzzy Logic Control of Fast Transient Response DC-DC Converter Middle East J Sci Res 23 (9) 2256-2263.
- Rajkumar A B Karthikeyan S Senthilkumar (2017) Fault Tree Based Reliability Analysis of Fast Response DC DC Converter International Journal of Applied Engineering Research 10 (85) 731-737.
- Shahid Syed Md (2005) Use of RFID technology in libraries A new approach to circulation, tracking inventorying and security of library materials.
- Sheikh Ghazala Shafi and Noman Islam (2012)Towards a contextaware smart library management system..
- Shyam D Premkumar K Thamizhselvan T Nazar Ali A Vishnu Priya M (2019) Symmetrically Modified Laddered H-Bridge Multilevel Inverter with Reduced Configurationally Parameters International journal of engineering and advanced technology Vol 9 issue 1.
- Sankara Subramanian A T P Sabarish A Nazar Ali A (2017) power factor correction based canonical switching cell converter for VSI fed BLDC motor by using voltage follower technique IEEE International Conference on Electrical Instrumentation and Communication Engineering (ICEICE) pp.1-8.
- Venkatesh V A NazarAli R Jaiganesh. V Indiragandhi (2019) Extraction and conversion of exhaust heat from automobile engine in to electrical energy Energy IOP Conference Series: Materials Science and Engineering, vol. 23.

Design and Implementation of Tera-Hertz Antenna for High Speed Wireless Communication

S. Prasad Jones Christydass^{1*}, S. Praveen², S. Naveen Kumar³, S. Rakesh Kumar⁴ and M.Periakaruppan⁵

¹Assistant Professor, ^{2,3,4,5}UG Scholars

^{1,2,3,4,5}Department of ECE, K. Ramakrishnan College of Technology, Trichy-621112, India

ABSTRACT

In this paper, a circular slot microstrip patch antenna is proposed for Tera-Hertz application. The entire structure is developed on substrate having 4.4 and 0.02 as relative permittivity ϵ_r and loss tangent 0.2 on FR4 substrate. The total size of the proposed antenna is $40 \times 40 \mu\text{m}^2$. The height of the substrate is $1.6 \mu\text{m}$. The proposed antenna has four resonating bands from 2.36 THz to 3.20 THz with the bandwidth of 2.69 THz, 3.92 THz to 5.38 THz with the bandwidth of 4.79, 7.36 THz to 8.70 THz with the bandwidth of 7.95 THz, 12.86 THz to 14.35 THz with the bandwidth of 13.70 THz. The Computer simulation tool an electromagnetic software is used for simulating the entire projected antenna. The simulated results such as return loss, VSWR, surface current, radiation pattern, gain and directivity are presented. The simulated results show that the presented antenna is the right choice for Tera-Hertz application.

KEY WORDS: FR4, MICROSTRIP PATCH ANTENNA, SLOTTED ANTENNA, TERA-HERTZ.

INTRODUCTION

In recent times, wireless data traffic is occurring at higher rate due to change in the creation, sharing and consumption of data. By this change there is a need for the highspeed wireless data transmission at anywhere any time. To overcome this, wireless terabit-per second (Tbps) are used to come within five years for which they could solve the wireless data traffic problems as they

could transmit for higher speed. For the short distance wireless communication, the (0.1 – 10 THz) Tera-Hertz range and sub- THz (0.1 – 0.3 THz) are widely used. THz communication links play a major role in which very high data rates are transmitted over short distance. The major disadvantage is small distance and but the transmission data rate will be higher when compared to long range data transmission. One of the major challenges faced at THz communication frequencies is that very high path loss will be imposed for the larger distance. The most important advantage of the THz frequencies is that the antenna size, where they are made to reduce to micrometers (mm). With the recognition of the photonic and semiconductor devices which operates in tera hertz mad it possible to implement communication devices which operates in THz band.

ARTICLE INFORMATION

*Corresponding Author: prasadjoness.ece@krct.ac.in
Received 15th April 2020 Accepted after revision 20th May 2020
Print ISSN: 0974-6455 Online ISSN: 2321-4007 CODEN: BBRCBA

Thomson Reuters ISI Web of Science Clarivate Analytics USA and Crossref Indexed Journal



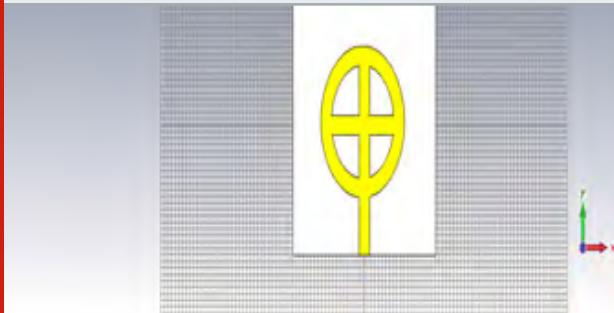
NAAS Journal Score 2020 (4.31) SJIF: 2020 (7.728)
A Society of Science and Nature Publication,
Bhopal India 2020. All rights reserved.
Online Contents Available at: <http://www.bbrc.in/>

Due to the shorter wavelengths of Tera-hertz, it suffers higher free space loss and attenuation. This can be overcome with the help of antennas with higher gain and directivity. The microstrip patch antenna meets the above requirements because of its low cost, easy fabrication and installation. In the literature various types of patch antennas are proposed for Tera-hertz application. Various types of nano antenna (Basyooni et al., 2018; Ding et al., 2019; Chen et al., 2017; Sadeghi et al., 2019) are studies in literature and most has complex structure. Metamaterials (Christophe Caloz et al., 2006), such as SRR (Prasad et al., 2017), CSRR (Prasad et al., 2017; Prasad et al,2019), S shaped, 8 shaped and omega shaped resonator (Boopathi et al., 2017; Choi et al., 2017; Suvadeep et al., 2017)are the artificial man-made structures that can ably enhance the EM properties of the antenna. The metamaterial has negative permittivity and permeability because of it structure and not based on its constituents.

MATERIAL AND METHODS

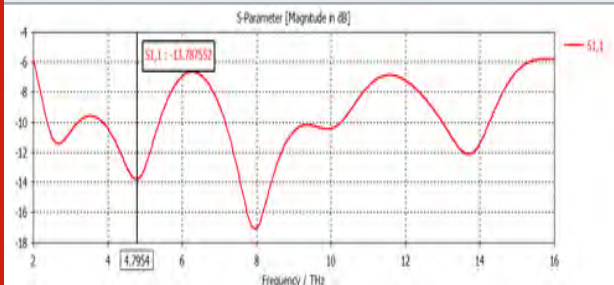
Tera-Hertz Antenna Design Results and Discussion

Figure 1: Design of Tera-Hertz antenna



The above Figure represents the design of Tera-hertz antenna where they are formed with a circular ring and plus ring inside to form an impedance matching at higher rates.

Figure 2: S parameter of the proposed antenna



The Figure 2 illustrates the s11 characteristics of the proposed antenna is presented from which it is observed that the proposed structure has four frequency band of operation which provided in the given Table 1 below.

Table 1. Frequency Band with bandwidth

Band	Lower Frequency	Upper Frequency	Band width
1	2.3686 THz	3.2043 THz	2.694 THz
2	3.9258 THz	5.3845 THz	4.7909 THz
3	7.3674 THz	8.7015 THz	7.9591 THz
4	12.865 THz	14.354 THz	13.707 THz

Figure 3: VSWR of the projected antenna

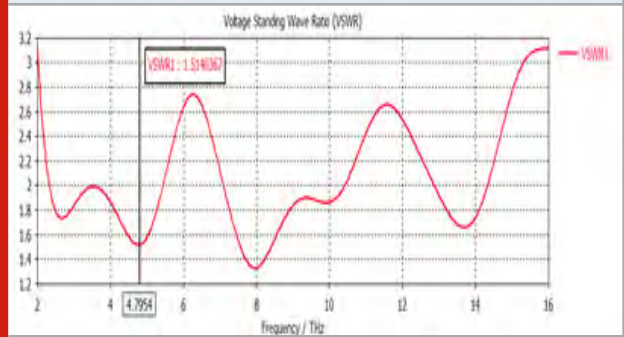


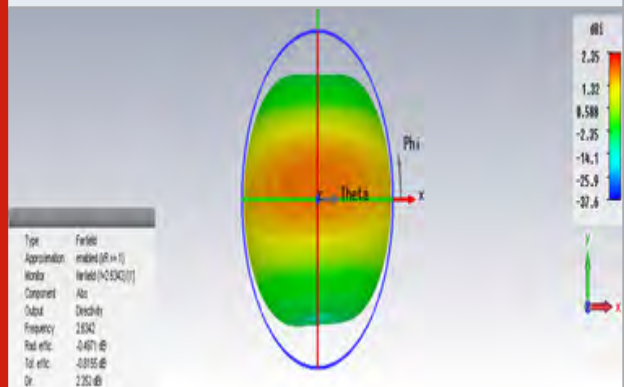
Figure 3 represents the Voltage Standing Wave Ratio characteristics of the projected antenna where all the resonating bands are having VSWR value less than 2. The value of VSWR in each band is provided in Table 2.

Table 2. Frequency Band with VSWR

Band	Lower Frequency	Upper Frequency	VSWR
1	2.3923 THz	3.2019 THz	0.69884
2	4.0217 THz	5.3375 THz	1.1418
3	7.3121 THz	8.7386 THz	1.5847
4	12.88 THz	14.37 THz	1.47898

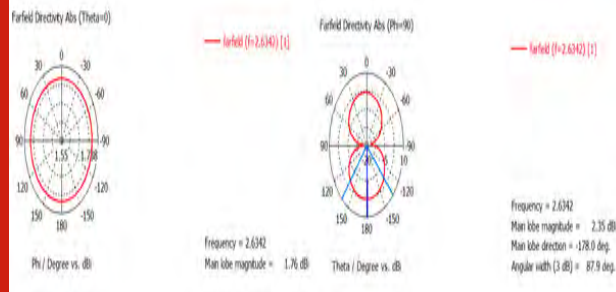
RESULTS AND DISCUSSIONS

Figure 4: 3D radiation pattern at 2.63THz



In the above Figure the Maximum Radiation pattern at 2.63THz is presented. From the Figure 4 it is clearly seen that the maximum radiation is perpendicular to the antenna axis.

Figure 5: E & H plane of the projected antenna at 2.63THz



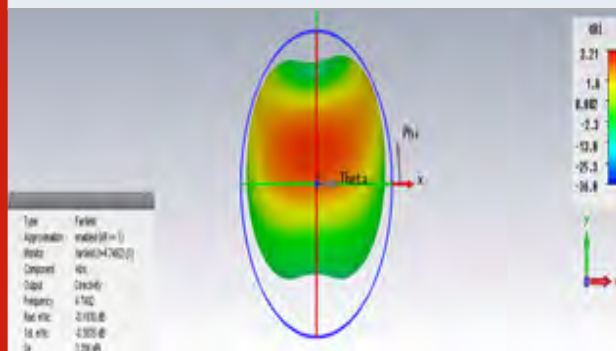
The E plane and the H plane are proposed on the Figure 5 where the E plane is has a omni-directional radiation pattern and the H plane has 8- shaped directional radiation pattern.

Figure 6: Surface current of the frequency 2.694 THz



In Figure 6 the surface current of the proposed antenna is presented from which it is observed that the maximum surface current is concentrated in the ring near the ground and therefore we conclude that the outer ring near the ground is responsible for the frequency band from the range 2.36- 3.2043THz with resonant frequency of 2.694THz.

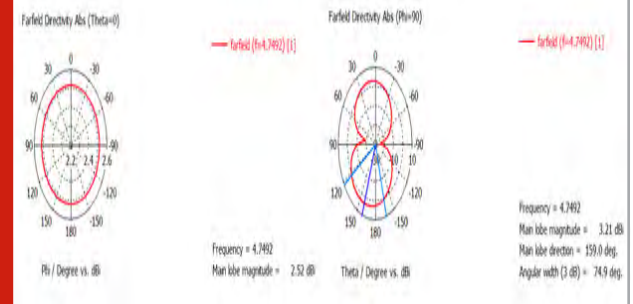
Figure 7: 3D radiation pattern at 2.63THz.



The 3D radiation pattern of the projected antenna is presented in above Figure 7 at 4.74THz and it is in

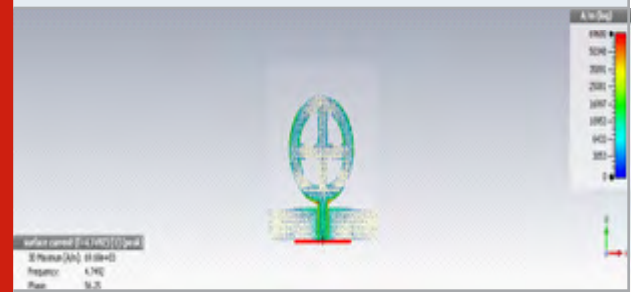
perpendicular direction to the antenna axis.

Figure 8: E & H plane of the proposed antenna at 4.74THz



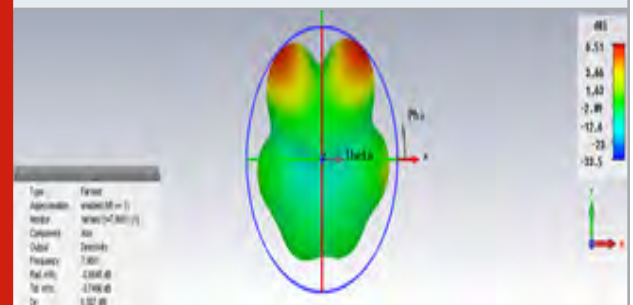
The E & H plane are proposed on the Figure 8 where the E plane is said to be in omni-directional and the H plane is said to be in 8- directional radiational pattern.

Figure 9: Surface current of the frequency 4.79 THz



In Figure 9 the surface current of the proposed antenna is presented from which it is observed that the max surface current is concentrated in the ring and in the ground and therefore we conclude that the outer ring near the ground is responsible for the frequency band from the range 3.92 THz - 5.38 THz with resonant frequency of 4.79 THz.

Figure 10: 3D radiation pattern at 7.96THz



The 3D radiation patten of the projected antenna is presented in Figure 10, it is clearly observed form the Figure that the radiation is has it maximum value in some directional points.

The E & H plane are proposed on the Figure 11 where the E plane is said to be in omni-directional and the H plane is said to be in 8- directional radiational pattern.

Figure 11: E & H plane of the proposed antenna at 7.95THz

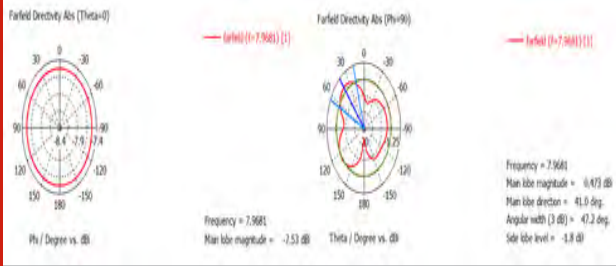
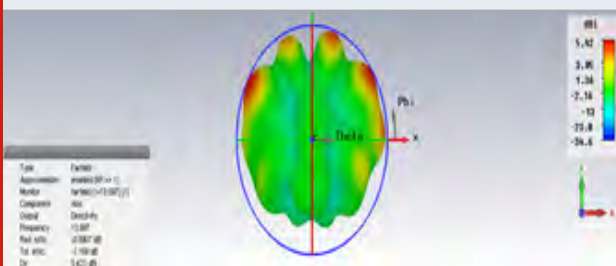


Figure 12: Surface current of the frequency 7.95 THz



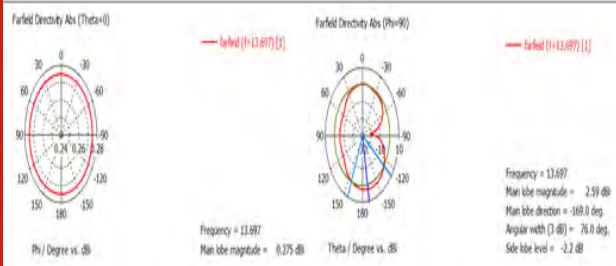
In Figure 12 the surface current of the proposed antenna is presented from which it is observed that the maximum surface current is concentrated in the ground and therefore we conclude that the ground is responsible for the frequency band from the range 7.36 THz - 8.70 THz with resonant frequency of 7.95 THz.

Figure 13: 3D radiation pattern at 13.70THz



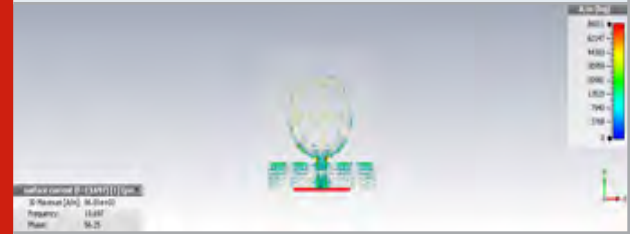
The 3D radiation pattern of the projected antenna is presented in Figure 13, it is clearly observed from the Figure that the radiation is has it maximum value in some directional points.

Figure 14: E & H plane of the proposed antenna at 13.70 THz



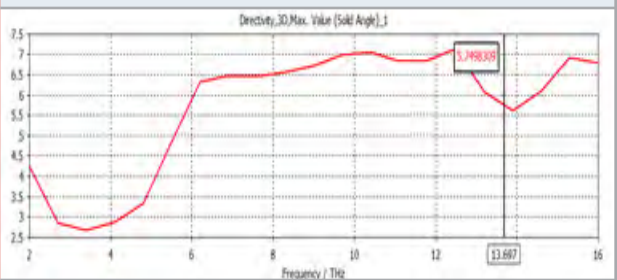
The E & the H plane are proposed on the Figure 14 where the E plane is said to be in omni-directional and the H plane is said to be in 8- directional radiational pattern.

Figure 15: Surface current when the frequency is 13.70 THz



In Figure 15 the surface current of the proposed antenna is presented from which it is observed that the maximum surface current is concentrated in the ground and therefore we conclude that the ground is responsible for the frequency band from the range 12.86 THz - 14.35 THz with resonant frequency of 13.70 THz

Figure 16: Directivity VS Frequency plot



In Figure 16, the directivity of the proposed antenna is presented. The maximum directivity is 6.51dBi. The directivity value for each resonating value is presented in Table 3. In Figure 17, the gain of the proposed antenna is presented and the maximum gain is 5.82 dBi. The gain value for each resonating frequency is presented in Table 4.

Table 3. Directivity of the proposed antenna

Band	Frequency of Resonance	Directivity (THz)
1	2.6342	2.9754
2	4.7492	3.301147
3	7.9681	6.5059818
4	13.697	5.7501439

Figure 17: Gain vs Frequency of the proposed antenna

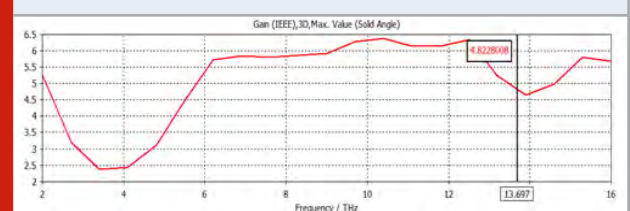


Table 4. Gain of the proposed antenna

Band	Frequency of Resonance (THz)	Gain
1	2.6342	3.397975
2	4.7492	3.056921
3	7.9681	5.8212989
4	13.697	4.8232034

CONCLUSION

A circular slot microstrip patch antenna is proposed for Tera-Hertz application. The entire structure is designed with relative permittivity ϵ_r 4.4 and loss tangent 0.2 substrate called FR4 substrate. The total size of the proposed antenna is $40 \times 40 \mu\text{m}^2$. The height of the substrate is 1.6 mm. The proposed antenna has four resonating bands from 2.36 THz to 3.20 THz with the bandwidth of 2.69 THz, 3.92 THz to 5.38 THz with the bandwidth of 4.79, 7.36 THz to 8.70 THz with the bandwidth of 7.95 THz, 12.86 THz to 14.35 THz with the bandwidth of 13.70 THz. The maximum directivity is 6.51 dBi and the maximum gain is 5.82 dBi. The simulated results show that the existing antenna is the right choice for Tera-Hertz application.

REFERENCE

- Basyooni A M Ahmed and M Shaban (2018) Plasmonic hybridization between two metallic nanorods *Optik* Vol. 172.
- Boopathi Rani and S.K. Pandey (2017) A CPW-fed circular patch antenna inspired by reduced ground plane and CSRR slot for UWB applications with notch band *Microw Opt Technol Lett.* Vol 59 Vol 745-749.
- Chen L Chang T Xiuqian X Xiao and H Chen (2017) Plasmonic quarter-wave plate with U-shaped nanopatches *Optik* Vol. 134 Vol 179–186.
- Choi ST Hamaguchi K Kohnor (2009) Small printed CPW-fed triangular monopole antenna for ultra-wideband applications *Microw Opt Technol Lett* Vol 51 Vol1180–1182.
- Christophe Caloz, Tatsuo Itoh. (2006) *Electromagnetic metamaterials: Transmission line theory and microwave applications* New York John Wiley & Sons Inc.
- Ding and K C Toussaint Jr (2019) Relaying of the local enhanced electric-field using stacked gold bowtie nanoantennas *Nanotechnology* Vol 30 Vol 36..
- Prasad Jones Christydass and N Gunavathi. (2017) Codirectional CSRR inspired printed antenna for locomotive short range radar *International Conference on Inventive Computing and Informatics (ICICI)*.
- Prasad Jones Christydass and N Gunavathi. (2017) Design of CSRR loaded multiband slotted rectangular patch antenna *IEEE Applied Electromagnetics Conference (AEMC)*.
- Prasad Jones Christydass and Manjunathan (2019) Pentagonal Ring Slot Antenna with SRR for Tri-Band Operation *Biosc. Biotech. Res. Comm, Special Issue* Vol 12, No 6 Vol 26-32.
- Prasad Jones Christydass and Pranit Jeba Samuel (2019) Metamaterial Inspired Slotted Rectangular Patch Antenna for Multiband Operation *Biosc. Biotech. Res. Comm, Special Issue* Vol 12 No 6 Vol 57-62.
- Sadeghi R R Gutha and H. Ali (2019) Super-plasmonic cavity resonances in arrays of flat metallic nanoantennas *Journal of Optics* Vol. 21.
- Suvadeep Choudhury and Akhilesh Mohan (2017) Miniaturized sierpinski fractal loaded QMSIW antenna with CSRR in ground plane for WLAN applications *Microw Opt Technol Lett.* Vol 59 Vol 1291-1265

TVS Based Technique for Efficient Web Document Clustering in Web Search

R Thalapathi Rajasekaran^{1*}, R. Ramesh², R. Menaka³ and Vanisri A⁴

^{1,2}Department of CSE, Chennai Institute of Technology, Chennai-600069, India.

³Department of ECE, Chennai Institute of Technology, Chennai-600069, India.

⁴Department of EEE, Chennai Institute of Technology, Chennai-600069, India.

ABSTRACT

Word grouping is significant for programmed thesaurus development, content order, what's more, word sense disambiguation. As of late, a few examinations have announced utilizing the web as a corpus. This paper proposes an unaided calculation for word bunching dependent on a word likeness measure by web tallies. Each pair of words is questioned to a web crawler, which delivers a co-event framework. By figuring the similitude of words, a word co-occurrence diagram is acquired. Another sort of chart grouping calculation called Newman bunching is applied for effectively distinguishing word bunches. Assessments are made on two arrangements of word bunches determined from a web registry and WordNet.

KEY WORDS: WEB SEARCH, CLUSTERING, TOPICAL, VISUAL STRUCTURAL (TVS).

INTRODUCTION

This work investigates another staggered Web information extraction based Topical, Visual Structural (TVS) web archive bunching for gathering the Web records. In spite of the fact that LVC-D bunching approach yielded persuading results, an another blend of a predominant Web highlights, for example, theme, visual and generally speaking structure are considered right now the TVS web report grouping is explored (Beil et al. 2002)

Overview of TVS Clustering: Web reports on the planet web are developing each day and their introduction is likewise evolving appropriately. The website specialists changing their style of introduction to assault the web

clients. Additionally the web clients produce various inquiries which must be taken care of in hopeful way. The advanced web client produces questions as indicated by their prerequisites and they search for various sort of assets. This acquaints difficulties with the web search tools and the web crawlers faces trouble in creating results to the client. Prior the web records are bunched or assembled by the metadata and now there are numerous scientists introduced web archive grouping calculations which utilizes the content highlights (Benjamin C.M et al,2003)

The techniques utilize diverse likeness gauges in distinguishing the class of the record and dependent on the similitude estimates utilized TVS strategy bunch the reports. Be that as it may, utilizing the content element alone would not help the web crawlers in creating customized results to the client. To give customized results to the client, the internet searcher needs to record the report in unexpected manner in comparison to the standard one. To accomplish this the bunching calculations needs to consider a few highlights like

ARTICLE INFORMATION

*Corresponding Author: thalapathr@citchennai.net
Received 15th April 2020 Accepted after revision 20th May 2020
Print ISSN: 0974-6455 Online ISSN: 2321-4007 CODEN: BBRBCA

Thomson Reuters ISI Web of Science Clarivate Analytics USA and Crossref Indexed Journal

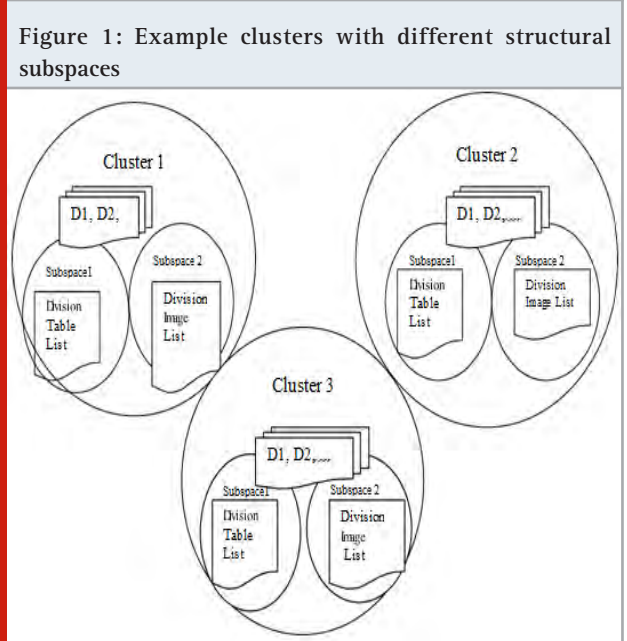


NAAS Journal Score 2020 (4.31) SJIF: 2020 (7.728)
A Society of Science and Nature Publication,
Bhopal India 2020. All rights reserved.
Online Contents Available at: <http://www.bbrc.in/>

topical, visual and auxiliary highlights. The auxiliary element speak to how the substance of the page is assembled and shown. In some cases the substance has been shown with no divisions and recognizing the class right now not a major issue (Cheng Xiang Zhai et al, 2008). In any case, when the record has been shown in divisions, passages and rundown, at that point it goes under various subspace of the class.

The pages with divisions, would be assembled into various subspace of a similar class. Likewise, the pages with numerous rundowns, sub divisions can be gathered into another subspace. For instance, the client might want to see the pages which shows the idea in various leveled way or the client might want to see the website pages in divisions. To create results to the client as indicated by their desire, the site pages must be grouped by their auxiliary highlights. By gathering the website pages as per the structure, the web search can without much of a stretch distinguish the related pages and produce results to the client(Da CruzeNassif et al,2013).

Figure 1 shows the example bunch being viewed as which has diverse basic sub classes which contains reports with various structures. The bunch gathered the equivalent basic reports of the root class into various subspace.



By gathering the reports as indicated by their structure the subspace of any class can be kept up. The web crawlers can recognize the resultant website pages dependent on the basic likeness (Divya 2014). The topical component speaks to the content element and this can be utilized to distinguish the class of the archive. The auxiliary component can be comparative for various class however the topical element has the effect and used to choose the class of the record. Each bunch has certain topical terms identified with the idea of the class. Be that as it may, not all the reports spread all the details of the point. A portion of the archives would talk about just the blueprint

of the point yet a portion of different reports would examine both diagram and explicit subtopic. Based this end product, the reports of the bunch would be gathered into subspaces. So that for the web internet searcher to deliver proficient outcomes on explicit exact question, the archives ought to be assembled into subclasses and under subspaces. For instance, on the off chance that the bunch is "Organizing", at that point the archives in the root catalog would examine just the blueprint as what is organizing and how it is performed. Be that as it may, the subclass "Systems administration Tools", would talk about the apparatuses and specialized methodologies in utilizing them. Additionally, the archives of the systems administration class could be divided into various subspaces. By remembering this, the topical measure must be estimated (Fisher et al,1987).

Figure 2: Example clusters with topical subspaces

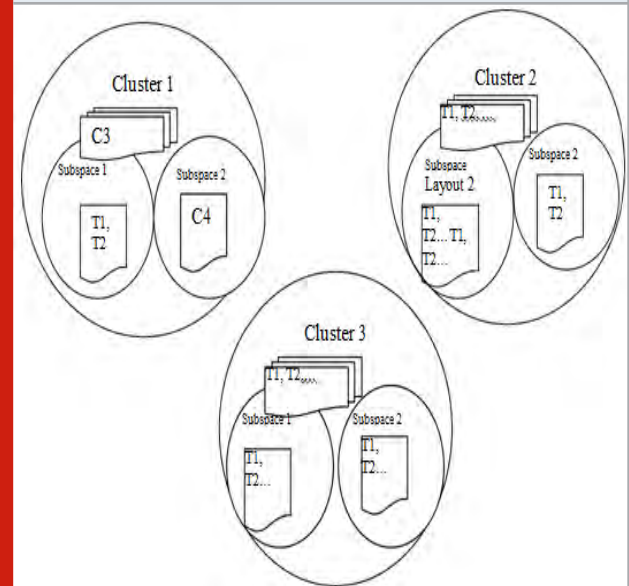


Figure 2 shows the groups with specific subspaces and every subspace has its own terms identified with the idea. By gathering the archives in various subspace as per the topical measure the issue of web record grouping can be drawn nearer in an effective way(Franz, M et al,2001). Like this, the visual element has extraordinary effect in grouping the web records. There are pages which presents the point dependent on visual substance. So the visual substance must be considered in web report bunching. The visual similitude can be assessed by tallying the quantity of visual components in the website page and the quantity of divisions of the site page. To perform bunching utilizing all the three highlights, first the calculation distinguishes various highlights present in the web report. At that point the strategy gauges distinctive comparability estimates like topical likeness, auxiliary closeness and visual similitude highlights. At that point dependent on these three highlights, the root class for the record and the subspace of the class are distinguished (Gennari et al, 1989; Hofmann 1999)

Figure 3 Block diagram of proposed TVS based web document clustering

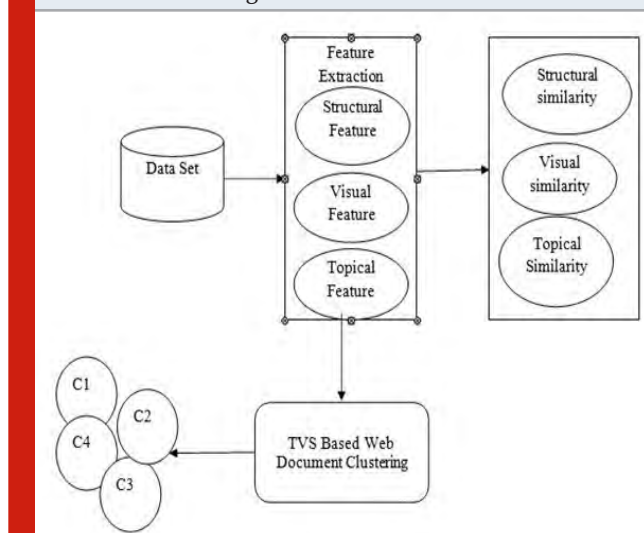
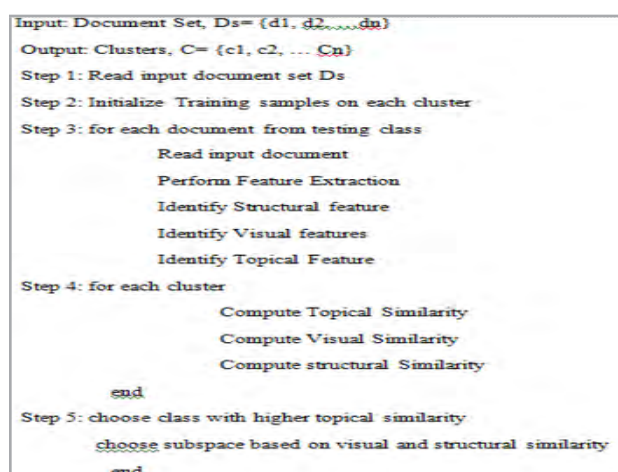


Figure 3 shows the general square chart of TVS based web record grouping calculation and shows diverse utilitarian stages. From Figure 3, the technique peruses the web record set and concentrates different highlights from the report. At that point the diverse closeness measures have been estimated. Utilizing the topical comparability measure the root class of the record has been distinguished and the rest of the highlights have been utilized to recognize the subspace of the report.

1. Feature Extraction
2. Structural Similarity Estimation
3. Visual Similarity Estimation
4. Topical Similarity Estimation
5. TVS clustering

MATERIALS AND METHODS

Algorithm for TVS clustering: Consider the record set $D_s = \{d_1, d_2, \dots, d_n\}$ with n number of archives and there exists a bunch $C = \{c_1, c_2, c_3, \dots, c_n\}$. Again each group C contains D number of reports $D = \{D_1, D_2, \dots, D_n\}$.



Each archive D contains visual highlights $V = \{v_1, v_2, \dots, v_n\}$, and different basic element $S = \{s_1, s_2, \dots, s_n\}$ and topical highlights as $T = \{T_1, T_2, \dots, T_n\}$. In light of this result, the archive from the informational index D must be distinguished for a bunch C_x , in view of TVS comparability measures.

Applying Feature Extraction

The element extraction assumes the underlying job in the TVS bunching calculation which extricates different highlights of the web record considered. The web archive would contain a few auxiliary highlights due to the nearness of records, tables, etc. It recognizes such highlights and split them from the web archive. Correspondingly, the nearness of visual highlights is distinguished and separated. At last, the topical highlights like content has been distinguished and removed from the web report. Other than the basic and visual highlights, the topical element are preprocessed to expel the stop words and stemmed to deliver unadulterated terms. Distinguished highlights have been utilized to gauge distinctive similitude towards the bunches considered.

Measuring Topical Similarity: The topical similitude speaks to the closeness of the archive as far as the idea being talked about. The basic and visual highlights would be comparable in various class archives however the key issue is the theme which has been talked about in the web report. For the report D_1 , the rundown of terms present can be recognized by applying stemming and grammatical feature labeling.

Likewise, the term set T_b can be produced by playing out the equivalent in the record D_2 . It isn't important that all the terms of archive D_1 ought to be available in the record D_2 . They would contain various terms of same class. Yet, so as to process the topical comparability, the utilization of WordNet lexicon and open index undertaking can be utilized. The word reference delivered can be utilized to appraise the topical measure. The Topical Term Set (TTS) contains the terms from WordNet and open registry venture scientific categorization.

Measuring Structural Similarity: The auxiliary closeness is a measure which speaks to the similitude of the reports as far as their structure. The site pages would have composed the substance in various structure which produces diverse structure to the site page. By processing the auxiliary closeness of the site pages the client intrigued result on specific structure can be produced. The basic similitude is the measure processed dependent on the structure of the site page given.

Each web archive would contain distinctive structure and from the basic components present in the web report, the Structural Similarity Measure (SSM) worth could be processed. For instance, the web archive D_i contains a structure S , at that point the basic comparability is processed towards various classes. The auxiliary comparability is figured by considering all the basic components of the web record.

Measuring Visual Similarity: The visual closeness speaks to similitude in the website pages as indicated by their visual components. A few pages would contain pictures and some of them would contain recordings. By estimating the visual similitude, the client solicitation can be satisfied in careful way. The web index would create result with progressively visual components. A few pages may depict the idea dependent on visual components and the client would search for progressively visual portrayals. In such cases the visual comparability based information recovery or grouping would help. To accomplish that, the visual closeness has been assessed between various records of the bunch.

Visual likeness is the measure processed dependent on the visual parts present in the web record. The info web record would contain number of pictures and visual documents of wave type. By distinguishing the visual substance present in the web record the VSM measure can be assessed.

TVS Clustering: The TVS grouping calculation peruses the web archive and concentrate the visual basic and topical highlights from the web record. At that point for each group c, the topical similitude measure is registered. In light of the assessed topical likeness measure, a solitary class has been distinguished and chosen. Later the visual and basic similitude measures are figured with the subspace of the class being recognized. In view of both the measures a solitary subspace has been recognized and recorded [15].

```

TVS Clustering Algorithm
Input: Document set, Ds
Output: Clusters, C = {c1, c2, ...}

Step 1: Read document set Ds.
Step 2: for each class C
    compute topical similarity measure Tsim.
end
Step 3: choose the class with higher topical similarity measure.
Step 4: for each level L
    compute visual similarity measure VSM.
    compute structural similarity measure SSM.
    compute weight measure, Wm = VSM×SSM
end
Step 5: choose the next level class according to the weight
    
```

The above discussed clustering algorithm computes different similarity measures and computes the weight. Based on the computed weight a single class is selected for assigning the document.

RESULTS AND DISCUSSIONS

Performance Evaluation

This segment presents the estimation of the proposed TVS

approach regarding exactness rates among assortment of datasets. The nature of each group parcel procured by this strategy is assessed against two diverse bunch likeness recognition informational collections GDS and SDS

Evaluation Criteria: The trial investigation is completed to watch the presentation of the TVS rather than two ordinary grouping calculations MDR and ViDRE. So as to break down the productivity of the proposed work, the last bunching aftereffects of every technique is assessed with its proper genuine names by utilizing the precision measurements.

Comparison of TVS with Existing Approaches: The recently proposed TVS Clustering strategy is contrasted with two bunching systems with assess its presentation.

ViDRE Based Clustering Method (ViDRE): The ViDRE based bunching calculation evaluates just the visual closeness of the info reports to perform web record grouping. This acquaints higher bogus order due with the absence of concerning different highlights.

MDR Clustering Method: The MDR bunching calculation consider just the substance and registers the information rate esteems to perform grouping dependent on the figured MDR values the web archives are bunched.

Experimental Results: The trial aftereffects of TVS shows the normal grouping precision of 99.4% which is 14.4% better bunching contrasted with MDR bunching and 1.0 % better contrasted with ViDRE grouping calculation as indicated by the GDS informational collection. So also, 21 % improvement has been accomplished in the SDS informational index contrasted with MDR calculation and 0.9% exactness has been improved than the ViDRE calculation.

Figure 4: Comparison of clustering accuracy of the proposed TVS method with the existing MDR and ViDRE methods

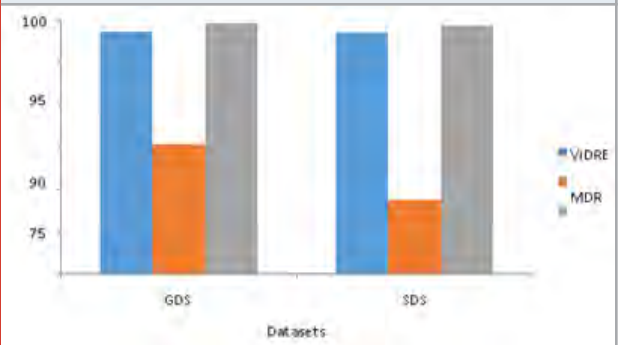


Figure 4 shows the correlation on exactness delivered by various strategies on two distinct informational indexes GDS and SDS. The outcome shows that the proposed TVS calculation has more noteworthy improvement in bunching precision than different techniques.

Performance Evaluation with other Metrics: The execution of the bunching calculation has been

estimated with different parameters like running time unpredictability and F-measure for the proposed TVS web report grouping calculation [19]. Figure 5 shows the correlation on time multifaceted nature delivered by various techniques on grouping 2 million records. The proposed TVS grouping calculation has created less time intricacy than different techniques. The TVS grouping calculation came about into bunches in 1433 seconds where different techniques considered finished in higher time contrasted with TVS grouping approach [20].

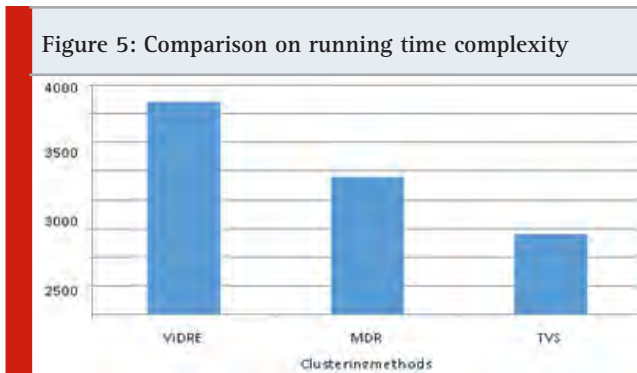
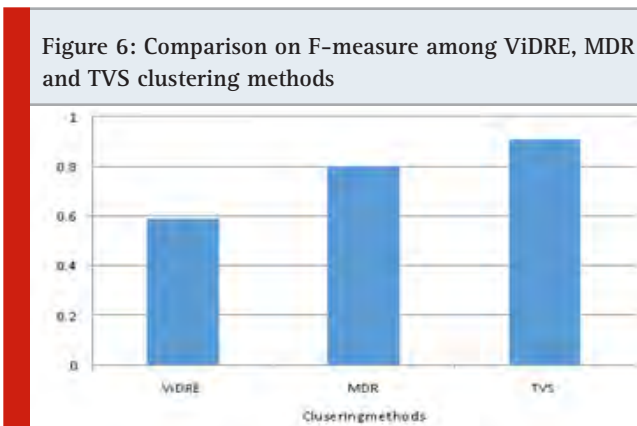


Figure 6 shows the comparison of F-measure produced by different methods. The proposed TVS algorithm shows better F-measure than the other methods.



CONCLUSION

The proposed TVS bunching calculation improves the exhibition of web record grouping dependent on the topical, visual and basic measures. The strategy shows preferred grouping results over different techniques considered for bunching the web archives. Consequently right now, (as level 1), visual (as level 2) and structure (as level 3) of web records are considered to bunch the reports into gatherings. The outcomes are very persuading as multilevels are removed cautiously for bunching process.

REFERENCES

- Beil et al (2002) Frequent term-based text clustering ACM SIGKDD international conference on Knowledge discovery and data mining Pages 36-442.
- Benjamin CM Fung Ke Wang & Martin Ester (2003) Hierarchical Document Clustering Using Frequent Itemsets In Proceedings SIAM International conference on data mining Pages 59-70.
- Cheng Xiang Zhai (2008) Statistical Language Models for Information Retrieval Foundations and Trends in Information Retrieval vol 2 no 3 Pages 137-213.
- Da CruzeNassif (2013) Document Clustering for Forensic Analysis: An Approach for Improving Computer Inspection IEEE Transactions on Information Forensics and Security vol 8 no 1 pp 234-238.
- Divya (2014) Text Clustering Using Novel Hybrid Algorithm Asian Conference on Intelligent Information and Database Systems ACIIDS 2014: Intelligent Information and Database Systems Pages 11-21.
- Fisher (1987) Knowledge Acquisition via incremental conceptual clustering presented COBWEB Springer Machine Learning vol 2 no 2 Pages 139-172.
- Franz M Ward T McCarley J & Zhu WJ (2001) Unsupervised and supervised clustering for topic tracking ACM SIGIR conference on Research and development in information retrieval Pages 310-317.
- Gennari & Langley (1989) Models of incremental concept formation Science Direct Artificial Intelligence vol 40 no 1-3 Pages 11-16.
- Hofmann (1999) Probabilistic Latent Semantic Indexing CM SIGIR conference on Research and development in information retrieval Pages 50-57.
- Liu YB Cai JR Yin J & Fu AWC (2008) Clustering Text Data Streams Springer Journal of Computer Science and Technology vol 23 no 1 Pages 112-128.
- Lu & Mei (2011) Investigating task performance of probabilistic topic models Springer Information Retrieval vol 14 no 2 Pages 178-203.
- Ma J Xu W Sun YH Turban E Wang S & Liu O (2012) An ontology-based text-mining method to cluster proposals for research project selection Systems Man and Cybernetics Part A: Systems and Humans IEEE Transactions on 423 2012 Pages 784-790.
- Ming & Wang (2010) Prototype hierarchy-based clustering for the categorization and navigation of web collections CM SIGIR conference on Research and development in information retrieval Pages 2-9
- Muhammad Rafi (2010) Document Clustering based on Topic Maps International Journal of Computer Applications vol 12 no 1 Pages 32- 36.
- Na & yongand (2010) Research on K-means Clustering Algorithm IEEE Third International Symposium on Intelligent Information Technology and Security Informatics IITSI

Pages 63-67.

Nadjet Kamel(2014) A Sampling-PSO-K-means Algorithm for Document Clustering Proceedings of the Seventh International Conference on Genetic and Evolutionary Computing ICGEC 2013 Prague Czech Republic Springer Genetic and Evolutionary Computing Pages 45-54.

Rege & Dong (2006) Co-clustering Documents and Words Using Bipartite Isoperimetric Graph Partitioning IEEE Data Mining ICDM 06.

Relevant Document Information Clustering Algorithm

for Web Search Engine International Journal of Advanced Research in Computer Engineering and Technology IJAR CET vol 1 no 8 pp 16-20. 20 Xu & Gong (2004) Document clustering by concept factorization ACM SIGIR conference on Research and development in information retrieval Pages 202-209.

Zhang & Ghahramani (2007) Probabilistic model for online document clustering with application to novelty detection ACM Neural Information Processing Systems Pages 1617-1624.

A Survey Paper on Different Feature Extraction Methods in Image Processing

N.Hemalatha^{1*}, T. Menakadevi² and A. Kavitha³

^{1*}Assistant Professor, Department of ECE, Sudharsan Engineering College, Pudukkottai-622501, India.

²Professor, Department of ECE, Adhiyamaan College of Engineering, Hosur-635109, India.

³Professor, Department of ECE, K. Ramakrishnan College of Technology, Trichy-621112, India.

ABSTRACT

Feature extraction incorporates reducing the quantity of datas required to define a gigantic arrangement of resources. Investigation of progressively number of factors requires immense measure of memory and computation power. The writing on feature extraction is very rich including numerous strategies with each methodology giving trade-offs between different variables. This paper looks at in a general sense on the various sorts of strategies that are existing and assembling it for a literature survey.

KEY WORDS: SVM, MATLAB, FPGA, XILINX ISE, ENHANCEMENT, VERILOG-HDL, BINARY DESCRIPTOR, FEATURE EXTRACTION, KEYPOINT DETECTOR, HCR, HAS, BRIEF, SURF AND SIFT.

INTRODUCTION

Feature extraction starts from an underlying arrangement of estimated data and builds determined expected to instructive and non-repetitive. At the point when the information to a calculation is exceptionally huge to be handled and it is suspected to be repetitive, at that point it might be changed into a decreased set of features. Deciding the subset of starting features is called feature selection. The picked features are depended upon contain the helpful data from the information, with the goal that the appetency assignment can be performed by utilizing the reduced representation instead of the total beginning information.

In picture classification, the local features of the picture are used to recognize the various pictures. These features are arranged on the different key segment of picture information like color intensity, edges of the articles present in picture, texture, and so on. The quality of the image processing is depends on the efficiency of the feature extraction process. These features can be utilized in picture matching, design acknowledgment and retrieval. These applications require the smaller and significant data to accomplish high level of exactness. An input picture groups huge complex and repetitive data. The procedure of transferring information to reduce the dimension of the feature is called as feature determination or feature selection. Picture examination is a procedure wherein feature of the pictures are separated and break down for further processing. It is not the same as other picture handling tasks like reclamation, coding and enhancement. Picture examination includes the detection, segmentation, extraction and classification techniques. Feature extraction system is utilized to separate the features without losing its original information for large image databases. Efficiency and effectiveness of feature choice and extraction are serious challenges presently. Various strategies are utilized to concentrate features like

ARTICLE INFORMATION

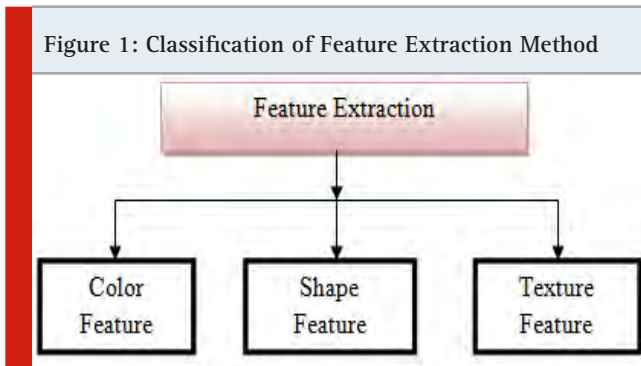
*Corresponding Author: hemalatha.n1985@gmail.com
Received 15th April 2020 Accepted after revision 20th May 2020
Print ISSN: 0974-6455 Online ISSN: 2321-4007 CODEN: BBRBCA

Thomson Reuters ISI Web of Science Clarivate Analytics USA and Crossref Indexed Journal



NAAS Journal Score 2020 (4.31) SJIF: 2020 (7.728)
A Society of Science and Nature Publication,
Bhopal India 2020. All rights reserved.
Online Contents Available at: <http://www.bbrc.in/>

shape, color and texture as feature vector. The strategies for feature extractions are arranged are appeared in Fig. 1.



Step1: The picture is predestined by utilizing quick color quantization calculation with cluster blending, and afterward a modest number of dominant colors and their rates can be acquired.

Step2: The spatial surface features are separated utilizing a steerable filter deterioration, which offers a capable and versatile estimation of early handling in the human visual framework.

Step3: The pseudo-Zernike snapshots of a picture are utilized for shape descriptor, which have better features representation limits and are added strong to noise than other moment representations.

Step4: The blend of the color, texture and shape features outfit a vigorous feature set for picture retrieval.

This paper investigated a few feature extraction methods to analyse the picture. Feature extraction techniques are delegated the low-level feature and a high state feature extraction. Low dimension feature has little information of the picture like point, line, edge and corner and so forth. Low dimension feature can be extracted naturally from the picture without knowing about shape. High state feature are based over low-level features to recognize items and bigger shapes in the picture

Image Feature Extractions Using Color Space Models
 Despite the fact that there are a few techniques executed for the extricating the features of pictures, however picture feature extraction utilizing color-based feature extraction is a significant strategy. In all the technique mean, skewness and standard deviation is figured with the goal that the features can be extracting effectively.

$$\mu_i = \frac{1}{N} \sum_{j=1}^N f_{ij}$$

$$\sigma_i = \left(\frac{1}{N} \sum_{j=1}^N (f_{ij} - \mu_i)^2 \right)^{\frac{1}{2}}$$

$$\gamma_i = \left(\frac{1}{N} \sum_{j=1}^N (f_{ij} - \mu_i)^3 \right)^{\frac{1}{3}}$$

The above equations are utilized to compute mean and standard deviation and skewness separately. Where f_{ij} is used for the color value and N denotes the number of pixels present in the picture.

The various kinds of color techniques that are described as per the following:

Table 1. Various Colors Space models for feature extraction

Color Method used for Extraction	Usages of the methodology
Histogram	Simple to Compute
CM	It is simple and robust to use.
Correlogram	It provides spatial information
CSD	It provides spatial information
CCV	It provides spatial information
SCD	It is adaptable and simple.
DCD	It is simple to use and robust too

Literature Survey of Image Feature Extraction Using Different Methods

1. Support Vector Machines Technique: In 2017, Abdelhak Boukharouba and Abdelhak Benniab proposed an effective handwritten digit recognition framework dependent on Support vector machines (SVM) procedure. A tale feature set dependent on progress data in the vertical and horizontal directions of a computerized picture collaborative with the well-known Freeman chain code was proposed. The fundamental lump of this feature extraction calculation is that it doesn't require any standardization of digits. These credits are easy but difficult to actualize stood out from various systems. They assessed their stratagem on 80,000 handwritten examples of Persian numerals and achieved extremely encouraging outcomes.

2. Binary Descriptor Coding Technique: In 2014, Pedro Monteiro, Joao Ascenso and Fernando Pereira proposed efficient binary descriptor coding technique. In a visual sensor network, countless camera hubs can gain and process picture information locally. Normally, camera hubs have serious imperatives as far as energy, bandwidth resources and handling abilities. Attaching these specific attributes, coding and transmission of the pixel-level depiction of the visual scene must be avoided, on account of the energy resources required. A promising approach is to passage at the camera centers, limited visual features that are coded to meet the information move limit and power necessities of the essential framework and gadgets. Since the full scale number of features extracted from a picture might be somewhat critical, they proposed a novel strategy to pick the important features before the real coding procedure. The arrangement depends on a score that estimate the exactness of every local feature. At that points, nearby features are positioned and just

the most relevant features are coded and transmitted. The selected features must expand the effectiveness of the picture analysis task yet additionally limit the required computational and transmission resources. Exploratory outcomes demonstrate that higher efficiency was accomplished when contrasted with the past best in class.

3. Feature Extraction Using Xilinx System Generator:

In 2014, Swapnil G. Kavitar and Prashant L. Paikrao proposed Feature Extraction Using Xilinx System Generator technique. Picture Features are the explanation behind by far most of the steady picture handling applications. Edge is the unique features of picture. It makes us dismember, infer and take decision in various picture handling applications. They proposed sobel and prewitts calculations over Field Programmable Gate Array (FPGA). Real time framework needs dedicated equipment for picture processing applications. FPGA has various exceptional features that fill in as a stage for processing constant calculations and gives generously better execution over programmable Digital Signal Processor (DSPs) and microchip. An exceptionally present-day approach of Xilinx System Generator was utilized for framework demonstrating and FPGA programming. Bit stream file (*.bit), netlist, timing and power analysis are generated by using XSG which is a tool of Matlab.

4. Image Enhancement Algorithms for Biomedical Image Processing:

In 2013, Praveen vanaparthi, Sahitya.G, Krishna Sree and Dr.C.D.Naidu discussed possible Image Enhancement algorithms for biomedical image processing. Advanced picture enhancement methods are to improving the visual nature of pictures. They proposed the Realtime equipment based diverse picture upgrade systems utilizing FPGA and concentrated on the usage of various calculations like brightness control, contrast stretching, negative transformation and thresholding. Sifting strategies on FPGA was a significant decision for superior advanced sign preparing applications. These calculations were effectively executed in Verilog HDL utilizing Xilinx ISE, MATLAB and MODELSIM. The aim of this work was to recreate and execute these calculations utilizing Verilog HDL. The gadget chose here for execution is (Spartan-3E) from Xilinx.

5. Binary-Descriptor-Based Image Feature Extraction Accelerator:

In 2016, Wenping Zhu, Leibo Liu, Guangli Jiang, Shaojun Wei and Shaojun Wei proposed new binary descriptor-based image feature extraction accelerator. Binary picture descriptors, which get picture feature description from the local picture fixes truly, are by and large grasped in the mobile and embedded applications on account of lower computational multifaceted nature and memory need. With the purpose of improving the count efficiency without corrupting affirmation execution, a lightweight binary descriptor was proposed subject to the examination of condition of-the art parallel descriptors in this paper. A directional edge recognition and advanced keypoint score function were created to refine the keypoints. Moreover, turn

invariance is accomplished by executing roundabout symmetric-based descriptor age and a coarse-grained direction computation procedure at the same time. The results shows that the proposed key point finder and double descriptor accomplish multiple occasions speedup and at any rate 23.6% improvement in handling speed with practically identical execution, separately. Moreover, huge scale integrate architecture was additionally structured dependent on in-depth investigation of bit-level and assignment level parallelism.

6. Feature Extraction for Handwritten Character Identification:

In 2015, Muhammad Arif Mohamad and Haswadi Hassan proposed Feature Extraction for Handwritten Character identification technique. The improvement of handwriting character Identification (HCI) is a fascinating zone with regards to design recognition. HCI framework comprises of various stages which are pre-preparing, feature extraction classification and pursued by the real recognition. It is commonly concurred that one of the principle components affecting execution in HCI is the assurance of a suitable course of action of features for addressing incorporate samples. This article provides an analysis of these advances. In a HCI, the choosing of features plays as main issues, as system in picking the significant feature that yields least order error. To overcome these issues and expand arrangement execution, numerous procedures have been proposed for reducing the dimensionality of the feature space in which information must be handled. These procedures, by and large meant as feature decline, might be partitioned into two principle classes, called feature extraction and feature selection. Incalculable papers and reports have just been distributed regarding this matter. In this article, we give an audit of a bit of the procedures and approach of feature extraction and determination. All through in this paper, we apply the examination and investigation of feature extraction and choice methodologies in order to get the present pattern. All through this article, likewise the audit of meta heuristic harmony search calculation (HSA) has provided.

7. Binary Morphological Processing for Image Feature Extraction:

In 2015, Sumera Sultana and R. Ganesh proposed Binary Morphological Processing for Image Feature Extraction technique. The present advanced world requires the necessity for picture feature extraction from pictures, recordings, moving thing, and so forward in the uses of medical, surveillance, authentication and automated industry assessment. The numerical morphology is a methodology of tolerating picture pixel esteems and performing algorithmic computations like enlargement, disintegration, opening, and shutting, and so forward. The scientific morphology can be organized and executed by using the product, Digital Signal Processing (DSP) and FPGA/ASIC. The Software and DSP usage are moderate in task and can't be used for quick applications. Thus, FPGA execution can be used for quick applications. The proposed arrangement acknowledges a data picture from a video/photograph and changes over into picture pixels network.

8. Feature Extraction of Moving Objects with Edge

Detection: In 2017, N. M. Wagdarikar and M. R. Wankhade proposed Feature Extraction of Moving Objects with Edge Detection technique. For some applications, for example, medicine, space investigation, observation, confirmation, mechanized industry examination and a lot more zones advanced picture processing is an expanding and dynamic territory with applications connecting into our regular day to day existence. Feature extraction and Edge location are the significant procedure in movement acknowledgment and it is required to be handled for structure rapid frameworks. Edge is a fundamental feature of a picture. Edges characterize the limits between districts in a picture by finding sharp discontinuities in pixel esteems, which assists with division and object recognition. Edge identification in pictures reduces the measure of information and filter through pointless data, while protecting the significant properties in picture. Consequently, edge location is in the front line of picture processing for object identification. This framework gives an account of Sobel Edge Detection algorithm and labelling algorithm to extract the features from images. And feature extraction moving images that is video is done using subtraction method.

9. Faster Image Feature Extraction Hardware: In 2016, Sherin Das, Jibu J.V and Mini Kumari G proposed new faster image feature extraction hardware. Scale Invariant Feature has numerous applications in various fields particularly in Computer vision. From that point onward, various procedures were proposed to improve filter includes by adding a few highlights to unique SIFT. SURF, n-dimensional SIFT, CSIFT, GSIFT are some of them. One of the significant constraints of SIFT in real time is its computational delay. In light of its computational complexity and enormous time delay its equipment execution is a difficult task. A few strategies were proposed to improve the speed of SIFT. In this paper they proposed new design to improve the speed of key point identification part of sift algorithm.

10. Image Processing using Xilinx System Generator (XSG)

in FPGA: In 2015, Himanshu Vaishnav, Ankita gupta and Himanshu Garg proposed new Image Processing strategy utilizing Xilinx System Generator (XSG) in FPGA. They broke down and gave the theoretical depiction of programming reenactment for picture processing by utilizing XSG and equipment. They additionally gave the hypothesis and reasonable parts of the technique, which gives a great deal of Simulink model for a few equipment tasks using different Xilinx that could be executed on different FPGA. They proposed a beneficial design for different picture preparing calculations for picture negatives, picture improvement; differentiate extending, Image Edge Detection, picture Brightness Control, Range Highlighting Transformation, Parabola change for grayscale and color pictures by using least possible System Generator Blocks. Exhibitions of theories structures executed in FPGA card XUPV5-LX110T prototyping Virtex5 were displayed.

11. A Comparative Study of Feature Extraction Methods

in Images Classification: In 2015, Seyyid Ahmed Medjahed proposed A Comparative Study of Feature Extraction Methods in Images Classification. Feature extraction is a significant part in picture processing. By utilizing this, we effectively represent the picture. In this paper, they unmistakably clarified the idea of a few feature extraction systems under various classifiers. For this, they utilize paired and multiclass characterizations and its deliberate regarding grouping exactness rate, review, accuracy, f-measure and other assessment measures. The goal is to locate the best strategy with improved exactness rate.

12. A Review of Feature Extraction Techniques for Image Analysis:

In 2017, Rajkumar Goel, Vineet Kumar, Saurabh Srivastava and A. K. Sinha proposed an audit of feature extraction systems for picture analysis. Feature extraction is the most significant advance in picture characterization. It helps in separating the feature of a picture as perfect as could be allowed. In this paper, they checked on different feature extraction methods. These techniques are named low-level feature extraction and High-level feature extraction. Low-level feature extractions depend on finding the points, lines, edge, and so forth while high state feature extraction techniques utilize the low dimension feature to give increasingly huge data to further processing of Image analysis. For the most part high level state feature extraction strategy utilizes the Artificial Neural Network (ANN) to separate the feature in numerous layers.

13. Recent Advances in Features Extraction and Description Algorithms:

A Comprehensive Survey: In 2017, Ehab Salahat and Murad Qasaimeh, proposed the ongoing advances in features extraction and depiction calculations: a comprehensive study. Computer vision is the most dynamic research fields in data innovation today. Enabling machines and robots to see and understand the including scene at the speed of sight makes ceaseless potential applications and openings. Feature location and description algorithms can be without a doubt considered as the retina of the eyes of such machines and robots. In any case, these calculations are commonly computationally raised, which shields them from accomplishing the speed of sight continuous execution. Also, they fluctuate in their abilities and some may support and work better given a specific kind of data contrasted with others. In that capacity, it is fundamental to minimalistically report their favourable circumstances and inconveniences just as their exhibitions and continuous advances. This paper is committed to giving a broad survey of the cutting edge and late advances in feature identification and depiction calculations. In particular, it begins by outlining essential thoughts. It then point thinks about, reports and inspects their presentation and capacities. The Maximally Stable Extremal Regions calculation and the Scale Invariant Feature Transform calculations, being two of the best of their sort, are picked to report their progressing algorithmic subordinates.

RECOMMENDATION FOR FUTURE WORK

Literature Review of the various image feature extraction algorithms lead to a wide research idea.

- VLSI architecture for medical image processing.
- VLSI architecture for colour image processing.
- Low power VLSI architecture for image scaling.
- Low power VLSI architecture for image scaling and noise reduction.

CONCLUSION

Subsequently some efficient feature extraction methods are presented. Feature extraction is utilized to minimize the dimension of picture and it is required to complete image coordinating and recovery quickly. To finish up, every one of the procedures are helpful for real time picture processing. Every method is unique and gives proper outcomes for every strategy. Every new strategy is advancing thus determination of appropriate method will prompt keep up the nature of the picture and achievement in feature extraction process. However, much more needs to occur in the territory of Image Processing. This field will develop and impact human life in unfathomable ways throughout the following decade.

REFERENCES

- Abdelhak Boukharouba and Abdelhak Bennia (2015), Novel feature extraction technique for the recognition of hardware digits, *Applied Computing and Informatics*, pp. 19-26.
- Pedro Monteiro, Joao Ascenso and Fernando Pereira (2014), Local feature selection for efficient binary descriptor coding, *IEEE Trans. Image process.*, pp. 4027-4031.
- Swapnil G.Kavitkar and Prashant L.Paikrao (2014), FPGA based image feature extraction using Xilinx System Generator, *IJCSIT*, vol.5 (3), pp. 3743-3747.
- Praveen Vanaparthi, Sahitya.G, Krishna Sree and Dr.C.D.Naidu (2013), FPGA implementation of image enhancement algorithms for biomedical image processing, *IJAREEIE*, vol.2, no.11 pp5747-5753.
- Wenping Zhu, Leibo Liu, Guangli Jiang, Shouyi Yin and Shaojun Wei (2016), Binary descriptor based image feature extraction accelerator, *IEEE Trans. Circuits and systems*, vol 26, no. 8, pp. 1532-1543.
- Muhammed Arif mohamad, Dewi Nasien, Haswadi Hassan and Habibollah Haran (2015), A Review on feature and extraction and feature selection for handwritten charactor recognition, *IJACSA*, vol. 6, No.2, pp. 204-212.
- Sumera Sultana and Ganesh.R (2015), FPGA implementation of binary morphological processing for image feature extraction, *IJERT*, vol. 4, No. 10, pp. 497-501.
- N.M Wagdarikar and M.R,Wankhade(2017) , Feature extraction of moving objects with edge detection, *IJAREEIE*, vol. 6, No. 7, pp. 5447-5456.
- Jibu J.V.Sherin Das, Mini Kumari.G (2016), Faster image feature extraction hardware, *IOSR-JCE*, pp. 33-38.
- Ankita gupta, Himanshu Vaishnav and Himanshu garg (2015), Image processing using Xilinx System Generator in FPGA, *IJRSI*, vol. 2, No. 9, pp. 119-125.
- Seyyid Ahmed Medjahed (2015), A Comparative Study of Feature Extraction Methods in Images Classification, *I.J. Image, Graphics and Signal Processing*, 2015, pp. 16-23, MECS.
- Rajkumar Goel, Vineet Kumar, Saurabh Srivastava and A. K. Sinha (2017), A Review Of Feature Extraction Techniques For Image Analysis, *IJARCCCE*, vol 6,no. 2, pp. 153-155.
- Ehab Salahat, and Murad Qasaimeh (2017), Recent Advances in Features Extraction and Description Algorithms: A Comprehensive Survey, *IEEE*.

Multi Input Dc-Dc Converter for Electric Vehicle Application

S. Dineshkumar^{1*}, K. Sureshkumar², S. Dheepak³, and B. Cibishanth⁴

^{1*}Assistant Professor,

^{2,3,4}UG Scholars Department of Electronics & Electronics Engineering, M.Kumarasamy College of Engineering, Karur, India

ABSTRACT

In recent development in electric vehicle technology mainly focus on technology. In single system the entire control is performed in simple control topology. The Key features of this system are three technical concepts. Electromagnetic, electrical, magnetic interfacing methods. In this article multi input sources because better performance of EV drive system with good efficiency, cost effective, very emerging power converting technics involved. Most collective information of the system is design multi input source of EV system and application DC/DC converter topology. MAT lab Simulink is used for verify the performance of the EV system which is Multi input DC to DC converter topology. The entire model is simulated and output of each system is evaluated.

KEY WORDS: DC/DC CONVERTER, MULTI INPUT DC, PHOTOVOLTAIC (PV), BATTERY.EV SYSTEM.

INTRODUCTION

The modern technology development Electric vehicle is major choice for all kind of users. Electric vehicle is majorly used as Pure battery operated electric vehicle, hybrid electric vehicle which is operate either fuel or battery operated electric vehicle. For charging of this type of vehicle charging station is established in globe. It is claiming that pollution free environment for users and globe. To overcomes the pollution the vehicle is operated in the new adoptive methodology of renewable energy supported Electric vehicle.

This type of vehicle is charging of battery is very easy through the renewable energy resource. Photovoltaic cell is

adopted in rooftop of the vehicle it cause the more efficient run when acceleration is needed. Standalone system is adopted in this vehicle for compact in size. Renewable energy resource adopted vehicle is continuously operate in flexible mode due to it depends weather. Solar power energy utilization based on irradiation output voltage is varies. For high level of irradiation optimum level of output is obtained from conversion process.

Cloudy and shaded condition solar energy output is vary to minimum output voltage level. Wind based energy system; energy harvesting is also cause the availability of wind sources. The output of wind energy system is also varies. The DC to DC converter is directly coupled to energy system; this may amplify the output into higher values or buck to lower levels. Various topologies recommended for the regulated output, especially during the lower input voltage conditions.

ARTICLE INFORMATION

*Corresponding Author: dhineshselvaraj@gmail.com

Received 15th April 2020 Accepted after revision 20th May 2020

Print ISSN: 0974-6455 Online ISSN: 2321-4007 CODEN: BBRCBA

Thomson Reuters ISI Web of Science Clarivate Analytics USA and Crossref Indexed Journal



NAAS Journal Score 2020 (4.31) SJIF: 2020 (7.728)

A Society of Science and Nature Publication,
Bhopal India 2020. All rights reserved.

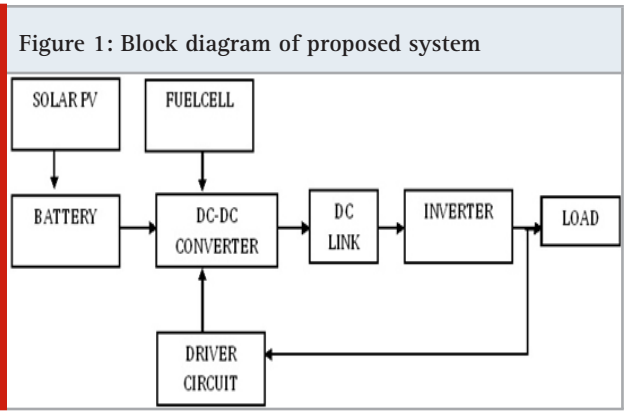
Online Contents Available at: <http://www.bbrc.in/>

Conventional topologies is proposed for mitigate the research gap hybrid multi input DC to DC converter is proposed here. Overall loss and voltage stress are concentrating the minimum voltage level. Multi input converter topology has more benefit minimum cost, power density and power management is very high.

Solar energy system dc to dc converter with multiple input system is utilizes battery and solar energy system as a input sources in the system classified into magnetically coupled system and electrically coupled system. Power transfer method on multi input converter leakage and phase angle are used to control the multi input converter for follow at each level. Galvanic isolation provides flexible output voltage levels.

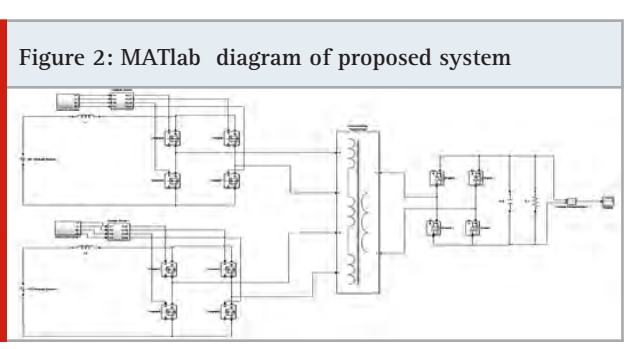
MATERIALS AND METHODS

Proposed System: Multi input DC – DC converter topology has two input energy sources. Renewable energy source (Solar PV) as one of the input energy source. Solar PV output voltage is regulated and output energy is used to store in battery. Second input energy source is fuel cell. Fuel cell output voltage is directly coupled to DC-DC converter. The block diagram refers to entire system.



DC – DC converter is operating in Buck and Boost mode of operation. Electric vehicle is operate in acceleration mode while it is run to claim with high requirement of supply energy. DC to DC converter is operate in boost mode of operation. Electric vehicle is operating in braking operation DC to DC converter is operating as Buck mode of operation. The regenerative energy is utilized for store into battery system.

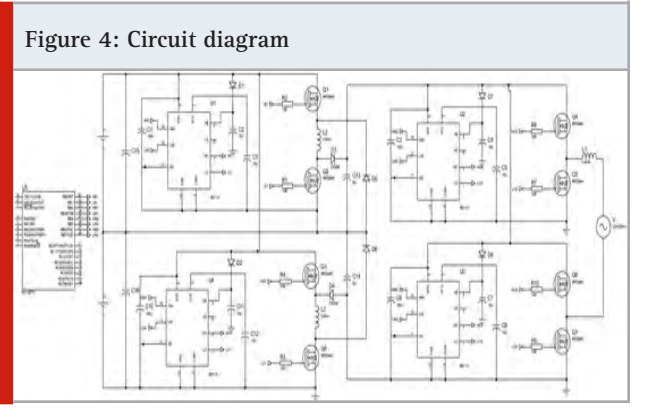
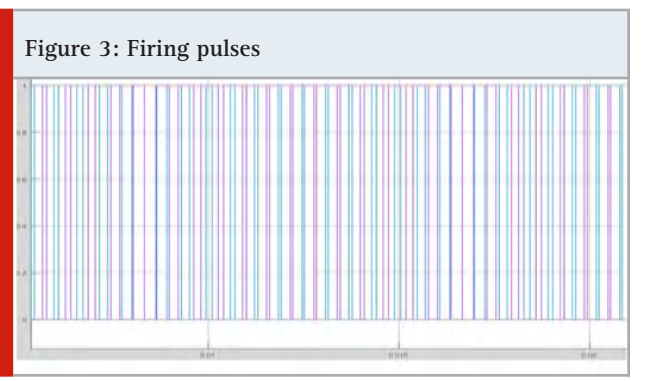
METHODOLOGY



In this Figure 2 shows about overall circuit model. Two type of converter are connected to two winding transformer. Firing pulse for that converter is provided by pulse generator. Switching frequency of each switch is calculated and firing pulse provided for those switches as per switching pattern.

In Figure 2 illustrate the switching firing pulses for all converter switches such as solar panel powered converter and fuel cell coupled converter. Each pulse are provided based on feedback signal .

RESULTS AND DISCUSSIONS

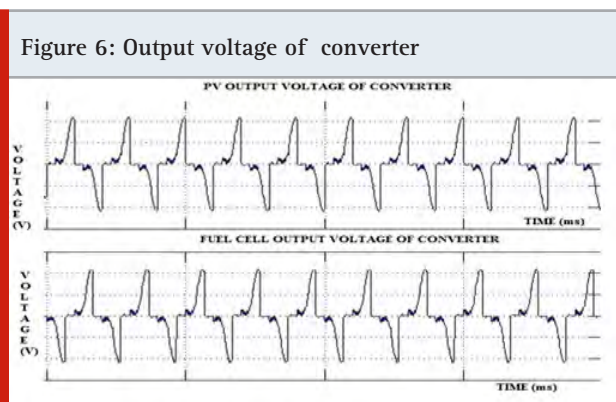
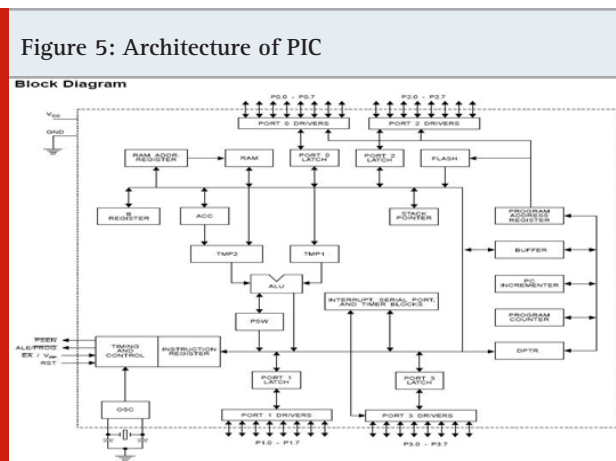


The converter switches are fired each switch is simultaneously operated. The above fig 4 shows firing circuit with help of firing circuit fuel cell is directly coupled to converter it seems that entire converter triggered based on output voltage get from fuel cell. The DC output voltage get from the fuel cell is converting into AC supply voltage.

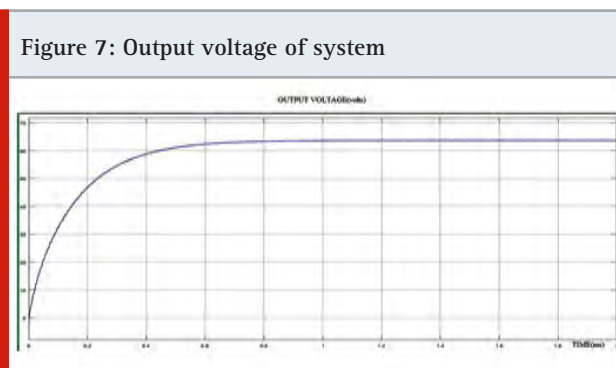
Solar PV output voltage is varied based on climatically change. Output voltage level is regulated and the supply output from Solar PV is stored in battery system. Solar output is regulated and provides the entire energy to the system which is coupled to battery. Battery gives the supply input of converter. DC-DC converter is control output voltage of the system .Converter firing pulse are feedback from load side voltage feedback. Based on the feedback signal microcontroller PIC16F72 is triggered each of MOSFET devices.

The Figure 6 shows the converter output voltage each converter gives output voltage of 25v.both converter

firing pulses are determined based on feedback signal of load side. Either the load side voltage variation is in low or high converter triggering pulse is also varied.



The Figure 7 shows output voltage of inverter circuit. Based on converter input supply voltage it gives corresponding output.



CONCLUSION

Multi input DC –DC converter is evaluated based on two input supply sources. In MATLAB Simulink model is used to verify the output of each input sources output. Both input DC sources output is linked with transformer. Transformer is used for get output of converter circuit and gives input voltage to inverter. Inverter output voltage is 63v.Each input source of Multi input converter is 25v each. The multi input transformer get the supply

input from converter circuit. Simulation output results shows the efficiency of the system

References

- A Bidram A Davoudi and R S Balog (2012) Control and circuit techniques to mitigate partial shading effects in photo voltaic arrays IEEE Journal Photovolt vol 2 no 4 m pp 532 to 546
- B Ji J Wang and J Zhao(2013) High-efficiency single phase transformerless PV H6 inverter with hybrid modulation method IEEE Trans Ind Electron vol 60 no 5 pp 2104 to 2115
- D Nguyen and B Lehman(2008)An adaptive solar photovoltaic array using model based reconfiguration algorithm IEEE Trans Ind Electron vol 55 no 7 pp 2644 to 2654
- G V Quesada F G Gispert R P Lopez M R Lumbreras and A C Roca(2009) Electrical PV array reconfiguration strategy for energy extraction improvement in grid-connected PV systems IEEE Trans Ind Electron vol 56 no 11 pp 4319 to 4331
- H Xiao and S Xie (2012) Transformerless splitinductor neutral point clamped threelevel PV gridconnected inverter IEEE Trans Power Electron vol 27 no 4 pp 1799 to 1808
- H Patel and V Agarwal (2008) Maximum power point tracking scheme for PV systems operating under partially shaded conditions IEEE Trans Ind Electron vol 55 no 4 pp 1689 to 1698
- N D Kaushika and N K Gautam(2003) Energy yield simulations of interconnected solar PV arrays IEEE Trans Energy Convers vol 18 no 1 pp 127 to 134
- R Gonzalez E Gubia J Lopez and L Marroyo (2008) Transformerless single phase multilevel-based photovoltaic inverter IEEE Trans Ind Electron vol 55 no 7 pp 2694 to 2702
- S Dineshkumar and PL Somasundaram (2017) Power Quality Improvement in Renewable Energy Source Interfacing with Main Grid by Implementation of Shunt Active Filter International journal of control theory and applications vol 10 Issue No 29 Pages 125 to 132
- S V Araujo P Zacharias and R Mallwitz (2010) Highly efficient singlephase transformerless inverters for ridconnected photovoltaic systems IEEE Trans Ind Electron vol 57 no 9 pp 3118 to 3128
- T Shimizu O Hashimoto (2003) A novel high-performance utility interactive photovoltaic inverter system IEEE Trans Power Electron vol 18 no 2 pp 704 to 711
- S Dinesh kumar J Praveen Daniel Dr N Senthilnathan(2015) Three phase shunt active filter using modified algorithm for interfacing renewable energy sources with main grid International Journal of Applied Engineering Research Vol 10 No 55 pp 3045 to 3049
- T Gowtham Raj and S Dinesh Kumar(2018) Total Harmonic Distortion In Three Phase Thirteen Level Voltage Source Inverter With Mpp Tracker And Sepic Converter For Solar Pv Array Journal of Chemical and Pharmaceutical Sciences Vol 4 Issue 3 Pages 304 to 311

MMCDM Based Approach for Efficient Web Document Clustering in Web Search

R. Siva¹, T. Thandapani², R. Ramesh³ and R. Balamurali⁴

^{1,4}Department of CSE, Chennai Institute of Technology, Chennai, Tamilnadu India.

^{2,3}Department of ECE, Chennai Institute of Technology, Chennai, Tamilnadu India

ABSTRACT

The assessment of grouping calculations is characteristically troublesome in view of the absence of target measures. Since the assessment of bunching calculations ordinarily includes different criteria, it very well may be displayed as a various criteria dynamic (MCDM) issue. This paper presents a MCDM-based way to deal with rank a choice of well known bunching calculations in the space of budgetary hazard examination. An exploratory examination is structured to approve the proposed approach utilizing three MCDM techniques, six bunching calculations, what's more, eleven bunch legitimacy lists more than three genuine credit hazard and hazard informational indexes. The outcomes show the viability of MCDM techniques in assessing bunching calculations and demonstrate that the rehashed separation strategy prompts great 2-way grouping arrangements on the chose money related hazard informational indexes.

INTRODUCTION

This examination presents a novel Multi quality Multi level Content Depth Measure (MMCDM) based web record bunching to help web search in a most effective way. As opposed to thinking about the structure, substance, subject and visual characteristics of a website page the real substance profundity for example semantic criticalness accumulates more noteworthy consideration among web clients. Thus, right now considering the various traits like structure, subject, visual and content profundity of the site page is estimated to rate and bunch the profoundly comparable web records. Separate metaphysics is worked to gauge the substance depthness of ideas. The comparable ideas are assembled to shape

bunches and those groups are returned back to the client during web search (Benjamin C.M et. al, 2003)

Overview of MMCDM: The modern web technology has great impact in the presentation layer and most of the designer concentrates on their presentation part by organizing the contents of the web page in various structures in various levels. For example, the web pages are organized by presenting the introduction in first level and the detailed parts in the next levels. Each level of the web page contains different information and each feature of the web document has certain depth. Some web pages present the information in top level by providing minimum structures and visual elements. But few web pages would present the content in depth by providing large structures and visual elements.

In order to cluster the web documents in an efficient manner, the multi features like visual, structural and concept are required to be considered as significant. However, multi levels such as concept depth and ontological levels (based on distance among the concepts) are also indeed significant along with the features for

ARTICLE INFORMATION

*Corresponding Author: thandapanit@citchennai.net
Received 15th April 2020 Accepted after revision 20th May 2020
Print ISSN: 0974-6455 Online ISSN: 2321-4007 CODEN: BBR CBA

Thomson Reuters ISI Web of Science Clarivate Analytics USA and Crossref Indexed Journal



NAAS Journal Score 2020 (4.31) SJIF: 2020 (7.728)
A Society of Science and Nature Publication,
Bhopal India 2020. All rights reserved.
Online Contents Available at: <http://www.bbrc.in/>

better clustering. By grouping the web pages based on their features the problem of web search can be approached efficiently. The web users always look to view web pages under certain constraints. Not all the web users have same set of requirements. For example, If there is a web user, who has great idea of particular technology and he does not look for the web pages with more visual and structural elements (Beil et al. 2002; Chi, D et al. 2010; Cheng Xiang Zhai et al.2008)

The user can understand the topic being discussed easily and does not require more pictorial representation. But when there is a web user, who has no idea about the topic considered, he would like to view the web pages with great presentation which requires large number of visual elements and pictorial representation. Also such web pages should contain lot of structural presentation, so that the requirement of the web user varies according to many constraints. Also the user looks for more personalized results from the web search engines(Goceri, E et al , 2012).

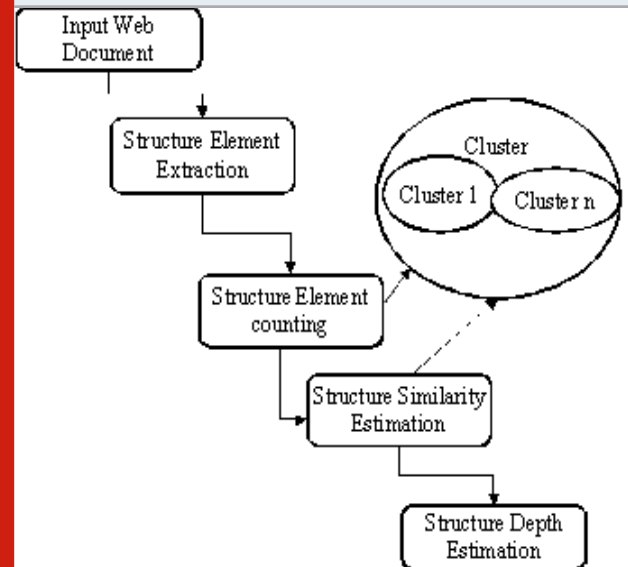
To provide more personalized results to the user, the search engines have the headache of grouping the web documents under several constraints. Also identifying the web pages with certain skeleton is not easier unless they have been grouped earlier. To achieve this, number of methods have been discussed earlier. Some methods consider only the concept or topic of the web document and the documents have been grouped based on the topic of the documents. When you consider the topic itself, then the terms present in the web documents and the taxonomy is sufficient. Based on the terms being identified from the documents, the similar documents of different classes can be identified. To compute the similarity of the document with the other documents of the cluster, several measures have been presented by different researchers. But considering the concept itself is not enough, so that the structural elements and the structure of the web pages is essential (Feng, Y et al.2015)

The structure is the way of organizing the web document content in specific skeleton. There are number of ways in organizing the content through different structures. The page differs greatly through the type of structure being used to organize the content of web page, so that the structural property could be a key in producing personalized results to the user. Some user would like to see the content in precise manner and in that case, the web search has the responsibility in producing the web result according to the user requirement. In particular, the user would like the content to be in precise order and more elements in a particular structure would be expected. In such case, the depth of the content in those elements are used to generate the personalized results.

Figure 1 shows the flow diagram of the structure similarity measurement estimation and shows the stages of the depth measure estimation.

Similarly, there are users who would expect the web pages to be effective with specific image elements and it must be the collection of different visuals. Not all the users would like the web pages to be presented in the collection of texts but some of them would look for the pages with more images and the concept to be presented in pictorial manner (Gunasundari, S et al., 2012).

Figure 1: Flow diagram of structure similarity estimation



This would bolster the client in understanding the idea of the site page. To register the comparability of the pages as far as their visual example, the visual likeness can be evaluated dependent on the visual parts present in the site page. To gauge the visual closeness, the image to picture likeness can be estimated. MMCDM gauges the visual comparability dependent on the photos/pictures present in the site page. On the off chance that the two pages contains comparative arrangement of pictures, at that point it very well may be considered as they are comparable in their visual surface. In the event that they have greater closeness in their visual surface, at that point their profundity in visual comparability is higher.

Figure 2: General block diagram of visual similarity estimation

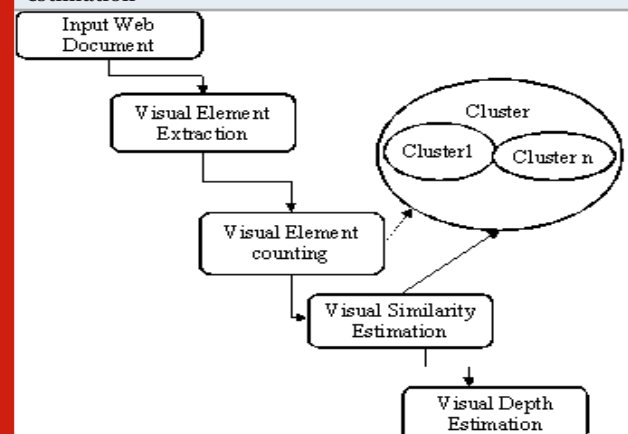


Figure 2 shows the general square outline of visual likeness estimation and shows the stages engaged with assessing the visual profundity measure.

The content profundity measure is the significant key in distinguishing the class of the archive. The web archives would examine different themes and a similar page would talk about various subjects. While arranging the website page, recognizing the subject of the site page is exceptionally basic. To recognize the subject of the page the scientific categorization can be utilized and to figure the profundity measure, the WordNet lexicon can be utilized what's more. By figuring the quantity of term matches with the term set recognized for the archive the profundity measure can be evaluated. The scientific classification would contain number of terms for the class which has been composed in various number of levels. At each level there will be number of terms and by processing the term recurrence in each level the profundity measure can be assessed.

Figure 3: General block diagram of MMCDM based web document clustering

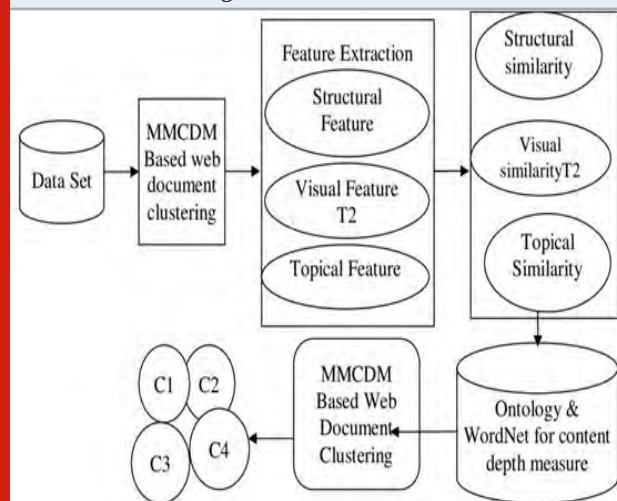
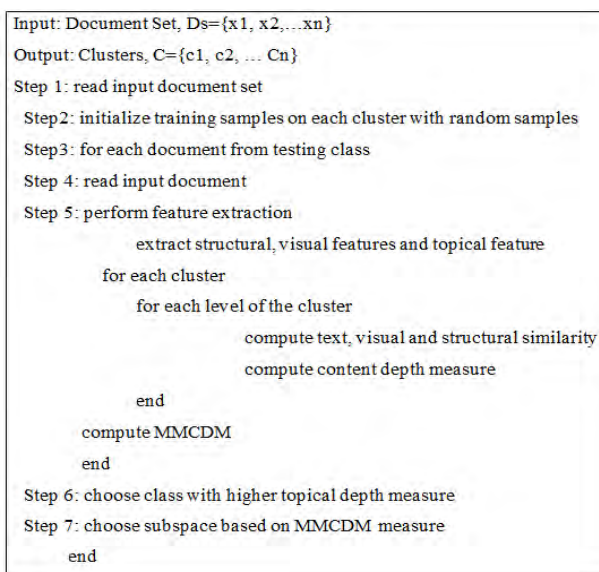


Figure 3 shows the general block diagram of multi attribute multilevel content depth measure based web document clustering and shows the functional stages involved.

1. Feature Extraction
2. Structural Similarity Estimation
3. Visual Similarity Estimation
4. Content Similarity Estimation
5. Measuring content depth using Ontology and WordNet
6. MMCDM Estimation
7. MMCDM Clustering

2. MATERIALS AND METHODS

2.1 Multi attribute multi level content depth measure based clustering: Let the web report informational index contains $X = \{x_1, x_2, \dots, x_n\}$ archives and expect the group C contains $\{c_1, c_2, c_3, \dots, c_n\}$ as a set, where each bunch c has number of records $\{D_1, D_2, \dots, D_n\}$.



Each record D from the bunch c has the visual highlights $V = \{v_1, v_2, v_n\}$, and auxiliary highlights $S = \{s_1, s_2, \dots, s_n\}$ and topical highlights as $T = \{T_1, T_2, \dots, T_n\}$. In light of this result, the record from the informational index x must be distinguished as bunch C , in view of MMCDM measure evaluated towards number of groups accessible.

The above examined calculation appraises the multi characteristic substance profundity measure at each degree of the group and dependent on the registered worth a solitary class has been chosen.

2.2 Performing Feature Extraction: The given web record set W_s has been perused and for each report D_i of W_s , the strategy peruses the substance. First the technique distinguishes the arrangement of terms T from the record D_i . Recognized terms T are added to the term set T_s . In the subsequent stage, the rundown of introduction labels is recognized and as per their pecking order the structures are distinguished. At last, the rundown of visual labels present in the web archive are recognized. All the highlights extricated are added to various arrangement of highlights and will be utilized to perform MMCDM estimation in the following stage. When the element extraction stage is finished, the calculation extricates the terms, visual components and basic elements.

The element extraction calculation distinguishes the rundown of literary terms, basic components and visual components from the web report. Recognized highlights are added to the concerned list of capabilities. The extricated highlights will be utilized to perform MMCDM estimation.

2.3 Measuring MMCDM Measure: The web archive has numerous highlights and the multi characteristic substance profundity measure shows the closeness of the record towards each class in each component. Right now, MMCDM first gauges the content profundity similitude dependent on the semantic cosmology. The literary profundity measure speak to how profundity the details of the class has been clarified or present in the web archive.

In the subsequent stage, the auxiliary profundity of the archive is evaluated dependent on the structure of the records. Finally, the visual basic comparably is assessed dependent on the visual conclusion of the reports from the class. Utilizing all these, the MMCDM estimates the multi credit content profundity measure to be utilized to perform bunching. The printed profundity measure shows the depthness of idea present in each level. The basic profundity measure, Sdm shows the closeness of the auxiliary components at each degree of the report present in the archive. The visual profundity measure, Vdm shows the profundity in similitude of the visual components present in the report towards the bunch records.

Figure 4: Flowchart of MMCDM estimation

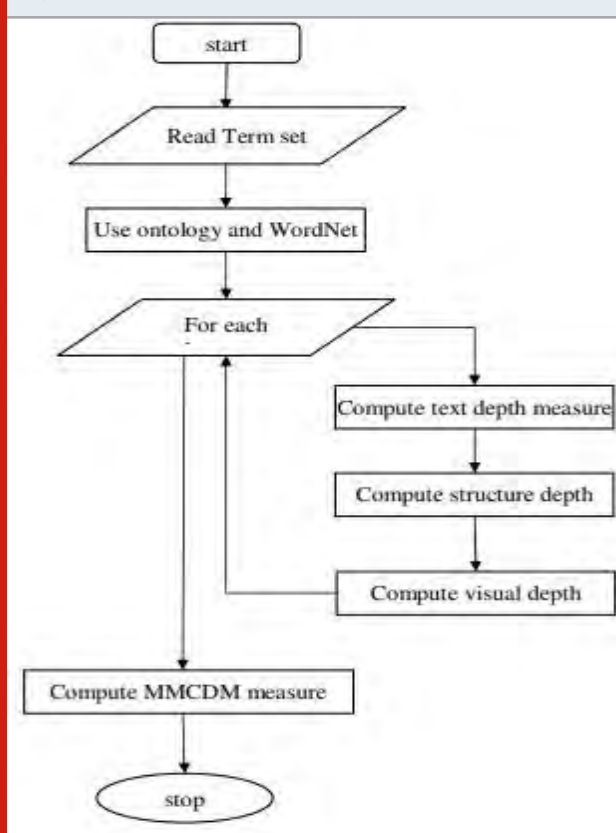
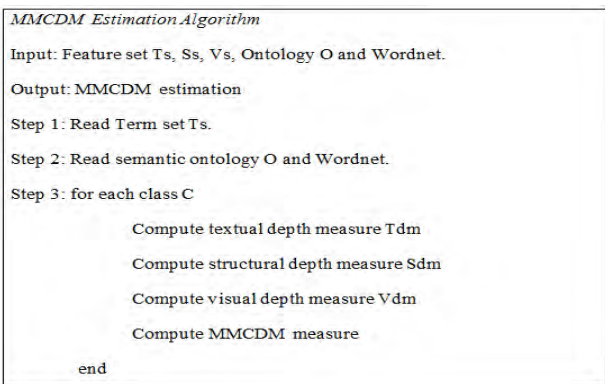


Figure 4 shows the flow chart of MMCDM estimation and the stages of estimating the MMCDM measure.



The above discussed algorithm computes the multi attribute content depth measure based on different feature depth measures. The computed MMCDM will be used to perform subspace clustering [15].

2.4 MMCDM Clustering: The web reports of the informational collection have been grouped by the MMCDM measure assessed. First MMCDM strategy processes the TextMatchMeasure (TMM) for each class to distinguish the root class. Later the MMCDM measure is evaluated. In light of the both the measures assessed, a solitary class will be chosen to allot the class mark. The grouping calculation chooses the class dependent on processed multi quality substance profundity measure [16].

The TMM is utilized as the way to distinguish the root class and it is figured as follows:

Figure 5: Flowchart of MMCDM clustering

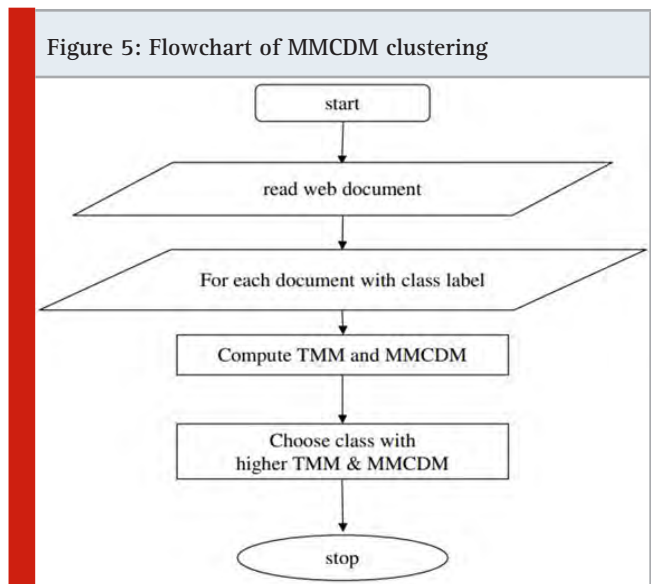
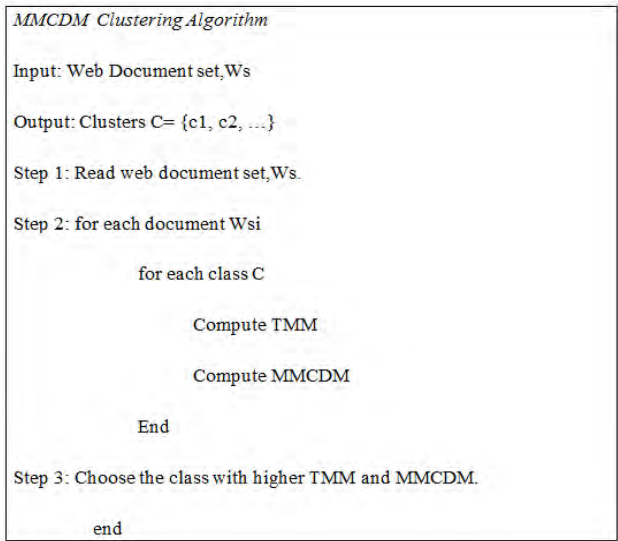


Figure 5 shows the detailed flow diagram of MMCDM clustering and the various stages involved in the process.



The above discussed clustering algorithm estimates the TMM and MMCDM for each class. Based on computed measures MMCDM method selects a single class and assigns the document to the class.

2.5 Ontology Construction: Cosmology is a formal express portrayal of a common conceptualization. Cosmology can fill in as an archive of all ideas in a space (Lei Zhang et al. 2010). The idea based metaphysics is created from the systems space which covers remote systems, sensor systems, appropriated systems, conventions, security methods, etc. Practically 1500+ words are included and the parent kid relationship is made. There are about 5+ layers of chain of command evolved through Protégé tool. Protégé is a free, open-source metaphysics editorial manager and structure for building shrewd frameworks. Right now, 4.1 is downloaded and introduced to fabricate disconnected cosmology. The procedure of cosmology development is physically done to remember the ideas for a layered methodology. The owl record in this manner made is parsed and used further to decide the separation between the terms extricated from the web archives.

2.6 Ontology gaining from web reports: Philosophy creation is done basically for information sharing. Philosophy Learning plans to computerize the ontology creation process. It utilizes strategies from different fields, for example, AI and inductive programming grouping and rule based. It's as yet far from being completely programmed and useable on a large scale by tenderfoots requires approval and contribution from the client all through the procedure (Jian Ma 2012). Ontology learning from content alone is finished by i) Natural language preparing of the information content to discover lexical and syntactic structure ii) Machine learning calculations used to determine metaphysics structure out of this structure. Machine learning further incorporates

- Clustering – utilizing client provided similitude measure
- Rule/format based information extraction
- Workbench apparatuses permit the utilization of various calculations

These guidelines are likely strong for Ontology Learning from Text. The issues recognized in the above said devices are reduced and even doesn't exist at times.

2.7 Online Vs. Disconnected cosmology: Online cosmology is a metaphysics that is commonly populated from idea maps, which thusly are produced on the fly from the records considered. It has a progressive structure. Since it isn't built by a specialist, it is less solid than disconnected philosophy. The benefits of an online philosophy lie in the realities that it is populated rapidly and that it can be for the most part made for a wide scope of spaces, that is, there is no area limitation in an online cosmology.

A philosophy that is practically comprehensive and built over some stretch of time, for the most part by a

specialist is disconnected metaphysics. The development of disconnected metaphysics is commonly a long length approach and isn't under a period limitation forced by the applications that utilize it. The benefits of disconnected cosmology exceed that of an online metaphysics therefore making it a perfect up-and-comer in helping bunching.

2.8 WordNet: WordNet is an enormous lexical database of English. Things, action words, descriptors and intensifiers are gathered into sets of intellectual equivalent words (synsets), each communicating a particular idea. Synsets are interlinked by methods for theoretical semantic and lexical relations (George A. Miller 1995). The subsequent system of definitively related words and ideas can be explored with the browser. In this proposed work, utilization of online WordNet to recognize the importance of terms separated is completed. Henceforth a blend of disconnected cosmology and online WordNet together empowers to quantify the substance depthness of the terms separated from the web records. Productive bunches are in this way created promising the theory.

3.1 Performance Evaluation: The presentation of the proposed MMCDM bunching calculation has been assessed dependent on different informational collections. The famous GDS and SDS informational indexes have been utilized as the info. The technique has created proficient outcomes in bunching and its presentation has been contrasted and various strategies. The GDS informational index has been taken from the planet web which contains 42 classifications of website pages which are gathered from various web crawlers. Thus, the SDS informational index has been taken from various sites and it has in excess of 100 web information bases.

3.2 Criteria of Evaluation: The presentation of the bunching calculation MMCDM has been assessed with the consequences of various grouping calculations for its bunching precision and F-measure. The grouping exactness has been estimated dependent on the equation.

3.3 Comparison with Existing Approaches: The presentation of the proposed MMCDM calculation has been contrasted and the current calculations to be specific ViDRE based bunching calculation which thinks about the visual comparability for the grouping of web archives. The ViDRE calculation produces poor arrangement precision because of the absence of considering huge number of features. Similarly, the MDR calculation registers the information pace of the page as the way to perform web archive bunching. In any case, it produces poor grouping precision.

3.4 Experimental Results: The result shows clearly that the proposed MMCDM clustering algorithm has produced higher clustering accuracy than MDR by improving the clustering accuracy upto 14.6% and it improves the accuracy upto 21.2 % on the GDS data set. Similarly,

the clustering accuracy is improved by 21 % with SDS data set and 21.2 % with GDS dataset when compared to ViDRE method.

3.5 Performance Evaluation with other Metrics: The presentation of the bunching calculation has been estimated with different parameters for the proposed MMCDM web archive grouping calculation. Figure 6 shows the correlation on running time multifaceted nature delivered by various techniques on grouping 2 million records. The proposed MMCDM bunching calculation has created less time multifaceted nature than different strategies .

Figure 6: Comparisons on running time complexity

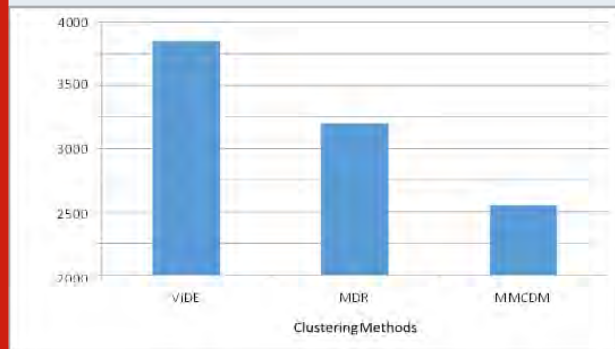
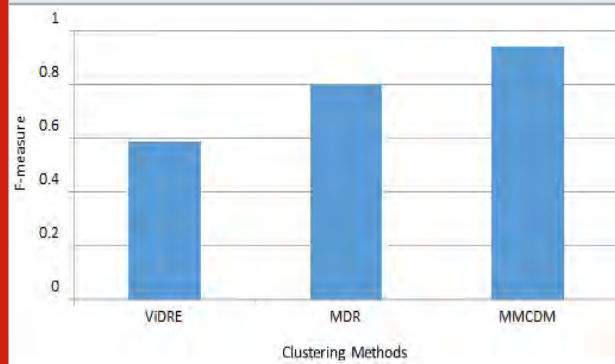


Figure 7: Comparison on F-measure among ViDRE, MDR and MMCDM clustering methods



CONCLUSION

Right now effective staggered multi trait content profundity measure based web archive grouping calculation is introduced. MMCDM strategy processes the content match measure to distinguish the root class of the web record given. At that point for each group, MMCDM registers the term profundity measure, visual profundity measure and auxiliary profundity measure. Utilizing these profundity measures MMCDM chooses the subspace of the reports hence creating productive outcomes than the other existing ViDRE and MDR techniques. The outcomes have been assessed and contrasted and existing ViDRE and MDR strategies.

REFERENCES

- Benjamin CM Fung Ke Wang & Martin Ester (2003) Hierarchical Document Clustering Using Frequent Itemsets In Proceedings SIAM International conference on data mining pp 59-70.
- Beil et al (2002) Frequent term-based text clustering ACM SIGKDD international conference on Knowledge discovery and data mining Pages 36-442.
- Chi D Zhao Y & Li M (2010) Automatic Liver MR Image Segmentation with Self-Organizing Map and Hierarchical Agglomerative Clustering Method" Image and Signal Processing Pages 1333-1337.
- Cheng Xiang Zhai 2008 Statistical Language Models for Information Retrieval Foundations and Trends in Information Retrieval vol 2 no 3 Pages 137-213.
- Deepa P & Suganthi M (2014) Performance Evaluation of Various Denoising Filters for Medical Image" International Journal of Computer Science and Information Technologies vol 5 no 3 Pages 4205-4209.
- Feng Y Qin XC Luo Y Li YZ & Zhou X (2015) Efficacy of contrast enhanced ultrasound without rate in predicting hepatocellular carcinoma differentiation" Ultrasound Med Biolvol 41 no 6 Pages 1553-1560.
- Goceri E Unlu MZ Guzelis C & Dicle O (2012) An automatic level set based liver segmentation from MRI data sets" Image Processing Theory Tools and Applications (IPTA) 3rd International Conference on 2012.
- Gunasundari S Suganya M & Ananthi (2012) „Comparison and Evaluation of Methods for Liver Tumor Classification from CT Datasets" International Journal of Computer Applications (0975 - 8887) vol 39 no 18.
- Kumar SS Moni RS & Rajeesh J (2012) „Liver Tumor Diagnosis by Gray Level and Contour let Coefficients Texture Analysis" Computing Electronics and Electrical Technologies Pages 557-562.
- Liu YB Cai JR Yin J & Fu AWC (2008) Clustering Text Data Streams Springer Journal of Computer Science and Technology vol 23 no 1 Pages 112-128.
- Lu & Mei (2011) Investigating task performance of probabilistic topic models Springer Information Retrieval vol 14 no 2 Pages 178-203.
- Li CM Xu CY Gui CF & FOX MD (2010) Distance regularized level set evaluation and its application to image segmentation" IEEE transactions on image processing vol 19 no 12.
- Massoptier L & Casciaro S (2007) Fully Automatic Liver Segmentation through Graph-Cut Technique"Engineering in Medicine and Biology Society Pages 5243- 5246.
- Mala K Sadasivam V & Alagappan S (2006) Neural Network based Texture Analysis of Liver Tumor from Computed Tomography Images at International Journal of Biological and Life Sciences vol 2 Pages 33-40.
- Muhammad Rafi (2010) Document Clustering based on Topic Maps International Journal of Computer

Applications vol 12 no 1 Pages 32- 36 Na & yongand
2010 Research on K-means Clustering Algorithm
IEEE Third International Symposium on Intelligent
Information Technology and Security Informatics IITSI
pp 63-67.

Miltzer A Hager A Jager F Tietjen C & Horneegger (2009)
Automatic detection and segmentation of focal liver
lesions in contrast enhanced CT images” Proceedings
international Conference on pattern recognition vol 10
pp 2524-2527.

Pavlidis T (2011) Image Analysis” Annual review of
Computer Science vol 3 Pages 121-146.

Rajeswari P & Sophia Reena G (2011) Human Liver

Cancer Classification using Microarray Gene Expression
Data International Journal of Computer Applications
(0975 – 8887) vol 34 no 6.

Ruskó L (2007) Fully Automatic Liver Segmentation
for ContrastEnhanced CT Images MICCAI Wshp 3D
Segmentation in the Clinic: A Grand Challenge.

Seo KS (2005) Improved fully Automatic Liver
Segmentation using Histogram tail threshold Algorithms
Springer Berlin Heidelberg vol 3516 Pages 822-825.

Singh KK & Singh A A Study of Image Segmentation
Algorithms for Different Types of Images International
Journal of Computer Science Issues vol 7 Pages 1-4.

Metamaterial Inspired MIMO Antenna for Radar, Satellite and Terrestrial Communications

S.Prasad Jones Christydass^{1*}, B. Monisha², S. Shanthini³ and R. Saranya⁴

¹Assistant Professor, ^{2,3,4}UG Scholars

^{1,2,3,4}Department of ECE, K.Ramakrishnan College of Technology, Trichy, Tamilnadu, India

ABSTRACT

In this research, two CSRR Metamaterial etched circular patch antenna with defected ground structure is proposed for X band application. The entire structure is designed with the substrate thickness of 0.51mm using FR4 substrate. The MIMO antenna is designed on the substrate with 50mm as its width and 24 mm as its length. The proposed antenna is having its resonating operating frequency band from 2.01 GHz to 2.15 GHz, 7.83 GHz to 8.52 GHz, 9.91 GHz to 10.01 GHz, 11.21 GHz to 12.84 GHz. The MIMO antenna is simulated using the CST electromagnetic software. The Simulated outputs are presented and all the results prove that the proposed structure is capable to use for the X band application.

KEY WORDS: CIRCULAR PATCH, CSRR, MIMO, METAMATERIAL, X BAND.

INTRODUCTION

One of the smartest antenna techniques used for satisfying the growing demand of high data rate with less complex communication system are the MIMO antenna. MIMO antenna technique is the method in which the system make use of more than one antenna the transmitting and receiving end in order to exploit the space diversity. With the help of space diversity this method can able to achieve the maximum data rate during the transmission. The patch antenna is widely used is because of its ease of fabrication and low cost. Metamaterials (Christoph et al., 2006) are the structure which are periodic in nature, which is used to enhance the various electromagnetic

characteristics. Various shapes (Prasad et al., 2017; Prasad et al., 2019; Prasad et al., 2019) are reported in the literature such as SRR, 8, S and omega shaped, CSRR. This metamaterials can able to enhance the electromagnetic property is because of its negative permittivity, permeability and refractive index (Kavitha et al., 2020; Shanthi et al., 2019; Suvadeep et al., 2017; Boopathi et al., 2017; Choi et al., 2009). In this paper, a novel metamaterial inspired MIMO antenna is proposed to operate in X band, which can be used in Radar, Satellite and Terrestrial communication application. Further the paper is elaborately discuss the evolution of the proposed MIMO antenna, the result at each evolution stage and the followed by the conclusion

ARTICLE INFORMATION

*Corresponding Author: prasadjoness.ece@krct.ac.in

Received 15th April 2020 Accepted after revision 15th May 2020

Print ISSN: 0974-6455 Online ISSN: 2321-4007 CODEN: BBRBCA

Thomson Reuters ISI Web of Science Clarivate Analytics USA and Crossref Indexed Journal



NAAS Journal Score 2020 (4.31) SJIF: 2020 (7.728)

A Society of Science and Nature Publication,
Bhopal India 2020. All rights reserved.

Online Contents Available at: <http://www.bbrc.in/>

METHODS AND MATERIALS

The projected MIMO antenna is having 4 stages of evolution namely antenna A, antenna B, antenna C and antenna D. Antenna A is a simple circular microstrip feed antenna with full ground which don't capable to achieve impedance matching. Antenna B is the modification of antenna A, two metamaterial shapes are etched in the circular patch, with the help of metamaterial antenna B can able to operate at four bands. Antenna C is designed by reducing the ground size of antenna B, by reducing the ground size the antenna c is operating at three bands with improved band width compared to antenna A and B. Finally, antenna D is the 2 element MIMO antenna which operates in 4 band. In figure 1a, figure 1b and Table 1, the evolution of MIMO antenna a for X band application, MIMO antenna unit cell with its parameter and its value are presented respectively.

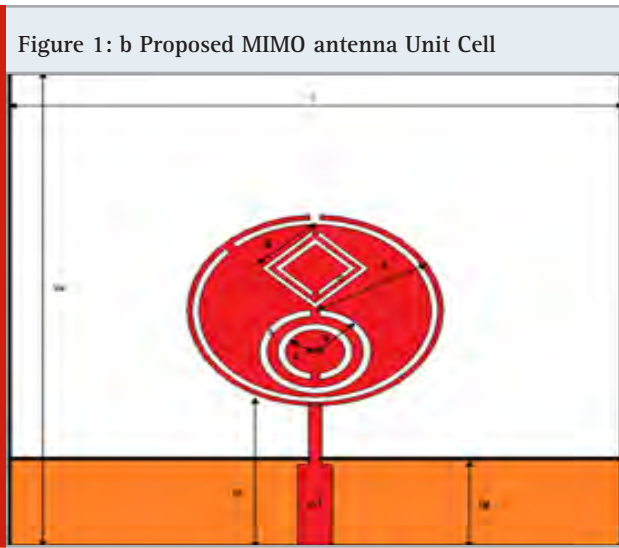
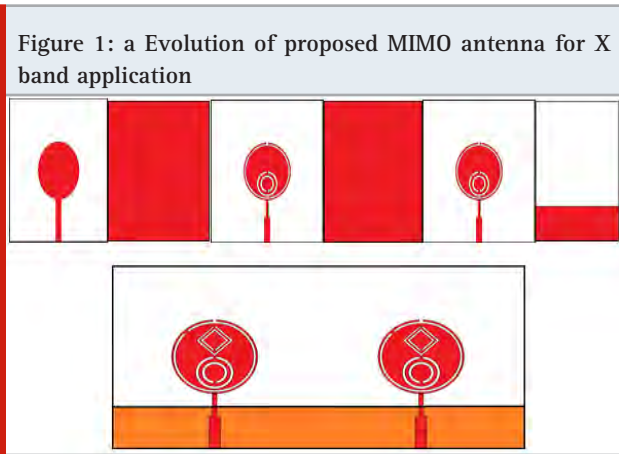
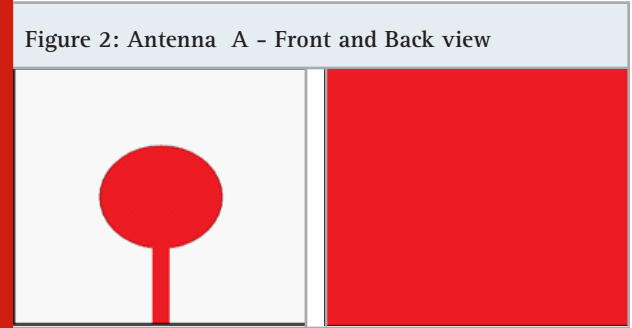


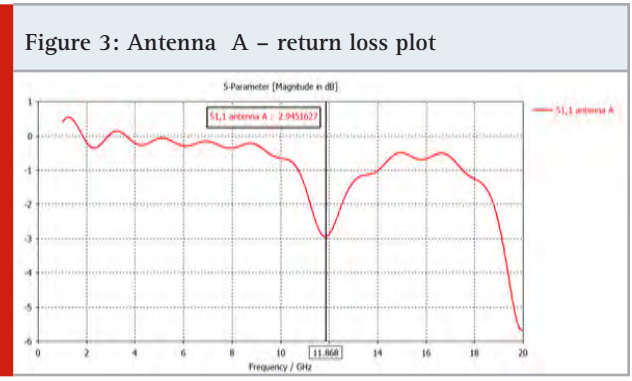
Table 1. Parameter value of MIMO antenna Unit Cell

w	l	wf	lf	lg	x
23	24	1.2	6	4.2	6
y	z	s	g	c	t
2	1	0.5	3	0.25	0.035

RESULT AND DISCUSSION



Initially, a circular antenna is designed to operate at X band with centre frequency of 11 GHz. The circular patch is feed with 50-ohm microstrip feed line. the circular patch is printed at one end and while the other end of the substrate is completely printed with ground. But the proposed structure impedance is not equal to the impedance of the feed file. Due to this impedance mismatching the proposed structure has no operating band of resonance. In figure 2 the initial design antenna A front and back view is depicted. In figure 3 the return loss plot of the antenna A is presented. From the figure we can clearly see that there is no resonance.



Then, in order to meet the impedance matching, the simple 50-ohm feed line is converted to quarter wave transformenr feed. Then two different shapaes CSRR is etched in the circular shape patch. This inclusion pf metamatrial make the aantenna B to resonate at four different frequency. The front and back view of the proposed antenna is dipited in figure 4. In figure 5, the s11 characteristics of antenna A and B is compared, form which we can observe that the proposed antenna B is having tetra band frequency of operation from 7.71 GHz to 7.79 GHz with 14 dB, 11.81GHz to 11.83 GHz with 11.46dB, 11.89 GHz to 12.01GHz with 15.62 dB and 14.89 GHZ to 15.02 GHZ with 13.21 dB as its return loss.

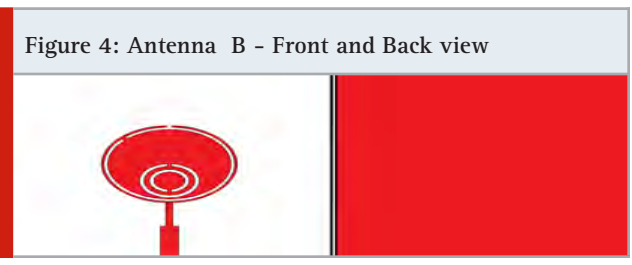


Figure 5: Comparison – Return loss plot of antenna A & B

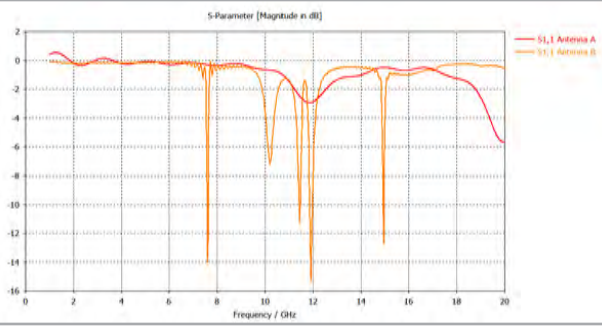


Figure 6: Antenna C – Front and Back view



Figure 7 Comparison – Return loss plot of antenna A,B & C

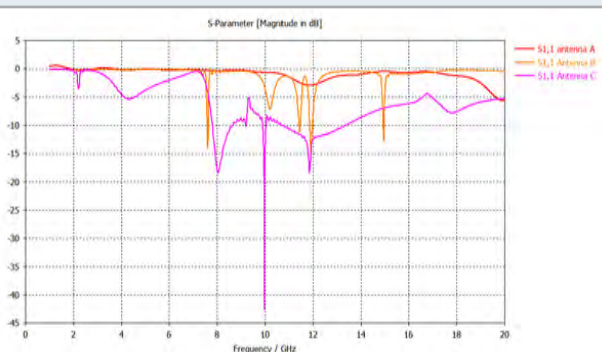
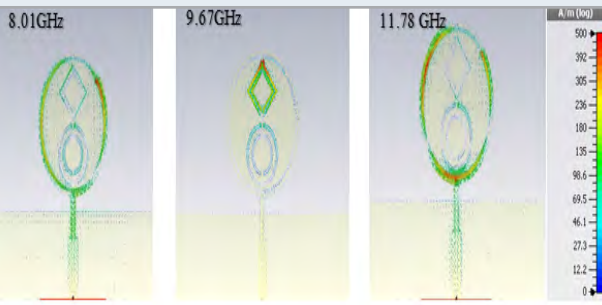


Figure 8: Surface current at various resonating frequency



Antenna B is having four band of operating frequency, but the major disadvantage is its bandwidth and its impedance matching is not good. In order to improve the bandwidth and impedance matching, the ground should be altered by defected ground structure. The evolved

design is capable to resonate at 3 operating frequency bands 7.83 GHz to 8.52 GHz with 18.25 dB, 9.91 GHz to 10.01 GHz with 43 dB and 11.21 GHz to 13.84 GHz with 18.16 dB as its return loss which observed in figure 7, which depicts the Comparison return loss performance of antenna A, B and C.

In figure 8, the surface current distribution of the antenna C which is used as the unit cell for the proposed MIMO antenna D. From figure 8, we can clearly observe that the surface current is concentrated more around the metamaterial structure in all the frequency band. The introduction of CSRR changes the current path by increasing the current path length and as a result the proposed unit cell antenna C is capable of resonating at triband frequency. Therefore the metamaterial introduces two new resonance bands at 7.83 GHz to 8.52 GHz with 18.25 dB, 9.91 GHz to 10.01 GHz with 43 dB and also improves the bandwidth of the three operating bands from 11.21 GHz to 13.84 GHz.

Figure 9: 3D, E plane and H plane Radiation pattern

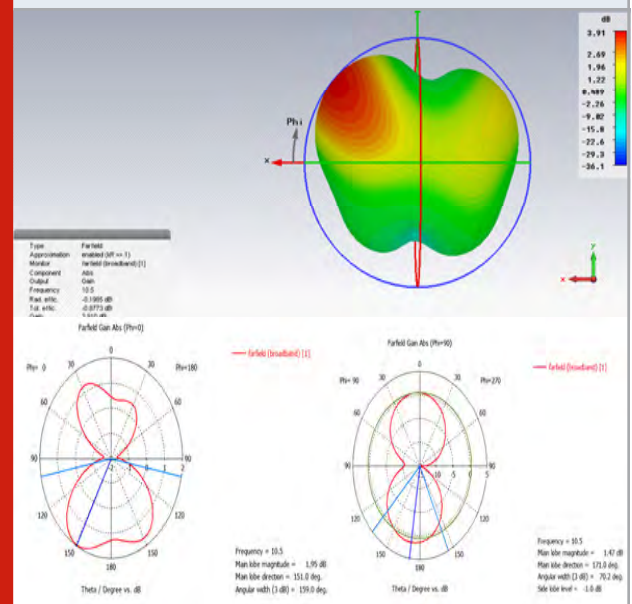


Figure 10: Directivity plot of antenna C

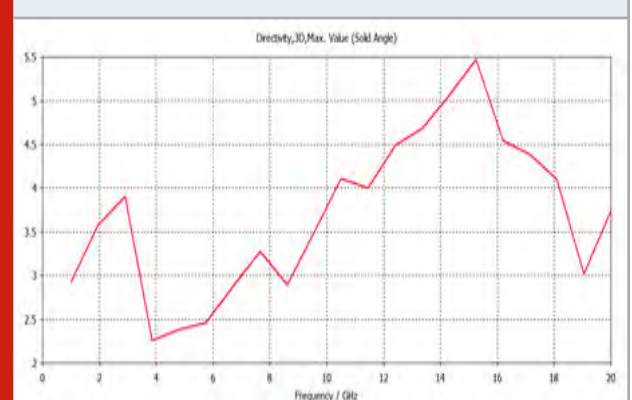


Figure 11: Gain plot of antenna C

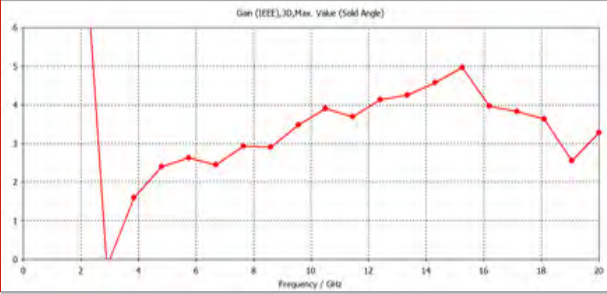


Figure 12: MIMO antenna for X band application

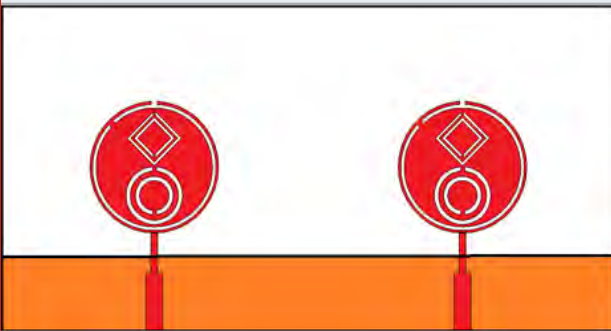


Figure 13: Comparison plot of s11 of antenna A,B,C with MIMO antenna for X band application

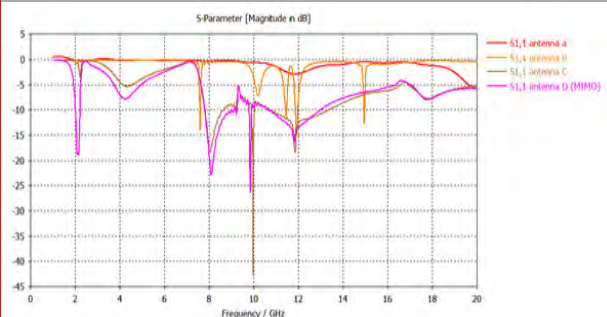


Figure 14: S parameter characteristics of the proposed MIMO antenna

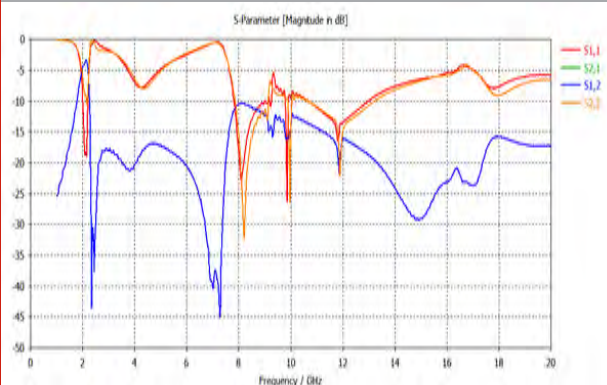


Figure 15: VSWR characteristics of the proposed MIMO antenna

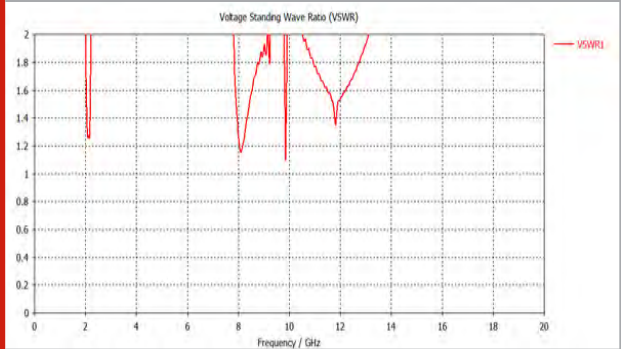


Figure 9 shows the radiation pattern such as 3-dimensional, E and H plane of the MIMO antenna for X band application. From, figure 9 the proposed MIMO antenna unit cell is capable to have an omnidirectional radiation pattern in the broadside direction of the MIMO antenna. Figure 10 and figure 11 depicts the directivity and gain plot of the MIMO unit Cell. Both gain and directivity is plotted with respect to the frequency, both are having positive values in all the operating band with the maximum value of 5.5 dBi and 5 dBi for directivity and gain respectively

Finally, the two antenna C is joined to form proposed antenna D which is the MIMO antenna for X band application. In Figure 12, the proposed MIMO antenna for the X band application is presented. This antenna is capable of operating at tetra bands from 2.01GHz to 2.15 GHz with 18.96 dB, 7.83 GHz to 8.52 GHz with 22.35dB, 9.91 GHz to 10.01 GHz with 26.12 dB and 11.21 GHz to 12.84 GHz with 16.19dB as it return loss. In figure 13 the return loss characteristics of the antenna A,B,C and proposed MIMO antenna for X band application (antenna D) is depicted. In figure 14, the S parameter of the MIMO antenna for x band application is presented, from the figure we can clearly see that the coupling between the element is maintained above 15dB in the all the operating bands. From Figure 15, it is observed that the proposed MIMO antenna for X band application having VSWR values less than 2 in all the operating frequency bands.

CONCLUSION

In this paper, metamaterial inspired circular patch antenna for X band application is presented. The projected MIMO antenna is having 4 stages of evolution namely antenna A, antenna B, antenna C and antenna D. Antenna A is a simple circular microstrip feed antenna with full ground which don't capable to achieve impedance matching. Antenna B is the modification of antenna A, two metamaterial shapes are etched in the circular patch, with the help of metamaterial antenna B can able to operate at four bands from 7.71 GHz to 7.79 GHz with 14 dB, 11.81GHz to 11.83 GHz with 11.46dB, 11.89 GHz to 12.01GHz with 15.62 dB and 14.89 GHz to 15.02 GHz with 13.21 dB as its return loss.. Antenna

C is designed by reducing the ground size of antenna B, by reducing the ground size the antenna c is operating at three bands with improved bandwidth from 7.83 GHz to 8.52 GHz with 18.25 dB, 9.91 GHz to 10.01 GHz with 43 dB and 11.21 GHz to 13.84 GHz with 18.16 dB as its return loss. Finally, antenna D is the 2 element MIMO antenna which operates in 4 band from 2.01GHz to 2.15 GHz with 18.96 dB, 7.83 GHz to 8.52 GHz with 22.35dB, 9.91 GHz to 10.01 GHz with 26.12 dB and 11.21 GHz to 12.84 GHz as its return loss. The Simulated result presented proves that the proposed structure is capable to use for the X band application.

REFERENCE

- Boopathi Rani and SK Pandey (2017) A CPW-fed circular patch antenna inspired by reduced ground plane and CSRR slot for UWB applications with notch band *Microw Opt Technol Lett* 59:Pages 745-749.
- Choi ST Hamaguchi K KohnoR (2009) Small printed CPW-fed triangular monopole antenna for ultra-wideband applications *Microw Opt Technol Lett*;51 Pages 1180-1182.
- Christophe Caloz Tatsuo Itoh 2006 *Electromagnetic metamaterials: Transmission line theory and microwave applications* New York: John Wiley & Sons Inc.
- Kavitha S Prasad Jones Christydass JSilamboli (2020) *Metamaterial Inspired Triple Band Antenna for Wireless Communication International Journal of Scientific & Technology Research* volume 9 issue 3.
- Prasad Jones Christydass and N Gunavathi (2017) Codirectional CSRR inspired printed antenna for locomotive short range radar *International Conference on Inventive Computing and Informatics (ICICI) coimbatore India* December 4-5.
- Prasad Jones Christydass and N Gunavathi (2017) Design of CSRR loaded multiband slotted rectangular patch antenna *IEEE Applied Electromagnetics Conference (AEMC) aurangabad india* January 2-5.
- Prasad Jones Christydass and Pranit Jeba Samuel (2019) *Metamaterial Inspired Slotted Rectangular Patch Antenna for Multiband Operation Biosc Biotech Res Comm Special Issue Vol 12 No(6) Pages 57-62.*
- Prasad Jones Christydass and Manjunathan (2019) *Pentagonal Ring Slot Antenna with SRR for Tri-Band Operation Biosc Biotech Res Comm Special Issue Vol 12 No(6) Pages 26-32.*
- Shanthi Dr T Jayasankar Prasad Jones Christydass Dr P Maheswara Venkatesh (2019) *Wearable Textile Antenna For Gps Application International journal of scientific & technology research* volume 8.
- Suvadeep Choudhury and Akhilesh Mohan (2017) *Miniaturized sierpinski fractal loaded QMSIW antenna with CSRR in ground plane for WLAN applications Microw Opt Technol Lett* 59 Pages 1291-1265.

Metamaterial Inspired Bandpass Filter for 5G Application

S. Prasad Jones Christydass^{1*}, A.S.Priyankka², S. Sugil³ and R. Soundharya⁴

¹Assistant Professor, ^{2,3,4}UG Scholars

^{1,2,3,4}Department of ECE, K.Ramakrishnan College of Technology, Trichy, Tamilnadu, India

ABSTRACT

Bandpass filter is very important part in any wireless communication system. In this paper a novel metamaterial inspired microstrip band pass filter is proposed for 5g application. The proposed filter has a frequency which covers the frequency from 3.42 GHz to 3.72 GHz and the band is used for 5G application. The microstrip BPF make use of loop metamaterial patches to achieve such frequency performance and the structure is fed by two port tapered feed. The entire structure is simulated using CST software. The total size of the proposed Metamaterial BPF is 12 x 10 x 1.6mm³ and fabricated on FR4 substrate. The simulated result proves that the proposed antenna has capacity to satisfy the 5G application requirements.

KEY WORDS: BANDPASS FILTER, COMPACT, METAMATERIAL, WIRELESS COMMUNICATION, 5G APPLICATION.

INTRODUCTION

In the recent trends in communication such as green communication and radar systems, the removal of RF noises becomes the key quality to be taken into care for the better performance of the systems (Hussaini et al., 2015). The planar band pass filters are the major components in the current 5G wireless communication which utilize various spectrum bands such as 700 MHz, 3.6 GHz and 26 GHz. Variety of techniques such as couple line technique, hair pin technique, combine technique, step and stub impedance (Srivastava et al., 2014) methods are reported in the literature.

Due to the peculiar EM property of the metamaterial the researches have attracted and various metamaterial

structure are developed in order to enhance the electromagnetic property of the RF devices. The planar filters are widely used to implement various types of filters such as low pass, high pass, band pass and band stop filters. The usage of planar filter is increased in because of its ease of fabrication and easy implementation with MIC. The various methods are implemented in order to enhance the filter performance but using the metamaterial (Prasad et al., 2017; Prasad et al., 2019; Prasad et al., 2019; Kavitha et al., 2020; Shanthi et al., 2019) to change the performance of the filter is not widely reported in the literature. In this paper a complementary split ring resonator is used in order to shift the frequency of operation is reported. Further the paper elaborately discuss the design methodology followed, result and finally conclusion.

ARTICLE INFORMATION

*Corresponding Author: prasadjoness.ece@krct.ac.in
Received 15th April 2020 Accepted after revision 20th May 2020
Print ISSN: 0974-6455 Online ISSN: 2321-4007 CODEN: BBRBCA

Thomson Reuters ISI Web of Science Clarivate Analytics USA and Crossref Indexed Journal



NAAS Journal Score 2020 (4.31) SJIF: 2020 (7.728)
A Society of Science and Nature Publication,
Bhopal India 2020. All rights reserved.
Online Contents Available at: <http://www.bbrc.in/>

MATERIALS AND METHODS

Design Methodology

The proposed filter has three stages of evolution namely filter A, filter B and filter C. Filter A has three simple

resonator patches namely resonator 1, resonator 2 and resonator 3. The structure is designed on a Fr4 substrate and feed with 2 tapered port from the lateral sides. The other one resonator act as parasitic elements. Then filter B, is designed by simply incorporating the single rectangular stub in resonator 3. Then proposed filter C is designed by imprinting the oval CSRR in Resonator 1 and resonator 2.

Figure 1: Evolution of the Metamaterial BPF

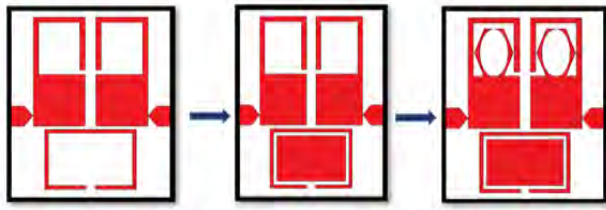


Figure 2: Parameters of the Metamaterial BPF

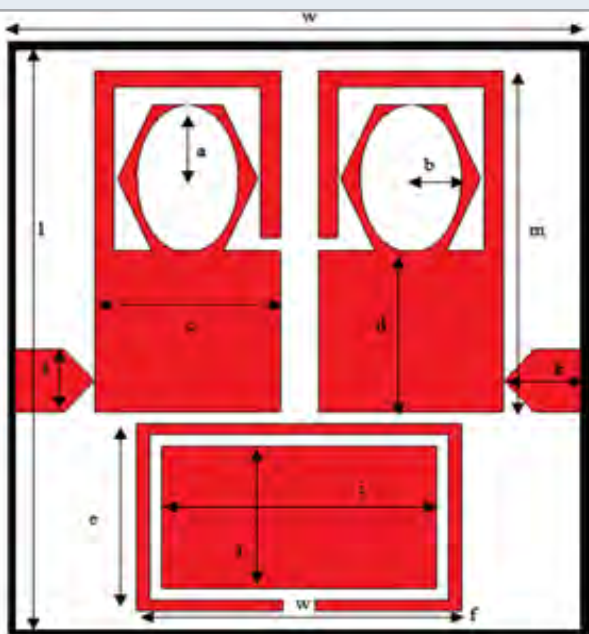


Table 1. Metamaterial BPF parameter Value

l	w	a	b	c	d	e
12	10	3	2	3	3.5	3
f	i	j	k	l	m	t
5	4.5	3.5	0.75	0.5	7	0.035

RESULTS AND DISCUSSION

Filter A

Filter A is having three resonators namely resonator 1, resonator 2 and resonator 3. In which resonator three is a simple split ring resonator which parasitic to resonator 1 and 2. The structure is feed at resonator 1 and 2. The

configuration of filter A is depicted in figure 3. In figure 4 the s parameter characteristic is presented. From the figure it is observed that the filter A is having resonance from 3.78 GHz to 4.26 GHz. the return loss of the filter in the resonant frequency is -29.89dB and the insertion loss is about 2dB.

Figure 3: Filter A configuration

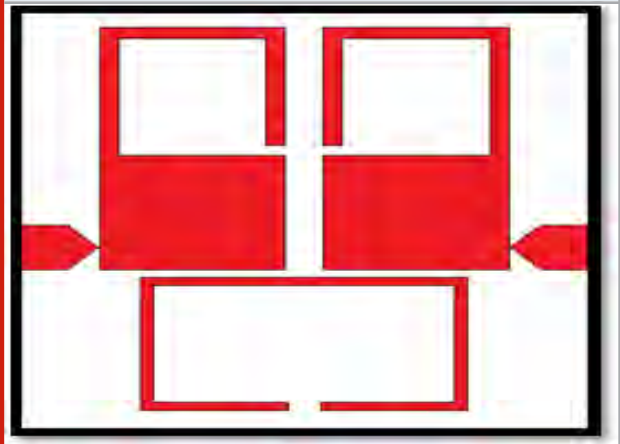
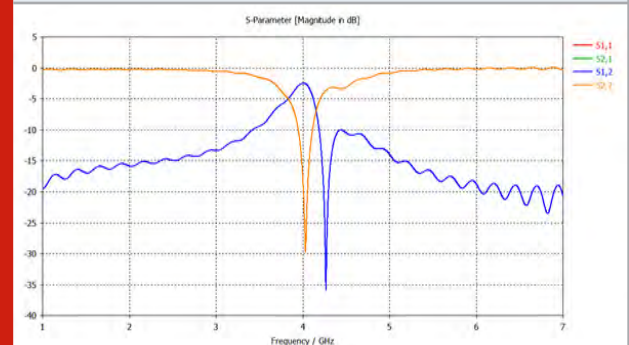
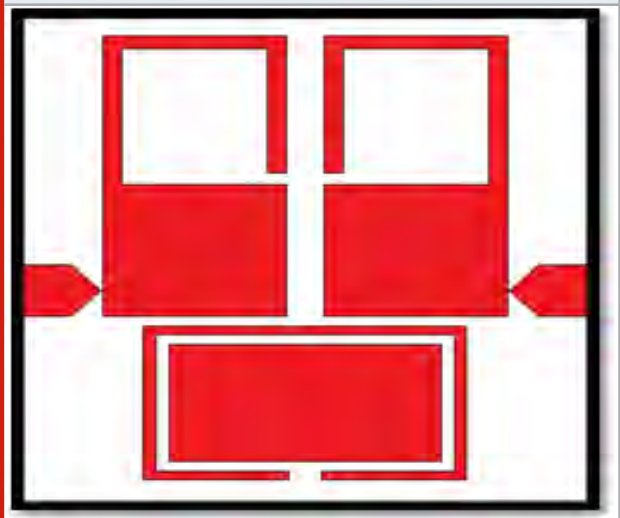


Figure 4: s parameter of the Filter A



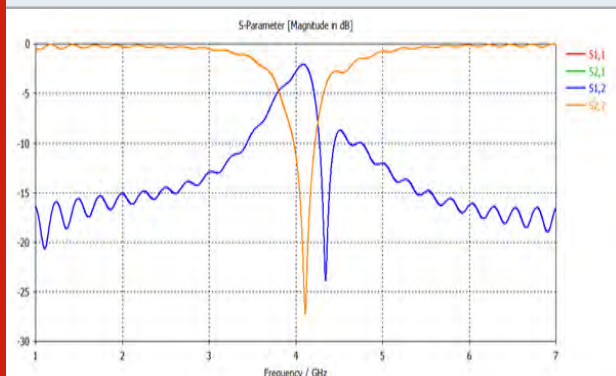
Filter B

Figure 5: Filter B Configuration



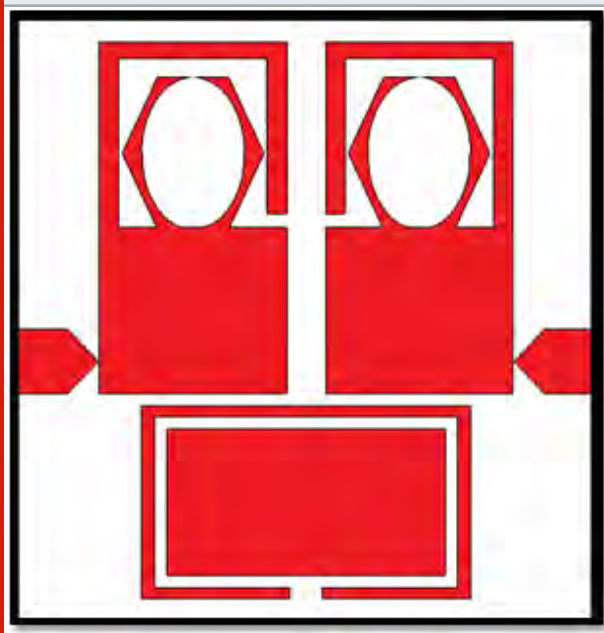
The filter B is the slight modification of filter A. a rectangular stub is included in side the resonator 3 in filter A to design filter B. the configuration of Filter B is depicted in figure 5 and in figure 6 the s parameter characteristics of the filter B is presented. The inclusion of rectangular stub increases the current path length and it also increases the capacitance. Because of this the resonance of the after B is shifted upward due to the inclusion of the rectangular stub. From the figure 6, it is observed that the filter A is having resonance from 3.96 GHz to 4.28 GHz. the return loss of the filter in the resonant frequency is -26.89 dB and the insertion loss is about 2.1 dB.

Figure 6: s parameter of the Filter B



Filter C

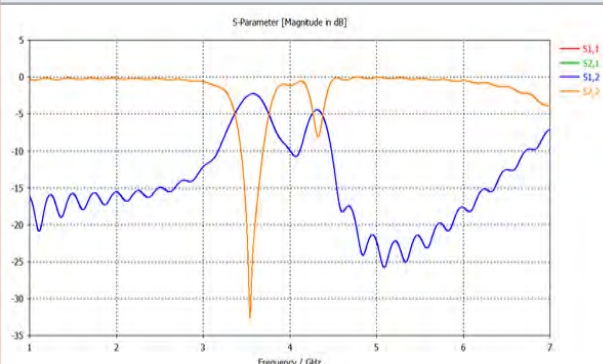
Figure 7: Filter C Configuration



Then proposed filter C is designed by imprinting the oval CSRR in Resonator 1 and resonator 2. The configuration of filter C is depicted in figure 7 and its s parameter characteristics is presented in figure 8. Further inclusion of the oval CSRR increases inductance and decreases the capacitance. Because of this the proposed filter C is

having resonance from 3.42 GHz to 3.72 GHz. The return loss of the filter in the resonant frequency is -33.16 dB and the insertion loss is about 1.5 dB.

Figure 8: s parameter of the Filter B



CONCLUSION

In this paper, Metamaterial BPF is proposed with size of $12 \times 10 \times 1.6\text{mm}^3$ and fabricated on FR4 substrate. The structure is designed on a Fr4 substrate and feed with 2 tapered port from the lateral sides. The proposed filter has three stages of evolution namely filter A, filter B and filter C. Filter A has three simple resonator patches namely resonator 1, resonator 2 and resonator 3 operating from 3.78 GHz to 4.26 GHz. The other one resonator act as parasitic elements. Then filter B, is designed by simply incorporating the single rectangular stub in resonator 3 operating from 3.96 GHz to 4.28 GHz. Then proposed filter C is designed by imprinting the oval CSRR in Resonator 1 and resonator 2 operating from 3.42 GHz to 3.72 GHz. The simulated result proves that the proposed antenna has capacity to satisfy the 5G application requirements.

REFERENCE

- Christophe Caloz Tatsuo Itoh (2006) Electromagnetic metamaterials: Transmission line theory and microwave applications New York: John Wiley & Sons Inc.
- Hussaini Y Abdulraheem k Voudouris B Mohammed R A AbdAlhameed H Mohammed I Elfergani A Abdullah D Makris J Rodriguez J M Noras C Nche and M Fonkam Green (2015) Flexible RF for 5G Fundamentals of 5G Mobile Networks John Wiley and Sons Pages 241–272 2015.
- Hong and M J Lancaster Microstrip Filters for RF/ Microwave vol 167 John Wiley and Sons 2004
- Kavitha SPrasad Jones Christydas JSilamboli (2020) Metamaterial Inspired Triple Band Antenna for Wireless Communication International Journal of Scientific & Technology Research volume 9 issue 3.
- Ofcom 8 February 2017 [Online] Available: <https://www.ofcom.gov.uk/>
- Prasad Jones Christydas and N Gunavathi (2017) Codirectional CSRR inspired printed antenna for

locomotive short range radar International Conference on Inventive Computing and Informatics (ICICI) coimbatore India December 4-5.

Prasad Jones Christydass and N Gunavathi (2017) Design of CSRR loaded multiband slotted rectangular patch antenna IEEE Applied Electromagnetics Conference (AEMC) aurangabad india January 2-5.

Prasad Jones Christydass and Pranit Jeba Samuel (2019) Metamaterial Inspired Slotted Rectangular Patch Antenna for Multiband Operation Biosc Biotech Res Comm Special Issue Vol 12 No(6) Pages 57-62.

Prasad Jones Christydass and Manjunathan(2019) Pentagonal Ring Slot Antenna with SRR for Tri-Band Operation Biosc Biotech Res Comm Special Issue Vol 12 No(6) Pages 26-32.

Shanthi Dr T Jayasankar Prasad Jones ChristydassDr P Maheswara Venkatesh (2019) Wearable Textile Antenna For Gps Application International journal of scientific & technology research volume 8.

Srivastava R K Manjunath and P Shanthi (2014) Design simulation and fabrication of a microstrip bandpass filter International Journal of Science and Engineering Applications vol 3 no 5 pages 1-4

Identification of Diseases in Plant Leaves Using Deep Learning Algorithm

R. Lalitha¹, S. Usha^{*2}, M. Karthik³, B. Pavithra⁴, P. L. Sivagaami⁵ and G. Madhumitha⁶

¹Professor, Department of Computer Science and Engineering, Rajalakshmi Institute of Technology, Chennai

^{2,3}Associate Professor, Department of Electrical and Electronics Engineering, Kongu Engineering College, Perundurai, Erode

^{4,5,6}UG students, Department of Computer Science and Engineering, Rajalakshmi Institute of Technology, Chennai.

ABSTRACT

Plant leaf diseases is one of the major threats to food security and it dramatically reduces the crop yield and compromises its quality. Accurate and precise diagnosis of diseases at an earlier stage is always a challenge for the farmers. The current advances in computing technologies have paved the way for diagnosing the diseases in plant leaves. In this paper, deep learning algorithm is used to detect the disease in leaves. The images of the plant leaves are captured and Convolution neural networks (CNN) model is used to diagnose the disease in the affected leaves. A variety of neuron-wise and layer-wise visualization methods are applied using CNN and trained with a publicly available plant disease given image dataset. The neural networks model captures the colors and textures of leaves and identify whether the leaves are healthy or affected. lesions specific to respective diseases upon diagnosis.

KEY WORDS: CONVOLUTIONAL NEURAL NETWORK, DATASET, DEEP LEARNING, IMAGE PROCESSING, LEAF DISEASE.

INTRODUCTION

An automation plays a vital role in today's social network and also perform a different task in various sector. In this paper the challenge of automating diagnosis of disease are tackled in plants from images of a particular leaf of a plant. It reviews and summarizes various techniques used for classification and detection of various bacterial, fungal and viral plant leaf diseases. The classification techniques help in automating the detection of plant

leaf diseases and categorizing them centered on their morphological features. Plant diseases reduces a major production in the agricultural industry. Hence, detecting the disease at an earlier stage helps to extent the life of the plant and produce greater yield to the farmers. Hence, this paper is focused towards detecting the plant leaf diseases by capturing the images of the leaves. The software created using CNN helps the farmers to get the correct information about the quality of plant leaves at any stage.

In deep learning approach, the CNN is a class of deep neural networks, most commonly used to analyze the visual image. Hence, CNN is considered to detect and diagnose the disease in the images of the leaves. The software development process has undergone three different modules for this purpose. In module 1, the

ARTICLE INFORMATION

*Corresponding Author: sushamangal@gmail.com
Received 15th April 2020 Accepted after revision 20th May 2020
Print ISSN: 0974-6455 Online ISSN: 2321-4007 CODEN: BBRCBA

Thomson Reuters ISI Web of Science Clarivate Analytics USA and Crossref Indexed Journal



NAAS Journal Score 2020 (4.31) SJIF: 2020 (7.728)
A Society of Science and Nature Publication,
Bhopal India 2020. All rights reserved.
Online Contents Available at: <http://www.bbrc.in/>

images are imported from the dataset. In module 2, the model is trained with the dataset. In module 3, the layers in CNN model are analyzed. With the results obtained. This approach will be very useful to farmers because the early detection of the plant disease in the farm can help the farmer to apply early prevention mechanisms to save cost and life of the plants.

MATERIALS AND METHODS

Literature Survey: Various algorithms and techniques have been proposed for plant disease detection and predicting accuracy in loss of damage to plants. The major finding from various researchers are discussed in this section.

(Umair Ayub et al., 2018) have made a study on various data mining techniques to identify crop disease and to predict the accuracy of loss or damage made by the disease. The techniques used by the study include Decision Tree, Random Forest, Neural Networks, Naive Bayes, Support Vector Machines, Gaussian Naïve Bayes and K-Nearest Neighbors. Sasirekha. Swetha (2015) have proposed the study that follows the Knowledge Discovery in Databases (KDD) process to identify disease occurrences at various levels of abstraction from dataset. The study created the concept of hierarchy using domain knowledge to incorporate it into the data mining process to improve performance. (Jitesh et al., 2016) have made a study on different types of plant diseases that occur on rice plant.

The images of various diseases such as Leaf blast, Brown spot, Leaf scald, Bacterial leaf blight, Sheath blight are used as datasets. Nikos (2016) have proposed a method which was implemented as a Windows Phone application in the Visual Studio 2015 using the Silver light library. It separate the spots from the rest of the leaf and the background. (Rakshitha et al., 2017) have presented a paper that mainly focuses on designing an UGV (Unmanned Ground Vehicle) for the purpose of disease detection of cutting pepper fruit. (Hemantkumar et al., 2019) have used this algorithm to predict pest Diseases of crops using machine learning techniques. (Mrunmaye et al., 2015) have proposed this algorithm to diagnose Pomegranate Plant Diseases. KNN clustering algorithms are used to detect, classify and also for cluster formation

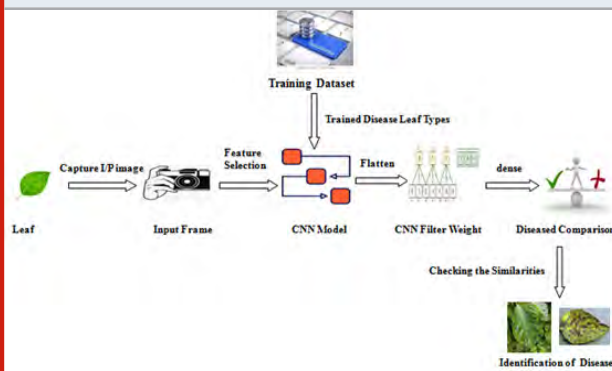
(Xiaoyan et al., 2018) have proposed a novel image segmentation model for plant diseases based on hybrid frog-hopping algorithm is proposed. Image Segmentation is the main step in feature extraction and diseases recognition of plant diseases images. The model could be used to extract the outcome from the background effectively. (Gulhane et al., 2014) proposed a model based on Principal Component Analysis Classifier. Predictions of diseases on cotton leaves by human service may be wrong in some cases. Utilizing machine vision techniques, it is possible to identify different kinds of diseases within visible as well invisible wavelength regions. After executing PCA/KNN multi-variable

techniques, it is possible to analyse a collection of numerical data related to the Green (G) channel of RGB image. The classification accuracy of PCA/KNN based classifier observed as 95%

Proposed System

To detect the plant leaf diseases deep learning approach is proposed in this paper.

Figure 1: Architecture of the system



The architecture of the software system is shown in Fig 1. The architecture is designed for the deep learning algorithm called Convolutional Neural Network which is called as ConvNet/CNN. It takes an input image of the plant leaf and assign the weights and biases to it to the various aspects and objects in the image of the leaf. This makes it possible to differentiate one from the other. After this, pre-processing is done. Based on this, CNN will learn these filters and characteristics.

Input Layer: The input layer in CNN contains the image data. Image data is represented by three dimensional matrices. It needs to reshape it into a single column. The captured images of different types of leaves of different plants are fed into the system.

Convo Layer: Convo layer is sometimes called feature extractor layer because features of the image are get extracted within this layer. A part of image of a leaf is connected to Convo layer to perform convolution operation. It creates the dot product by calculating the dot product between receptive field and the filter. Result of the operation is single integer of the output volume. Similarly, it filters over the next receptive field of the same input image by a stride and do the same operation again. It will repeat the same process again and again until it goes through the whole image of the leaf. The output will be the input for the next layer.

Pooling Layer: The spatial volume of the input image after convolution is reduced in the pooling layer.

Fully Connected Layer: A Fully connected layer contains the weights, biases, and neurons. It connects neurons in one layer to neurons in another layer. This layer will classify the images between different categories by training the model.

Softmax / Logistic Layer: Softmax or Logistic layer is the last layer of CNN. It resides at the end of fully connected layer. The Logistic layer is used for binary classification of the images and softmax is for multi-classification of the images.

Output Layer: Output layer produces the required output for the user with the comparative analysis.

Module Description: The modules in the proposed system is described as follows;

1. Build model for training datasets
2. Build model for CNN test accuracy
3. Implementation of CNN model
4. Plant disease identification
1. Build model for training datasets

Training dataset is created to train the system with CNN and how to apply neural network concepts to produce results. Here the images are trained by using dataset classifier and fit generator function. Fit generator function accepts the datasets, performs back propagation and update the weights in the proposed model. By using this function, the dataset can be easily classified and trained. In this module the grayscale base and edge base are used to identify the model loss and model accuracy.

2. Build model for CNN test accuracy: The trained dataset is used in this module to train the CNN model so that it can identify the test image and the disease type. CNN has different layers like dense, dropout, activation, flatten, convolution 2D, and Max pooling 2D. After the model is trained successfully, the software can identify the disease if the plant species is connected in the dataset. Here the convolution 2D layer is used to combine the image into multiple images activation. This is called as activation function. and Max pooling 2D is used to max pool the value from the given size matrix and also check the similarity and give it to dense. Flatten layer is used to generate the fitting function of an image after convolution 2d image is obtained. Dense layer is mainly used for classification. These processes will run in a hidden layer. By using these layers, it is easy to predict the disease and also find the accuracy.

3. Implementation of CNN model: In this module, the trained dataset images and the sample valid images are compared for obtaining results. It generates the result with the diseased leaf name. It also shows the accuracy and loss percentage in the output. Loss percentage shows the dissimilarity between the images. With a large dataset and efficient training method, more accurate results can be obtained.

4. Plant disease identification: The input images are given through a using preprocessing package. That input image converted into array value and image to array function package. We have already classified disease of leaf in our dataset. Compare both as did in module 3. Then we have to predict our leaf diseases using predict function.

RESULTS AND DISCUSSIONS

The proposed model predicts whether the leaf is diseased or healthy leaf. If the leaf is diseased, the result will provide the type of disease as classified by the CNN algorithm. The model is tested with dataset of 58 images of different leaves. The accuracy of the prediction is more than 98%. The result inferred from the proposed work is given in Fig 2.

Figure 2: Input leaf image



The accuracy of the model is shown is shown in Fig 3 and the loss is shown in Fig 4. The sample code for identifying and diagnosing the leaves of a tomato plant is shown in Fig 5. The tomato plant leaves are categorized as bright, bold, spotted leaf, yellow leaf, brown leaf and accordingly the viruses affected in the leaves are diagnosed as mosaic virus, Septoria leaf spot, early blight, late blight etc. Accordingly, for the input image given in Fig 2, it diagnoses and detects that the leaf is affected with Septoria leaf spot virus and creates a warning measure to the farmer. The risks involved to the plant yield and to the life time of the plant are also shown to the farmer.

Figure 3: Model accuracy

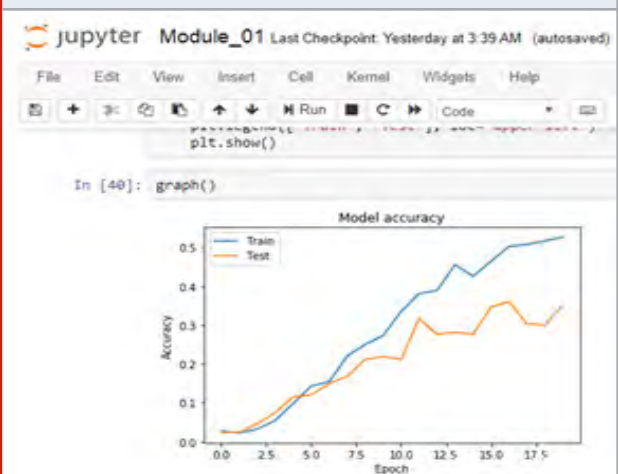
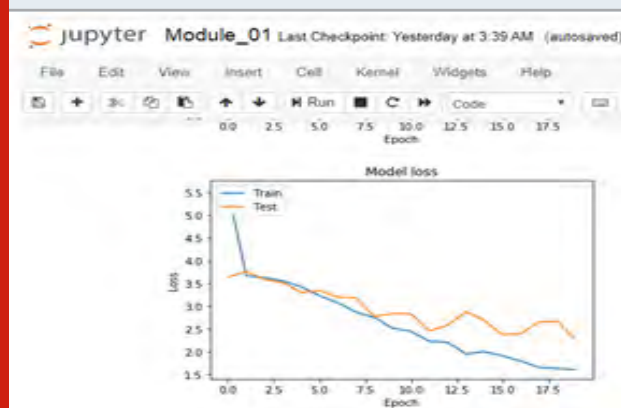


Figure 4: Model Loss



The sample code to detect the type of virus in a tomato plant leaf is shown in Fig 5

Figure 5: Sample code

```
elif output['Tomato_Late_blight']==1.0:
    print("Tomato_Late_blight")
elif output['Tomato_Leaf_Mold']==1.0:
    print("Tomato_Leaf_Mold")
elif output['Tomato_Septoria_leaf_spot']==1.0:
    print("Tomato_Septoria_leaf_spot")
elif output['Tomato_Spider_mites_Two-spotted_spider_mite']==1.0:
    print("Tomato_Spider_mites_Two-spotted_spider_mite")
elif output['Tomato_Target_Spot']==1.0:
    print("Tomato_Target_Spot")
elif output['Tomato_Tomato_Yellow_Leaf_Curl_Virus']==1.0:
    print("Tomato_Tomato_Yellow_Leaf_Curl_Virus")
elif output['Tomato_Tomato_mosaic_virus']==1.0:
    print("Tomato_Tomato_mosaic_virus")
elif output['Tomato_healthy']==1.0:
    print("Tomato_healthy")
```

Potato_Late_blight

CONCLUSION

This software provides a clear information about the conditions of the leaves of a plant. With a smart phone, the images of a plant can be easily captured and can be given as input to the system. With a few minutes, the system will detect whether the leaf is healthy or not. If is affected with a virus, it also gives warning to the farmers about the significance of immediate treatment and care needed for the plant to provide a good yield with a long life.

REFERENCE

- Balasubramanian Vijayalakshmi and Vasudev Mohan (2016) Kernel based PSO and FRVM: An automatic plant leaf type detection using texture, shape and color features Computer and Electronics in Agriculture vol 125 Pages 99-112.
- Bin Liu, Yun Zhang Dong Jian He and Yuxiang Li (2017) Identification of Apple Leaf Diseases Based on Deep CNN Symmetry vol 10 no 11.
- Chit Su Hlaing ,Sai Maung Maung Zaw (2017)Plant Diseases Recognition for Smart Farming Using bModel-based Statistical Features IEEE.
- Dheeb Al Bashish MalikBraik and SuliemanBani-Ahmad (2010) A Framework for Detection and Classification of Plant Leaf and Stem Diseases International Conference on Signal and Image Processing.
- Dong Pixia and Wang Xiangdong (2013) Recognition of Greenhouse Cucumber Disease Based on Image Processing Technology Open Journal of Applied Sciences, vol. 3. GodliverOwomugisha and Ernest Mwebaze (2016) Machine Learning for Plant Disease Incidence and Severity Measurements from Leaf Images IEEE.
- Gavhale U Gawande and K O Hajari (2016) Unhealthy region of citrus leaf detection using image processing techniques International Conference on Convergence of Technology I2CT Pages 1-6.
- HarshalWaghmare, RadhaKokare and YogeshDandawate (2016) Detection and Classification of Diseases of Grape Plant Using Opposite Colour Local Binary Pattern Feature and Machine Learning for Automated Decision Support System 3rd International Conference on Signal Processing and Integrated Networks (SPIN).
- HemanthkumarWani and NilimaAshtankar (2017) An Appropriate Model Predicting Pest/Diseases of Crops Using Machine Learning Algorithms International Conference on Advanced Computing and Communication Systems.
- Joshi and B. D. Jadhav (2016) Monitoring and Controlling Rice Diseases Using Image Processing Techniques 2016 International Conference on Computing, Analytics and Security Trends (CAST) College of Engineering Pune.
- Jadhav and S. B. Patil (2015) Grading of Soybean Leaf Disease Based on Segmented Image Using K-means Clustering International Journal of Advanced Research in Electronics and Communication Engineering (IJARECE) vol 4 no 6 Sensing Pages 1693- 1706.
- Jitesh P. Shah and Vipul K. Dabhi, Dharmsinh (2016) A Survey on Detection and Classification of Rice Plant Diseases IEEE.
- MrunmayeeDhakate and Ingole,(2015) Diagnosis of Pomegranate Plant Diseases using Neural Network A.B IEEE.
- Nikos Petrellis (2016) Plant Lesion Characterization for Disease Recognition window phone application IEEE.
- Nikos Petrellis (2017) A Smart Phone Image Processing Application for Plant Disease Diagnosis Network with

shuffle frog leap algorithm IEEE.

Pujari R Yakkundimath and A S Byadgi (2014) Identification and classification of fungal disease affected on agriculture/horticulture crops using image processing techniques IEEE International Conference on the Computational Intelligence and Computing Research.

Rakshitha N Rekha H S Sandhya S Sandhya V and S Sowndeswari (2017) Pepper Cutting UGV and Disease Detection using Image Processing IEEE.

Sasirekha, N. Swetha. (2015) An Identification of Variety of Leaf Diseases Using Various Data Mining Techniques International Journal of Advanced Research in Computer and Communication Engineering Vol 4

Issue 10.

Umair Ayub and Syed Atif Moqurrab (2018) Predicting Crop Diseases Using Data Mining Approaches: Classification IEEE 2018

Viraj A Gulhane and Maheshkumar H Kolekar (2014) Diagnosis Diseases on Cotton Leaves Using Principal Component Analysis Classifier IEEE.

Wang M Zhang J Zhu and S Geng Spectral prediction of Phytophthora infestans infection on tomatoes using artificial neural network (ANN) International Journal of Remote.

Xiaoyan Guo Ming Zhang Yongqiang Dai (2018) Image of plant disease segmentation model based on pulse coupled neural network IEEE 2018

Smart Portable Kidney Dialysis Control and Monitoring System

A. SenthilKumar¹, G.Keerthi Vijayadhasan² D.Rashiga³ and K. Swetha⁴

^{1,3,4}Dept. of ECE, Chennai Institute of Technology, Chennai, Tamilnadu, India

²Dept. of EEE, Chennai Institute of Technology, Chennai, Tamilnadu, India

ABSTRACT

In recent years, kidney dialysis takes place through the process of using the Hemodialyzer (artificial kidney) to clear away the lavish and extra fluid from the hemoglobin and return back the filtered blood to the body. During blood transplant, the blood exposure is detected through the blood exposure detector. If a blood leak develops through the dialysis membrane, and the appropriate alarm is activated. The Disadvantage of the existing dialyzer is that some obstacles may arise which is due to the cuprophane membrane makes the toxic membrane in the dialyzer to be activated, so that the dialyzer can be dangerous sometimes. The Proposed System is that the blood which is to be purified is by heating unit having LM35. After fully purified, while dispatching the sanguine fluid it can analyse whether it blood can be fissure or not by using Photo interrupter Transmitter and Receiver. The alert signal is transmitted to the health care unit so that they can take appropriate actions. This is done through the IOT based transmission of the information to the cloud, with the help of cloud we can analyze the patient's entire process. From analysis we are using a DA tool which is inexpensive compared to the existing systems.

KEY WORDS: LM35, PHOTO INTERRUPTER, DA TOOL.

INTRODUCTION

For the past years, the procedure of dialysis has experienced in the significant creating and the created countries. This dialysis should be possible with the different ways like Haemodialysis, Peritoneal dialysis, and kidney transplantation. A Profitable Blood introduction identifier is by and by starting at now available which requires an identifying force of under 1ml of blood, and the

blood presentation ballgame can be knowledgeable about 1~2 seconds. The ballgame of the blood introduction is a direct result of the distinction in automated advancement in the circuit, which involve two tossing joins segregated by an opening.

When the blood flows in the aperture, the electrical connection is being created between the two cables and so with this the blood exposure is detected. The currently using product is insubstantial blood exposure device, which cannot be restate. Moreover, the quantity of blood required for suspect the blood exposure can be enhanced. By adding to this, the fare of such products are not economical for the normal victims and thus cannot be familiarize.

ARTICLE INFORMATION

*Corresponding Author: senthilkumara@citchennai.net
Received 15th April 2020 Accepted after revision 20th May 2020
Print ISSN: 0974-6455 Online ISSN: 2321-4007 CODEN: BBRCCA

Thomson Reuters ISI Web of Science Clarivate Analytics USA and Crossref Indexed Journal



NAAS Journal Score 2020 (4.31) SJIF: 2020 (7.728)
A Society of Science and Nature Publication,
Bhopal India 2020. All rights reserved.
Online Contents Available at: <http://www.bbrc.in/>

There is no monitoring for the Blood Leakage in the Hospital for a patient. If the blood leakage is more the patient health will be more critical. Outwardly the dialysis, leads to the increase of the toxins in the blood leads to the condition called the uraemia. The victim will receive the necessary medication to manage the uremia and other medical conditions.

In Proposed Work, the Victim who is having the impure blood, is collected in a Container. After collecting the impure blood which is having some disease like Diabetes, High blood pressure, etc. In order to remove those diseases, here we have a connected heating unit for heating the blood. Here we have used LM35 as a Temperature sensor to monitor the blood condition of heating. After heating the blood, it can send it to the blood purifier unit for the purification of blood. After fully purified it can be sent to the victim through a pumping motor, while sending the blood it can be audited whether it can be Exposed or not by using a Photo Interrupter, Transmitter and Receiver. Photo Interrupter is used as a sensor for detecting the blood leakage and combined with a Wi-Fi for the function of wireless transmission.

The blood leakage spotter can be made to be given with the small batch so it can be wearable, which is uncomplicated and modest way for the monitoring of the blood leakage during remediless treatment. The alert is made whenever the leakage is detected and the sound and the warning message is made to be sent to the health care unit. With this message the healthcare workers can get the knowledge of what the Victim is getting to do. This also sends the message when the victim is more sensitive to handle the device and he is nervous. The Photo Interrupter sensing element is used for the detection of the light changes and it alters the original voltage signal appropriately.

Here the IOT for moving data to the cloud is used, with the assistance of cloud we can break down the patient's whole procedure. From investigation we are utilizing a DA apparatus. It is an interfering observing gadget, which empowers an easy induction of the indicator on the human plasma to expel all destructed blood.

Literature Survey: (Davita et al, 2017). Dialysis patients frequently experience the ill effects of cardiovascular infection. Heart pressure beats enter the extracorporeal blood circuit of a dialysis machine and proliferate through the vascular framework, where the weight sensors are utilized to catch beats. The cardiovascular heartbeats are the more grounded pressure beats beginning from the peristaltic blood siphon. The venous weight sign will remove the cardiovascular sign. This technique perform less at low heart pressure. At present, a novel strategy utilize both blood vessel and venous weight sensor. The outcomes propose that pulse can be evaluated all the more precisely from pressure signals with lower heart signal abundancy when both blood vessel and venous weight are utilized, contrasted with when just the venous sign is utilized.

The introduction of the methodology using both vein and venous signs and the past system using only the venous was surveyed concerning typical heartbeat estimation for each I-min fragment, with beat chose from the PPG-signal as reference. The beat calculation relied upon heartbeat starting events. The heartbeat starting events was resolved as the time snapshot of the mid plentifulness motivation behind each heartbeat for both the normal cardiovascular part $e(J)(t)$ and the PPG-signal. The top to top adequacy of each heartbeat was figured as the differentiation in plentifulness of the apex succeeding the mid ampleness point, and the valley going before the mid abundancy point (C. Carissa Stephens 2017).

The new technique empowers consistent internet checking of a patient's pulse additionally for patients with low cardiovascular sign plentifulness. In Machine learning approach for expectation of hematic parameters in hemodialysis patients, According to Cristoforo Decaro, A spectroscopic arrangement was set up for obtaining of blood absorbance range and tried in an operational domain. This arrangement is non intrusive and can be applied during dialysis meetings. A help vector machine and a counterfeit neural system, prepared with a dataset of spectra, have been executed for the expectation of hematocrit and oxygen immersion.

The calculations were prepared by directed learning: targets were given by rotator to Hct and hemo-gas analyzer for sO_2 . All the preparation set of absorbance spectra, estimated by spectrometer during dialysis tests, have shaped the info information. Hematocrit and oxygen immersion levels of blood tests were anticipated by models dependent on help vector machine and fake neural systems procedures. At long last, the help vector machine and the fake neural system were thought about through assessment parameters, to confirm the exactness of the two models.

Relapse plot examination work contrasts real yields of two calculations and the relating wanted ones (targets). Right now, pivot speaks to the objective qualities, y-hub speaks to the anticipated qualities, line speaks to the ideal fitting among target and anticipated qualities, while disperse focuses speak to test tests. These outcomes show that SVM and ANN can execute a model which predicts with great exactness hematocrit levels utilizing absorbance range inputs. A decent forecast exactness of Hct was accomplished by the two models ($r^2 = 95\%$). A similar examination was performed for oxygen immersion.

The precision of these techniques is higher for oxygen immersion than for hematocrit forecast. Results are astounding for both the AI based calculations, they give precise expectations. For the two calculations, the coefficient of assurance is equivalent to 99%, so models report elite. Figure 7 shows exactness of the models with test information. The two strategies give proficient expectations, however SVM is, once more, the best AI calculation, in light of the fact that MSE and MAE are lower than the ones of ANN. These outcomes show that

both SVM and ANN strategies can foresee precisely hematocrit and oxygen immersion.

The arrangement here proposed, comprising in the utilization of small spectrometer and AI methods, permits results which are similar with other non-obtrusive sensors, for expectation of hematocrit and oxygen immersion. This paper shows the use of an AI approach joined with a basic and ease spectroscopic based arrangement for checking hematic parameters of blood, for example, hct and sO₂, during dialysis and other extra mortal medicines. A help vector machine and a counterfeit neural system have been executed and applied to information got through spectrometry in the noticeable and approach infrared of various blood tests. Results exhibit that SVM and ANN models accomplished great learning exhibitions and both demonstrate the capacity to learn connection among information and targets. In term of precision, the most encouraging calculation is SVM, however both AI techniques can expand exact prescient models. As for other non-obtrusive methods which utilize just not many prompt information of the range and which play out the estimations with direct adjustment.

In an examination for assessing the appropriateness of peritoneal dialysis(PD) patients, as indicated by Wang-Chin To decide the dialysis strategy for the patient, it is important to utilize the clinical expert point of view to pass judgment on not just whether the patient 's state of being is reasonable or not , yet in addition whether the dialysis technique is " tweaked" to coordinate the patient's life. As needs be, in 2006, the National Health Insurance actualized the Pre-ESRD program , which is a case the board , permits clinical staff to give proficient treatment guidance to patients for various life circumstances . The reason for this plan is to rearrange the examination of patients before case the board . Right now the specialists utilize the writing audit technique to focus on the patient 's word related status .This examination additionally expects to accomplish the motivation behind permitting the nursing staff to rapidly comprehend the circumstance of the patient case . So as to present the consequent defense the board progressively productive, it can likewise make the patient's work smoother and have a superior quality.

In Effects of Obesity on Heart Rate Variability in Consistent Ambulatory Peritoneal Dialysis Patients, Natchanon Promprasit says that Both weight and interminable kidney sickness (CKD) replaced with constant versatile peritoneal dialysis (CAPD) have been known as the purpose behind cardiovascular autonomic brokenness (CAD) anyway there has been no examination on these the two conditions affecting the CAD. Right now, purpose behind examination is the effects of weight on beat variability (HRV) in CKD superseded with CAPD patients. There are 77 Thai subjects, orchestrated from their weight record (BMI) as; normal prosperity (NH) gathering, CAPD run of the mill (CN) social event, and CAPD heavy (CO) gathering. As the results, differentiating among CO and CN social occasions, found that the higher augmentation of mindful tactile framework (SNS) of CO

bundle has been showed up by the tallness of systolic circulatory strain (SBP) and heartbeat (HR) stood out from the CN gathering. In this manner, the CAPD patients with huskiness have been plainly demonstrated that they have more CAD than CAPD patients with normal body weight. When the data were destitute down for relationship, the results showed that basic logarithm of high repeat (lnHF) is on the other hand related to triglyceride (TG) level with $r = - 0.553$, $p = 0.014$, however, ordinary logarithm of low repeat (lnLF) is really related to TG level with $r = 0.489$, $p = 0.033$. Along these lines, it might be prescribed that TG level may be a pointer for CAD in CAPD fat patients (Muthukumar, B et al,2019).

They demonstrated that the huge people has higher of these two parameters of diabetes mellitus than common sound. The relative result that the more raised degree of TG in CO bundle appeared differently in relation to CN social affair may be the result from the alteration of the bounty glucose and blood lipid. The examination of M.A. Paschoal et al., demonstrated that the weight pack through and through greater addition in TG and VLDL while greater reduction in HDL. Sadly, the current data found that solitary the TG ascent of the CO pack was found. The examination of M. Cignarelli et al, and M.A. Paschoal et al [15]., prescribed that the atherosclerosis from hyperlipidemia has the ischemic effects the various organs, for instance, kidney, heart, and cerebrum. Particularly, the renal ischemia is the typical implication for the hypertension by the commencement and emanation of the renin hormone. In addition, the CAD may be occurred from either heart or cerebral ischemia. The more noticeable lessening of time zone including pNN50 of the CO pack when

stood out from the CN bundle indian; $r = - 0.553$; $p = 0.014$

lnLF; $r = 0.489$; $p = 0.033$,lnLF/HF extent: $r = 0.546$; $p = 0.016$

cated that the chubbiness may grow the CAD in the CAPD patients with weight. Notwithstanding the way that, it has been inspecting, the proposed framework may be a result of the effect of leptin hormone.

MATERIALS AND METHODS

Proposed System

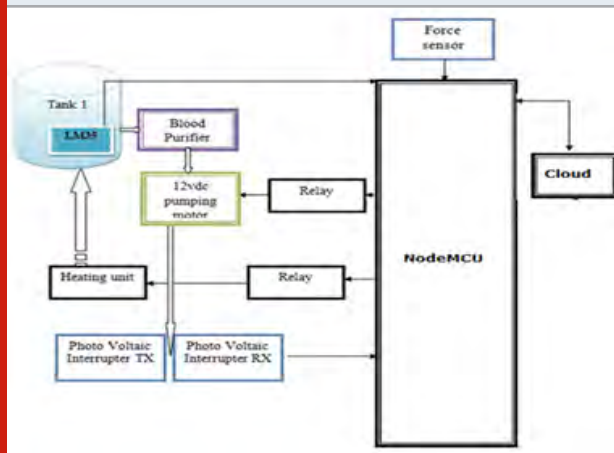
The proposed method comprises of 4 phases:

- i) Phlebotomy
- ii) Dialysis Process
- iii) Blood Leakage detector
- iv) Alert through IOT

i) Phlebotomy: Phlebotomy is when someone uses a needle to take blood from a vein, usually in the patients arm. The Blood of the Patient whose blood is to be dialyzed is made to be taken out through the 12v dc pumping motor. The blood is pumped out through this motor and is collected in a tank which consist of the

LM35. The purpose of collection of the blood in the tank is for the purification process of the blood where the dialysis takes place.

Figure 1: The Block diagram represents the Smart Portable Kidney Dialyzer



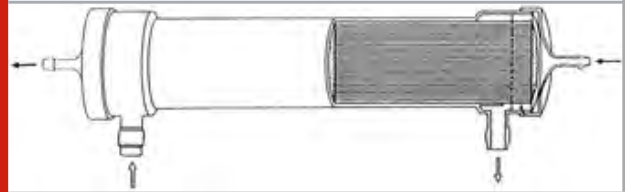
ii) Dialysis process: The tank which acts as the purification agent in the dialysis that consist of the LM35. Inside the tank, the dialysis takes place by passing the blood into the semipermeable membrane that purifies the blood and the purified blood is made to be passed through the outlet of the tube which should be returned to the another arm of the patients body. The blood flows through the tubules, while the dialysate flows countercurrent in the spacing between the tubules. Solutes are driven through the pores of the membrane from one fluid to another fluid by concentration gradient. The most important characteristic of dialyzers is their overall mass transfer coefficient (KKO), a measure of how effective a dialyzer is at transporting a particular solute across a fixed area of its membrane. In turn, KKO (in conjunction with the surface area (AA) and the flow rates) can be used to calculate the clearance (KK), the rate at which blood is cleaned.

a) Dialysate: Dialysate is the fluid that runs the blood through the dialyzer. The composition of the dialysate is very significant in the removal of solutes from the blood based on the concentration gradient. Substances that are to be removed have little presence in the dialysate, while substances that are to be left in the blood are present in dialysate. In between those two extremes are the substances that must be carefully balanced – the blood is not to be entirely cleaned of their presence, so the dialysate still contains a quantity of that particular substance. The substances that commonly appear in commercial dialysate solutions are sodium, potassium, calcium, magnesium, chloride, acetate, bicarbonate, and glucose.

The LM35 is placed in order to monitor the temperature of the patient and the temperature notification is sent to the mobile device through the wireless network.

iii) Blood Leakage Detector: After purification, blood can be sent to the patient through a pumping motor. During that period, blood leakage will be checked by Photo interrupter Transmitter and Receiver. The sensor used for blood leakage detecting is Photointerrupter and wireless transmission made by using Wi-Fi. In the circuit, the arm jeweler coordinated with blood spillage identifier which is utilized to screen the blood spillage during the hemodialysis treatment. The Alert framework will be started quickly with a sound and cautioning light in the wake of distinguishing the blood leakage. Then the alarm sign will be transmitted to the medicinal services, it will be a fitting activity for human services laborers to forestall any dangers. The retentive material close to the photointerrupter detecting component will detect the light and the first voltage signal. This changes in the voltage signal is sent to caution segments and the Wi-Fi module.

figure 2: A typical dialyzer. The blood enters on the right and travels through thousands of tiny tubules before exiting on the left. The dialysate enters on the bottom left, fills the spacing around the tubules and exits on the bottom right



iv) Alert through IOT: The force sensor is made to be connected to the device which sends the information to the health care unit when the patient is nervous to perform the dialysis process. When he is more sensitive he can't perform the dialysis process at that time the force sensor placed at the circuit sends the alert to the healthcare unit that the patient is not fit for the dialysis process. The process is then put to hold so that the patient should be recovered from the sensitiveness and should continue with the process of the dialysis. Through the LM35, the body temperature of the patient is noted and it is displayed in the mobile device which acts as the receiver unit. If the blood leakage is detected that is also sent as the notification to the healthcare unit. With the help of the cloud we can analyze the patient's entire process. From analysis we are using a DA tool.

IV) RESULT AND DISCUSSION

There is no monitoring for the Blood Leakage in the Hospital for a patient. If the blood leakage is more the patient's health will be more critical. The sensor used here is the Photointerrupter. It is used for recognizing the blood exposure and united with a wifi which is due to the cellular conveyance. In the event that the spotter detects the introduction of blood, the warning framework will be activated immediately, such that the alarm sound and the notice message is sent to the Healthcare unit. With this message from the device the healthcare unit, the healthcare workers can know about the status of the

Victim. They are also notified if the victim is not fit for performing the dialysis process when they nervous, so it provides certain time limit so that the victim can settle down and perform the dialysis process.

Additionally it is an intruding checking gadget, which empowers an easy instatement of the locator on the human plasma to expel all destructed blood and it is convenient. The blood purification is done with the heating unit placed inside the tank and the temperature can be sensed with the temperature sensor. Those details are displayed through the receiver module of the cloud data in mobile app. So it is easy for the healthcare unit to take further action on the patients health. This device overcomes the advantage of the existing dialysis system which is more convenient and portable to the patients and moreover everyone nowadays are familiar with smartphones so the information sent through the cloud through the wireless system will be useful for the healthcare units in order to monitor the patients dialysate level.

Figure 3: Inputs of the system model

Parameter Name	Variable	Units
Blood flow rate	Q_B	mL/min
Dialysate flow rate	Q_D	mL/min
Dialyzer properties	K_0A	mL/min
Trade-off coefficient	α	-
Urea generation rate	\dot{G}	mg/min
Residual kidney function	$GFR\%$	-
Total blood volume	V_B	mL
Total dialysate volume	V_D	mL
Incoming blood urea concentration	C_{B_i}	mg/mL
Incoming dialysate urea concentration	C_{D_i}	mg/mL
Dose length	t_1	min or hours
Time between doses	t_2	min or hours
Ultrafiltration coefficient	K_{UF}	mL/min/mmHg
Dialyzer blood pressure	P_B	mmHg
Dialyzer dialysate pressure	P_D	mmHg

Figure 4: Parameters calculated by the system model

Parameter Name	Variable	Units
Dialysate flow rate	Q_D	mL/min
Dialysance	D	mL/min
Dialyzer clearance	K	mL/min
Total dialysate volume	V_D	mL
Outgoing blood concentration	C_{B_o}	mg/mL
Outgoing dialysate concentration	C_{D_o}	mg/mL

1. Blood flow rate is one of the most important variables in hemodialysis. Because of the large volume of blood in the body, the only way to sufficiently remove urea in a satisfactory time scale is to increase the blood flow rate. Unfortunately, a home-based system is limited to blood flow rates below 100 mL/min due to the types of blood ports that must be used in a non-clinical setting. Any system that is embodied must work around this limiting flow rate.

2. Optimal dialysate flow rate is closely tied to the blood flow rate. At slower blood flow rates, the dialysate flow rate does not need to exceed about a one-to-one ratio.

This actually works in the favor of a home hemodialysis system. At high blood flow rates, the best dialysate flow rate can be double the blood flow rate, vastly increasing the volume of dialysate needed. Since one of the goals of this chapter was to devise a system that uses less dialysate, having a system with a slower blood flow rate is advantageous.

3. Peristaltic pump abundance is more serious for pumps in the movement rate dimension required for dialysis. For machines that are plugged into the wall, this is inconsequential. However, if a battery-powered system were developed, designing a pump that is more efficient would be important. The effect of pump power on the system was not integrated into the Simulink model, but its importance is noted.

4. The immensity of the dialyzer has a negligible smash on the consent of urea at the process of hemodialysis. Because the physical size of a large dialyzer (with a Q of 1600 mL/min) is not limiting, at this point in the design process there is no reason not to use the largest available dialyzer. Portable systems that rely on slow blood flow rates need all the help in urea clearance available.

CONCLUSION

Nowadays, kidney failure is found to be a major disease among everyone. Haemodialysis, Peritoneal dialysis, and kidney transplantation are the different variety of therapy methods for kidney failure. The currently available therapy for kidney failure has a specific commercial blood leakage detector which detects sensitivity of blood and leakage condition of blood can be detected within a seconds. The sensor which senses based on the changes of the voltage signal. It also has a detector with two electrodes spaced, each generates a source via lead by connecting to the signal. The signal processing unit in this device detects the change of the state by introduction of fluid across the electrodes and the alarm is initiated. The nonconductive material in cathode can be reused after cleaning. The different items are associated with detecting and identification of blood spillage of roughly 1 ml of blood. The blood spillage can be distinguished by change in electrical conductance which contains two metal wires that are isolated by a cut. The portable kidney machine is very efficient and adaptable for this generation in order to do dialysis for the kidney renal failure patients. The healthcare unit through IOT can have the ability to measure the temperature of the patient.

REFERENCES

- Android Studio 3.0 Android Developers Blog 2017. [Online]. Available: <https://android-developers.googleblog.com/2017/10/android-studio-30.html>. [Accessed: 05- Nov- 2017].
- Davita.com. (2017). The history of dialysis - DaVita. [online] Available at: <https://www.davita.com/kidney-disease/dialysis/motivational/the-history-ofdialysis/e/197> [Accessed 5 Sep. 2017].
- C. Carissa Stephens Dialysis: All You Need to Know

Medical News Today, 2017. [Online]. Available: <https://www.medicalnewstoday.com/articles/152902.php>. [Accessed: 04- Nov- 2017].

Chronic kidney disease - Symptoms and causes - Mayo Clinic Mayoclinic.org, 2017. [Online]. Available: <https://www.mayoclinic.org/diseases-conditions/chronickidney-disease/symptoms-causes/syc-20354521> [Accessed: 05- Nov- 2017].

Dialysis The National Kidney Foundation 2017. [Online]. Available: <https://www.kidney.org/atoz/content/dialysisinf> [Accessed: 13- Nov- 2017].

H. Garden and S Electronics How Microcontrollers Work What is a Microcontroller? How Microcontrollers Work | HowStuffWorks, 2017. [Online]. Available: <https://electronics.howstuffworks.com/microcontroller1.htm> [Accessed: 02- Nov- 2017].

Dr R Menaka, Dr R Janarathanan, Dr K Deebea,(2020)

FPGA implementation of low power and high speed image edge detection algorithm, Microprocessors and Microsystems, Volume75 2020 103053

Kidney Health Australia. (2017) Types of dialysis | Kidney Health Australia. [online] Available at: <http://kidney.org.au/your-kidneys/support/dialysis/types-ofdialysis> [Accessed 1 Sep. 2017].

Kidney dialysis Broughttolife.scienceuseum.org.uk, 2017 [Online] Available: <http://broughttolife.scienceuseum.org.uk/broughttolife/techniques/kidneydialysis>. [Accessed: 12- Nov- 2017].

Muthukumar, B Dhanagopal R & Ramesh R (2019) KYP modeling architecture for cardiovascular diseases and treatments in healthcare institutions. J Ambient Intell Human Comput.

Implementation of Recurrent Controller with Seven Stage Cascaded Converter for Micro Grid Solar Photovoltaic Battery with Reduced Number of Switches

M. Hari Prabhu¹, K. Sundararaju², S. Nagarajan³, N. D. Arun⁴, M. Bhuvaneshwaran⁵, and A. Mariya Joseph Sathish⁶

¹Assistant Professor,

²Professor

^{3,4,5,6}UG Scholars, Department of Electrical and Electronics Engineering, M.Kumarasamy College of Engineering, Karur – 639113, India.

ABSTRACT

This paper introduces a recurrent control system for the reduced seven-level cascaded inverter switch for reactive and responsive power management with a better power output. The suggested repetitive control approach is extended to the RSCI and the output is checked on a grid-connected micro grid combined with solar panel for the battery. To obtain full efficiency, an incremental conductance method (IfC)-based control technique is suitable for efficient use operation of MPPT. The Energy storage system of battery is regulated by recurrent managed based RSCI for photovoltaic for efficient energy management. A changeable radiance input to the photovoltaic unit is considered to demonstrate the viability and stability in operation of the proposed solution. In order to clarify the technical applicability of the solution offered and to satisfy the IEEE-1547 energy quality limitations, an LCL filter is identified to reduce the amount of harmonic distortion in the grid side current. The enhanced output of the proposed technique is explained by providing results of simulation compared with respect to a neutral point clamped inverter with proportional integral controller (PI). The feasibility of the proposed solution is tested by simulation using MATLAB software during constant and changing irradiance condition

KEY WORDS: FLYING CONDENSER INVERTER (FCI), MAXIMUM POWER POINT TRACKING (MPPT), MULTILEVEL INVERTERS, NEUTRAL POINT CLAMPED INVERTER (NPC), SEVEN LEVEL CASCADED INVERTER.

ARTICLE INFORMATION

*Corresponding Author: hariprabhum@gmail.com

Received 15th April 2020 Accepted after revision 20th May 2020

Print ISSN: 0974-6455 Online ISSN: 2321-4007 CODEN: BBRCBA

Thomson Reuters ISI Web of Science Clarivate Analytics USA and Crossref Indexed Journal



NAAS Journal Score 2020 (4.31) SJIF: 2020 (7.728)

A Society of Science and Nature Publication,
Bhopal India 2020. All rights reserved.

Online Contents Available at: <http://www.bbrc.in/>

INTRODUCTION

Due to the global emissions and energy crisis, distributed generation has been integrated in the electricity generation field as a solution with advanced semiconductor-electronic power devices and smart grid technology. Although the electricity distribution system performs a significant role in the electricity sector, it also has the challenges of looking forward to seeking an optimal control and security solution. PV framework has more appealing functionality for which it is generally recognized and widely deployed in different power sectors in various countries. For clean energy fields, PV is chosen primarily for a distribution grid because it allows for small power generators to be installed and provides low to medium voltage levels. Single-stage and two-stage converters are used by enhanced technology electronic devices based on voltage source for power conversion systems. In real-time Photovoltaic applications, battery based micro grid. In a two-level transformation scheme,

One converter transforms pulsating direct current to constant direct current, and the second converter is used to adjust constant direct current to alternate current for improved energy quality and performance. To run the single-stage conversion method, it is better to incorporate a multi-level inverter instead of the traditional voltage source inverter (VSI), because it provides more voltage levels while decreasing voltage errors and harmonics. Many approaches are ideal for uniform and differing levels of irradiance. The incremental conductivity system is commonly used to monitor the inverter to deliver full power supply to the load. In most instances, the desirable aspect behind its choice is better performance and easy to execute in a remote system. In most cases, the desirable aspect behind its choice is better performance and easy to incorporate in a remote system.

Specific topologies of multi-level inverters (MLI) are proposed by different researchers focused on a Neutral Point Clamped Inverter, Flying Condenser Inverter and Cascaded Inverter (CI). The key drawback to work on a suitable alternative for these types of inverters, though, is the need of a huge range of electronic power switches, capacitors, and diodes. In comparison, the number of components is also rising with the increase in the voltage rate. At the design stage, always it is important to concentrate on setup and integrated converter management aspects and find solutions for basic construction, cost-effectiveness, enhanced power management and power efficiency problems.

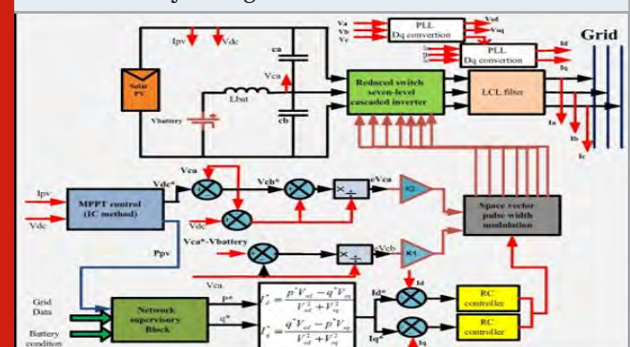
Because of its simple interface mechanism and cost-effectiveness the PI controllers are commonly used in real-time applications. Nevertheless, the efficiency of such controllers depends on their benefit parameters. Such controllers struggle to demonstrate their best efficiency because of usage of constant gain parameters with a design shift and adjustments in feedback in various working conditions. Numerous solutions are suggested by different writers to improve the controller

efficiency and to address the related shortcomings of PI controllers, In addition to power management, removing the THD often includes the inverter management. In this regard, recurrent control could effectively check or completely remove transient signals, specifically when employing closed loop model. Thanks to its superior error cancelation characteristics, recurrent control based controller is efficient in detecting and removing any regular signals including other order harmonics. Application of RC controller to multilevel inverter was thoroughly investigated in this paper. The LCL filter enhances the amplitude and current of the inverter side (AC) harmonic distortion, as well as to preserve the ability to prevent any unexpected voltage changes due to harmonics.

Their volatile, non-linear, and fluctuating existence is one of the big Photovoltaic battery issues powered grid systems. Service quality problems are weakening the system's operating efficiency because of heavy use of electronic control tools. The immediate needs of industrial sectors with heavy power demand include a low to maximum voltage delivery grid with improved energy storage, change in frequency and voltage control. Power system connected renewable systems with storage battery and effective inverter power for solving all of the mentioned problems. This paper concerns design as well as analysis of a three phase solar photovoltaic system and reduced seven level cascaded inverter switch connected to grid. The performance of the introduced method is achieved in conditions of non-varying and changing radiance. The suggested control solution focused on repeated regulation and gradual conductance have a potential to regulate the conditions for MPPT, harmonic removal, enhanced power management, and battery charging and discharge. The suggested solution is tested and findings show a better regulation of the power flow with improved power consistency, improved performance and reliability.

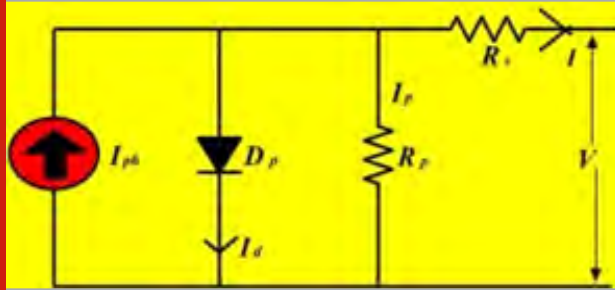
Modeling: For the testing of the proposed solution, the test device consisting of a photovoltaic battery powered grid with grid supports inverter power is checked. Figure.1. Display the entire device and also other important components like the sensor, the photovoltaic battery and a controller present in the block diagram representation

Figure 1: Control device block diagram which combines PV and battery storage



Photovoltaic System Modeling: In Fig (2), Corresponding diagram of a PV cell model and diode has a light produced picture current, diode, parallel resistor, and series resistor.

Figure 2: Equivalent circuit of Photovoltaic cell with single diode



To a good photovoltaic cell, the cumulative current (I) is measured as (1) $I = I_{ph} - I_{oeq} \left[\exp\left(\frac{V - IR_s}{N_s a V_{T_w}}\right) - 1 \right] - V + IR_s R_p$ where 'I_d' states the current of the photovoltaic cell that is expressed as: (2) $I_d = I_{oeq} \left[\exp\left(\frac{V}{a V_{T_w}}\right) - 1 \right]$ here I_o is dark current of the cell saturation (A), Q is electron charge (C), Boltzmann constant is K, Working temperature of the cell is T_w and Ideal factor of the system is 'a'. The current 'I_{ph}' also rests on the operating temperature and the solar radiation, and could be measured as follows: (3) $I_{ph} = G_w G_{ref} \left[I_{sc} + K_1 (T_w - T_{ref}) \right]$ here N_s is expressed as the many series attached photovoltaic cells, T_{ref} is the temperature that is used as reference of the PV cell,

Short circuit temperature coefficient of the current is K_i, Short circuit current of the cell is I_{sc}, reference temperature coefficient are G_w and G_{ref}. The current (I_o) of cell saturation depends on cell temperature (4) $I_o = I_{on} \left[\frac{T_w}{T_{ref}} \right]^3 \exp\left(\frac{q_a K E_g}{T_w T_{ref}} - \frac{E_g}{T_w T_{ref}}\right)$, where I_{on} is cell's history of back saturation at particular temperature (K) and solar irradiance (W / m²). E_g, T_w is the PV-cell's substance band difference (eV). E_g, T_w has a low temperature dependency and is measured as: (5) $E_g, T_w = E_g, T_{ref} \left[1 - 0.0002677(T_w - T_{ref}) \right]$ with E_g, T_{ref} being 1.121 eV for silicon cells.

Regardless of the tacit existence of aforementioned equation; at a constant temperature and irradiance, that is not possible to find empirical solutions to the photovoltaic parameters. The current is greater than level of saturation's cell and thus the leakage level and narrow diode under short circuit situations are ignored. The current in the short circuit is almost same to the picture current produced by the light and is defined as: (6) $I_{ph} = I_{sc}$. For the state of open circuit, voltage of the open circuit is determined by taking the zero output voltage. Reverse saturation current (I_{on}) at a reference temperature is ignored by the opposite leakage current (I_p): (7) $I_{on} = I_{sc} \exp\left(\frac{V_{oc}}{N_s a V_{T_w}}\right) - 1$ the given figure shows the output characteristics of the PV model as voltage vs and power vs. current. These are the results of the test under varying temperature and irradiance conditions.

Reduced switch seven level cascaded inverter modeling:

Reduced switch seven level cascaded inverter includes a complete three-phase inverter and one cascade-connected condenser circuit for selection. The inverter works in both the lower and upper half cycles (+ ve) and also in -ve cycles. Electric diodes and switches are expected to be optimal if the voltage in between both condensers are equal and constant to respectively V_{dc3}, 2V_{dc3}. The output power delivers from the generator side photovoltaic is in line with the grid power, the inverter side result current (RSCI) is also in line with the grid voltage. The inverter operation is generally divided into 8 operating modes: four operating modes represent the upper half cycle (+ ve) and a further four modes represent the lower half cycle (-ve). Fig.5. displayed a two step RSCI circuit diagram.

Figure 3: Curves of PV characteristics performed at various levels of irradiance

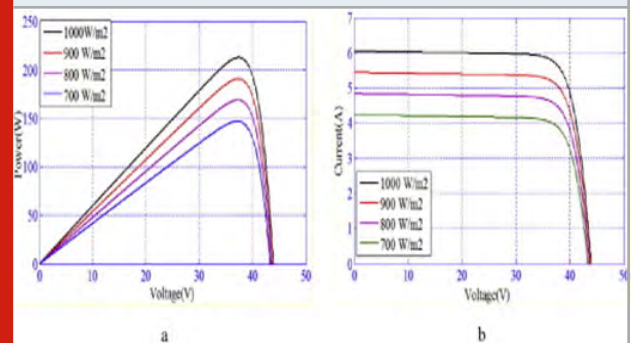


Figure 4: Curves of PV characteristics performed at various temperature conditions

(a) Power (W) vs. Voltage (V) curve
(b) Current (A) vs. Voltage (V) curve

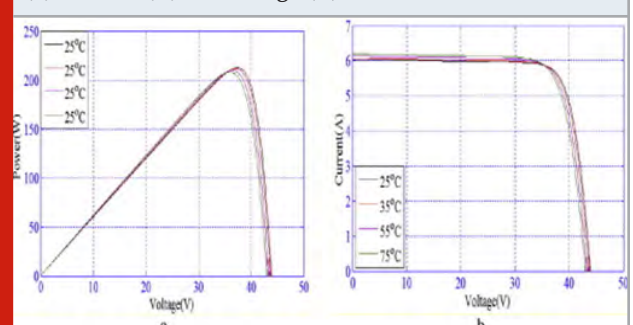
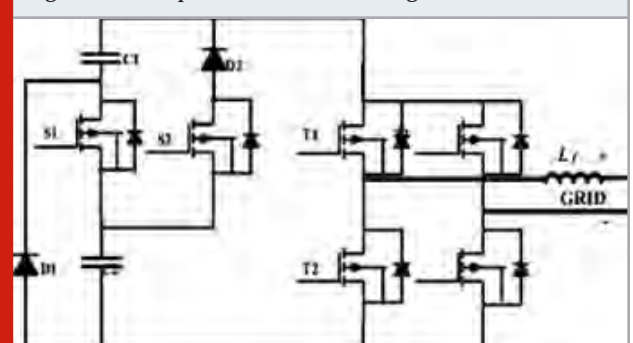
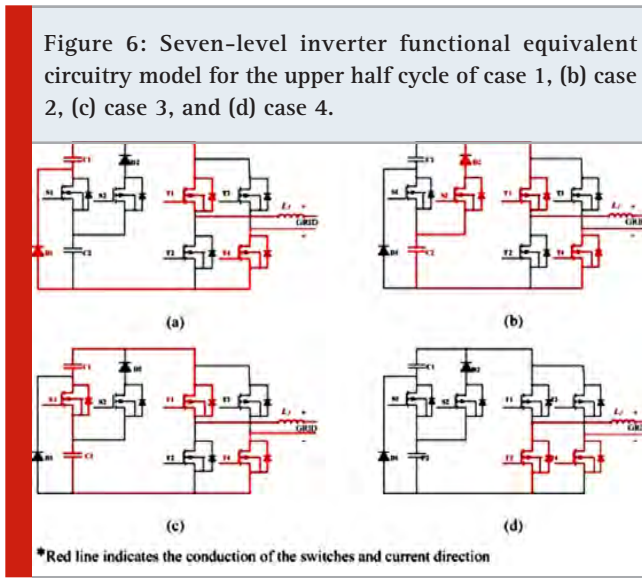


Figure 5: Two phase RSCI circuit diagram



The seven-level inverter functional equivalent circuitry model for the upper half cycle of (A) case 1, (B) case 2, (C) case 3, and (D) case 4 are illustrated in Fig (6)



Upper half cycle (+ve):

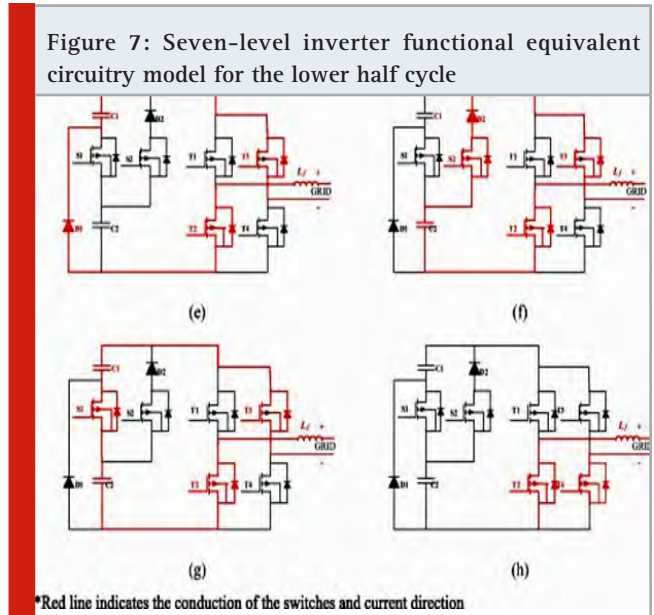
Case1- As we seen in Fig. 6(a) in this case, the S_1 and S_2 both switches are turned off, because of that C_1 condenser discharges power from D_1 at same time, and the diode is low. The capacitor's output voltage is V_{dc3} . During this operation the voltage source inverter control electronic switch T_1 and T_4 is ON load. At the moment, the voltage output of RSCI is same as the voltage output of the condenser range, which means the output voltage of RSCI is V_{dc3} .

Case2- As we seen in Fig. 6(b) in this case, the turn S_1 is turned off and S_2 is turned on and at the time S_2 and D_2 were short, the condenser C_2 unloaded the current flow through S_2 and D_2 . The capacitor output voltage is $2V_{dc3}$ due to this condition. Below, as in the previous example, the transition at the same time T_1 and T_4 are ON state. Hence the output voltage for reduced switch seven level cascaded inverter is $2V_{dc3}$.

Case3- As seen in Fig. 6(c) in this case, the condition for turn s_1 is turned on. The D_2 is skewed in reverse since the S_1 is turned ON. The current flow cannot be opposed by the switch S_2 as it is ON condition during this time. The switch can be ON or OFF to prevent transitioning from S_2 . Here, the condensers C_1 and C_2 are concurrently unloaded and the output voltage V_{dc} is given. The T_1 and T_4 keys, as in the previous example

Case4- As we seen in Fig. 6(d) in this case, the s_1 and S_2 both switches are turned off, and the V_{dc3} condenser output voltage. Here t_4 is turned on, and then RSCI's positive current passes along the inductor filter. The anti parallel diode of the switch t_2 is expected to be in on condition to perform conduction continuously to the filter current of inductor. RSCI voltage is zero then.

The output voltage of RSCI in the upper half cycle produced is V_{dc3} , $2V_{dc3}$, V_{dc} and zero respectively, after observing the above cases. Unlike the upper half cycle, Output voltage of RSCI is ideal in the lower half cycle but has an opposite symbol. The seven-level inverter half-cycle working equivalent circuit diagram is shown in Fig. 7.



RSCI process in the lower half cycle often split into further four instances. When contrasting Characters. 6 and 7. The collection circuit of the condenser is the same with both the half cycle and a variation instead of t_1 and t_4 , t_2 and t_3 are conditional. T_2 is on in the last 8th event and For the continuous conduction of the inductor current, the anti- diode of the t_4 turn. The inverter provides seven voltage stages, such as: $\pm V_{dc3}$, $\pm 2V_{dc3}$, $\pm V_{dc}$ and nil. The modulation of the space vector pulse width (SVPWM) strategy tracks transition conduction at RSCI.

As seen on Fig.5, configuration includes two switches called S_1 and S_2 and one voltage source inverter for VSI service. Furthermore, two extra diodes and condensers also are used. By adding two additional switches in Fig. 8 shows RSCI tri-phase functional diagram. By changing the angle of conduction, the switches are controlled. All the parallel alternating states for both the upper and lower half periods are included in table 1 and 2.

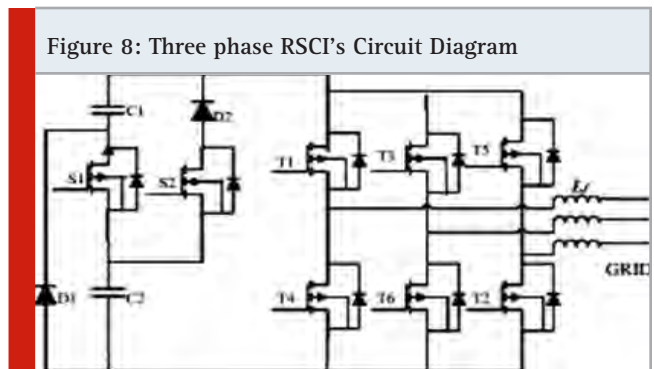


Table 1. Upper half cycle (+ve): switching states (three phase)

S ₁	S ₂	T ₁	T ₃	T ₅	T ₄	T ₆	T ₂	V _{out} (+)
X	X	✓	X	X	X	✓	✓	V _{dc3}
X	✓	✓	X	X	X	✓	✓	2V _{dc3}
✓	X	✓	X	X	X	✓	✓	V _{dc}
X	X	X	X	X	X	X	✓	0

Table 2. Lower half cycle (-ve): switching states (three phase)

S ₁	S ₂	T ₁	T ₃	T ₅	T ₄	T ₆	T ₂	V _{out} (+)
X	X	X	✓	✓	✓	X	X	V _{dc3}
X	✓	X	✓	✓	✓	X	X	2V _{dc3}
✓	X	X	✓	✓	✓	X	X	V _{dc}
X	X	X	X	✓	X	X	X	0

The switch ON and OFF condition is represented by '✓' and 'X' respectively.

RSCI has to be divided into two groups, depending on the utility side requirement. One of the voltage thresholds is higher than the usage voltage to increase the limited current, and another voltage level is smaller than the usage voltage to reduce the limited current. In order to trace the reference current, RSCI's output current can be regulated in the above way.

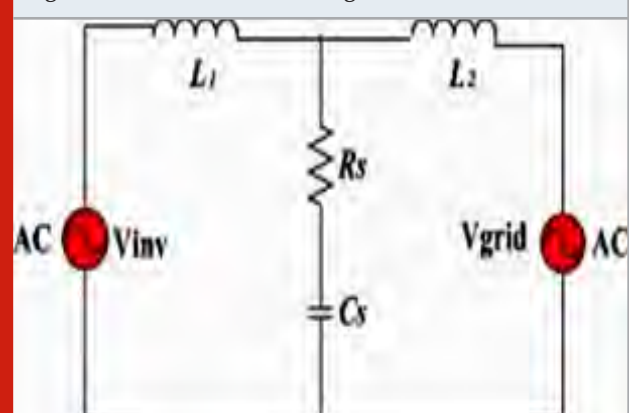
LCL filter: According to device requirement LCL filter is designed to minimize the harmonics generated by the nonlinear loads and converter. To the corresponding LCL filter circuit diagram KVL law is applied, as seen in Fig. 9:

$$(8) V_{inv} = V_{grid} + LdI_{in} \quad V_{dt} = V_{grid} + LdI_{gridt}$$

(9) $I_{grid} = 1L(V_{in} V_{ref} - V_{grid})dt + 1L(V_{inh})dt$ (10) $I_{gridh} = 1L - 2(I_{sgn} I_{inv})$
 $t_d V_{dc} T_{sw}$ where I_{grid} , I_{gridh} , t_{sw} , and t_d represents current in the grid, harmonic current in the current, time of delay, and time of switch accordingly. Through line to line inverter output voltage, the architecture components of LCL filters R_s , C_s , L_1 and L_2 are measured in voltage

unit, phase to phase voltage in voltage unit'; level real power in 'w'; direct current contact voltage (V_{dc}) in voltage units; frequency in the grid is represented as f_{grid} in 'hz', frequency of switching in 'hz,' frequency of resonance; str frequency of angular (along str). The capacitance and base impedance and are determined by taking the following parameters as: (11) $Z_b = VL L_2 Pr$, (12) $C_b = 1_{grid} Z_b$

Figure 9: LCL filter Circuit Diagram



The scale of the condenser (Cs) is measured as: (13) $C_s=0.01/(0.05C_b)$ here in Eq. (14), the power factor variance of the grid is presumed below 5 per cent for the configuration of the filter condenser. RSCI's overall current ripple (benefit $I_{1, \max}$) is expressed as: (14) inverter side filter, $\max=2V_{dc3}L_1(1-m)$ filter of the converter side and SVPWM index modulation respectively.

The average current ripple can be determined with respect to Eq, considering the magnitude of m as 0.5.

$$(15) I_{L, \max} = V_{dc6} F_{sw} L_1 \text{ For the estimation of } L_1.$$

$$(16) I_{L, \max} = 0.1 I_{L, \max}$$

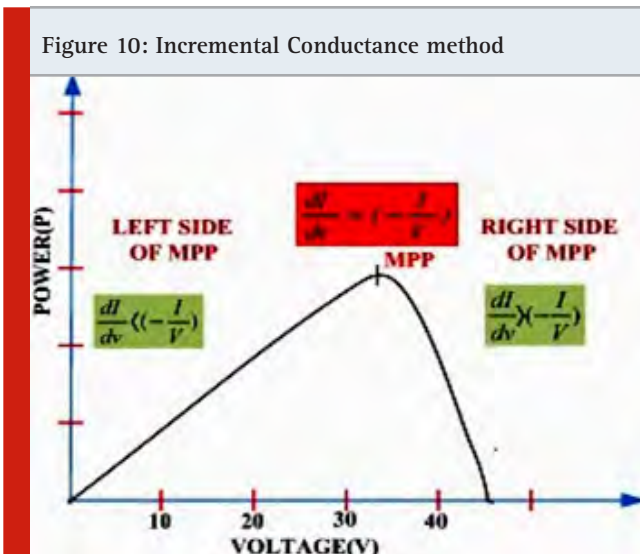
$$(17) I_{\max} = P_{r23} V_{ph}$$

$$(18) L_1 = V_{dc6} F_{sw} I_1$$

Predicted current ripple is intended to limit to 20% by the LCL filter and given that the desired attenuation factor 'Ka' calculates the L2: The 'Rs' resistor is coupled with the condenser to protect the device from resonance condition and the switching frequency ripple is eliminated by the resistor. 'Rs' value is determined as: (20) $R_s=13res Cs$ where $res=L_1+L_2L_1L_2Cs$.

Control Techniques: Various control techniques integrated into the present analysis are discussed in this section. To obtain the optimum power an IC-based MPPT function algorithm is adapted. To increase the performance and regulation of the device, a feedback regulation technique based on the structure of the d_q is applied also for management of battery energy. In addition, a repeated control technique is implemented with the goal of removing harmonic distortion in modulation of the width of the space vector pulses.

MPPT Algorithm Using Incremental Conductance



By differentiating the Photovoltaic output power from voltage and by rendering it zero, the algorithm is formulated for achieving MPP. (21) $d_p d_v = ddV(VI)=I+VdIdV=0$ The following equation renders approximately, (22) everywhere, ' V_m ' and ' I_m ' signify the voltage and current in MPP. That means location of the operational point can be determined, whether it is far away or close to MPP. Therefore the operational point can be reached to MPP by cautiously measuring the growth 'M.' Mathematically, the whole cycle could be interpreted as follows in the region of current source and voltage source area: (23) $dIdV < -IVM = M+QM$ (left side MPP) (24) $dIdV > -IVM = M-Q_M$ (MPP in right side) (25) At MPP, $dIdV = -IV_M = m$.

Battery power management control: Because of the block of control network as seen in Figure.1, The proposed inverter (RSCI) control system controls the required reactive energy and active energy production for the load unit. the photovoltaic parameters, power system parameters and the parameters for battery are taken into account, the aforementioned conditions should be satisfied. The d-q axis represents the reactive power active power components using the transformation of Park in terms of voltage and current.

$$(26) P = V_{sd}d + V_{sq}q$$

$$(27) q = V_{sq}d - V_{sd}q \text{ where } 'V_{sd}' \text{ and } 'V_{sq}'$$

denote grid voltages (V) of the d-q axis; I d' and 'iq' denote the responding converter power of the dq axis. Using Eqs, the corresponding d and q axis current from inverter could be obtained by using Eqs in the value of the expected reactive and active power. (26), (27) as follows:

$$(28) id = pV_{sd} - qV_{sq} V_{sd2} + V_{sq2}$$

$$(29) iq = qV_{sd} - pV_{sq} V_{sq2} + V_{sd2}$$

The desired voltage vector on the inverter is determined using a decoupled control technique and applied using the RC controller. To convert a specified amount of power, the battery acts in two operating modes. The battery derives the electricity during charging state from the energy surplus generated from PV. In the discharging operation condition, it assists the PV system when it is unable to supply the necessary electricity. Within this analysis, the battery feature plays an auxiliary support role within improving the stability and productivity of photovoltaic power by using power of surplus during the breakdown of power.

Suggested regulation of the test device by battery energy is shown in Figure (1). Under control of this topology, when an surplus of electricity is present in the grid, the battery must consume electricity, and generate power equally when the grid cannot accommodate the required output.

In the vector diagram the measured voltage example vector is then used for evaluating the relevant field. For the relative errors of condenser voltages to be correctly chosen shortest vector is required as in Eqs. (30), (31).

$$(30) eV_{Ca} = VCa - V_{Ca} V_{Ca}$$

$$(31) eV_{Cb} = V_{Cb} - V_{Cb} V_{Cb}$$

with the required capacitor voltage (V), V_{Ca} and V_{Cb} explains the real voltage of capacitor (V) through the condensers 'ca' and 'cb' respectively.

Through this method, the shortest vector range as discussed before is evaluates condenser collection for loading mode or unloading mode. The choice of selecting correct short vector often relies on the short relative vector, relative condenser voltage and their relevance to the actions of the control device. A decision function 'E' is constructed as follows by using this method:

$$(32) E = K_{1c} V_{Ca} - K_{2c} V_{Cb}$$

To decide the decision function, every relative error of the voltage in the capacitor is connected to the gain 'k₁' and 'k₂' values. The related gains values 'K₁' and 'K₂' are so determined that the resulting relative condenser voltage loss enables greater regulation of the selected voltage of capacitor. The corresponding 'k₁' and 'k₂' values need to have the same example voltage to equate the condenser voltage. However, in this application, in case of unbalanced condenser voltage systems, that is recommended to apply different values of k₁ and k₂ entirely based on voltage capacitors.

The solar device was operated by the process of IC and the power 'Ca' was operated for enabling the loading and unloading of batteries using the Equations (34).

$$(33) V_{Ca} \text{ distribution} = V_{bat}$$

$$(34) V_{ref} - V_{Ca} = V_{Cb}$$

In each phase, short vector selection depends on the 'E' polarity. In any time phase, In case of positive sign of 'E', according to the equations, the respective vector collection the loading 'ca' or unloading 'cb.' Likewise, In the case of negative sign of 'E', the respective vector collection can load 'cb' or discharge 'Ca' during time phase.

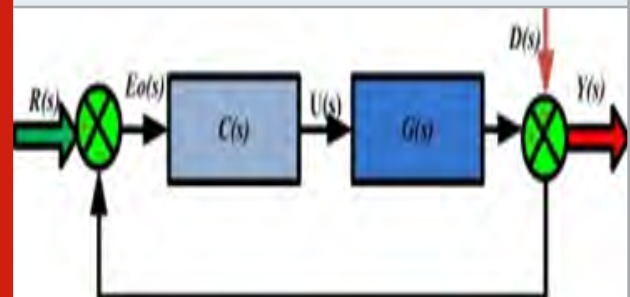
By using the respective vector voltage and the related real timing of the voltages according to the introduction of control system, as seen in Figure(1), the respective active power (pb) is provided by RSCI and reactive power (qb) also provided by RSCI. In comparison, MPPT regulation has made an effort on the generation side to gain rigorous regulation of VCb (K₂ u K₁) with a reference value of (V_{dcu} - V_{Ca}). In addition VCa is flexibly operated with the reference value of the battery voltage 'Vbat'. By using the decision function 'E' along with the necessary example values you can determine the appropriate

short voltage vector to implement the required voltage vector. Maximum available power will be provided by machines by means of the optimum MPPT function. It is possible to achieve the desired power at the generator by producing the expected vector voltage on the generator side. The suggested scheme of control also controls VCa dynamically, supplying the surplus power to the battery, and extracting input from the energy supply during the input deficit.

The battery inductor is used in the proposed method to regulate the current of the load, especially during the disruption situations. A broad range of the inductor level could be used for the operation, but lowering the inductor value will raise the battery overflow and even this quality depends completely on the condenser quality and the voltage fluctuation. Considering the size and rate, the inductor value is selected as 5 milli Henry.

Recurrent controller: Recurrent frequency domain regulation (RC) technique is discussed here. This is constructed and evaluated depends on Fourier transform at the domain of Z at a discrete time [30],[31]. Closed loop feedback controller of RSCI block diagram description is shown in the Figure (11). In the practical method, disturbances caused by some means, such as fluctuation in the grid and non-linear loads, non linear time of delay, produce harmonics of lower order. That was not enough to remove the harmonics of lower order that appear to insert high into the waveforms output by using traditional LC and LCL filters.

Figure 11: RSCI control of closed loop



To mitigate the harmonics of the lower order and to achieve improved the power system output voltage; a suitable controller must be built. The representation of the system's state space model could be expressed:

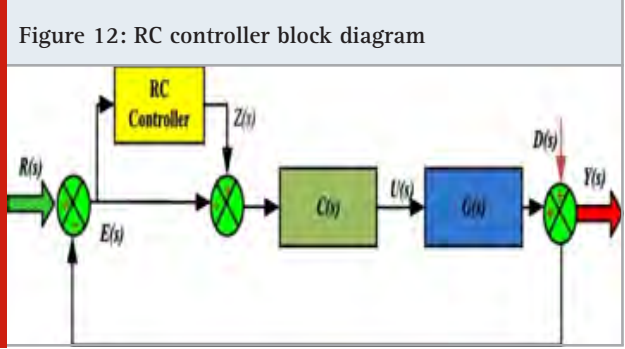
$$(35) Y(s) = G(s)R(s) + D(s)$$

$$(36) U(s) = C(s)R(s) - Y(s)$$

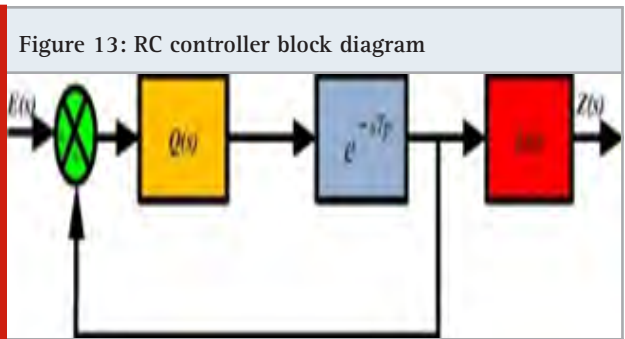
As illustrated in Figure 12, where the input example signal is r(s), the output of the loop is y(s), the controller is c(s), inverter is g(s), the distortion is d(s).

The finding error E0(s) of the closed loop method is given by:

(37) $E_0(s) = R(s) - D(s)1 + C(s)G(s)$ due to control input $U(s)$ and $D(s)$;



The Fig.12 Presents a closed loop device diagram of the controller RC implementation. Upon feeding to the main system controller the monitoring mistake is again changed by controller. Fig.13 Demonstrates RC Controller topology. The $L(s)$ filter serves as a learning filter to balance the transition as used by the controller RC. The 'Q(s)' filter function is used to minimize the error in the real system between 'L(s)' and the error.



Alternatively, inside the defined RC controller boundary $q(s)$ aims to restrict frequency. By changing the periodic signal generator's delay of time 'q(s)' phase delay can be compensated. In case of the signal of periodic, the operation of the controller is to produce output frequencies as k_p with cyclic frequency and number of integers. You will measure the time span T:

$$(38) T_p = 2p.$$

Transfer function of closed loop can be given in:

$$(39) h(s) = c(s)g(s)1 + c(s)g(s).$$

Tracking error 'e(s)' of controller RC can be given in:

$$(40) e(s) = E_0(s)$$

without RC at the same time as error $e_0(s)$ the system.

RESULT AND DISCUSSION

To test and verify the feasibility of the solution, In MATLAB a model of simulation is built. Between RSCI and three level neutral point clamped inverter using

controller PI with the repeated controller comparative tests were reported then evaluated under set and variable irradiance condition. Table 3 shows the model function for the proposed method.

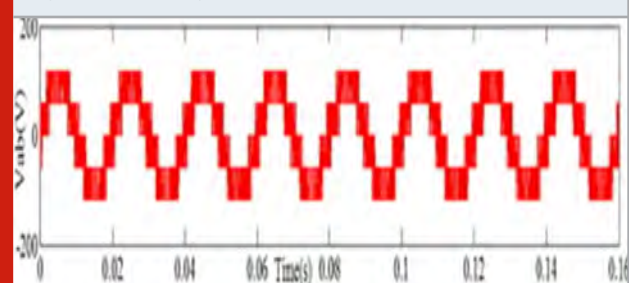
Table 3. parameters of the system

Photovoltaic system data (273 K+1000 W/m ² , 25)	
Characteristics	Values
Voltage at max power (V _{max})	37.5 V
Typical maximum power (P _{max})	210.1 W
Short circuit current (I _{sc})	6.04 A
Current at maximum power (I _{max})	5.602 A
Resistance in series(R _s)	0.221 Ω
Current open circuit (V _{oc})	44V
Boltzmann constant(K)	415.405 Ω1.38065 * 10 ⁻²³ J/K
Resistance in parallel (R _p)	415.405 Ω
Material band gap	1.12 eV
Charge of electron (q)	1.602 * 10 ⁻¹¹ C
Temperature coefficient of short-circuit current (K _i)	0.0032 A/K
idealist factor (a)	1.3 eV
Filter data of LCL	
Phase to phase voltage (V _{ph})	117.3 V
Line to line inverter output voltage (V _{LL})	143.66 V
Switching frequency (F _{sw})	40 * 10 ³ Hz
Rated active power (P _r)	558 W
Information of the Battery	
Inductor of battery (L _{Bat})	5 mH
Voltage of battery (V _{bat})	60 V

Case1: PI controller with three level neutral point clamped inverter

Fixed condition of irradiance: For producing the required voltage level topology of the NPC MLI consisted of 4 electronic switches then 2 diodes of clamping in one side, thus having six clamping diodes, twelve switches, two condensers. The device produces the power system current and voltage necessary for the inverter output, considering PI controller with topology. Fig.14. Thevoltage components of zero, positive and negative sequence which fit the method are demonstrated

Figure 14: Voltage of a three level inverter



The output current is shown in Fig at inverter and grid side rail. 15.15. This leads to Pg. 15(a) shows harmonic disturbances in the inverter current and which is eliminated by the LCL filter of integrated is seen in Figure (15)(b). Illustration Figure (16), Figure(17).The harmonic evaluation of the converter current for four cycles at a fundamental frequency of 50 Hz is analysed and revealed by the fast Fourier Transform. According to the IEEE 1541 standard, the 5.38 percent THD is too high and therefore needs to be further improved for real time deployment especially for photovoltaic based power grid system.

Figure 15 (a): NPC inverter output current (b) Grid output current

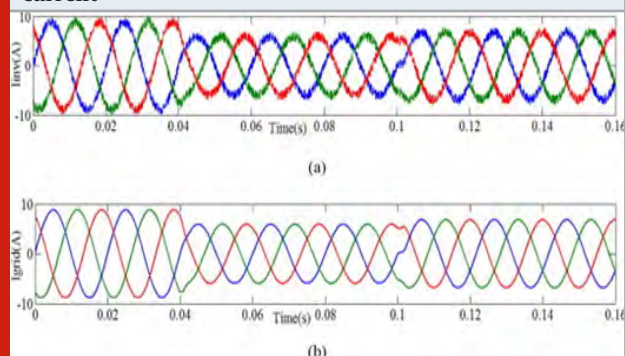


Figure 16: Calculation of THD of Current in inverter

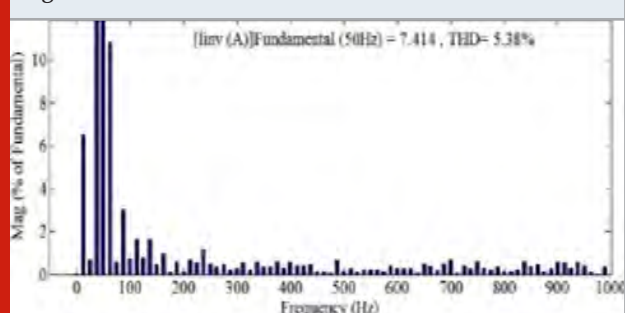
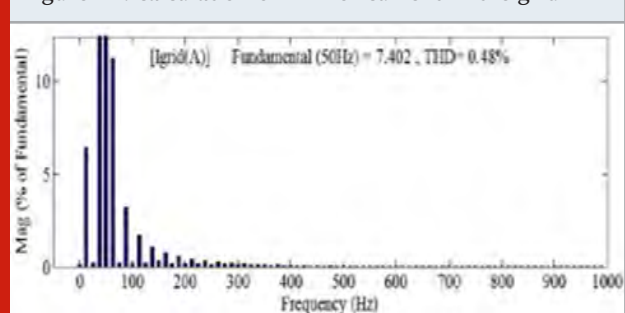


Figure 17: calculation of THD of current in the grid



Changing condition of irradiance: LCL filter output is evaluated under different irradiance conditions for the same system. Illustration. 18 Shows power system side and converter side current simulation results. The results from Fig. 18(a) specifically show the harmonic distortion. In the inverter current case, due to the existence of nonlinearity.

Nonetheless, the effect of usage of the filter LCL for minimizing the amount of harmonics to given quality of energy problem was expressed in the current in the power system side grid, as seen in Figure (18)(b). This experiment was verified by measuring the inverter side current's THD value using technique of FFT for cycles of four at a simple frequency of 50 Hz. Illustration. 19, War. By applying the LCL filter, 20 imply a large removal of the value of THD from 5.7 per cent to 0.2 per cent. From conclusions in the above analysis, restriction such as the need for filter of LCL for achieving three level voltages is expressed in the behaviour for MLI in addition to more switches of operations. This motivates the design of the MLI switch in addition to reduced reliance on the integrated model filter, by incorporating above limitation into solution nominated.

Figure 18 (a): Inverter current output (b) Grid current output

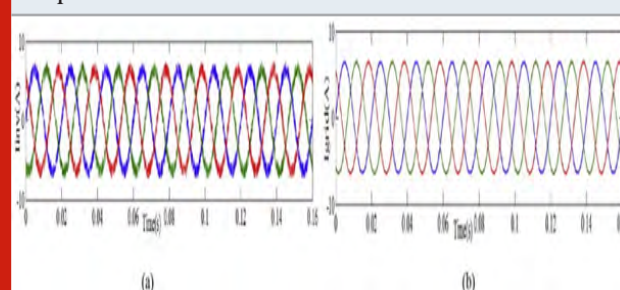


Figure 19: Calculation of the THD in current of inverter side

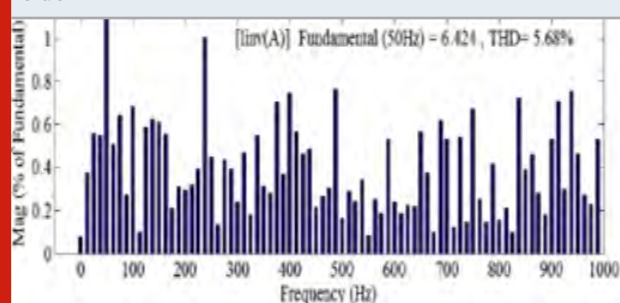
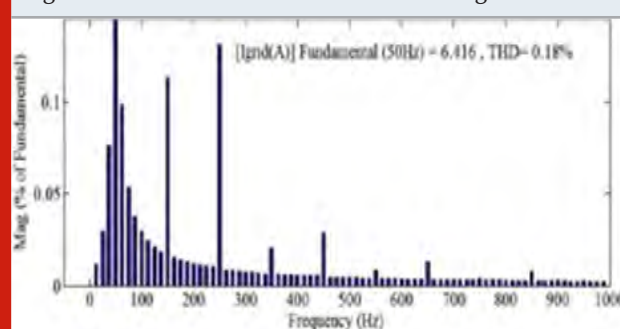


Figure 20: Calculation of THD incurrent of grid side

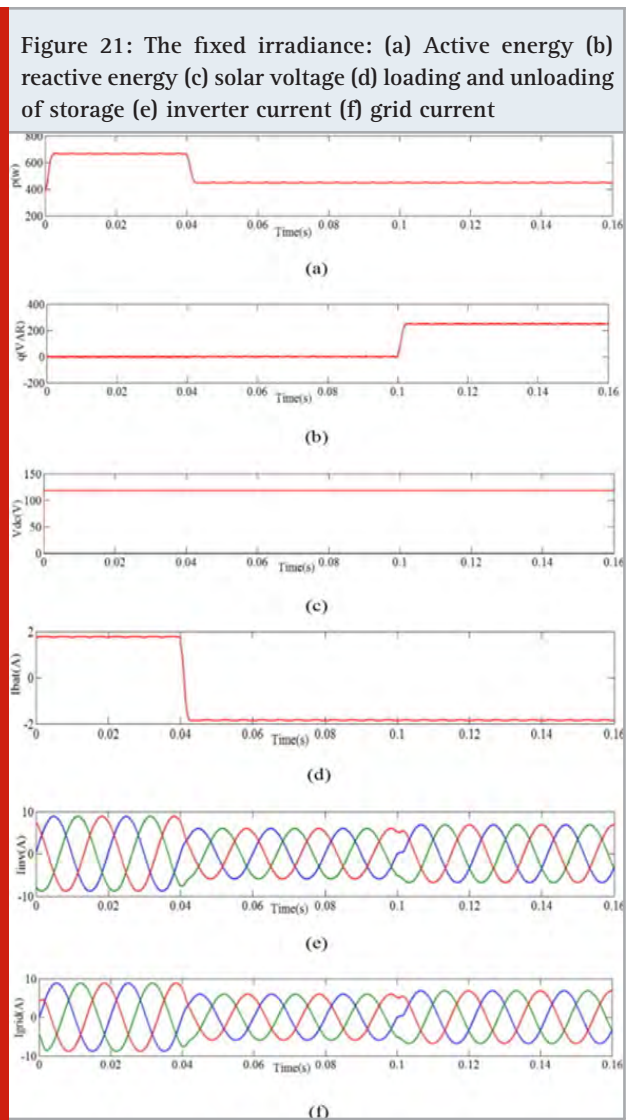


Case2: Recurrent controller with CSIR

Fixed Irradiance Condition: Fig. 21 displays difference of the time of the reactive energy and active energy, the solar voltage output and the inverter current output,

the system output and the battery power charging then discharge. Three of the photovoltaic units are attached as series format into the network for creating a photovoltaic board. Analysis in above, that was estimated that radiation in the rated PV device will achieve $I_{ph} = 5.6A$ and the voltage output will be 117.2 voltage, and the output current will be 4.74 ampere.

Lastly, to the time interval $t = 40$ ms, the all real energy of 558 watt was produced which initially differs between 663 watts and 444 watts as shown in Figure 21(A). Illustration 21(B) equally demonstrates variance of the re active energy and displays the original variance of the reactive power is sent to the power system from 0 to 251 var in the interval period of $t = 100$ ms.



Machine was producing reactive energy required due to the presence of a condenser. Fig. 21(c) shows PV module output dc variance voltage. In the case of a PV powered micro grid, energy storage is important for increasing performance and reliability. The management policy and preparation to load the energy storage in operating time then to drain energy storage capacity for fulfilling electricity shall be enforced. The time difference for

using storage power is seen in Figure 21(D). Current value gets 1.8 ampere in period interval 0 ms to 41ms in the battery discharge process and during the loading phase the power approaches -1.8 ampere in period interval 41 ms to 99ms.

The feasibility for suggested solution is seen as Figure 21 (E to F) on the harmonic minimisation, passing the device properties near to similar behaviour. That reveals small reliance for the filter LCL relative for the 3 level inverter (NPC) in case-1. The study of FFT explicitly shows this by displaying a decreased THD ratio of 0.46 per cent to that of using the filter LCL is seen in Figure(22). Even so, at Pg. 23A more increased efficiency is obtained by using the grid side current in THD-level, LCL filter into 0.22 percent. In the proposed solution, the inclusion of LCL filter is considered because of its device safety gain under sudden voltage transition.

Figure 22: Calculation of THD current of inverter side

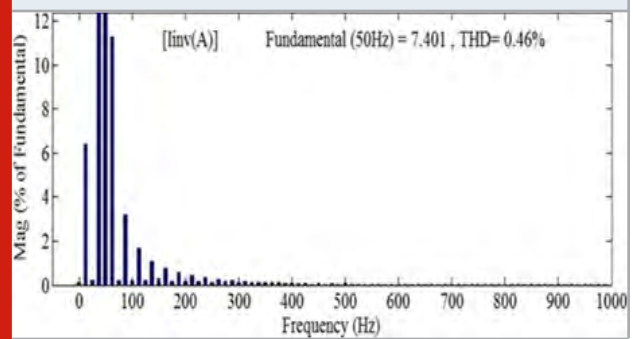


Figure 23: calculation of THD current of grid side

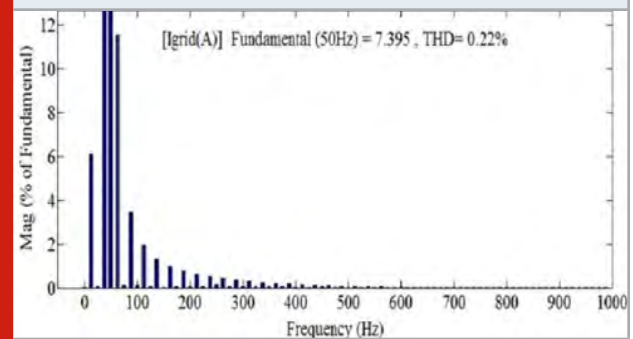


Figure (24) Displays the phase to phase variation for the voltage of converter, the midpoint amplitude of the converter, and the reduced voltage phase of the converter. The suggested RSCI dependent RC controller produces high level amplitude relative for the clamped converter, seen in Figure 24(a) and (b). The suggested inverter's remover voltage phase as per centre point is shown as diagram. 24(C) Zero distortion of harmonics.

Figure 24: The irradiance (a) phase to phase inverter amplitude (b) converter phase voltage (c) Filtered inverter phase voltage

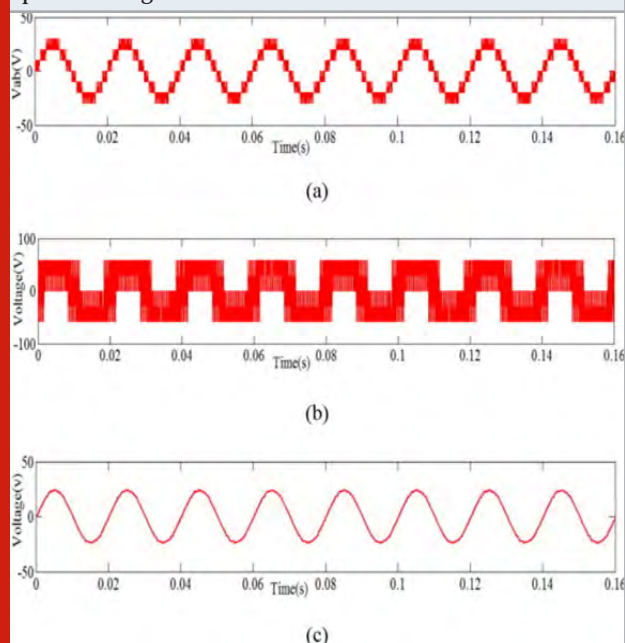
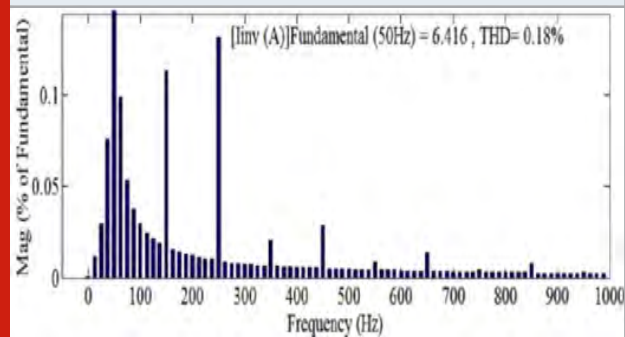


Figure 25: Calculation of THD current of inverter



CONCLUSION

This paper recommends a many stage PV micro grid network supported RSCI based inverter for storing power. Furthermore, an incremental conductance algorithm based MPPT technique is implemented to recover the full usable energy for defined and variable irradiance conditions. A repetitive control technique is applied in place of controller PI with RSCI for further boost the performance. The harmonic rates are determined by seeking THD value by FFT analysis to ensure the chance of real-time use, and are established in within standard of IEEE1547. For remaining enhancement of the efficiency of the power, integration of the filter LCL was explored; while the suggested solution results satisfactorily. In addition, the proposed controller will evaluate the battery's efficacy in improving overall device efficiency. The simulation findings suggest the enhanced efficiency of the introduced topology of converter and strategy of control in better power level, decreased flips, removable

error in steady state and harmonic level also minimized as opposed to the NPC inverter with PI transmitter.

REFERENCE

- B Van Zeghbroeck (2004) Principles of Semiconductor Devices Colorado University.
- D Rekioua E Matagne Optimization of Photovoltaic Power Systems Modelization Simulation and Control.
- HL Tsai CS Tu YJ Su (2008) Development of generalized photovoltaic model using MATLAB/SIMULINK in Proceedings of the world congress on Engineering and computer science vol 2008 Pages 1-6.
- HR Teymour D Sutanto KM Muttaqi P Ciufo (2014) Solar PV and battery storage integration using a new configuration of a three level NPC inverter with advanced control strategy IEEE Trans Energy Converters 29 (2) Pages 354-365.
- J Leuchter V Rerucha AF Zobaa (2010) Mathematical modeling of photovoltaic systems in Power Electronics and Motion Control Conference (EPE/PEMC) 14th International 2010 Sep 6 IEEE Pages S4-1.
- M Bragard N Soltau S Thomas R W De Doncker (2010) The balance of renewable sources and user demands in grids power electronics for modular battery energy storage systems IEEE Trans Power Electron 25 (12) (2010 Dec) Pages 3049-3056.
- MG Villalva J R Gazoli E RuPagesert Filho (2009) Modeling and circuit-based simulation of photovoltaic arrays in Power Electronics Conference 2009 COBEP'09 Brazilian 2009 Sep 27 IEEE Pages 1244-1254.
- MG Villalva J R Gazoli Filho E RuPagesert (2009) Comprehensive aPagesroach to modeling and simulation of photovoltaic arrays IEEE Trans Power Electron 24 (5) (2009 May) Pages 1198-1208.
- M Hariprabhu K Sundararaju Performance (2019) Improvement of Grid Connected Photovoltaic Power Generation System using Robust Power Balanced Control (RPBC) Technique with active Power Line Conditioning International Journal of Recent Technology and Engineering (IJRTE) ISSN 2277-3878 Volume 7 Issue 5S3 February 20.
- M Hariprabhu Dr K Sundararaju Sophisticated Fuzzy Rule Set (SFRS) based MPAGEST Technique for Grid Connected Photovoltaic Power Plant with DC-DC Boost Converter Journal of Advanced Research in Dynamical and Control Systems Vol 9 Sp- 18 / 2017 PAGES 2612 - 2637.
- O Hachana K E Hemsas G M Tina C Ventura Comparison of different meta heuristic algorithms for parameter identification of photovoltaic cell/module J Renew Sustain Energy 5 (5) (2013 Sep) p 053122.
- O M Toledo D Oliveira Filho A S Diniz Distributed photovoltaic generation and energy storage systems a review Renew Sustain Energy Rev 14 (1) (2010 Jan 31) Pages 506-511.
- R Banos F Manzano Agugliaro F G Montoya C Gil A Alcaide J Gomez Optimization methods aPageslied

to renewable and sustainable energy a review *Renew Sustain Energy Rev* 15 (4) (2011 May 31) Pages 1753-1766.

S Punitha K Sundararaju Voltage stability improvement in power system using optimal power flow with constraints 2017 IEEE International Conference on Electrical Instrumentation and Communication Engineering (ICEICE) Pages 1-6.

S Jain V Agarwal Comparison of the performance of maximum power point tracking schemes aPageslied to single-stage grid-connected photovoltaic systems *IET Electron Power APagesl* 1 (5) (2007 Sep 1) Pages 753-762.

T Salmi M Bouzguenda A Gastli A Masmoudi Matlab/Simulink based modeling of photovoltaic cell *Int. J.*

Renew. Energy Res. (IJRER) 2 (2) (2012 May 12) Pages 213-218.

W De Soto S A Klein W A Beckman Improvement and validation of a model for photovoltaic array performance *Solar Energy* 80 (1) (2006 Jan 1) Pages 78-88.

X Zhang Z Shao F Wang P Liu K Ren Zero-sequence circulating current reduction for three-phase three-level modular photovoltaic grid-connected systems in *Zhongguo Dianji Gongcheng Xuebao (Proceedings of the Chinese Society of Electrical Engineering)* 2013 Mar 25 Chinese Society for Electrical Engineering vol 33(9) Pages 17-24.

FPGA Implementation of Adaptive LMS Lattice Filter

Sasikala S¹, Gomathi S², Naveen Kumar D³, Praveenraaj R. K⁴ and Priyadharshini B⁵

¹Associate Professor, ²Assistant Professor, ^{3,4,5}UG Scholar

Department of ECE, Kongu Engineering College, India

ABSTRACT

An adaptive filter is a procedure device that iteratively models the link between the input and output signals of the filter. An adaptive filter is a system with a linear filter that has a transfer function controlled by variable parameters and a means to adjust those parameters according to an optimization algorithm. This paper presents an approach for implementing an adaptive lattice LMS filter which gives less delay and improved SNR than traditional adaptive filter. Adaptive noise cancellation is realized using lattice form, which is developed around the lattice basic structure. Least Mean Square (LMS) based adaptive filters are widely deployed for removing noise in Electrocardiogram (ECG) due to less number of computations. The ECG signal along with Power Line Interference (PLI) noise is taken as input and signal to noise ratio analysis for lattice LMS structure is performed. Combinational delay of 4 tap and 8 tap lattice LMS filter is improved by 3.5% and 14.33% respectively.

KEY WORDS: ADAPTIVE FILTER, ECG SIGNAL, FPGA IMPLEMENTATION, LATTICE FILTER, LEAST MEAN SQUARE, POWER LINE INTERFERENCE NOISE, SIGNAL TO NOISE RATIO.

INTRODUCTION

An adaptive filter plays a vital role in statistical signal processing. In practical situations, the system is operating in an uncertain environment where the input condition is not clear and the unexpected noise exists. Under such circumstances, system should have the flexibility to modify the system parameters and make adjustments based on the input signal and other relevant signal to obtain optimal performance. The main characteristics of the adaptive filter is the adjustment of filter coefficient

with respect to the input signal. Adaptive filter adjusts their coefficient to minimize an error signal and can be realized as finite impulse response, infinite impulse response, lattice and transform domain filter. The lattice structure is incorporated in the filter structure to improve the SNR and reduce the delay.

Various research work has been done in the area of adaptive filter using various algorithm. Design and analysis of Noise Signal Cancellation using Adaptive Algorithms (Abhishek et al. 2014; Anjana et al. 2014). Modified Model and Algorithm of LMS Adaptive Filter for Noise Cancellation (Awadhesh et al. 2018). Denoising ECG signal using Adaptive filter Algorithm. The targeted FPGA is Altera Cyclone IV (Chinmay et al. 2012). The filter design results in superior performance, greater data sample frequency and less logic occupation using hardware Description Language (HDL) (Malarmanan et

ARTICLE INFORMATION

*Corresponding Author: sasikalapriyaadarsan@gmail.com
Received 15th April 2020 Accepted after revision 20th May 2020
Print ISSN: 0974-6455 Online ISSN: 2321-4007 CODEN: BBRBCA

Thomson Reuters ISI Web of Science Clarivate Analytics USA and Crossref Indexed Journal



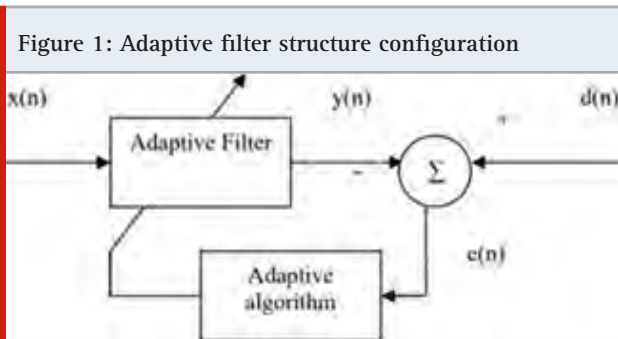
NAAS Journal Score 2020 (4.31) SJIF: 2020 (7.728)
A Society of Science and Nature Publication,
Bhopal India 2020. All rights reserved.
Online Contents Available at: <http://www.bbrc.in/>

al. 2010).Two adaptive filters using Least Mean Square (LMS) and Normalized Least Mean Square (NLMS) are applied to remove the noises and the results are compared in terms of different performance parameters such as, Power Spectral Density (PSD),frequency spectrum and convergence (Sachin et al. 2010). Four types of AC and DC noises is mixed with ECG signal and nullify the signals using LMS and RLS algorithm (Zhao et al. 2013; Syed et al. 2009; Gomathi et al. 2020). Adaptive filter can exist in three forms such as direct, transposed and hybrid forms. The main reason for the LMS algorithms popularity in adaptive filtering is its computational simplicity (Bansal et al. 2011), making it easier to implement than all other commonly used adaptive algorithms. The only disadvantage is its weak convergence.

The rest of paper is as follow: The detailed description of existing and proposed system is described in section II and III Results of 4 tap and 8 tap LMS adaptive and Lattice filter using Xilinx ISE FPGA design suite are illustrated in section IV followed by conclusion in section V.

MATERIAL AND METHODS

Existing System: The adaptive filter uses the least mean square algorithm which uses a technique called “method of steepest descent” and continuously estimates results by updating filter weights is shown in fig. 1.



Filter Output: $y(n)=wT(n)x(n)$ (1)

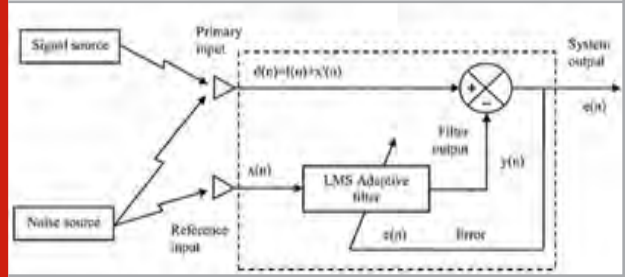
Error Signal : $e(n)=d(n)-y(n)$ (2)

Weight Update Equation:

$w(n+1)=w(n)+2\mu c(n)e(n)x(n)$ (3)

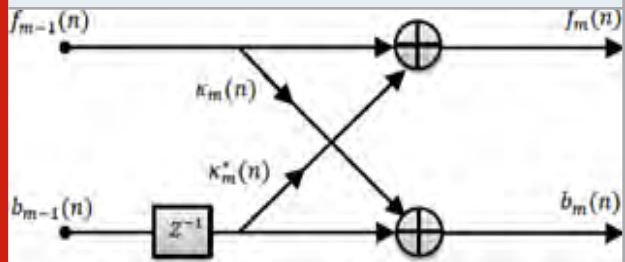
Fig. 1. shows the building blocks of the adaptive filter and the equation explains the functioning of the filter. The input signal or signal source is combined along with the noise signal and given to the adder and the output is given to the LMS adaptive filter (Sasikala et al. 2017; Sathya et al. 2015) for which the noise signal is given as input. The output from the LMS adaptive filter is given as feedback is shown in fig. 2.

Figure 2: LMS adaptive filter structure



Proposed System: Adaptive system can be realized using lattice form, which is developed around the lattice basic structure shown in figure 3. The input-output relation of such a building block is characterized by the coefficient. A Lattice filter is a highly efficient structure for generating the sequence of forward prediction error and corresponding sequence of backward prediction errors at the same time. The various stages of a lattice predictor are “Decoupled” from each other. This decoupling property shows the backward prediction errors produced by the various stages of a lattice predictor are “orthogonal” to each other for wide sense stationary input data. The lattice filter is modular in structure. Hence, if we are required to increase the order of the predictor, we simply add one or more stages without affecting earlier computations. All the stages of lattice predictor have a similar structure; consequently such a predictor lends itself to the use of very large scale integration (VLSI) technology if that technology is considered beneficial to the application of interest.

Figure 3: Lattice structure



The order-update equations for forward and backward reduction errors are recursively specified by

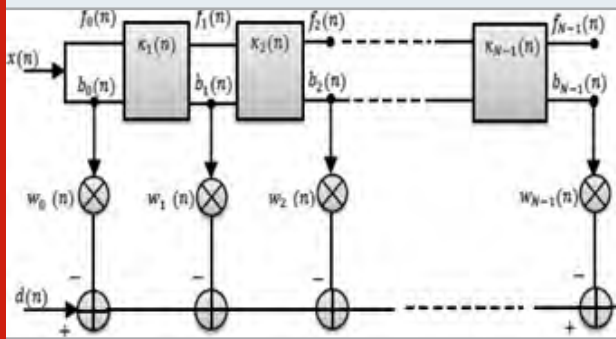
$f_m(n) = f_{m-1}(n)-k_m(n)b_{m-1}(n-1)$ (4)

$b_m(n) = b_{m-1}(n-1)-k_m(n)f_{m-1}(n)$ (5)

Fig. 3. Shows the lattice structure which is incorporated in the direct form adaptive filter to make it into lattice filter.

Along with the lattice structure the LMS algorithm is incorporated to for adaptive lattice LMS filter is shown in fig. 4.

Figure 4: Lattice joint process estimator



RESULTS AND DISCUSSION

Filter Design: Fig. 5 shows four tap direct form LMS filter structure is designed and simulated in Xilinx System generator [13]. The blocks used in this structure are adder, multiplier, unit delay, divider, math function, constant, signal from workspace and scope. The Gate way in and Gate way out used to connect the Simulink block to Xilinx block and Xilinx block to Simulink block respectively with filter order N=4.

Figure 5. 4: tap FIR filter

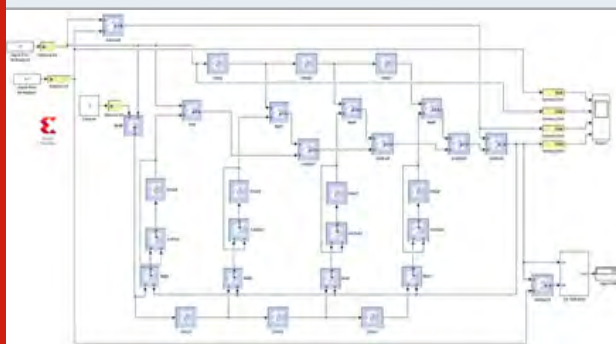


Figure 6.4: tap lattice filter

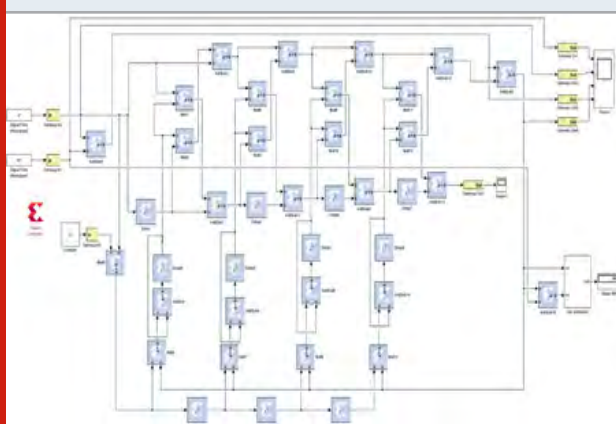


Fig. 6 shows four tap Lattice LMS filter structure is designed and simulated in Xilinx System generator. The blocks used in this structure are adder, multiplier, unit delay, divider, math function, constant, signal from

workspace and scope. The Gate way in and Gate way out used to connect the Simulink block to Xilinx block and Xilinx block to Simulink block respectively with Filter order N=4.

Simulation Results: PLI noise of 50-60 Hz is added to the input ECG signal. The Simulation is done using system generator and synthesis is executed using FPGA design suite.

Figure 7: Simulation output of 4 tap direct form LMS filter structure



Simulation output of 4 tap direct form LMS filter structure is given in fig. 7. In this simulation input is the ECG signal and PLI noise is mixed with it and the noise is filtered using 4 tap direct form adaptive filter and output is obtained.

Figure 8: Simulation output of 4 tap lattice LMS filter structure



Simulation output of 4 tap Lattice LMS filter structure is given in fig. 8. In this simulation input is the ECG signal and PLI noise is mixed with it and the noise is filtered using 4 tap Lattice LMS adaptive filter and the output is obtained.

Simulation output of 8 tap direct form LMS filter structure is given in fig. 9. In this simulation input is the ECG signal and PLI noise is mixed with it and the noise

is filtered using 8 tap direct form adaptive filter and the output is obtained.

Figure 9: Simulation output of 8 tap direct form LMS filter structure

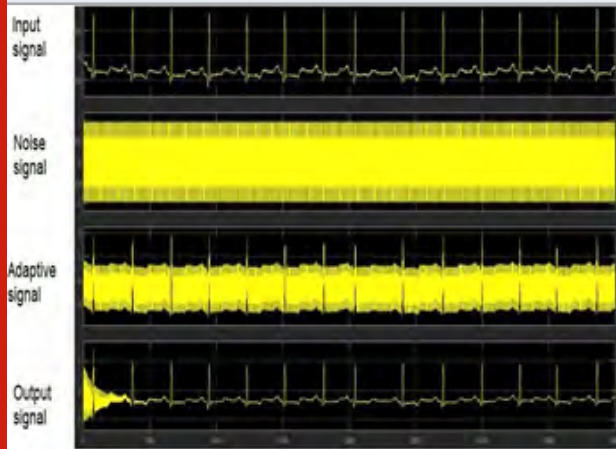
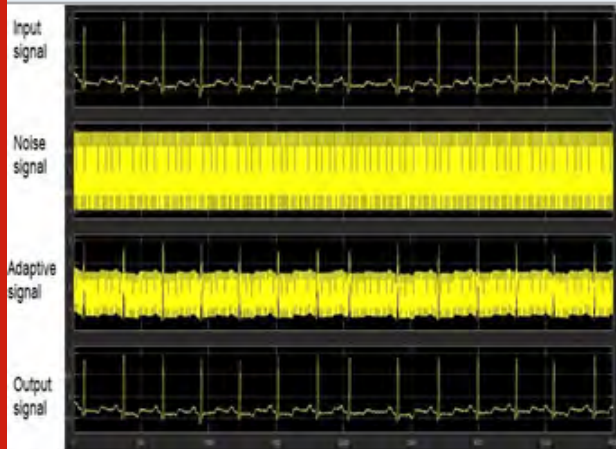


Figure 10: Simulation output of 8 tap lattice LMS filter structure



Simulation output of 8 tap Lattice LMS filter structure is given in fig. 10. In this simulation input is the ECG signal and PLI noise is mixed with it and the noise is filtered using 8 tap Lattice LMS adaptive filter and the output is obtained.

Signal to Noise Ratio Calculation for ECG Signals: The signal to noise ratio (SNR) is considered to an important parameter when denoising the signal. Signal to Noise Ratio for ECG signals is compared and tabulated in Table 1, for direct form and lattice LMS Adaptive Filter Structures.

From Table 1, it is observed that the SNR of 4 tap lattice and 8 tap lattice adaptive filters improved by 54.79% and 55.39% compared to FIR filter. Area and Time Delay Analysis for Various Filters

Table 1. SNR Calculation with ECG Signals between Direct Form and Lattice LMS Adaptive Filter Structures for 4 Tap and 8 Tap

INPUT ECG SIGNALS	SNR in dB			
	4 Tap		8 Tap	
	Adaptive LMS	Lattice LMS	Adaptive LMS	Lattice LMS
100.dat	25.62	86.99	25.83	72.42
101.dat	26.03	72.98	26.11	68.15
105.dat	26.37	65.71	26.09	63.82
108.dat	25.08	87.21	25.39	72.46
200.dat	24.62	32.77	25.2	33.51
203.dat	29.09	42.47	28.07	43.12
208.dat	30.2	43.59	29.11	44.18
228.dat	23.36	86.75	23.83	72.33
Average	26.29	64.80	26.20	58.74

Table 2. Comparison of Area and Delay for Various Filters

Filter Length/Parameter	FILTER LENGTH 4		FILTER LENGTH 8	
	FIR	Lattice	FIR	Lattice
Number of Slice LUTs	16	96	16	96
Number of Slice Registers	40	57	72	121
Total delay (ns)	17.433	16.815	25.488	21.834

The proposed lattice LMS filters provide reduction in combinational delay when compared to the direct form LMS filter. From table 2 the combinational delay of 4 tap and 8 tap lattice LMS filter is improved by 3.5% and 14.33% respectively.

CONCLUSION

Two forms like direct form and lattice LMS adaptive filters were designed and implemented in Xilinx system generator. Here LMS adaptive filters were realized in a digital environment using Xilinx ISE tool. Simulation is performed with various ECG signals obtained from MIT BIH database as input to the designed filters and its SNR is obtained. From the analysis, it is observed that the SNR value for lattice LMS filters are 60% greater than the normal direct form of LMS filters for ECG signal denoising. The proposed lattice LMS filters provide reduction in combinational delay when compared to the direct form LMS filter. Combinational delay of 4 tap and 8 tap lattice LMS filter is improved by 3.5% and 14.33% respectively.

REFERENCES

- Abhishek Chaudhary and Amit Barnawal (2014) Analysis of Noise Signal Cancellation using Adaptive Algorithms, International Journal of Engineering Research and General Science Vol.2 Issue-6 Pages.2091-2730.
- Anjana S and Anitha Mary X (2014) Noise Cancellation using Adaptive Filters in FPGA, Research Journal of recent Science Vol.3 Pages.4-8.
- Awadhesh Kumar Maurya, Priyanka Agrawal and Shubhra Dixit (2018) Modified Model and Algorithm of LMS Adaptive Filter for Noise Cancellation Vol. 38 Issue-5 Pages.2351-2368.
- Bansal and Singh(2011) Analysis of Adaptive LMS Filtering in Contrast to Multirate Filtering IEEE 4th International Conference on Emerging Trends in Engineering and Technology Pages.22-26.
- Chinmay Chandrakar and Kowar M.K (2012) Denoising ECG signal using Adaptive filter Algorithm, International Journal of Soft Computing and Engineering ISSN:2231-2307, Vol.2, Issue-1.
- H. Zhao, S. Hu, L. Li and X. Wan (2013) NLMS adaptive FIR filter design method, IEEE International Conference of IEEE Region 10 Pages. 1-5.
- Malarmannan and Malarvizhi (2010) FPGA implementation of Adaptive Filtering and its performance analysis International Journal of Engineering and Technology, Vol. 5 No.3.
- Sachin Singh and Dr.K.L.Yadav (2010) Performance evaluation of different Adaptive filters for ECG signal processing International Journal of Computing and Engineering Vol.2 No.5 Pages.1880-1883.
- Syed Zahurul Islam and Syed Zahidul Islam (2009) Performance Study of Adaptive Filtering Algorithms for Noise Cancellation of ECG Signal 7th IEEE Conference. on Information Communications and Signal processing.
- S. Sasikala and G. Murugesan, G (2017) Efficient Digit Serial Architecture for Sign Least Mean Square Adaptive Filter for Denoising of Artifacts in ECG Signals International Journal of Biomedical Engineering and Technology Vol. 23 no. 2/3/4 Pages 335-344.
- C. Sathya, S. Sasikala, G. Murugesan (2015) Denoising ECG signal using combination of ENSLMS and ZALMS algorithms Proceedings of 3rd International Conference on Signal Processing, Communication and Networking
- Gomathi Swaminathan, G.Murugesan, S.Sasikala, L.Murali(2020) A novel implementation of combined systolic and folded architectures for adaptive filters in FPGA Microprocessors and Microsystems, Elsevier Vol.74.

Secured IoT with Network Intrusion Detection Traffic Control by Data Routing Protocol in WSN Using Genetic Algorithm

S. Manikandan¹, P. Pushpa² and S. Sathish Kumar³

^{1,2,3}Lecturer, Jiangxi Engineering Laboratory on Radioactive Geo science and Big Data Technology, East China University of Technology, Nanchang, 330013, Jiangxi, China.

ABSTRACT

Internet of Things security targets around secure network enabled devices that interface with one another on wireless network. IoT security is the secure component attached to the Internet of Things, and it endeavors to ensure IoT devices and systems against cybercrime. The Internet of Things is a developing pattern, with a cascade of new components hitting the market. As this grows widely there occurs an issue: When you're associated with everything, there are many approaches to hack your private data. That can make you an appealing objective for individuals who need to make a benefit off of your own information. Each associated devices you possess can include another protection concern, particularly since the majority of the interface with your cell phone. Any innovation accessible today has not come to its 100 % capacity. It generally has a hole to go. Thus, we can say that Internet of Things has a huge innovation in a world that can assist different advances with reaching its exact and finish 100 % ability also. This is widely called network intrusion which means an intruder steals one's private data over the network. IoT energizes the correspondence between devices, also popularly known as Machine-to-Machine (M2M) communication. Along with this, the physical devices can remain associated. Due to association of physical devices, there occurs network traffic which leads to denial of services and bottleneck. To overcome these consequences in wireless sensor network, data routing protocols are implemented. This proposed system emphasizes how data traffic over wireless network are regulated by data routing protocol using genetic algorithm with the traffic information collected through IoT devices.

KEY WORDS: WSN, IOT, DATA ROUTING PROTOCOLS, GENETIC ALGORITHM, INTRUSION DETECTION.

ARTICLE INFORMATION

*Corresponding Author: prasadjoness.ece@krct.ac.in
Received 15th April 2020 Accepted after revision 20th May 2020
Print ISSN: 0974-6455 Online ISSN: 2321-4007 CODEN: BBRBCA

Thomson Reuters ISI Web of Science Clarivate Analytics USA and Crossref Indexed Journal



NAAS Journal Score 2020 (4.31) SJIF: 2020 (7.728)
A Society of Science and Nature Publication,
Bhopal India 2020. All rights reserved.
Online Contents Available at: <http://www.bbrc.in/>

INTRODUCTION

The IoT security framework turns into need of effective arrangement of IoT framework. The identification of interlopers is one of the significant advancement in guaranteeing the security of the IoT systems. The association of IoT devices is possible through only network layer which is the backbone for data transmission, yet in addition it gives chances for deploying network based security mechanisms, for example, Network Intrusion Detection Systems (NIDS). To enhance the number of hidden layers and the neurons in the network layer is proposed by an advanced intrusion detection system of IoT genetic algorithm into learning network. The improved genetic algorithm is applied for various kinds of hit, principle number of hidden layers with neurons in a hidden layers are recursively generated. By this the system complexity is diminished however much could be expected by guaranteeing location rate. By utilizing the results obtained from the issues of learning network is used to design the intrusion detection system which has more prominent improvement in execution (Ying Zhang et al., 2019). The genetic algorithm with the memory function and adjustment function of immune genetic algorithm are used for further calculation. Other than improved algorithm, the operators of genetic algorithm is used. The improved algorithm provides improved wide search capability and searching operation with greater efficiency (Yingchen Wang et al., 2018).

The legitimacy and sanity of the improved model are evaluated in examination with existing outcomes. Genetic algorithm reflects procedure of characteristic selection process utilizing bio-motivated operators like crossover and mutation. The process of genetic algorithm depends upon hypothesis of fitness function. Genetic algorithm deals with generation of solution. The fitness of every population produced is determined by assessing fitness procedure with corresponding solution. The existence of individual to abutting iteration simply depends on fitness estimation of individual. The individuals with less fitness estimation is expelled from population. Great attributes obtained from parent solutions are proliferated to abutting population by applying mutation and crossover. The importance of genetic algorithm for explaining the scheduling problem is experienced in the proposed system (Diya Thomas et al., 2018). The objective of research is to propel the existing state of the art in IoT research by distinguishing various domains where IoT is intensely utilized, the security necessities and difficulties that IoT is currently confronting, and the current security solutions that have been proposed or actualized with their impediments (Syed Rizvi et al., 2018).

The protective measures are significant concern of internet of things biological framework. For revitalizing the back bone of security measures and protection of internet of things. Actually, block chain has genuinely comprehensive which is distinguished by scientists from organization and scholarly worldwide are applying blockchain in various ways on regular basis (Mahdi H. Miraz et al., 2018). The procedure in genetic algorithm

is introduced to examine multi located data sources and single point by decision utilizing vehicle queue at four bearing roadway signal crosspoint. The research have been shown with arduino pack and ordinary traffic framework is contrasted by smart traffic framework. The results from proposed framework encourage infuriate free travel by withdrawing waiting time for green light and mishaps (P. Kuppusamy et al., 2018). The genetic algorithm is one of significant method for fuzzy system which profits ideal element subset. The procedure of genetic algorithm work recursively with lot of applicant results for issue is otherwise called population. The procedure in genetic algorithm cycle is reshaped until it ranges to final statement. The procedure in genetic algorithm computes the fitness esteem by utilizing fitness function. The estimation relies on nature of result of each and individual generation, where the fitness function (capacity of the issue) is likewise used to assess best competitor result (Archana P. Kalea et al., 2018).

The growth in field of internet of things, the degree of innovative work for wireless network and wireless sensor network is being developed definitely. The transmission of data which is called as routing of data packets in a network is a decisive process, and lot of vitality is spared if routing of data packets is prepared adequately in the network which leads to an advancement issue along with numerous requirements similarly, vitality in a hub, connecting quality, traffic, and so on. To overcome this type of issues, genetic algorithms which is incorporated with genetic procedures over given network consisting population would provide ideal solution. In such case, efficiency of algorithm is blocked because of improper union, so they were not capable to pass through search area with huge number of solution for ideal energy retaining. To handle the above mentioned disadvantages, an advanced genetic algorithm utilizing local searching method is adjusted. Right now, an altered genetic algorithm is called as enhanced genetic algorithm utilizing search method component with sleep wakeup system. This improves the wireless network to an extent that vitality protection with augmentation of network existence is powerful, and recognizing data transmission imperatives and energy utilization of sensor during network communication (Aishwarya S Hampiholi et al., 2018).

Internet of things is comprised of devices which are capable to detect, impart, process, and even control their condition. The internet of things devices are progressively turning into part of complicated, dynamic, and circulated systems, for example, power or versatile systems. An assortment of sensors in IoT can catch various parts of the condition that they screen continuously. This proposes a one-class support tucker machine (OCSTuM) and an OCSTuM dependent on tensor Tucker machine and a genetic algorithm called GA-OCSTuM. The procedure in genetic algorithm selects a component subset of device sensor data and quest for ideal design parameters. The proposed genetic algorithm based OCSTuM calculation can spare computational productivity, yet improves the irregularity identification exactness of OCSTuM (Xiaowu

Deng Peng et al., 2018). IoT top security concerns: cloning of device, exposure of sensitive data, denial of service attack, illegal access to devices and control, tampering of data. This exploration research achieves the requirement to relieve IoT device cloning with security measures and exposure of sensitive data (Swapnil Naik et al., 2017).

MATERIALS AND METHODS

Related Work: The utilization of wireless sensor communication, which permits easier intrusion between communication by attackers, together with the Internet of Things (IoT) or Web of Things (WoT) additionally prompts attackers to uncover confidential data and to control information. It is vital to find efficient and successful techniques to balance such intrusion. Something else, all the benefits of the IoT will be relinquish. So as to address these difficulties, first, a profound security investigation of the current advances is expected to find the root cause along with the analysis strategies that permit verification of the security of the network (Stefan Marksteiner et al., 2017). A technique for friendship network in interpersonal organizations utilizing genetic algorithm. This is to respond to two primary inquiries. The first thing is that how the connections are formed in the interpersonal network and the subsequent one is that why links are framed in the social network. They utilized the possibility of genetic algorithm to build up a companion proposal framework. As asserted, their methodology brought about more excellent companions list which are significant and suitable for the further future connections. Utilize a human interpersonal organization and examine it, build an informal community of items by extricating data from such system, use attributes from the system so as to run a model which can produce engineered systems with comparative properties, The last advance is applying the methodologies and dissecting the outcomes (Wail Mardini et al., 2017).

The primary goal in the IoT is that each article in the IoT can utilize its friendship networks to scan for specific administration. The proposed work tends to issue of connection selection of associations, breaks down few procedures in the review. At that point it proposes a connection determination methodology utilizing procedure of genetic algorithm to find relatively ideal result. The results show an improvement over reviewed methodologies regarding few parameter (Wail Mardini et al., 2017). The crafty systems are the variations of delay tolerant network. Such networks are considered to be valuable for direction of data packets where there are less number of base stations in long distance travel of data packets. In a capitalist system, when hubs move apart or turn off capacity for energy moderation, communications might be upset or diminished intermittently. Such occasions bring about discontinuity in availability of data. The segmentation of system happens when there is no way existing between the source and destination. In such a way, hubs can communicate with one another by sharp links through store convey forward activity. Right now, present the plan of an incorporated keen framework

for IoT gadget determination and arrangement in crafty systems utilizing Fuzzy Logic and genetic algorithm (Miralda Cuka et al., 2017).

The hereditary calculation is a populace based enhancement strategy. It utilizes the general standards of common determination. It tends to be utilized for both compelled and unconstrained issues. The calculation iteratively changes the populace by utilizing three administrators: selection, crossover and mutation. At each progression, the genetic algorithm chooses parent chromosomes and creates the new population by applying genetic operations (Ilhan Aydin et al., 2017). The internet of things has picked up fame in successive years for syndetic of devices such as sensors, gear, software programming, and services of data. Through the web it enhances the correspondence between these devices. The ideal components associated with internet of things are: distinguishing proof, detecting, correspondence, administrations and semantics. The distinguishing proof component coordinates the administrations with the interest. The detecting component acquires the data from different items inside the system at that point, it transmits detected information back to the database (Ankush B. Pawar et al., 2016). The internet of things contains an intricate framework of brilliant devices, which often transmits data through the network. The major advancements of internet of things technology is worldview, which is comprised of security fundamental tasks and delicate data to be published in the network and the dimension of security is vital.

This system contemplates security of system that matters in astute home, human services and hauling areas. The interference that happens in IoT devices is conceivable during activity making them in shutdown mode. The research categorization of security threats in internet of things systems is designed to help IoT designers for better acquaintance with security defects and better assurances will be consolidated (MukrimahNawir et al., 2016). The internet of things systems discover increasingly more wide conveyance in numerous territories. Significant element of the IoT systems are huge number of information sources, hubs of the IoT arrange have constrained processing assets, information move from sources to the focal gadgets, various sorts of systems are utilized(internet, remote, wire, etc.). These highlights do rather genuine the issue of equal preparing of numerous gathered information in IoT. This issue incorporates in itself two different issues: Big information handling and making of versatile systems. The hereditary calculation is utilized for finding the ideal plan of the appropriation of CEP administrators on IoT arrange has. Trial results indicated that the use of the offered approach permits to get an increase in throughput to 50 percent. Simultaneously, the activity of the genetic algorithm doesn't abuse the ongoing scale (Igor Kottenko et al., 2016). The internet of things environment is fundamental for making a proficient official between data services and internet of things in order to execute a composite task effectively.

Right now, propose service asset portion approach which limits information transmissions between client's cell phones and which successfully manage the requirements of these sorts of situations. The tasks issue into a variation of the degree-obliged least crossing issue and applied the procedure of genetic algorithm to diminish the point expected for creating a close ideal arrangement. The fitness algorithm and cipher strategy to apply the procedure of genetic algorithm in productive way. Also, it takes fundamentally less time than the beast power approach (MinHyeop Kim et al., 2015). There are loads of PCs, physical gadgets, and cell phones. To finish a mind boggling task, the undertaking might be disintegrated into a ton of straightforward errands, and be doled out to heaps of gadgets in IoT, which can improve the entire execution of the framework. Be that as it may, by along these lines, the specialized gadgets in the IoT should make a parity one another, accordingly to build the framework execution while balance all the assets. Numerous scientists have checked that the problem is NP-hard. Right now, propose a genetic algorithm for understanding the planning in IoT framework. Trial results show the proficiency of the proposed calculation (Junqing Li et al., 2013).

Motivation: Location of malignant associations in PC systems has been a developing issue persuading across the board inquire about in software engineering to grow better intrusion detection system (IDS). Right now, present an AI approach known as genetic algorithm (GA), to distinguish such unsafe associations. The algorithm mulls over various highlights in organizing the associations, for example, kind of convention, arrange administration on the goal and status of the association to create a grouping rule set. Each standard in rule set recognizes a specific attack type. For this trial, we actualized a GA and prepared it on the informational index to create a standard set that can be applied to the IDS to distinguish and group various kinds of intrusions. A genetic algorithm is a hunt method utilized in processing to discover genuine or rough answers for streamlining and search issues. Genetic algorithm is categorized as worldwide inquiry heuristics. Genetic algorithm is a specific class of transformative algorithms. The transformative algorithms are applied to PC systems to network intrusion and data traffic brought about by data transfer.

Each attainable solution can be set apart by its estimation of the wellness of the issue. Genetic algorithm is begun with a lot of solutions called populations which means organizing network traffic. It is utilized to focus another population and gives progressively appropriate and more opportunities to choose. This is rehashed until best solution is given. Fundamentally, a fitness function is utilized to assess and to recognize the fittest individuals which finds the elective course to move the information instead of clogged system. It is a procedure that accepts the population produced as information and reproduces the appropriateness of population as result. The subordinate procedure involved in genetic algorithm is given below.

STEPS IN GA

- Step 1: Choose a procedure to signify population parameters //selection operator, crossover operator, mutation operator, population size, crossover probability and mutation probability.
 - Step 2: Initialize random population with strings of size l, pmax, set p = 0.
 - Step 3: Evaluate each and every string in generated population.
 - Step 4: If $p > p_{max}$ and other termination criteria is satisfied, then terminate the procedure.
 - Step 5: Perform reproduction process over the produced population.
 - Step 6: Perform crossover operation on random pair of string.
 - Step 7: Perform mutation process on every string.
 - Step 8: Analyze strings in newly generated population. Set $p = p + 1$ and go to Step 3.
 - Step 9: CIPHERING of population in binary string. // Steps in fitness function.
 - Step 10: Random generation of a population.
 - Step 11: Fitness value of each population is calculated.
 - Step 12: Use fitness value to select pairs of parent strings.
 - Step 13: Generate new string //crossover and mutation is performed until a new population has been produced.
 - Step 14: Repeat steps 10 to 13 until satisfying solution is obtained.
 - Step 15: The newly produced population is further examined and analyzed for termination process.
 - Step 16: If the termination criteria is not met, the population is recursively performed.
 - Step 17: Choose a random point from parents. // Crossover
 - Step 18: Split the parents at the crossover point.
 - Step 19: Create new population by exchanging tails of the parents.
- //Generally setting crossover probability with a value 0.5 produces good results and its typical range is 0.3 to 1.

Figure 1: Flowchart for Genetic Algorithm



Existing System: An intrusion detection system is a framework which is used to organize traffic for apprehensive movement and issues alerts when such a suspicious activity is found in the network. Intrusion detection system is a software application that filters a system for suspicious movement or breaching of strategy. An malignant venture or contravention is regularly exposed either to an oversee or gather centralized system utilizing a security information and event management framework. A security management framework coordinates outputs received from various locations and uses alert filtering procedures to detach malignant accomplishment from false alert. Despite this the intrusion detection system screens networks for possibly malevolent activity and additionally approved to false alerts. Subsequently, enterprises need to calibrate their intrusion detection system framework when they initially propose them. This implies an appropriate setting up of the intrusion detection system to perceive the difference between ordinary traffic on the system resembles with malevolent movement.

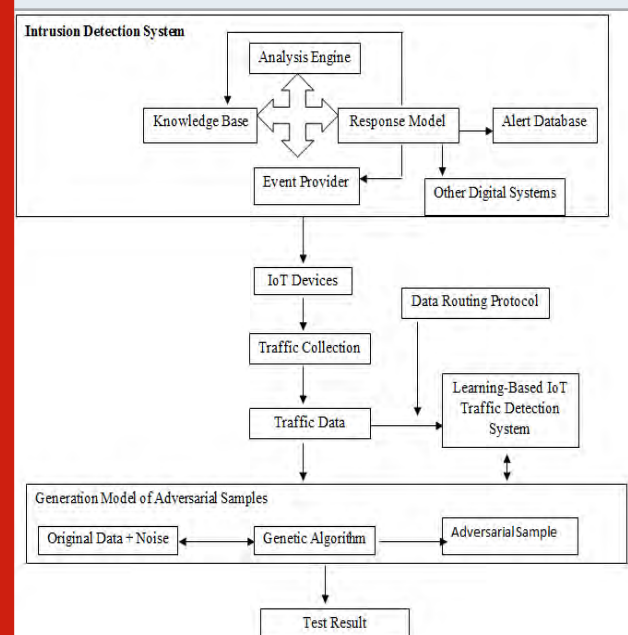
Intrusion detection system additionally screens and organizes data packets inbound to the system to analyze noxious activity associated with it and on the double sends the admonition notices. Wireless sensor network is a system that comprises of minor, unpredictable and huge number of sensors and at least one base station or hub. Most testing issue in wireless sensor system is the constrained battery intensity of sensor hubs utilized in the system. To build the vitality of sensor hubs, vitality is ideally administered all through the wireless sensor system. So the way to advance the existence time of the system is to plan successful and vitality conventions. Routing protocol can be a structure based or convention activity based. Right now, instructional exercise of existing routing protocol in wireless sensor systems is completed. Testing issues for WSNs are energy utilization and system life time.

Proposed Methodology: Figure 2 shows the monitoring of network intrusion detection by IoT devices and network traffic control by genetic algorithm. Routing in the internet of things - Sensors or wireless sensor networks comprise of a fundamental piece of IoT since sensors can be constrained by end clients and information can be transmitted to far off locales through Internet. IoT information conventions are utilized to interface low power IoT devices. The IoT devices will commonly transmit information over the worldwide Internet. Business IoT, where nearby correspondence is commonly either Bluetooth or Ethernet (wired or remote). The IoT devices will ordinarily communicate with neighborhood devices. These protocols furnish point-to-point communication with the equipment at the client side with no internet connection. Availability in IoT data protocol is through a wired or a cellular network. There are numerous application zones of wireless sensor networks, for example, battle field reconnaissance, psychological militant following and roadway traffic observing. These applications gather sensed information from sensor hubs to screen events in the domain of intrigue. One of the

significant issues in these applications is the presence of the radio-jamming zone between source hubs and the base station. Based on the routing protocol, transmission of the detected information may not be delivered to the base station.

To take care of this issue, we propose a genetic algorithm based routing protocol for dependable transmission while considering the fair energy exhaustion of the sensor hubs. The genetic algorithm finds an effective routing by considering the radio-jamming zone, transmission separation, normal outstanding vitality and bounce check. There are a few applications known for wireless sensor networks, and this assortment requests improve the routing protocol. The lifetime of system and energy utilization for routing which assume key role in each application are represented by some prominent parameters. The procedure of genetic algorithm is one of the optimized technique of nonlinear methodology and generally a good choice of effectiveness for huge scope of application. The current work attempts to apply an extensive improvement in every single operational phase of a wireless sensor network including hub position, coverage of network, and aggregation of data and accomplished a perfect solution of routing protocol parameters and application based sensor networks. By utilizing genetic algorithm which is dependent on the consequences produced by reproductions in network, a particular fitness function was accomplished, upgraded, altered for all operational phases of sensor networks. Figure 1 shows the execution procedure of genetic algorithm.

Figure 2: IoT for Network Intrusion Detection by Traffic Control



Intrusion detection system of sensor network setup at point located within the system to monitor traffic produced from other devices of the system. It provides

a perception of traffic on the whole subordinate network and analyzes the traffic that is produced from the subnet to the collection of known threats. When an attack is renowned or an intrusion is detected, an alert is sent to the executive. A network intrusion detection system is introducing the alert system on the subnet where firewalls are situated which is to check whether someone is intruding the firewall system. The intrusion detection system runs on independent devices located on the system. The intrusion detection system screen the imminent and dynamic data packets received from devices and will produce alert messages to the administrator if pernicious attack is recognized. This shows a preview of existing system and contrast the past depiction. The logical intrusion detection system records were distorted, an alert message is transmitted to the manager to examine. The utilization of intrusion detection system is notified on crucial devices, which are not expected to configure their design.

The intrusion detection system includes a framework that would reliably resides at the front end server, controls and deciphers the protocol used between client and server system. Intrusion detection system is attempting to make sure about server by normally checking the hyper text transfer protocol. As protocol is decoded before and entering in to the next layer of network, then the framework would require to present the interface to utilize the data transfer protocol. The intrusion detection system is a operator that dwells large inside a group of servers. Protocol recognizes the intrusions by observing and decoding the communication using data transfer protocol. This may screen query based protocol expressed to the centralized layer as it is executed with database in the server. In the intrusion detection system, the procedure to build up a total perspective on the system framework associated to organize information in the network.

Detection Method of IDS: The intrusion detection system distinguishes attacks with respect to the premise of the particular examples, for example, bytes produced, 1's or 0's produced in the traffic system. It additionally identifies the definitely realized malevolent guidance succession which is utilized by the attackers. The recognized instances in the intrusion detection system are known as signatures. The intrusion detection system can easily differentiate the attacks whose design exists in framework yet it is difficult to distinguish new suspicious attacks. The intrusion detection system was familiar that recognizes the ambiguous suspicious attacks as new threat or intrusion are grown quickly. In intrusion detection system, there is utilization of machine learning to provide a trustful activity model is contrasted with that model and it is considered as malware in the event that it isn't discovered in new model. IoT based strategy has a advanced property in contrast with intrusion detection system as these models can be prepared by the applications and equipment designs.

ALGORITHM

Step 1: Start
Step 2: Security administrator configure perspectives and Network behavior monitoring.

Step 3: Data packet capture by preprocessing module.
// The Intrusion detection system.

Step 3.1: If, it is normal data detection, then discard normal data.

Step 3.2: Else, misuse of detection module is identified.
// the data from Step 2 and Step 3.2 is provided to another preprocessing module.

Step 4: Collected is provided is checked with training database.

Step 5: Calculate inferior and superior limit.
Step 6: Abnormal data detection, alert response module.

// Implementation of GA.
Step 7: Generate initial population for time interval.
//Selection process

Step 8: Estimate the fitness of each chromosome.
// Fitness test.

Step 8.1: If, termination criterion is satisfied, Repeat Step 2.

Step 8.2: Else, proceed with next step.
// Generation of new population, Reproduction.

Step 9: Select a pair of strings for mating.

// crossover.
Step 10: Exchange parts of 2 selected strings and create 2 offsprings using crossover probability.

Step 11: Randomly change the gene values in 2 offspring chromosome using mutation probability.
// Mutation.

Step 12: Include the resulting chromosome in the new population.

Step 12.1: If, the size of new population is equal to existing chromosome.

Step 12.1.1: Replace the current string population with new population, Repeat Step 8. //Replacement

Step 12.2: Else, Repeat Step 9.

Step 13: End.

RESULTS AND DISCUSSION

Wireless sensor network are accomplishing with progression of time. Out of immense utilization of wireless sensor networks, few applications request fast data transfer with least interruption. A few applications offer significance to throughput and they don't need to deal with delay. The data on network structure and routing

protocol is significant and it ought to be fitting for the necessity of the utilization. The protocols are dependable approaches to build lifetime of the systems, in spite of the fact that these leads to more energy utilization by heads of cluster. Consequently, to build system lifetime, heads of cluster must be reorganized during every time of design of cluster. Regardless, the protocol guarantees usage of a successful layout of cluster, they neglect to ensure optimization of the best hub as cluster head. Through enhancement, the layout decreases the energy utilization and subsequently improves effectiveness and

lifetime of the system. In the end, the data transformation and inquiries between the principle stations, data sink is another significant issue in wireless sensor network. A basic procedure for transmission of data is the immediate data transmission between the base stations. The single step adaptation procedure is excessively exorbitant, the separation between the hub and base station, the more energy is required and subsequently the lesser the lifetime of system. Table 1 explains the detection of network intrusion by intruders using genetic algorithm.

Table 1. Network Intrusion Detection by Genetic Algorithm

DURATION		PROTOCOL	SOURCE PORT	DESTINATION PORT	SOURCE IP ADDRESS				DESTINATION IP ADDRESS				ATTACK TYPE
Hours	Mins				0	1	2	3	0	1	2	3	
Secs													
0	0	File transfer protocol	1890	23	191	162	1	191	162	0			
12					32			50					
0	0	Simple mail transfer protocol	1800	26	191	162	1	191	162	0			
0					32			50					
0	0	RSH	1020	901	191	162	1	191	162	0	RCP		
1					32			50					
0	0	TELNET	1900	25	191	162	1	191	162	0	GUESS		
0					32			50					
0	0	RLOGIN	1000	415	191	162	1	191	162	0	RLOGIN		
0					32			50					
0	0	RSH	1801	551	191	162	1	191	162	0	RSH		
0					32			50					
0	0	File transfer protocol	1899	901	191	162	0	191	162	0	GUESS		
0					41			50					
0	0	TELNET	4562	25	191	162	1	191	162	0			
0					31			50					
0	1	TELNET	5672	56	191	162	0	191	162	0			
0					41			50					
0	0	File transfer protocol	2345	701	191	162	0	191	162	0			
0					41			50					
10													

Another procedure for data transfer is multistep oriented transfer for a particular range. This procedure spares significant energy consumption and decreases impact in

the system to a lot, in spite of the fact that, \contingent upon the spot of utilizing routing protocols, but they have a few impediments. Primary explanation that makes

specialists progressively keen on the data organization and data transmission protocol is significant energy expended at this level. The huge consumption of energy is by radio communication. Along with this, a clear study on this stage, vows to advance wireless sensor network with reference to energy utilization and system lifetime. Improvement of the parameters referenced above eventuates in an advanced wireless sensor network. There are various techniques, for example, evolutionary algorithm and gratitude to its better outcomes for the scope of systems and the final algorithm that was produced towards the end, the procedure of genetic algorithm is a general one. The accessibility of ultimate algorithm makes algorithm valuable and provide support for clients. Consequently, the current investigation utilizes the procedure of genetic algorithm for configuring and customization of systems.

Table 2. Intrusion detection system of network by IoT based on Genetic algorithm

TRAFFIC	TRAINING SET	TESTSET
Normal	67892	9610
Denial of Service	45632	7231
Probe	12377	2254
R2L	889	2671
U2R	46	150
Total	126836	21916

the technique of genetic algorithm, the fitness work, by definition, is a strategy for scoring each chromosome reliant on their ability.

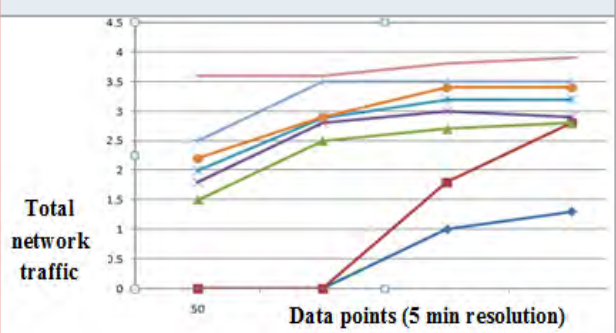
The selected score is a characteristic for continuation of further engendering. Reliance on issue by the fitness work is broad, so that if there ought to be an event of specific issues, it is ludicrous to hope to portray the issue. Typically, populaces are permitted to go to the progressive age reliant on their fitness esteem. Right now, score coordinates the predetermination of solutions. During every dynamic generation, another generation is made through grasping people from the current age to mate on the bases of their fitness esteem. The population with higher fitness score has higher opportunities for being picked, the system which realizes specific gathering of the best arrangement. Bigger piece of the limits consolidate a stochastically organized segment for grasping humble number of less fit individuals for motivation behind keeping arranged assortment in the people. The hybrid procedure builds up the huge development toward creation.

Figure 3 shows the network traffic prediction by genetic algorithm. The reproductive procedure by which acquired attributes are starting with a generation then onto the successive generation is mimicked. In the reproductive procedure, crossover process embraces two or three

Table 2 provides explanation on intrusion detection system of network by IoT devices based on genetic algorithm. A worldwide heuristic algorithm, different populations are created by assessment of perfect arrangement by genetic algorithm multiplication process. The methodology of fitness work is one of the huge strategies utilized in genetic algorithm to compute fitness of the recently produced solutions. The genetic algorithm starts with a fundamental solutions that contains self assertive sets that fuses characteristics by gathering of 0 s or 1 s. The fitness work count drives solutions to achieve a perfect arrangement by the means for monotonous methodology including hybrid and determination administrators. There are two unique approaches to develop another masses: steady state genetic algorithm and generational genetic algorithm. A couple of individuals in the solutions are superseded and at the same time, the generational genetic algorithm replaces all the new individuals of generation. By using

population by selection process of parents. The procedure keeps on arriving at the ideal size in the new generation. A few crossover process causes, every one of which with various points. The most direct way is single session, where an irregular cross section is embraced to isolate new generation. The bit succession of the next generation is reproduced as the succession generation population.

Figure 2



The fitness of population decides degree to which the utilization of vitality is limited and inclusion is expanded. Some significant fitness calculations in wireless sensor network is evaluated. Direct separation to base station - it alludes to whole of direct separation between sensor hubs. Utilization of vitality, sensibly, is dependent upon the quantity of hubs and for huge wireless sensor network the vitality is extraordinary. Also, DDBS is worthy for littler systems where number of close hubs isn't impressive. Cluster based separation: The absolute heads of cluster and base station separations and sum of the separation between the decided part hubs and cluster. The arrangement suits systems with an enormous number of broadly dispersed hubs.

Table 3 explains the characteristics of data routing protocols for network traffic detection. Higher cluster separation prompts higher energy utilization. For minimization of energy utilization, the cluster distance

must not be excessively huge. The thickness of the clusters is constrained by embracing this estimation, while thickness is included of hubs in each group. Group based separation standard - rather than a normal cluster separation, standard inference quantifies the progressions of separations of the group. Group based separation is a component of the arrangement of sensor hubs. There

are groups with various sizes in irregular situation so a cluster inside a predetermined variety in the cluster separation is satisfactory. Provided that this is true, the distinctions in cluster separation are not null, whereas the variety is dependent on solution of data. At any rate, under deterministic solution with uniform spread of center point positions,

Table 3. Data routing protocols for Network data traffic detection

Routing Protocols	Classification	Power Consumption	Data Aggregation	Scalability	Query based	Overhead	Data model	QoS
RPT SPEED	Source initiated Location	Limited	No	Limited	No	Less	Demand driven	Yes
RIP	Low Destination initiated	Yes Limited	Limited No	No Limited	Less No	Geographic High	No Event driven	Yes
IGRP	Flat	Low	No	Limited	No	Low	Continuously	Yes
OSPF	Data centric	High	No	Limited	No	Medium	Event driven	Yes
GEAR EGP	Location	Limited	Yes	Limited	No	Medium	Event driven	Yes
	Source initiated	High	No	Limited	No	High	Continuously	Yes
SPAN	Hierarchical/ Location	Low	Yes	Limited	High	High	Continuously	Yes
BGP	Location	Low	Yes	Good	Low	Medium	Continuously	Yes
GAF	Hierarchical/ Location	High	Yes	Limited	Good	Medium	Query driven	Yes
IS - IS	Location Yes	High	No	Good	No	Good	Virtual grid	
SMTP	Hierarchical	Limited	Good	No	Yes	Low	Continuously	Yes
HTTP	Data-centric	High	No	Yes	No	High	Continuously	Yes
VGA	Flat	Low	Yes	Yes	Low	Good	Complex	Yes
IGP	Location	Maximum	Yes	Limited	Good	Good	Complex	No

cluster division configuration must be constrained. All things considered, changes of uniform cluster based partitions show that the framework is poor. Move essentialness: it is proportion of used imperativeness required for moving all the accumulated data to the base station. Let n be the amount of related center points in a gathering. Number of transmissions with everything taken into account, the base station coordinates the amount of transmissions that occurs at each checking period. This measure is obtained subject to the conditions and the imperativeness level of the framework; thus t speaks to a long time mastermind which the common perfect response for enhancing and a fair response for minimization are sufficient. The idea of the best course of action or chromosome chooses the show of hereditary calculation based arrangement. In what using genetic algorithm, a fitness capacity to improve each key operational pieces of remote sensor organize is introduced. Toward fitness capacities are the most part used to improve vitality use and lifetime parameters. Diversion results certified improvement of the directing conventions.

CONCLUSION

From the audit, it is comprehended that there are numerous advancements that empower IoT integration in reality. For example wireless sensor network is one of them which are essential to detect devices that produce immense information caught and sent to IoT based Internet servers. Right now, it is imperative to comprehend the efficiency of routing protocol for information dispersal or steering and the efficiency to sent information safely. The proposed technique to consider distinctive routing protocols and their productivity as far as throughput, delay time and data routing protocol overhead.. Genetic algorithm requires increasingly computational time. Huge number of hubs can be conveyed in this system, the predetermined number of hubs access the channel and data packets and head of clusters communicate locally occurs when data transmission between hubs are boundless. Higher energy utilization is a result of the occasional migration. In any case, obligations of cluster head might be appropriated among every other hub through occasional migration, which brings about lower energy utilization. The information gathered by group individuals are collected in cluster head and sent

to the sink. In this way, utilization of routing protocol in wireless sensor network by application of genetic algorithm, network traffic is detected and diminished.

ACKNOWLEDGMENT

This Paper is sponsored by Jiangxi Engineering Laboratory on Radioactive Geo science and Big Data Technology, East China University of Technology, Nanchang, 330013, Jiangxi, China.

REFERENCES

- Aishwarya S Hampiholi and Dr. Vijaya Kumar B P (2018) Efficient routing protocol in IoT using modified Genetic algorithm and its comparison with existing protocols IEEE Third International Conference on Circuits, Control, Communication and Computing.
- Ankush B. Pawar and Dr. Shashikant Ghumbre (2016) A SURVEY ON IoT APPLICATIONS, SECURITY CHALLENGES AND COUNTER MEASURE 978-1-5090-1338-8/16/\$31.00 ©2016 IEEE.
- Archana P. Kalea and Shefali P. Sonavaneb (2018) IoT based Smart Farming : Feature subset selection for optimized high- dimensional data using improved GA based approach for ELM Elsevier B.V.
- Diya Thomas and Binsu C. Kovoorb (2018) A Genetic Algorithm Approach to Autonomous Smart Vehicle Parking system Published by Elsevier B.V.
- Igor Kottenko and Igor Saenko (2016) An approach to Aggregation of Security Events in Internet-of-Things Networks Based on Genetic Optimization DOI 10.1109/UIC-ATC-ScalCom-CBDCoM-IoP-SmartWorld.2016.147.
- Ilhan Aydin Mehmet Karakose Ebru Karakose (2017) A Navigation and Reservation Based Smart Parking Platform Using Genetic Optimization for Smart Cities 978-1-5090-5938-6/17\$31.00 IEEE
- Junqing Li Yuting Wang Tao Sun (2013) A HYBRID GENETIC ALGORITHM FOR TASK SCHEDULING IN INTERNET OF THINGS ICIT 2013 The 6th International Conference on Information Technology.
- Kuppusamy P. Kamarajapandian M. S. Sabari and J. Nithya (2018) Design of Smart Traffic Signal System Using Internet of Things and Genetic Algorithm https://doi.org/10.1007/978-981-10-7200-0_36.
- Mahdi H. Miraz and Maaruf Ali (2018) Blockchain Enabled Enhanced IoT Ecosystem Security © ICST Institute for Computer Sciences, Social Informatics and Telecommunications Engineering https://doi.org/10.1007/978-3-319-95450-9_3.
- Miralda Cuka Donald Elmaz Ryoichiro Obukata Kesuke Ozer, Tetsuya Oda and Leonard Barolli (2017) An Integrated Intelligent System for IoT Device Selection and Placement in Opportunistic Networks using Fuzzy Logic and Genetic Algorithm IEEE DOI 10.1109/WAINA.2017.178.
- MinHyeop Kim and In-Young KoAn (2015) Efficient Resource Allocation Approach based on a Genetic Algorithm for Composite Services in IoT Environments DOI 10.1109/ICWS.2015.78.
- Mukrimah Nawir Amiza Amir Naimah Yaakob Ong Bi Lynn (2016) Internet of Things (IoT): Taxonomy of Security Attacks 978-1-5090-2160-4/16/\$31.00 ©2016 IEEE.
- Stefan Marksteiner Víctor Juan Expósito Jiménez Heribert Vallant Herwig Zeiner (2017) An Overview of Wireless IoT Protocol Security in the Smart Home Domain 978-1-5386-3197-3/17/\$31.00 ©2017 IEEE.
- Swapnil Naik and Vikas Maral (2017) Cyber Security – IoT IEEE International Conference On Recent Trends in Electronics Information & Communication Technology (RTEICT) 978-1-5090-3704-9/17/\$31.00 © 2017 IEEE.
- Syed Rizvi Joseph Pfeffer Andrew Kurtz and Mohammad Rizvi (2018) Securing the Internet of Things (IoT): A Security Taxonomy for IoT IEEE DOI 10.1109/TrustCom/BigDataSE.2018.00034.
- Wail Mardini Yaser Khamayseh Montaha Hani Khatatbeh (2017) Genetic Algorithm for friendship selection in Social IoT 978-1-5090-6778-7/17/\$31.00 ©2017 IEEE.
- Wail Mardini Yaser Khamayseh Muneer Bani Yassein Montaha Hani Khatatbeh (2017) Mining Internet of Things for intelligent objects using genetic algorithm 0045-7906/© 2017 Elsevier Ltd.
- Xiaowu Deng Peng Jia Xiaoning Peng and Chunqiao Mi (2018) An Intelligent Outlier Detection Method with One Class Support Tucker Machine and Genetic Algorithm towards Big Sensor Data in Internet of Things DOI 10.1109/TIE.2018.2860568 IEEE Transactions on Industrial Electronics.
- Ying Zhang Peisong Li and Xinheng Wang (2019) Intrusion Detection for IoT Based on Improved Genetic Algorithm and Deep Belief Network DOI 10.1109/IEEE Access.
- Yingchen Wang Xiaoxiao Geng Fan Zhang and Junhu Ruan (2018) An Immune Genetic Algorithm for Multi-Echelon Inventory Cost Control of IoT Based Supply Chains DOI 10.1109/IEEE Access.

Design and Implementation of Solar Powered Electric Bicycle

P. Karthikeyan¹, Major P. S. Raghavendran² and V. Kumaresan³

¹Assistant Professor,

²Associate Professor,

³Assistant Professor,

Department of Electrical and Electronics Engineering, Kongu Engineering College, Tamilnadu, India.

ABSTRACT

For the past 100 years, vehicle industries played crucial role in developing public transportation, healthcare, agriculture and medicine related vehicle. The vehicle used in irrespective of all sectors is oil as fuel for vehicle propulsion. The fuel not only generates mechanical energy but also generate environment hazards. One among them is CO₂ emission which creates a dangerous effect to the environment in terms of polluting air, increasing temperature level of atmosphere and cause of climate changes. One of the immediate steps to stop the emission level of CO₂ in vehicle industries is to stop production of vehicles. It is no practically viable as on this modern era. So the alternate way is to drive the vehicle by electricity which is also not generated conventionally as generation of energy from fossil fuels. The production of electricity does not pollute environment in case it is produced non conventional way. So the vehicle has to be driven by non polluting sources. There are many to generate non polluting energy source. One of them is solar energy in particularly solar photovoltaic which convert energy from solar into electric energy. In this proposed work a design and implementation of solar powered bicycle has been discussed. The design of each part in proposed method is finalized after considering the problems in existing methods. Thus the proposed solution of solar powered bicycle can become an alternative to the conventional fuel based automobiles

KEY WORDS: BATTERIES, ELECTRIC VEHICLE, POWER CONVERTERS, SOLAR ENERGY.

INTRODUCTION

The birth of the electric vehicle: It's hard to say only one innovator had invented electric vehicle in one country because at the starting of 1800 century many innovator

started to work on electric vehicle and created small scale electric vehicle (Rizzo et al., 2013). Robert Anderson was developed first basic electric carriage during that time (Chan et al., 2013). Electric vehicle uses electric motors as prime mover rather than conventional engine to provide required motive force. The solar powered electric vehicles (Chia Chen Lin et al., 2019) utilize energy from sun and convert it into electrical energy. The PV cells generate sufficient electrical energy only day time in particularly when the sun is energy adequate. The charge present in the battery supply ample electrical power to the vehicle during the lack of sunlight and also not energy conversion operation of PV cell.

ARTICLE INFORMATION

*Corresponding Author: pmanjukarthick@gmail.com

Received 15th April 2020 Accepted after revision 20th May 2020

Print ISSN: 0974-6455 Online ISSN: 2321-4007 CODEN: BBR CBA

Thomson Reuters ISI Web of Science Clarivate Analytics USA and Crossref Indexed Journal



NAAS Journal Score 2020 (4.31) SJIF: 2020 (7.728)

A Society of Science and Nature Publication,

Bhopal India 2020. All rights reserved.

Online Contents Available at: <http://www.bbrc.in/>

Figure 1: Thomas Parker and his electric car for First crude electric carriage



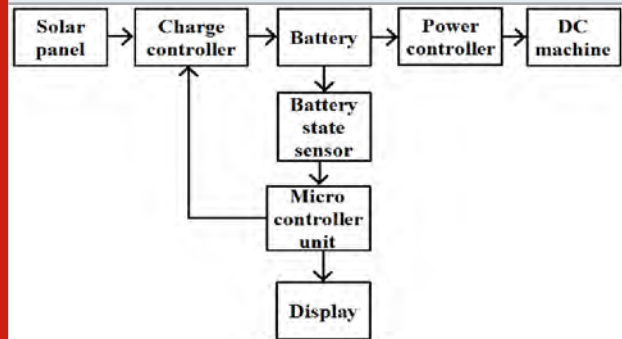
The electrical energy to the electric vehicle may possibly from off vehicle sources, self vehicle with battery bank and electric utility. Off vehicle source may be conventional or nonconventional energy it depends on availability of resources. Self contained source must be on the vehicle itself so that it generates required electrical energy for propulsion. Off vehicle sources may be on domestic places or a place in which maximum amount electricity generated by renewable way. Based on degree of electrical energy connected to vehicle, it can be classify into three categories. One is Battery Electric Vehicles, second one is plug in Hybrid Electric Vehicles and the final one is Hybrid Electric Vehicles (HEV). Battery Electric Vehicles more commonly called EVs (Rajashekara et al., 1994; Chan et al., 1993; Chan et al., 2001) and, are completely electric vehicles with rechargeable batteries and nonexistence of gasoline engine.

Battery Electric Vehicles are utilizing the stored energy in batteries for electric vehicle propulsion. The ultimate role of gasoline engine is removed by an electric motor. The electric motor obtained its power from rechargeable batteries through a charge controller. The battery power is utilized to run the electric motor with abet of all onboard electronics. BEVs do not produce any dangerous emissions and hazards caused by conventional gasoline powered vehicles. The batteries in the vehicles are charged by on board supply as solar energy or off board solar hub/solar energy supplier or energy from electricity. Indian Pollution control board recent announced that Delhi is one of the most polluted cities in India. It shows that pollution due to road dust and vehicles account for about 50% of the total pollution. Fine particles matter from vehicles is the main reason for air pollution.

It causes severe health problems such as high blood pressure, child and maternal malnutrition and diabetes. Environmental vulnerability (Singh Gupta et al., 2008) is a matter of great concern, especially in India. In this proposed method, solar powered electric cycle design part as well as implementation part is discussed. Since a bicycle is traffic free and pollution free transport for most the people, the solar powered electric bicycle is proposed.

Block Diagram Of The Proposed System

Table 1. Frequency Band with bandwidth



The block diagram of proposed system is shown in figure 2. It's consist three parts namely source part, battery and charge controller part and DC machine part. The solar panel gets solar energy as light energy and converts it into electrical energy in the form of DC. The DC output from solar panel is inherently small value or high value and based upon the intensity of the solar energy. Batteries (Sibrandus Stratingh et al., 2015) present in the proposed system get charged by solar panel through charge controller. It maintains the charge level of batteries while charging of batteries or discharging with help of battery state sensor and microcontroller. During day time in particularly high light intensity period, solar panel will generate maximum electrical energy. Batteries get charged during that time and its charging level is limited by charge controller. The battery state sensor (BSS) continuously measures the charge level of the battery and send control signal to charge controller.

The operation of charge controller depends on the signal from microcontroller. Based on microcontroller signal, the charge controller performs either step up or step down operation. Once the battery gets charged it read to perform its operation ie its supply required value of DC voltage to motor for propulsion. When the sunlight is amply available, the battery is charged efficiently to run the motor. Without sunlight, the motor runs by using the stored energy in the battery. The PIC16F877A microcontroller is interfaced with the LCD display. The voltage level of the battery is measured continuously and sent as the analog value to the microcontroller so that the remaining voltage value and the battery empty period are being displayed to the users. The speed of the motor is controlled by power controller, which in turn controls the speed of the bicycle.

Proposed System: Circuit diagram of the proposed system: The circuit diagram of the proposed system is shown in figure 3. A 75W, 18V solar panel is used in this proposed method. The solar panel output is connected to a battery through a charge controller. MOSFET based charge controller (Bortis Ortiz et al., 2011) is used. This CC performs the step and step down the operation of the output of solar PV. So, the required input supply is given to the battery. Two 12V, 7.2Ah batteries are connected in series. Thus the solar panel able to supplies

adequate electrical energy to a 24V battery via a charge controller. The energy stored in the battery can be used to supply and run the dc motor. A 250W and 24V dc motor are used in this proposed method. The high resistive resistors are being connected in parallel with the battery. By potential divider rule, the drain voltage level of the battery is measured and the analog value is sent to the microcontroller. This controller generates a control signal and it will act as a control signal for the charge controller. The remaining voltage and the empty time of the battery are measured. The port B of the microcontroller is interfaced with the LCD. Hence the measured values are displayed to the users.

Design of charge controller:

Figure 3: Circuit diagram of the proposed system

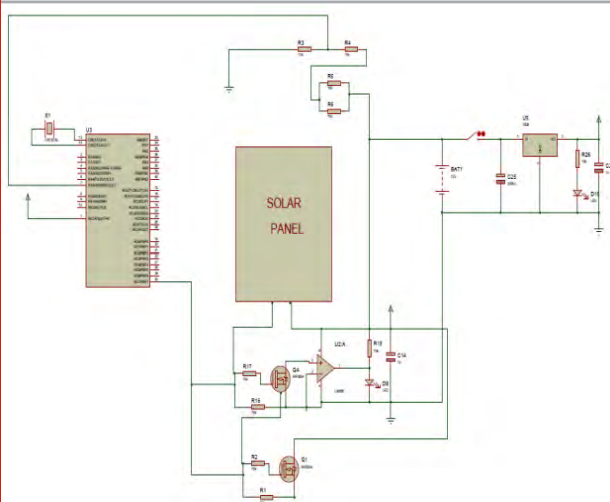


Figure 4: Circuit diagram of the charge controller

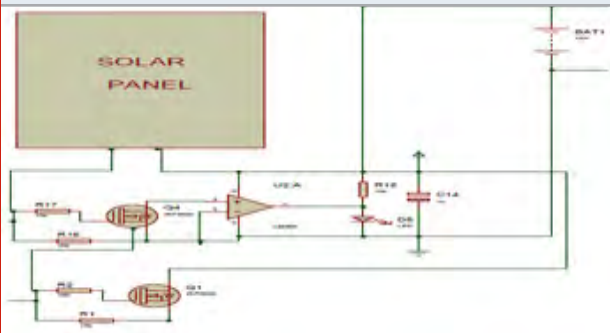
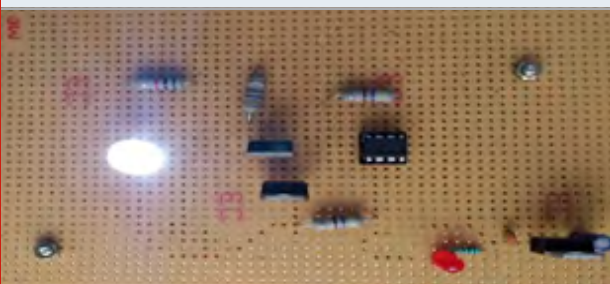


Figure 5: Charge controller on PCB



The most important purpose of the charge controller is regulating the amount of electric power connected to and drawn from batteries (Rohith et al., 2018). Under normal condition, the charge controller stops the battery from over charging and completes discharging operation. MOSFET based charge controllers are used in this proposed method since it is voltage controlled devices.

Design of battery state measurement

Figure 6: Circuit diagram of battery state measurement

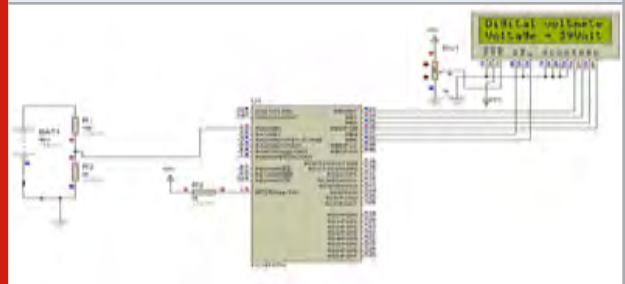
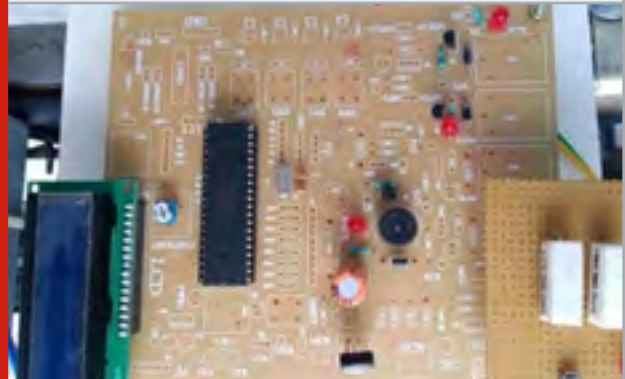


Figure 7: Battery state measurement on PCB



The drain voltage of the battery (Cao Schofield et al., 2008) is measured by the potential divider rule and the analog value is sent to the microcontroller. The LCD is interfaced with the microcontroller. The remaining charge and the empty time of the battery (Krein, 2007) is calculated and displayed to the user as digital value.

Hardware setup

Figure 8: Solar bicycle side view



Figure 9: Top view of bicycle



Figure 10: Solar panel setup



Figure 11: LCD display



RESULT & CONCLUSION

In this proposed system we have designed a solar electric bicycle and found a solution for the environmental problems. Solar energy creates absolutely no pollution. This is perhaps the most important advantage that makes solar energy so much more practical than oil. Usage of conventional vehicle and burning oil may release dangerous gases into our precious atmosphere. Solar energy is an entirely renewable resource. Some days we may be unable to get solar energy because of bad weather conditions such as cloudy and stormy days. But the next day we will get constant and consistent solar power source. For pollution free environment, noiseless road transport and zero percentage air pollution, Electric vehicles are needed in this globalization era. The people who are using vehicle for their transportation, they must look into the causes of conventional vehicle. The world environment climate change society reported that by

2030 the conventional vehicle will contribute major role in world climate change issues. N

not too early and not too late, this is exactly correct time to change over from conventional vehicle to electric vehicle which are powered by non renewable energy sources such as solar, wind and hybrid. Our government along with environment climate controlling society may focus more attention in electric vehicle manufacturing industries and provide sufficient subsidy to promote more startup company. The philosophy, technical features, and design of solar bicycle were discussed. In future, wind can also be used as one of the energy sources by placing wind turbine at the convenient place. Hybrid bicycle can also be modified further and we can make it to use for physically disabled people. Even bicycle can be digitalized by fitting indicators, advance sensors, navigation system etc. Gear variation system can also be implemented to increase torque and to control the speed.

REFERENCES

- Bortis Ortiz Kolar and Biela (2011) Design procedure for compact pulse transformers with rectangular pulse shape and fast rise times IEEE Trans. Dielectr. Electr. Insul Vol. 18 Pages 1171–1180.
- Cao Schofield and Emadi (2008) Battery balancing methods: A comprehensive review in Proc IEEE Vehicle Power Propuls Conf (VPPC) Pages 1–6.
- Chan (1993) Present status and future trends of electric vehicles in Proc 2nd Int Conf. Power Syst. Control, Oper Manage Pages 456–469.
- Chan and Chau (2001) Modern Electric Vehicle Technology Oxford, U.K.: Oxford Univ Press
- Chan Fellow (2013) IEEE The Rise & Fall Of Electric Vehicles In 1828– 1930: Lessons Learned Proc. IEEE Vol.101 Pages 206–212.
- Chia Chen Lin Ying Chuan Lai ChihChiang Wang et al., (2019) Development and Implementation of Solar-Assisted Electric Bicycle with GPS Tracking Service over Cloud IEEE International Conference on Consumer Electronics - Taiwan (ICCE-TW).
- Greenhouse Gas Emissions from a Typical Passenger Vehicle (2013) EPA Office of Transportation and Air Quality EPA420-F-05-004
- Krein (2007) Battery management for maximum performance in plug-in electric and hybrid vehicles in Proc Keynote Presentation IEEE Vehicle Power Propuls Conf Arlington TX Pages 2–5
- Lucian Nicolae Demeter Valer Turcin Mihai Hanek et al., (2017) Modular solution for charging the batteries of electric bikes parked on public domain Electric Vehicles International Conference (EV)
- Rohith S Prabhu Neeraj Vasudev Nandu et al., (2018) Design and Implementation of A Power Conversion System On A Bicycle With Utilisation By Sensors

Rajashekara (1994) History of electric vehicles in general motors IEEE Trans. Ind Vol. 30 Pages 897–904
Rizzo (2013) Automotive Applications of Solar Energy Available: http://www.dimec.unisa.it/leonardo_new/documents/Survey_Paper_AAC10_GRizzo.pdf
Rydh and Sanden (2005) Energy analysis of batteries in photovoltaic systems Part I: Performance and energy requirements Energy Convers Manag Vol 46 1Pages 957–1979
Sibrandus Stratingh (2015) Professor of Chemistry and Technology University of Groningen Groningen

The Netherlands DiOrio Dobos and Janzou Economic analysis case studies of battery energy storage with SAM Nat Renewable Energy Lab Washington DC USA
Singh Alapatt and M Abdelhamid (2012) Green energy conversion & storage for solving India's energy problem through innovation in ultra large scale manufacturing and advanced research of solid state devices and systems in Proc Int Conf Emerg Electron Pages 1–8
Singh Gupta and Poole (2008) Global green energy conversion revolution in 21st century through solid state devices in Proc 26th Int Conf Microelectron Nis Serbia May 11–14 Vol 1 Pages 45–54

CSRR Inspired UWB Antenna for Breast Cancer Detection

V. Vedanarayanan¹, G. Arulselvi², D. Poornima³ and D. Joshua Jeyasekar⁴

¹Assistant Professor, Dept. of ETCE, Sathyabama Institute of Science and Technology (Deemed to be University), Chennai.

²Associate Professor, Department of CSE, Faculty of Engineering and Technology, Annamalai University, Chidambaram.

³Research Scholar, Department of CSE, Faculty of Engineering and Technology, Annamalai University, Chidambaram.

⁴Assistant Professor, Department of ECE, Jeppiaar Institute of Technology, Sriprumbudur, Chennai.

ABSTRACT

In this paper, a rectangular CSRR inspired microstrip antenna is proposed for the breast cancer detection. The proposed rectangular antenna is capable to have ultrawideband performance, when the proposed resonating structure is feed with a 50-ohm microstrip line. The resonating frequency of the projected UWB CSRR antenna is from 2.31 GHz to 12.18 GHz. The proposed UWB CSRR antenna is fabricated on a FR4 substrate. The antenna is simulated using a EM tool called CST and the all the simulated results such as return loss, VSWR, E plane, H plane, 3D radiation patterns are presented. The SAR analysis are also presented with two size of tumor with same breast size is presented. All the above simulated results show that the presented antenna is the right choice for the detection of breast cancer at early stages.

KEY WORDS: BREAST CANCER, CSRR, METAMATERIAL, RECTANGULAR MICROSTRIP, UWB.

INTRODUCTION

The detection of contrast between the normal and the cancer tissue is the basis for any cancer detection methods (Lazebnik et al, 2007). Here in UWB Radar technology the dielectric contrast between the tumor tissue and the normal tissue is detected in order to identify

the cancer tissue. For this the major requirement is the antenna for transmitting and receiving the UWB band. The various clinical methods used for diagnosis such as X-ray, Ultrasound and MRI are not cost effective, this limitation motivate the researchers to find an alternate way for clinical diagnosis imaging. In the literature various number of antennas are proposed but they are having complex shapes (Ojaroudi et al, 2014). The rectangular microstrip patch antenna (Shanthi et al, 2019) is the simplest form of planar antennas. It is widely used because of its easy fabrication and its compatibility with the MIC.

ARTICLE INFORMATION

*Corresponding Author: veda77etce@gmail.com
Received 15th April 2020 Accepted after revision 20th May 2020
Print ISSN: 0974-6455 Online ISSN: 2321-4007 CODEN: BBRBCA

Thomson Reuters ISI Web of Science Clarivate Analytics USA and Crossref Indexed Journal



NAAS Journal Score 2020 (4.31) SJIF: 2020 (7.728)
A Society of Science and Nature Publication,
Bhopal India 2020. All rights reserved.
Online Contents Available at: <http://www.bbrc.in/>

Metamaterial (Christophe et al., 2006) are the artificial periodic structure which with negative parametric characteristic. The negative mu and epsilon are achieved with the help of the structures and not by the constituents. In the literature various shapes of metamaterial from SRR (Prasad, et al, 2019), CSRR (Prasad, et al, 2017; Kavitha et al, 2020), omega shaped, eight shaped and ELC (Prasad, et al, 2017) are investigated widely. In this paper we propose a UWB CSRR antenna for imaging in biomedical application. The proposed antenna is having a total designed size equal to 20 x 35 x1.6 mm³. The proposed structure is fabricated on substrate having 4.4 as it permittivity value and 0.02 as its loss tangent value which is called as FR4 substrate. Further the paper contains the details of materials and methods in section 2, result and discussion in section 3 and finally conclusion in section 4.

MATERIALS AND METHODS

Design of UWB CSRR antenna for Breast cancer detection:

The proposed UWB CSRR antenna is having three stages of evolution namely antenna A, antenna B and antenna C. Antenna A is a simple microstrip patch antenna a with full ground and it is fed with 50-ohm offset feed. The proposed antenna is having a triple band operating frequency bands from 2.56 GHz to 4 GHz, 5.85GHz to 7.12 GHz and 8.52 GHz to 14.21 GHz. Then, the antenna B is designed such that the ground is altered by reducing the size of the ground to lg and introducing slot of size a x b mm². The designed antenna B is capable of resonating at dual band with frequency range from 2.95 GHz to 12.12 GHz & 13.72 GHz to 14.35 GHz. And finally, the antenna C is designed by introducing a complementary split ring resonator with two slits exact opposite to each other. The proposed UWB- CSRR antenna has two operating band with the operating frequency range from 2.61 GHz to12.35 GHz & 13.62 GHz to 14.56 GHz. In Figure 1, the three stage evolution of the projected UWB -CSRR antenna is presented. The Parameter value of the UWB -CSRR antenna (antenna C) is given in Table 1.

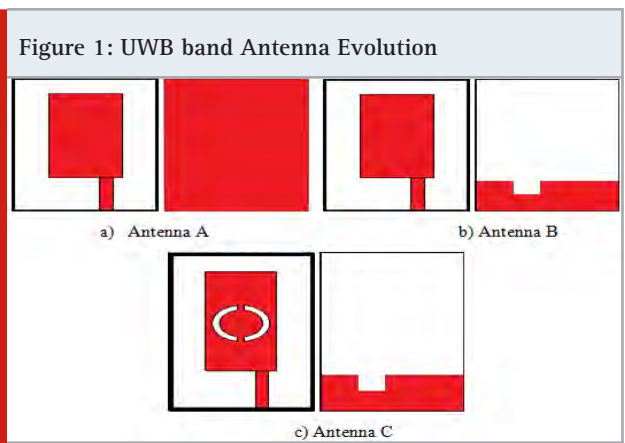
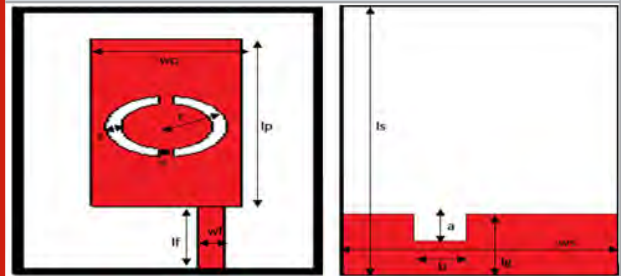


Table 1. UWB-CSRR antenna Parameter value

w	l	wp	lp	wf	lf	a
20	35	9.9	22	1.8	9	3.5
b	lg	s	v	r	t	h
2	8	1	1	4	0.035	1.6

Figure 2: UWB-CSRR antenna and its parameters



In figure 2, the proposed UWB-CSRR antenna for breast cancer detection is presented. The proposed structure is having a rectangular radiating element of size wp x lp mm². The structure is feed with a feed line of length lf and width wf. The entire radiating element and feed line is designed on top of the substrate and at the bottom of the substrate the defected ground structure along with slot of size a x b mm². In the rectangular patch, a complementary split ring resonator is etched at the centre. The slit is introduced in the CSRR at opposite to each other. With out the metamaterial structure and defected ground structure the antenna is having tri band frequency response. Once the ground is altered and after the inclusion of the metamaterial structure CSRR the proposed antenna exhibits an ultrawide band response. The response is due to the change in the direction of current flow because of the ground alteration and the CSRR introduction. In Figure 3, the s11 characteristics of the proposed antenna is presented. From the figure we can observe that the UWB-CSRR antenna proposed is having a dual band resonance from 2.61 GHz to 12.35 GHz & 13.62 GHz to 14.56 GHz. The maximum return loss value of the UWB-CSRR is -25dB. In Figure 4, the comparison return loss graph of the three stage of the proposed UWB-CSRR antenna is depicted. From, the figure it is observed that because of the defected ground structure and inclusion of CSRR the current path length increases which directly affects the resonant pattern of antenna A. Since the CSRR is included, it creates the extra resonance because of the inductance and capacitance.

As a result, the proposed antenna UWB- CSRR is having the wide and resonance. A simple rectangular patch antenna is converted into ultra-wideband antenna with the inclusion of CSRR and defected ground structure. In figure 5, the voltage standing wave ratio is presented.

From the figure it is noted that in the entire operating band of the UWB-CSRR antenna from 2.61 GHz to 12.35 GHz & 13.62 GHz to 14.56 GHz the value of VSWR is less than 2. Therefore, the impedance is matched in the entire operating band of frequency operation.

Figure 3: UWB CSRR antenna s11 characteristics

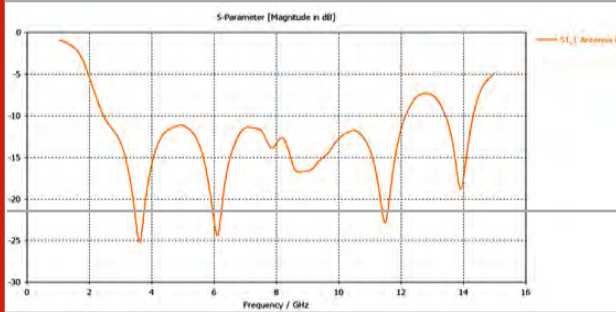


Figure 4 s11 Comparison of Various stages of the UWB CSRR antenna

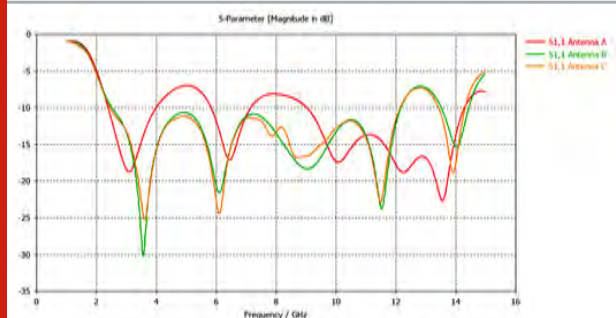


Figure 5: Voltage Standing Wave Ratio of the proposed antenna

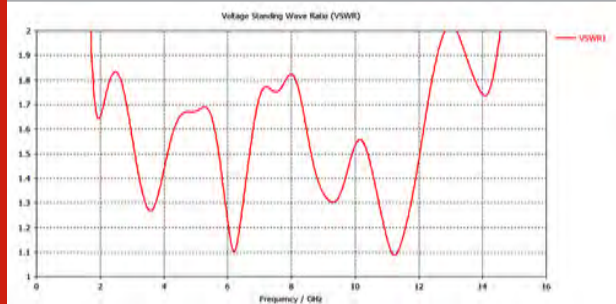


Figure 6: 3D radiation pattern of the UWB-CSRR antenna

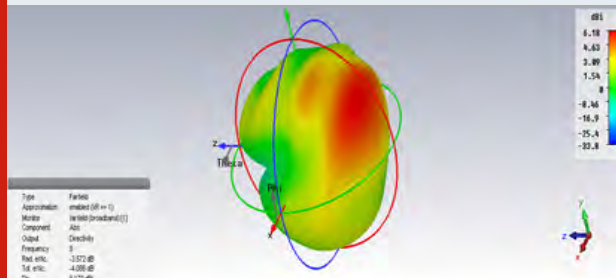
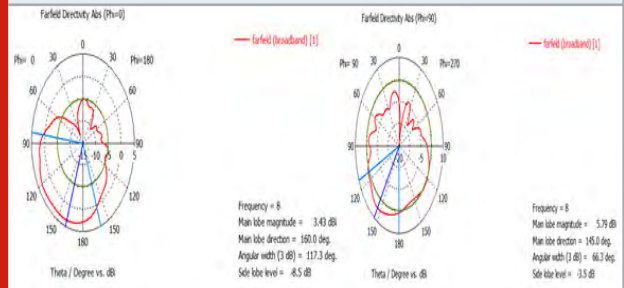


Figure 7: E & H plane of the UWB CSRR antenna



RESULT AND DISCUSSION

In Figure 6, the 3-dimensional gain pattern of the projected UWB-CSRR antenna is presented. From the figure it is noted that the maximum gain is in the broad side direction of the antenna axis. In Figure 7, the E & H plane radiation pattern is presented which has Omnidirectional and eight shaped pattern.

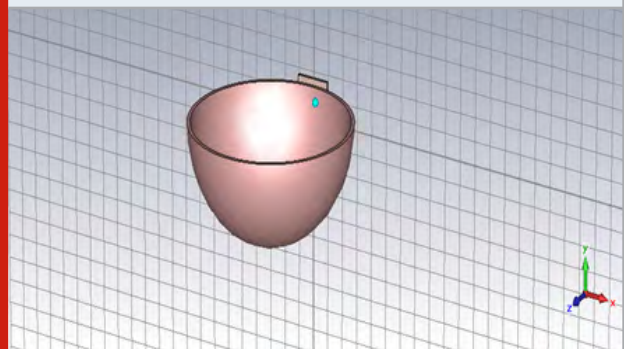
SAR Analysis with and without tumor: The implementation of the proposed antenna for the breast cancer detection is done by calculating the SAR value. SAR is specific absorption rate, which is the amount of total power absorbed by per mass tissue. The point where the value of SAR is high then that cell area is composed of tumor cell.

$$SAR = d/dt(dW/dm) = d/dt(dW/\rho dV) \quad (1)$$

From electric field it is calculated as

$$SAR = \sigma |E|^2 / \rho \quad (2)$$

Figure 8: Breast CAD model with tumor in CST environment



In figure 8, the breast CAD model along with proposed antenna and tumor designed in CST studio is depicted. The size of the breast used for the simulation is 60 mm. The distance between the antenna and the breast is equal to 10 mm. There are two types of tumor is used in the simulation of size 2 mm and another tumor of size 3 mm. It is clearly observed that with out the tumor the

SAR analysis of the proposed breast model is presented in Figure 9. From the figure we can observe that there is no deviation in the SAR value at the surface of the breast. Then, in the same breast the tumor is introduced, because of it there is variation in the SAR value in the breast at the point where the tumor is introduced. In Figure 10 and 11, the SAR analysis of the proposed antenna along with various size of tumor and breast antenna is presented. In table 2 , the point and max SAR values for 2mm tumor and 3 mm tumor is presented . From that table it is clearly observed that when the tumor size is increased then automatically the SAR value also increased. Similarly in Table 3 the location of the tumor placed and detected is presented, from which it is observed that the placed and detected location are nearly equal to each other.

Table 2. Point and Max SAR values for 2mm and 3 mm

Size of the breast	60 mm breast			
	2 mm		3 mm	
Size of the tumor	2 mm		3 mm	
Frequency (GHz)	Point SAR W/Kg	MAX SAR W/Kg	Point SAR W/Kg	MAX SAR W/Kg
3	11.8	6.35	12.5	9.13
5	17.2	5.70	18.8	6.11
7	28.3	1.53	33.6	4.15
9	25.7	2.31	42.5	2.83
11	26.4	1.47	35.8	4.78

Figure 9: SAR without the tumor

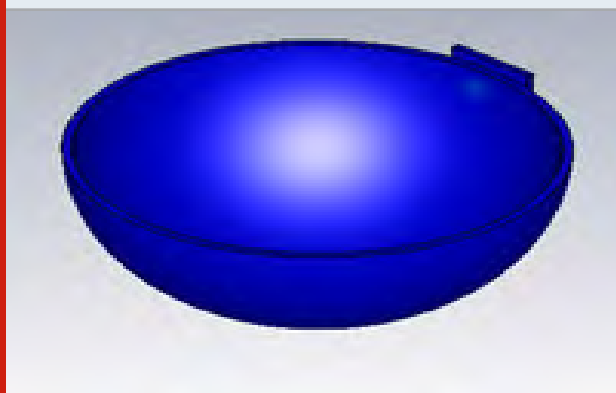


Figure 10: SAR with 2 mm tumor

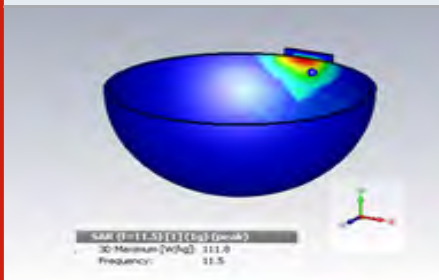


Figure 11: SAR with 4mm tumor

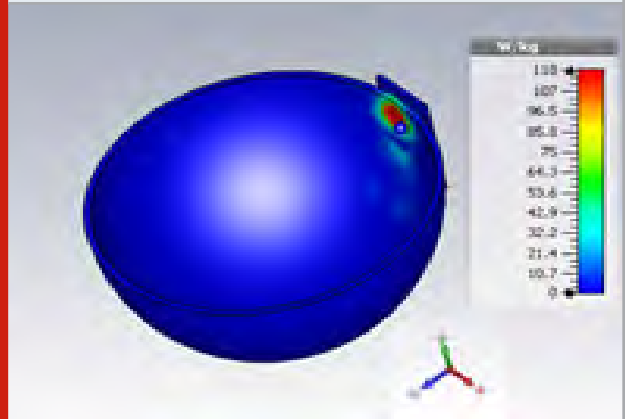


Table 3. Location of tumor cell placed and detected

Tumor cell place at the location	Tumor cell detected at the location
21,32,42	21.51,31.98,42.12
10,48,52	10.28,47.97,52.49

CONCLUSION

In this paper, a compact rectangular microstrip Antenna A is having a triple band operating frequency bands from 2.56 GHz to 4 GHz, 5.85GHz to 7.12 GHz and 8.52 GHz to 14.21 GHz. Then, the antenna B is designed such that the ground is altered by reducing the size of the ground to lg and introducing slot of size a x b mm² with operating frequency range from 2.95 GHz to 12.12 GHz & 13.72 GHz to 14.35 GHz. The proposed antenna C is designed by introducing a complementary split ring resonator with two slits exact opposite to each other with the operating frequency range from 2.61 GHz to 12.35 GHz & 13.62 GHz to 14.56 GHz. Then the breast CAD model along with proposed antenna and tumor designed in CST studio. The size of the breast used for the simulation is 60 mm. The distance between the antenna and the breast is equal to 10 mm. Two types of tumor is used one is 2 mm and another is 3 mm. The tumors are placed at different location and SAR values are calculated. The maximum SAR point location is nearly as same as the tumor location, from this we can conclude that the proposed antenna is the excellent choice for the breast cancer detection

REFERENCE

- Christophe Caloz, Tatsuo Itoh (2006) Electromagnetic metamaterials: Transmission line theory and microwave applications New York John Wiley & Sons Inc.
- Kavitha S.Prasad Jones Christydass and J.Silamboli (2020) Metamaterial Inspired Triple Band Antenna for Wireless Communication International Journal of

Scientific & Technology Research Vol 9 issue 3.

Lazebnik, M. D. Popovic L McCartney (2007) A large-scale study of the ultra-wideband microwave dielectric properties of normal, benign and malignant breast tissues obtained from cancer surgeries *Physics in Medicine and Biology* Vol 52 No 20 Pages 6093–6115.

Ojaroudi N M Ojaroudi and Y Ebazadeh UWB/Omni-directional microstrip monopole antenna for microwave imaging applications(2014) *Progress In Electromagnetics Research C* Vol 47,Pages 139–146.

Prasad Jones Christydass and N Gunavathi. (2017) Codirectional CSRR inspired printed antenna for locomotive short range radar *International Conference on Inventive Computing and Informatics (ICICI)*.

Prasad Jones Christydass and N Gunavathi. (2017) Design of CSRR loaded multiband slotted rectangular patch antenna *IEEE Applied Electromagnetics Conference (AEMC)*.

Prasad Jones Christydass and Manjunathan (2019) Pentagonal Ring Slot Antenna with SRR for Tri-Band Operation *Biosc. Biotech. Res. Comm, Special Issue* Vol 12 No 6 Pages 26–32.

Prasad Jones Christydass and Pranit Jeba Samuel (2019) Metamaterial Inspired Slotted Rectangular Patch Antenna for Multiband Operation *Biosc. Biotech. Res. Comm, Special Issue* Vol 12 No 6 Pages 57–62.

Shanthi Dr T Jayasankar, Prasad Jones Christydass Dr P Maheswara Venkatesh (2019) Wearable Textile Antenna For Gps Application *International journal of scientific & technology research* Vol 8 Issue 11

A Novel Control Approach for PV-Grid System in various Atmospheric Conditions

Dr. K Balachander^{1*}, Dr. A. Nagamani Prabu² and Dr. B. Janarthanan³

¹Department of Electrical and Electronics Engineering, Faculty of Engineering,

^{2,3}Department of Physics, Faculty of Arts, Science and Humanities, Karpagam academy of Higher Education , Coimbatore, India

ABSTRACT

This paper presents a design idea of Fuzzy Logic Controller (FLC) based Maximum Power Point Tracking (MPPT) with global and local MPP (Maximum Power Point) Monitoring. The proposed system is formed from a Photovoltaic (PV) array coupled with a grid through a boost converter (BC). A monitoring has been made by Proportional Integral controller (PIC) based Partial Power Converter (PPC) with FLC algorithm in tracking MPP under partial shading conditions. The effectiveness of the proposed control in terms of high accuracy, fast dynamics, and stable transitions improvement. Performance analysis such as power stability, peak overshoot, undershoots and settling time, etc. of the overall system is carried out.

KEY WORDS: FUZZY LOGIC CONTROLLER; MAXIMUM POWER POINT TRACKING; PARTIAL POWER CONVERTER; PROPORTIONAL INTEGRAL CONTROLLER

INTRODUCTION

A solar PV array's efficiency depends on the degree of temperature and irradiance and the characteristics of the PV array. At present operation of MPPT is important for connected PV systems to increase energy efficiency. About PV system grid integration includes a power electronics interface with DC conversion capability. Various configurations and topologies were developed with the goal of increasing the conversion efficiency in PV systems. The Frequency based control is implemented using PLL for the synchronization of frequencies. The internal current loop is implemented with FLC control

and it helps to produce the inverter AC voltage reference. Due to its in-ability to monitor the reference signal with accuracy under static frame, the FLC controller realized for dq reference quantity is achieved. Transformation of abc-dq converts the AC signal into DC by varying from static to rotating frame. This paper introduces a PPC that extracts a portion of the entire power of the system and provides the rest of the power directly to the output end. The Phase Locked Loop (PLL) is used for the synchronization of grid frequencies, and Synchronous Reference Frame (SRF) is used to boost stability.

MATERIALS AND METHODS

Existing System and disadvantages: The existing system (Fig. 1) consists of PV Module, PPC with MPPT and Single Phase Inverter with control structure. In this method a high-performance active power control scheme was proposed by restricting the maximum feed-in capacity of PV systems. In this approach, a high-performance active

ARTICLE INFORMATION

*Corresponding Author: kaybe.ind@gmail.com
Received 15th April 2020 Accepted after revision 20th May 2020
Print ISSN: 0974-6455 Online ISSN: 2321-4007 CODEN: BBRCSA

Thomson Reuters ISI Web of Science Clarivate Analytics USA and Crossref Indexed Journal



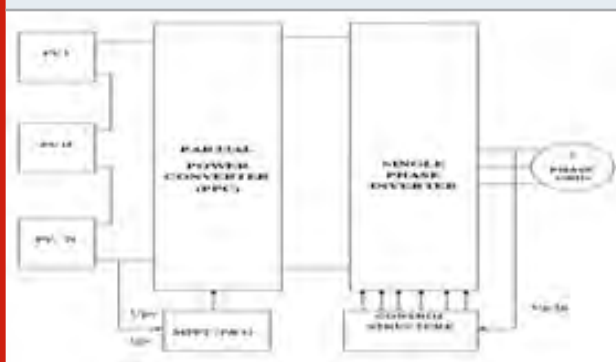
NAAS Journal Score 2020 (4.31) SJIF: 2020 (7.728)
A Society of Science and Nature Publication,
Bhopal India 2020. All rights reserved.
Online Contents Available at: <http://www.bbrc.in/>

power control scheme was proposed by restricting the maximum feed-in power of PV systems. The solution proposed can ensure steady operation of constant power generation. Compared to the conventional methods, this control technique allows the PV systems to work at the left side of the highest power point, and therefore it can achieve a stable operation as well as smooth transitions.

Tests of simulation have confirmed the efficacy of the proposed control solution in terms of reduced overshoots, decreased power losses and rapid dynamism. In order to increase the reliability of the injected power in PV-NRF the control technique is modified to PI-CC. The main drawbacks of this system in less accuracy, high power loss, failure to work under complex shading, weather shifts, complexity in design of control circuit, reduced system performance and low efficiency.

need of additional control circuits and improve system performance and efficiency.

Figure 1: Existing PV Grid-connected system



Proposed System: The non-polluting and strong deployment versatility, PV technology has been at the core of interest. In efficiency of the PV system is affected by irradiation and temperature. Thus, when partial shading occurs from the surroundings, the incident shadow decreases the irradiation and reduces the power produced. Since outmoded MPPT methods have not been capable to recognize the global maximum power of the characteristic VI curve, a new tracking method with a proposed converter is required.

The system proposes (fig. 2) a global MPPT method with shading detection and the slope-pattern from each segment of the curve. The proposed system results show that it is better than current system outputs. Results from simulation have checked the efficacy of the proposed control solution in terms of reduced overshoots, decreased power losses, improved performance and rapid dynamism

Changed to SRF control technique with FLC to increase the stability of injected power in PV-NRF. Some of the advantages of proposed system are MPPT accuracy, fast-tracking time, less power loss, ability to operate at dynamic changes of shading and weather conditions, no need of irradiation and temperature sensors, no

Figure 2: Proposed FLC System

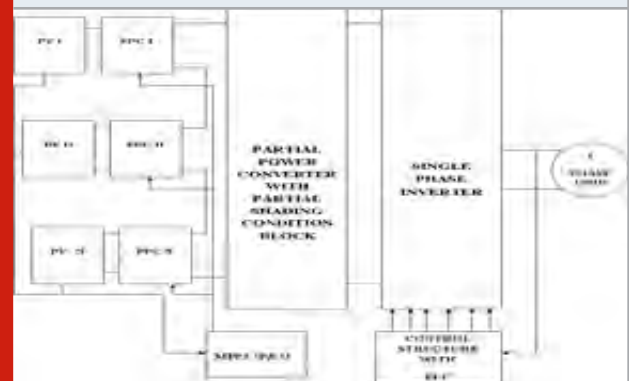


Figure 3: Simulation Diagram of Partial Power Converter

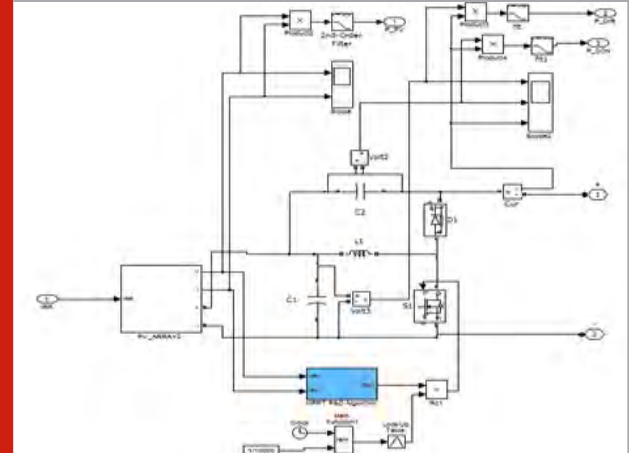
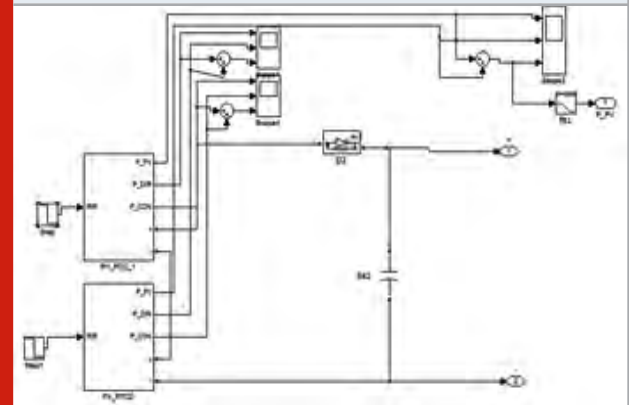


Figure 4: Simulation Diagram of PV- Partial Power Converter



RESULT AND DISCUSSION

Simulation: Simulations are done by MatLab. Fig. 3 and 4 describes Simulation Diagram of Partial Power Converter and of PV- Partial Power Converter. Three PV

modules (PV1, PV2 and PV3) are connected. Owing to the stage that is added, the global conduction, switching and magnetic losses see an increase. Hence, the efficacy found in two-stage configurations is lesser in comparison with single-stage configurations. Also, the overall power that is generated by the system is dealt with by the converter that also minimizes the conversion efficacy. With the aim of overcoming the lesser efficiency, few authors have introduced various solutions depending on interleaved connections.

Figure 5: Simulation Diagram of PV based Partial Power Converter with Control Structure for Grid Connected System

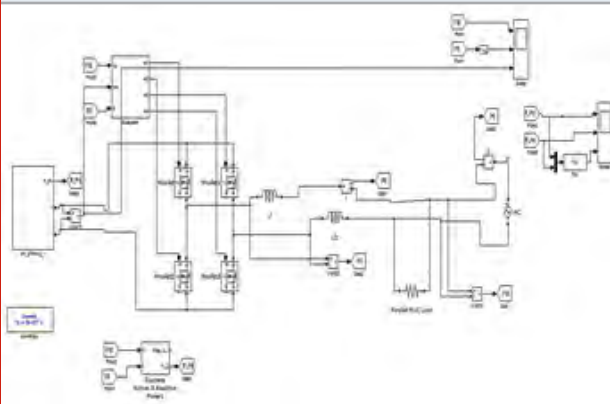


Figure 6: Simulation Diagram of Control Loop Structure (Fuzzy Logic Control)

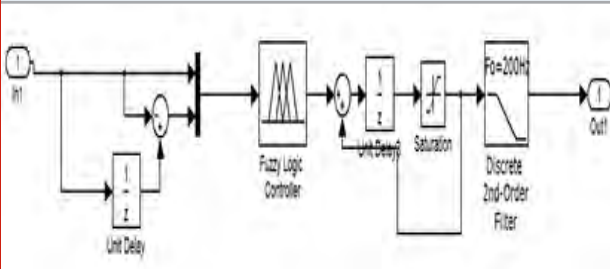
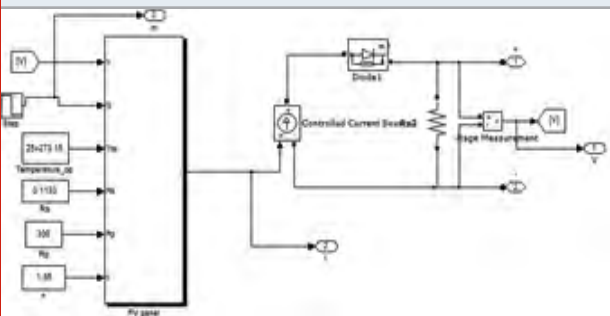


Figure 7: PV Panel Step Input



The fig. 5 shows the simulation Diagram of PV based Partial Power Converter with Control Structure for Grid Connected System. The method of partial power processing, where just a fraction of the overall power

is necessary for elevating the input voltage, can considerably decrease the converter size and power loss. Simulation Diagram of Control Loop Structure (Fuzzy Logic Control) and PV Panel Step Input is shown in fig. 6 and 7.

5. Output and Results: With the aim of comparing the performance of the newly introduced configuration, a simulation of a partial power converter is done for the same operating point. Fig. 8 and 9 shows the Output Current and Voltage Waveform of PV1-PPC and PV2-PPC. The converter operates at the same parameters, except the voltage and current sizing for the semiconductors and the power ratings, such that they get optimized for attaining their maximum efficacies. It is observed that the partial power converter not just offers a better efficacy, but the needs for the semiconductors are also less.

Figure 8: Output Current and Voltage waveform of PV1 – PPC

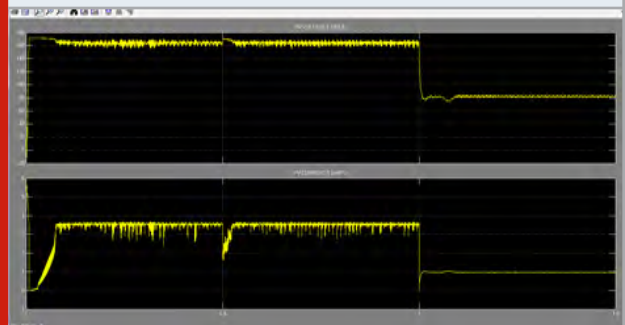


Figure 9: Output Current and Voltage waveform of PV2 – PPC

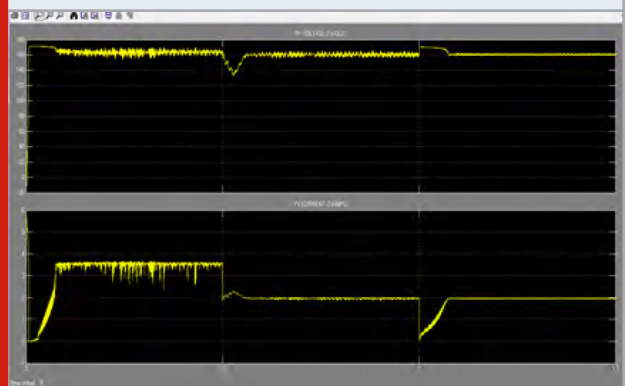
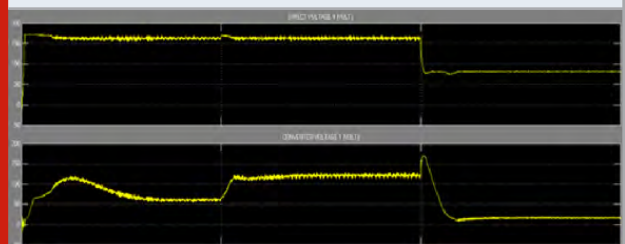


Figure 10: Output voltage waveform of Direct1 and Converter1

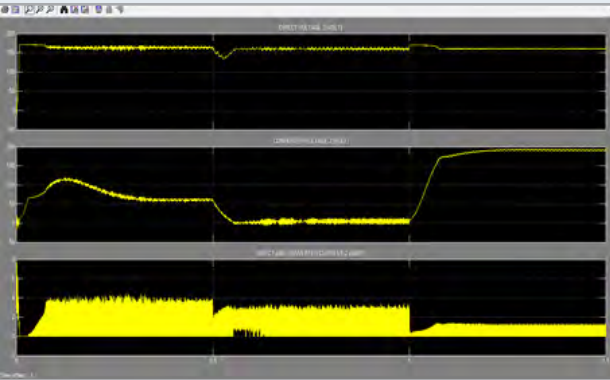


This aspect may result in an increased reliability of the grid system along with good efficiency and less losses. Figure 10 and 11 describes Output voltage waveform of Direct1 and Converter1 and Output current waveform of Direct1 and Converter1. Output voltage and current waveform of Direct 2 and Converter 2 (PI Controller) is shown in fig. 12.

Figure 11: Output current waveform of Direct1 and Converter1



Figure 12: Output voltage and current waveform of Direct 2 and Converter 2 (PI Controller)



The overall system performance increases in comparison with the available partial power converter with PI controller (PPC-PI) and also the new system (PPC-FLC) attains greater conversion efficiencies in comparison with the PPC-PI configuration (power stability, Peak overshoot, Undershoot and settling time). Fig. 13 and 14 illustrates the Output power waveform of PV 1 and 2 Power (PI Controller) Output power waveform of Direct Power from PV 1 and 2 to Inverter (PI Controller).

Figure 13: Output power waveform of PV 1 and 2 Power (PI Controller)

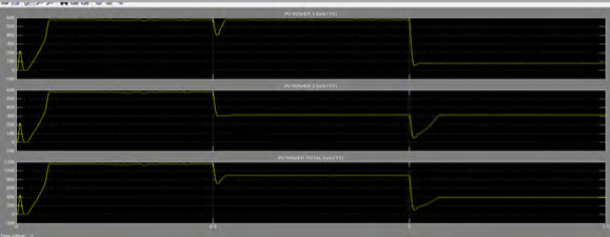


Figure 14: Output power waveform of Direct Power from PV 1 and 2 to Inverter (PI Controller)

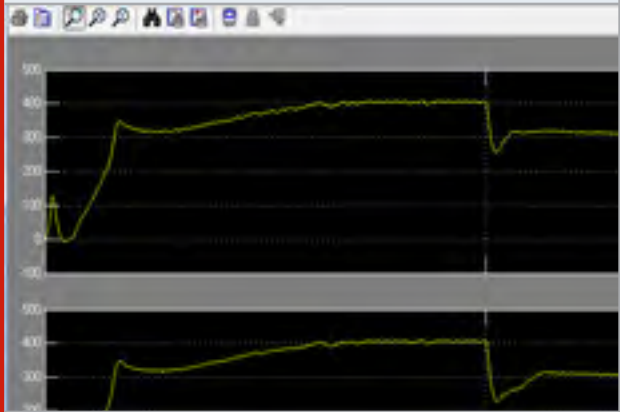


Figure 15: Output power waveform of Converter Power from PPC 1 & 2 to Inverter (PI Controller)

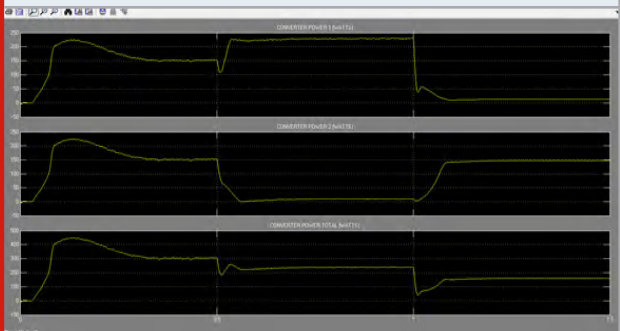


Figure 16: Output voltage and current waveform of Inverter and DC Bus Voltage (PI Controller)

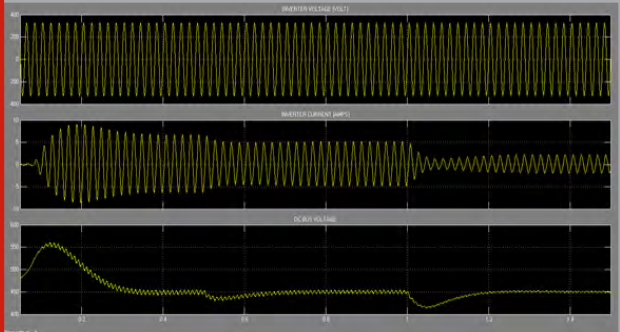
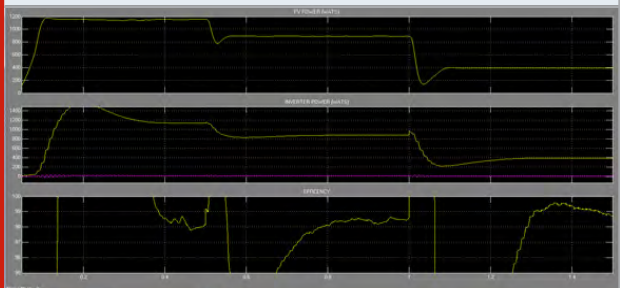


Figure 17: Output Waveform of PV/ Inverter Power and Efficiency (FLC Controller)



Output power waveform of Converter Power from PPC 1 & 2 to Inverter (PI Controller) and Output voltage and current waveform of Inverter and DC Bus Voltage (PI Controller) shown in fig. 15 and 16. From the graphs we analyzed the maximum peak overshoot, undershoot and settling time parameters. Output Waveform of PV/ Inverter Power and Efficacy (FLC Controller) is shown in fig. 17. When using PPC-FLC system there is no peak overshoot and undershoot occurred as well as settling time of the system is also quick when compared to existing system (PPC-PI).

CONCLUSION

A simple, high efficient dc/dc boost converter with MPPT control using Perturb and Observe algorithm along with Fuzzy logic control (FLC) desirable for medium to large scale PV systems is introduced. Higher efficiency of the converter is accomplished through partial power processing also through the collaborative operation of the converter along with fuzzy logic control (FLC)-current control loop structure. In addition, the overall efficiency of the plant was observed to be increased by using MPPT. The reliability was found to increase by the design of the newly introduced converter. The simulation of converter proposed was done for testing the performance parameters inclusive of the efficiency, reliability, switching operation, MPPT performance and simultaneous operation. From the results, it can be concluded that for partial shading condition fuzzy logic base MPP algorithm gives better response compared to PI controller. Fuzzy Logic base MPPT algorithm only dependent on the information and knowledge of the model at various atmospheric. As for partial shading condition, the local MPPT differs from global MPPT. In PI controller as the duty cycle is already decided at the peak of some MPPT, under such situation it cannot track the global MPPT, which differs from local MPPT. The variation of duty cycle is also less in case of fuzzy logic base MPPT algorithm. It helps to minimize the oscillations of output power of the converter.

The results of simulation indicate that performance and satisfaction of the work goals are achieved. At last, the overall system performance increases in comparison with the available partial power converter with PI controller (PPC-PI) and also the new system attains greater conversion efficiencies in comparison with the PPC-PI configuration (power stability, Peak overshoot, Undershoot and settling time).

REFERENCES

- Abdullah M Noman Khaled E Addoweesh, Hussein M Mashaly (2012) A Fuzzy Logic Control Method for MPPT of PV Systems IEEE Industrial Electronics Society.
- Alajmi, K H Ahmed S J Finney B W Williams (2013) A Maximum Power Point Tracking Technique for Partially Shaded Photovoltaic Systems in Microgrids IEEE transactions on industrial electronics vol 60 no 4.
- Bidram A Davoudi R S Balog (2012) Control and Circuit Techniques to Mitigate Partial Shading Effects in Photovoltaic Arrays IEEE journal of photovoltaics vol 2 no 4.
- Bidram A Davoudi and R S Balog (2012) Control and circuit techniques to mitigate partial shading effects in photovoltaic arrays IEEE J Photovolt vol 2 no 4 Pages 532-546.
- Bounechba, A. Bouzid, K. Nabti and H. Benalla (2014) Comparison of perturb & observe and fuzzy logic in maximum power point tracker for PV systems Science Direct Elsevier Energy Procedia 50 Pages 677 - 684.
- Chen S Tian Y Cheng L Bai (2014) An Improved MPPT Controller for Photovoltaic System Under Partial Shading Condition IEEE Transactions on Sustainable Energy vol 5 no 3.
- Choudhury P K Rout (2015) Comparative Study of M-FIS FLC and Modified P&O MPPT Techniques under Partial Shading and Variable Load condition IEEE India Conference.
- Choudhury P K Rout (2015) Adaptive Fuzzy Logic Based MPPT Control for PV System under Partial Shading Condition International Journal Of Renewable Energy Research, vol 5 no 4.
- El-Helw A Magdy M I Marei (2017) A Hybrid Maximum Power Point Tracking Technique for Partially Shaded Photovoltaic Arrays IEEE Access vol 5Pages 1900-11908.
- Esram and P L Chapman (2007) Comparison of photovoltaic array maximum power point tracking techniques IEEE Trans. Energy Conv vol 22 no 2 Pages 439 - 449.
- Jiang, D R Nayanisiri D L Maskell and D M Vilathgamuwa (2015) A hybrid maximum power point tracking for partially shaded photovoltaic systems in the tropics Renew. Energy vol. 76 Pages 53-65.
- Mahamudul M Saad M I Henk (2013) Photovoltaic System Modeling with Fuzzy Logic Based Maximum Power Point Tracking Algorithm International Journal of Photo energy.
- Nabil Karami, Nazih Moubayed, Rachid Outbib (2017) General review and classification of different MPPT Techniques Elsevier Renewable and Sustainable Energy Reviews 68 Pages 1-18.
- Patcharaprakiti S Premrudeepreechacharn and Y Sriuthaisiriwong (2005) Maximum power point tracking using adaptive fuzzy logic control for grid-connected photovoltaic system Renew. Energy, vol 30 no 11 Pages 1771-1788.
- Sha, R Chudamani,(2012) A Novel Algorithm for Global Peak Power Point Tracking in Partially Shaded Grid Connected PV System IEEE International Conference on Power and Energy.
- Shah, C. Rajagopalan (2016) Experimental evaluation

of a partially shaded photovoltaic system with a fuzzy logic-based peak power tracking control strategy IET Renewable Power Generation vol 10 no1.

Shiqing Tang Yize Sun Yujie Chen Yiman Zhao Yunhu Yang and Warren Szeto (2017) An Enhanced MPPT Method Combining Fractional Order and Fuzzy Logic Control IEEE Journal of Photovoltaics Pages 2156-3381.

Srivalli, D. Venkatesh (2017) A Global MPPT and Fuzzy Controller for Photovoltaic System under Partial Shading Condition International Journal of Advanced Technology And Innovative Research vol. 09 no 07.

Tawfik Radjai Lazhar Rahmani Saad Mekhilef Jean

Paul Gaubert (2014) Implementation of a modified incremental conductance MPPT algorithm with direct control based on a fuzzy duty cycle change estimator using dSPACE Science Direct, Elsevier Solar Energy 110 Pages 325-337.

Vaishnavi P Deshpande Sanjay B Bodkhe (2016) Analysis of Various Connection Configuration of Photovoltaic Module Under Different shading conditions International Journal of Applied Engineering Research vol 12 no 16.

Villalva J R Gazoli and E R Filho (2009) Comprehensive approach to modeling and simulation of photovoltaic arrays IEEE Trans Power Electron vol. 24no 5 pp 1198-1208

Enhancing Security Using 3-Kae Algorithm In Wireless Sensor Networks

R.Balamurali^{1*}, S. Rajesh Kannan², R Thalapathi Rajasekaran³ and R. Ramesh⁴

¹Department of ECE, Chennai Institute of Technology, Chennai, Tamilnadu, India.

^{2,3,4}Department of CSE, Chennai Institute of Technology, Chennai, Tamilnadu India.

ABSTRACT

Creation of a network environment for Wireless Sensor Network is much related to conventional networks. Security requirements that contain the parameters such as confidentiality, integrity, availability and authenticity play an important role in the study of security for WSN. Not all security solutions considered for conventional networks can be applied directly to WSN because of its few said limitations like, energy and battery power. Moreover, the belief was that the Public Key Cryptography (Asymmetric Encryption) is not well- suited for WSN because of its above said constraints, but later through studies of encryption algorithms, researchers have found that algorithms based on curves i.e Elliptic Curve Cryptography (ECC) was one of the feasible technique to be applied for such energy constrained devices.

INTRODUCTION

Wireless Sensor Networks possesses a large number of sensor nodes organized solidly in a closed environment to collect data for some specific function based on requirements. Sensor devices are enabled with limited memory capacity, computational ability, and limited transmission power. The sensors are mostly pre-programmed to sense and collect the data and forward it to the base station through defined communication channel (Abdur Rahaman Sardar et al, 2015). If the information sensed seems to be sensitive, the sensor nodes and communication channel should also be trust worthy. The Sensor Network also holds the self-organizing ability, if the positions of nodes are not

prearranged. Each node must trust the succeeding node, irrespective of its topology, and if any node is found to be mistrustful, the resultant node should be capable of taking alternative path to reach the destination (Adnan Ahmed et al, 2016).

Sensor Networks are vulnerable to many sort of attacks (attacks at various layers of Sensor Network is well explained in introduction part). All these attacks are said to be internal attacks i.e nodes either act malicious or performs some malfunction like, not forwarding packets or selectively forwarding packets in order to save its energy (Ahmad Abed et al, 2012). But all these sorts of attacks can be addressed by identifying the node as malicious and not performing any further communication via that particular node or by taking some preventive measures by avoiding those nodes from carrying sensitive data (Akyildiz et al, 2007). Such internal attacks on these small tiny devices are performed based on the deployed region of these nodes. Nodes deployed non-manually cannot be replaced at any cost, and such nodes on dissipation of its energy will enter in to die state. Unnecessary depletion

ARTICLE INFORMATION

*Corresponding Author: balamurali@citchennai.net
Received 15th April 2020 Accepted after revision 20th May 2020
Print ISSN: 0974-6455 Online ISSN: 2321-4007 CODEN: BBRBCA

Thomson Reuters ISI Web of Science Clarivate Analytics USA and Crossref Indexed Journal



NAAS Journal Score 2020 (4.31) SJIF: 2020 (7.728)
A Society of Science and Nature Publication,
Bhopal India 2020. All rights reserved.
Online Contents Available at: <http://www.bbrc.in/>

of energy caused based on attacks between nodes will also make a node die.

One such possible attack on WSNs is called node capture by tampering the data from node where an opponent takes full control over nodes through undeviating physical access. Many newer security mechanisms for WSNs focus on other sorts of network attacks and do not take node capture into account. It is usually assumed that physically having access to nodes and tampering data is “easy” and will not make much harm to the network system (Akyildiz et al,2002). But over a 100 x 100m field, deployment of sensor nodes may fall over a Vulnerable Region or so called border region nodes. Here Vulnerable Region is said for nodes which may fall both under the coverage area of specified network as well as outside the network (Akyildiz et al,2002).

When nodes under Vulnerable Region or border region have a physical access to an opponent, it may cause a serious damage to the other nodes which fall in the secure region (nodes that are within the required coverage area) thus resulting in decrease of throughput and degrading the overall performance of the network both at the transmission end and the receiver end(Aliouat, Z et al,2012). The proposed work carried out in this thesis mainly focuses on the physical access to nodes and provides a prevention mechanism to overcome such attack thus showing the performance analysis of the designed algorithm. However, to the best, no solution has been found for such attack in Wireless Sensor Network.

The next step is to calculate the distance between the destination nodes by using Euclidean distance. Let d be the distance between nodes A and B. Let the coordinates of nodes A and B be (x_1, y_1) and (x_2, y_2) . Then the Euclidean distance between node A and B is given by,

$$d = \sqrt{(x_2 - x_1)^2 + (y_2 - y_1)^2}$$

The same distance calculation is done for all one hop neighbours in the network. The destination index of all nodes is compared with the current destination index stored in source node. If it is found to be equal then the communication flag (comm_flag) is set to true. Finally, communication over secure region to secure region begins by different key generating algorithms that are given below.

Duty Key and Public Key Generation Algorithm

input : Keyval, Sourceid, CHid output : Keytr , KeyDuty

$N = \text{Size}(\text{Keyval})$

calculate euclidean distance $d = || \text{Sid} - \text{CHid} ||$ if d is in secure region // Public Key Generation

temp.key <- Create a random key of size $N-1$ gen.diag.matrix[$N-1$ $N-1$] = [temp.key]

find : det = det(diag.matrix)

Pukey = det * temp.key else // Duty Key Generation

temp.dkey <- Create a random key of size N gen.diag.

matrix[N N] = [temp.key]

find : det1 = det[(diag.matrix)*(dia.matrix)]

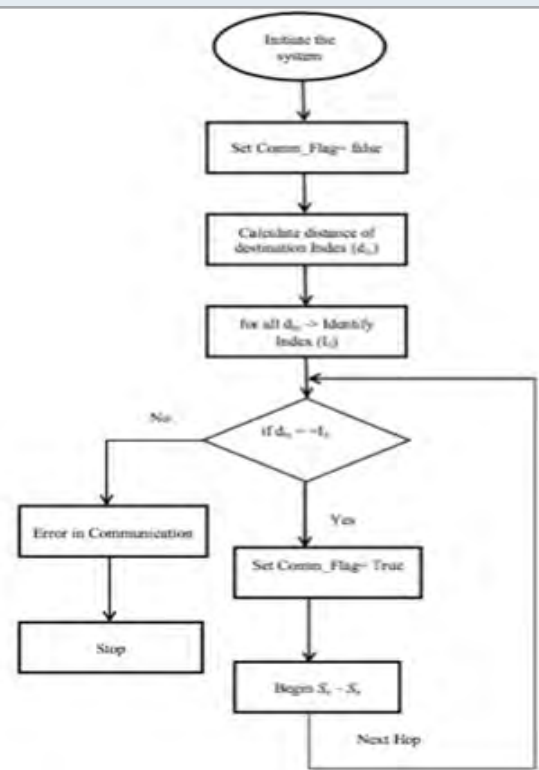
KeyDuty = det1 * temp.dkey

find : det2 = det[(diag.matrix)-1*(dia.matrix)]

Keybackduty = det2 * temp.dkey endif

The proposed model consists for five different types of keys, but the use of too many keys also lead to more overhead at the node level. Therefore, in order to reduce the complexity, dk is generated only if the communicating node falls in the Vulnerable Region. To say clearly, nodes that fall in secure regions communicate with Public Key (pk). As a first step, distance between source node and destination node is calculated using Euclidean distance as the location coordinates are stored by network manager and it is broadcasted to all nodes. However, all nodes know the location of all other nodes for security reason; all nodes will also know the location of Vulnerable Region node too which is initially broadcasted to all nodes by NM. Here, (Alper Bereketi et al,2009) Vulnerable Region node is also said to be secure node and communication take place similar to other secure region nodes until they are compromised. After calculating the distance d , if d falls in the secure region, a random value N of 64 bits is generated (Amir Sepasi Zahmati et al,2007). The values are stored in one dimensional array and stored in a temporary variable. A two-dimensional array of matrix is generated and the values are placed diagonally where the other places of matrix is replaced with 0 in order to reduce complexity. Determinant of diagonal matrix is computed and multiplied with the respective stored temporary key.

Figure 1



Performance Evaluation: nodes and the values are recorded by slowly inserting the malicious nodes by the count of

Table 1. Simulation Parameters

Parameters	Description
No of Nodes	100
Area size	100 x 100
Packet size	512 bits
Key size	64 bits
MAC	IEEE 802.15.4
Traffic Source	CBR
Energy Level	0.5nJ
Malicious nodes	0 to 10
Simulation Time	100 secs

SIMULATION RESULTS

Algorithm Comparison: The proposed algorithm is compared with both symmetric and asymmetric techniques as shown in graph 1, and the corresponding values are stored in the table 1. The proposed model takes 512 bits of data and 64 bits of key size. The other traditional algorithms shown in the graph are also of 512 bits of data but vary in their key size (Dhanagopal, R et al, 2019) The time taken for the algorithm execution is compared with the proposed algorithm running time and it is found that the proposed algorithm value seem to be less when compared to other algorithms. The algorithm comparison shown in graph 4.5 (b) shows a slight variation between ECC and the proposed 3-KAE. Elliptic curve is found to be better than RSA, both during encryption and decryption. Key length of RSA is greater than ECC because, ECC key size is reduced during the encryption process. Likewise, decryption of RSA takes more time than ECC, only because of factoring of large numbers. Three types of attack are possible on RSA, (i) timing attack, (ii) Mathematical attack and (iii) brute force attack. Likewise elliptic curves uses discrete logarithm for locating by varying its key size to 112 bits or 109bits with respect to its applications which is possible by mathematical attack and quantum computing attacks.

Table 2

Key bits in size	Sipke Jack (64)	RC5 (64)	AES (128)	Spritz (64)	Proposed 3-KAE (64)
Encryption	1.15	1.89	1.78	0.85	0.82
Decryption	1.25	2.02	1.95	1.95	1.2

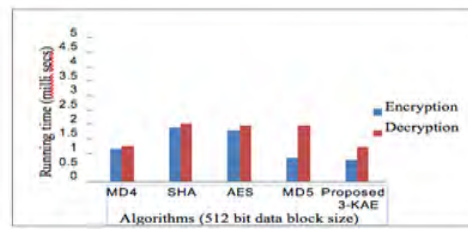


Figure 1 Running Time comparison of Symmetric algorithms with Proposed 3-KAE

An algorithm is said to be good only based on the running time and how long it take for a key to get compromised. In that case, the existing algorithms like RSA and ECC are vulnerable to attack moreover such traditional algorithms are not well suited for sensor applications too. The proposed model is found to be performing well both in case of running time and time taken for compromising the key. The time taken for compromising the key is large compared to other cryptographic techniques, thus proving that 3-KAE is well suited for sensor applications.

Table 2 Algorithm comparison with proposed model

Key bits in size / Running Time(ms)	RSA	ECC	Proposed 3-KAE
Encryption	2.35	1.45	1.3
Decryption	4.32	2.35	1.98

Figure 2

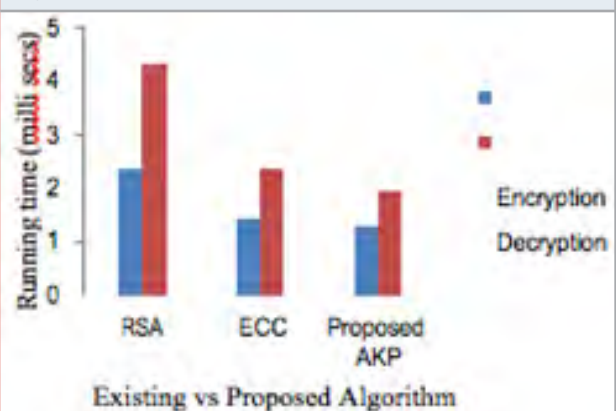
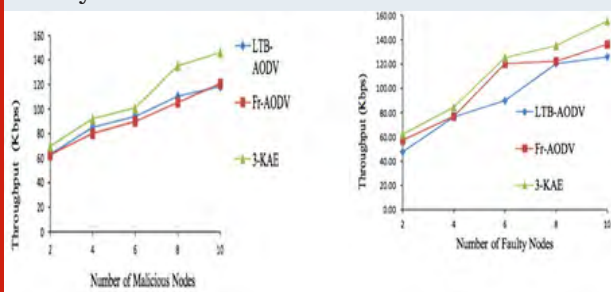


Figure 3: Network vs malicious node (b) Network vs Faculty node



CONCLUSION

Recent trends of using internet application globally leads to a major threat to secure communication. So it is passion to say that, stronger the algorithm stronger will be the security to the data. Moreover, when working with WSN, the nodes are mainly inclined to node capture or physical access attack, because of random deployment of nodes mainly in tall buildings, public places etc. Once an adversary takes control through physical access to these small tiny devices, the node becomes vulnerable and the launching of various types of attacks by the adversary are conceivable leading to improper functioning of the whole network. The aim of the antagonist is to take away the secret keying materials and tries to attack the algorithm involved. This happens by taking control over the node and producing a huge number of replicas by sharing the details of compromised node to all the other nodes in the network. Moreover, not noticing this type of attack on a node will lead to algorithm failure, data leakage and malfunctioning of whole network.

Internally it also leads to decrease of network lifetime and efficiency. Security parameters like integrity and confidentiality will fail due to this unattended nature. However, such type of physical node capturing attack is possible only with static sensors and not applicable to mobile devices. The proposed Three Keying architecture model using Asymmetric Encryption (3-KAE) provides a solution to this type of physical access or node capture attack by first dividing the region into secure and vulnerable, based on the location parameters and the area where sensors are deployed. Separate key mechanism is used between secure region -to- secure region and another keying mechanism is used over Vulnerable Region. The proposed 3-KAE algorithm gives a solution to betterment of prevention from such sort of attacks in sensor enabled devices.

Over the decades, the constraints in Sensor Networks revolve around power consumption and memory utilization. Due to these limitations, nodes are vulnerable and an attack can affect the network usage to some extent (sometimes it may affect the whole system). Hence, providing security measures for WSN becomes more important. Though the proposed model of physical access is found to be best against performance of existing models, security parameters are not completely met.

When secured communication is preferred as a major requirement with in sensor devices, authentication over Vulnerable Region is yet another important role to be inculcated in sensor nodes. Moreover, these devices are cheap without any physical protection i.e still no trusted platform is incorporated on such devices. Trust management system helps in decision making process in the network. It helps the members in the network to find the misbehaving nodes and thereby disconnects them from the network. The trust level of a node is estimated based on the lifetime of a sensor node, communication ratio and consistency level, therefore Vulnerable Region nodes are closely monitored.

REFERENCES

- Abdur Rahaman Sardar Jamuna Kanta Sing & Subir Kumar Sarkar (2015) An Attack Monitoring Framework Design for Clustered WSN using OMNet++ International Journal of Electronics Communication and Computer Engineering vol 6 no 5 Pages 5-7.
- Adnan Ahmed Kamalrulnizam Abu Bakar Muhammad Ibrahim Channa & Abdul Waheed Khan (2016) A Secure Routing Protocol with Trust and Energy Awareness for Wireless Sensor Network Mobile Network and Applications Springer vol 22 no 2 Pages 272-285.
- Ahmad Abed Alhameed Alkhatib & Gurvinder Singh Baicher (2012) Wireless Sensor Network Architecture International Conference on Computer Networks and Communication Systems vol 35 Pages 11-15.
- Akyildiz IF Melodia T & Chowdhury K (2007) A Survey on Wireless Multimedia Sensor Networks Computer Networks vol 51.
- Akyildiz IF Su W Sankarasubramaniam Y & Cayirci E (2002) Wireless Sensor Networks: a survey Computer Networks vol 38 no 4 Pages 393-422.
- Akyildiz IF Weilian S Sankarasubramaniam Y & Cayirci E (2002) A survey on Sensor Networks IEEE Communications Magazine vol 40 no 8 pp 102-114.
- Aliouat Z & Aliouat M (2012) Effective Energy Management in Routing Protocol for Wireless Sensor Networks in NTMS.
- Alper Bereketli & Ozgur B Akan (2009) Event-to-Sink Directed Clustering in Wireless Sensor Networks IEEE Communications Magazine vol 40 no 8 Pages 398-403.
- Amir Sepasi Zahmati Bahman Abolhassani Ali Asghar Beheshti Shirazi & Ali Shojaee Bakhtiari (2007) An Energy Efficient Protocol with Static Clustering for Wireless Sensor Networks International Journal of Electronics Circuits and Systems vol 1 no2.
- Amis A Prakash R Vuong T & Huynh D (2000) Max-Min D- Cluster Formation in Wireless Ad Hoc Networks IEEE proceedings vol 75 no 1 Pages 156-167.
- Anastasia G Contib M Francescoa MD & Passarella

A (2008) Energy conservation in Wireless Sensor Networks: A survey Ad Hoc Networks vol 7 no 3 pp 537-568.

Anis Koubaa Mário Alves & Eduardo Tovar (2005) Lower Protocol Layers for Wireless Sensor Networks: A Survey

IPPHURRAY Technical Report Pages 1-14.

Dhanagopal R Muthukumar B(2019) A Model for Low Power High Speed and Energy Efficient Early Landslide Detection System Using IoT Wireless Pers Commun.

Development of Industrial Monitoring System Based on Embedded HTTP Host Using Raspberry Pi

S.Bhuvaneshwari^{1*}, R. Raghuraman², T. Thandapani³ and A. Sivabalan⁴

^{1,3,4}Department of ECE, Chennai Institute of Technology, Chennai, Tamilnadu India

²Department of EEE, Chennai Institute of Technology, Chennai, Tamilnadu India

ABSTRACT

The industry for embedded systems is expected to grow rapidly and it drive the continuous development of Internet of Things. The cognitive embedded system will be the major impact of latest trends such as reduced energy consumption, improved security for embedded devices and visualization tools with real time data. The impact of embedded systems is further improved by connecting it with internet. In this project, we developed a Embedded HTTP Host for Industrial monitoring purpose. Parameters like temperature and humidity, gas are captured lively and stored in the web server. The captured values in stored in inbuilt storage and uploaded via internet and it can be accessed via HTTP URL using the web browser. Clients can track and manage the performance of all the industrial machines remotely via local browser.

KEY WORDS: RASPBERRY PI 4, ETHERNET, LAN, HTTP, RIDE7.

INTRODUCTION

An Embedded system is an integrated microprocessor-based computer hardware system with dedicated function within a larger mechanical or electrical system. It can work as an individual system or as a part of a large system. It is an integrated circuit which includes hardware and mechanical parts are specifically designed to perform complex real time tasks(Aiping Tan et al,2019). The complexity of an embedded system varies significantly depending on the tasks that need to be performed. Nowadays it controls many devices in common. Demand will be huge when embedded devices are connected with

internet to enable the remote accessing capability of the I/O devices.

In existing setup, ATmega32A 8 bit AVR microcontroller, Zigbee Pro module and Ethernet module are used for monitoring network. An Industrial Ethernet Module is setup using an Alter Cyclone III FPGA processor (Chetna Singhal et al, 2020).It is responsible for processing the EtherNet/IP protocol and to transfer the data to the host interface. There were certain performance drawbacks existing in this when comparing Atmega controller with the latest Raspberry Pi 4 board.

The paper includes an architecture and development of a HTTP Web Host using Raspberry Pi 4 board. Ethernet interface is linked to system using STARTECH C6ASPAT10 cable. STM32WLE5 Microcontroller will be managing the sensors to capture Temperature, humidity, Gas, pressure, motion, and speed parameters. Parameters captured would be useful for different kind of industrial

ARTICLE INFORMATION

*Corresponding Author: sbhuvaneshwari@citchennai.net
Received 15th April 2020 Accepted after revision 20th May 2020
Print ISSN: 0974-6455 Online ISSN: 2321-4007 CODEN: BBRCBA

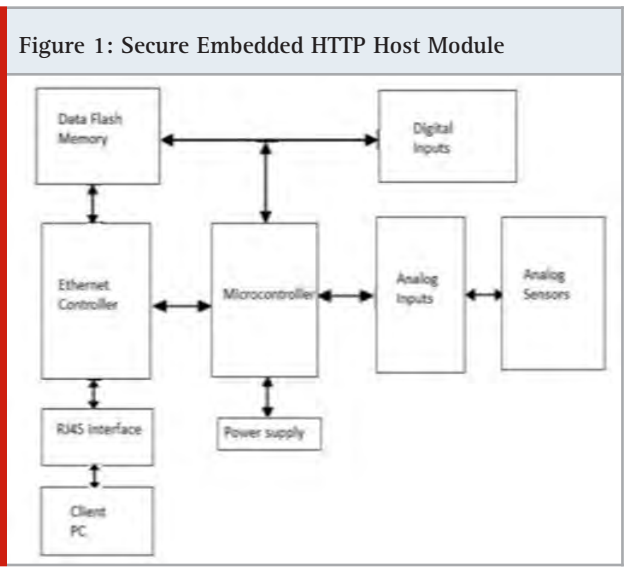
Thomson Reuters ISI Web of Science Clarivate Analytics USA and Crossref Indexed Journal



NAAS Journal Score 2020 (4.31) SJIF: 2020 (7.728)
A Society of Science and Nature Publication,
Bhopal India 2020. All rights reserved.
Online Contents Available at: <http://www.bbrc.in/>

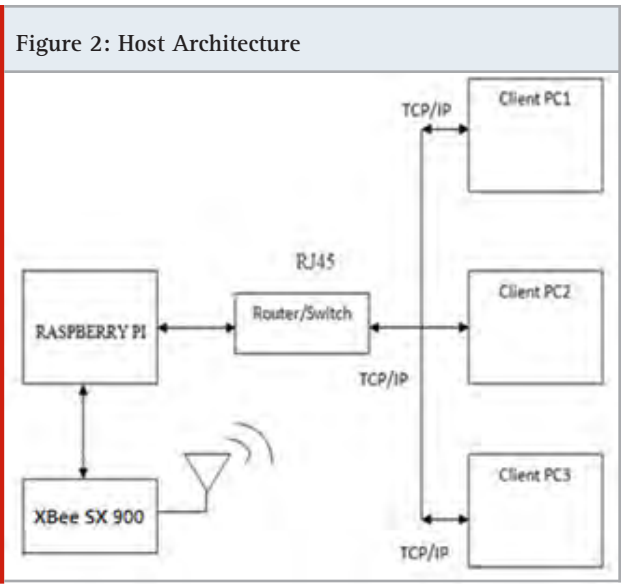
sectors. In our project embedded systems are integrated with Internet technology to create an Embedded web Technology system which is emerging recently(Clive Seguna et al, 2019) .The medium of communication used in our project is Transmission Control Protocol/Internet protocol. Network Communications are performed as per IEEE 802.3 Ethernet standard and it is an emerging technology of Embedded systems. ARM based Embedded HTTP Host running on Raspberry Pi 4 is capable of faster execution and latest Ethernet standard can make internet performance faster(Elizabeth Kadiyala et al , 2017). This developed system is apt for optimizing industrial sectors very secure by remotely monitoring various industrial applications without direct access.

Embedded Http Host: Embedded HTTP Host is used to implement a embedded internet technology. It process on embedded system with high performance computational configuration to perform remotely including passive and active information about the connected system to the end user. It is possible to integrate different electrical devices to web Host to enable real time tracking and to control the electrical equipments remotely without any restriction via website released by embedded HTTP Host(Iqra Qasim et al,2020). It is developed using an embedded processor connected with Ethernet networking standard. The embedded host made of ARM processor with inbuilt Ethernet controller. End user system will be connected to the Ethernet controller via STARTECH C6ASPAT10 interface.TPC packets are used to send and receive data from arm processor.



The end user can access the Host using the assigned IP. End users have local area network connectivity that transfer the required info to the router that processes and search for the system which is configured with assigned IP address(Jorge F et al,2020). Secure session will be established with corresponding host using TRANSMISSION CONTROL PROTOCOL/INTERNET PROTOCOL. Once session established, end user can able to monitor and control the devices remotely.

System Description: The overall setup of Industrial monitoring system has individual architecture setup for sensor and server as follows. Sensor architecture model consists of STM32WLE5 MC and XBee SX 900. Host architecture model consists of Raspberry Pi 4 with inbuilt Ethernet connectivity and DigiXBee SX900(Mauricio David Perez et al,2020) . Industrial system is monitored via Graphical user interface module on PC. Fig 2&t3 depicts the architecture of sensor and host.



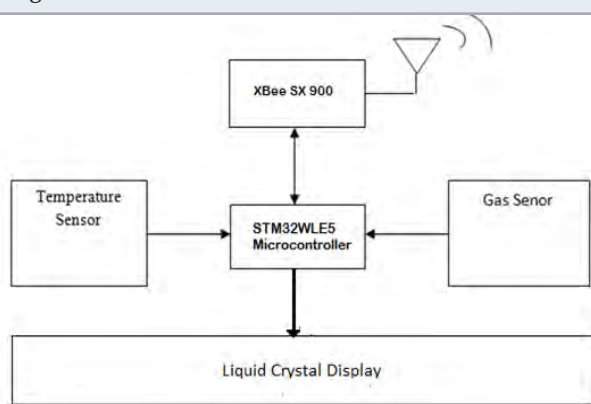
In sensor architecture model, multiple sensors nodes are developed to capture the various performance parameters of industrial equipments. i.e. temperature humidity and gas respectively. STM32WLE5 MC is used to integrate all the sensor units to collect the analog data from it(Pinjia Zhang et al,2020). The collected data will be digitalized using PCF8591 Analog to Digital converter and gets the digitalized information via I2C bus. It transmits the digitalized information to the Host node via wireless technology. Also inbuilt 10 bit ADC converts the analog data from sensors and converts it into digital data to display in LCD screen. GUI on PC will display the captured values which are transmitted to it(Phanumat Saatwong et al,2020). GUI can be accessed using the defined IP address in the any of the web browser. IP's are secured using login credentials. Once user accesses the IP via local browser, it will prompt for user credentials. User have to login with proper credentials to view the monitored parameters.

System Design: The system design consists of various hardware's and software's. Hardware kit includes Raspberry Pi 4, GROVE-AHT20 I2C, MQ-6, STM32WLE5 MC and XBee SX 900 connector.

Raspberry Pi 4: Raspberry Pi 4 development kit is shown in fig 4. It is a tiny pocket computer with dual display. It is invented by Raspberry Pi Foundation[4]. The performance speed is increased in new Raspberry Pi 4 when comparing it with the earlier models. It has a Broadcom BCM2711, Quad core Cortex-A72 (ARM v8)

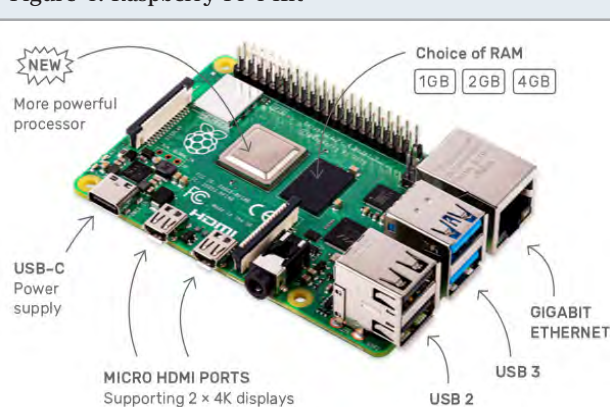
64-bit SoC clocks at 1.5GHz. It comes with GB Ethernet, along with onboard wireless networking and Bluetooth 5.0. SD cards are used for booting and persistent storage purpose since it does not have built in storage. It is an energy efficient model which runs silently and use less power when compare to other computers.

Figure 3: Sensor Module



Temperature and humidity Sensor - GROVE – AHT20 I2C: Grove AHT20 Temperature and Humidity sensor is based on AHT20, compared with Grove - Temperature & Humidity Sensor Pro (AM2302/DHT22), AHT20 is a new generation of temperature and humidity sensor embedded with a dual-row flat and no-lead SMD package. AHT20 is fabricated with a latest application-specific integrated circuit chip with an optimized Micro Electro Mechanical Systems semiconductor capacitive humidity sensor, and a latest on-chip temperature sensor. The output is I2C protocol with the Grove interface. The performance of AHT20 is more stable in harsh environments compared with the previous generation of temperature and humidity sensor, AHT20 is suitable in most industrial scenarios.

Figure 4: Raspberry Pi 4 Kit



MQ-6 Module: The MQ-6 module is a simple circuit which is used as a gas leakage detector device specifically fabricated for an industrial area. It has a high sensitivity to multiple gases. It can also be used to identify the

presence of alcohol, cooking fumes, and cigarette smoke. It gives out the concentration of the gases as a analog voltage equivalent value. It can be easily integrated with Raspberry Pi board and also it respond very quickly. To make it work, the heater coil should be powered with 5V and load resistance must be added. The output of MQ-6 should be connected with an ADC to obtain the digital value.

Microcontroller-STM32WLE5: STM32WLE5 microcontroller is one of the Ultra-low powered multi-modulated with wireless technology. It has an Arm Cortex - M4 core processor clocks at 48 MHz. It is optimized for Low-Power Wide Area Networks. It consists of various communication features including 43 GPIOs, integrated switched-mode power supply and multiple low-power modes to maximize battery life. It includes embedded security hardware functions as well.

XBee SX 900: XBee SX 900 module has maximum power, security, and flexibility which can be used for complex network design. It includes powerful 1-Watt 900 MHz Digi XBee-PRO SX 900 and battery-optimized 20 mW Digi XBee SX 900 modules for critical designs. It uses DigiMesh networking topology to enable redundancy and reliability. It is made for secured and reliable data communications between multiple devices. Software part includes below mentioned software's.

Raspbian OS -Buster: It is one of Debian based distribution computer OS dedicated for Raspberry Pi processor. It includes several versions of OS such as Buster and Stretch. It is highly optimized for the Raspberry Pi line's low-performance ARM CPUs. We use Buster as an OS in our system.

RIDE7

Ride7 is software used for writing, compiling and debugging application code from a single user interface. It controls the Raisonance C/Assembler tool sets for various processors. It also can be used for Post-link code size optimization. It has high-level language debugging tools with views of symbols, locals, disassembly, registers, peripherals, etc. It have Syntax highlighting code editor and it make it user friendly.

Embedded C: Embedded C programming language is developed on top of C programming language dedicated to use in embedded systems. It uses the same syntax as the C programming language. It is used for limited resources like RAM and ROM. It is used for cross development and hardware dependent.

Putty: PUTTY is an open-source terminal which is used to load the code into the processor. It supports multiple network protocols such as SCP, SSH, Telnet and rlogin along with an xterm terminal emulator to transfer files.

Internet Protocol Suite: TCP/IP is a group of defined protocols managing interaction among all the systems over the internet[4]. Packaged information will be sent

and received to destination as per the definition. It is a combination of TCP and IP protocols. The Internet Protocol standard control the movement of packets sent out over networks and it route the packets where to go and how to get there. IP allows any computer on the Internet to forward a packet to another computer that's one or more intervals closer to the packet's recipient. The Transmission Control Protocol is responsible for ensuring the reliable transmission of data across various networks. In our project HTTP protocol is used for data transmissions between client and serve. An end user initiates a request to a host to view required information.

Code Compilation: The code developed for whole system is written in Embedded C language using RIDE7 application. First ADC unit script help to converts the analog data from sensor into digital data. Second is Universal Asynchronous Receiver/Transmitter module and it is used to transfer the data to system via RS232. Third is LCD unit, which is used to show the actual values received from the sensor. Its compiled using RIDE7 interface as mentioned in Fig 6. Fourth unit is to route the monitored data to the web page. Developed codes are compiled using Raspbian compiler. All the developed codes are loaded into Raspbery development kit by via Putty console. Web Host GUI provides an interface between web Host and program that generate the web content.

as Host. Collected data will be displayed in webpage GUI based on end user request.

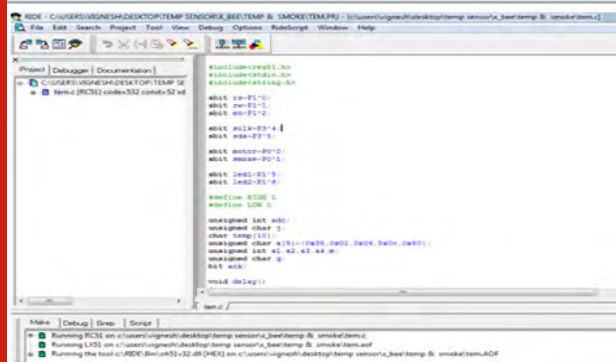
Figure 6: Remote Sensor Architecture



Figure 7: Embedded HTTP Host model

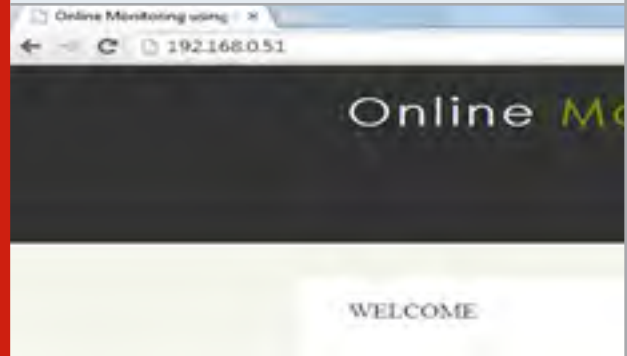


Figure 5: LCD Module Compilation Using Ride7



Hyper Text Transfer Protocol is utilized to communicate between Host and system browser. The HTML web page can be accessed using IP 192.168.0.51 on the system browser is shown. User need to login with user credentials to read the required information.

Figure 8: Embedded HTTP Host Login UI



RESULTS

The unit testing of individual components is done and developed the complete system by integrating it in the proper manner. The complete system was deployed in industrial environment and tested. Fig 7 and Fig 8 display how the setup was done to make it work.

The temperature, humidity and gas sensor sense the respective parameters of the deployed area and convert it into digital signal using ADC. Integrated MC is configured to read those respective values and store it. Data would be displayed in LCD by configuring the MC. XBEE SX 900 will transfer the data to RPI which is acting

It displays the information about the temperature, humidity and concentration of CO in the remote industrial location.

Figure 10: Embedded HTTP Host UI



CONCLUSION

Advanced monitoring system is implemented using Raspberry Pi4 with faster response which can be used day today life. It can also interact with any system through serial communication ports. It can be enabled in Private Network and also in Public Network. This system has been developed at low budget so maintenance made easier. In future we can integrate any number of Sensors based on requirement with this monitoring system. We tested it in industrial environment but we can also implement this system in hospital, home, etc., via Internet. This work can be further leveraged by deploying high end rack servers with wireless sensor networks and increased number for parameters using high end sensors for wide area management.

REFERENCES

Aiping Tan Shoubin Wang Ning Xin Yan Shi Yuhuai Peng (2019) A Multi-Channel Transmission Scheme in Green Internet of Things for Underground Mining Safety Warning.
Chetna Singhal A Rajesh (2020) Review on cross-layer

design for cognitive ad-hoc and sensor network IET Communications (Volume 14 Issue 6 41).

Clive Seguna Luke Tanti Jeremy Scerri Kris Scicluna (2019) A Low-Cost Real Time Monitoring System for an Industrial Mini-Climatic Chamber IECON - 45th Annual Conference of the IEEE Industrial Electronics Society.
Elizabeth Kadiyala Shravya Meda Revathi Basani S Muthulakshmi (2017) Global industrial process monitoring through IoT using Raspberry pi.
Israel Vieira Ferreira Jeferson André Bigheti Eduardo Paciencia Godoy (2019) Development of a Wireless Gateway for Industrial Internet of Things Applications IEEE Latin America Transactions (Volume 17 Issue 10 October).

Iqra Qasim Muhammad Waseem Anwar Farooque Azam Hanny Tufail Wasi Haider Butt Muhammad Nouman Zafar (2020) A Model-Driven Mobile HMI Framework (MMHF) for Industrial Control Systems.
Jorge F Schmidt Denis Chernov Christian Bettstetter (2020) Towards Industrial Ultra-Wideband Networks Experiments for Machine Vibration Monitoring.
Mauricio David Perez Seung Hee Jeong Sujith Raman Daniel Nowinski Zhigang Wu Syaiful MS Redzwan Jacob Velander Zhiwei Peng Klas Hjort Robin Augustine (2020) Head-compliant microstrip split ring resonator for non-invasive healing monitoring after craniostosis-based surgery Healthcare Technology Letters Volume 7 Issue 12.

Pinjia Zhang Yang Wu Hongdong Zhu (2020) Open ecosystem for future industrial Internet of things (IIoT) Architecture and application CSEE Journal of Power and Energy Systems Volume 6 Issue 1.

Phanumat Saatwong Surapong Suwankawin (2020) An Interoperable Building Energy Management System With IEEE1888 Open Protocol for Peak-Load Shaving.

Device Authentication for IoT Devices using ECC

Krithiga J^{1*}, Krishnan S², Sai Nithisha M², Jeevika Shree A³ and Lokeswari S⁴

^{1,3,4}Department of ECE, Chennai Institute of Technology, Chennai-600069, India.

Department of EEE, Chennai Institute of Technology, Chennai-600069, India.

ABSTRACT

IoT devices are a part of the larger concept using in different domains including health care, home automation, environmental monitoring and also being deployed in various public and private environments. IoT holds the key role in Automation and machine learning. Authentication is recognized as predominant task throughout the IoT, as the tens of millions of the users connect to internet and start sharing their information. In IoT locale authentication can be provided mainly between three categories, they are: IoT appliance – IoT appliance, IoT gateway–mobile client and IoT gateway – IoT appliance. In the Internet of Things environment for communication between two sensing devices we need a secure protocol. The purpose of this project is to provide a latitudinous outline of the security hazards. Here we addressed the authenticity operation between IoT gateway -IoT appliance. Over the laborious security analysis, the results signify that the propounded proposal come up with limited computational overheads together with hefty credentials privacy and key security capabilities in comparison to distinct similar schemes.

KEY WORDS: ECC, MUTUAL AUTHENTICATION, IOT, SECURITY.

INTRODUCTION

In a digital world through digital devices and digital networks, the most of the information is between users or systems immediately without involvement of human – computer interaction or person to person interaction (Goutham Reddy, A et al,2018). The Advanced technology such as IoT are reason behind the smart city which greatly

improves efficiency and user satisfaction(Boyko, V et al,2000; Chaturvedi, A et al,2012). Undoubtedly, rapid change of IoT has made a significant change in the economic and social growth of the society. As internet is an unrestricted construction, it also has few faults through which wire tappers perform various cyber-threats over communicated messages. There are high chances for hacking as every device shares their data through online. With the help of cryptographic techniques, we can restrain those attacks

Cryptography is the primary building block of network security and study of designing the techniques for secrecy, securing data and communications through the use of codes(Chen, C et al,2012). ECC is one type of cryptography which uses public key cryptography. Cryptography

ARTICLE INFORMATION

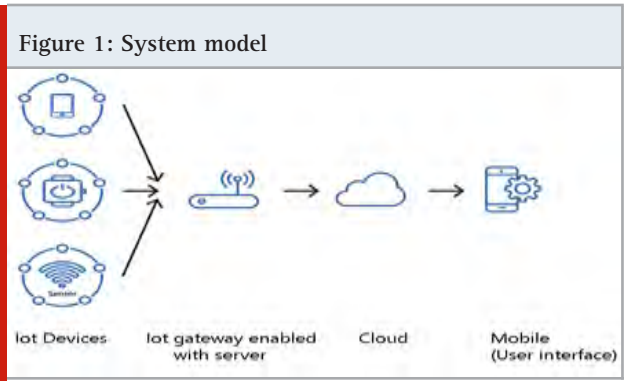
*Corresponding Author: krithigaj@citchennai.net
Received 15th April 2020 Accepted after revision 20th May 2020
Print ISSN: 0974-6455 Online ISSN: 2321-4007 CODEN: BBRCBA

Thomson Reuters ISI Web of Science Clarivate Analytics USA and Crossref Indexed Journal



NAAS Journal Score 2020 (4.31) SJIF: 2020 (7.728)
A Society of Science and Nature Publication,
Bhopal India 2020. All rights reserved.
Online Contents Available at: <http://www.bbrc.in/>

encrypt plaintext into cipher text and then decrypt back into plaintext. The latest encryption method, the Elliptic curve cryptography algorithm provides vigorous security. ECC defines both the public key as well as private key based on using the points on the curve (Hankerson, D et al,2006; Hsieh, W et al,2012).



Literature review: From PAK-X protocol, the client and server stores the password in different version where the client has the password which is in the form of plaintext that is stored in it and verifier of that password is stored in the server. The PAK-X provides additional security even if the server is not taken in account. Authentication and Key agreement (AKA) protocols provides security against various known attacks. Also it provides comparison in terms of computation overheads [4]. Smart card authentication method which is authorised by user provides authentication between the user and it also keeps the original information of the user (Chen, B et al,2014). The hashing module provides a specified protection in data security with reduced computations. Also it enhances the level of security with the help of attribute biometrics(Chen, C et al,2012).

ID based method which is accessed by user remotely in between client and server provides authenticity by providing key agreement which is randomly generated i.e, session key. This method employs a greater security, secrecy in forward condition and no keys are shared between the client and the server(Das, A. K. et al,2011). The two factor methodology provides authentication which is more secure and efficient than the other authentication methods. It protects the user by generating random codes using pseudo random number generator thereby reducing the complexity of re-registration (Han, L et al,2006). The remote based login method provides mutual authentication which is error free, also it has the advantages in terms of power and security (Hsieh, W et al,2012).

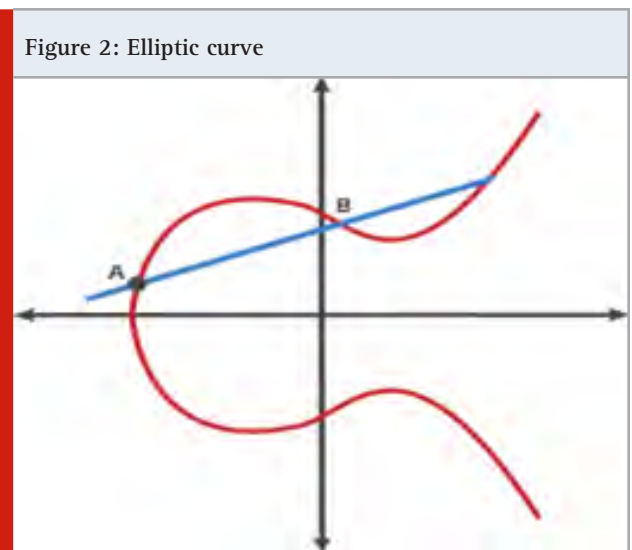
System Model: Generally, automatic control of home appliances is an IoT build system that consist of countless devices that are connected to the internet services. The major components forming an IoT network are its sensing capability, data processing and storage, services provided at the application layer and some additional security mechanism. The authenticated client and the server interact to one other and share information via

Internet. The devices use various etiquettes to collect info and share that gathered information to the gateways. These gateways are components that allow easy and fast access to the IoT world. The authorized users now access this data by providing their legitimacy.

Now we designed a model that includes many IoT appliances attached to the gateway and end-users have mobile phones for interface. Here all things are connected to IoT and possess sufficient computing capabilities. For example, consider a smart irrigation system deployed in afield, whenever an intrusion happens the proposed scheme identifies the data from the malicious node. Farmer can use mobile client anywhere to monitor the records and updates of the field remotely. It makes users ease and efficient by providing distinct services such as healthcare and secure monitoring and energy conservation.

Mathematical Elementals: Here, there is brief discussion about the mathematical concepts for better understanding.

Elliptic curve Equation: General Equation for elliptic curve is $y^2=x^3+ax+b$, this equation is known as cubic equation as the highest power is 3, The curve is given in Figure 1 :



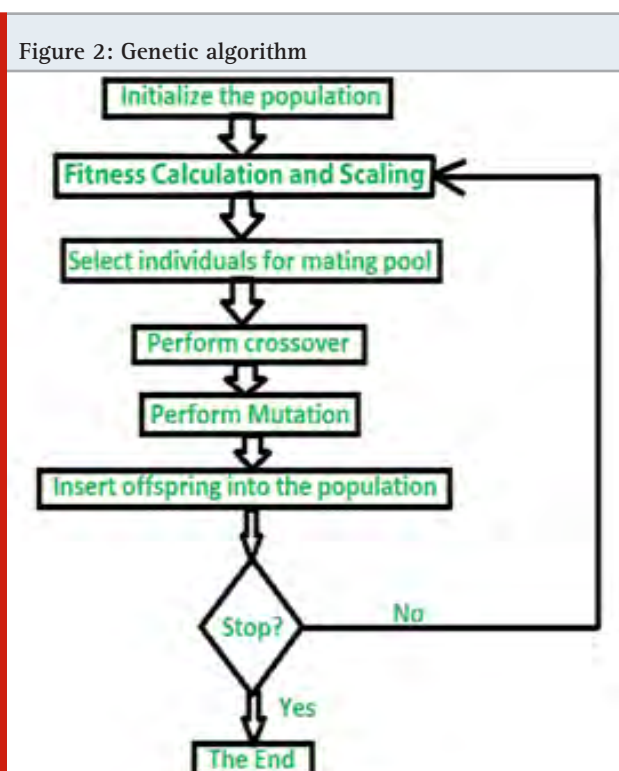
$y^2 \text{ mod } P=(x^3+ax+b) \text{ mod } P$, here $(a,b \in \mathbb{Z}_p)$ and $(4a^3+27b^2) \text{ mod } P \neq 0 \text{ mod } P$. The additive group is formed by points in the curve and special point O known as point at infinity.

Now take an equation $q=kP$ where k is less than P and $q, p \in E_p(a,b)$. it will be easy to calculate q when k and P are known, but it will be relatively difficult to determine the k if P and q are known. This is known as discrete algorithm problem for a given elliptic curve. Generally, k will be big number to avoid feasible hazards. Here P is the prime number of 128 bit. In the above equation kP is Scalar multiplication that is calculated as repeated addition $kP=P+P+P+\dots +P$ (k times).

MATERIALS AND METHODS

Proposed Work: This work consists of two phases. The first phase deals with identifying new elliptic curves. The second phase provides an authentication mechanism to authenticate a mobile client or IoT device when connecting to IoT gateway.

1. Curve Identification: Given a prime number p identifying parameters a and b that maximizes the field can be formularized as an optimization problem. The fitness can be derived from Schoof's algorithm which estimates the no. of points on the curve. This range normally lies between $p-2\sqrt{p}$ and $p+2\sqrt{p}$. We applied genetic algorithm to find the near optimal solution for this considered optimization problem. The aim of this work is not to identify a perfect elliptic curve but identify a curve that can satisfy the encryption needs.



2. Authentication Mechanism: This introduces a key agreement protocol which is mutually authenticated between client and server for IoT device. This scheme typically contains two participants. They are named IoT Appliance which act as Client, and an IoT gateway enabled with Server. This protocol comprises of three stages called system initial login, registration of client and mutual authentication [8].

1. System Initial login phase:

In Initial login phase, when the server starts up the following parameters are generated by S.

- (1) Both Elliptic curve equation $E_p(a,b)$ over a finite field with prime number (p) and the base point

Pbase is chosen by the server with order n .

- (2) Server chooses hash functions H and chosen x as private key of S.
- (3) The public key is computed by $P_s = x * P_{base}$, where x is some random number.
- (4) The server will publish $\{E_p(a,b), P, H, P_{base}, P_s\}$ and x is kept as private.

Table 1

Security (bits)	Minimum size (bits) of Public Keys		Key Size Ratio	Valid
	DSA / RSA	ECC		
80	1024	160-223	1:6	Until 2010
112	2048	224-255	1:9	Until 2030
128	3072	256-383	1:12	Beyond 2031
192	7680	384-511	1:20	
256	15360	512+	1:30	

2. Registration of client stage: A new client will complete registration at server and then obtain the parameters at this phase. The server receives chosen $\{ID_c, PW_c\}$ that has been sent by the client through a secured channel, where ID_c is the identity and PW_c is password of Client. After getting this, server will check for the authenticity of ID_c and computes Hash Function H , it also checks whether the information is already existing in database. If exists Server will acknowledge for distinct identity. Then server starts to compute the set of virtual-identity, that are corresponding to secret keys and identity, password of the client. Then S sends them over a secured channel, that will be stored in the device [8]. Where C is client and S is server.

3. Mutual authentication stage: A session key which was common has been generated by allowing both client as well as the server to mutually authenticate with one another for upcoming communication through the open channel. Initially the server receives a request to login from the client. Now server will verify login request of the client. The authentication message is sent back to client from server, if that request is authentic [1]. This message helps to prove the legitimacy of the server. By this way both client as well as server will have secured and uninterrupted transmission of data, through open channel.

Performance Analysis: This is the analysis between the RSA and ECC. Elliptic curves which produce cryptosystems are a substitute to the cryptosystems of RSA [8]. Integer factorization problem is responsible for safety of RSA cryptosystems as well as elliptic curve discrete logarithm problem is accountable for safety of an ECC [7]. The best acclaimed algorithm for finding a solution is ECC, since IFP of RSA doesn't take full exponential time to find the solution where ECLDP takes. RSA is not preferable

REFERENCES

- Boyko V MacKenzie P & Patel S (2000) Provably secure password-authenticated key exchange using Diffie-Hellman *Advances in cryptology – Eurocrypt 2000* Springer Pages 156–171.
- Canetti R & Krawczyk H (2001) Analysis of key-exchange protocols and their use for building secure channels *Advances in cryptology – EUROCRYPT* Pages 453–474.
- Chaturvedi A Mishra D Jangirala S & Mukhopadhyay S (2017) A privacy preserving biometric-based three-factor remote user authenticated key agreement scheme *Journal of Information Security and Applications* 32 Pages 15–26.
- Chen B-L Kuo W-C & Wu L-C (2014) Robust smart-card-based remote user password authentication scheme *International Journal of Communication Systems* 27(2) Pages 377–389.
- Chen C-L Lee C-C & Hsu C-Y (2012) Mobile device integration of a fingerprint biometric remote authentication scheme *International Journal of Communication Systems* 25(5) Pages 585–597.
- Das A K (2011) Analysis and improvement on an efficient biometric-based remote user authentication scheme using smart cards *IET Information Security* 5(3) Pages 145–151.
- Goutham Reddy A Suresh D Phaneendra K Sun Shin J & Odelud V (2018) Provably secure pseudo-identity based device authentication for smart cities environment *Sustainable Cities and Society* 41 Pages 878–885.
- Han L Tan X Wang S & Liang X (2016) An efficient and secure three-factor based authenticated key exchange scheme using elliptic curve cryptosystems *Peer-to-Peer Networking and Applications* Pages 1–11.
- Hankerson D Menezes A J & Vanstone S (2006) *Guide to elliptic curve cryptography* Springer Science & Business Media.
- Hsieh W-B & Leu J-S (2012) Exploiting hash functions to intensify the remote user authentication scheme *Computers & Security* 31(6) Pages 791–798.

Detection of Glucose Using Non-Invasive Method and Food Analysis for Diabetic Patients Using IoT

N. Suriya^{1*}, S. Pavithra², K Santhosh Solomon³ and Yaswanth Reddy⁴

^{1,3,4}Department of ECE, Chennai Institute of Technology, Chennai-600069, India.

²Department of CSE, Chennai Institute of Technology, Chennai-600069, India.

ABSTRACT

In current trends of smart wearables, there are lot of smart devices for healthcare systems. Among them the detection of Glucose from the patient is tested using blood sample by pricking the finger. This paper demonstrates a device to test the blood glucose level using non-invasive method of not pricking the finger. A Node MCU 32S is used as microcontroller to obtain the readings from the blood glucose detector, temperature sensor and heart rate sensor. The Glucose detector contains PIC16LF178X chip and has two electrodes to send and receive data bits. The electrodes are placed on the tongue where one electrode sends a certain bit of data. The data bits when passed through the blood in the tongue, certain amount is lost due to the presence of glucose. The remaining bits are detected at the second electrode. The difference between these values gives the amount of glucose in the blood. The temperature sensor detects body temperature. The pulse sensor detects the heart rate and blood pressure. These readings are displayed on the mobile application which is connected to the microcontroller via internet. Based on these readings, the microcontroller sends alerts in the mobile application. The dietary suggestions are given to the patient through the mobile application in order to maintain normal glucose levels and also to reduce in times of high glucose levels. A list of foods which should be taken is displayed on the mobile application

KEY WORDS: DIABETES, GLUCOMETER, HEALTH MONITORING, WEARABLE SENSORS, MOBILE APPLICATION.

INTRODUCTION

These days certain diseases are more common to people and are less concern about it. Some are terminal diseases which cannot be cured completely but can be well controlled. One such disease is Diabetes. According to the IDF, the number of people affected by diabetes in the world are about 365 million people, which is 8.5% of the global population. (Global Health Report, WHO) Around

2.2 million deaths are caused due to high blood glucose in 2012. Study shows that diabetes is the seventh leading cause of death as of 2016. Diabetes causes substantial economic loss to people with diabetes and their families. It has been noted that the prevalence of diabetes is more in low- and middle-income countries. Diabetes causes many complications in human body. It creates a risk of dying prematurely. Some may include heart attack, stroke, vision loss, kidney failure, leg amputation, nerve loss etc. In pregnancy, un-controlled diabetes leads to fetal death and other complications.

Diabetes can be treated and its consequences can be avoided or delayed with proper diet, physical activity such as exercises, medication for health issues and regular screening and treatment for complications

ARTICLE INFORMATION

*Corresponding Author: suriyan@citchennai.net
Received 15th April 2020 Accepted after revision 20th May 2020
Print ISSN: 0974-6455 Online ISSN: 2321-4007 CODEN: BBRCBA

Thomson Reuters ISI Web of Science Clarivate Analytics USA and Crossref Indexed Journal



NAAS Journal Score 2020 (4.31) SJIF: 2020 (7.728)
A Society of Science and Nature Publication,
Bhopal India 2020. All rights reserved.
Online Contents Available at: <http://www.bbrc.in/>

The feasibility research of estimating glucose concentration using mm-wave has been performed in (Doojin Lee et al., 2017). Using mm-wave generated by Soli-Radar system which contains 2 Tx and 4 Rx with 8mm x 10mm package. They used EMR to get raw value ADC to sampling signal. It requires blood samples and has 60% accuracy. The Health monitoring system referred in (Luka Bartoli'c et al., 2018) consists of a web API enabling automated data acquisition for glucose levels. It uses Bluetooth to communicate between glucometer or fitness bracelet. But, the usage of web application built on php, JavaScript, html and CSS makes access to the system complicated and not simple. In (Md Koushik Chowdhury et al., 2014), the Fast Fourier Transform (FFT) domain and peak to peak voltage amplitude is performed by a renounced software toolbox. It also controls all the data processing and programming of the device. The input was obtained from Infrared Light source and ultrasound transmitter but resulted in time delayed output.

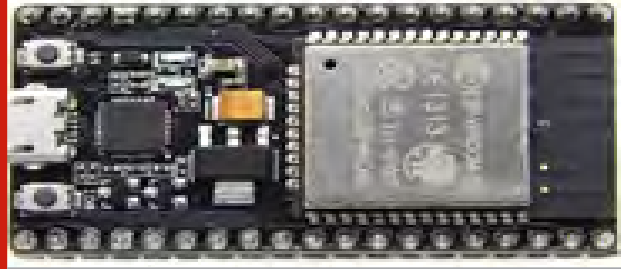
Moreover, 45 blood samples for blood glucose measurements were required and 225 data-based signals were recorded and examined. The generation of Personalized Diet in (Wahidah Husain et al., 2011) is quite different where a Genetic Algorithm was developed which takes its input from user database and food database to create a diet menu for the patients. It was a simulation application yet it was highly feasible and has high accuracy. In (Abu Sadat Sabbir et al., 2016) and (S.S.Mule et al., 2016) the Arduino Uno is used to connect with glucometer and Bluetooth device. The Analog voltage is read after 2 seconds of blood detection (Abu Sadat Sabbir et al., 2016). It had functions of Glucose monitoring, diet control, physical activity monitoring, insulin usage, and other services but lacks the usage of non-invasive methods for glucose detection. The recent research made in (Toshiya Arakawa et al., 2018) using mercury sphygmomanometers at fingertip sensors for calculating blood pressure was accurate but highly complicated. The android based health monitoring in (Shivam Trivedi et al., 2011) uses photoplethysmography technique and gets input from pulse sensor and temperature sensor to display the readings. It does not use IoT but uses Bluetooth and hence it is easy to use and able to measure signals at real time.

MATERIAL AND METHODS

NODE MCU 32S: The Figure 1 represents the Node MCU 32S microcontroller developed by NodeMcu. It ESP32 chip supports Wifi and Low Power Input. The power to the MCU is supplied via the micro USB Type-B present on-board or directly through the VIN pin. Its operating voltage ranges between 6 to 20 volts if external supply. But heat issues occur when operated beyond 12V thereby causing damage. Therefore, supply voltage between 7 to 12V is recommended.

The serial-to-usb chip present on the device allows programming and opening the UART of the ESP32 MCU. It is programmed using Embedded C language.

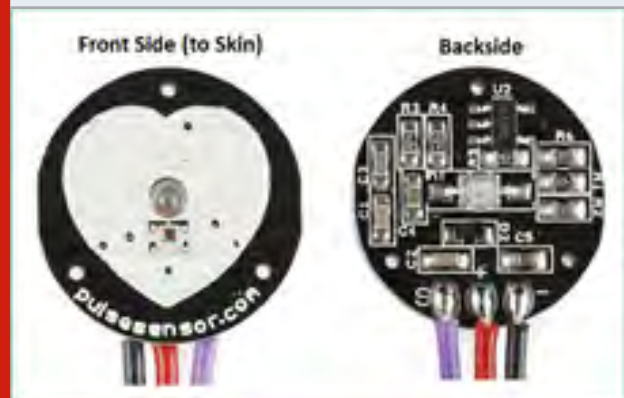
Figure 1: Node MCU ESP32S microcontroller



The program contains Wifi credentials to connect to the specific network for internet access. The Virtual Pins are assigned to pulse sensor, Temperature sensor and Blood Glucose Sensor respectively. The normal values of the readings detected by these sensors are also declared. A list of food items which should be taken at various glucose levels are written. The program contains conditions to check the current reading and display the respective food items as dietary suggestions to the patients in order to maintain normal glucose levels. It is also programmed to display alerts to visit doctor if the temperature, heart beat, blood pressure or blood glucose levels are out of range or abnormal.

Pulse Sensor

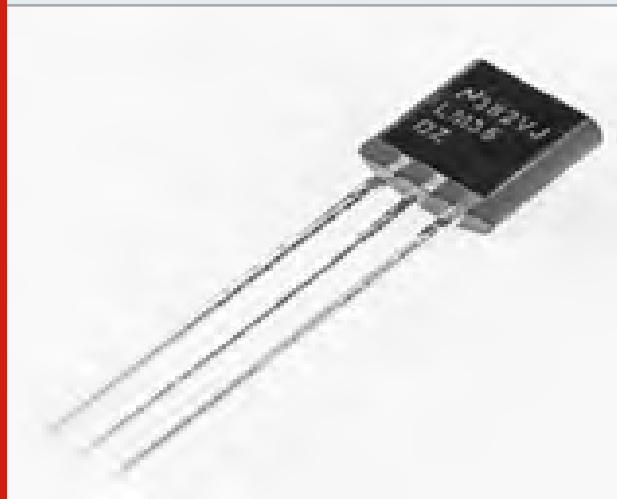
Figure 2: Pulse sensor



The Figure 2 represents the pulse sensor. It is made up of an optical heart rate sensor coupled with amplification circuit and a noise cancellation circuit. The sensor has two sides. On the front side (to skin) an LED is placed along with an ambient light sensor. On the backside, the noise cancellation and amplification circuitry are located. The frontside which consists of the LED should be placed over a vein in our body. Mostly it is placed on the fingertip or ear tips but it should be on top of a vein. The veins have blood flow due to the pumping action of the heart i.e. whenever the heart muscles contract the blood is pumped through the veins. Therefore, if we monitor the flow of blood, we can determine the heart beat as well. Whenever there is a flow of blood, the light sensor will pick up more light since light is reflected by the presence of blood cells. This minor change in the light reflected is analysed to determine the heartbeat. The

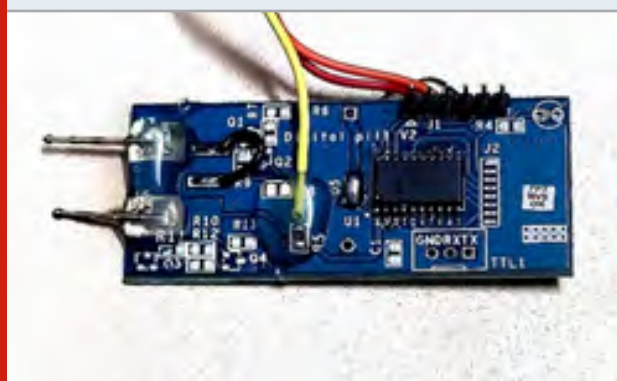
operating voltage of the pulse sensor is between 3.3V to 5V and the drawing current is 4mA.

Figure 3: LM35 Temperature Sensor



LM35: The LM35 is an integrated-circuit that can be used to measure temperature in centigrade temperature which is shown in Figure 3. The advantage of using LM35 is due its accuracy which is greater than a thermistor. The sensory circuit present is sealed hence it is not subjected to oxidation. The output voltage need not be amplified as it generates higher output voltage in general. The LM35 is rated to be operated between -55°C to 150°C . It draws around 60mA from its supply for operation which is regarded as the biggest advantage. Unlike other devices, the LM35 has low self-heating capability therefore it has $\pm 0.4^{\circ}\text{C}$ accuracy.

Figure 4: Blood Glucose Sensor



Blood Glucose Sensor: The blood glucose sensor shown in Figure 4 consists of PIC16LF178X chip. It is used to determine the concentration of glucose. The glucose concentration is measured in milligram per decilitre (mg/dl) or millimole per litre (mmol/L). It operates at a voltage range between 1.8 to 5.5 V thereby making it a low power chip. It contains two electrodes: working electrode and counter electrode. The working electrode provides 8 bit which when placed on the Tongue, passes

through the blood and few bits of data are lost due to the presence of glucose in the blood. The remaining bits are captured by the other electrode. Therefore, the difference between the input and output is considered for analysing the amount of glucose present in the blood.

Mobile Application: Blynk is an open source mobile application which is designed for IoT. It has in-built features such as remote-control hardware, display readings from sensor, store data from external devices and much more. The Blynk app contains predefined widgets which can be used to create interfaces for our application. The data communication between the application and the hardware is maintained by the Blynk server. Blynk supports direct pin manipulation without writing any additional code thereby it is easy to integrate and add new functionality using the virtual pins. To uniquely identify our requests in blynk server, an Auth Token is sent during creation of your Blynk account. This Auth Token is a unique identifier allocated by the server which is needed to connect our hardware to the smartphone.

RESULTS AND DISCUSSIONS

The device consists of a microcontroller, a temperature sensor, a heartbeat sensor, a blood glucose sensor and a mobile application. The ESP32s Dev Kit V1 node mcu is used as a microcontroller. It has built in WiFi module thereby enabling to connect to the internet. The microcontroller is programmed using embedded C programming language used largely in microcontrollers. The entire functioning of the device is controlled by the microcontroller. The readings from the connected components are processed and sent to the mobile application.

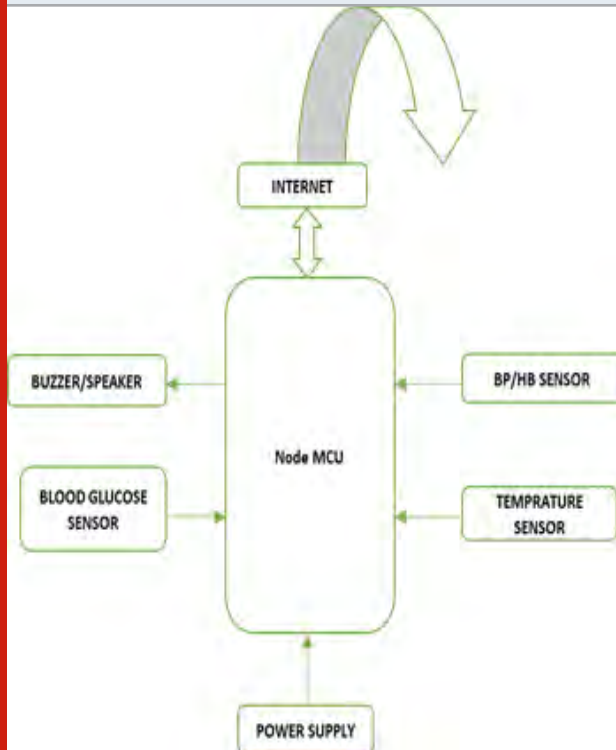
The AN1560 which consists of PIC16LF178X chip is used as blood glucose sensor. It contains two electrodes: working electrode and counter electrode. The working electrode provides 8 bit which when placed on the Tongue, passes through the blood and few bits of data are lost due to the presence of glucose in the blood. The remaining bits are captured by the other electrode. Therefore, the difference between the input and output is considered for analysing the amount of glucose present in the blood. The Analog data is converted to digital as it is connected to A/D convertor pins in the board. The readings are mapped to respective values in the code dumped in the microcontroller.

The pulse sensor is used to detect the heartbeat rate from the individual when placed on his skin. The heart rate values are used to also determine the blood pressure of the individual. The pulse sensor is connected to the microcontroller to send the readings for processing.

The temperature sensor LM35 is used to detect the temperature of the individual. It is placed to the individual's The power to the MCU is supplied via the micro USB Type-B present on-board or directly through the VIN pin. Its operating voltage ranges between 6 to

20 volts if external supply. But heat issues occur when operated beyond 12V thereby causing damage. Therefore, supply voltage between 7 to 12V is recommended. The serial-to-usb chip present on the device allows programming and opening the UART of the ESP32 MCU. The sensor is connected to the microcontroller to send the readings for processing.

Figure 5: Architecture Of Proposed Solution



The mobile application used here is an open source platform. Blynk is an IoT platform with mobile apps, private clouds, device management, data analytics, and machine learning. Basically, it is an open source mobile application meant for catering IoT needs. The application is configured and authenticated to receive the data from the microcontroller through internet and display them on the mobile application respectively as shown in Figure 6.

Figure 6: Mobile Application Connectivity

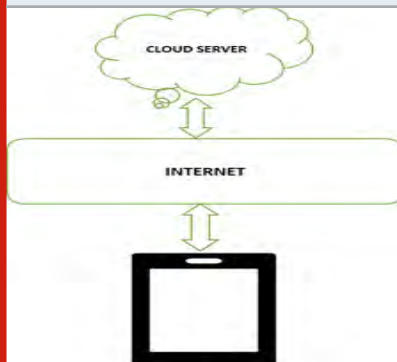
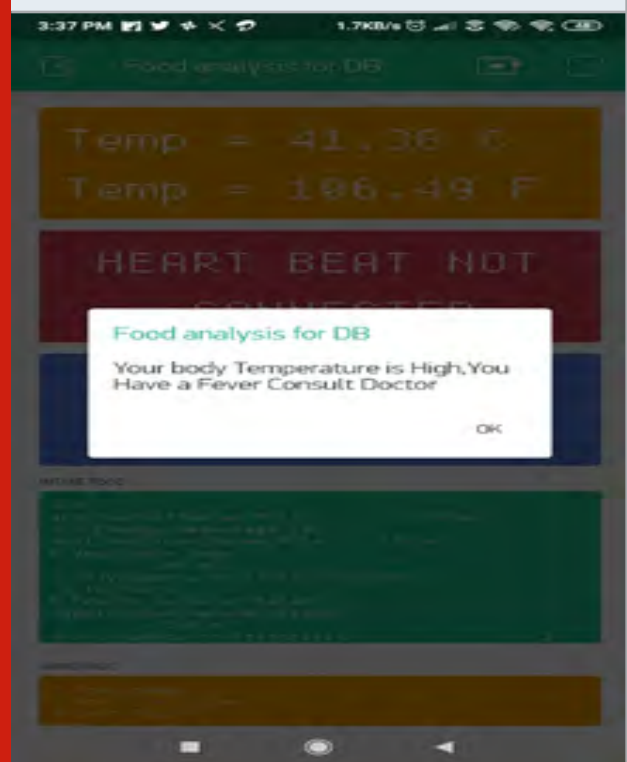


Figure 7: Readings from various sensors displayed on the mobile application



Figure 8: Alert is displayed when readings are abnormal



CONCLUSION

This work has presented, the continuous monitoring of Blood Glucose levels, Temperature, Heart beat and Blood Pressure of diabetic patients. The usage of non-invasive method of detecting blood glucose levels without pricking the finger is introduced. The dietary suggestions are carefully developed and programmed to identify the correct foods to be taken to maintain balanced blood glucose levels. Alerts in the form notifications are sent to the patient in case of abnormal readings. To the best of our knowledge, there is not any device which brings the above parameters in the form of "smart wearables" and accessing through a mobile application.

REFERENCES

- Bruno Zori'c Faculty of Electrical Engineering Computer Science and Information Technology Osijek J J Strossmayer University of Osijek Osijek Croatia
- Goran Martinovi'c Faculty of Electrical Engineering Computer Science and Information Technology Osijek J J Strossmayer University of Osijek Osijek Croatia.
- Doojin Lee Glucose Concentration Estimation using Electromagnetic Waves Department of Mechanical and Mechatronics Engineering University of Waterloo Ontario Canada
- Karly Smith Biomedical Engineering Department of Systems Design Engineering University of Waterloo Ontario Canada
- Clement Csech Department of Biomechanics and Bioengineering Universite de Technologie de Compiegne Compiegne France.
- E-Gluko A Ubiquitous System for Health Status Monitoring And Tracking In Diabetes Patients Luka Bartoli'c Faculty of Electrical Engineering Computer Science and Information Technology Osijek J J Strossmayer University of Osijek Osijek Croatia.
- Md Koushik Chowdhury Anuj Srivastava Neeraj Sharma And Shiru Sharma The Potential Application of Amplitude Modulated Ultrasound With Infrared Technique For Blood Glucose Level Determination In Non Invasive Manner School Of Biomedical Engineering Indian Institute Of Technology (Banaras Hindu University) Varanasi Uttar Pradesh - 221 005 India.
- Muthukumar B Dhanagopal R Et Ramesh R KYP (2019) modeling architecture for cardiovascular diseases and treatments in healthcare institutions J Ambient Intell Human Comput.
- SSMule THMujawar MSKasbe and LPDeshmukh Microcontroller Based Blood Glucose Meter Design and Development Department of Electronics Science Solapur University Solapur MS India.
- Shivam Trivedi Alice N Cheeran Android based health parameter monitoring Department of electrical engineering Veermata Jijabai Technological Institute Matunga Mumbai India.

Framework for Cancer Detection using Deep Wavelet Autoencoder & Neural Network in Brain Images

M. Kavitha^{1*}, S. B.Rajdakshan², S. Tamilselvan³ and M.Mohamed Fardhin⁴

^{1*}Professor,

^{2,3,4}UG Scholars

^{1,2,3,4,5}Department of ECE, K. Ramakrishnan College of Technology, Trichy-621112, India

ABSTRACT

This paper focuses on cancer detection in brain images using neural networks and comparison of other classifiers has been done. Image processing plays an important role for diagnosing diseases. It mainly focuses on the brain anatomy and also deals with the functions of brain. It consists of three phases such as deep neural network, classification and segmentation task. A framework has been developed for cancer detection in brain images using neural network and autoencoder. The features are selected from the brain images and they are trained and classification has been done. The performance of deep wavelet neural network classifier was compared with other classifiers. The experimentation is carried out using the brain image database to prove the results against the proposed technique. From the results obtained in the proposed method, it can be inferred that our technique has achieved good results and it is efficient.

KEY WORDS: BRAIN IMAGES, SEGMENTATION, DEEP NEURAL NETWORK.

INTRODUCTION

Cancer cells originates from the tissue. The objective classification tool using neural networks for detecting and classifying the brain cancer. Machine learning algorithms help us better classification tool. A neural network consists of an neurons and it processes information for computation. Neural networks are statistical data modeling tools. Some investigations done in the past,

it has identified images based on their colour, gray level and their high contrast. Because the color of images vary among different patients in different photographs and therefore those method would not suitable in all images used in clinical.

The contribution of the proposed technique is 1.design of autoencoder 2. Using deep neural network. Cancer detection is a critical problem in the segmentation. The accuracy is maintained for detecting malignant tumors etc. Deep neural networks (DNN) have fascinated so many scientists. Auto encoder is basically Artificial Neural Network (ANN)[6]. It is used for efficient data encoding in an unsupervised algorithm. Auto encoder is typically robust, whereas wavelet function has a variation in the features and frequency. When it is combined, they are not able to solve many problems in real time applications.

ARTICLE INFORMATION

*Corresponding Author: kavitha79ramar@gmail.com
Received 15th April 2020 Accepted after revision 20th May 2020
Print ISSN: 0974-6455 Online ISSN: 2321-4007 CODEN: BBRCBA

Thomson Reuters ISI Web of Science Clarivate Analytics USA and Crossref Indexed Journal



NAAS Journal Score 2020 (4.31) SJIF: 2020 (7.728)
A Society of Science and Nature Publication,
Bhopal India 2020. All rights reserved.
Online Contents Available at: <http://www.bbrc.in/>

The aim of this paper is to build a architecture that helps in cancer detection through the neural network classification. A DWA is used for extracting features. The deep wavelet autoencoder was finally tested and compared with many other existing methods. DWA performs high accuracy[7] when compared with the other existing techniques. This is the easiest way.

Related Works: Mohammad Amazad Hossain[1] proposed the template based K means and fuzzy c means clustering algorithm. Steps such as preprocessing, dilation and erosion techniques and texture analysis methods were applied to the brain images to detect the features and for classification fuzzy c means clustering algorithm has been used, The detection results were validated by comparing with experts. Dr.C.Pande[2] have considered the brain imaging techniques for different modalities. Segmentation techniques such as K means clustering, morphological operations such as dilation erosion considered for brain images. It is survey methods all segmentation techniques applied to the brain images. Gawande[3] have some tumour diagnosis using image processing techniques. In this methods the efficiency and accuracy is very low when compared to the other techniques. Palani[8] proposed the techniques for diabetic detection using neural network especially SVM classifier. In this technique, sensitivity, accuracy are calculated. The percentage of accuracy of detection is 80% only. Wrapper approach[4] use induction algorithm and handle complex data sets. It produces minimum error rates and reduce misclassifications. Menon[5] provide a detailed review about brain segmentation methodologies. It gives a clear idea for the purpose of analysis[12] in brain images.

Proposed Method: Figure 1 represents the block diagram for Brain MRI image classification based on Deep Wavelet Auto encoder. In medial DICOM images are taken for processing. Slices of DICOM image are taken and it is preprocessed. The preprocessing images[8] are converted into flattened matrix array and then converted into several arrays. The o/p arrays are passed through auto encoder. Reconstruction of arrays[13] has been done. Encoded image is passed through deep neural network. The images resolution is very high. The features are taken and they are tested and trained[9] for classification whether the image abnormal or normal. Figure 1 shows the proposed model. They are several encoders such auto encoder, sparse encoder and denoising auto encoder.

Autoencoder

Figure 2: Shows simple autoencoder with 3 layers

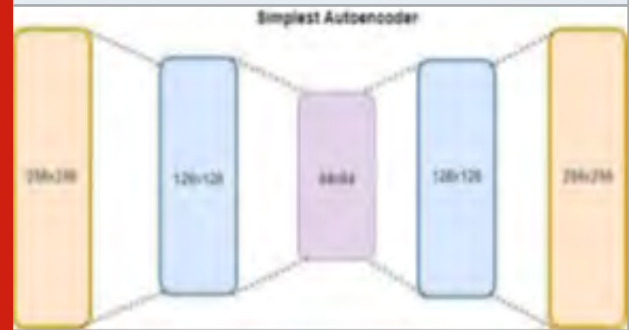


Figure 2 shows simple autoencoder . It acts as best preprocessing for image analysis.

Figure 3: Shows sparse encoder

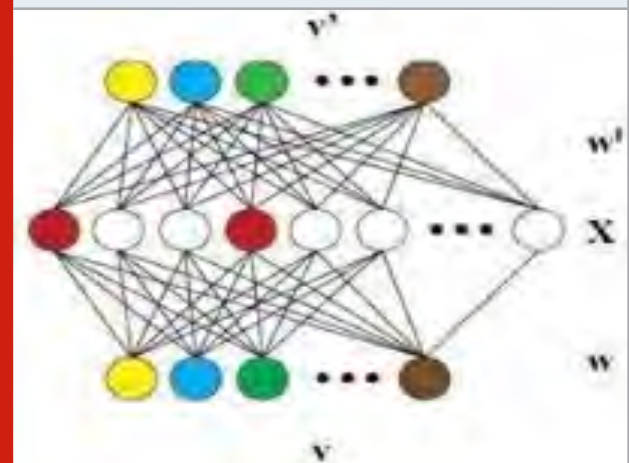


Figure 4: shows denoising autoencoder



Figure 5: Proposed architecture of a single layer of DWA

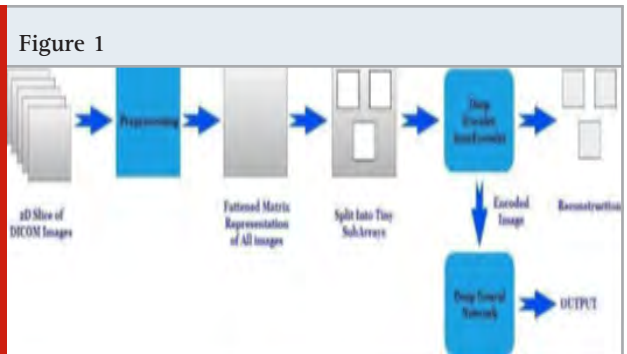
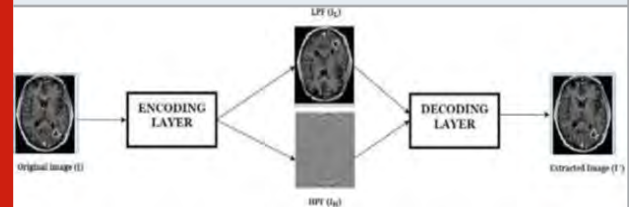


Figure 5, represents a proposed DWA architecture. In this technique, dicom images are encoded and then it is passed through the LPF[10], for decoding it is passed through the HPF the image is extracted. Further the features are extracted for classification[11] using deep neural network and autoencoder.

RESULTS AND DISCUSSION

Figure 6: Shows the deep neural network based brain tumour based classification

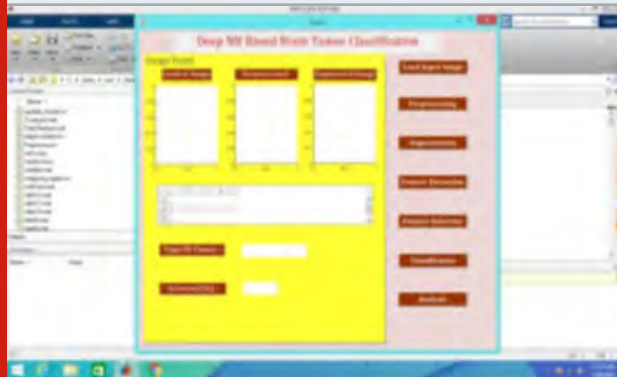


Figure 6 shows the deep neural network based brain tumour based classification. This window shows the icon of load image, segmentation, feature extraction and neural network classification.

Figure 7: Shows the neural network applied to DICOM images

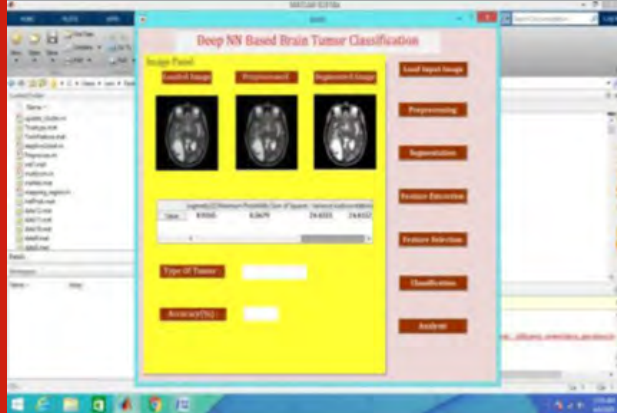


Figure 8: Classification performance of brain images for cancer detection

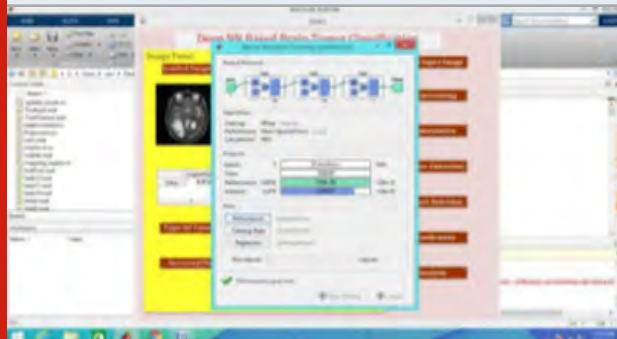


Figure 9: Performance of the classifier in Dicom images



Figure 10: cancer affected image

Magenta: Initial; Green: Final after 100 iterations

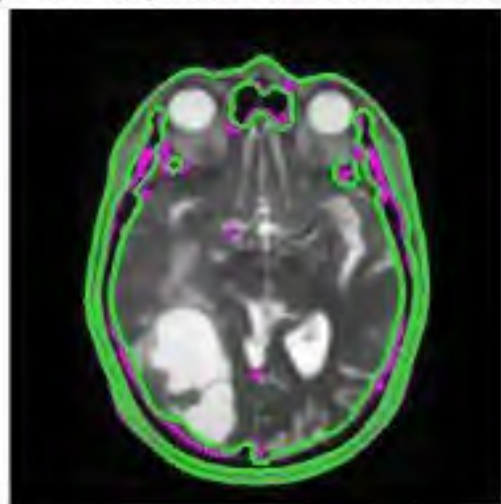


Figure 11: Segmented image

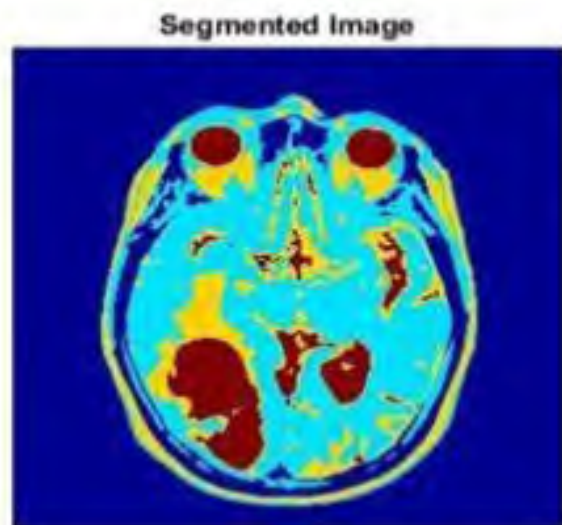
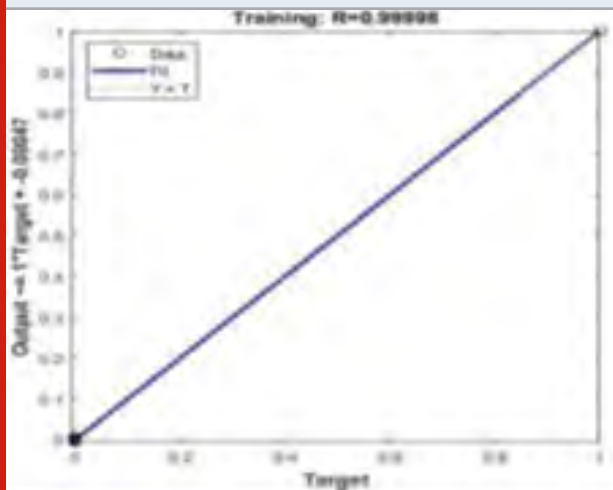


Figure 12: Training phase classification performance



CONCLUSION

Cancer detection using neural network and the deep wavelet auto encoder has been done. Here the features were taken. The process testing and training has been done in similar manner. Finally the classification has been done compared with the existing classifiers. In order to find the accuracy, sensitivity, specificity are calculated using neural network specifications. The quality of the images has been improved. The types of images taken are Dicom images i.e medical image. The accuracy is also very high. So the method using auto encoder and neural network plays a vital role. The accuracy of this method is 96%.

REFERENCES

- Alhadidi B, Zu'bi Mohammed Hussain, Suleiman HN (2007) Mammogram Breast Cancer Image Detection Using Image Processing Functions. *Information Technology Journal* 6(2): 217-221.
- Dr.C.Pande, Xu C and Princo JL (2000) A Survey On Current Methods In Medical Image Segmentation, *Annual Review of Biomedical Engineering* 2.
- Suraj.S.,Gawande ,Langote VB, Chaudhuri DS (2012) Segmentation Techniques for Image Analysis.

International Journal of Advanced Engineering Research and Studies 2(1): 252255.

Sathya A, Wrapper, Senthil S, Samuel A. (2012) Segmentation of breast MRI using effective Fuzzy C- Means method based on Support Vector Machine. *Information and Communication Technologies (WICT)* 67-72.

Singh M, Verma A, Sharma N, Menon (2018) An Optimized cascaded stochastic resonance for the enhancement of Brian MRI. *Innovation and Research in BioMedical Engineering (IRBM)* 39(5): 334-342.

Pham TX, Siarry P, Oulhadj H (2018) Integrating fuzzy entropy clustering with an improved PSO for MRI brain image Segmentation. *Applied Soft Computing* 65: 230-242.

Tong J, Zhao Y, Zheng P, Chen L, Jiang L (2018) MRI brain tumor segmentation based on texture features and kernel sparse coding. *Biomedical Signal Processing and Control* 47: 387-392

M.Kavitha,Dr.S.Palani(2014) , Blood vessel, optic disk and damage area based features for diabetic detection from retinalimages, *Arabian journal of science and Engineering*, vol39, pg.no: 7059-7071.

M.Kavitha, Dr.S.Palani(2014) , Hierarchical classifier for soft and hard exudates detection, *Journal of intelligent and fuzzy systems*, vol 27, pg.no. 2511-2528.

M.Kavitha, R.Jaiganesh(2019), Facilities navigation and patient monitoring system using ibeacon technology , *International Journal of Mechanical and Production Engineering Research and Development*, issue. vol. 9, special, issue 1, jan 2019, 562-570

M.Kavitha, R.Jaiganesh(2019), Hierarchical classifier for Breast cancer diagnosis, *Journal of Advanced Research in Dynamic and control systems*,vol-11,04-special issue,2019(page no.607-611).

M.Kavitha, A.Kavitha(2019), BBRC Bioscience biotechnology research communication, Framework for the merging of thermal and visible images in Real time Recognition Application Issue vol12 no (6)Nov 2019.

Dr.M.Kavitha, Dr.S.Palani(2020), Analysis of retinal images with public data base, *International journal of business information systems*.

Design of Inverted – Dual Band F MIMO Antenna Structure

J. Deepa^{1*}, S. Syedakbar^{2*} and S. Geerthana^{3*}

^{1,2,3*}Assistant Professor,

^{1,2,3}Department of ECE, K. Ramakrishnan College of Technology, Trichy-621112, India

ABSTRACT

This paper explains a twofold band revamped F numerous information select yield (MIMO) getting twine with predominant remoteness, covering the 2.4/5-GHz remote neighbourhood systems (WLAN) band. The fate MIMO yielding twine is set up out of two indistinguishable winding rearranged F radio twine modules. There are two beneficiary segments. This collector parts are unflinchingly isolated with almost 0.a hundred and fifteen λ_0 of the lower band. The high imprisonment is done through structure decoupling devices, a twisting boisterous division and a particular T-shaped zone engraved at the floor for the higher band and the diminishing band, independently. Moreover, U-formed cuts accomplishing better impedance getting sorted out are cut at the 50- Ω fortifying strains to widen the realities move capacity of the over the top band. The proposed reversed F-MIMO radio wire in the impedance data verbal trade covers 2.4–2.forty eight GHz(decrease band) and 5.15–5.825 GHz(upper band).This reception apparatus achieves 15-dB disconnection arranged the 2.4-and 5-GHz WLAN gatherings. This builds up a perilous improvement thought nearly to the straightforward structure of the MIMO reception apparatus. This rearranged F-MIMO reception apparatus is genuine suitable for WLAN programs which demonstrates by means of the enhancement and estimation results

KEY WORDS: DECOUPLING, DOUBLE BAND RADIO WIRE, INVERTED F RECEIVING WIRE, NUMEROUS INPUT-VARIOUS-OUTPUT (MIMO) ANTENNA, (WLAN).

INTRODUCTION

With the quick development of wireless neighbourhood network (WLAN) that slot in with the 802.11a and 802.11b standard to perform ordinary country of throughput and wonderful omni directivity, the interest on high facts charges and excessive unwavering first-class is rather terrible. Various input – several output (MIMO) innovation has pulled in much consideration for its terrific properties

as a ways as dependability and increasing the channel limit. Notwithstanding, due to the restrained space, it's hard to location various antennas together closely even as maintaining high isolation. Step with the aid of step commands to enhance the segregation among antennas progresses closer to becoming a basic trouble.

To realize first rate execution of twin band dual difficulty WLAN MIMO antenna, the ports must be as unrelated as could pretty be expected. Much attention has been centered around some uncommon processes increasing isolation. Many decoupling designs had been accounted for, consisting of electromagnetic band gap (EBG), defected floor shape (DGS), a simple resonator, parasitic additives, etc. The receiving wires planned (Chattha et al., 2012; chen et al., 2005; Haruki et al.,

ARTICLE INFORMATION

*Corresponding Author: shanjeya008@gmail.com

Received 15th April 2020 Accepted after revision 20th May 2020

Print ISSN: 0974-6455 Online ISSN: 2321-4007 CODEN: BBRBCA

Thomson Reuters ISI Web of Science Clarivate Analytics USA and Crossref Indexed Journal



NAAS Journal Score 2020 (4.31) SJIF: 2020 (7.728)

A Society of Science and Nature Publication,

Bhopal India 2020. All rights reserved.

Online Contents Available at: <http://www.bbrc.in/>

2005) were meant for Multiple input and multiple output software by stepped forward separation, then the transfer speeds of those reception apparatuses have been missing aimed at the complete WLAN range. In (Chattha et al., 2012), the separation become expanded in means of including a attached decoupling networks between the dual firmly put radio twine components.

An opened wind strains resonator planned in (chen et al., 2005) to improve the remoteness amongst dual antennas additives in micro strip repair receiving twine exhibits. In (Haruki et al., 2005) an aloof resonator become positioned between tightly divided planar reversed F antennas to decrease the multiple connection. Sponging additives what's more, DGS were likewise effective to decouple as exhibited in (Gao et al., 2005; Huynh et al., 2003) however those innovations aren't commonly appropriate, furthermore, the antennas are somewhat extensive as discussed in (Syedakbar et al., 2017; deepa et al., 2016; syed akbar et al., 2017) An folded arrangement and a split-ring resonator have been displayed in (Li et al., 2003; Looby et al., 2007) separately. Be that because it may, the systems are excessively puzzled.

In this letter, a reduced twin band wireless fidelity MIMO reception equipment with progressed disconnection is planned, and also the polarity of the planned version is direct polarity. The antenna form remains advanced since the wandering changed F antenna. Through consisting of winding monopoles, a wireless fidelity information measure is accomplished. A high isolation between 2 antenna additives is obtained by method of etching a reversed T-slot on the ground and a winding resonant branch. The exhibitions of the antenna, like S-Parameters, patterns of radiation, and envelope coefficient of correlation (ECC), are analysed, and also the consequences reveal a wireless fidelity MIMO antenna with high detachment is effectively accomplished. Whatever stays the message is remote into 4 sections. In Segment II, a stylish interpretation in underlying form of wireless fidelity Multiple input and multiple output antenna is specified, Segment III particulars the procedure, the imitation and estimated effects square measure examined in Segment IV, associate degree an stop remains certain lastly.

MATERIALS AND METHODS

Basic Design Of The Twin-Band Mimo Antenna: The pure mathematics of the projected initial structure of twin band inverted F LAN MIMO antenna equipment is appeared in Fig. 1. Antenna sets by concerning $D = \text{zero.1 one}$ and $D = \text{zero.2 one}$ area unit examined for varied coupling conditions (where D speaks to the gap between 2 antenna components), for this example D equals with zero.115 λ_0 , that is around 1/8 one (where the wavelength is at a pair of.4 GHz) therefore on diminish the final dimension of the antenna framework. The antenna is imprinted arranged the simplest coating of a tokenish effort FR4 substrate ($\epsilon_r = \text{four.4}$, $\tan\delta = 0.02$) with the mensuration of fifty two metric linear unit (W

\times seventy seven.5 mm(L) \times one.6 mm(T). the 2 antenna parts area unit nourished in the 50- Ω microstrip strokes by the dimension as two.5 mm, and also the improved antenna measurements area unit recorded in the first table. Primer arrange of the represented reversed F twin band antenna have assessed & improved by utilizing the Ansoft HFSS 16.1 programming. The estimated parameters(S) of the underlying arrange of Multiple input multiple output antennas area unit appeared in Fig. 2. It tends to be seen that the S11 is less than less than from a pair of.4 to 2.48 GHz and from five.18 to 5.84 GHz, also, the S21 between the reception antennas is around -6 decibel at a pair of.4 Giga hertz also, -eight decibel at 5-Giga hertz band, that the separation doesn't see financial necessities.

Figure 1: F-MIMO Antenna Structure

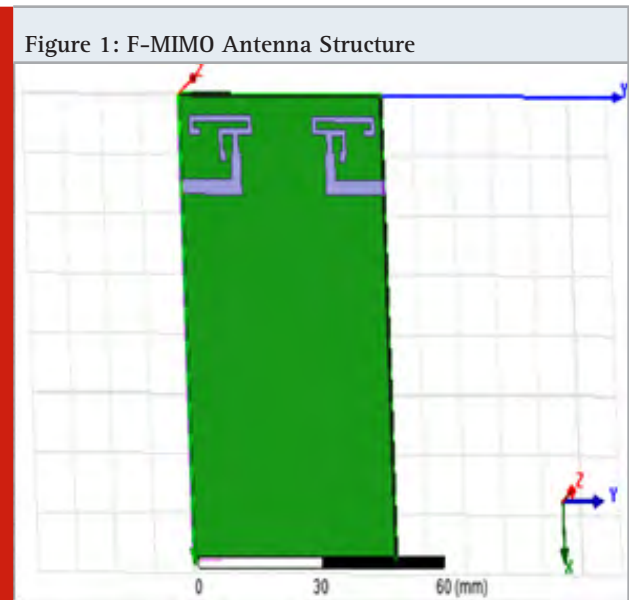
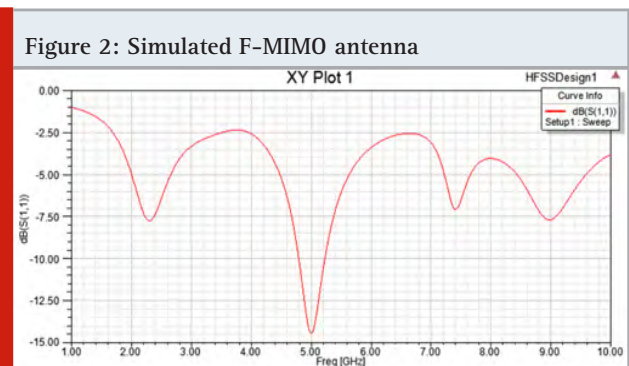


Table 1. Dimensions of F-Mimo Antenna

Adjus table	Esti mated	Adjus table	Esti mated	Adjus table	Esti mated
L1	2.8	L6	14.5	W1	1
L2	2.5	L7	4.7	W2	1.25
L3	3	L8	4.7	W3	1.5
L4	5.7	L9	7	W4	2.5
L5	8.7	L10	5	H	7.5

Figure 2: Simulated F-MIMO antenna



RESULT AND DISCUSSION

Reversed T-Stub on the Ground: To rise the remoteness, an reversed T-stub resonator with a entire period of approximately $\lambda/4$ at 2.4 Giga hertz is scratched in floor as regarded in Fig. 3. In Fig.4 the remoted S-parameters of the T-Stub are appeared. It tends to stay visible as remoteness have efficiently expanded via 12 decibel at 2.4 Giga hertz contrasted with the Antenna 1 with the aid of inclusive of a T-stub, yet the detachment of the frequency with high band is sort of changed.

Figure 3: T-Stub Structure

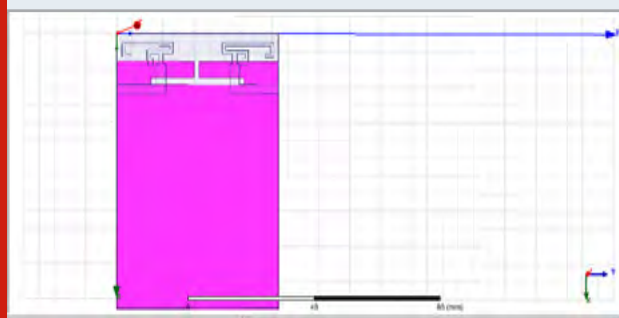
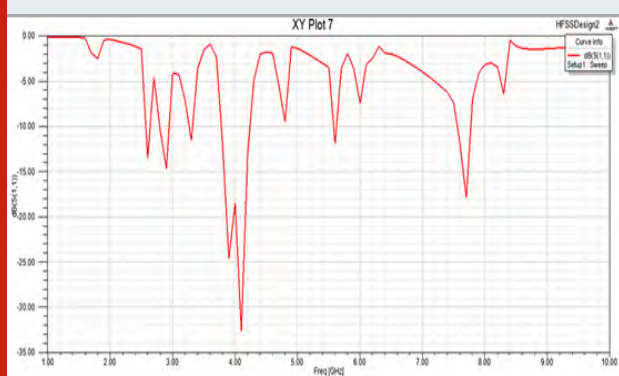


Table 1. Dimensions of F-Mimo Antenna

Adjus table	Esti mated	Adjus table	Esti mated	Adjus table	Esti mated
L1	2.2	L6	15.15	L11	10
L2	17.1	L7	9.68	L12	12.5
L3	1.6	L8	9.68	G1	7.9
L4	13.1	L9	10	S1	0
L5	12.65	L10	1.6	H	7.3

Figure 4: T-stub Antenna



Verification of Radiation Pattern: To extra conveniently define the functioning device of the planned structure, in Fig. 5 the sampled radiation of the tested antenna are given and vertical and paralleled lane evaluating in working frequencies of 2.4, 5.2, and 5.8 GHz, individually. F-mimo return loss has appeared in Fig. 6 It can be

viewed that the examples are semi omni directional, which is sensible for faraway conversation terminals to get indicators from any bearing, so the methodology of energizing detonate attribute modes on the physique is acquired to scale back the sample connection.

Figure 5: F-MIMO Radiation Pattern

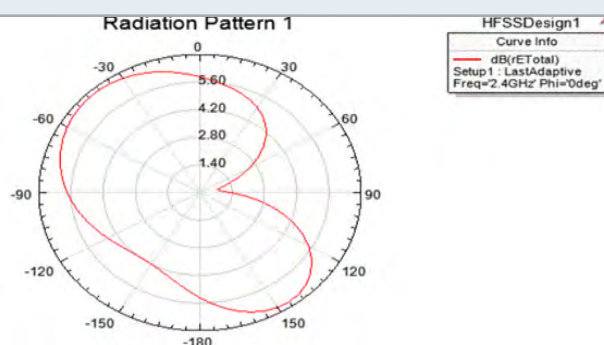
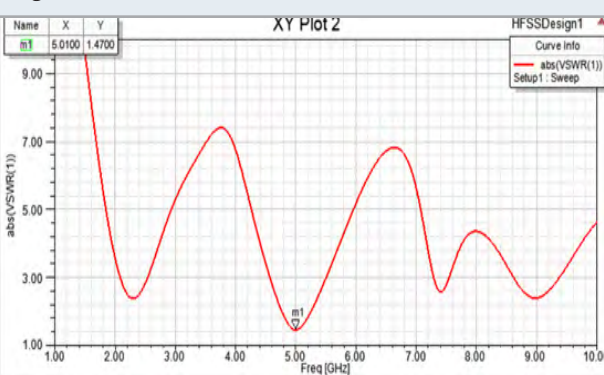


Figure 6: F-MIMO VSWR



CONCLUSION

A twin band reversed F Multiple input multiple output reception equipment by antenna arrangements working by each 2.4-and 5-GHz LAN band is planned, estimated, and investigated in our paper. At 15dB the antennas have segregated and enhanced via imparting a modified T-stub and a wander line resonance branch. The proposed reception equipment has been efficaciously motivated and estimated, and the effects exhibit that it ought to outstanding high-quality device for application of the WLAN.

REFERENCES

- Chattha Y Huang M Ishfaq and S Boyes (2012) A Comprehensive Parametric Study of Planar Inverted-F Antenna Wireless Engineering and Technology Vol 3 No 1 Pages 1-11.
- Chen and Y F Lin (2005) Exploratory and Simulated Studies of Planar Inverted-F Antenna IEEE International Workshop on Antenna Technology Singapore Pages 299-302 7-9.
- Deepa S.Suganthi G Shenbaga Ranjani J Candice Freeda and M. Jayaprabha (2016) Multiband Planar MIMO

Antenna for GSM1800/ LTE2300/ WiMAX/WLAN Applications International Journal of Engineering Research & Technology (IJERT) Vol 4 No19 Pages 38-43.

Haruki and Kobayashi (2005) The Inverted-F Antenna for Portable Radio Units Conv Rec. IECE Japan (in Japanese) Pages 613,

Gao C C Chiau X Chen and C G Parini (2005) A Compact Dual-Element PIFA Array for MIMO Terminals Loughborough Antennas and Propagation Conference Loughborough Pages 4-5.

Huynh and W Stutzman (2003) Ground Plane Effects on Planar Inverted-F Antenna (PIFA) Performance IEE Pro-ceedings Microwave Propagation Vol 150 No 4 Pages 209-213

Lobby E Lee and C T P Tune (2007) Planar Reversed-F Antennas, Chapter 7 In: by R. Waterhouse, Ed., Printed

Antennas for Wireless Communications, John Wiley and Sons, Hoboken.

Li, Y. Rahmat-Samii and T. Kaiponen (2003) Data exchange limit Study of a Dual Band PIFA on a Fixed Substrate for Wireless Communication IEEE Transactions on Antennas and Propagation Vol 1 Provo Pages 22-27.

Syedakbar S. Ramesh J Deepa Ultra wide band monopole planar MIMO antenna for portable devices IEEE International Conference on Electrical Instrumentation and Communication Engineering 2017.

Syedakbar A. Muthulakshmi G. Monika Dharani J. Aarthy Unit cell structure for multiport ultra wide band (UWB)antenna International Conference on Innovations in Information Embedded and Communication Systems ICII ECS-2017.

Powering Smart Street Lighting Cities Using Visible Light Communication and Light Fidelity

D. Sivamani¹, P. Thirusenthil Kumaran², C. Gnanavel³ and L. Nagarajan⁴

^{1,2,3,4}Assistant Professor, Department of EEE

^{1,2}Rajalakshmi Engineering College,

³AMETdeemed to be university

⁴K. Ramakrishnan College of Technology.

ABSTRACT

As energy saving sparing turns into the hotly debated issue now a days in the entire world, gigantic electric power consumption is devoured by the road lights because of its persistent working all through evening. energy saving sparing could be accomplished through the lighting as it is one of the most force utilization electrical gadgets. The lights turn on before people on walk and vehicles comes to reduce power when there is nobody in the street or yard. The controlling of the lights is done at the light's premises utilizing remote and pyro electric infrared sensors. The idea of a self-governing appropriated controlled light framework, in which the lights turn on before people on walk or vehicles comes and lessen brilliance to spare electric force when there is no traffic. A conveyed sensor organize is utilized to identify walkers or vehicles. Our shrewd road light framework comprises of a HB-LED light, a brilliance sensor, a movement sensor and a short-separation correspondence arrange VLC is developing field in optical remote correspondence which uses LED to transmit information. One of the most significant favorable circumstances of HB-LED lighting, specifically its powerful proficiency. The future scope of VLC will be presented. In street lamps, Li-Fi hotspots provide better Communication, Monitoring and Controlling of data.

KEY WORDS: ENERGY SAVING ,VLC,OWC,HB-LED,LI-FI.

INTRODUCTION

Assemble a vitality sparing keen lighting framework with incorporated sensors and controllers. Planning to save lighting framework which is perfect and adaptable with other business item and computerization system. Build an energy saving sparing shrewd lighting framework with coordinated sensors and Arduino controllers(Ron Lenk et al,2011). Plan a keen lighting framework with LED, which

makes the framework versatility and expandability. Wise lighting control and vitality the executives' framework is an ideal answer for vitality sparing, particularly in broad daylight lighting the board. It understands remote on/off and darkening of lights, which can spare vitality by 40%, spare lights upkeep costs by half, and drag out light life by 25%. The framework application in streetlight control will diminish in streetlight power and upkeep cost, and increment accessibility of road light. It is necessary to determine (A. Nazar Ali et al,2014) to diminish in a specific zone or inside a specific time range, this framework assists with darkening the lights likewise. On the off chance that the walker traffic diminishes fundamentally state somewhere in the range of 1:00AM and 5:00AM, at that point darkening the lights is the correct arrangement. In developing newer techniques (D.Shyam et al,2019) diminish the brightening of the

ARTICLE INFORMATION

Received 15th April 2020 Accepted after revision 20th May 2020
Print ISSN: 0974-6455 Online ISSN: 2321-4007 CODEN: BBRCBA

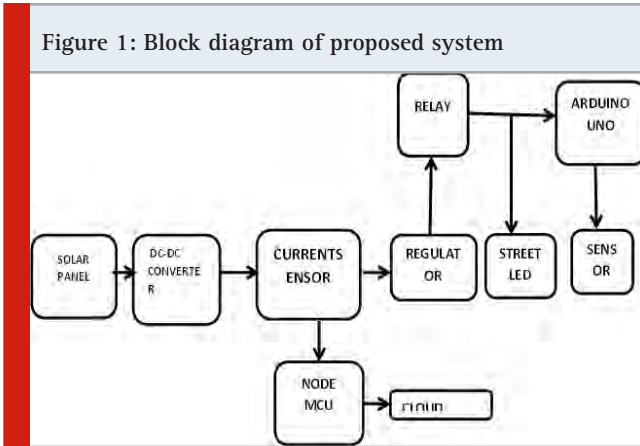
Thomson Reuters ISI Web of Science Clarivate Analytics USA and Crossref Indexed Journal



NAAS Journal Score 2020 (4.31) SJIF: 2020 (7.728)
A Society of Science and Nature Publication,
Bhopal India 2020. All rights reserved.
Online Contents Available at: <http://www.bbrc.in/>

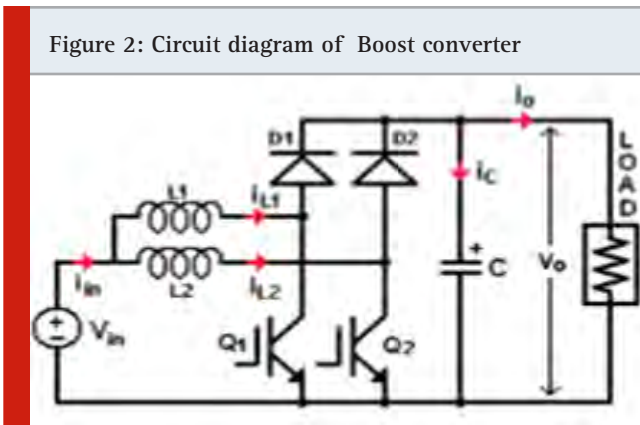
road lights to 20% at whatever point no person on walk or vehicle was distinguished, there is sparing of energy saving and improving the performance of the system(A.Nazar Ali et al,2015; AT Sankara Subramanian et al,2017).

Block Diagram



The proposed block diagram of the complete powering smart street light system with visible light communication and LIFI shown in figure1. The proposed module consists of solar panel, DC-DC converter, Regulator,relay,Node MCU, cloud storage, street light as HB LED,Arduino m The lamp module should be communicate (S.R.Paveethra et al,2019) and control through wireless.

Working of Boost Converter: The proposed converter made up of two single-stage help converters associated in equal and shown in figure2. The two PWM signal contrast is 180 deg when each switch is controlled with the interleaving technique (C.Kalavalli et al,2020). Since every inductor current extent is diminished by one for every stage, we can decrease the inductor size and inductance when the info current moves through two lift inductors. The information current wave is diminished in light of the fact that the info current is the total of every current of inductor L1 and L2 (Premkumar et al,2015).



At the point when the switch is shut, current courses through the inductor clockwise way and the inductor

stores the vitality. Extremity of the left half of the inductor is sure. At the point when the switch is opened, current will be diminished as the impedance is higher. Accordingly, change or decrease in current will be restricted by the inductor. The extremity will be turned around (implies left half of inductor will be negative at this point). Along these lines two sources will be in arrangement making a higher voltage charge the capacitor through the diode(Premkumar et al,2018).

The modes of operation are explained as below.

MODE 1:

At Initial time, Q₁ is closed and Q₂ is opened. The current flow through the inductor L₁ starts to rise.

The rate of change of L₁ is

$$L_1 (di/dt) = V_i / L,$$

while the rate of change of L2 is

$$L_1 (di/dt) = (V_i -V_o) / L_2$$

MODE 2 :

At time T₁, Q₁ and Q₂ are opened. The inductors L₁ and L₂ discharge through the load.

$$L_1 (di/dt) = L_2 (di/dt) = (V_i -V_o) / L$$

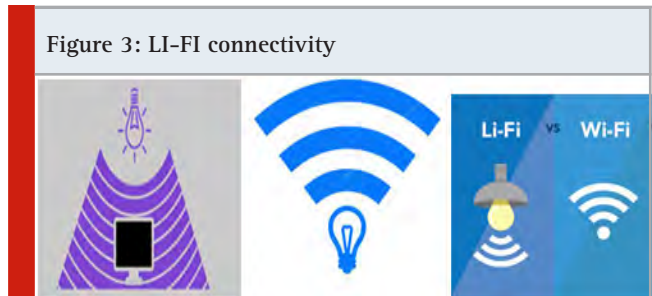
MODE 3:

At time T₂, Q₂ is closed while Q₁ still opened. The current of the inductor L₂ starts to rise, while L₁ continues to discharge.

MODE 4:

At time t₃, Q₂ is opened and Q₁ still opened. The situation is same as state b. The inductors L₁ and L₂ discharge through the load. Due to the symmetry of the circuit, the next state is similar to the previous.

4.LI-FI



Light Fidelity or Li-Fi is a Visible Light Communications (VLC) framework running remote interchanges going at extremely high speeds. The on-off movement of LEDs empowers a sort of information transmission utilizing double codes mode anyway the natural eye can't see this change and the LEDs seem to have a consistent force. Li-Fi can work submerged where Wi-Fi bombs totally.

MATERIALS AND METHODS

Hardware and Software Implementation

a. Integration Of The Sensors With Arduino: Sensors are directly interfaced to the controller whose sensed values predict the movement of vehicles or pedestrians. The

Infrared sensors and the Relay pins are connected to the digital pins of Arduino. The 3 IR sensor's out pins are connected to D2, D3, D4 pins of Arduino respectively. The IN1, IN2, IN3 pins of 4-channel Relay are connected to D5, D6, D7 pins of Arduino respectively. The IR sensor's VCC and GND are connected to the 5V and GND pins of Arduino. The VCC and GND pins of 4-channel Relay are connected to the 5V and GND pins of Arduino.

b. INTERFACING OF Nodemcu: NodeMCU is an open source IoT platform which acts as a network processor which can be connected to the nearest Wi-Fi hot spot for internet connectivity. The processed data from the sensors are sent to the cloud using the NodeMCU interfaced with Arduino. The VCC and GND pins of Current sensor (ACS712) are connected to the 3V and GND pins of NodeMCU. The out pin of Current sensor is connected to the A0 pin of NodeMCU.

C. Uploading To The Cloud: The data which is sent to the NodeMCU controller is finally uploaded to the cloud. The data in the cloud is displayed for the user in a web server. The data of the power usage in the cloud can be viewed in the form of graphs with a minimum time delay of one second (X. Yin et al,2016). The data can also be generated as a report in an excel sheet between the particular dates, months and years. It can be accessed anywhere in live by the authorities and public at any time using the URL (Ran Wang et al,2014; J.M.Alonso et al,2011).

RESULT AND DISCUSSION

SIMULATION AND ITS OUTPUT

Figure 4: Simulation of proposed converter

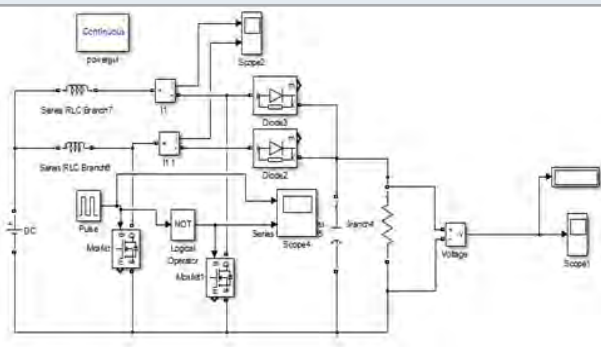
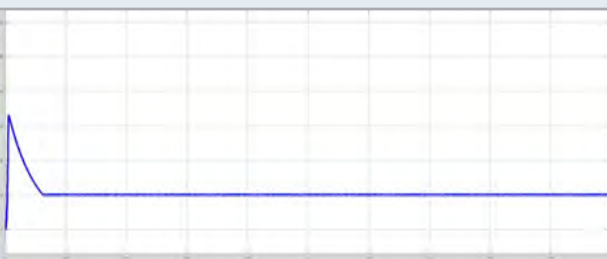


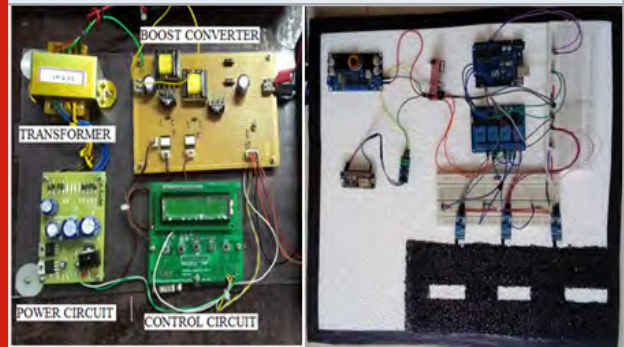
Figure 4, the proposed converter is simulated in open loop and closed loop operations.

Figure 5: Output Waveform for Boost converter



HARDWARE IMPLEMENTATION

Figure 6: prototype for proposed system



Battery is connected to supply the Boost converter. The output of the converter is connected to the current sensor and the voltage regulator. The input voltage of the converter is 1.2V and the output voltage of 5V is given to the regulator. The current sensor is connected to sense the current in the circuit. The Regulator voltage of 3.3V and 5V are connected to the NO and NC contacts of relay and the OUT pin is connected to the LED. When the IR sensor1 detects vehicle movement the nearest LED glows high i.e. with 5V supply, after the passing of vehicle the LED glows with 3.3V supply. The dimming of LED is implemented by the switching of relay using an Arduino program. Similarly, when the IR sensor2 and IR sensor3 detect vehicle movement the adjacent LED goes HIGH and when no movement is detected it goes to LOW state i.e. 3.3V. Here the LED goes to OFF state only in the morning. This work deals with (A.Nazar Ali et al,2019) value of current measured is fed to the nodeMCU and the corresponding voltage, current and power usage are uploaded in the cloud (M.V.Mreno et al,2017).

Figure 7: Sensor output



Hardware Output

a.SENSOR OUTPUT DISPLAYED IN SERIAL MONITOR:

The reading of the car or vehicle passing is viewed in the serial monitor of Arduino IDE. When no movement is detected the data output is 1 and when movement is detected the data output changes to 0.

b.GRAPHICAL REPRESENTATION IN CLOUD: The graph of the Voltage is shown in ,current measured which is shown in Figure7 and power usage is shown in Fig.8. The data can be (V.Venkatesh et al,2019) uploaded using the

Wi-Fi hotspot and can be accessed anywhere in live by the authorities and public at any time using the URL.

Figure 8: Graphical representation of voltage

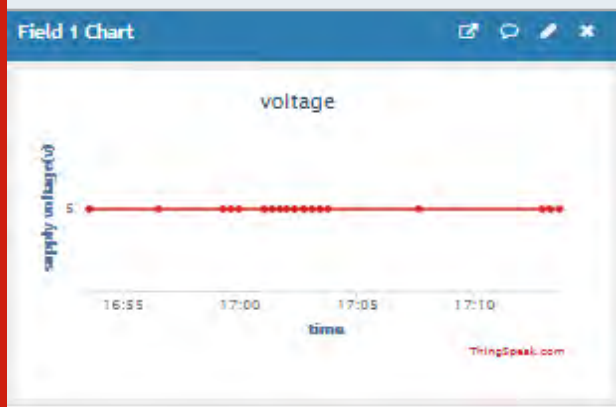
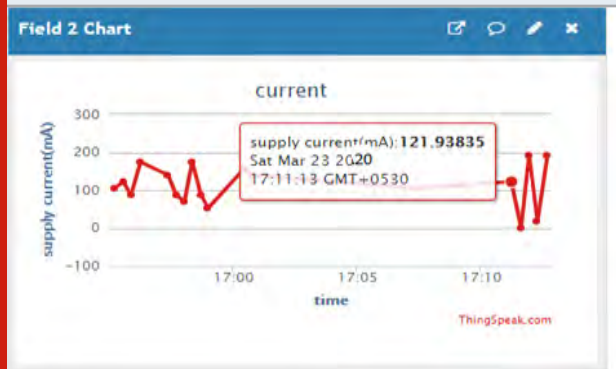


Figure 9: Supply frequency vs Time



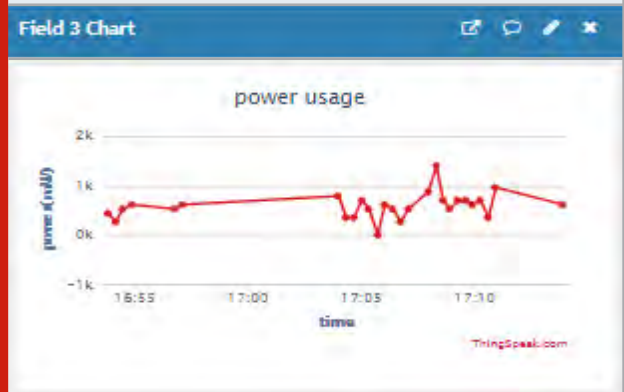
Figure 10: Current vs time



CONCLUSION

This framework is one of the practical lighting arrangements. The solid element of this framework is adaptability, expandability, vigor and similarity. The controlling road light makes the simplicity mix of lighting control and sensors into various sorts of modules that is input module and light module. This independent model can be applying on the light module relies upon various kinds of circumstance in industry open yard zone

Figure 11: Graphical representation of power usage



In this way, in future work advancement, more modules can be configuration to deal with more framework, for example, cooling, security framework and so forth.

REFERENCES

- A Ali Nazar R Jayabharath MD Udayakumar (2014) An ANFIS Based Advanced MPPT Control of a Wind-Solar Hybrid Power Generation System International review of modelling and simulations vol.7 no. 4 pp. 638-643.
- A.Nazar Ali and R. Jayabharath (2014) Performance Enhancement of Hybrid Wind/Photo Voltaic System Using Z Source Inverter with Cuk-sepic Fused Converter Research Journal of Applied Sciences Engineering and Technology 719 p. 3964-3970.
- AT Sankara Subramanian P Sabarish, A Nazar Ali(2017) A power factor correction based canonical switching cell converter for VSI fed BLDC motor by using voltage follower technique| IEEE International Conference on Electrical, Instrumentation and Communication Engineering (ICEICE) pp.1-8.
- A Nazar Ali D Sivamani R Jaiganesh M Pradeep (2019) Solar powered air conditioner using BLDC motor, IOP Conference Series: Materials Science and Engineering, vol. 23.
- M V Moreno et al., (2017) Applicability of Big Data Techniques to Smart Cities Deployments in IEEE Transactions on Industrial Informatics, vol. 13 no. 3 pp. 800-809
- .C.Kalavalli S.R.Paveethra S.Murugesan Dr.A.Nazar Ali, (2020) Design And Implementation Of High Efficiency H6 PV Inverter With Dual Axis Tracking, International Journal of Scientific & Technology Research Vol 9 issue 02 pp. 4728-31.
- J M Alonso A J Calleja D Gacio J Cardesin and E López (2011) A longlife high-power-factor HPS-lamp LED retrofit converter based on the integrated buck-boost buck topology IECON 2011 - 37th Annual Conference of the IEEE Industrial Electronics Society Melbourne VIC pp. 2860-2865.
- Premkumar, Kamaraj et al. (2018) Antlion Algorithm Optimized Fuzzy PID Supervised On-line Recurrent

Fuzzy Neural Network Based Controller for Brushless DC Motor Electric Power Components and Systems 45 20 pp.2304-2317.K

Premkumar et al. (2018) Novel bacterial foraging-based ANFIS for speed control of matrix converter-fed industrial BLDC motors operated under low speed and high torque Neural Computing and Applications 21 12 pp.1411-1434.

.Premkumar et al. (2015) GA-PSO optimized online ANFIS based speed controller for Brushless DC motor Journal of Intelligent & Fuzzy Systems 28 6 pp.2839-2850.

Ran Wang Choice on Control System Technology of Intelligent Lighting. Electrical & Intelligent Building, 2014 1-2: 79-81.

Shyam D Premkumar K Thamizhselvan T Nazar Ali A Vishnu Priya M(2019) Symmetrically Modified

Laddered H-Bridge Multilevel Inverter with Reduced Configurationally Parameters International journal of engineering and advanced technology Vol 9 issue 1.

S.R.Paveethra, C.Kalavalli, S.Vijayalakshmi, Dr.A.Nazar Ali, D.Shyam (2020) Evaluation Of Voltage Stability Of Transmission Line With Contingency Analysis, International Journal of Scientific & Technology Research Vol 9 issue 02 pp. 4018-22

V Venkatesh A Nazar Ali R Jaiganesh. V Indiragandhi (2019) Extraction and conversion of exhaust heat from automobile engine in to electrical energy Energy| IOP Conference Series: Materials Science and Engineering vol. 23.

X. Yin and S. L. Keoh, Personalized ambience: An integration of learning model and intelligent lighting control 2016 IEEE 3rd World Forum on Internet of Things (WF-IoT) Reston VA 2016, pp. 666-671.

Performance Analysis of Various Photovoltaic Configurations Under Uniform Shading and Rapid Partial Shading Formations

A. T. Sankara Subramanian^{1*}, P. Sabarish², M. D.Udayakumar³ and T. Vishnu kumar⁴

^{1,2,3,4}Assistant Professor,

^{1,2,3,4}Department of EEE, K. Ramakrishnan College of Technology, Trichy-621112, India.

ABSTRACT

In this work, Different PV alignments are simulated with different patterns of shading condition are simulated using MATLAB Simulink and the Outputs are analyzed based on the factors Shading loss, Mismatch loss and Fill factor of the array. Energy requirement is an ever increasing factor throughout the world with global development taking place in all sectors. Sufficient generation of power to meet the increasing demand and to get rid of crisis is always observed to be a challenging task. Though the fossil fuel based power generation satisfies the maximum demand in the 20th century, it is well aware that the fossil fuels cannot be obtained instantly and not long repeatedly. So, power sectors now mostly depends on the renewable sources of power generation especially Solar. Ecofriendly Solar energy is abundant and available for free for power generation. There are plenty of means of extracting power from solar energy. Photovoltaic arrays are used to convert the irradiance from the sun light to electrical energy. But the perplexing factor is that the irradiance of the sunlight is not uniform throughout the day and that to because of the presence of natural or manmade obstacles it is also not spread uniformly over the PV array resulting in partial shading condition. This in turn affects the performance of the system introducing many local maxima in the nonlinear Power versus voltage characteristics of the panel. Also this non uniform shading results in shading loss in the Net output of PV array

KEY WORDS: PHOTOVOLTAIC, PARTIAL SHADING, PV CONFIGURATION, FILL FACTOR.

INTRODUCTION

Power demand is a major factor which any country in the world wants to address without affecting the reliability and continuity. When this is the situation, the cause need to be satisfied without any more increase in pollution, that

is the usage of fossil fuels for power generation need to come down and the green energy should be emphasized. In this regard, solar energy is identified to be the surplus source of energy and the electrical power can be extracted from it on two different ways. The first way is to make use of solar glass collectors or solar thermal method and the second is by using Photovoltaic arrays. The first method is very cheap but less reliable whereas the second method is slightly costly when it comes to large scale installation but relatively more reliable. But the major Problem associated with the power generation based on solar its poor conversion efficiency of less than 20%. It attracts the attention of many researchers and many literatures

ARTICLE INFORMATION

*Corresponding Author: sankar1490@gmail.com

Received 15th April 2020 Accepted after revision 20th May 2020

Print ISSN: 0974-6455 Online ISSN: 2321-4007 CODEN: BBR CBA

Thomson Reuters ISI Web of Science Clarivate Analytics USA and Crossref Indexed Journal



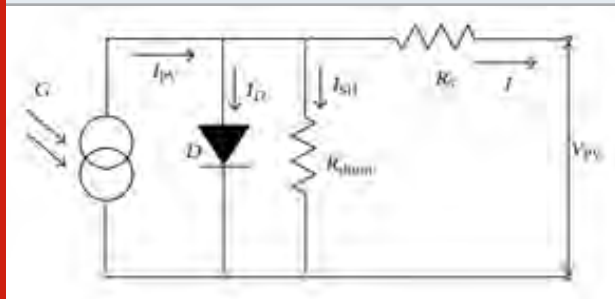
NAAS Journal Score 2020 (4.31) SJIF: 2020 (7.728)

A Society of Science and Nature Publication,
Bhopal India 2020. All rights reserved.

Online Contents Available at: <http://www.bbrc.in/>

already addressing the most suitable way to extract the highest possible wattage from the PV array.

Figure 1: PV Cell model using a Diode



One of the main factor which will affect the maximum power generation is the Array Alignment starting from simple series to complicated Honey womb formation of PV alignments. Though many researches address this issue under uniform irradiance available over the array, only few emphasis on the variation in irradiance due to natural reasons such as passing of clouds, Shadows of infrastructures and trees etc. It severely affects the chance of finding the global highest wattage point of an array by providing more local maxima for different irradiance level. Though it is an unavoidable phenomena, by selecting suitable PV array alignment, the maximum possible Power can be obtained from the array.

PV Cell Model with one diode: Figure 1 shows the modelling of PV cell using one diode, the irradiance of the cell is mentioned in the model as ‘G’, which is meant to be a current source with Ipv source current which in turn divides into ID and IP with the presence of Parallel diode and an internal Resistance Rp or Rshunt. These is an series cell resistance of Rs is also connected where Rs is less when compared to Rshunt. The output voltage is mentioned as Vpv. The silicon based PV cells will have a cell voltage of 0.7 volts. The cells are connected in different alignments to obtain the array.

Figure 2: PV module Equivalent circuit

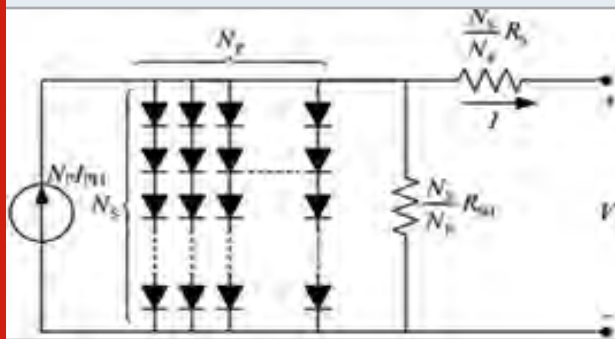


Figure 2 describes the approximate equivalent circuit of Photovoltaic array which comprises of Ns number of cells connected in series and Np number of cells connected in parallel. The total number of cells present in the module will be the product of Ns and Np. For example, in a 6x6 PV

array there will be 36 cells. The net open circuit voltage and short circuit current of module depends on how the 36 cells are connected. The impact of change in PV alignment cannot be much differentiated when the cells receives irradiance uniformly but under partial shading formations the case is different and each alignment provides different Maximum wattage points based on the local maxima obtained due to non-uniform shading formation over the module.

For a PV Cell, the equation which addresses the relationship between voltage and current is as follows,

$$I_{out} = I_{pv} + I_0 \left[e^{\left(\frac{q}{kTA} (+IR_{se}) - 1\right)} \right] - \frac{(V+IR_{se})}{R_{Par}} \quad (1)$$

where I_{pv} is the photon made current, I_0 is the saturation cell dark amperes, A is the diode constant, k refers Boltzmann’s constant (1.38×10^{-23} Joule/Kelvin), T is the internal working temperature of the PV cell measured in kelvin and q is the electron charge (1.6×10^{-19} Coulomb). The dependency of PV based generation on the factors of temperature and irradiance is described by the following equation,

$$I_{pv} = [I_{sc} + KI_{out} (T - T_{ref})] GC / G_{nom} \quad (2)$$

where I_{sc} refers to the PV current when the terminals short circuited, KI_{out} is the SC current-Temp coefficient of PV cell, G_c shows the available irradiance to the cell and G_{nom} refers the nominal irradiation the PV cell in W/m^2 .

The value of current which saturates depends hardly on the temperature of the cell and it is given by the expression,

$$I_0 = I_{nom} \left(\frac{T_{ref}}{T}\right)^3 \left[e^{\left(\frac{-1.12q}{kA} \left(\frac{1}{T_{ref}} - \frac{1}{T}\right)\right)} \right] \quad (3)$$

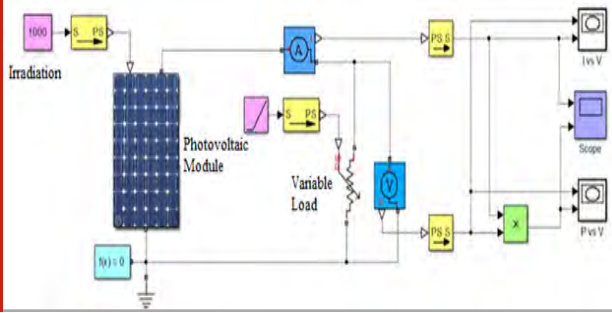
For a PV Cell, the equation which addresses the relationship between voltage and current can be also expressed as follows,

$$I_{out} = N_{ph} I_{ph} + N_p I_0 \left[e^{\left(\frac{q}{kTA} \left(\frac{V}{N_s} + \frac{IR_{ser}}{N_p}\right) - 1\right)} \right] - \frac{\left(\frac{N_s V}{N_s} + IR_{ser}\right)}{R_{Par}} \quad (4)$$

From the above equation it is clear that the number of cells connected in series and parallel will have a major impact in the output current of the PV module.

Figure 3 shows the basic simulation diagram of PV module which is meant to simulate the required model of PV series PVCLU50FC and to study the P-V and I-V characteristics of the desired PV module. The specification as mentioned by the vendor is mentioned in Table 1. The simulation can be also extended to partial shading condition by making changes in the irradiance value of each cell as per the sample patterns discusses in this work.

Figure 3: Simulation diagram of PV module in MATLAB Simulink



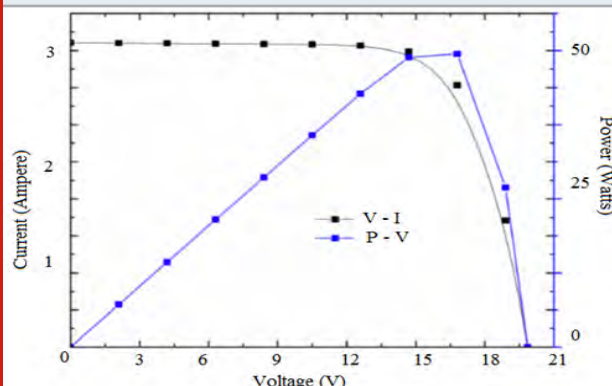
The Specifications of PVCLU50FC – an 50W Monocrystalline PV module as given by the manufacture is shown in table 1 as follows,

Table 1. Specification of selected PVCLU50FC PV module

Description	Rating/ Specification
Type of cell	Monocrystalline
No. of cells	36 Cells
Pmax (Maximum Power)	50W
O.C Voltage (V_{oc})	22.2 Volts
S.C Current (I_{sc})	3.4 Amps
Voltage corresponding to Pmax (V_{mp})	17.8 Volts
Current corresponding to P_{max} (I_{mp})	2.7 Amps
Efficiency of PV Module	15.1%
Maximum voltage of system	DC 600 Volts

Based on the realization of the PV module in the MATLAB software, the characteristics of I-V and P-V obtained are shown in the following figure 4, Which shows the variation of module power and module current with the module voltage. It resembles the specifications given in the above table 1 and thus the simulation for partial shading formation can be proceeded without any deviation.

Figure 4: Simulation output showing the I-V and P-V Characteristics of the PV module



Photovoltaic alignments under consideration: As given in figure 5, five different PV alignments are considered for discussion in this paper which includes Series, Series Parallel, Total-Cross-tied, Bridge linked and the Honey womb formations.

Each alignment is studied based on the available literatures and the observations are summarized as follows,

Series alignment: All the cells are connected in series. It offers high voltage and low current output.

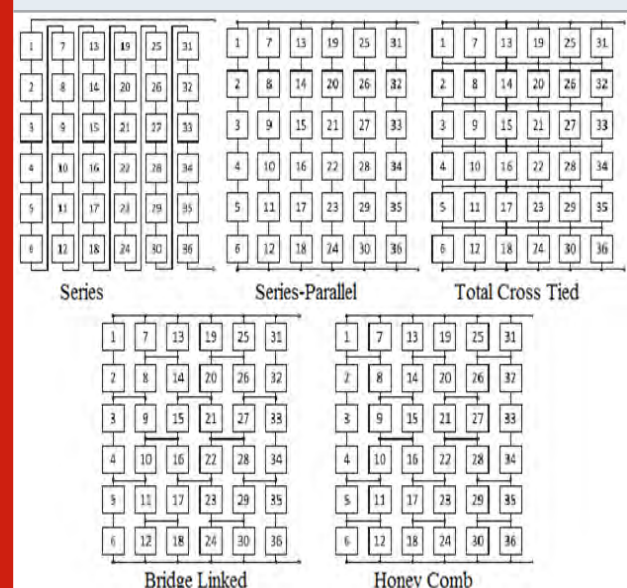
Series Parallel: This alignment is meant to overcome the drawback of series alignment by connecting all the cells in a column serially and then connecting all columns in parallel.

Total-Cross-tied: This alignment is formed by row-wise connection of all the cross-ties in Series parallel connection as shown in figure 5.

Bridge linked: Here four modules are connected as in figure 5 to form bridges. So it has a fixed bridge size. Two connected serially followed by two in parallel.

Honey Womb: It is an altered version of Bridge linked, here the difference is that there is no fixed bridge size.

Figure 5: Various PV Alignments under consideration



MATERIALS AND METHODS

Analysis of PV alignments under Uniform irradiance and Partial Irradiance cases: Based on the simulation done with different PV alignments as mentioned in figure 5, the I-V and P-V characteristics for different irradiance is shown in the figure 6. It is observed that the in I-V characteristics, with the increase in the irradiance from 200W/m² to 1000W/m², there is a gradual increase in

the module current i.e at 1000 W/m² the module current is 3.2 A whereas it gets reduced to 0.7 A for 200 W/m². Similarly in P-V characteristics it is observed that the maximum output module power increases with increase in the irradiance. i.e for 200 W/m² the P_{max} is 8 W whereas for 1000 W/m² the value rises upto 48.5 W.

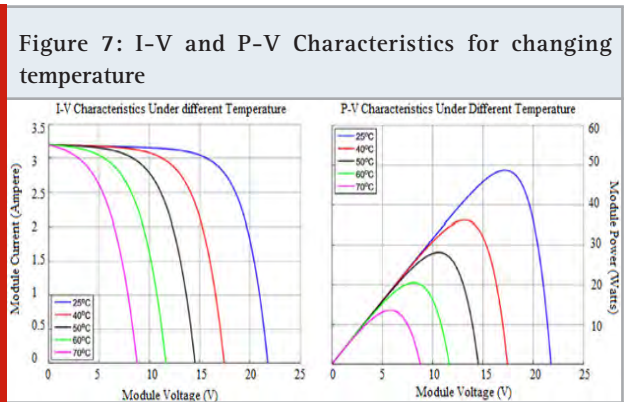
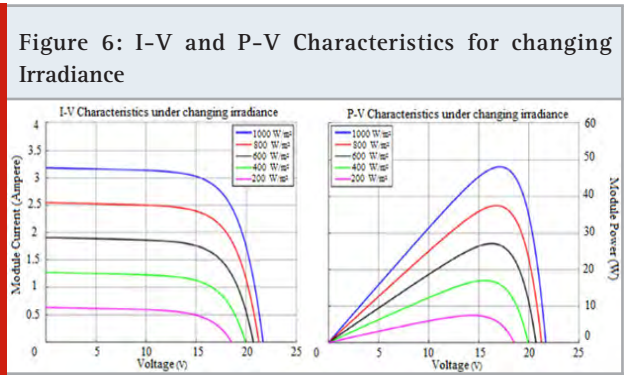


Figure 7 shows the impact of change in temperature on the I-V and P-V characteristics of the PV module. It is observed that the in I-V characteristics, with the increase in the temperature from 25°C to 70°C, there is a gradual decrease in the module voltage i.e at 25°C the module voltage is 22 V whereas it gets reduced to 8.6 V for 70°C. Similarly in P-V characteristics it is observed that the maximum output module power decreases with increase in the temperature. i.e for 25°C the P_{max} is 48 W whereas for 70°C, the value drops to 12.5 W. So it is observed clearly that suitable heat sinks need to be provided so as to obtain maximum wattage from the PV module and also it prevents the PV module from getting affected.

For the standard operating condition with the irradiance of 1000W/m² and at 25°C, the Values obtained through simulation is mentioned in the table 2

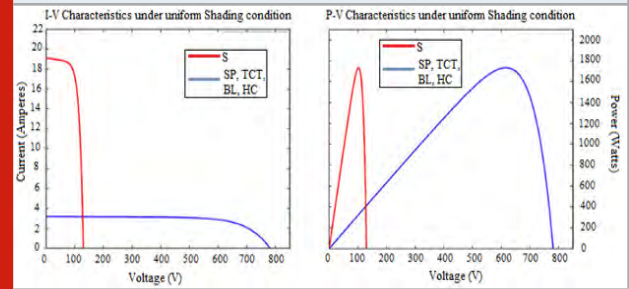
It is observed that at uniform irradiance all the PV alignments are providing same maximum wattage value of 1735 W. Series Alignments offers high voltage of 615V and low current of 2.856 A and other alignments are producing same characteristics as shown in figure 8. Hence the impact is emphasized more on Partial shading cases.

The impact of partial shading can be analyzed by framing following 6 shading formations in a 6 x 6 PV array with the specification as given earlier in table 1 is discussed as follows,

Table 2. Results of Various PV alignments under 1000W/m² and at 25°C

Alignment	(P _{max} -UC) (Watts)	Maximum Voltage (V)	Maximum Current (A)
Series	1735	615.4	2.856
Series Parallel	1735	101.8	16.89
Total Cross Tied	1735	101.8	16.89
Bridge Linked	1735	101.8	16.89
Honey Comb	1735	101.8	16.89

Figure 8: I-V and P-V Characteristics of various PV alignments under Uniform Shading



Shading formation 1 (Realization 1): 1st column has 1000W/m², 2nd and 3rd Column has 600W/m² and Last 3 columns has 400W/m² irradiance as shown in figure 9.

Shading formation 2 (Realization2): Left top 6 cells has 1000W/m², Right bottom 6 cells has 600W/m² and Remaining has 400W/m² irradiance as shown in figure 9.

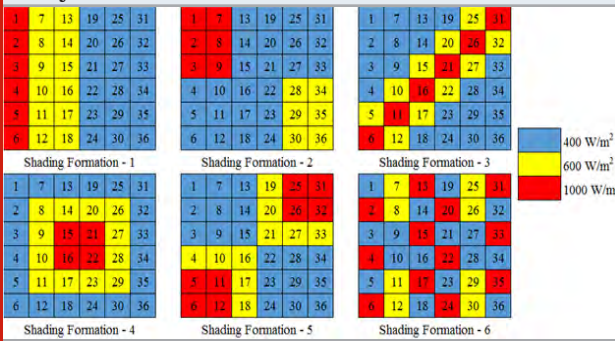
Shading formation 3 (Realization3): Diagonal cells has 1000W/m², nearby diagonal cells has 600W/m² and Remaining has 400W/m² irradiance as shown in figure 9.

Shading formation 4 (Realization4): Centre 4 cells has 1000W/m², nearby outer 12 cells has 600W/m² and Remaining has 400W/m² irradiance as shown in figure 9.

Shading formation 5 (Realization 5): Right top 4 cells and left bottom 4 cells has 1000W/m², nearby L- Shaped shading has 600W/m² and Remaining cells has 400W/m² irradiance as shown in figure 9.

Shading formation 6 (Realization 6): Right top 4 cells and left bottom 4 cells has 1000W/m², nearby L- Shaped shading has 600W/m² and Remaining cells has 400W/m² irradiance as shown in figure 9.

Figure 9: Sample Partial Shading formations under study



Under Partial shading formations, the maximum wattage experiences many local maxima which in turn together produces the global Pmax as shown in figure 10. It shows the comparison of P-V Characteristics of Shading formation 1 with that of the normal uniform shading that is discussed earlier. From the observations made the sum of maximum Wattages of separate modules are tabulated for different shading formations in Table 3.

Table 3. Data Obtained on P_{max}-I

Shading Formation in Module	ΣP _{max} Individual modules (P _{max} -I) (Watts)
Realization 1	1265.46
Realization 2	1392.8
Realization 3	1304.6
Realization 4	1338.4
Realization 5	1335.8
Realization 6	1068.4

RESULTS AND DISCUSSION

The observation is made by considering three important factors namely Shading loss, Mismatch Loss and Fill factor

Shading loss is the difference between the Maximum Wattage of the PV module during uniform irradiance and the sum of maximum wattages of separate modules.

$$\text{Shading loss} = P_{\text{max}} - \text{UC} - \Sigma P_{\text{max}} \text{ Individual modules (P}_{\text{max}}\text{-I)} \quad (5)$$

Mismatch Loss is the difference between the sum of maximum wattages of separate modules and Global Maximum wattage of the module.

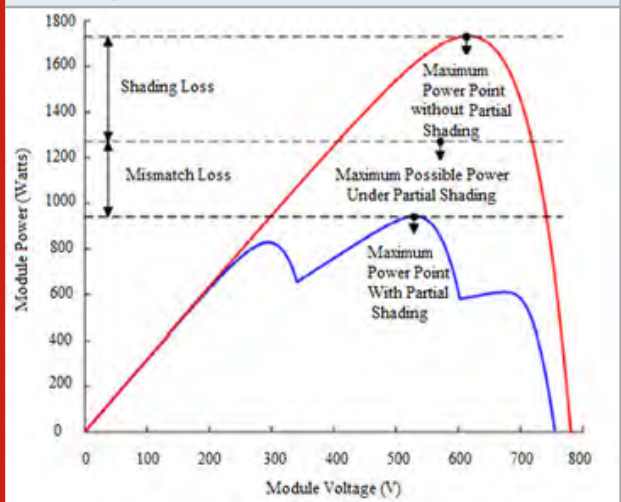
$$\text{Mismatch Loss} = \Sigma P_{\text{max}} \text{ Individual modules (P}_{\text{max}}\text{-I)} - P_{\text{GMP}} \quad (6)$$

Fill factor is calculated by the ratio of Global Maximum wattage of the module and the Product of O.C voltage and S.C Current of the module.

$$\text{Fill factor} = (P_{\text{GMP}}) / (\text{Voc} \times \text{Isc}) -$$

Table 4 shows the Performance data related to the P-V characteristics of various PV alignments under different shading formations.

Figure 10: P-V characteristics for shading formation 1 as a Sample



From Table 4 it is observed that at Realization 1, Honey comb has the highest Power of 1245 W whereas Series has the worst value of 943.35 W. In all other realization from 2 to 6, the Total Cross tied alignment has the highest power ranging at 1346.9 W, 896.5W, 1168.2W, 1159.6W and 1004.5W in Realizations 2 to 6 respectively. Hence it is clear that the Total cross tied alignment will offer more Pmax for partial shading formations. Table 5 shows the final results of this work as a comparison of Shading loss, Mismatch loss and Fill factor values calculated based on formulae given in equations 5,6 and 7.

Figure 11: Shading loss comparison of various PV alignments subjected to different shading formations

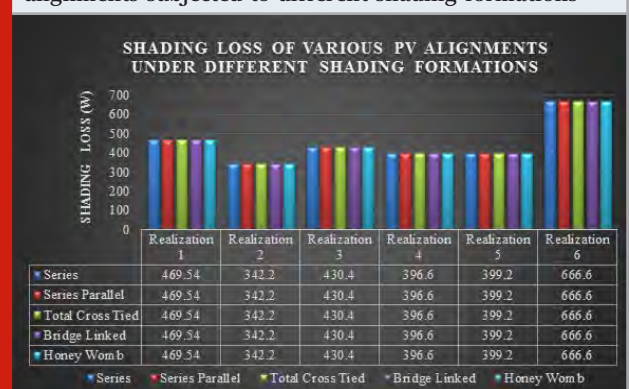


Table 4. Data Obtained from P-V curves of different PV alignments subjected to defined shading formation

Shading Formation	Alignment	Maximum Power (Watts)	Maximum Voltage (V)	Maximum Current (A)	GMP (W)	O.C Voltage (V)	S.C Current (A)
Realization 1	Series	943.35	535.2	1.78	942.4	754.2	3.14
	Series Parallel	1245	98.2	12.46	1244	127.9	14.53
	Total Cross Tied	1245	98.2	12.46	1244	127.9	14.53
	Bridge Linked	1245	98.2	12.46	1244	127.9	14.53
	Honey Comb	1245	98.2	12.46	1244	127.9	14.53
Realization 2	Series	1125	401.2	2.72	1126	762.4	3.16
	Series Parallel	1114.6	102.6	10.68	1112.6	128.32	10.64
	Total Cross Tied	1346.9	98.46	13.57	1345	128.92	11.8
	Bridge Linked	1174.4	106.8	11.05	1178.6	128.42	10.66
	Honey Comb	1168.5	105	11.01	1165.2	128.62	10.85
Realization 3	Series	556.86	634.4	0.865	554.8	761.2	1.96
	Series Parallel	724.8	88.6	8.28	726.2	123.16	16.06
	Total Cross Tied	896.5	100.7	8.94	897.6	123.96	12.38
	Bridge Linked	736.6	84.8	8.62	735.8	123.4	14.65
	Honey Comb	784.2	102.6	7.66	775.2	123.63	15.54
Realization 4	Series	1016.8	578.9	1.75	1016.5	760.1	3.16
	Series Parallel	1104.8	103.2	10.56	1102.6	127.12	19.01
	Total Cross Tied	1168.2	102.9	11.16	1164.9	128.2	19.65
	Bridge Linked	1105.4	102.4	10.64	1106.2	127.42	19.43
	Honey Comb	1136	102.2	10.88	1136	127.84	19.62
Realization 5	Series	1006.7	568.4	1.67	1008.9	758.45	2.96
	Series Parallel	1098.2	103.7	10.68	1095.2	126.3	18.56
	Total Cross Tied	1159.6	104.6	11.18	1158.6	127.1	18.74
	Bridge Linked	1118.3	104.8	10.86	1118.2	126.5	19.1
	Honey Comb	1104.2	103.5	10.72	1102.9	126.9	18.24
Realization 6	Series	725.6	416.5	1.76	728.02	744.5	3.17
	Series Parallel	682.8	48.98	13.96	692.4	123.5	18.96
	Total Cross Tied	1004.5	102.7	9.74	1003.2	124	14.54
	Bridge Linked	732.86	104.6	7.08	734.5	123.6	15.68
	Honey Comb	742.97	105.2	7.12	742.8	123.7	17.48

Figure 12: Mismatch loss comparison of various PV alignments subjected to different shading formations

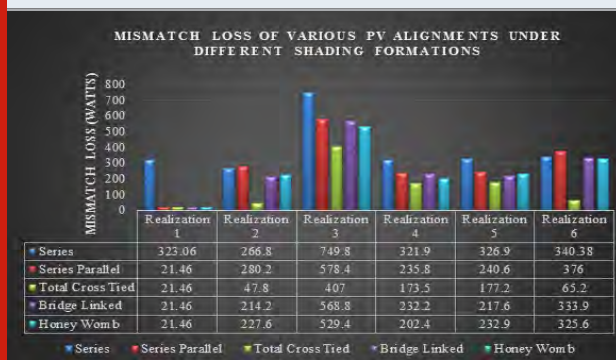


Figure 13: Fill Factor comparison of various PV alignments subjected to different shading formations

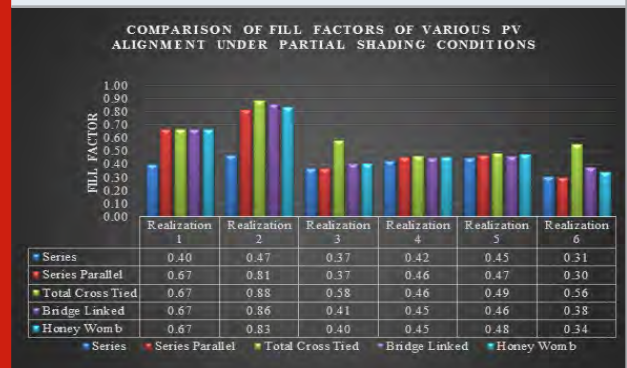


Table 5. Calculated values of Shading loss, Mismatch loss and Fill factor of various PV alignments subjected to different shading formations

Shading Formation	Factors	Series	Series Parallel	Total Cross Tied	Bridge Linked	Honey Comb
Realization 1	Shading losses (W)	469.54	469.54	469.54	469.54	469.54
	Mismatch Loss (W)	323.06	21.46	21.46	21.46	21.46
	Fill Factor	0.40	0.67	0.67	0.67	0.67
Realization 2	Shading losses (W)	342.2	342.2	342.2	342.2	342.2
	Mismatch Loss (W)	266.8	280.2	47.8	214.2	227.6
	Fill Factor	0.47	0.81	0.88	0.86	0.83
Realization 3	Shading losses (W)	430.4	430.4	430.4	430.4	430.4
	Mismatch Loss (W)	749.8	578.4	407	568.8	529.4
	Fill Factor	0.37	0.37	0.58	0.41	0.40
Realization 4	Shading losses (W)	396.6	396.6	396.6	396.6	396.6
	Mismatch Loss (W)	321.9	235.8	173.5	232.2	202.4
	Fill Factor	0.42	0.46	0.46	0.45	0.45
Realization 5	Shading losses (W)	399.2	399.2	399.2	399.2	399.2
	Mismatch Loss (W)	326.9	240.6	177.2	217.6	232.9
	Fill Factor	0.45	0.47	0.49	0.46	0.48
Realization 6	Shading losses (W)	666.6	666.6	666.6	666.6	666.6
	Mismatch Loss (W)	340.38	376	65.2	333.9	325.6
	Fill Factor	0.31	0.30	0.56	0.38	0.34

From Table 5, It is observed that the Shading loss will not be affected by selection of PV alignment since the values remains equal as mentioned in figure 11 for any specific realization. When it comes to Mismatch loss for all realization it is found from figure 12 that the Total cross tied is having the lowest loss among all PV Alignments under discussion about 7% to 12.5%. In terms of Fill factor, the Total cross tied is possessing highest value among all alignments in any shading pattern as per figure 13. Hence it is very much justifiable to Choose Total Cross tied alignment for Partial shading cases

CONCLUSION

After detailed data analysis using MATLAB Simulink, it is observed that Total Cross Tied alignment will provide most desirable solution, though the selection of PV alignments will not bring change in the Shading losses under different shading conditions, TCT found to be best suited for partial shading formations as it offers only less mismatch loss and Better fill factor when compare to other PV Alignments. Hence Selection of PV alignment will impact strongly on the Performance of PV in terms of its efficiency, Mismatch loss and Fill factor. It is also noted based on the available data that not only the PV alignment but also the value of irradiance, Shading formation and Temperature affects the efficiency of the Photovoltaic system. By Choosing Total cross tied Alignment with Suitable MPP method will yield improved efficiency and performance in Photovoltaic systems.

REFERENCES

Edwin M et al (2019) IOP Conf Ser Mater Sci Eng 623

012022.

Jai Ganesh R S Kodeeswaran M Kavitha T Ramkumar Performance analysis of piezoelectric energy harvesting system employing bridgeless power factor correction boost rectifier.

Kalavalli C SR Paveethra S Murugesan Dr A Nazar Ali Dr V Venkatesh (2020) Design and Implementation Of High Efficiency H6 PV Inverter With Dual Axis Tracking International Journal Of Scientific & Technology Research Volume 9 Issue 02 Issn 2277-8616.

Kavitha M and R Jai Ganesh Hierarchical Classifier for Breast Cancer Diagnosis Journal of Advanced Research in Dynamical and Control Systems Volume 11- 04 Special Issue Pages 607-611 1943-023X.

Kavitha M R Jai Ganesh & A Rajkumar (2019) Facilities Navigation And Patient Monitoring System Using Ibeacon Technology International Journal Of Mechanical And Production Engineering Research And Development (Ijimperd) Issn (P) 2249-6890 Issn (E) 2249-8001 Vol 9 Special Issue 1 562-570.

Nazar Ali A et al (2019) IOP Conf Ser Mater Sci Eng 623 012010.

Okan Bingol Burçin Ozkaya (2018) Analysis and comparison of different PV array configurations under partial shading conditions Solar Energy.

Paveethra SR C Kalavalli S Vijayalakshmi Dr A Nazar Ali D Shyam (2020) Evaluation Of Voltage Stability Of Transmission Line With Contingency Analysis International Journal Of Scientific & Technology Research Volume 9 Issue 02 February 2020 Issn 2277-8616.

Pradeep M et al (2019) IOP Conf Ser Mater Sci Eng 623 012017.
Sabarish P et al (2019) IOP Conf Ser Mater Sci Eng 623 012011.
Sankara Subramanian AT et al (2019) IOP Conf Ser Mater Sci Eng 623 012012.
Subramanian A & Ali Nazar (2017) A power factor correction based canonical switching cell converter for VSI fed BLDC motor by using voltage follower technique 1-8 101109/ICEICE20178191932.
Thirusenthil Kumaran P P Pushpakarthick G V Chidambarathanu M Venkatachalam Xavier Raja Durai R Jaiganesh (2019) Power quality in distribution

grids International Journal of Innovative Technology and Exploring Engineering (IJITEE) ISSN 2278-3075 Volume-9 Issue-1.
Udayakumar M D et al (2019) IOP Conf Ser Mater Sci Eng 623 012018.
Venkatesh A et al (2019) IOP Conf Ser Mater Sci Eng 623 012009.
Vijayalakshmi S P Sabarish SR Paveethra Dr PR Sivaraman Dr V Venkatesh (2020) Exploration And Applications Of Electronic Balance For High Power Discharge Lamps At High Frequency Through Power Factor Modification International Journal Of Scientific & Technology Research Volume 9 Issue 02 Issn 2277-8616.

Design of FIR Filter Using High Speed Wallace Tree Multiplier with Fast Adders

Dr. A. Kavitha^{1*}, S. Suvathi Priya², S. Naveena³, B. Vijiyaprabha⁴ and S. Prasheetha⁵

^{1*}Professor, ^{2,3,4,5}UG Scholars

^{1,2,3,4,5}Department of ECE, K. Ramakrishnan College of Technology, Trichy-621112, India.

ABSTRACT

-In present day scenario, the need of high-speed applications and computational Systems in Digital Signal processing applications is drastically increased with increased mobile computing and multimedia applications. Whereas the finite impulse response (FIR) filters is the basic building block of any communication system. FIR filter consists of various blocks. One of the most important blocks in the filter design is multiplier. Different types of multipliers are existing in the digital circuits. But to have a high performance in speed, design of efficient multiplier is essential. To meet out the best performance in speed, Wallace tree multiplier with Kogge-stone adder is designed using verilog hardware description language. The designed high speed multiplier is used for implementing high speed Finite Impulse Response (FIR) filters in order to minimize the hardware complexity and latency. This paper aims at additional reduction of the latency and power of FIR filter. The designed filter is simulated with xilinx simulation tool for verification and synthesis report also taken for the analysis purpose. The simulation and synthesis report helps in finding the performance of FIR filter using Wallace tree multiplier with carry look-ahead and Kogge-stone adders.

KEY WORDS: FINITE IMPULSE RESPONSE FILTER, WALLACE TREE MULTIPLIER, CARRY LOOK-AHEAD ADDER, KOGGE-STONE ADDER.

INTRODUCTION

In all kind of signal processing and communication systems, filters play a major role. Filters find its extensive usage in communication systems and signal processing applications such as noise reduction, channel equalization, audio and video processing and also in biomedical signal processing applications. Finite impulse response (FIR) filters are used extensively for the implementation

purpose in many applications. Generally a digital filter accepts a digital input, provides a digital output and consists of digital components. Software working on a digital signal processor (DSP) reads input samples from an A/D converter, executes the mathematical calculations for the necessitate filter type and provides the output through a D/A converter in a digital filtering application. By contrast, an analog filter works directly on the analog inputs and which is completely built with analog components.

Digital signal processing applications are so extensive which mainly play a role in television sets, house entertainment systems, sound reproduction audio equipments and in all information systems. The digital filter is an significant element in all kind of mathematical operations on a sampled, discrete-time signal to improve

ARTICLE INFORMATION

*Corresponding Author: kavithakrct@gmail.com

Received 15th April 2020 Accepted after revision 20th May 2020

Print ISSN: 0974-6455 Online ISSN: 2321-4007 CODEN: BBRBCA

Thomson Reuters ISI Web of Science Clarivate Analytics USA and Crossref Indexed Journal



NAAS Journal Score 2020 (4.31) SJIF: 2020 (7.728)

A Society of Science and Nature Publication,
Bhopal India 2020. All rights reserved.

Online Contents Available at: <http://www.bbrc.in/>

the certainty of a signal. The digital filter is characterized by its transfer function (C. Y. Yao et al., 2012). Two types of digital filters available which are named as are infinite impulse response (IIR) and finite impulse response (FIR).

The order of an FIR filter mainly decides the width of the transition-band. So that, when the order of the filter is higher, the transition is more sharper between a pass-band and adjacent stop-band. Most of the applications such as frequency channelization, channel equalization in digital communication, adaptive noise cancellation in speech processing, noise cancellation in seismic signal processing and some other part of signal processing need higher order FIR filters (G.Parameswara Rao et al., 2011).

As the number of multiply-accumulate (MAC) operations involved per filter output raises linearly with the order of the filter, implementation of filters with large size orders is a difficult task. Besides the scaling of semiconductor device, semiconductor memories have become lesser in cost, higher in speed and more power-efficient. In addition, as per the international technology roadmap for semiconductors, the presence of embedded memories in the system-on-chips (SoCs) (Choi et al., 2017; W.B.Ye et al., 2017) is more dominating, which may go beyond 90%, of the total Soc content (W. B. Ye and Y. J. Yu et al., 2014). Filters are the fundamental block of communication systems. Filters are used to eliminate noise and interference from the signal and are also employed to modify different characteristics of the signal. Among analog and digital filters, digital filters are more precise and invariable. There are two types of filters in communication systems, 1. Finite Impulse Response Filter 2. Infinite Impulse Response Filter.

MATERIALS AND METHODS

Related Works: FIR filter with Wallace tree multiplier and carry select adder is designed to reduce the delay and area in VLSI circuits. New technique called folded filter is designed for better performance, where adder, multiplier, filters, transposed flip flops are used. These designed models are known as CSLA with D-latch. The combination of Wallace tree multiplier with carry select adder occupies less area (B.sakthivel et al., 2018).

Every DSP processor must have high speed multiplier. Thus the speed of a circuit depends upon its multiplier. FIR filter requires addition, multiplication and signal delay, which can be done by nikhilam sutras in vedic multiplier. This paper compares the performance of urdhava triyakbhyam and nikhilam sutras in the vedic multiplier. Finally, nikhilam sutra has less number of simplified mathematical calculation when compared to the other. It is coded in verilog hardware description language and simulated in xilinx 12.1 where the terms of power, time delay and area are reduced (Y.angelin jasmine et al., 2018). Dada multipliers are faster than Wallace tree multipliers because it has less number of bit-interconnects and it does not require any external

hardware. This paper deals with the comparison of dada, full-dada and Wallace tree multiplier. Due to the reduced number of initial stages, area is minimized (vikas kaushik and Himanshi saini et al., 2018). Various types of multiplications are used with FIR filter along with various adders. Also, to have optimal delay and area, shift and add method was used for multiplication. To minimize the complexity of the designed filter, canonical signed digit was used rather than binary (Anubhuti Mittal et al., 2017).

Memory based structures are more convenient than other multipliers in FIR designing. In digital signal processing applications, memory structures such as look up tables are used with APC (anti-symmetric product coding) and OMS (odd-multiple-storage) techniques. It is implemented in Xilinx 9.2 tool and the results are shown with less delay and area when compared with other conventional multipliers (R.Dhayabaran et al., 2013). In digital signal processing, FIR filter is the fundamental building block of communication systems. This method overcomes the disadvantages of other multiplier and adder by reducing area, delay and power. Thus the combination of vedic multiplier and kogge stone adder is faster than vedic and ripple carry adder. Because it has less slices than that of vedic and the full adder. It performs faster filter operations (s.Rooban, Shadik et al., 2019).

Proposed System: There are many techniques to overcome the problems in mobile computing and portable multimedia applications. As technology is evolving, the size of the transistor goes on decreasing. In our paper, we choose the complex architecture like Wallace tree to overcome the problems and further enhancement for effective communication. FIR filter is one of the essential building blocks of communication systems and we can use this filter to overcome area and delay problems. To optimize delay and filter area, for addition operation, we are using Kogge-stone adder and for multiplication technique we are using Wallace tree multiplier. In the proposed method, parallel prefix adder is used because which is more flexible and higher in speed than other type of adders like Ripple carry adder.

To reduce delay, mainly parallel prefix adders are the most excellent ones. In the proposed method, we choose Kogge-Stone adder among all parallel prefix adders which gives less delay than other type of adders. Brent-Kung adder (A. G. Dempster et al., 2010) which takes up less area but provides maximum delay compared to Kogge-stone adder. Han-Carlson adder which takes up less area but creates maximum delay comparing all the other parallel prefix adders. For the proposed filter, Wallace Tree is used as it is well known for high speed multiplication which employs half adders and full adders for the addition of two numbers and three numbers respectively. In the proposed system, both carry look-ahead and kogge-stone adders are used with Wallace tree multiplier when designing FIR filter.

Kogge-Stone Adder: Kogge-stone adder is a parallel prefix (the output of the operation is based on the initial

inputs) from carry look ahead adder and is shown in the given figure 1. It generates carry in time and this type of adder is called as fastest adder and which is known for low depth and faster performance. This type of adders are mostly used for high performance circuits in industries.

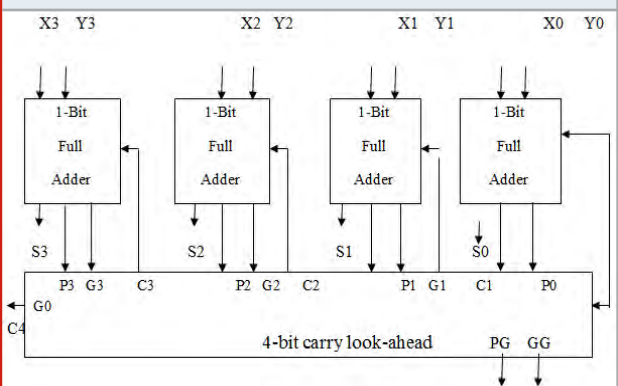
Wallace Tree Multiplier: It is an proficient and well organized hardware implementation of a digital circuit which multiplies two integers and it is shown in figure 2. The Wallace tree has three steps:-

- Multiplying every bit of one data with every bit of another data.
- Decrease the number of products to two by the layers of half adders and full adders.
- Joining the wires in two numbers and adds them with the adder.

Having less delay is the major advantage of Wallace tree multiplier and it decreases the number of logic levels to carry out the summation. But it is complex in its layout and also has irregular wires. The Wallace tree multiplier performs multiplication on any order of bits only in three steps which makes the computations to be performed to decrease. The input A of n bits and B of m bits are given as inputs to the Wallace tree multiplier it produces a product term of n+m bits.

Carry Look-Ahead Adder: A carry look-ahead adder (CLA) or fast adder is a type of adder employed in digital logic design. Figure 3 is a structure of carry look-ahead adder which gets better speed by decreasing the quantity of time used to estimate carry bits. The carry look-ahead adder computes one or more carry bits before the sum, which decreases the wait time to estimate the result of the larger size bits of the adder.

Figure 3: Block diagram of carry look-ahead adder



RESULT AND DISCUSSION

The designed filter is simulated with xilinx simulation tool and also synthesised with Xilinx to analyse various parameters. The simulation and synthesis report helps in finding the performance of FIR filter designed using wallace tree multiplier with carry look-ahead and kogge-stone adders. Following are the Simulation results obtained:

Figure 1: Block diagram of kogge-stone adder

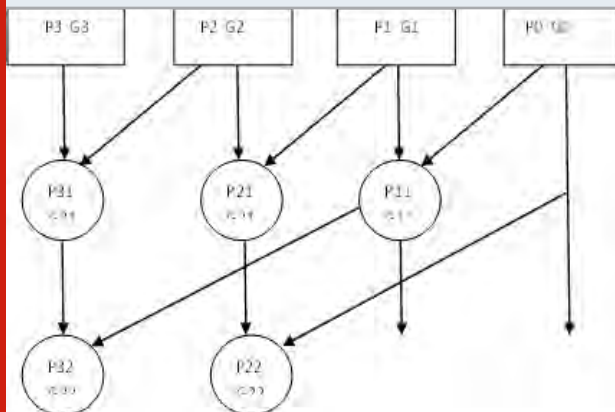


Figure 2: Block diagram of Wallace tree multiplier

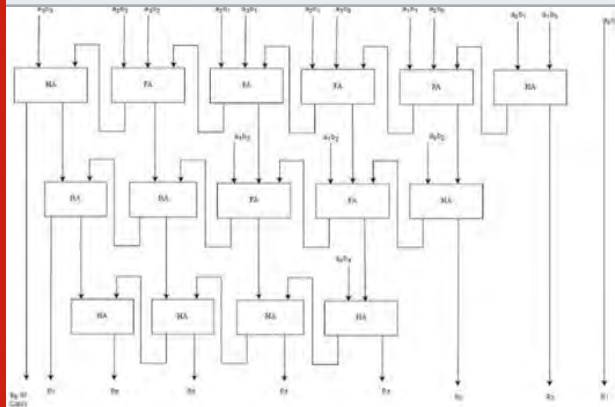


Figure 4: Simulation of FIR filter

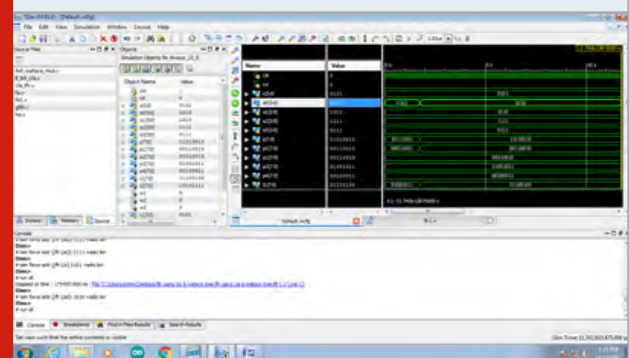


Figure 4 shows the simulation report of the designed FIR filter and figure 5 shows the RTL view for the same filter.

Figure 5: Detailed RTL structure of FIR filter

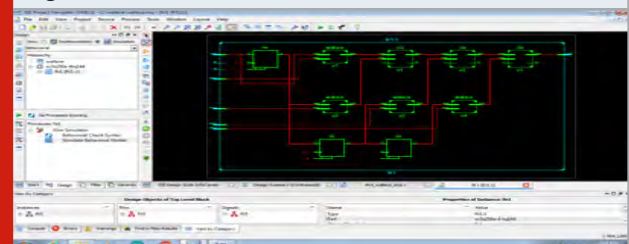


Figure 6 shows the synthesis report of designed filter which provides the information about number of slices, LUT and details about delay. Figure 7 shows the power report of the designed filter.

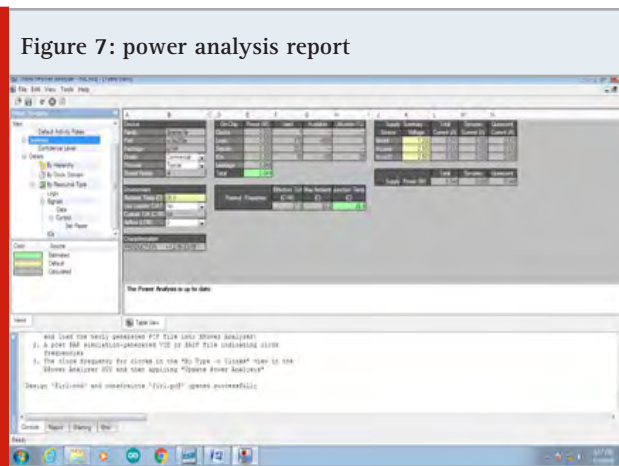


Table 1 shows the detailed analysis about the various parameters for the designed FIR filter using Wallace tree multiplier with carry look ahead and Kogge-stone adders.

Attributes	FIR filter with Wallace tree multiplier and carry look-ahead adder	FIR filter with Wallace tree and kogge-stone adder
Logical Delay	8.411 ns	5.421 ns
Routing Delay	10.13 ns	8.155 ns
Total Delay	18.541 ns	13.576 ns
No. of Slices	53	49
Bonded IOBs	25	25
No. of 4 input LUTs	98	87
Power	0.058w	0.049w

CONCLUSION

Number of slices, LUTs, delay and power are compared for the FIR filter designed with Wallace tree and carry look-ahead adder and also with Kogge-stone adder. The designed filter is verified with xilinx simulation tool and synthesis report also taken for analysis. We have found that the filter combination of the Wallace tree and the Kogge-stone adder has the faster response than other adder. Even though we have got very less difference for smaller order of bits used, the difference will be much larger when the length of the bits increases. Compared with the conventional type of filters, the proposed filter gives better performance and which can be used in all kind of digital signal processing applications.

REFERENCES

Anubhuti Mittal Ashutosh Nandi Disha Yadav(2017) Comparative study of 16-order FIR filter design using different multiplication techniques IET Circuits Devices Syst Vol 11 Iss 3 pp 196-200 © The Institution of Engineering and Technology.

A G Dempster and M D Macleod (1995) Use of minimum-adder multiplier blocks in FIR digital filters IEEE Trans Circuits Syst II vol 42 no 9 pp 569-577.

B Sakthivel Athulya PS Amrutha Suresh Akshaya T Pavithra (2018) A Design and analysis of FIR filters using Wallace tree multiplier and carry select adder IJRTER.

Parameswara Rao(2011) Design and Implementation of 32-bit high level Wallace Tree Multiplier 2011

R Dhayabarani M Poovitha (2013) Modified Reconfigurable FIR filter design Using Look up TableIJERT vol 2.

S Rooban Shaik Saifuddin SLeelamadhuri Shadik Waajeed (2019) Design of FIR filter using wallace multiplier with kogge-stone adderIJITEE vol-8 Issue-6.

Vikas Kaushik and Himanshi Saini (2018) The proposed full-Dadda multiplier IJRST vol 4.

W B Ye and Y J Yu (2014) Bit-level multiplier FIR filter optimization incorporating sparse filter technique IEEE Trans Circuits Syst I vol 61 no 11 pp 3206- 3215.

X Lou Y J Yu and P K Meher (2016) Lower bound analysis and perturbation of critical path for area-time efficient multiple constant multiplications IEEE Trans Comput-Aided Design Integr Circuit Syst.

Y Angelin Jasmine and C Chitra (2018) Low power high speed FIR filters using vedic multiplierInternational journal vol 118 No 20.

A New Methodology of Arterial Blood Clot Removal Using Bio Molecular Devices for ATPase Nuclear Motors

P. Sabarish^{1*}, A. T. Sankara Subramanian², S. Murugesan³ and V. Sureshkumar⁴
^{1*,2,3,4}Assistant Professor

^{1*,2,3,4}Department of EEE, K. Ramakrishnan College of Technology, Trichy-621112, India.

ABSTRACT

In this paper it is practically nothing; The induced biological machines do designers contribution in a living organisms and creature cells joining such on individuals. The induced biological machines might possibly experience the living creatures, filling in a convenient medication stores. The architects jump forward in planning a nuclear motor in a manufacture method at the Nano-scale, two or three billions of a meter in size. The chief facilitated sub-nuclear motor in molecule of the synthetic ATPase coupled to a metallic substrate with a genetically structured controlled ran of 40 minutes at 3 to 4 cycles of consistently. Nuclear motors are not so much new. The ATPase nuclear motors are little bodies in the cells are practically all living creatures are found in the layers of mitochondria. ATP is the fuel for the sub-nuclear motor's development. Imperativeness opens up the atomic bonds between phosphates particles are broken during hydrolysis to change over ATP into ADP. Throughout the ATP hydrolysis, the rightward way turns to an end; it rotates rightward during ATP association from ADP. The controlled is for joining the ATPase motors, Nano-fabricated metallic substrates which is combined of histamine and other amino acids. The histamine combines the sub-nuclear motors to attach the Nano-fabricated instances of gold, copper or nickel the three constant cerebrums until the sub-nuclear motors are joined to additionally create Nano-fabricated devices that can give headings

KEY WORDS: BIONIC MACHINES, NANO, ATP HYDROLYSIS, ATPASE NUCLEAR MOTOR.

INTRODUCTION

The prefix "nano-" (from the Greek root nanos, or overshadow) implies one-billionth of something. The expression "nanotechnology" alludes most by and large

to innovation on the size of a billionth of a meter, or a nanometer (a nanometer is ~6 carbon molecules wide). Thus, the words "nanomachine," "nanorobot," "nanomotor" and "nanocomputer" may allude to complex designed articles created by situating matter with sub-atomic control.

This creating field of research is made arrangements for extending Nano scale size (1 to 100nm) at any rate of one estimation. This technology, right now, a lot of creating methods in material science,science,structuring and

ARTICLE INFORMATION

*Corresponding Author: prasadjoness.ece@krct.ac.in
Received 15th April 2020 Accepted after revision 20th May 2020
Print ISSN: 0974-6455 Online ISSN: 2321-4007 CODEN: BBRCBA

Thomson Reuters ISI Web of Science Clarivate Analytics USA and Crossref Indexed Journal



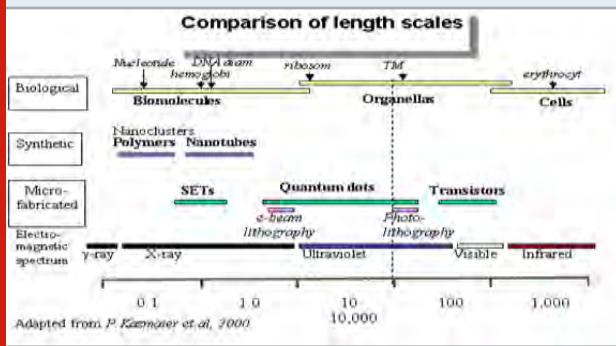
NAAS Journal Score 2020 (4.31) SJIF: 2020 (7.728)
A Society of Science and Nature Publication,
Bhopal India 2020. All rights reserved.
Online Contents Available at: <http://www.bbrc.in/>

microelectronics that are prepared for controlling issue at the minutes of degrees. In this request we have to achieve the improvement of recently developed, legitimate data and headways regions reaching out from ICT to drug and bio technology.

Figure 1: View of Nanorobot in Brain enhancer



Figure 2: Comparison of length scales

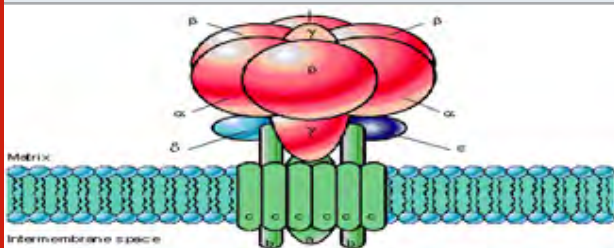


METHODS AND MATERIALS

Biological Motor Powered Nano mechanical Devices:

Logical headways in nanofabrication innovation presently give the capability of designing utilitarian cross breed natural/inorganic Nano mechanical frameworks. ATPase is an unavoidable compound in basically alternate living being. It involves two parts, (1)F0 hydrophobic film limit section at risk for proton translocation. (2) F1 hydrophilic portion is liability for ATP blend and hydrolysis. The protons travel through the F0, the y monetary unit of the F1-ATPase turns rightward.

Figure 3: Synthesis of ATP from Y subunit



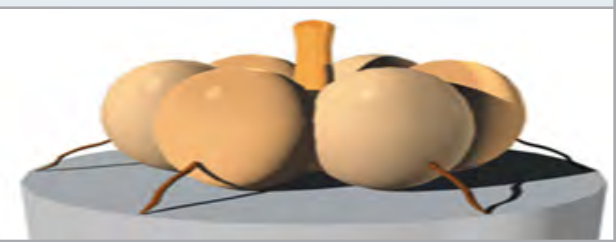
During hydrolysis, counter clockwise rotation of the y monetary unit provides interaction with y monetary unit in the order.

Figure 4: Hydrolysis operation



The specific component of collaboration presently can't seem to be resolved. Crystallization of the F1-ATPase has uncovered that each of the three locales must contain bound nucleotides altogether for revolution of the y subunit to happen. Further, the y subunit is uprooted from its focal hub during revolution. The power created by ATPase engine protein was >100 pN, which is among the best of any known atomic engine. With a determined no-heap rotational speed of 17 r.p.s. furthermore, a breadth of under 12 nm, the F1-ATPase protein is a customized Nano-engine. These properties, combined with F1-ATPase consequently prompts potential for making synthetically controlled Nanomechanical gadgets.

Figure 5: ATPase motor



The effect of engine created squander items just as the impacts of burden on the presentation and life of the engine should be distinguished. An assessment of the designing properties of the F1-ATPase engine protein give steady estimations of the exhibition of the F1-ATPase engine protein under various working conditions.

Integration of Biological Motors and NEMS: Stages for the creation of both bio sub-atomic engines and NEMS must be set up so as to incorporate these advancements and produce half breed frameworks. Beginning endeavors have concentrated on the improvement of these stages. What's more, we likewise have started assessing the designing properties of F1-ATPase.

Figure 6: Cell's sensory system



With the coordination of bio atomic engine gadgets and cell-flagging frameworks by building ,an auxiliary restricting site custom fitted to a phone's flagging course specialists intend to utilize the cell's tangible framework to control Nano devices embedded in living cells.

Figure 7: Attachment of Nano cells

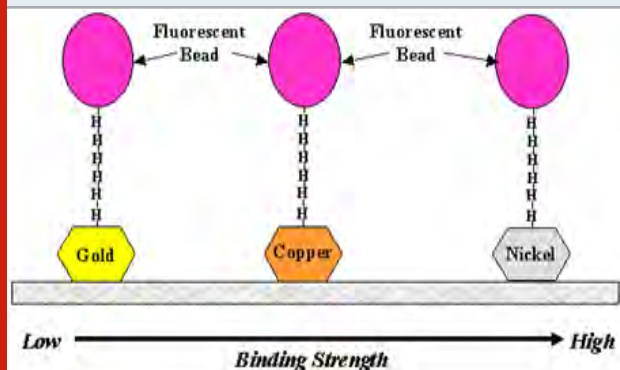


RESULT AND DISCUSSION

Attachment of Biological Molecules to Nanofabricated Substrates: The target of this test was to assess the official of natural atoms to nanofabricated substrates. Electron bar lithography was used to carve an exhibit design on a 25 mm coverslip that had been covered with an oppose bilayer. Coverslips then were designed with metal substrates utilizing evaporative affidavit of gold, copper, or nickel. Consequently, the bilayer was evacuated to uncover the cluster.

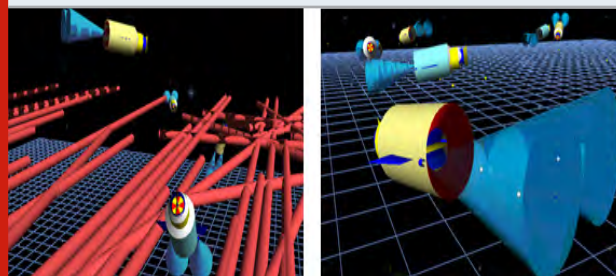
A six His-label peptide was covalently coupled to carboxylate-adjusted 1 mm fluorescent microspheres utilizing a water-solvent carbodiimide. The His-labeled microspheres were permitted to connect to gold-, copper-, and nickel-covered coverslips for 15 minutes at room temperature. Unattached microspheres were evacuated through a progression of washes, and coverslips were watched utilizing fluorescence microscopy. His-labeled microspheres appended to every one of the three substrates; be that as it may, connection was most as often as possible saw with nickel-covered coverslips.

Figure 8: Binding Strength of Nano Fabricated Structures



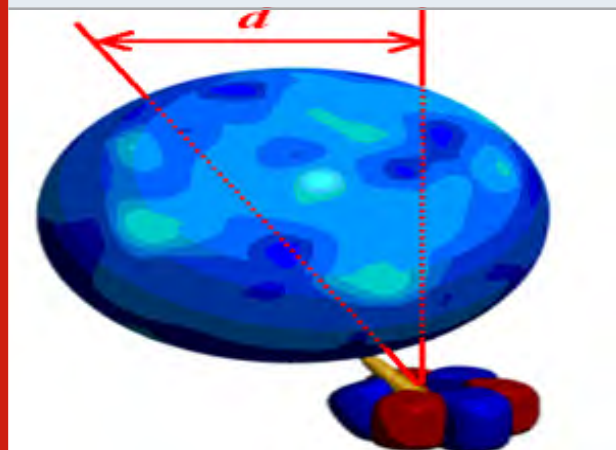
Attachment and Movement of Individual Bimolecular Motors: It incorporates connect ATPase to a nanofabricated substrate and it measure the rotational speed in point of disfigurement of the y monetary unit. The ATPase proposes in the y monetary unit of uprooted in the focal hub around turn a separation greater than a 20 Å.

Figure 9: 3-D view of Individual Biomolecular Motors



By connecting a 1 mm Nano-sphere to the y monetary unit, the displacement and angle of deformation of the y monetary unit must be fixed. In this angle of deformation will provide valuable insight on the mechanism behind rotation of the y monetary unit.

Figure 10: 3D view of Displacement and Phase Angle of Motors

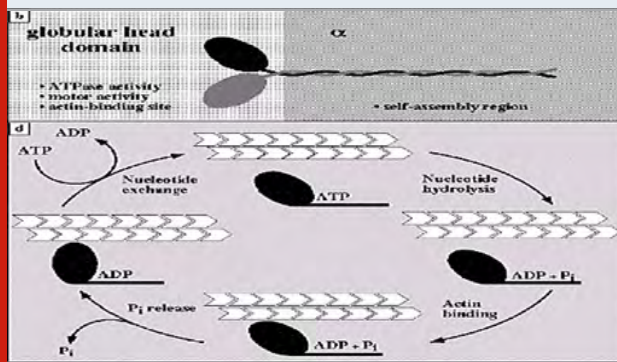


Biologicalmotor For Arterial Blood Clot Removal: Late improvements of Nano-technology has revealed chance of making in Nano scale gadget those might have the option to precisely granulate out blood vessel clumps brought about by atherosclerosis. A few normally happening bio sub-atomic engines have been examined. These engines are fuelled by ATP, which is totally alright for the body, and they are amazingly effective. The various types of engines are talked about underneath.

Types of bio molecular motors: In these fundamental kinds of bio molecular engines are the actin-based sliding engines or microtubule-based straight engines

and revolving engines. In these sliding engines of the system utilized in skeletal muscle to deliver development. An improved new model of that engine includes some kinds of fibers spherical protein and Motor protein, which slide more than each other. The dainty actin fibers are made out of protein monomers connected together to shape chains.

Figure 11: ATP cycle of myosin heads binding to actin



The Motor proteins fibers contain numerous dynamic nob units in cooperate with spherical protein to frame forward spans. The Motor engine particles in the nob bunches are stimulated by the dephosphorylating pattern of ATP.

Figure 12: Actin and Myosin Filament

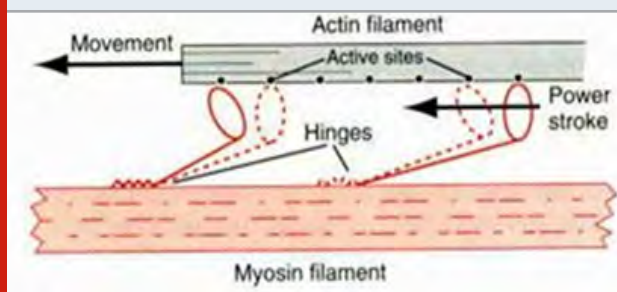


Figure 13: A Cross-section of the Complete Nanogrinder

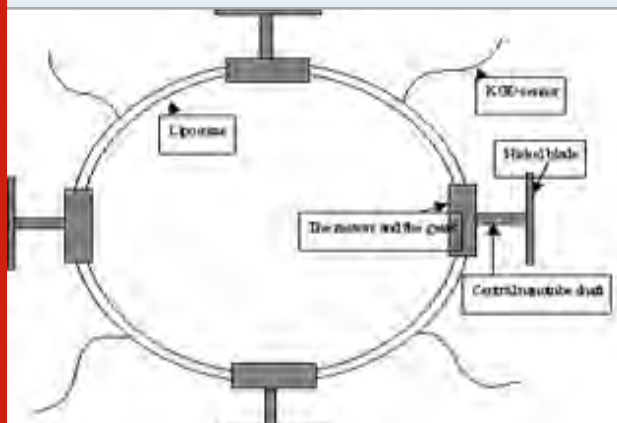


Figure 14: The Motor-Nanotube-Blade Assembly

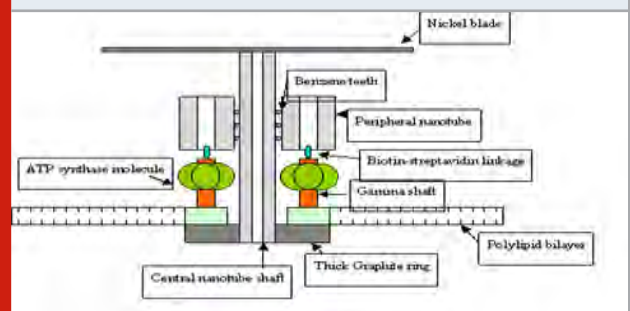


Figure 15: Virus Finders



Figure 16: Artery cleaners



Nano grinder: The gadget planned right now of an artificially-prepared spherical vesicle installed with six engine nanotube-edge congregations and with various interface sensor groupings. The sensors are utilized to tie the gadget to coagulation with the goal that granulating can be focused on. A nickel sharp edge related with a carbon Nano-rod and benzene gears is turned by six ATPase structures which is joined to carbon Nano-rod and benzene engines outfits by methods for biotin-streptavidin linkages. The benzene engine and Nano-rod gathering are held simultaneously with in a graphite plate to include auxiliary security. The nickel sharp edge is covered with titanium and all parts are covered with PEG and superoxide dismutase which is used for biocompatibility.

CONCLUSION

To improve the plans for commercializing nanotechnology for Nano scale devices and the applications of creation

in nuclear machines and gathering of limit at the nanometre level. Any individual who considers the future should purchase Nano structures, for this is the significant clarification of nanotechnology. Regardless of whether we make well or truly, we and our beneficiaries should then live in our creation. Nano systems give us a reasonable and all around study of a rich new vein of the feasible.

REFERENCES

- A T Berg S F Berkovic M J Brodie (2014) Revised terminology and concepts for organization of seizures and epilepsies report of the ILAE Commission on Classification and Terminology Epilepsia
- Dalton S Patel A R Chowdhury M Welsh T Pang S Schachter (2012) Detecting epileptic seizures using wearable sensor technologies In Proc of the First AMA-IEEE Medical Technology Conference on Individualized Healthcare
- Edwin M et al (2019) IOP Conf Ser Mater Sci Eng 623 012022
- Fisher R Boas W Blume W Elger C Genton P Lee Epileptic seizures and epilepsy(2009) Definitions proposed by the International League against Epilepsy ILAE and the International Bureau for Epilepsy IBE Epilepsies 46 4
- Jai Ganesh R S Kodeeswaran M Kavitha T Ramkumar Performance analysis of piezoelectric energy harvesting system employing bridgeless power factor correction boost rectifier
- Kalavalli C SR Paveethra S Murugesan Dr A Nazar Ali Dr V Venkatesh (2020) Design and Implementation Of High Efficiency H6 PV Inverter With Dual Axis Tracking international journal of scientific & technology research volume 9 issue 02 february issn 2277- 8616
- Kavitha M and R Jai Ganesh Hierarchical Classifier for Breast Cancer Diagnosis Journal of Advanced Research in Dynamical and Control Systems Volume 11- 04 Special Issue Pages 607-611 1943-023X
- Kavitha M R Jai Ganesh & A Rajkumar (2019) Facilities Navigation And Patient Monitoring System Using Ibeacon Technology International Journal of Mechanical and Production Engineering Research and Development (IJMPERD) ISSN (P) 2249-6890 ISSN (E) 2249-8001 Vol 9 Special Issue 1 562-570
- Nazar Ali A et al (2019) IOP Conf Ser Mater Sci Eng 623 012010
- Paveethra SR C Kalavalli S Vijayalakshmi Dr A Nazar Ali D Shyam (2020) Evaluation Of Voltage Stability Of Transmission Line With Contingency Analysis International Journal Of Scientific & Technology Research Volume 9 Issue 02 Issn 2277-8616
- Pradeep M et al (2019) IOP Conf Ser Mater Sci Eng 623 012017
- Sabarish P et al (2019) IOP Conf Ser Mater Sci Eng 623 012011
- Sankara Subramanian AT et al (2019) IOP Conf Ser Mater Sci Eng 623 012012
- Subramanian A & Ali Nazar (2017) A power factor correction based canonical switching cell converter for VSI fed BLDC motor by using voltage follower technique 1-8 101109/ICEICE20178191932
- Thirusenthil Kumaran P P Pushpakarthick G V Chidambarathanu M Venkatachalam Xavier Raja Durai R Jaiganesh (2019) Power quality in distribution grids International Journal of Innovative Technology and Exploring Engineering (IJITEE) ISSN 2278-3075 Volume-9 Issue-1.
- Udayakumar M D et al (2019) IOP Conf Ser Mater Sci Eng 623 012018
- Venkatesh A et al (2019) IOP Conf Ser Mater Sci Eng 623 012009
- Vijayalakshmi S P Sabarish SR Paveethra Dr PR Sivaraman Dr V Venkatesh (2020) Exploration And Applications Of Electronic Balance For High Power Discharge Lamps At High Frequency Through Power Factor Modification International Journal Of Scientific & Technology Research Volume 9 Issue 02 Issn 2277-8616

Fractional Order Controlled Multilevel Boost Hybrid Converter

S.Jeyasudha*¹, A. Anton Amala Praveen² and B. Geethalakshmi³

^{1,3}Associate Professor, ²Assistant Professor

^{1,2}Department of EEE, K. Ramakrishnan College of Technology, Trichy, Tamilnadu, India.

³Department of EEE, Pondicherry Engineering College, Puducherry, India.

ABSTRACT

The field which is gathering research momentum in the recent days is the achievement of multilevel output for huge voltage and power renewable applications. Especially, multilevel inverter (MLI) for solar photovoltaic (SPV) has gained more attention. The main advantages of MLI are reduced total harmonic distortion and improved quality of output voltage. These MLI produce only AC output. But the SPV residential system requires both AC and DC outputs. This is achieved by proposing a multilevel boost hybrid converter (MBHC) which generates simultaneous multilevel AC output and three single DC outputs. This configuration increases the output voltage more than twice that of the conventional MLI, with the same number of power switches. Thus it increases the reliability and efficiency of the system. The demonstration of proposed system is verified successfully using MATLAB/Simulink simulation. The closed loop control of the proposed system is developed by using fractional order proportional integral (FOPI) controller, integer order proportional integral (PI) controller. Both PI and FOPI controller based MBHC, were tested with reference, load and line variation. With these two controllers, the frequency response of MBHC is also compared and presented. The compared results show that the FOPI based MBHC is superior than the conventional controller based MBHC.

KEY WORDS: CLOSED LOOP, HYBRID CONVERTER, CONTROLLER DESIGN, MULTILEVEL INVERTER, MULTILEVEL BOOST HYBRID CONVERTER.

INTRODUCTION

In the last few decades, the attention has increased for non conventional energy sources such as solar, wind, hydro, and biomass which result in clean and green power generation system. The major source is a solar energy

photovoltaic (SPV) source, because it has the advantages of free of cost and high level availability, and also it is environmental friendly (Xing, et al., 2017). The output of the SPV system is very less so it will be boosted for high DC power and inverted for AC power system (WAN, et al., 2017). An output of the voltage source inverter's (VSI) is equal to the input applied to that. So this is used in low power applications. This voltage source inverter is cascaded for producing high power and high voltage applications which is called multilevel inverter (MLI) (Zhang, et al., 2018).

Multilevel inverter for solar photovoltaic system is a recent solemn research in the modern days. Flying

ARTICLE INFORMATION

*Corresponding Author: jeyasudhas.eee@krct.ac.in

Received 15th April 2020 Accepted after revision 20th May 2020

Print ISSN: 0974-6455 Online ISSN: 2321-4007 CODEN: BBRCBA

Thomson Reuters ISI Web of Science Clarivate Analytics USA and Crossref Indexed Journal



NAAS Journal Score 2020 (4.31) SJIF: 2020 (7.728)

A Society of Science and Nature Publication,
Bhopal India 2020. All rights reserved.

Online Contents Available at: <http://www.bbrc.in/>

capacitor MLI and Neutral point clamped MLI are conventional single phase MLI's, which increases device count with increase of number in levels (Vijeh, et al., 2019). Compared to the above said MLI's the cascaded MLI reduces component count (Ye, Z, et al., 2018). All the MLI's are switched by PWM, SPWM, SVM, SHEWM and sliding mode control strategy (Zeb, et al., 2018) and (Ali, et al., 2017). But these control strategies with the conventional MLI produces only multilevel AC outputs and the peak value of this output is depended on the sum of the input sources used. This is overcome by the proposed multilevel boost hybrid converter (Jeyasudha, et al., 2018).

The MBHC is a multilevel inverter and boost converter combination. This circuit consists of a three boost derived hybrid converter (BDHC) connected serially. The BDHC produces both the AC and DC outputs and it is constructed using conventional boost converter which has only one switch which is replaced by a four switch bridge network (Ray, et al., 2013). Thus reduction in the switching count results in reduced switching losses, increased reliability and increased power processing capability. The proposed MBHC has three BDHC connected in cascade for the AC output to produce the seven-level MLI and separate DC outputs. The presence of inductor in each converter circuit makes the AC voltage as high as compared to the conventional H bridge MLI. The DC and AC output of the MBHC fluctuates when it is sourced from the SPV, or when the load varies. Therefore it has to be controlled with the suitable controller.

This paper elaborates the closed loop control operation of multilevel boost hybrid converter (MBHC). The proportional integral (PI) controller has been the most commonly used controller for regulating the converter output (De Keyser, et al., 2018). The most basic and important requirement of any system design is the stability and robustness. But PI controller has its limitations to achieve the required stability. With fractional order proportional integral (FOPI) controller better stability can be achieved. The FOPI controller is generally represented as PI^λ , where λ is the fractional order of the integrator (Sheng, et al., 2018). The PI and FOPI controller parameters are designed and the resultant outputs are compared for the proposed converter.

By seven Sections of title is given in this proposed system. The operation of the circuit is explained in Section 2 and closed loop PI controller design and FOPI controller design are focused in Section 3. The simulated results and comparison of both the controller are explained in Section 4. The transient analysis MBHC is described in Section 5. Finally, Section 6 provides the summary of all the Sections.

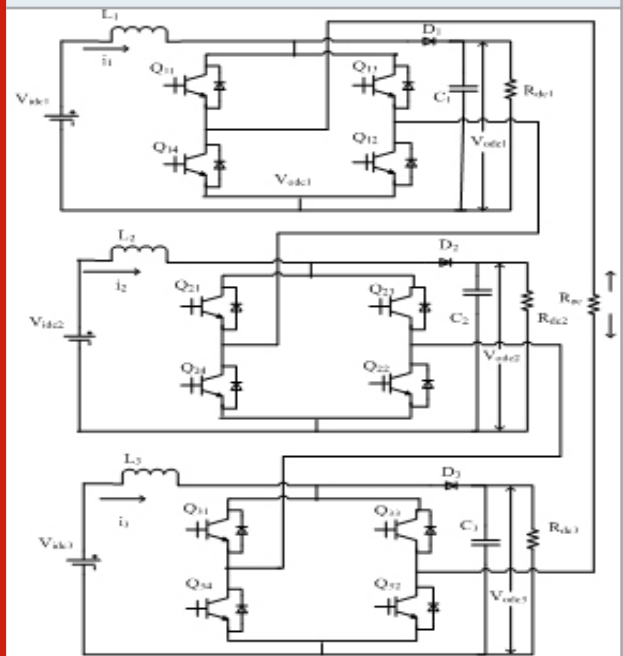
MATERIALS AND METHODS

Principle operation of MBHC:

Configuration and Operating Principle of MBHC: Fig. 1 shows the construction of multilevel boost hybrid converter. Multilevel AC output and DC output are

produced by the connecting three single BDHC seriously. The boost circuit elements $L_1, C_1, D_1, L_2, C_2, D_2, L_3, C_3, D_3$ and three load resistors $R_{dc1}, R_{dc2},$ and R_{dc3} are operated for DC output; load resistor R_{ac} is operated for AC output. Twelve switches Q_{31} to Q_{34}, Q_{21} to Q_{24}, Q_{11} to Q_{14} and the three input sources V_{dc1}, V_{dc2} and V_{dc3} are operated for AC and DC output. AC and DC loads share the same set of switches and are dividing the current and so the summation of the AC and DC output power results in total power of the circuit. The main aim of this MBHC is, to boost the multilevel AC output compared to the conventional MLI output. In this MBHC, the output is sum of the boosted input, but in the traditional MLI, the output voltage is the total input source voltage only. So this topology is called as multilevel boost hybrid convert (MBHC). Simultaneously each bridge will act as a boost converter so it produces the DC boost outputs.

Figure 1: Proposed MBHC circuit



In MBHC the following considerations are made: Voltage across capacitors $V_{ode1} = V_{ode2} = V_{ode3}$, Input inductors $L_1=L_2=L_3$, DC load resistors $R_1=R_2=R_3$, Output capacitors $C_1=C_2=C_3$, Inductors current $iL_3 = iL_2 = iL_1$, and input voltages $V_{dc3} = V_{dc2} = V_{dc1}$. As in the traditional 7 level multi level inverter phase output voltage is given in the

$$V_{oac} = V_{-idc1} + V_{idc2} + V_{idc3} \quad (1a)$$

$$V_{oac} = V_{ode1} + V_{ode2} + V_{ode3} \quad (1b)$$

The output voltages across each DC loads are given in equation (2) as the traditional boost converter

$$V_{odc1} = \frac{V_{idc1}}{1-\delta}; V_{odc2} = \frac{V_{idc2}}{1-\delta}; V_{odc3} = \frac{V_{idc3}}{1-\delta} \quad (2)$$

In order to derive the equation for the boost seven-level MBHC, the basic equation of the MLI (1b) and the boost converter equation (2) are combined and is given in (3)

$$V_{oac} = \frac{V_{idc1}}{1-\delta} + \frac{V_{idc2}}{1-\delta} + \frac{V_{idc3}}{1-\delta} \quad (3)$$

Here duty cycle is δ , V_{odc} is DC output voltage and V_{oac} is AC output voltage. This equation is again written as for n-level MBHC output voltage is given in equation

$$V_{oac} = \sum_{n=1}^m \frac{V_{idcn}}{1-\delta} \quad (4)$$

Circuit operation: Two modes of operation are followed in the MBHC one is boosting mode and another one is the inverting mode. Boosting mode is a high frequency switching as like in the traditional boost converter. Low frequency switching is done for the inverting mode and it is worked as a conventional voltage source inverter. Both the modes happen simultaneously. The boosting mode is again divided into shoot-through and power interval mode. For the shoot-through interval mode the switches Q_{11} , Q_{21} , Q_{31} and Q_{14} are ON, so the inductor stores energy and the diode gets reverse biased and it opens as shown in Figure 2a, and no current flows in the DC and AC loads. To maintain the continuous conduction, the capacitor C_1 supplies current to DC load and the capacitor C supplies current to AC load. For the power interval mode the switches Q_{11} and Q_{12} are ON which is depicted in the Figure 2b. in this mode diode gets forward biased, so current flows in the DC load and at the same source current flows AC load also. The conduction of different switches for each level is tabulated in the Table 1.

Figure 2a: Shoot-through interval mode

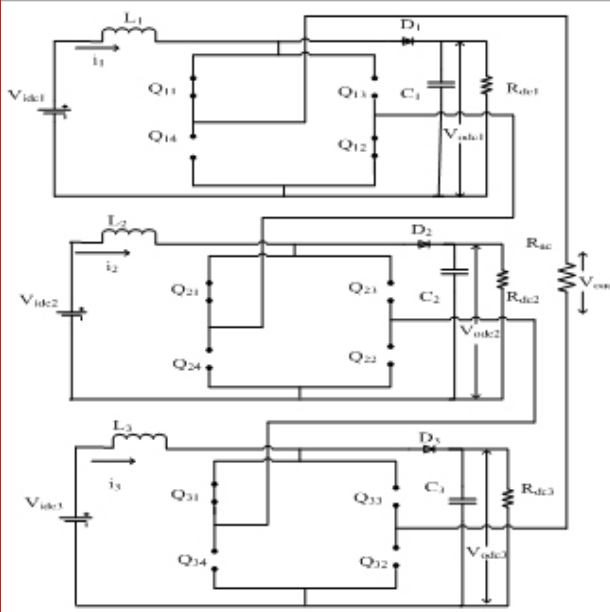


Figure 2b: Power interval mode

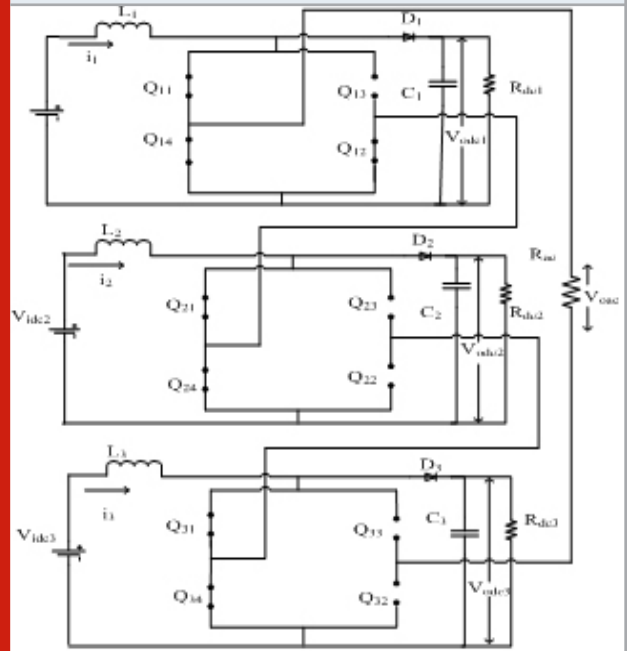
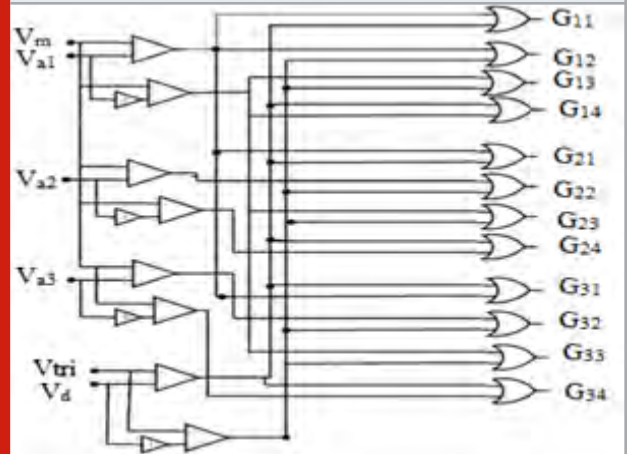


Figure 2c: Logic diagram for control pulses



Switching Strategy of MBHC: The switches are operated in accordance with the sequence which is given in the Table 1. This sequence is developed by comparing carrier triangular waves V_{tri} with a DC signal V_d . This DC signal used so the boosting interval is maintained as in (Jeyasudha, et al., 2018). By comparing the three DC signal V_1 , V_2 and V_3 with the sinusoidal signal, the multilevel AC output is maintained. Thus the The output comparison signals are added to generate the corresponding gate signals of G_{11} to G_{14} , G_{21} to G_{24} and G_{31} to G_{34} as shown in the Figure 2c from the switches Q_{11} to Q_{14} , Q_{21} to Q_{24} , and Q_{31} to Q_{34} respectively.

Dynamic model of MBHC: The transfer function of the MBHC is developed by deriving the dynamic model of the converter to form the closed loop operation of the MBHC. For level one shoot-through interval period is

represented by δ which is the duty ratio of boosting operation. The power interval period is represented by $1-\delta$. Both are shown in the Figure 2a and 2b respectively. By applying the KVL and KCL, the set of dynamic model of boosting mode equations are described in (5) to (11), all the equations are for positive half cycle of the inverter.

$$L_1 \frac{di_1}{dt} = V_{idc1} - V_{odc1}(1-\delta) \tag{5}$$

$$L_2 \frac{di_2}{dt} = V_{idc2} - V_{odc2}(1-\delta) \tag{6}$$

$$L_3 \frac{di_3}{dt} = V_{idc3} - V_{odc3}(1-\delta) \tag{7}$$

$$C_1 \frac{dV_{odc1}}{dt} = i_1(1-\delta) - \frac{V_{odc1}}{R_{dc1}} \tag{8}$$

$$C_2 \frac{dV_{odc2}}{dt} = i_2(1-\delta) - \frac{V_{odc2}}{R_{dc2}} \tag{9}$$

$$C_3 \frac{dV_{odc3}}{dt} = i_3(1-\delta) - \frac{V_{odc3}}{R_{dc3}} \tag{10}$$

For inverting mode equation is given in (11)

$$L_1 \frac{di_{ac}}{dt} = V_{idc1}(1-\delta) - R_{ac}i_{ac}(1-\delta) \tag{11}$$

Likewise, the boosting interval equations for level 2 and level 3 is same as that of the level 1 equations as in the equations (5) to (10), but the inverting mode level 2 and level 3 equations are varied and it is given in (12) and (13) respectively.

For level 2

$$(L_1 + L_2) \frac{di_{ac}}{dt} = (V_{idc1} + V_{idc2})(1-\delta) - R_{ac}i_{ac}(1-\delta) \tag{12}$$

For level 3

$$(L_1 + L_2 + L_3) \frac{di_{ac}}{dt} = (V_{idc1} + V_{idc2} + V_{idc3})(1-\delta) - R_{ac}i_{ac}(1-\delta) \tag{13}$$

All these equations are also same for the negative half cycle, but the input sources are negatively signed.

Experimental verification of Open loop of MBHC: From the equations (5) to (13) the state-space model is developed and the circuit is simulated with MATLAB/Simulink for the values tabulated in the Table 2 as in (Ray, et al., 2013) and the state-space numerical model is validated as in (Jeyasudha, et al., 2018). The output DC and AC voltages are observed and shown in the Figure 3a and 3b respectively.

In the Figures. 3a and 3b, for a input voltage of 40V and 0.62, 0.3 as a duty cycle and modulation index, the simulated DC and AC output voltages are 81.63V and 244.8V (205.8V RMS) respectively. The input current of 8.329A and the DC output current of 4A and AC output current of 0.633A RMS are also observed from the simulation.

The proposed MBHC is tested by experimental demonstrations to verify its open loop outputs. For open loop operation, the digital gate pulses are generated by writing the codes in the VHDL in the Xilinx platform and it is implemented with the FPGA development board. The gate pulses G11 to G34 are generated and transmitted to the gate driver. The driver circuit is to fire the IGBT switches for proper operation. The details of the circuit parameters used in the hardware set up is given in Table 3. The prototype of the MBHC converter is demonstrated and the open loop outputs are noted and shown in Figure 4a and Figure 4b.

Transfer function of MBHC: Linearizing (5) to (10) and (13) around the equilibrium point and separating the dynamic ac small signal terms from the dc steady state component, the following dynamic model (14) is obtained.

Table 1. MBHC switching operation sequences

Levels	Condition of switches												V _{oac} AC output voltage	
	Q11	Q12	Q13	Q14	Q21	Q22	Q23	Q24	Q31	Q32	Q33	Q34		
Positive half Cycle	0	B	0	0	B	B	0	0	B	B	0	0	B	0V
	1	1	1	0	B	1	0	0	B	1	0	0	B	V _{idc1} / (1-δ)
	2	1	1	0	B	1	1	0	B	1	0	0	B	(V _{idc1} + V _{idc2}) / (1-δ)
	3	1	1	0	B	1	1	0	B	1	1	0	B	(V _{idc1} + V _{idc2} + V _{idc3}) / (1-δ)
Negative half cycle	0	0	B	B	0	0	B	B	0	0	B	B	0	0V
	1	0	B	1	1	0	B	1	0	0	B	1	0	-V _{idc1} / (1-δ)
	2	0	B	1	1	0	B	1	1	0	B	1	0	-(V _{idc1} + V _{idc2}) / (1-δ)
	3	0	B	1	1	0	B	1	1	0	B	1	1	-(V _{idc1} + V _{idc2} + V _{idc3}) / (1-δ)

$$\frac{d\hat{x}}{dt} = A\hat{x} + B\hat{u} + E\hat{\delta} \tag{14}$$

where A is the state matrix and B is the input matrix is the input matrix corresponds to δ . Using the equation (14) and Table 2 the input to control transfer function is developed and is given in the equation (15)

$$\frac{V_{dc}(s)}{\delta(s)} = \frac{s^6 - 8.07 \times 10^2 s^5 - 5.3 \times 10^4 s^4 - 7.7 \times 10^7 s^3 - 1.06 \times 10^{10} s^2 - 2.12 \times 10^{13} s + 2.7 \times 10^4}{s^7 + 1.4 \times 10^3 s^6 + 1.44 \times 10^6 s^5 + 1.94 \times 10^9 s^4 + 2.2 \times 10^{10} s^3 + 9.06 \times 10^{13} s^2 + 9.89 \times 10^{16} s + 1.3 \times 10^7} \tag{15}$$

Table 2. MBHC model parameters

Parameters	Values
I/P Voltage (V_{idc1} to V_{idc3})	40V
I/P Inductor (L_1 to L_2)	5mH
Capacitor C_1	1mF
Load resistor (R_{dc1} to R_{dc3})	20 Ω
Load resistor (R_{ac})	200 Ω
Frequency for switches	10KHz

Figure 3a: Open loop input and output voltage waveform

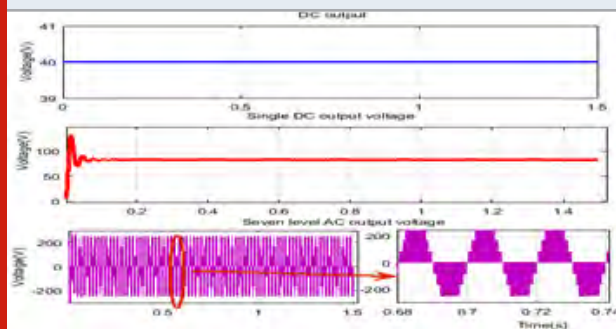
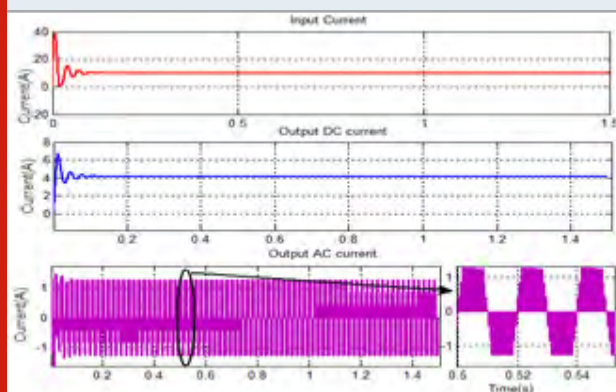


Figure 3b: Open loop input and output current waveform



The transfer function exhibits the seventh order dynamic. Using voltage mode feedback of DC signal, the control parameters are tuned by the Zeigler - Nichols method.

Table 1. Frequency Band with bandwidth

Components	Manufacturer/No.
IGBT Switches	FGL40N120AND IGBT (Fairchild)
Diode	MUR3060 (Multicomp)
Driver Circuit	TLP 320 IC
FPGA Board	Spartan 6 (Xilinx)
Current Sensor	IC7840
Voltage Sensor	LV 25-P

Figure 4a: Output DC voltage and output DC current

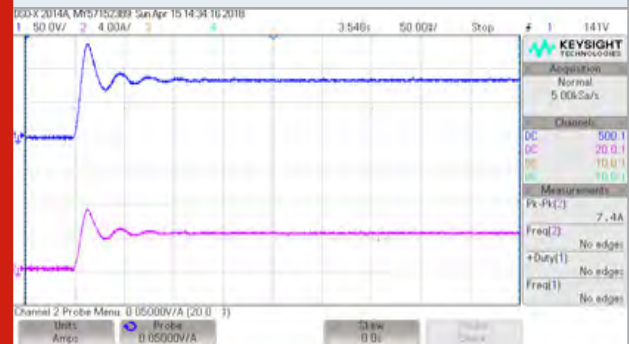


Figure 4b: Output AC voltage and current waveform

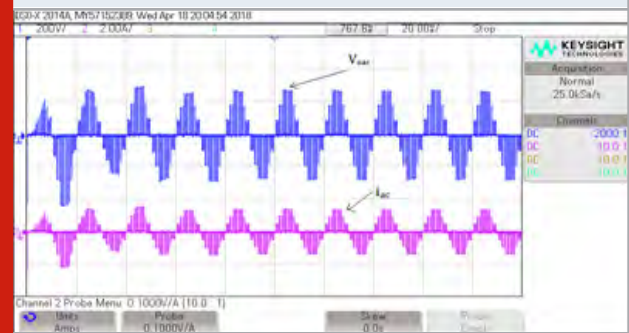


Figure 5a: MBHC with PI Controller

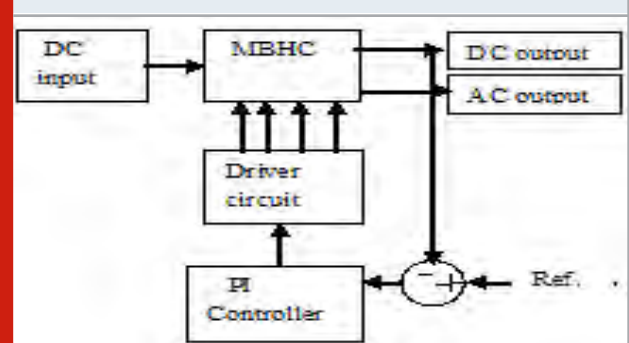
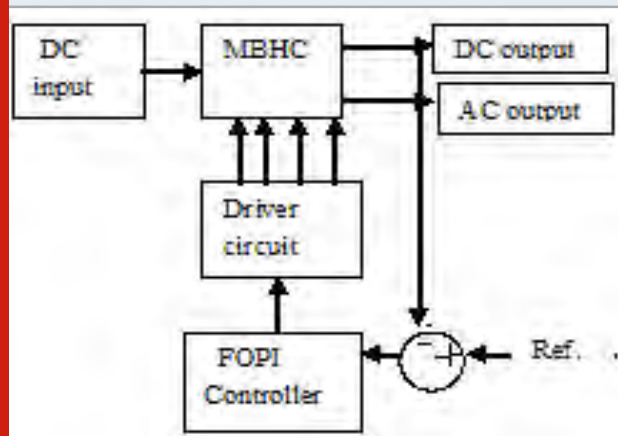


Figure 5b: Closed loop FOPI controller



Closed loop control of MBHC

PI controller design: The closed loop MBHC is depicted in the Figures 5a and 5b. The PI controller process the error created by comparing the reference voltage with the generated output voltage of MBHC. The MBHC system transfer function which is given in (15) is used to derive the PI controller parameters with Zeigler Nichols method (Paraskevopoulos, 2017). The tuned parameters and are obtained from Zeigler Nichols oscillation method. This K_p and K_i values are applied in the closed loop control circuit of the MBHC and the simulation results are compared with fractional order controller based MBHC in the Section 4.

Fractional order control of MBHC: PI controllers are used in industries for speed control applications. Due to its simplicity of design, good performance in small settling time and low percentage overshoot, it is considered the best controller. For slow industrial process and lagging of robustness, the PI controller can be further improved by appropriate settings of fractional-I and fractional-D values. This paper attempts to study the behaviour of fractional order PI controllers (Roy, et al., 2017; Jeyasudha, et al., 2018; Jeyasudha, et al., 2017) over integer order PI controllers. Figure 5b represents the FOPI closed loop block diagram of the MBHC. The FOPI controller tuning parameters K_p , K_i and λ which give more flexibility for accomplishing the control objective by the expansion shown in equation (16)

$$G_c(s) = \frac{U(s)}{E(s)} = K_p + K_i s^{-\lambda} \tag{16}$$

This equation is implemented by the MATLAB simulation. A range of different values which are chosen for the control parameters K_p , K_i and λ to minimize the error. In this work, the controller parameters are optimized by Genetic Algorithm (GA) (Nemati, et al., 2018), which is a global optimization, easy and accurate. The integral absolute error of the controller is taken as an objective function of the GA. The following parameter values are

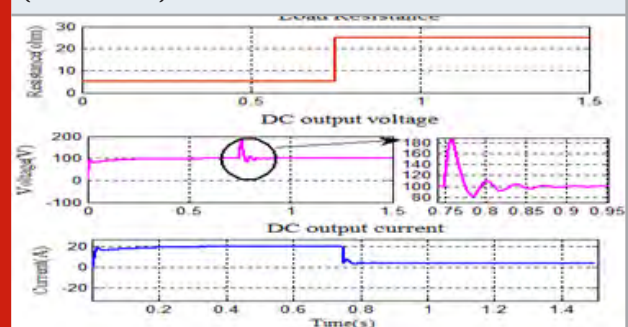
optimized for the FOPI controller: $K_p = 0.001$, $K_i = 0.01$ and $\lambda = 0.93$.

RESULT AND DISCUSSION

Simulation Results and Analysis

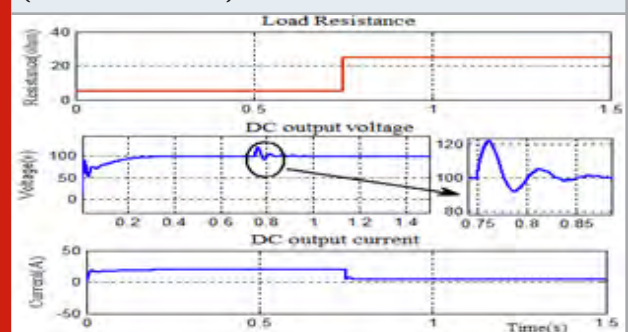
Load Regulation: For the closed loop operation the input voltage, the DC reference voltage and AC reference voltage are set as 40V, 100V and 212.2V (RMS) respectively. For verifying this condition, the DC load is varied from 5Ω to 25Ω with an interval of 0.75 sec. The sudden variation in the load resistance enhance the output voltage which makes the changes in the preferred set value of 100V. Thus controller of the converter acts upon the duty cycle value and make the output as same as that of the reference voltages value with a settling time of $t_s=0.25$ sec as shown in the Figure 6b. The corresponding load current has also been presented in Figure 6c.

Figure 6: Load variation DC output voltage and current (PI controller)



Similarly, the fractional order control load variation output voltage and current waves are shown in the Figure 7. The peak overshoot value of the DC output voltage is less for FOPI controller than the PI controller.

Figure 7: Load variation DC output voltage and current (Fractional order PI)



Similarly, AC load resistance R_{ac} is varied from 200Ω to 150Ω at the time $t=0.75$ sec for PI and FOPI controlled MBHC. For a sudden decrease in load resistance and to maintain the output voltage as the reference value the controller is activated to adjust the duty ratio and regulate the output voltage as shown in Figures. 8b and 9b for PI and FOPI respectively. The load current is

correspondingly varied and depicted in the Figures. 8c and 9c respectively.

Figure 8: AC output load variation voltage and current (PI controller)

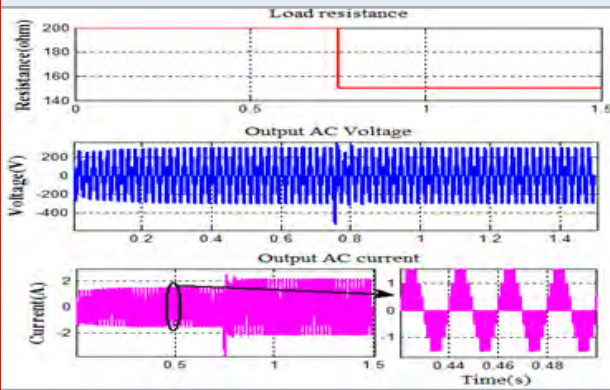
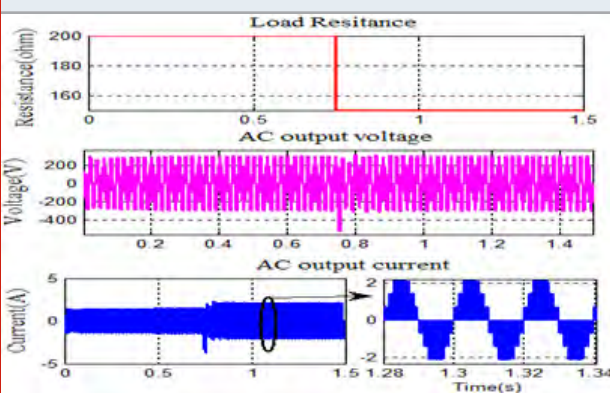
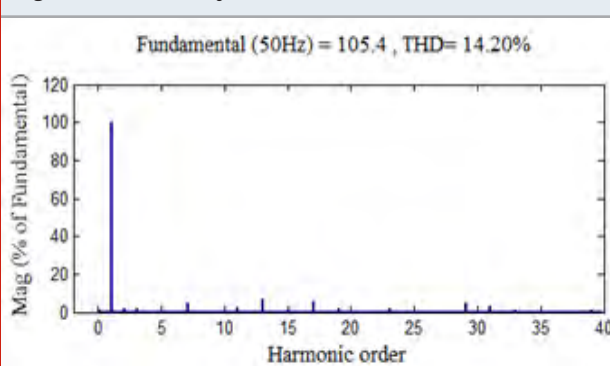


Figure 9: AC output load variation voltage and current (FOPI)



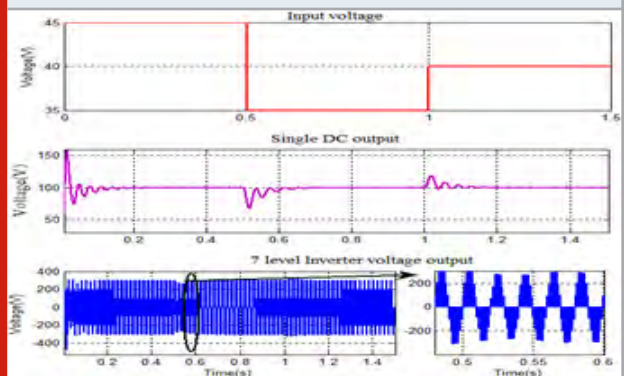
The FFT is used to acquire the harmonic spectrum of the output voltage waveform. Figure 10 shows the harmonic spectrum of seven-level BMHC output voltage with load variation. It is observed that the third and fifth order harmonics are less for the load variation voltage. The THD of the load variation voltage of MBHC is 14.20 %.

Figure 10: FFT analysis of Load variation



Line Regulation: To verify the performance of the controller under supply variations, the load resistance is kept at a fixed value of $R_{dc} = 20\Omega$ and $R_{ac} = 200\Omega$, variation is incorporated only in the supply side. The desired set voltage across the dc load is 100V. The supply voltage is maintained at 45V until $t=0.5$ sec and a step change is given to vary the input voltage to 35V. One more step variation is given at $t=1$ sec and the supply voltage switches to 40V. In order to regulate the dc output voltage to 100 V the controller changes the duty ratio from 0.57 to 0.44 at $t = 0.5$ sec and from 0.44 to 0.51 at $t = 1$ sec. The corresponding output voltage plot is depicted in Figure 11b. Similarly, the ac output voltage is also regulated as shown in the Figure 11c. It is found that variation in modulation index is not significant, since, the AC output voltage depends both on duty ratio as well as modulation index. The FOPI controlled supply variation is also shown in the Figure 12.

Figure 11: Supply variation of PI controller



The harmonic spectrum of the source variation is shown in the Figure 13. The THD of the source variation is 13.67%.

Figure12: Supply variation of FOPI controller

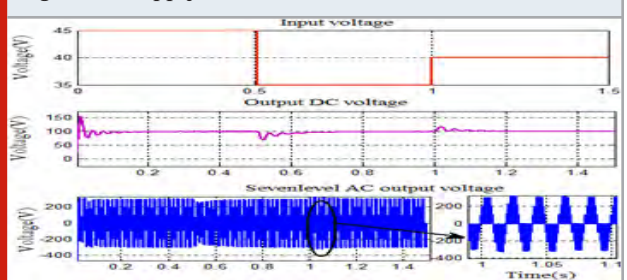
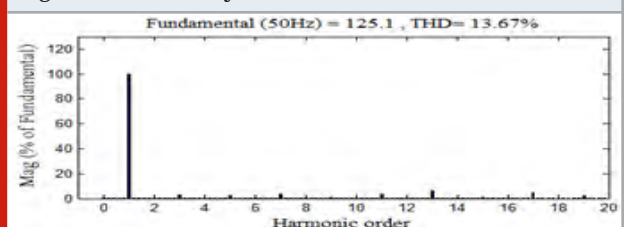
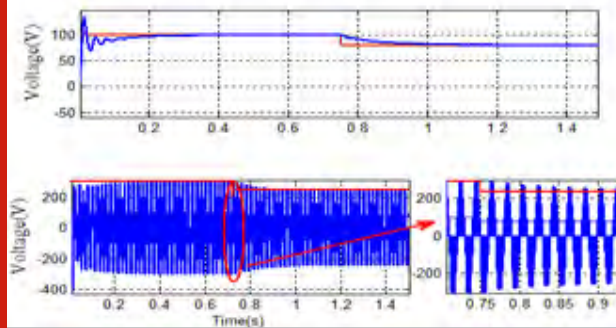


Figure 13: FFT analysis of source variation



Reference Variation: The input voltage and DC load resistance and AC load resistance is taken as 40V, $R_{dc}=20\Omega$ and $R_{ac}=200\Omega$ respectively for the variation of the reference value. The DC reference voltage is changed from 100V to 80V at $t = 0.75\text{sec}$, and the AC reference voltage is varied from 212.2V rms to 106.1V rms at $t=0.75 \text{ sec}$. according to the variation of the reference value the DC and AC output voltages are changed and follow the reference voltages as depicted in the Figure 14 for PI controller.

Figure 14: Reference variation-PI controller

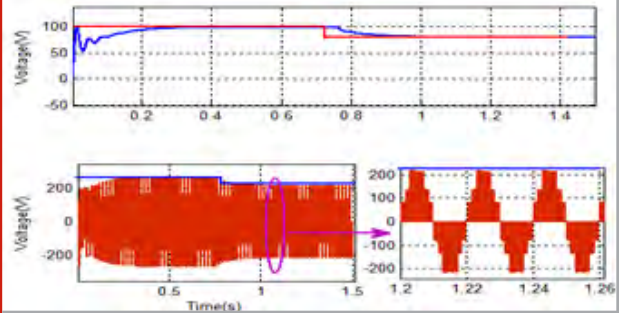


The harmonic spectrum of the source variation is shown in the Figure 16. The THD of the reference variation is 13.48%.

Transient analysis of MBHC: The transient performance criterion considered for the PI and FOPI controllers are the peak overshoot (M_p), settling time (t_s), and the integral absolute error (IAE).

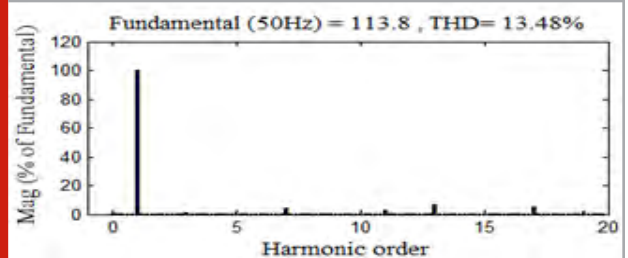
These parameters are measured and compared for both PI and FOPI controller of MBHC to prove the robustness of the converter. The transient performance analysis of this topology it tabulated in Table 4. All transient parameters

Figure 15: Fractional order reference variation



Compared to the PI controller, it is observed that the depicted result, as shown in the Figure 15, of FOPI illustrates better performance of the proposed converter.

Figure 16: FFT analysis of reference variation



are less for FOPI controller compared to the integer order PI controller. The peak overshoot of the FOPI controller is reduced to 74%, 14%, and 00% for load variation, supply variation and reference variation respectively. Likewise, the settling time is reduced to 21.8%, 25%, and 14% for the above attributes respectively and IAE is reduced to 88%, 60%, 83% for load variation, supply variation and reference variation respectively.

Table 4. Transient analysis of MBHC

Attributes	Peak overshoots M_p (%)		Settling time t_s (s)		Integral absolute error (IAE)	
	PI	FOPI	PI	FOPI	PI	FOPI
Load variation	81	21	0.32	0.25	0.009	0.001
Supply variation	58	50	0.2	0.15	0.02	0.008
Reference variation	60	0	0.22	0.19	0.003	0.0005

CONCLUSION

This paper has proposed closed loop controller for a novel Multilevel boost hybrid Converter that is capable of supplying DC and multilevel AC output simultaneously for high power residential applications. The conventional PI and FOPI controller design of the MBHC has been done and subjected to the line regulation, load regulation and reference regulation. From the results it is concluded

that the FOPI controller has better performance than the integer order PI controller in regulating the output of the MBHC of the PV applications.

REFERENCES

- Ali N Priyadarshini K S Sathiyapriya S Soundaryalakshmi D & Suganya V (2017) A Performance Analysis of Switched Capacitor Multilevel DC/AC Inverter using

- Solar PV Cells International Journal for Modern Trends in Science and Technology 3 104-109.
- De Keyser R Muresan C I & Ionescu C M (2018) An efficient algorithm for low-order direct discrete-time implementation of fractional order transfer functions ISA transactions 74 229-238.
- Jeyasudha S & Geethalakshmi B (2017) Modeling and analysis of a novel boost derived multilevel hybrid converter Energy Procedia 117 19-26.
- Jeyasudha S & Geethalakshmi B (2017 April) Modeling and control of integrated photovoltaic module and converter systems In 2017 Innovations in Power and Advanced Computing Technologies (i-PACT) (pp 1-7) IEEE.
- Jeyasudha S & Geethalakshmi B (2018) Fractional-Order Controller Design and Analysis of SEPIC Converter In Intelligent and Efficient Electrical Systems (pp 47-63) Springer Singapore.
- Nemati M Braun M & Tenbohlen S (2018) Optimization of unit commitment and economic dispatch in microgrids based on genetic algorithm and mixed integer linear programming Applied energy 210 944-963.
- Paraskevopoulos P N (2017) Modern control engineering CRC Press.
- Ray O & Mishra S (2013) Boost-derived hybrid converter with simultaneous DC and AC outputs IEEE transactions on Industry applications 50(2) 1082-1093.
- Roy A & Srivastava S (2016 March) Design of optimal PIAD δ controller for speed control of DC motor using constrained particle swarm optimization In 2016 International Conference on Circuit Power and Computing Technologies (ICCPCT) (pp 1-6) IEEE.
- Sheng D Wei Y Cheng S & Wang Y (2018) Observer-based adaptive back stepping control for fractional order systems with input saturation ISA transactions 82 18-29.
- Vijeh M Rezanejad M Samadaei E & Bertilsson K (2019) A general review of multilevel inverters based on main submodules: Structural point of view IEEE Transactions on Power Electronics 34(10) 9479-9502.
- Wan X F Dai Y C Liu Q Du L P & Hu W (2017) MPPT study of PV array with multi-peak based on combination of perturbation method and SVR Chinese Journal of Power Sources (5) 37.
- Xing X Zhang C He J Chen A & Zhang Z (2017) Model predictive control for parallel three-level T-type grid-connected inverters in renewable power generations IET Renewable Power Generation 11(11) 1353-1363.
- Ye Z Jiang L Zhang Z Yu D Wang Z Deng X & Fernando T (2017) A novel DC-power control method for cascaded H-bridge multilevel inverter IEEE Transactions on Industrial Electronics 64(9) 6874-6884.
- Zeb K Uddin W Khan M A Ali Z Ali M U Christofides N & Kim H J (2018) A comprehensive review on inverter topologies and control strategies for grid connected photovoltaic system Renewable and Sustainable Energy Reviews 94 1120-1141.
- Zhang Y Wang H Wang Z Yang Y & Blaabjerg F (2018) Simplified thermal modeling for IGBT modules with periodic power loss profiles in modular multilevel converters IEEE Transactions on Industrial Electronics 66(3) 2323-2332.

Design of Triple Layered Antenna for 5G Millimeter Wave Applications

Syedakbar. S¹, Geerthana. S², Arthy. R³, Eniyal. S⁴ and Mathumitha.B⁵

^{1,2}Assistant Professor, Department of Electronics and Communication Engineering,

^{3,4,5}UG Scholar, Department of Electronics and communication Engineering,

K. Ramakrishnan College of Technology, Samayapuram, Tiruchirappalli.

ABSTRACT

A printed patch antenna is proposed for 5G broadband millimeter-wave (mm-Wave) applications. The antenna is able to resonate at two different frequencies with multiple resonance, in this paper we introduce two slots are etched to reduce the undesirable modes. It also provide good impedance around a Ka-band. We can able to obtain TM₂₀ mode without affecting TM₁₀ mode. This printed patch with minute etches is good and attractive candidate or 5G mm wave applications.

KEY WORDS: MM-WAVE,PATCH ANTENNA, TLY SUBSTRATE, 5G.

INTRODUCTION

Due to vast development in mobile wireless communication, very high data trafficking in the communication channel. So, we are in need of wide band spectrum for data transmission in the millimeter wave frequency bands namely 5G communications (Sharma et al.,2008; Rachmansyah et al., 2011) The existing traditional micro-strip antennas are surveyed because of their simpler structure, less weight, low cost and it is easily fabricated using printed circuit board (PCB) process, these are very attractive parameters in the design of millimeter wave antennas. Bandwidth, return loss, gain are the major parameters of the antenna design, various techniques were evolved for improving the bandwidth of the antennas such as tapered feed, L-Probe, T-shaped

feed line, substrate integrated waveguides (Ramya Vijay et al., 2018; Syedakbar.S et al.,2017).

The different patch structures slots like U-shaped slots, E-slots, spiral antenna are also evolved based on the design equation for the design antenna to be operated in the expected frequency and gain adjustment (Afsar Uddin.M, et al.,2015; Rakesh Kumar Tripathi 2011). Novel design methodology also incorporated in the design of printed patch using the concept of negative permeability and permittivity concepts called as meta-material for features enhancements.(F. Yang et al.,2001; S. Prasad Jones Christydass et al., 2017; T. S. Rappaport 2013; Syedakbar.S et al,2017). The size of the antenna is reduced with simpler structure by means of multiple layer of the substrates. In the proposed work, the antenna is proposed to 5G millimeter wave application with an existing low profile by introducing the slot in the longitudinal direction to have broad side radiation pattern. The center line E-shaped patch is altered to suppress the undesirable mode of operation. The paper is divided into multiple sections. Section I deal with an

ARTICLE INFORMATION

*Corresponding Author: akbarkrct@gmail.com
Received 15th April 2020 Accepted after revision 20th May 2020
Print ISSN: 0974-6455 Online ISSN: 2321-4007 CODEN: BBR CBA

Thomson Reuters ISI Web of Science Clarivate Analytics USA and Crossref Indexed Journal

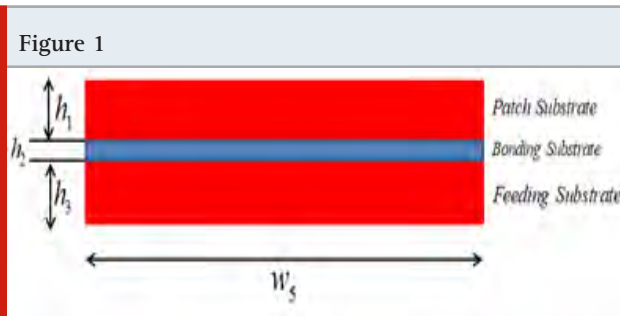


NAAS Journal Score 2020 (4.31) SJIF: 2020 (7.728)
A Society of Science and Nature Publication,
Bhopal India 2020. All rights reserved.
Online Contents Available at: <http://www.bbrc.in/>

introduction to this work, Section II explains the design methodology, and Section III explains result analysis of the proposed work followed by conclusions.

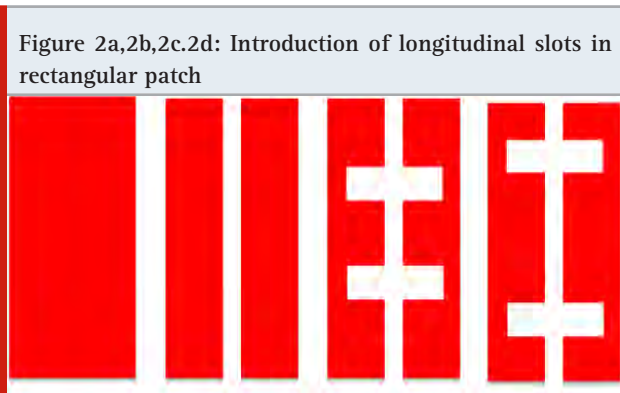
MATERIALS AND METHODS

Design Methodology: The design millimeter wave antenna is evolved from the basic micro-strip patch antenna. The millimeter wave antenna has an two different substrate: Layer 1 and Layer 3 is Taconic TLY substrate with the dielectric constant of $\epsilon_r=2.2$, whose thickness is $h_1=h_3=0.508\text{mm}$, in one of the layer the feeding is given. Layer 2 is Rogers 4450 with a dielectric constant is $\epsilon_r=2.2$, whose thickness is $h_2=0.1\text{mm}$, which is used to bond the two layers of Taconic TLY Substrate. The figure 1.a explains the substrate dimensions were antenna designed.

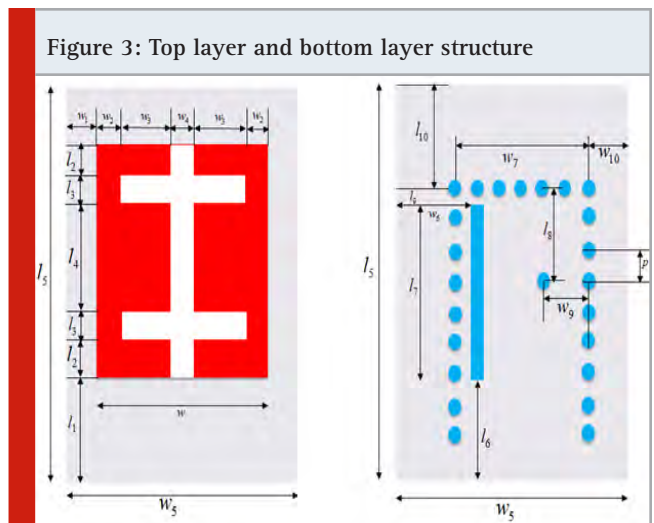


Initially the radiating patch is obtained as normal rectangular patch which fed by means of SIW feed, since it suitable for millimeter wave frequency antennas [Ramesh-----] which is an appropriate feed to match the impedance between the feeding part and the radiating part. The figure 2 explains the design of radiating patch is elaborated into three portions, they are of

- a) In figure 2b, the a longitudinal slot is introduced at the rectangular patch by which the multi mode operation is obtained.
- b) In figure 2c, the radiating slots were introduced so that we can able to obtain wider bandwidth of the obtained frequency is expanded
- c) In figure 2d the unwanted resonance also suppressed by increasing the gap between two radiating slots in the rectangular patch



The figure 3 explains the structure and dimensions of radiating structure and feeding structure substrate with transverse slots in the feeding substrate.



RESULTS AND DISCUSSION

The analyzed and designed antenna and feed structure is printed on 12.50x12.50 mm² substrate of three layers feed structure layer is Taconic TLY layer of width 0.508mm and the patch is structure is also fabricated in the same material as such the feed substrate, to have a contact we introduced a substrate of Roger with the thickness of 0.1mm. Therefore the entire antenna thickness of the antenna is 1.116mm. The antenna is said to good candidate for millimeter wave communication by means of key parameters such as return loss, VSWR, gain and radiation pattern. The figure 4 explains the better return loss less than -10dB and the VSWR is also less than 2 at the specific millimeter wave frequency. The better radiation pattern and the gain is also obtained.

Table. 1 The dimensions of the entire antenna is discussed in the table 1

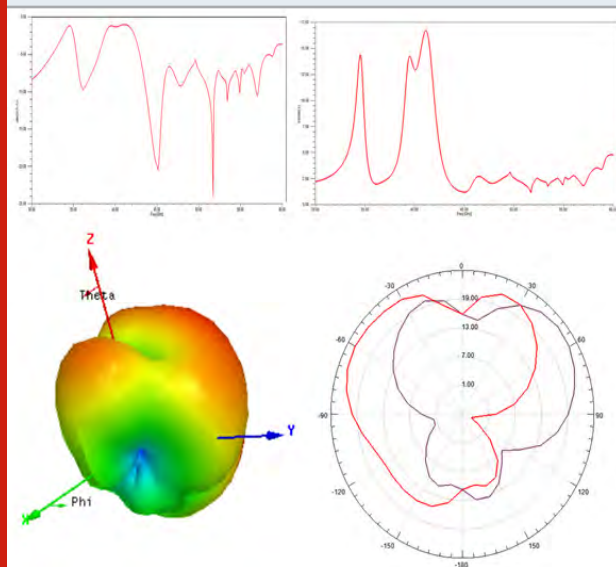
Parameter	Values (mm)	Parameter	Values (mm)	Parameter	Values (mm)
w_1	4.58	l_1	3.61	w_1	1.27
w_2	0.48	l_2	0.52	w_{10}	5.47
w_3	1.08	l_3	0.48	l_9	0.25
w_4	0.25	l_4	3.28	l_{10}	4.46
w_5	12.50	l_5	12.50	$h_1 h_3$	0.508
w_6	6.12	l_6	4.71	h_2	0.1
w_7	4.35	l_7	3.09	p	0.60
w_8	0.29	l_8	1.60	d	0.30

CONCLUSION

The novel printed patch antenna is designed to address millimeter wave application is presented in this paper. The significant feature of the design approach is its

compactness of total substrate dimension of 12.50mm x 12.50mm. The designed is good candidate based on the better simulated results on S-parameters, radiation patterns, gain of Thus, the proposed design is a suitable candidate for 5G millimeter wave applications to avoid network trafficking.

Figure 4: Return loss, VSWR, #D and 2D radiation pattern of the designed antenna



REFERENCES

Afsar Uddin M M Humayan Kabir M Javed Hossain and M A Rahman Khan (2015) Designing High Bandwidth Connected E-H and E-Shaped Micro strip Patch Antennas for S-band Communication International Journal of Computer Science and Information Security Vol 13 No 6.
F Yang X-X Zhang X Ye and Y Rahmat-Samii Wide-band

E-shaped patch antennas for wireless communications IEEE Trans Antennas Propag vol 49 no 7 pp 1094–1100 2001

S Prasad Jones Christydas ; N Gunavathi (2017) Design of CSRR loaded multiband slotted rectangular patch antenna 2017 IEEE Applied Electromagnetics Conference (AEMC)

Rachmansyah Antonius Irianto and A Benny Mutiar (2011) Designing and Manufacturing Micro strip Antenna for Wireless Communication at 24 GHz IJCEE Vol 3 No 5 Pages 33.

Rakesh Kumar Tripathi (2011) Dual Frequency Wideband Rectangular Microstrip Patch Antenna for Wireless Communication Systems Thapar University Pages 25
Ramya Vijay ; Thipparaju Rama Rao (2018) Design of penta-band antenna with integrated LNA circuit for vehicular communications IET Circuits Devices & Systems Volume: 12 Issue: 3

Sharma and G Singh (2008) Design of Single Pin Shorted Three-dielectric layered Substrates Rectangular Patch Microstrip Antenna for Communication Systems Progress In Electromagnetics Research Letters Vol 2 157–165.

Syedakbar S S Ramesh J Deepa (2017) Ultra wide band monopole planar MIMO antenna for portable devices IEEE International Conference on Electrical Instrumentation and Communication Engineering.

Syedakbar S A Muthulakshmi G Monika Dharani J Aarthy (2017) Unit cell structure for multiport ultra wide band (UWB) antenna International Conference on Innovations in Information Embedded and Communication Systems ICIECS-2017.

T S Rappaport S Sun et al (2013) Millimeter wave mobile communications for 5G cellular: It will work! IEEE Access vol 1 pp 335–349.